

Cover Page



Universiteit Leiden



The handle <http://hdl.handle.net/1887/21063> holds various files of this Leiden University dissertation.

Author: Ewing, Mark McConnell

Title: Post-interventional atherosclerotic vascular remodeling : preclinical investigation into immune-modulatory therapies

Issue Date: 2013-05-23

Post-interventional atherosclerotic vascular remodeling

Preclinical investigation into
immune-modulatory therapies

Mark M. Ewing

Post-interventional atherosclerotic vascular remodeling

Preclinical investigation into
immune-modulatory therapies

Proefschrift

ter verkrijging van
de graad van Doctor aan de Universiteit Leiden,
op gezag van de Rector Magnificus prof. mr. C.J.J.M. Stolker,
volgens besluit van het College voor Promoties
te verdedigen op donderdag 23 mei 2013
klokke 15.00 uur

door

Mark McConnell Ewing

geboren te Alkmaar
in 1986

Promotiecommissie

Promotor: Prof. dr. P.H.A. Quax
Co-promotor: Prof. dr. J.W. Jukema

Overige leden: Prof. dr. R.E. Toes
Prof. dr. J. Hamming
Prof. dr. P.J. van den Elsen
Prof. dr. J. Kuiper (LACDR, Leiden University)

The research described in this thesis was performed the departments of Surgery and Cardiology in the Leiden University Medical Center, Leiden, The Netherlands.

Het verschijnen van dit proefschrift werd mede mogelijk gemaakt door steun van de Nederlandse Hartstichting.

Financial support for the printing of this thesis was provided by Boehringer Ingelheim BV, Boston Scientific, ChipSoft, Daiichi Sankyo Nederland BV, Diabetes Fonds, J.E. Jurriaanse Stichting, familie Van Mourik, MSD Nederland BV, Roche Nederland BV and Servier Nederland Farma BV.

Happiness lies in the joy of achievement and the thrill of creative effort.

Franklin D. Roosevelt
1882-1945

Aan mijn ouders & Hinka

Cover design: M.M. Ewing
Inspired by the London Underground map and reproduced with the
kind permission of Transport for London.

Printing: Wöhrmann Print Service

ISBN: 978-94-6203-331-3

Mark M. Ewing
Post-interventional atherosclerotic vascular remodeling: preclinical investigation into
immune-modulatory therapies.

Proefschrift Leiden
Met literatuur opgave en Nederlandse samenvatting.

© 2013 M.M. Ewing
No parts of this thesis may be reproduced or transmitted in any form or by any
means without prior permission of the author.

Table of contents

	Page
Chapter 1 General introduction	11
Chapter 2 Potential biomarkers for accelerated atherosclerosis and other post-interventional remodeling <i>Biomark Med. 2012;6:53-66</i>	39
Chapter 3 Small animal models to study restenosis and effects of (local) drug therapy <i>Coronary stent restenosis, Editor: IC Tintoiu. Bucharest: The Publishing House of the Romanian Academy. 2011</i>	61
Chapter 4 Part I Annexin A5 in accelerated atherogenesis Annexin A5 therapy attenuates vascular inflammation and remodeling and improves endothelial function in mice <i>Arterioscler Thromb Vasc Biol. 2011;31:95-101</i>	83
Chapter 5 Annexin A5 prevents post-interventional accelerated atherosclerosis development in a dose-dependent fashion <i>Atherosclerosis 2012;221:333-340</i>	107
Chapter 6 Part II Innate and adaptive immunity in vascular remodeling Optimizing natural occurring IgM antibodies for therapeutic use: inflammatory vascular disease treatment with anti-phosphorylcholine IgG <i>Submitted for publication</i>	127
Chapter 7 Blocking toll-like receptors 7 and 9 reduces postinterventional remodeling via reduced macrophage activation, foam cell formation, and migration <i>Arterioscler Thromb Vasc Biol. 2012;32:e72-80</i>	161
Chapter 8 T-cell co-stimulation by CD28-CD80/86 and its negative regulator CTLA-4 strongly influence accelerated atherosclerosis development <i>Int J Cardiol. 2013; In press</i>	189
Chapter 9 Part III PCAF in post-interventional vascular remodeling Genetic variation in PCAF, a key mediator in epigenetics, is associated with reduced vascular morbidity and mortality: evidence for a new concept from three independent	219

	Page
prospective studies <i>Heart. 2011;97:143-50</i>	
Chapter 10 The epigenetic factor PCAF regulates vascular inflammation and is essential for accelerated atherosclerosis development. <i>Submitted for publication</i>	237
Chapter 11 The lysine acetyltransferase PCAF is a key regulator of arteriogenesis. <i>Submitted for publication</i>	259
Chapter 12 Summary and general discussion	285
Nederlandse samenvatting	292
List of publications	299
Curriculum Vitae	302

Chapter 1

General introduction

Introduction

Atherosclerotic cardiovascular disease

Cardiovascular diseases are the leading cause of death worldwide responsible for an estimated 16.7 million deaths annually which can be primarily attributed to atherosclerosis, a chronic inflammatory disease of the large and medium-sized arteries¹. Atherosclerosis lies at the basis of coronary heart disease (CHD) and cerebrovascular pathologies, which both do not become manifest until the development of an acute thrombotic vascular occlusion. In the United States alone, atherosclerosis is responsible for 610.000 new and 325.000 recurrent cases of myocardial infarction every year². Fortunately, the mortality of CHD has been steadily declining in the past 20 years, by almost 33% in the Netherlands alone due to improved primary prevention and treatment strategies³. Nevertheless, current incidence rates continue to stress the importance of ongoing research into the improvement of prevention and treatment of these atherosclerosis-related pathologies.

An atherosclerotic plaque is comprised of a subendothelial accumulation of lipids and infiltrated leukocytes such as monocyte-derived macrophages, mast cells and B and T lymphocytes, covered by a fibrous cap build up from smooth muscle cells (SMC) and extracellular matrix (ECM) deposition. Lesion formation is initiated by a qualitative change in the endothelial monolayer by irritating stimuli such as dyslipidaemia, hypertension, and pro-inflammatory mediators that lead to the exposure of adhesion molecules⁴. Local leukocyte adhesion and infiltration follows with continuing cellular activation and pro-inflammatory mediator and enzyme production, leading to a localized chronic inflammatory state supported by continuing cholesterol accumulation. Over time, apoptosis and necrosis occur which lead to the formation of a necrotic core containing cellular debris and free cholesterol crystals. Coronary plaque progression causes luminal stenosis and ischemia in distal tissues, evoking clinical symptoms of angina pectoris. Eventual plaque rupture and endothelial erosion can trigger local arterial thrombosis due to the exposure of underlying thrombogenic material to the circulation causing platelet aggregation and humoral coagulation, resulting in occlusive thrombus formation⁵. Such atherothrombosis events elicit brain or myocardial infarction as life-threatening complications, often requiring lesion revascularization through angioplasty, bypass-grafting or thrombolysis.

Target lesion revascularization and post-interventional vascular remodeling

Revascularization strategies are comprised of percutaneous coronary intervention (PCI), coronary artery bypass-grafting (CABG) surgery and thrombolysis. PCI is primary choice of revascularization strategy in patients presenting with objective myocardial ischemia due to occlusive CHD, diagnosed when presented with two out of the following three markers: clinical symptomatic presentation, typical changes on electrocardiography (ECG) and of circulating cardiac markers⁶.

Transluminal angioplasty was invented by the American Charles Dotter in 1964, who applied this technique to re-open blocked arteries in the lower extremities of patients and improve blood flow. PCI for the treatment of obstructive coronary artery disease was first performed by the cardiologist Andreas Guentzig and colleagues in Zurich in 1977, who used Dotter catheters modified by adding an inflatable balloon to allow dilation of occluded coronaries⁷. Despite initial benefits, renewed obstruction termed

'restenosis' developed in 30-60% of all cases due to elastic recoil and negative remodeling of the injured artery⁸. Restenosis following angioplasty has been the major problem limiting the success rate of coronary interventions and tremendous efforts have been made to target this problem⁹.

The introduction of bare-metal stents (BMS), which are deployed in the lesion segment during balloon inflation, prevented elastic recoil and have reduced the incidence of restenosis to 16-44%¹⁰, but also led to the development of neointimal hyperplasia and in-stent restenosis (ISR) (figure 1).

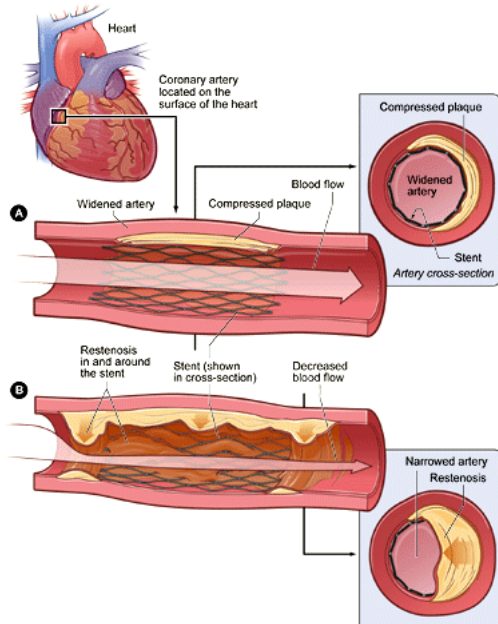


Figure 1.1 In-stent restenosis development

Stent expansion during therapeutic angioplasty compresses the atherosclerotic plaque into the arterial wall, re-establishing blood flow (panel A). The inset displays a cross-section of the compressed plaque and stent-widened artery. Over time, inflammation and accelerated atherosclerosis support fibrous tissue deposition, SMC migration and proliferation and foam cell formation. This can cause renewed (partial) blockage of the artery and distal ischemia (panel B). The inset shows a cross-section of the tissue growth around the stent.

This results from SMC migration and proliferation at the site of injury and extracellular matrix (ECM) formation by these cells. BMS struts serve as scaffolds to keep injured intimal and medial flaps from protruding into the lumen. Drug-eluting stents (DES) and drug-coated balloons have been developed to counter this phenomenon¹¹. DES struts are coated with polymers which can release anti-proliferative drugs such as sirolimus and paclitaxel to prevent SMC proliferation. These significantly reduced ISR incidence, although rates of 5-10% are still reported, responsible for over 200.000 revascularizations annually in the United States alone¹². Advantages of drug-coated balloons over stents are high drug concentration delivery per square millimeter of balloon surface and application possibilities in locations anatomically unfavorable for stent placement, such as bifurcations, small vessels and coronary

ostia. However, the lack of continued presence of both drug and polymer is the most important difference with stents. They reduce the chance of local hypersensitivity reactions, but also run the risk of an insufficient sustained period of drug-release to be fully effective¹¹.

Primary PCI has been shown to be clinically superior to thrombolysis with less major adverse events and with increased preservation of myocardium, particularly when applied in the period 3-12h after onset of symptoms. Thrombolysis however remains a viable alternative to primary PCI if it can be delivered within 3h after symptom onset⁶.

PCI is less invasive and generally preferable above CABG surgery except in cases such as chronic total occlusion, three-vessel or left main stem disease with distal vessel disease or ostial stenosis, provided patients are presented in a hospital with PCI facility and an experienced team. PCI only treats a spot, whereas CABG surgery into the distal third of the artery treats the entire vessel¹³. Nevertheless, PCI and CABG surgery both provide good symptom relief and clinical trials have so far been unable to show a significant difference in mortality 1-8 years after revascularization. The original trend favoring CABG disappeared, despite a reduction in mortality, due to the introduction of stenting to PCI. Recommendation of either PCI or CABG surgery will be guided by technical improvements in cardiology or surgery, hospital expertise and patients' preference⁶.

Restenosis risk factors

The underlying causes of post-PCI restenosis can be divided into four general categories, namely biological, arterial, stent and implantation factors^{14, 15}. Biological factors are comprised of the natural vascular wall resistance to antiproliferative drugs, the development of a sustained hypersensitivity reaction directed towards the polymer or metallic stent platform and local concentration of proteinases that stimulate SMC proliferation and migration. Arterial factors that can influence restenosis development are unfavorable (low) coronary artery wall shear stress levels, the progression of primary atherosclerotic lesion growth within a segment treated with angioplasty, as well as previous positive vascular remodeling¹⁵. Stent factors that determine ISR risk are the antiproliferative drug concentration and duration of sustained drug release. The stent gap, strut thickness and polymer disruptions, cracking and fractures are all major risk factors for ISR¹⁰. Above all, carefully-conducted technical implantation is highly important for adequate therapeutic effectiveness and factors such as barotrauma, inadequate stent expansion and geographical misses, where the stent is deployed proximally or distally from the lesion and deployment of a DES in a clot-laden arterial segment are all factors that contribute to ISR risk^{10, 14}.

Animal models for restenosis

Over the past decade, positive results have been obtained with sirolimus and paclitaxel-eluting stents (SES and PES respectively), although studies investigating other anti-restenotic drug were unable to provide similar results. Animal models that mimic the pathophysiology of post-interventional vascular remodeling allow for testing of new potential anti-restenotic drugs and evaluation of their therapeutic effectiveness, as well as effects of arterial wall integrity, atherosclerotic lesion initiation and progression and plaque stability¹⁶. Genetically-modified mouse strains allow for

screening of genes of interest concerning their role in lesion development, even in a dyslipidemic setting¹⁷. One well-defined model is the femoral arterial cuff model for post-interventional vascular remodeling and, during hypercholesterolemia, accelerated atherosclerosis development in which a non-constrictive cuff is surgically placed around the mouse femoral artery. This model allows for drug-eluting cuff placement to mimic DES deployment. This and other animal models to investigate restenosis and effects of (local) drug therapy are described in detail in chapter 3.

Arterial thrombosis

Arterial thrombosis lies at the basis of myocardial infarction in patients and their ischemia-related symptoms. In addition, catheter insertion into the thrombotic blocked coronary artery during PCI, balloon dilatation and stent deployment all favor the development of progressive and renewed arterial thrombosis. For this reason, anti-platelet drugs are the cornerstone of adjunctive medication⁶.

Thrombocyte adhesion, activating and aggregation result from contact to tissue other than the intact endothelium containing von Willebrand factor, but also from thrombin and epinephrine. Upon activation, platelets release prothrombotic mediators such as serotonin, thromboxane A₂ and ADP which cause vasoconstriction and platelet aggregation. Signaling through intracellular transduction pathways leads to the extracellular expression of the GPIIb/IIIa-complex which enables fibrinogen binding and clot formation. Currently often applied anti-platelet therapy consists of acetylsalicylic acid, clopidogrel and abciximab, also used in combination. Acetylsalicylic acid irreversibly acetylates cyclo-oxygenase, necessary for the formation of prostaglandin thromboxane A₂ from arachidonic acid, whilst the thienopyridine clopidogrel irreversibly blocks the adenosine phosphate (ADP) receptor on platelets necessary for GPIIb/IIIa-complex activation¹⁸ and the monoclonal antibody abciximab binds the GPIIb/IIIa-complex¹⁹. Despite the increased risk for bleeding complications, anticoagulant therapy has been shown to be very effective in reducing myocardial infarction, PCI and CABG-surgery-related arterial thrombosis and mortality¹⁸, also in combination with oral anticoagulant therapy (e.g. vitamin K antagonists) when sustained for at least 2 weeks following intervention⁶. Platelet aggregates facilitate leukocyte tethering and rolling²⁰, supporting the eventual leukocyte infiltration and local inflammatory response responsible for arterial inflammation and remodeling.

Annexin A5

The cellular membrane consists of a phospholipid bilayer that contains positively- and negatively charged phospholipids. Viable and healthy (endothelial) cells and platelets actively express the negatively charged phosphatidylserine (PS) on the inner cytosolic cellular membrane leaflet. Certain circumstances lead to a loss of membrane symmetry and translocation of PS to the outer membrane side, for example platelet activation and collagen adherence, but also erythrocyte aging, microparticle shedding and apoptosis^{21, 22}. Platelet-expression of PS enables the assembly of the prothrombinase complex comprised of factors Va, Xa and II (prothrombin). This complex promotes the conversion of prothrombin into the proteolytically active thrombin which cleaves fibrinogen to form fibrin polymers that lead to thrombus formation²³. Annexin A5 is a member of the annexin family, a group of highly-conserved proteins that are able to bind to negatively-charged phospholipid membranes in the presence

of Ca^{2+} ions. Annexin A5 resides intracellularly and is released upon injury and binds reversibly, specifically and with high affinity to PS²⁴. For this reason annexin A5 has been used diagnostically world-wide for the detection of apoptosis and atherosclerosis both in vitro and in vivo. PS serves as an 'eat-me' signal on apoptotic cells for circulating phagocytes and annexin A5 binds PS forming two-dimensional crystals and may thereby act as a lattice shielding PS from phagocytes and from interacting in phospholipid-dependent coagulation reactions^{22, 25}. The binding between annexin A5 and PS is uncompromised by circulating heparin, although annexin A5 can bind to the heparin oligosaccharide complex²⁶. Annexin A5 was originally discovered as an anticoagulant and antithrombotic protein and has been shown to be essential in the maintenance of placental integrity, where the pro-coagulant apical surfaces of syncytiotrophoblasts possess many binding sites for annexin A5. Its binding is crucial for the continuous blood flow and fetal viability²⁷. Annexin A5 has since also been shown to associate with the interferon γ receptor and prevent inflammatory cellular responses to secreted interferon γ ²⁸. This inflammatory cytokine is produced by natural killer (NK) and T-cells and is involved in monocyte recruitment and activation, central in pro-atherogenic cellular responses and inflammation²⁹.

In addition to its strong anti-coagulant properties, annexin A5 binds with high affinity to oxidized low-density lipoprotein (oxLDL) cholesterol particles and is therefore present in high concentrations in atherosclerotic lesions^{30, 31}. Circulating annexin A5 plasma levels are inversely related to the severity of coronary stenosis and are indicative of atherosclerotic plaque extent³², but are also elevated in hypertensive patients with systolic dysfunction³³ and following acute myocardial infarction³⁴. The binding of annexin A5 to oxLDL cholesterol particles, to apoptotic cells and the inhibitory effects on inflammation and coagulation have identified annexin A5 as a protein with high clinical anti-atherosclerotic and anti-restenotic potential.

The innate immune system in atherosclerosis

Immune responses against circulating and local immunogenic antigens in the arterial wall play a critical role in the initiation of inflammatory processes that characterize accelerated atherosclerosis development. The immune system can be divided into the innate and adaptive systems which are closely linked together and are tightly regulated. Innate immunity forms the first line of defense and exerts a fast although unspecific immune response to invading micro-organisms, whilst adaptive immunity reacts more slowly, but targets highly specific antigen-bearing targets on foreign intruders³⁵.

The innate immune system is comprised of the complement system, various toll-like and scavenger receptors and natural antibodies that target pathogenic antigens. Their activation evokes responses that are comprised of both internalizing and signaling pathogen recognition receptors (PRRs) that recognize pathogen- and damage-associated molecular patterns (PAMPs and DAMPs respectively) leading to inflammation (figure 2)³⁶.

Complement

The complement system consists of a group of liver-synthesized proteins, membrane-bound receptors and regulatory enzymes designed to increase antibody-mediated clearance of pathogens from the body and complement component C3 has a

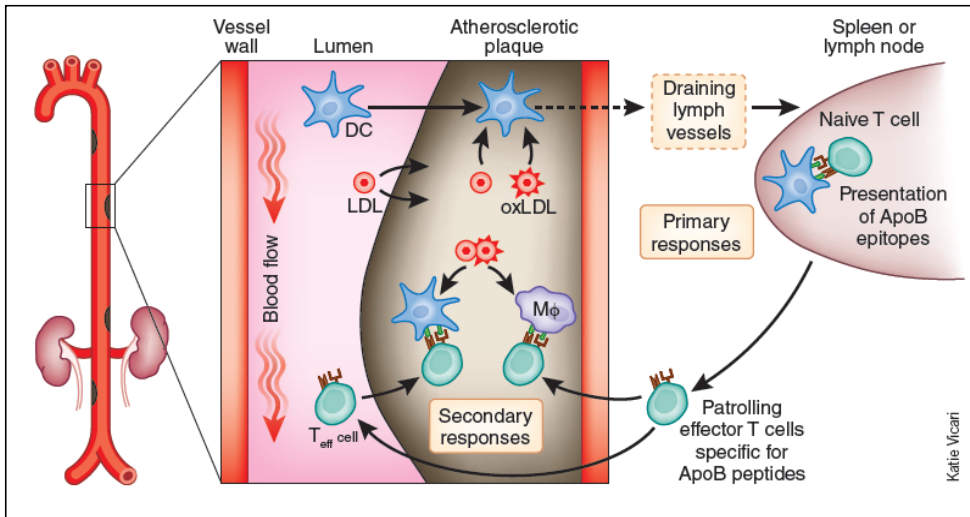


Figure 1.2 Innate and adaptive immunity in (accelerated) atherosclerosis development⁵³

Endothelial damage at sites of arterial atherosclerosis or interventional injury can cause platelet adherence and expression of adhesion molecules that enable recruitment and infiltration of leukocytes bearing pathogen recognition receptors such as dendritic cells. These can ingest immunogenic antigens such as oxLDL particles and TLR-ligands and travel to draining lymph nodes where antigens are presented to naive T-cells in the presence of co-stimulatory factors. Activated effector T-cells enter the blood stream and travel to the site of inflammation, where they engage in secondary inflammatory responses in co-operation with residing macrophages.

central function in this process. C3 cleavage by convertases into C3a and C3b is induced by specific substrates through either the classic, alternative or lectin pathways. C3b binds to the surface of pathogenic cells, enabling increased phagocytosis through opsonization^{37, 38}. The classic pathway is activated by binding of the C1 complex to antibodies bound to antigen-presenting bacterial cells. The three pathways initiate a cascade that results in C5 activation and formation of terminal complement component C5b-9, the membrane attack-complex that causes bacterial and cell lysis and the chemotactic factor C5a that supports leukocyte recruitment³⁹. Many complement triggers reside in the tunica intima in atherosclerotic segments and complement inhibition has been shown to result in reduced accelerated atherosclerotic lesion formation⁴⁰.

Toll-like receptors

Toll-like receptors (TLRs) form a major component of innate immunity, innate-adaptive crosstalk and reactions towards infectious and immunogenic auto-agents and are localized on both the internal and external sides of the cellular membrane. Situated on the cellular outer membrane leaflet, TLRs 2, 4 and 5 recognize exogenous PAMPs that originate from bacteria or viruses such as lipopolysaccharide (LPS) or flagellae (TLR5), whilst TLRs 7 and 9 on the inner cellular membrane recognize both pathogenic and endogenous ligands released after tissue damage or cell stress⁴¹. Myd88-dependent signaling is the dominant activation pathway of TLR signaling leading to nuclear factor kappa B (NFκB) transcription and expression of pro-inflammatory chemokines and cytokines^{42, 43}. Endothelial TLR4 activation by LPS on

circulating Gram-negative bacteria during bacteremia leads to nitric oxide production and vasodilation that can initiate hypotensive septic shock⁴⁴. DAMPs recognized by TLR4 include heat shock proteins⁴⁵, fibronectin extra-domain A⁴⁶, tenascin C and high mobility group box (HMGB) 1⁴⁷. TLR2 and/or 4 deficiency and inhibition are associated with reduced atherosclerosis and vascular remodeling, whilst increased signaling aggravates inflammation and atherogenesis, highlighting the importance of these receptors in the innate immune response.

Endosomal TLRs like TLRs 3, 7 and 9 recognize viral and bacterial DNA and (double-stranded) RNA (TLR3) fragments and possibly also damaged self DNA/RNA that might result from during interventional procedures including PCI and CABG-surgery. Arterial presence and activation of TLR7 and TLR9⁴⁸ leads to upregulation of interferon γ , interleukin (IL) 6, IL-12 or tumor necrosis factor (TNF) α by innate immune cells such as macrophages⁴⁹. These TLRs also recognize immune complexes containing self nucleic acids in autoimmune diseases and are localized in human arteries. Development of atherosclerotic plaques and PCI-induced injury cause a release of self RNA/DNA or proteins that enhance the recognition of nucleic acids by intracellular TLRs and can activate TLR7 and 9 signaling, by which these important parts of the innate immune system contribute strongly to arterial inflammation^{50, 51}. Indeed, septic shock can also develop when bacterial unmethylated CpG DNA binds TLR9, highlighting TLR7 and 9 as therapeutic targets to prevent restenosis. Surprisingly, TLR3 is suggested to have a protective role in atherosclerosis development.

Scavenger receptors

LDL cholesterol is the most important risk factor for cardiovascular disease (CVD) and cholesterol lowering therapy alone such as HMG-CoA reductase inhibitors (statins) can reduce CVD-risk by 30-40%. Once trapped in the arterial wall, LDL oxidation by enzymes such as lipoxygenases occurs. Oxidative modification of phospholipid fatty acids, degradation of apoB-100 into peptide fragments and modification of these structures by aldehydes derived from oxidized fatty acids leads to development of immunogenic neo-antigens⁵². Intramural oxLDL particle accumulation stimulates oxLDL-uptake by scavenger receptors such as scavenger receptor (SR) A-1, SRA-2, SR-B1 and cluster of designation (CD)36 on monocyte-derived macrophages. Scavenger receptors are multifunctional PRRs that clear the environment of cellular debris and microbes and are responsible for oxLDL particle ingestion by macrophages. Cholesterol efflux, termed efferocytosis, is controlled by ABC-type cassette transporters that mobilize cholesterol into high-density lipoprotein (HDL) particle for transport to the liver⁵³. A defective balance between cholesterol influx and efflux in these cells leads to excessive intracellular cholesterol accumulation which is stored in lipid droplets and promotes foam cell formation and lesion progression⁵⁴. Continuous influx of monocytes is observed throughout lesion progression and they are referred to as being signature cells in atherogenesis that are both central and detrimental in lesion progression.

Unfolded protein response

Many exogenous and endogenous sources of cellular stress have been identified, including stress that arises from the accumulation of unfolded protein in the endoplasmic reticulum (ER). In response to this stress, eukaryotic cells possess a

three-pronged signal transduction pathway collectively known as the unfolded protein response (UPR). This is made up of the IRE-1, PERK and ATF-6 axes⁵⁵. Sustained intracellular UPR is designed to relieve cell stress and reduce amino-acid biosynthesis, but UPR itself can lead to cell pathology and tissue dysfunction. In the arterial wall, saturated fatty acids, oxidative stress and oxysterols, but above all intracellular cholesterol accumulation, all lead to chronic UPR and inflammation in intimal macrophages and endothelial cells⁵⁶. This supports plaque progression and CHOP-induced foam cell apoptosis and necrotic core development^{57, 58}, but occurs in all stages of atherosclerotic lesion formation⁵⁹. Overall, it is clear that the UPR is fundamental in the pathogenesis of inflammatory diseases and could serve as a target of therapy for modulating cellular stress and inflammation⁶⁰.

Natural (auto-) antibodies

Natural antibodies are immunoglobulins that arise spontaneously without prior immune exposure or infection and even occur in specific-pathogen-free mouse strains. Natural antibodies occur predominately of the IgM isotype and are produced by B-1 cells in the spleen and act as the humoral equivalent of PRRs⁶¹. They are suggested to aid the homeostasis of the internal milieu by binding to protein determinants of dying cells, such as PS and to facilitate C3b deposition on pathogens aiding their elimination and that of immunogenic auto-antigens⁶².

In both mouse and man, natural IgM and IgG antibodies occur towards malondialdehyde (MDA) and copper-oxidized LDL cholesterol. To investigate their origin, B cell lines were isolated from spleens from non-immunized ApoE^{-/-} mice on high-fat diets⁶³. The resulting monoclonal antibodies, termed E0 antibodies were tested for their ability to recognize oxLDL. Gene sequence analysis unexpectedly identified that the genes encoding for the IgM anti-Cu oxLDL E06 antibody were completely similar to a classic B cell clone expressing T15 antibodies directed towards phosphorylcholine (PC) present on *Streptococcus pneumoniae* bacteria⁶⁴. Of all reported anti-PC antibodies, T15 antibodies are most effective in clearance of pneumococci pathogen infections⁶⁵ and they occur frequently in inbred mouse strains⁶⁶. This discovery identified complete molecular mimicry between oxLDL particles and *Streptococcus pneumoniae* bacteria that express the same PC moiety (figure 3)⁶⁷.

Anti-PC IgM T15 and E06 antibodies were found to be functionally equal in their ability to recognize PC on oxidized phospholipids but not on native LDL⁶⁸. This was confirmed when immunization of hypercholesterolemic LDL-receptor (r)^{-/-} mice against *Streptococcus pneumoniae* raised plasma titers of anti-PC IgM antibodies and prevent native atherosclerosis formation⁶⁹. They are suggested to act by passing through the endothelial barrier and binding to PC on oxLDL particles, thus blocking their uptake by scavenger receptor bearing macrophages and foam cells, preventing their expression of pro-inflammatory cytokines, matrix metalloproteinases (MMPs) and co-stimulatory molecules for T cell activation. In addition, anti-PC IgM may bind and lead to clearance of circulating oxLDL particles, rendering them unavailable for plaque formation and protect endothelial cells from the harmful oxidative properties of oxidized phospholipids (figure 4)⁷⁰. Immunization studies to prevent native atherosclerosis formation in mice have thus far been performed through active vaccination using *Streptococcus pneumoniae*⁶⁹, with PC bound to keyhole limpet hemocyanin (KLH)⁷¹ and through oral administration with oxLDL and MDA-LDL⁷², but also through

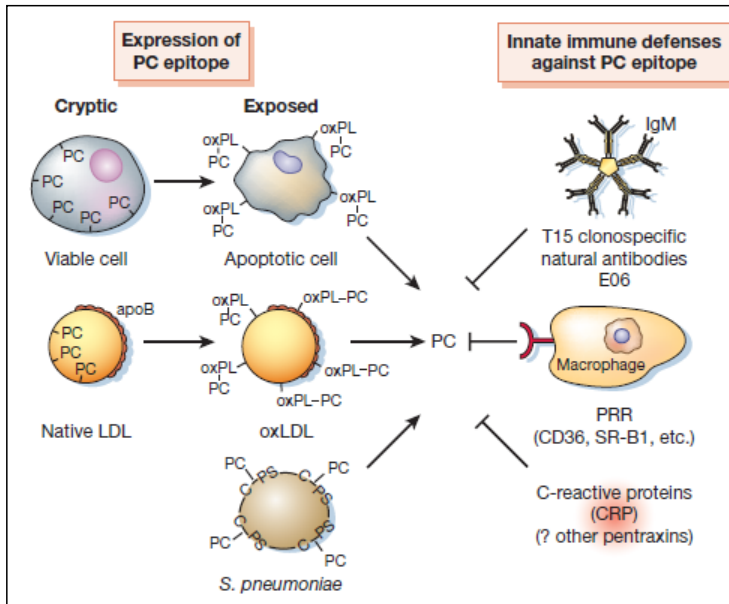


Figure 1.3 Molecular mimicry of pathogen associated molecular patterns³⁶

The immunogenic phosphorylcholine (PC) epitope is expressed by apoptotic cells, by oxidized LDL particles and by *Streptococcus pneumoniae* bacteria, which share molecular mimicry. These are recognized by various parts of the innate immune defenses such as natural antibodies of the T15/E06 type, macrophage scavenger receptors CD36 and SR-B1 and by C-reactive protein.

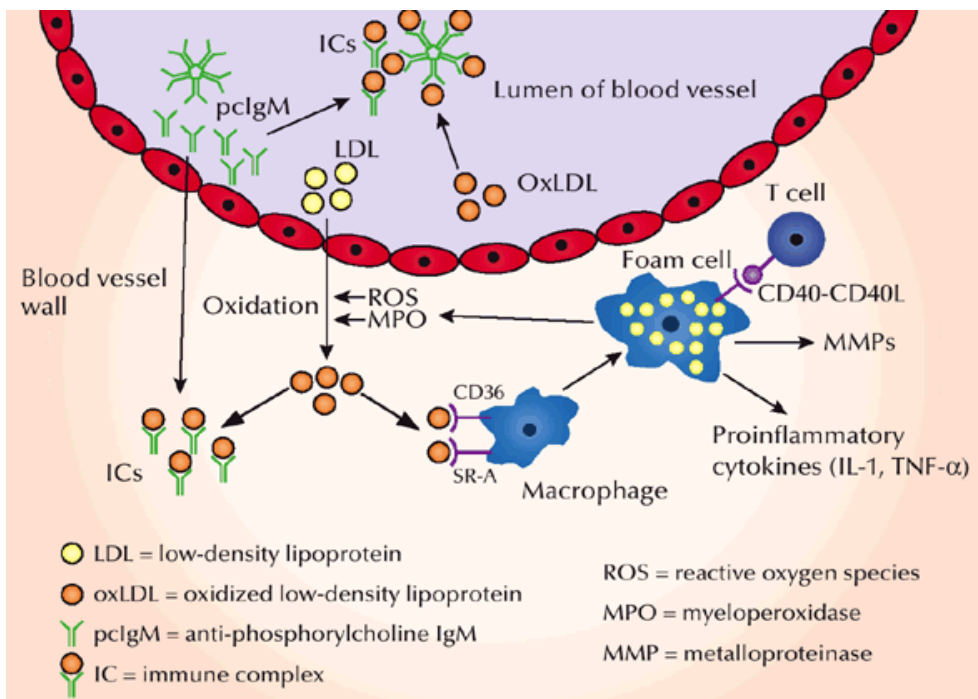


Figure 1.4 Proposed role of anti-PC IgM T15/E06 antibodies in preventing atherosclerosis⁷⁰

Atherosclerosis develops due to scavenger-mediated uptake of LDL cholesterol oxidized by reactive oxygen species leading to lipid-laden foam cell formation. These produce proinflammatory cytokines, MMPs and myeloperoxidase and express co-stimulatory molecules for T-cell activation. Pneumococcal vaccination (in mice) enhances anti-phosphorylcholine (PC) IgM antibodies that cross the endothelium where they bind to oxLDL particles to form immune complexes and prevent oxLDL uptake and foam cell formation. Additionally, anti-PC IgM can bind circulating oxLDL, facilitating its clearance and rendering it unavailable for plaque formation.

passive vaccination with two types of recombinant IgG1 against MDA-modified apoB 100⁷³ (including regression of existing lesions⁷⁴), with anti-PC IgM antibodies⁷⁵ and using oxLDL-pulsed mature dendritic cells⁷⁶.

Interestingly, recent investigations into the mechanisms of recognition that govern T-cell responses to LDL particles yielded surprising results. Research into T-cell hybridomas from human apoB100 transgenic mice immunized with oxLDL revealed they no longer recognized oxLDL, but solely LDL particles. Nevertheless, serum from these animals did contain anti-oxLDL IgG, indicating that T-cell responses to LDL lead to anti-oxLDL antibody production by plasma cells. The hypothesis behind these findings states that ingested and degraded oxLDL particles by scavenger receptor-expressing cells are co-expressed with MHC class II on the cell surface where they subsequently be recognized by CD4+ (TRBV31+ T-cell receptor bearing) T-cells. These CD4+ T-cells can stimulate macrophages, but also plasma cells to produce simultaneously anti-LDL and anti-oxLDL and related (PC) atheroprotective antibodies⁷⁷, emphasizing that such an antibody response is not just confined to oxLDL, but also extent towards native LDL particles.

Advantages of active vaccination are life-long protection and the need for only relative few immunizations, whilst passive immunization allows the induction of a fast and controlled immune response against the desired antigen. Fully human monoclonal antibodies are ideal for such passive immunization strategies and are preferred above re-engineered, de-immunized or rodent monoclonal antibodies. They can be generated using phage display platforms, which allow for identification of clinical candidates selected for their optimal desired functions⁷⁸. Previously, such recombinant antibody libraries have proven to serve as an excellent source of active and well tolerated experimental therapeutics⁷⁹.

Natural antibodies in CHD

Over the past twenty years, many basic and epidemiological studies have suggested a role for indolent infections such as *Chlamydia pneumoniae* in atherosclerosis progression, although clinical trials using antibiotics failed to reduce CHD incidence⁸⁰. Thus far, a clinical study in healthy human volunteers (both smokers and non-smokers) was unable to show an increase in serum anti-PC or anti-oxLDL immunoglobulines following the application of widely-used adult pneumococcal polysaccharide vaccine, despite an increase in antibodies directed towards surface capsular polysaccharides⁸¹. Another study identified that hospital-administered patients suffering from myocardial infarction were less likely to have received a pneumococcal polysaccharide vaccine than patients admitted for other causes, suggesting vaccination might protect from myocardial infarction. However, effects are likely to result from a reduced incidence of pneumonia, which has been shown to trigger myocardial infarction⁸², and thus acute events triggering infarction rather than through reduced

atherogenesis. Indeed, in contrast to chronic infections, prevention and adequate treatment of acute infections may prevent abrupt and severe inflammatory changes in high-risk patients groups and reduce myocardial infarction incidence⁸³. Nevertheless, a save immunization protocol that can elicit a proper and sustained immune response or the development of fully human antibodies towards PC, preferably of the IgG isotype, could prove very effective in the prevention of both native and post-interventional accelerated atherosclerosis formation in clinical setting.

The adaptive immune system in atherosclerosis

The adaptive immune system can recognize an almost infinite number of molecular structures and depends on the vast variety of B and T cell receptors and immunoglobulines, generated by somatic rearrangement processes in blast cells. In contrast to PRRs, an almost infinite number of receptors exists and is capable of interacting with infiltrating pathogens.

Effector T-cells

Most T-cells in the atherosclerotic lesion are CD3+ and CD4+ T-helper (Th) cells that express the $\alpha\beta$ T-cell antigen receptor (TCR) and have a Th1 phenotype. These cells are identified by their production of interferon (IFN) γ and IL-2 and are derived from native major histocompatibility complex (MHC) class-II CD4+ T-cells following presentation with specific antigens and co-stimulatory signals in the presence of cytokines such as IL-12 and IFN γ ⁸⁴. Cytotoxic MHC class I-recognizing CD8+ T-cells are also present in the lesions, although their function remains unclear. CD4+ T-cells recognize class-II presented peptides by antigen-presenting cells (APCs) such as oxLDL particles, heat shock proteins 60 and 65, but also exogenous pathogens such as *Chlamydia pneumoniae*. An extensive body of evidence exists identifying the direct role of pro-inflammatory Th1 T-cells in atherosclerosis development^{77, 85, 86}. IgG2a antibodies in plasma dominate early atherosclerotic lesion progression, indicating predominant Th1 involvement. The two most important effector molecules produced by Th1 cells are membrane-bound CD40 ligand and the pleiotropic cytokine IFN γ that contribute to monocytes-differentiation and activation. IFN γ is highly produced in atherosclerotic lesions by not only Th1 cells, but also macrophages and NKT cells⁸⁷. These molecules in turn stimulate pro-inflammatory IL-1, TNF α and MMP expression by macrophages and contribute substantially to local inflammation (IL-6 and C-reactive protein), lesion growth and fibrous cap thinning⁸⁸. Indeed, strong atherosclerotic lesion reduction was found in ApoE^{-/-} mice with genetic CD40 ligand disruption⁸⁹ and IFN γ deficiency⁹⁰ as well as following anti-CD40 ligand antibody treatment⁹¹. Finally, daily IFN γ administration significantly augmented lesion growth in hypercholesterolemic ApoE^{-/-} mice⁹².

Th2 cells primarily produce IL-4, IL-5, IL-10 and IL-13 and stimulate B-cell antibody production, but are not detected in large quantities in atherosclerotic lesions. IL-10 itself has strong anti-inflammatory and anti-atherosclerotic and restenotic effects⁹³. Nevertheless, Th2 specific IgG1 antibodies are only detected in plasma at the advanced stages of atherosclerotic lesion progression. Studies involving Th2 cells have shown that Th2 cells in general inhibit atherogenesis²⁹.

Regulatory T-cells

Regulatory T-cells (Tregs) have a T-cell suppressive function and contribute effectively to maintenance of immunological response and auto-reactivity. They comprise approximately 5-10% of all peripheral CD4⁺ T-cells and are defined as the cell population expressing CD4⁺CD25⁺CD127^{low} markers on their extracellular membrane surface and intracellular forkhead box (Fox) P3, vital for their suppressive function⁹⁴. Mice genetically deficient for FoxP3 develop an autoimmune-like lymphoproliferative disease, emphasizing the suppressive function of Tregs in maintaining peripheral tolerance⁹⁵, whilst humans lacking FoxP3 suffer from severe autoimmune disease that develops in infancy.

Tregs exert suppressive function through inhibition by cytokines, cytolysis, metabolic disruption and intervention in dendritic cell maturation. Thymus-derived Tregs express inhibitory cytokines IL-10, IL-35 and transforming growth factor (TGF) β , which stimulates collagen synthesis and is fibrogenic⁹⁶. They migrate towards an atherosclerotic lesion similarly to Th1 cells, but the local pro-inflammatory microenvironment favors Th1 cell survival, causing an imbalance in T-cell adaptive immunity⁹⁷. Tregs constitutively express cytotoxic T-lymphocyte antigen 4 (CTLA-4)⁹⁸, acting as physiological dendritic-cell-mediated co-stimulation inhibitor and have been shown to control the development of atherosclerotic lesions through regulation of Th1 and Th2 responses⁹⁹ and is vital for their suppressive function¹⁰⁰. Indeed, loss of adequate CTLA-4 function with blocking monoclonal antibodies produces auto-immune disease in mice similar to CD4⁺CD25⁺ Treg depletion and abolishes their protective function both in vitro and in vivo, since these cells can no longer block TCR and CD28-mediated co-stimulatory signals leading to Th1 activation, even to immunogenic self auto-antigens⁹⁸. CTLA-4 on Tregs has also been shown to induce the enzyme indolamine 2, 3-dioxygenase (IDO) through CD80 and CD86 interaction on dendritic cells, which catalyzes the conversion of tryptophan to kynurenine¹⁰¹ that has potent immunosuppressive effects on dendritic cells, and thus T-cell activation¹⁰².

T-cell co-stimulation

T-cell mediated immune responses are initiated in lymphoid tissues where they are stimulated by APCs and can then interact with B cells to promote an antibody response or migrate to peripheral tissues to engage infiltrated pathogens or immunogenic antigens. A small portion of these cells become memory T-cells, to enable a quick response during re-infection. Their activation is described by the two-signal model which is composed of the presentation of MHC complex-bound peptides, as well as co-stimulatory signals provided by accessory molecules¹⁰³. Activation of the two principal pathways leads to IL-2 regulated T-cell proliferation and their effector function acquisition. Since T-cell activation leads to TCR internalization, native T-cells require prolonged antigen exposure. The dominant co-stimulatory receptor CD28 is constitutively expressed on resting T-cells and binds CD80 (B7-1) and CD86 (B7-2) on dendritic cells, B cells, and monocytes/macrophages. CD80 and CD86 have both been shown to strongly contribute to atherosclerotic lesion formation¹⁰⁴. Their function is required for an adequate T-cell response to atherosclerotic antigens and their expression of IFN γ . TCR binding in absence of CD28 ligation leads to T-cell anergy or even apoptosis, preventing non-specific T-cell activation and auto-immunity (figure 5)¹⁰⁵.

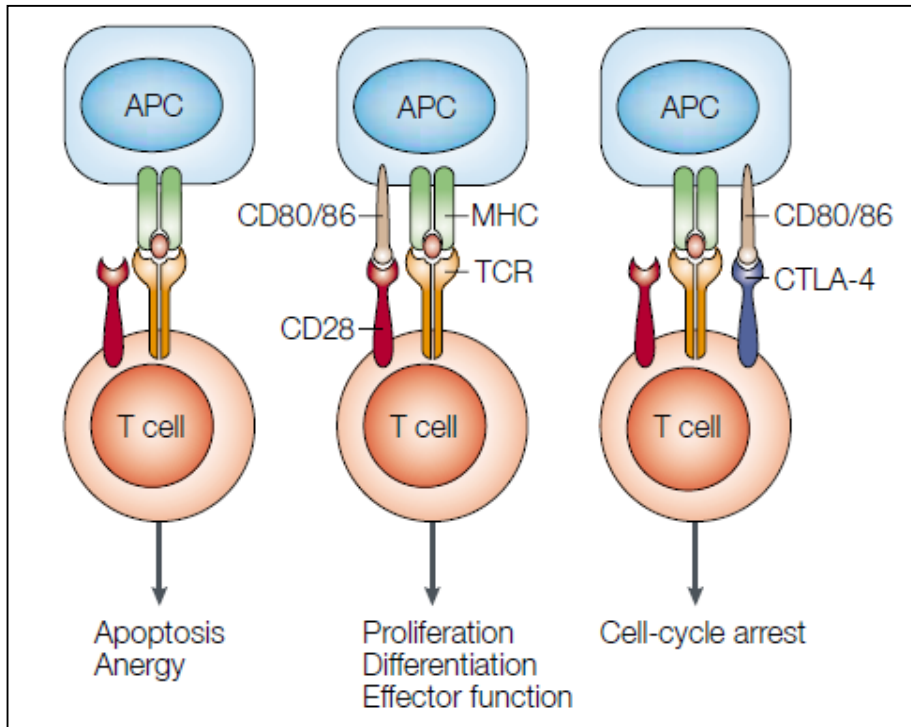


Figure 1.5 T-cell fate under various T-cell receptor engagements¹⁰⁷

Adequate T-cell stimulation requires simultaneous interaction between a specific major histocompatibility (MHC)-peptide complex and the T-cell receptor and CD28 ligation by the B7-1 (CD80) or B7-2 (CD86) receptors on the antigen-presenting cell (APC). Absence of simultaneous interaction leads to T-cell apoptosis or anergy. After successful activation, T-cells upregulate cytotoxic T-lymphocyte antigen 4 (CTLA-4; CD152) that outcompetes CD28 for CD80/86 binding and results in cell-cycle arrest.

Cytotoxic T-lymphocyte antigen (CTLA)-4 and co-inhibition

CTLA-4 (CD152) is a co-inhibitory receptor expressed on activated T-cells and is homologous to CD28 and binds either a CD80 or CD86 mono- or heterodimer on APCs with approximately 100 times higher affinity than CD28¹⁰⁶. Most CTLA-4 is expressed intracellularly rather than at the cell surface, thus limiting its engagement to CD80/86 and preventing a premature termination of an immune response¹⁰⁷. During an ongoing immune response, CTLA-4 is upregulated and outcompetes CD28 for binding to CD80 and CD86, leading to T-cell proliferation inhibition and termination of IL-2 production, IL-2 receptor expression and arresting T-cells in the G1-phase of their cell cycle¹⁰⁵.

The importance of the CD28/CTLA-4 pathways has become evident by generating mice genetically deficient in CTLA-4, which develop fatal lymphoproliferative disease with progressive polyclonal T-cell accumulation in peripheral lymphoid and solid organs such as the heart, liver and pancreas¹⁰⁸. This is prevented by crossing CTLA-4^{-/-} mice with Rag^{-/-} and with CD80^{-/-}CD86^{-/-} animals¹⁰⁹. CTLA-4 has the maximal inhibitory effects in primed rather than naïve T-cells and decreases the proportion of cytokine-secreting T-cells in stead of the response magnitude per T-cell, explaining that more APCs are necessary to generate a detectable cytokine response

during CTLA-4 ligation¹⁰⁷. In contrast to full-length CTLA-4, transgenic expression of tailless CTLA-4 mutant protein only reduced lymphocytic infiltration in solid, but not lymphoid, organs in CTLA-4^{-/-} mice¹¹⁰, but transfected mutant CTLA-4 constructs into Jurkat cells indicated scavenging of CD80/86¹¹¹. These findings support the balanced view that CTLA-4 receptors act by both scavenging C80/86 away from CD28 on APCs as well as through direct intracellular pathways and are vital for maintaining T-cell homeostasis and preventing auto-immune reactions.

Unlike activated effector T-cells, Tregs constitutively express CTLA-4 and since blocking CTLA-4 antibodies prevent their inhibitory effects, CTLA-4 is required for their suppressive function¹¹². Treg function was shown to be completely inhibited following acute CD80 and CD86 inhibition, further confirming the essential role for co-stimulation and inhibition in controlling adequate Treg function⁹⁹.

A second co-inhibitory receptor expressed by T-cells and shown to be involved in atherogenesis is programmed-death (PD)-1. PD-1 is a family member of CD28 which can bind either PD-1-ligand 1 or 2 (PD-L1 and PD-L2 respectively), expressed on either solely hematopoietic cells (PD-L2) or both non- and hematopoietic cells (PD-L1)^{106, 113}. PD-1^{-/-} mice also develop lupus-like proliferative arthritis and glomerulonephritis with IgG deposition¹¹⁴. Similarly to CTLA-4, PD-1 signaling inhibits T-cell proliferation and activation and their signaling has an important function in downregulating pro-atherogenic T-cell responses¹¹⁵.

Clinical significance of CTLA-4

Rheumatoid arthritis (RA) is a chronic inflammatory disease that leads to progressive joint damage and disability and activated T-cells were shown to play a central role in inflammation progression¹¹⁶. The potential for CTLA-4 to interrupt T-cell co-stimulatory signals was harnessed by fusing the extracellular domain of human CTLA-4 to the modified Fc portion of human IgG1, creating the soluble fusion protein CTLA-4Ig named abatacept¹¹⁷. Circulating abatacept has been shown to prevent CD28-CD80/86 co-stimulation of follicular Th-cells¹¹⁸ and subsequently decreasing T-cell production of TNF α , IFN γ and IL-2 and has been approved for the treatment of mild to severe RA in patients who respond insufficiently to other disease-modifying antirheumatic drugs, including methotrexate, and TNF α inhibitors¹¹⁷. Abatacept displays little immunogenicity, with <3% of patients developing an antibody response¹¹⁹. Interestingly, soluble CTLA-4Ig has also been shown to effectively prevent T-cell mediated lymphoproliferative disease in CTLA-4^{-/-} mice¹²⁰.

B lymphocytes and dendritic cells

Co-stimulatory and -inhibitory receptors are not restricted to T-cells, but are also expressed on B lymphocytes. These cells are present at the base of early fatty streaks and thereafter constitutively in the adventitia of human coronary lesions. At first, they were suggested to have a protective function against atherogenesis, since splenectomy increased atherosclerotic lesion size in hypercholesterolemic mice due to loss of B-cell produced protective anti-oxLDL antibodies¹²¹. However, acute B-cell depletion using anti-CD20 antibodies was since then shown to reduce atherosclerotic lesion size by reducing pathogenic T-cell responses whilst preserving the production of protective anti-oxLDL IgM, rather than IgG, antibodies. This reduced production of IFN γ and enhanced that of IL-17¹²². Very recently, the important role of CD28 in

this process was elucidated. The half-life of antibodies is days to weeks, whereas long-term immunity against infection through antibody production by plasma cells continues of a life-time. It was shown that CD28-expressing long-lived plasma cells (LLPCs) residing in the bone-marrow, but not splenic short-lived plasma cells, require continuous CD28 signaling through CD80 or CD86 for their function and loss of the CD28-CD80/86 pathway strongly reduces LLPCs half-life^{123, 124}. Since these cells are the producers of protective natural antibodies (e.g. against oxLDL particles), CD28 is suggested to be important in maintaining adequate antibody titers associated with atherosclerosis risk.

Dendritic cells express co-stimulatory molecules such as CD80 and CD86 and accumulate in the intima of atherosclerotic lesions and two distinctive types have been identified, namely classic myeloid dendritic cells (mDC) which mainly recognize endogenous and exogenous bacterial signatures through TLR2 and 4 and can produce MMPs and IL-12, leading to recruitment of cytotoxic T-cells¹²⁵. Plasmacytoid dendritic cells (pDC) specifically recognize viral fragments through TLR9 and can produce large amount of IFN γ ¹²⁶, leading to TLR4 upregulation on other APCs and increases atherosclerotic lesion development¹²⁷. pDC presence in the shoulder region of atherosclerotic lesions contributes strongly to plaque instability and rupture²⁹.

Epigenetic regulation of inflammation

Post-interventional atherosclerotic vascular remodeling results from local arterial-inflammatory processes that are tightly regulated by local gene expression profiles immediately after vascular interventions such as PCI and CABG-surgery. Inflammation results from increased transcription of inflammatory genes and is limited by the extent of chromatin accessibility to gene-regulatory proteins and transcriptional factors. Chromatin consists of DNA wrapped around histones (called nucleosomes) and non-histone proteins¹²⁸ and can display various degrees of compactness. This is controlled by the amount of histone modifications exerted by epigenetic factors that cause acetylation and methylation of lysine residues¹²⁹, but also DNA methylation at CpG dinucleotides. Since they determine gene expression independently of DNA sequence, their actions can even lead to notably different gene expression patterns between monozygotic twins¹³⁰.

Low-density chromatin, termed euchromatin, consists of active genes and is associated with hypomethylation of CpG dinucleotides in DNA and acetylated histones^{131, 132}, whilst compact chromatin (heterochromatin) is a hallmark of silent genes and is associated with hypermethylation of CpG dinucleotides in DNA and non-acetylated histones. Epigenetic factors have counterbalancing and reversible actions and vital epigenetic factors that control the degree of chromatin methylation and acetylation are histone methyltransferases and demethylases and lysine histone acetyltransferases (KATs) and deacetylases (KDACs)^{133, 134}.

KATs are nuclear enzymes that are recruited to gene promoter regions by gene regulatory proteins such as class II transactivator (CIITA) in leukocytes and can serve as master switches by increasing general inflammatory gene accessibility. Examples of KAT-regulated genes involved in atherosclerosis development include MHC class II and nuclear factor kappa-beta (NF κ B), a pivotal transcription factor in inflammation¹³⁵. KATs are considered to act dominantly in the nucleus of injured endothelial and SMCs immediately following vascular injury, such as occurs during PCI or CABG-

surgery. Intervention in the function of these KATs and their accessory molecules could affect the local arterial inflammatory response in the acute setting, affecting the degree of post-interventional vascular remodeling and the need for re-intervention in the long term¹³⁶.

P300/CBP-associated factor (PCAF)

P300/CBP-associated factor (PCAF/KAT2B) is a transcriptional co-activator with KAT-activity and regulates histone acetylation of NF κ B-regulated inflammatory genes¹³⁷. PCAF can bind the cyclooxygenase (COX)-2 promoter region following cellular exposure to inflammatory mediators and regulates the cellular inflammatory response through prostaglandin H2 formation¹³⁸. Furthermore, PCAF also enhances the p65-mediated increase in TNF α promoter activity¹³⁹ and both TNF α and COX-2 regulate the cellular inflammatory responses by leukocytes that lead to atherosclerosis (figure 6)^{140, 141}.

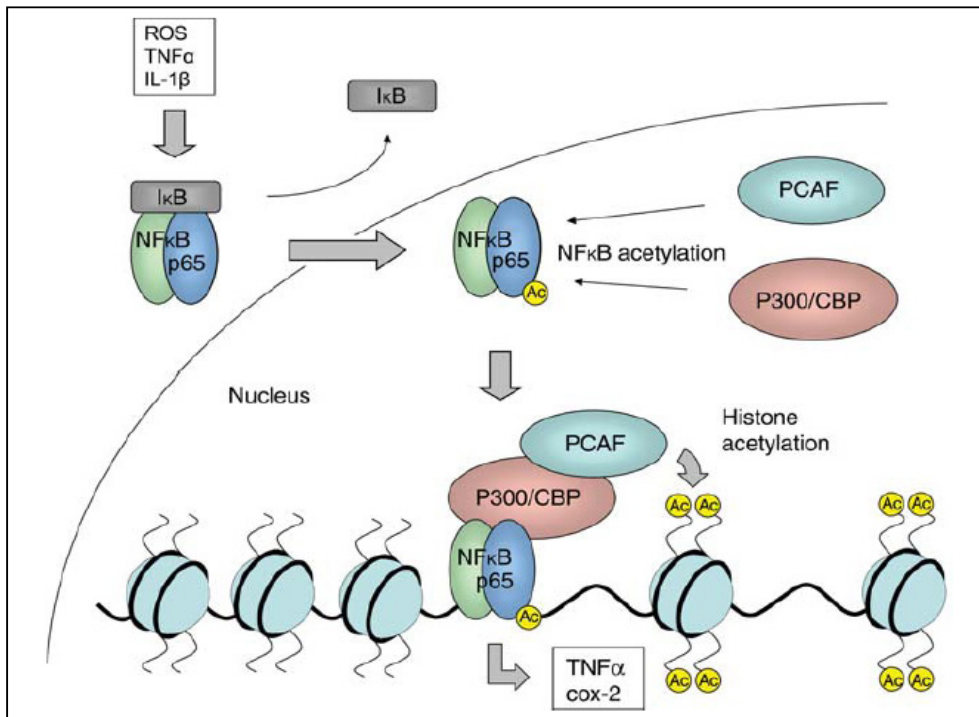


Figure 1.6 The role of PCAF in inflammation¹³⁶

The role of p300/CREB binding protein (CBP)-associated factor (PCAF) in the activation of nuclear factor kappa B (NF κ B)-mediated gene transcription is initiated by NF κ B stimulators such reactive oxygen species (ROS), tumor necrosis factor (TNF) α and interleukin-1 β . PCAF and P300 can act as factor acetyltransferases and acetylate NF κ B directly, but also enable NF κ B-target gene transcription through histone-acetylation at promoter regions of target genes such as TNF α and cyclo-oxygenase-2 involved in inflammation.

PCAF^{-/-} mice are developmentally normal without a distinct phenotype, although levels of PCAF-B are drastically elevated in lung and liver tissue. In contrast, PCAF-B deficiency is embryonically lethal and PCAF-B^{-/-} mice die between 9-12 days of

gestation¹⁴². However, when PCAF^{-/-} mice reach 6-12 months of age, they develop amyloid toxicity^{143, 144} and short-term memory deficits and exaggerated responses to acute stress¹⁴⁵, confirming that PCAF histone acetylase activity is involved in life-long chromatin remodeling processes by post-translational histone modification.

PCAF in clinical CHD

Recently, association between the -2481G→C SNP in the promoter region of the PCAF gene and reduced CHD mortality and restenosis was shown in three independent large prospective studies¹⁴⁶⁻¹⁴⁸. A meta-analysis of the dataset showed that patients heterozygous for the low-risk allele had approximately a 20% reduction in risk for cardiovascular events, compared with 40% in patients homozygous for the allele¹⁴⁹. The SNP might affect binding of a nuclear protein, but could similarly be a mere proxy marker for a functional SNP elsewhere in the PCAF locus due to linkage disequilibrium¹⁵⁰. This finding has nonetheless added to the growing body of evidence that epigenetic regulation of inflammatory gene expression in activated leukocytes is vital for the process of atherosclerosis and restenosis development and could serve as a target of therapy or as diagnostic risk marker to improve patient screening.

Aim of the thesis

The aim of this thesis was to investigate the role of the immune system in the pathophysiological process leading to the development of post-interventional atherosclerotic vascular remodeling. This research enabled the evaluation of the effectiveness of specific immunomodulatory therapies in the prevention of accelerated atherosclerosis development, which could be applied during PCI or CABG-surgery in the clinical setting.

The development of post-interventional atherosclerotic vascular remodeling can be divided into specific phases of chronic tissue inflammation elicited by the activated immune system. First, intervention for established occlusive atherosclerotic disease induces arterial injury which elicits the expression of pro-coagulant factors and arterial thrombosis. This provides the scaffold for cells and mediators from the innate immune system to undergo local adhesion, infiltration and activation into the arterial wall (phase 1). Innate immune responses are directed towards (self) immunogenic molecular patterns that are present in the subendothelial space such as oxLDL particles and TLR ligands and lead to a pathological inflammatory response (phase 2). These activated cells not only stimulate the process of vascular remodeling and ECM deposition through expression of inflammatory mediators such as cytokines, but also travel to draining lymphoid tissues to recruit residing naïve cells that belong to the adaptive immune system. To this end, intercellular communication through specific receptor-ligand interactions and co-stimulatory signals leads to activation of naïve lymphocytes that enter the circulation to engage their specific antigen-bearing targets (phase 3). Their additive effects at the site of vascular injury to local infiltrated cells, antigen-antibody complexes and pro-inflammatory chemo- and cytokines promotes transcription of their inflammatory genes, enabled by tightly-controlled epigenetic regulation processes (throughout phases 2-3). This ultimately leads to accelerated atherosclerosis development and secondary clinical presentation.

Outline of the thesis

Hallmark events of immune system-mediated inflammatory reactions and their derived factors that could serve as future clinical biomarkers of CVD progression are described in **chapter 2**. The underlying factors that are causally related to inflammatory vascular remodeling are discussed and investigated for their possible application as (additive) biomarkers for adequate risk assessment and patient evaluation with the aim of improved patient screening and enabling future tailor-made treatment. Preclinical small animal models to study restenosis and effects of systemic and local drug therapy are reviewed in **chapter 3**, with special focus on the murine femoral arterial cuff model that encompasses a pathophysiology highly-resembling that of (in-stent) restenosis development. This ensures an ideal intervention model for the screening of candidate genes and new (locally applied) anti-restenotic drugs, especially when investigated in a hypercholesterolemic mouse strain such as the ApoE3*Leiden mouse.

The therapeutic effectiveness of the PS-binding protein annexin A5, which is well-known for its anti-thrombotic properties and usefulness as apoptotic marker, is evaluated in **chapter 4** in three different mouse models for vascular inflammation, remodeling and dysfunction. It was found that systemic annexin A5 treatment led to annexin A5 accumulation at the site of injury and prevented the initiation of a local inflammatory response with major beneficial therapeutic effects. In **chapter 5**, association between polymorphisms in the annexin A5 gene and restenosis risk in patients undergoing PCI is investigated in patients enrolled in the GENDER study, with further investigations into dose-response effectiveness of annexin A5 at the time of revascularization.

Chapter 6 describes the investigations into therapeutic application of optimized naturally occurring anti-PC IgM antibodies by harnessing the anti-inflammatory PC-binding properties in a clinically applicable format using recombinant monoclonal chimeric antibodies. This strategy was pursued further with fully human IgG antibodies towards PC that were identified and produced using phage display techniques, which allowed careful selection for the most optimal anti-inflammatory antibody properties. In this line, **chapter 7** shows the therapeutic efficacy of a newly-synthesized dual TLR7/9 antagonist in the prevention of post-interventional atherosclerosis development through prevention of inflammatory cytokine expression and oxLDL particle-uptake by macrophages during TLR7/9 stimulation *in vitro*. The novel TLR7/9 antagonist also increased secretion of the anti-inflammatory cytokine IL-10, responsible for reduced oxLDL particle-uptake through scavenger receptors expressed by macrophages.

The importance of T-cells and the co-stimulatory and co-inhibitory pathways is displayed in **chapter 8**, where knock-out mouse strains were used to confirm the importance of CD4 T-cells and the CD28-CD80/86 pathway in vascular remodeling. Blocking anti-CTLA-4 antibodies and abatacept, a soluble CTLA-4Ig that prevents CD28-mediated T-cell activation and is registered for treatment of clinical rheumatoid arthritis, were applied to elucidate the role of CTLA-4 signaling in accelerated atherosclerosis development. The powerful inhibitory effects on CD4+ T-cell status are investigated in the T-cell populations in the spleen and draining lymph nodes in hypercholesterolemic mice.

Chapter 9 identifies strong association between genetic variation in PCAF, a key mediator in epigenetics, and vascular morbidity and mortality in three independent patient cohorts is discussed in, which provides evidence for new concepts in the epigenetic regulation of genetics responsible for the processes of inflammation and proliferation during atherogenesis. The causal role of PCAF in this process is investigated in **chapter 10**, in which PCAF knock-out mice are subjected to surgical cuff-induced vascular injury and inhibitory effects of PCAF deficiency on leukocyte activation and functional cytokine expression were investigated. Additionally, it is shown that perivascular delivery of the only potent natural PCAF inhibitor garcinol at the time of surgery can protect against neointimal formation. Finally, **chapter 11** describes the important role of PCAF in inflammation and vascular remodeling in general, with significantly impaired arteriogenesis in PCAF knock-out mice compared to controls allowing careful assessment of its contributory role in neovascularization.

Reference List

1. Dahlof B. Cardiovascular disease risk factors: epidemiology and risk assessment. *Am J Cardiol* 2010;105(1 Suppl):3A-9A.
2. Lloyd-Jones D, Adams RJ, Brown TM et al. Heart disease and stroke statistics--2010 update: a report from the American Heart Association. *Circulation* 2010;121(7):e46-e215.
3. Atary JZ, de VM, van den Dijk R et al. Standardised pre-hospital care of acute myocardial infarction patients: MISSION! guidelines applied in practice. *Neth Heart J* 2010;18(9):408-15.
4. Hansson GK. Inflammation, atherosclerosis, and coronary artery disease. *N Engl J Med* 2005;352(16):1685-95.
5. Libby P, Ridker PM, Hansson GK. Progress and challenges in translating the biology of atherosclerosis. *Nature* 2011;473(7347):317-25.
6. Silber S, Albertsson P, Aviles FF et al. Guidelines for percutaneous coronary interventions. The Task Force for Percutaneous Coronary Interventions of the European Society of Cardiology. *Eur Heart J* 2005;26(8):804-47.
7. King SB, III. Angioplasty from bench to bedside to bench. *Circulation* 1996;93(9):1621-9.
8. Landau C, Lange RA, Hillis LD. Percutaneous transluminal coronary angioplasty. *N Engl J Med* 1994;330(14):981-93.
9. van der Hoeven BL, Pires NM, Warda HM et al. Drug-eluting stents: results, promises and problems. *Int J Cardiol* 2005;99(1):9-17.
10. Farooq V, Gogas BD, Serruys PW. Restenosis: delineating the numerous causes of drug-eluting stent restenosis. *Circ Cardiovasc Interv* 2011;4(2):195-205.
11. Gray WA, Granada JF. Drug-coated balloons for the prevention of vascular restenosis. *Circulation* 2010;121(24):2672-80.
12. Garg S, Serruys PW. Coronary stents: current status. *J Am Coll Cardiol* 2010;56(10 Suppl):S1-42.
13. Barner HB. Operative treatment of coronary atherosclerosis. *Ann Thorac Surg* 2008;85(4):1473-82.
14. Dangas GD, Claessen BE, Caixeta A, Sanidas EA, Mintz GS, Mehran R. In-stent restenosis in the drug-eluting stent era. *J Am Coll Cardiol* 2010;56(23):1897-907.
15. Weintraub WS. The pathophysiology and burden of restenosis. *Am J Cardiol* 2007;100(5A):3K-9K.
16. Pires NM, Jukema JW, Daemen MJ, Quax PH. Drug-eluting stents studies in mice: do we need atherosclerosis to study restenosis? *Vascul Pharmacol* 2006;44(5):257-64.
17. Zadelaar S, Kleemann R, Verschuren L et al. Mouse models for atherosclerosis and pharmaceutical modifiers. *Arterioscler Thromb Vasc Biol* 2007;27(8):1706-21.
18. von BN, Taubert D, Pogatsa-Murray G, Schomig E, Kastrati A, Schomig A. Absorption, metabolism, and antiplatelet effects of 300-, 600-, and 900-mg loading doses of clopidogrel: results of the ISAR-CHOICE (Intracoronary Stenting and Anti-thrombotic Regimen: Choose Between 3 High Oral Doses for Immediate Clopidogrel Effect) Trial. *Circulation* 2005;112(19):2946-50.
19. Varon D, Spectre G. Antiplatelet agents. *Hematology Am Soc Hematol Educ Program* 2009;267-72.
20. de Boer HC, Verseyden C, Ulfman LH et al. Fibrin and activated platelets cooperatively guide stem cells to a vascular injury and promote differentiation towards an endothelial cell phenotype. *Arterioscler Thromb Vasc Biol* 2006;26(7):1653-9.
21. Balasubramanian K, Schroit AJ. Aminophospholipid asymmetry: A matter of life and death. *Annu Rev Physiol* 2003;65:701-34.
22. van Genderen HO, Kenis H, Hofstra L, Narula J, Reutelingsperger CP. Extracellular annexin A5: functions of phosphatidylserine-binding and two-dimensional crystallization. *Biochim Biophys Acta* 2008;1783(6):953-63.
23. Monroe DM, Hoffman M, Roberts HR. Platelets and thrombin generation. *Arterioscler Thromb Vasc Biol* 2002;22(9):1381-9.
24. Boersma HH, Kietselaer BL, Stolk LM et al. Past, present, and future of annexin A5: from protein discovery to clinical applications. *J Nucl Med* 2005;46(12):2035-50.
25. Cederholm A, Frostegard J. Annexin A5 multitasking: a potentially novel antiatherothrombotic agent? *Drug News Perspect* 2007;20(5):321-6.
26. Capila I, Hernaiz MJ, Mo YD et al. Annexin V--heparin oligosaccharide complex suggests

- heparan sulfate--mediated assembly on cell surfaces. *Structure* 2001;9(1):57-64.
27. Wang X, Campos B, Kaetzel MA, Dedman JR. Annexin V is critical in the maintenance of murine placental integrity. *Am J Obstet Gynecol* 1999;180(4):1008-16.
28. Leon C, Nandan D, Lopez M, Moeenrezakhanlou A, Reiner NE. Annexin V associates with the IFN-gamma receptor and regulates IFN-gamma signaling. *J Immunol* 2006;176(10):5934-42.
29. Weber C, Zernecke A, Libby P. The multifaceted contributions of leukocyte subsets to atherosclerosis: lessons from mouse models. *Nat Rev Immunol* 2008;8(10):802-15.
30. Cederholm A, Frostegard J. Annexin A5 in cardiovascular disease and systemic lupus erythematosus. *Immunobiology* 2005;210(10):761-8.
31. Ewing MM, de Vries MR, Nordzell M et al. Annexin A5 therapy attenuates vascular inflammation and remodeling and improves endothelial function in mice. *Arterioscler Thromb Vasc Biol* 2011;31(1):95-101.
32. van Tits LJ, van Heerde WL, van der Vleuten GM et al. Plasma annexin A5 level relates inversely to the severity of coronary stenosis. *Biochem Biophys Res Commun* 2007;356(3):674-80.
33. Ravassa S, Gonzalez A, Lopez B et al. Upregulation of myocardial Annexin A5 in hypertensive heart disease: association with systolic dysfunction. *Eur Heart J* 2007;28(22):2785-91.
34. Peetz D, Hafner G, Blankenberg S et al. Annexin V does not represent a diagnostic alternative to myoglobin for early detection of myocardial infarction. *Clin Lab* 2002;48(9-10):517-23.
35. Hartvigsen K, Chou MY, Hansen LF et al. The role of innate immunity in atherogenesis. *J Lipid Res* 2009;50 Suppl:S388-S393.
36. Binder CJ, Chang MK, Shaw PX et al. Innate and acquired immunity in atherogenesis. *Nat Med* 2002;8(11):1218-26.
37. Walport MJ. Complement. First of two parts. *N Engl J Med* 2001;344(14):1058-66.
38. Walport MJ. Complement. Second of two parts. *N Engl J Med* 2001;344(15):1140-4.
39. Niculescu F, Rus H. The role of complement activation in atherosclerosis. *Immunol Res* 2004;30(1):73-80.
40. Schepers A, de Vries MR, van Leuven CJ et al. Inhibition of complement component C3 reduces vein graft atherosclerosis in apolipoprotein E3-Leiden transgenic mice. *Circulation* 2006;114(25):2831-8.
41. Michelsen KS, Doherty TM, Shah PK, Arditi M. Role of Toll-like receptors in atherosclerosis. *Circ Res* 2004;95(12):e96-e97.
42. Hollestelle SC, de Vries MR, van Keulen JK et al. Toll-like receptor 4 is involved in outward arterial remodeling. *Circulation* 2004;109(3):393-8.
43. Michelsen KS, Wong MH, Shah PK et al. Lack of Toll-like receptor 4 or myeloid differentiation factor 88 reduces atherosclerosis and alters plaque phenotype in mice deficient in apolipoprotein E. *Proc Natl Acad Sci U S A* 2004;101(29):10679-84.
44. Hansson GK, Edfeldt K. Toll to be paid at the gateway to the vessel wall. *Arterioscler Thromb Vasc Biol* 2005;25(6):1085-7.
45. Hochleitner BW, Hochleitner EO, Obrist P et al. Fluid shear stress induces heat shock protein 60 expression in endothelial cells in vitro and in vivo. *Arterioscler Thromb Vasc Biol* 2000;20(3):617-23.
46. Arslan F, Smeets MB, Riem Vis PW et al. Lack of fibronectin-EDA promotes survival and prevents adverse remodeling and heart function deterioration after myocardial infarction. *Circ Res* 2011;108(5):582-92.
47. Li W, Sama AE, Wang H. Role of HMGB1 in cardiovascular diseases. *Curr Opin Pharmacol* 2006;6(2):130-5.
48. Edfeldt K, Swedenborg J, Hansson GK, Yan ZQ. Expression of toll-like receptors in human atherosclerotic lesions: a possible pathway for plaque activation. *Circulation* 2002;105(10):1158-61.
49. Pryschep O, Ma-Krupa W, Younge BR, Goronzy JJ, Weyand CM. Vessel-specific Toll-like receptor profiles in human medium and large arteries. *Circulation* 2008;118(12):1276-84.
50. Kawai T, Akira S. The role of pattern-recognition receptors in innate immunity: update on Toll-like receptors. *Nat Immunol* 2010;11(5):373-84.
51. Boule MW, Broughton C, Mackay F, Akira S, Marshak-Rothstein A, Rifkin IR. Toll-like receptor 9-dependent and -independent dendritic cell activation by chromatin-immunoglobulin G complexes. *J Exp Med* 2004;199(12):1631-40.
52. Miller YI, Choi SH, Wiesner P et al. Oxidation-specific epitopes are danger-associated

- molecular patterns recognized by pattern recognition receptors of innate immunity. *Circ Res* 2011;108(2):235-48.
53. Hansson GK, Hermansson A. The immune system in atherosclerosis. *Nat Immunol* 2011;12(3):204-12.
 54. Chou MY, Hartvigsen K, Hansen LF et al. Oxidation-specific epitopes are important targets of innate immunity. *J Intern Med* 2008;263(5):479-88.
 55. Todd DJ, Lee AH, Glimcher LH. The endoplasmic reticulum stress response in immunity and autoimmunity. *Nat Rev Immunol* 2008;8(9):663-74.
 56. Sanson M, Auge N, Vindis C et al. Oxidized low-density lipoproteins trigger endoplasmic reticulum stress in vascular cells: prevention by oxygen-regulated protein 150 expression. *Circ Res* 2009 13;104(3):328-36.
 57. Tabas I. Macrophage death and defective inflammation resolution in atherosclerosis. *Nat Rev Immunol* 2010;10(1):36-46.
 58. Tabas I. The role of endoplasmic reticulum stress in the progression of atherosclerosis. *Circ Res* 2010;107(7):839-50.
 59. Zhou J, Lhotak S, Hilditch BA, Austin RC. Activation of the unfolded protein response occurs at all stages of atherosclerotic lesion development in apolipoprotein E-deficient mice. *Circulation* 2005;111(14):1814-21.
 60. Zhang K, Kaufman RJ. From endoplasmic-reticulum stress to the inflammatory response. *Nature* 2008;454(7203):455-62.
 61. Baumgarth N, Herman OC, Jager GC, Brown L, Herzenberg LA, Herzenberg LA. Innate and acquired humoral immunities to influenza virus are mediated by distinct arms of the immune system. *Proc Natl Acad Sci U S A* 1999;96(5):2250-5.
 62. Binder CJ, Silverman GJ. Natural antibodies and the autoimmunity of atherosclerosis. *Springer Semin Immunopathol* 2005;26(4):385-404.
 63. Palinski W, Miller E, Witztum JL. Immunization of low density lipoprotein (LDL) receptor-deficient rabbits with homologous malondialdehyde-modified LDL reduces atherogenesis. *Proc Natl Acad Sci U S A* 1995;92(3):821-5.
 64. Shaw PX, Horkko S, Chang MK et al. Natural antibodies with the T15 idiotype may act in atherosclerosis, apoptotic clearance, and protective immunity. *J Clin Invest* 2000;105(12):1731-40.
 65. Briles DE, Forman C, Hudak S, Clafin JL. Anti-phosphorylcholine antibodies of the T15 idiotype are optimally protective against *Streptococcus pneumoniae*. *J Exp Med* 1982;156(4):1177-85.
 66. Mi QS, Zhou L, Schulze DH et al. Highly reduced protection against *Streptococcus pneumoniae* after deletion of a single heavy chain gene in mouse. *Proc Natl Acad Sci U S A* 2000;97(11):6031-6.
 67. Binder CJ, Shaw PX, Chang MK et al. The role of natural antibodies in atherogenesis. *J Lipid Res* 2005;46(7):1353-63.
 68. Horkko S, Bird DA, Miller E et al. Monoclonal autoantibodies specific for oxidized phospholipids or oxidized phospholipid-protein adducts inhibit macrophage uptake of oxidized low-density lipoproteins. *J Clin Invest* 1999;103(1):117-28.
 69. Binder CJ, Horkko S, Dewan A et al. Pneumococcal vaccination decreases atherosclerotic lesion formation: molecular mimicry between *Streptococcus pneumoniae* and oxidized LDL. *Nat Med* 2003;9(6):736-43.
 70. Rose N, Afanasyeva M. Autoimmunity: busting the atherosclerotic plaque. *Nat Med* 2003;9(6):641-2.
 71. Caligiuri G, Khallou-Laschet J, Vandaele M et al. Phosphorylcholine-targeting immunization reduces atherosclerosis. *J Am Coll Cardiol* 2007;50(6):540-6.
 72. van Puijvelde GH, Hauer AD, de VP et al. Induction of oral tolerance to oxidized low-density lipoprotein ameliorates atherosclerosis. *Circulation* 2006;114(18):1968-76.
 73. Schiopu A, Bengtsson J, Soderberg I et al. Recombinant human antibodies against aldehyde-modified apolipoprotein B-100 peptide sequences inhibit atherosclerosis. *Circulation* 2004;110(14):2047-52.
 74. Schiopu A, Frendeus B, Jansson B et al. Recombinant antibodies to an oxidized low-density lipoprotein epitope induce rapid regression of atherosclerosis in apobec-1(-)/low-density lipoprotein receptor(-) mice. *J Am Coll Cardiol* 2007;50(24):2313-8.
 75. Faria-Neto JR, Chyu KY, Li X et al. Passive immunization with monoclonal IgM antibodies against phosphorylcholine reduces accelerated vein graft atherosclerosis in apolipoprotein

- E-null mice. *Atherosclerosis* 2006;189(1):83-90.
76. Habets KL, van Puijvelde GH, van Duivenvoorde LM et al. Vaccination using oxidized low-density lipoprotein-pulsed dendritic cells reduces atherosclerosis in LDL receptor-deficient mice. *Cardiovasc Res* 2010;85(3):622-30.
77. Hermansson A, Ketelhuth DF, Strothoff D et al. Inhibition of T cell response to native low-density lipoprotein reduces atherosclerosis. *J Exp Med* 2010;207(5):1081-93.
78. Hoogenboom HR. Selecting and screening recombinant antibody libraries. *Nat Biotechnol* 2005;23(9):1105-16.
79. Lonberg N. Fully human antibodies from transgenic mouse and phage display platforms. *Curr Opin Immunol* 2008;20(4):450-9.
80. Madjid M. Acute infections, vaccination and prevention of cardiovascular disease. *CMAJ* 2008;179(8):749-50.
81. Nguyen JT, Myers N, Palaia J, Georgopoulos A, Rubins JB, Janoff EN. Humoral responses to oxidized low-density lipoprotein and related bacterial antigens after pneumococcal vaccine. *Transl Res* 2007;150(3):172-9.
82. Lamontagne F, Garant MP, Carvalho JC, Lanthier L, Smieja M, Pilon D. Pneumococcal vaccination and risk of myocardial infarction. *CMAJ* 2008;179(8):773-7.
83. Madjid M, Musher DM. Preventing myocardial infarction with vaccination: myths and realities. *JAMA* 2010;303(17):1751-2.
84. Robertson AK, Hansson GK. T cells in atherogenesis: for better or for worse? *Arterioscler Thromb Vasc Biol* 2006;26(11):2421-32.
85. Zhou X, Stemme S, Hansson GK. Evidence for a local immune response in atherosclerosis. CD4+ T cells infiltrate lesions of apolipoprotein-E-deficient mice. *Am J Pathol* 1996;149(2):359-66.
86. Zhou X, Caligiuri G, Hamsten A, Lefvert AK, Hansson GK. LDL immunization induces T-cell-dependent antibody formation and protection against atherosclerosis. *Arterioscler Thromb Vasc Biol* 2001;21(1):108-14.
87. Kleemann R, Zadelaar S, Kooistra T. Cytokines and atherosclerosis: a comprehensive review of studies in mice. *Cardiovasc Res* 2008;79(3):360-76.
88. Hansson GK, Libby P, Schonbeck U, Yan ZQ. Innate and adaptive immunity in the pathogenesis of atherosclerosis. *Circ Res* 2002;91(4):281-91.
89. Lutgens E, Gorelik L, Daemen MJ et al. Requirement for CD154 in the progression of atherosclerosis. *Nat Med* 1999;5(11):1313-6.
90. Whitman SC, Ravisankar P, Daugherty A. IFN-gamma deficiency exerts gender-specific effects on atherogenesis in apolipoprotein E-/- mice. *J Interferon Cytokine Res* 2002;22(6):661-70.
91. Mach F, Schonbeck U, Sukhova GK, Atkinson E, Libby P. Reduction of atherosclerosis in mice by inhibition of CD40 signalling. *Nature* 1998;394(6689):200-3.
92. Whitman SC, Ravisankar P, Elam H, Daugherty A. Exogenous interferon-gamma enhances atherosclerosis in apolipoprotein E-/- mice. *Am J Pathol* 2000;157(6):1819-24.
93. Eefting D, Schepers A, de Vries MR et al. The effect of interleukin-10 knock-out and overexpression on neointima formation in hypercholesterolemic APOE*3-Leiden mice. *Atherosclerosis* 2007;193(2):335-42.
94. Fontenot JD, Gavin MA, Rudensky AY. Foxp3 programs the development and function of CD4+CD25+ regulatory T cells. *Nat Immunol* 2003;4(4):330-6.
95. Brunkow ME, Jeffery EW, Hjerrild KA et al. Disruption of a new forkhead/winged-helix protein, scurf1, results in the fatal lymphoproliferative disorder of the scurfy mouse. *Nat Genet* 2001;27(1):68-73.
96. Vignali DA, Collison LW, Workman CJ. How regulatory T cells work. *Nat Rev Immunol* 2008;8(7):523-32.
97. Mallat Z, Taleb S, Ait-Oufella H, Tedgui A. The role of adaptive T cell immunity in atherosclerosis. *J Lipid Res* 2009;50 Suppl:S364-S369.
98. Sakaguchi S. Naturally arising CD4+ regulatory t cells for immunologic self-tolerance and negative control of immune responses. *Annu Rev Immunol* 2004;22:531-62.
99. Ait-Oufella H, Salomon BL, Potteaux S et al. Natural regulatory T cells control the development of atherosclerosis in mice. *Nat Med* 2006;12(2):178-80.
100. Salomon B, Lenschow DJ, Rhee L et al. B7/CD28 costimulation is essential for the homeostasis of the CD4+CD25+ immunoregulatory T cells that control autoimmune diabetes. *Immunity* 2000;12(4):431-40.

101. Fallarino F, Grohmann U, Hwang KW et al. Modulation of tryptophan catabolism by regulatory T cells. *Nat Immunol* 2003;4(12):1206-12.
102. Munn DH, Sharma MD, Mellor AL. Ligation of B7-1/B7-2 by human CD4+ T cells triggers indoleamine 2,3-dioxygenase activity in dendritic cells. *J Immunol* 2004;172(7):4100-10.
103. Baxter AG, Hodgkin PD. Activation rules: the two-signal theories of immune activation. *Nat Rev Immunol* 2002;2(6):439-46.
104. Buono C, Pang H, Uchida Y, Libby P, Sharpe AH, Lichtman AH. B7-1/B7-2 costimulation regulates plaque antigen-specific T-cell responses and atherogenesis in low-density lipoprotein receptor-deficient mice. *Circulation* 2004;109(16):2009-15.
105. Chen L. Co-inhibitory molecules of the B7-CD28 family in the control of T-cell immunity. *Nat Rev Immunol* 2004;4(5):336-47.
106. Gotsman I, Sharpe AH, Lichtman AH. T-cell costimulation and coinhibition in atherosclerosis. *Circ Res* 2008;103(11):1220-31.
107. Alegre ML, Frauwirth KA, Thompson CB. T-cell regulation by CD28 and CTLA-4. *Nat Rev Immunol* 2001;1(3):220-8.
108. Tivol EA, Borriello F, Schweitzer AN, Lynch WP, Bluestone JA, Sharpe AH. Loss of CTLA-4 leads to massive lymphoproliferation and fatal multiorgan tissue destruction, revealing a critical negative regulatory role of CTLA-4. *Immunity* 1995;3(5):541-7.
109. Mandelbrot DA, McAdam AJ, Sharpe AH. B7-1 or B7-2 is required to produce the lymphoproliferative phenotype in mice lacking cytotoxic T lymphocyte-associated antigen 4 (CTLA-4). *J Exp Med* 1999;189(2):435-40.
110. Masteller EL, Chuang E, Mullen AC, Reiner SL, Thompson CB. Structural analysis of CTLA-4 function in vivo. *J Immunol* 2000;164(10):5319-27.
111. Carreno BM, Bennett F, Chau TA et al. CTLA-4 (CD152) can inhibit T cell activation by two different mechanisms depending on its level of cell surface expression. *J Immunol* 2000;165(3):1352-6.
112. Takahashi T, Tagami T, Yamazaki S et al. Immunologic self-tolerance maintained by CD25(+) CD4(+) regulatory T cells constitutively expressing cytotoxic T lymphocyte-associated antigen 4. *J Exp Med* 2000;192(2):303-10.
113. Blank C, Brown I, Marks R, Nishimura H, Honjo T, Gajewski TF. Absence of programmed death receptor 1 alters thymic development and enhances generation of CD4/CD8 double-negative TCR-transgenic T cells. *J Immunol* 2003;171(9):4574-81.
114. Nishimura H, Nose M, Hiai H, Minato N, Honjo T. Development of lupus-like autoimmune diseases by disruption of the PD-1 gene encoding an ITIM motif-carrying immunoreceptor. *Immunity* 1999;11(2):141-51.
115. Gotsman I, Grabie N, DaCosta R, Sukhova G, Sharpe A, Lichtman AH. Proatherogenic immune responses are regulated by the PD-1/PD-L pathway in mice. *J Clin Invest* 2007;117(10):2974-82.
116. Fiocco U, Sfriso P, Oliviero F et al. Co-stimulatory modulation in rheumatoid arthritis: the role of (CTLA4-Ig) abatacept. *Autoimmun Rev* 2008;8(1):76-82.
117. Moreland L, Bate G, Kirkpatrick P. Abatacept. *Nat Rev Drug Discov* 2006;5(3):185-6.
118. Platt AM, Gibson VB, Patakas A et al. Abatacept limits breach of self-tolerance in a murine model of arthritis via effects on the generation of T follicular helper cells. *J Immunol* 2010;185(3):1558-67.
119. Haggerty HG, Abbott MA, Reilly TP et al. Evaluation of immunogenicity of the T cell costimulation modulator abatacept in patients treated for rheumatoid arthritis. *J Rheumatol* 2007;34(12):2365-73.
120. Tivol EA, Boyd SD, McKeon S et al. CTLA4Ig prevents lymphoproliferation and fatal multiorgan tissue destruction in CTLA-4-deficient mice. *J Immunol* 1997;158(11):5091-4.
121. Caligiuri G, Nicoletti A, Poirier B, Hansson GK. Protective immunity against atherosclerosis carried by B cells of hypercholesterolemic mice. *J Clin Invest* 2002;109(6):745-53.
122. Ait-Oufella H, Herbin O, Bouaziz JD et al. B cell depletion reduces the development of atherosclerosis in mice. *J Exp Med* 2010;207(8):1579-87.
123. Rozanski CH, Arens R, Carlson LM et al. Sustained antibody responses depend on CD28 function in bone marrow-resident plasma cells. *J Exp Med* 2011;208(7):1435-46.
124. Nair JR, Carlson LM, Koorella C et al. CD28 expressed on malignant plasma cells induces a pro-survival and immunosuppressive microenvironment. *J Immunol* 2011;187(3):1243-53.
125. Niessner A, Weyand CM. Dendritic cells in atherosclerotic disease. *Clin Immunol* 2010;134(1):25-32.

126. Niessner A, Sato K, Chaikof EL, Colmegna I, Goronzy JJ, Weyand CM. Pathogen-sensing plasmacytoid dendritic cells stimulate cytotoxic T-cell function in the atherosclerotic plaque through interferon-alpha. *Circulation* 2006;114(23):2482-9.
127. Niessner A, Shin MS, Pryshchep O, Goronzy JJ, Chaikof EL, Weyand CM. Synergistic proinflammatory effects of the antiviral cytokine interferon-alpha and Toll-like receptor 4 ligands in the atherosclerotic plaque. *Circulation* 2007;116(18):2043-52.
128. Wu C. Chromatin remodeling and the control of gene expression. *J Biol Chem* 1997;272(45):28171-4.
129. Wierda RJ, Geutskens SB, Jukema JW, Quax PH, van den Elsen PJ. Epigenetics in atherosclerosis and inflammation. *J Cell Mol Med* 2010;14(6A):1225-40.
130. Fraga MF, Ballestar E, Paz MF et al. Epigenetic differences arise during the lifetime of monozygotic twins. *Proc Natl Acad Sci U S A* 2005;102(30):10604-9.
131. Yoo CB, Jones PA. Epigenetic therapy of cancer: past, present and future. *Nat Rev Drug Discov* 2006;5(1):37-50.
132. Kaminsky ZA, Tang T, Wang SC et al. DNA methylation profiles in monozygotic and dizygotic twins. *Nat Genet* 2009;41(2):240-5.
133. Grunstein M. Histone acetylation in chromatin structure and transcription. *Nature* 1997;389(6649):349-52.
134. Kuo MH, Allis CD. Roles of histone acetyltransferases and deacetylases in gene regulation. *Bioessays* 1998;20(8):615-26.
135. Barnes PJ, Karin M. Nuclear factor-kappaB: a pivotal transcription factor in chronic inflammatory diseases. *N Engl J Med* 1997;336(15):1066-71.
136. Pons D, de Vries FR, van den Elsen PJ, Heijmans BT, Quax PH, Jukema JW. Epigenetic histone acetylation modifiers in vascular remodelling: new targets for therapy in cardiovascular disease. *Eur Heart J* 2009;30(3):266-77.
137. Vogel NL, Boeke M, Ashburner BP. Spermidine/Spermine N1-Acetyltransferase 2 (SSAT2) functions as a coactivator for NF-kappaB and cooperates with CBP and P/CAF to enhance NF-kappaB-dependent transcription. *Biochim Biophys Acta* 2006;1759(10):470-7.
138. Deng WG, Zhu Y, Wu KK. Role of p300 and PCAF in regulating cyclooxygenase-2 promoter activation by inflammatory mediators. *Blood* 2004;103(6):2135-42.
139. Miao F, Gonzalo IG, Lanting L, Natarajan R. In vivo chromatin remodeling events leading to inflammatory gene transcription under diabetic conditions. *J Biol Chem* 2004;279(17):18091-7.
140. Monraats PS, Pires NM, Schepers A et al. Tumor necrosis factor-alpha plays an important role in restenosis development. *FASEB J* 2005;19(14):1998-2004.
141. Narasimha AJ, Watanabe J, Ishikawa TO et al. Absence of myeloid COX-2 attenuates acute inflammation but does not influence development of atherosclerosis in apolipoprotein E null mice. *Arterioscler Thromb Vasc Biol* 2010;30(2):260-8.
142. Yamauchi T, Yamauchi J, Kuwata T et al. Distinct but overlapping roles of histone acetylase PCAF and of the closely related PCAF-B/GCN5 in mouse embryogenesis. *Proc Natl Acad Sci U S A* 2000;97(21):11303-6.
143. Duclot F, Meffre J, Jacquet C, Gongora C, Maurice T. Mice knock out for the histone acetyltransferase p300/CREB binding protein-associated factor develop a resistance to amyloid toxicity. *Neuroscience* 2010;167(3):850-63.
144. Duclot F, Jacquet C, Gongora C, Maurice T. Alteration of working memory but not in anxiety or stress response in p300/CBP associated factor (PCAF) histone acetylase knockout mice bred on a C57BL/6 background. *Neurosci Lett* 2010;475(3):179-83.
145. Maurice T, Duclot F, Meunier J et al. Altered memory capacities and response to stress in p300/CBP-associated factor (PCAF) histone acetylase knockout mice. *Neuropsychopharmacology* 2008;33(7):1584-602.
146. Monraats PS, Pires NM, Agema WR et al. Genetic inflammatory factors predict restenosis after percutaneous coronary interventions. *Circulation* 2005;112(16):2417-25.
147. Shepherd J, Blauw GJ, Murphy MB et al. Pravastatin in elderly individuals at risk of vascular disease (PROSPER): a randomised controlled trial. *Lancet* 2002;360(9346):1623-30.
148. Shepherd J, Cobbe SM, Ford I et al. Prevention of coronary heart disease with pravastatin in men with hypercholesterolemia. West of Scotland Coronary Prevention Study Group. *N Engl J Med* 1995;333(20):1301-7.
149. Pons D, Trompet S, de Craen AJ et al. Genetic variation in PCAF, a key mediator in epigenetics, is associated with reduced vascular morbidity and mortality: evidence for a new

150. concept from three independent prospective studies. *Heart* 2011;97(2):143-50.
Xiao Q, Ye S. The genetics of epigenetics: is there a link with cardiovascular disease. *Heart* 2011;97(2):96-7.

Chapter 2

Future potential biomarkers for post-interventional restenosis and accelerated atherosclerosis

M.M. Ewing^{1,2,3*}, J.C. Karper^{2,3*}, J.W. Jukema^{1,3}, P.H.A. Quax^{2,3}

1 Dept. of Cardiology, Leiden University Medical Center (LUMC), Leiden, The Netherlands

2 Dept. of Surgery, LUMC, Leiden, The Netherlands

3 Einthoven Laboratory for Experimental Vascular Medicine, LUMC, Leiden, The Netherlands

* Both authors contributed equally

Abstract

New circulating and local arterial biomarkers may help the clinician with risk stratification or diagnostic assessment of patients and selecting the proper therapy for a patient. Additionally they may be used for follow-up and testing efficacy of therapy, which is not provided by current biomarkers. Processes leading to post-interventional restenosis and accelerated atherosclerosis are complex due to many biological variables mediating the specific inflammatory and immunogenic responses involved. Adequate assessment of these processes requires different and more specific biomarkers. Post-interventional remodeling is associated with cell stress and tissue damage causing apoptosis, release of damage-associated molecular patterns (DAMPs) and upregulation of specific cyto/chemokines that could serve as suitable clinical biomarkers. Furthermore, plasma titers of pathophysiological process-related (auto)antibodies could aid in the identification of restenosis risk or lesion severity. This review provides an overview of a number of potential biomarkers selected on the basis of their role in the remodeling process.

Introduction

The current concept that inflammation plays a key role in the development of (post-interventional) atherosclerotic vascular remodeling has led to the investigation of inflammatory factors to serve as biomarkers for cardiovascular risk prediction. Multiple local arterial and blood-based biomarkers have been identified and selected for their association with a more adverse cardiovascular risk profile independently of known traditional risk factors such as dyslipidemia, hypertension, diabetes and smoking. Many of these markers have been incorporated into risk prediction models to improve risk assessment accuracy in addition to current diagnostic strategies¹. Of these, C-reactive protein (CRP) is currently the best-validated inflammatory biomarker. Despite the value of plasma lipoprotein profiling and CRP measurements the picture is not yet clear. Many patients but not all continue to develop vascular remodeling following revascularization procedures and ongoing investigations into newer and more accurate or combined biomarker risk profiles remain necessary². This review retracts the underlying pathophysiology of atherosclerosis and post-interventional vascular remodeling and the value of recently discovered inflammatory biomarkers³ in the prediction of cardiovascular events in the biological context that require target lesion revascularization, highlighting their potential clinical value. Other biomarkers including genetic differences such as polymorphisms are not taken into account in this review.

Background of atherosclerosis and restenosis

Native atherosclerosis

Atherosclerosis is a chronic inflammatory disease of the large and medium-sized arteries and is initiated by a qualitative change in the endothelial monolayer by irritative stimuli such as dyslipidemia, hypertension, and pro-inflammatory mediators that lead to the exposure of adhesion molecules and infiltration of circulating leukocytes into the arterial wall⁴. Such mediators could be of high value when measured as biomarkers of lesion progression and stage of severity. Changes in endothelial permeability provoke the retention of cholesterol-containing low-density lipoprotein (LDL) particles that are endocytosed by monocytes-derived macrophages leading to foam cell and atheromatous lesion formation in the arterial tree^{5, 6}. Tunica media-derived smooth muscle cell (SMC) migration and proliferation and extracellular matrix deposition lead to the formation of a fibrous cap overlying a necrotic core due to inefficient efferocytosis^{5, 7}. Physical disruption of the plaque exposes the underlying thrombogenic material to the circulation triggering thrombosis formation, that may be monitored as biomarkers, and luminal occlusion with progressing ischemia in distal tissues⁶, eventually leading to infarction requiring angioplasty or bypass-grafting^{6, 8}.

Post-interventional restenosis

Restenosis following angioplasty and stent implantation has been the major problem limiting the success rate of coronary interventions and tremendous efforts have been made to target this problem⁹. Acute and long-term vessel occlusion requiring target lesion revascularization following balloon angioplasty occurred in 30-60% of all pa-

tients due to elastic recoil and negative remodeling. The introduction of bare-metal stents (BMS) prevented elastic recoil and has reduced this incidence of restenosis to 16-44%, but also led to the development of neointimal hyperplasia¹⁰. Drug-eluting stents (DES) have been developed to counter this phenomenon, although incidence rates of 5-10% of in-stent restenosis (ISR) are still reported, encompassing over 200.000 revascularizations annually in the United States alone¹¹. Inflammation has been shown to be the driving factor behind these remodeling processes, pointing to a role as biomarker for this factor in the analysis of disease progression. DES have been successful in the prevention of neointimal hyperplasia, but have not been able to completely prevent the process of ISR. These figures support the need for development of new biomarker assays that allow careful screening of patients at risk for restenosis.

Restenosis is defined as more than 50% luminal loss at follow-up angiography with clinical restenosis defined as recurrence of symptoms such as angina pectoris or ischemia at rest, requiring repeat revascularization¹². It has been proposed to be the result of an overshooting healing response that originally occurred in three distinctive phases: early loss due to elastic recoil, which occurs within minutes and has been successfully countered by the application of intracoronary stenting, followed by neointimal hyperplasia and eventually accelerated atherosclerosis development¹³.

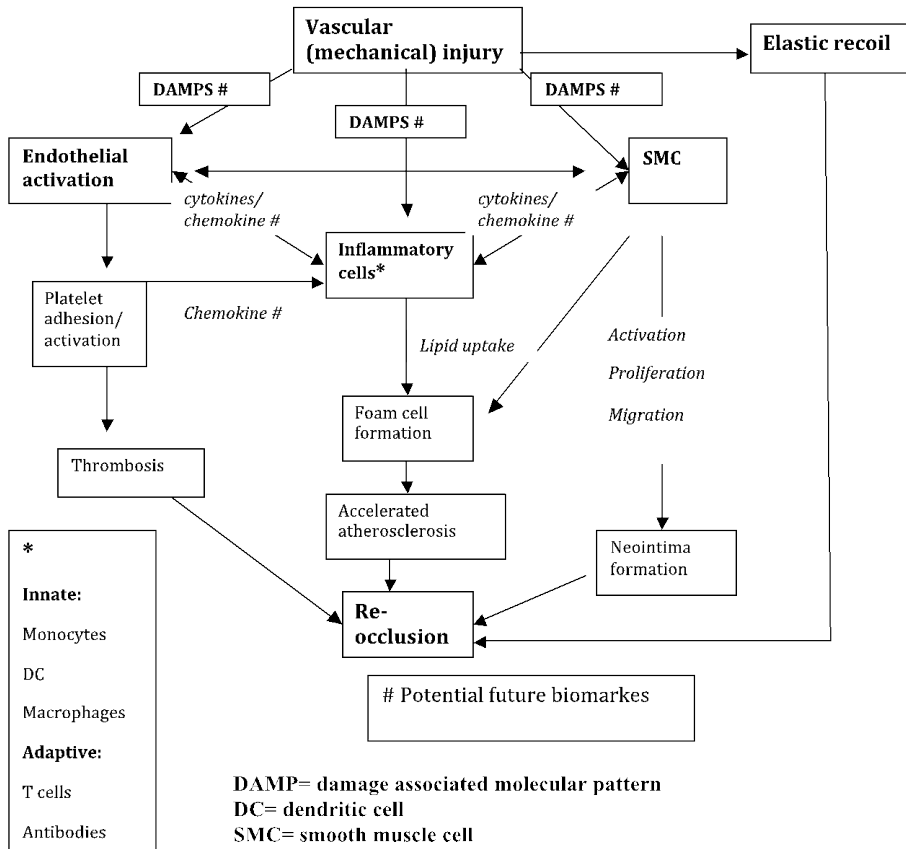


Figure 2.1 Post-interventional restenosis development

Neointimal hyperplasia is evoked by injury to the endothelium and underlying atherosclerotic plaque, with exposure of thrombogenic content to flowing blood, supporting the adhesion and activation of thrombocytes and thrombosis. Platelets release mitogens, which can be traced throughout the plasma to serve as biological markers of thrombosis extent, and promote SMC migration and proliferation to the tunica intima with local extracellular matrix deposition¹⁴. This process is prevented or delayed (e.g. by many years) by DES compared to BMS implantation through the release of drugs that affect SMC migration and proliferation. This process is ultimately followed by a phase of vascular remodeling, in which accelerated atherosclerosis and concentric adventitial compression together further comprise lumen patency¹³.

Underlying causes of restenosis

The underlying causes of restenosis can be divided into four general causes, namely biological, arterial, stent and implantation factors^{10, 12}. Biological factors encompass the natural (genetic) vascular wall resistance to anti-proliferative drugs and the development of a sustained hypersensitivity reaction directed towards the polymer or metallic stent platform. Additionally, the initial levels of proteinases that determine SMC proliferation and migration are of great importance to treatment success¹⁰. These effects of proteinase of SMC proliferation and migration may be direct or indirect effects. In vascular remodeling matrix metalloproteinases may regulate migration, proliferation, and death of vascular smooth muscle cells by degrading matrix and non-matrix substrates¹⁵, but also may play a role in activating other factors such as growth factor or other pericellular proteases¹⁶. Arterial factors that influence the vascular response are comprised of factor regulated by local wall shear stress levels, the progression of original atherosclerosis lesions growth within a stented segment, but also previous positive vascular remodeling. Stent factors that contribute to the development of ISR are the specific type of coating used, drug concentration and sustained period of release and to a lesser extent the drug of choice^{17, 18}. Differences between effectiveness rates of specific drugs are determined by their ability to meet the biological threshold that exists and determines the initiation of an inflammatory response and the eventual occurrence of neointimal hyperplasia, which could be tracked with biomarker levels in plasma¹⁰. The stent gap, strut thickness and possible polymer disruption or cracking and eventual fractures are all important for proper stent effectiveness in the prevention of ISR¹⁰. Finally, technical implantation factors can limit therapeutic effectiveness that stenting could offer, such as an incomplete stent expansion and geographical misses, where the stent is deployed short of or beyond the complete lesion area¹². During every interventional procedure the eventually of barotrauma to unstented segments and the deployment of a DES in a clot-laden arterial segment remains, that raise the chance of ISR after discontinuation of anti-thrombotic drugs. These factors support the search for biomarkers that could offer diagnostic insight at the time of procedure. These markers should be an adequate reflection of acute vessel injury.

Inflammation status as biomarker

The overall requirement of a cardiovascular disease biomarker is to enhance the ability to optimally manage the patient, identification of patients, to differentiate

patients, assess the likelihood of a therapeutic response, the risk of future recurrences and progression of disease¹⁹. The use of BMS or DES may have different effects on the pathophysiological process initiated and thereby on the inflammatory response and eventual potential biomarkers related to restenosis or in-stent thrombosis. For potential novel biomarkers it would be of major importance to be easily detectable and that levels correlate with disease progression. Since inflammation is importantly involved in vascular disease many studies focused on CRP as a biomarker. CRP is a strong marker of inflammation and upregulated in response to pro-inflammatory cytokines. No association was found for major cardiovascular events and high sensitivity-CRP, IL6 or TNF α by Sukhija and co-workers²⁰. However, CRP seemed to be an excellent marker for post-stenting inflammation since it was produced mostly in response to pro-inflammatory cytokines released as a response upon the vascular damage initiated by the procedure¹. In addition pre-procedural serum CRP-level proved to be an independent predictor of adverse outcome after coronary stent implantation, suggesting that a systemically detectable inflammatory activity is associated with proliferative responses within successfully implanted stents²¹. Higher baseline CRP levels of patients undergoing BMS implantation are a predictor of restenosis²². Interactions were also found between CRP levels, statin treatment and restenosis-incidence²³. No clear association of CRP and restenosis was found during application of drug-eluting stents¹. A study on first cardiovascular events and death based on the Framingham Offspring Study by Wang and co-workers showed that the most informative circulating biomarkers for predicting death proved to be B-type natriuretic peptide, C-reactive protein, homocysteine, renin, and the urinary albumin-to-creatinin ratio². Other studies focused on CRP levels did not find a direct relation with restenosis²⁴. Currently the limitation of existing biomarkers is that even in combination, they only add moderately to the prediction of risk in an individual person². This statement is confirmed by Ware who explains that a risk factor must have a much stronger association with the disease outcome than we ordinarily see in etiologic research if it is to provide a basis for early diagnosis or prediction in individual patients. Most studies are of limited value for the risk stratification of individual patients as we have discovered new biologic variables that lie on the complex pathway leading to chronic disease and death²⁵. Therefore the role of experimental research is very important in identifying novel biomarkers since it provides the tools to focus more specifically on the pathophysiological process. Currently a lot of contradicting data is available of using CRP as a biomarker in cardiovascular disease, a notion merely worsened by the use of different stents types. The approaches thus far may not be specific enough to serve as good reflectors of the pathophysiological process that is initiated by the interventional procedure. CRP is possibly just an indirect reflection of inflammation which is easily become upregulated by other underlying inflammatory processes. The application of individual biomarkers only contributes moderately to risk assessment of individual patients. The prospect of combining multiple known markers could possibly contribute significantly more to the optimization of patient selection and individual tailor-made treatment¹. The future success of biomarker strategies in this field could possibly depend on the discovery of new biomarkers to complement the current markers and diagnostic strategies. The identification of patients at elevated risk based upon biomarker assessment could be of additive value for the management of patients

receiving stent implantation. In this review, we provide an overview of considered novel potential biomarkers in post-interventional atherosclerotic vascular remodeling with the emphasis on inflammation.

Future biomarkers

Circulating Factors

Several factors involved in the pathophysiological process of post-interventional remodeling may be detected in the circulation soon after the interventional damage, thereby forming potential biomarkers that are easily available such as damage-associated molecular patterns (DAMPs). DAMPs are endogenous structures that can be released upon tissue damage and can be recognised by receptors on inflammatory cells e.g. Toll Like Receptors. Balloon angioplasty with or without stent placement will cause damage to the vessel wall that will cause a release of DAMPs and activate toll-like receptors that cause a release of several inflammatory cytokines and chemokines^{26, 27}. Also antibodies may be formed upon (auto-) antigens that become present after the intervention. Original papers on this subject are summarized in the citation overview below.

Citation overview	
Biomarker	References
AnnexinA5	28-35
DAMPS	26, 27, 36-62
Cytokines/chemokines	1, 22, 26, 39, 63-85
Plasma antibodies	86-96

Annexin A5

Annexin A5 is a member of the annexin family, a group of highly-conserved Ca²⁺-dependent proteins that bind to negatively-charged phospholipid surfaces. Annexin A5 is primarily an intracellular protein that is released upon injury and binds specifically and with high affinity to phosphatidylserine (PS)²⁸. PS becomes externalized and presented upon the outer cellular membrane during the process of apoptosis, but also during platelet activation and erythrocyte aging²⁹. For this reason annexin A5, alone and bound to contrast agents, has been used world-wide for the detection of apoptosis in vitro and in pilot experiments in vivo in patients²⁸.

PS serves as an 'eat-me' signal on apoptotic cells for circulating phagocytes. Annexin A5 then binds PS leading to the formation two-dimensional crystals. Annexin A5 thereby may act as a lattice shielding PS from phagocytes and from interacting in phospholipid-dependent coagulation reactions^{30, 31}. In addition to its anti-thrombogenic properties, annexin A5 binds with high affinity to oxLDL cholesterol which together with apoptotic cells is present in native atherosclerotic and restenotic lesions in high concentrations³². For this reason, annexin A5 is also detectable in high concentrations in (accelerated) atherosclerotic lesions³³.

Next to its presence in the vascular wall, annexin A5 has been suggested in the prevention of pro-inflammatory microparticle formation. Stimulated platelets and

apoptotic cells expressing PS on their membrane have been shown to shed PS-containing membrane-derived microparticles. Annexin A5 is able to inhibit the formation of microparticles by binding to PS on these cells³⁰.

Annexin A5 is partially removed from the circulation by binding to specific components of atherosclerotic tissues, such as oxLDL and activated or damaged cells. Measurement of plasma annexin A5 concentration requires only limited amounts of venous blood and is therefore an easy-to-perform diagnostic test. Although this information does not allow discrimination between a restenotic and a de novo atherosclerotic lesion, it could certainly be of much additive value to current diagnostic strategies and screening purposes. In addition, it was found that the prognostic value of the oxLDL / annexin A5 ratio is even more sensitive than annexin A5 alone, stressing the importance of combined biomarkers for disease screening³⁴. The presence of high concentrations of annexin A5 in atherosclerotic lesions leads to annexin A5 release in the circulation following myocardial infarction³⁵. Increased annexin A5 levels are therefore indicative of the extent of myocardial tissue damage. Since annexin A5 levels provide both information on plaque severity in the stable period of atherosclerosis and on infarction severity during acute episodes of plaque rupture, annexin A5 is a highly potential future biomarker of cardiovascular disease progress.

Damage Associated Molecular Patterns (DAMPs)

Restenosis is a late process, although it is believed that events that take place within 72 hours after intervention are already triggering the restenosis process. The intervention will cause severe damage to the vessel wall leading to a release of DAMPs. DAMPs can be seen as endogenous fragments that are recognized by the immune system by toll-like receptors (TLR)²⁶. During the whole process of restenosis a continuous process of cell stress, lipid influx, inflammation and matrix degradation, the release of DAMPs will continue. The last decade much focus has been towards the involvement of TLR in cardiovascular disease where the TLRs were predominantly found on circulating cells and in vascular lesions³⁶⁻³⁸. TLRs are membrane-bound receptors located on a variety of immune and non-immune cells including macrophages, endothelium, SMCs and platelets. Release of the DAMPs as endogenous TLR ligands may have serious consequences due to the activation of the TLR signalling pathway on variety of cells carrying TLRs. These cells may then initiate a severe inflammatory response with direct activation of the vessel wall but also platelet activation and infiltration of inflammatory cells^{26, 39, 40}. A causal role for TLR4 in post-interventional vascular remodeling was previously demonstrated. Neointima formation, arterial outward remodeling as well as vein graft remodelling were decreased by in TLR4 deficient mice, and TLR4 ligands and TLR4 silencing tools could modify these processes⁴¹⁻⁴³. Furthermore TLR4 is importantly involved in the sterile inflammatory response upon CD36 activation by oxLDL particles⁴⁴. Two very important DAMPs that can be linked to multiple TLRs are high mobility group box 1 (HMGB1) and fibronectin-EDA (FN-EDA) that also come available in the circulation upon their release. These DAMPs may potentially serve as ideal biomarkers since they are only upregulated in response to tissue damage, have direct inflammatory effects via multiple TLRs and can also be detected in the plasma^{27, 49-51}. Nuclear HMGB1 may become present in the cytoplasm or even outside the cell

where it is known to act as TLR2 and TLR4 ligand^{45, 49}. Not only can this release be initiated upon cell stress but also activated macrophages are capable of releasing HMGB1^{26, 49-51}. Previously our group was able to detect intra- and extra-nuclear HMGB1 in remodeled vein grafts⁴². Furthermore presence of HMGB1 was detected in atherosclerotic plaques. Although the number of macrophages increased markedly in fatty streaks and fibrofatty lesions, the proportion that expressed HMGB1 did not alter significantly. However, the proportion of macrophages containing HMGB1 in both cytoplasm and nuclei increased markedly⁵². Others showed that elevation of serum HMGB1 level is associated with severe cardiac remodeling complications such as pump failure, cardiac rupture, and eventually in-hospital cardiac death. This was in association with an increased serum C-reactive protein level in these patients. However, in an animal model for myocardial infarction blockade of HMGB1 caused impaired infarct healing and marked scar thinning thereby worsening left ventricular remodelling⁵³. Furthermore, HMGB1 serum levels are markedly increased upon surgical thoracic aortic aneurysm repair⁵⁴. HMGB1 is also of interest in other inflammatory disease processes like SLE and kidney ischemia reperfusion^{55, 56}. HMGB1 also has pro-thrombogenic features by increasing tissue factor expression on monocytes and inhibiting anti-coagulant protein C pathway *in vitro*. *In vivo* the combined administration of thrombin and HMGB1 caused prolonged plasma clotting times⁵⁷. The effect of HMGB1 on platelets via direct TLR4 activation is still unknown. Fibronectin is a part of the extracellular matrix that undergoes severe stress during interventional procedures. Fibronectin-EDA (FN-EDA) is an adhesive glycoprotein spliced from fibronectin and is important in wound healing and can be produced by activated endothelium and fibroblasts. FN-EDA has been implicated in fibroblast differentiation, proliferation and migration and is capable of monocytes activation and induction of inflammation through upregulation of cytokines like interleukin-1 α and β and matrix metalloproteinases. Interestingly, FN-EDA is the only spliced variant of FN that binds and activates TLR4^{58, 59}. FN-EDA targets antigen to TLR4-expressing cells and induces cytotoxic T cell responses⁶⁰. FN-EDA is also considered to be a TLR2 ligand and therefore has the potential to activate the two most important TLRs in vascular disease. We showed that lack of FN-EDA prevents myocardial remodeling and preserves pump function after infarction⁶¹. FN-EDA was also found in restenotic lesions with features of accelerated atherosclerosis and in the myocardium in the early phase of the remodeling process following infarction⁶¹. Additionally absence of FN-EDA reduced atherosclerosis formation. In normal aortas the spliced FN-EDA could not be found, although FN-EDA was found in atherosclerotic plaques and in plasma of atherosclerotic mice. FN-EDA was shown to have effects in both plasma lipoprotein metabolism and in macrophage foam cell formation^{59, 62}. Studies with atherosclerotic mice that lack FN-EDA indeed showed that cholesterol levels were lowered^{59, 62}. In addition, FN-EDA may influence post-interventional remodeling directly via inducing an inflammatory reaction but also via effects on lipid metabolism.

Cytokines and chemokines

Cytokines and chemokines are important mediators of inflammatory responses and can be easily measured in serum. Both lowered and elevated concentrations of cytokines and chemokines are associated with cardiovascular risk profiles and specifically post-interventional vascular remodeling due to accelerated

atherosclerosis development. Nevertheless their levels can strongly differ due to different pathophysiological processes initiated by different treatment strategies. The treatment strategy (BMS vs. DES) therefore may have strong influence on the reliability of a selected cytokine or chemokine as biomarker^{1,22}. Interestingly conditions after acute myocardial infarction could exacerbate post-angioplasty restenosis by stimulating signaling via TNF α ⁶³. This may cause differences for patients that undergo scheduled PCI versus patients that had an acute myocardial infarction before PCI. It may therefore be important to look for combinations of specific cytokines besides a selected biomarker. Activation of innate immune response via TLRs will lead to nuclear factor kappa B (NF κ B) activation followed by upregulation of cytokines and chemokines^{26, 39}. Many different cytokines have been studied in relation to post-interventional remodeling and may be used in combination with specific biomarkers to correlate DAMP presence with remodeling related cytokines. Additionally this may provide better insight in the underlying mechanism of the pathophysiological process and thereby indications for proper treatment strategies. Cytokines could also be interesting to measure the effect of these treatment strategies by checking ratios of pro- and anti-inflammatory cytokines. Here we discuss a few cytokines/chemokines that have been intensively researched in relation to cardiovascular disease and have showed biomarker potential

Tumor necrosis factor α

Tumor necrosis factor (TNF) α is a pro-inflammatory cytokine that is importantly involved in inflammatory responses. Multiple cells including endothelial cells, vascular smooth muscle cells and monocytes-derived macrophages can secrete it. Several studies have shown that blockade of TNF α caused a reduction in neointimal formation via acceleration of endothelium repair, found increased mRNA expression of TNF α in the neointima of damaged vessels which may be upregulated 4000 times compared to resting levels. These kinds of studies also showed a relation with accelerated atherosclerosis^{64, 65}.

Interestingly, the local delivery of thalidomide as a potent TNF α biosynthesis inhibitor demonstrated a powerful reduction of the neointima formation in mice. In humans single nucleotide polymorphisms in the TNF α gene were found and showed associations with an increased clinical and angiographic risk for restenosis⁶⁶. Angioplasty in peripheral arterial segments gave increased levels of TNF α within 1 hour, although no statistically significant correlation was found between failed angioplasty and the following inflammatory response⁶⁷. Kubica et al stated that the combined analysis of CRP and TNF α might be an effective approach to the clinical restenosis prediction and long-term outcome is markedly influenced by the periprocedural activation of inflammation⁶⁸.

Monocyte chemoattractant protein 1

Monocyte chemoattractant protein (MCP)-1 binds to its receptor CC chemokine receptor 2 (CCR2) that belongs to the family of G-coupled receptors and is a chemokine that is capable of attracting immune cells like monocytes. Upon vascular injury MCP-1 recruits monocytes, memory T cells and dendritic cells to the injured site. Attracted monocytes infiltrate the vessel and contribute importantly to neointima formation⁶⁹. MCP-1 is strongly expressed locally in different stages of the remodeling

process. Furthermore, it has strong influence on SMC proliferation. Both mouse models for arterial restenosis as for vein graft remodeling showed a MCP-1 inhibitor showed sufficient reduction in neointima formation. Furthermore studies in which the receptor for MCP-1 was targeted gave similar results⁷⁰⁻⁷². No differences in MCP-1 concentrations between patients with acute MI, patients with stable coronary artery disease and healthy individuals were found⁷³. However, an inverse correlation was found between MCP-1 concentration at baseline and the time to reperfusion, and a significant decrease in MCP-1 concentration immediately after PCI and lower MCP-1 concentrations over time in patients who developed restenosis within 6 months were found⁷³. Elevated baseline level of MCP-1 was associated both with traditional risk factors for atherosclerosis as well as an increased risk for death or myocardial infarction, independent of baseline variables. Interestingly MCP-1 levels are not associated with CRP levels indicating the importance of selecting specific inflammatory markers in stead of general markers like CRP⁷⁴. MCP-1 levels are different amongst patients that received a BMS versus a DES⁷⁵. Furthermore in the same study they found increased monocyte CCR-2 expression 24 hr and 48 hr after stenting in the BMS but not the DES group and changes in plasma MCP-1 after stenting correlated significantly with in-stent lumen loss. Previously another Japanese study already showed a correlation between MCP-1 and the risk for restenosis after stenting⁷⁶.

Interleukin 10

Interleukin 10 (IL-10) is one of the most prominent anti-inflammatory cytokines. It may suppress antigen presentation and is capable of inhibiting pro-inflammatory cytokine production. Different animal models for restenosis and atherosclerosis showed protective effects of IL-10 by the use of recombinant human IL-10 or using animals deficient in IL-10.

In humans three polymorphisms significantly increased the risk of restenosis in patients and demonstrate that IL-10 is associated with restenosis⁷⁷⁻⁷⁹. IL-10 is however upregulated together with pro-inflammatory cytokines to maintain a balance between pro- and anti-inflammatory cytokines. Most of the time upregulation of pro-inflammatory cytokines exerts the upregulation of IL-10. Peripheral therapeutic angioplasty gave no difference in IL-10 levels compared to patients that underwent only angiography⁶⁷. In a study using BMS after PCI a significant low IL-10 levels was associated with an increase in restenosis after 6 months⁸⁰. The use of undergoing zotarolimus-eluting (zotarolimus is a semi-synthetic derivative of rapamycin that works as immunosuppressant) stent implantation combined with pioglitazone significantly reduced neointimal hyperplasia within the stented lesion and attenuated total plaque burden in the in-segment regions of the stent at the 8-month follow-up. These changes were preceded by an elevated IL-10 concentration 10 days after implantation⁸¹.

RANTES/CCL5

CCL5 (RANTES) deposition was involved in wire-induced intimal hyperplasia and blocking of RANTES receptors attenuates neointima formation and macrophage infiltration in animal studies⁸². Two clinical studies focused on the relation of RANTES levels and restenosis. While one of these studies found a decrease of RANTES in

time in the non-restenosis group another found a significant time-dependent increase in the restenosis group^{83, 84}. No association was found between RANTES promoter genotype and restenosis⁸⁵.

Plasma antibodies

Recent results from murine interventional studies indicate that inflammation and (auto)immune mechanisms are both strong contributors to the development of post-interventional restenosis development have led to the hypothesis that (auto) antibodies are both causally related to restenosis development, and titers could serve as biological biomarkers for the identification of restenosis risk or lesion severity. Longitudinal studies will be required to determine both the diagnostic and predictive values of antibody profiles, but promising candidates have emerged over the past decade, which will be discussed below.

The immune system can be divided into the innate and adaptive systems, which are closely linked and regulated. The innate immunity forms the first line of defense and offers a quick but unspecific response to invading microorganisms, whilst adaptive immunity takes longer to develop, but targets highly specific antigen-bearing foreign intruders. To this end, the former system is comprised of various toll-like receptors, the complement system and cytokines and chemokines, whilst the latter depends on the vast variety of B and T cell receptors and antigen-specific immunoglobulines.

Anti-oxidized LDL and phosphorylcholine antibodies

Immune responses against oxidized forms of cholesterol-containing LDL particles play a critical role in activation and regulation of the inflammatory process that characterizes all stages of atherosclerosis⁸⁶. LDL cholesterol is the most important risk factor for cardiovascular disease and cholesterol-lowering therapy (statins) alone can reduce CVD-risk by 30-40%. LDL has been found to play a key role in lesion development and LDL oxidation by enzymes such as lipoxygenases primarily occurs in the extracellular matrix in the arterial wall. Oxidative modification of phospholipid fatty acids, degradation of apoB-100 into peptide fragments and modification of these structures by aldehydes derived from oxidized fatty acids leads to the development of immunogenic neo-antigens^{87, 88}. These contain pathogen-associated molecular patterns (PAMPs) that are recognized by the pathogen recognition receptors (PRRs) from the immune system, of which TLRs and scavenger receptors are considered to be the most important. TLRs occur both intra- and extracellular and are activated by lipopolysaccharide (LPS) and various other (viral) micro-biological antigens, but also by endogenous ligands such as heat shock proteins and fibronectin extra-domain A⁸⁹. Their activation stimulates MyD88-dependent and independent intracellular cascades that eventually all lead to increased NFκB transcription and inflammation. In both mouse and man, natural anti-oxLDL IgM and IgG antibodies occur, whilst in vitro, antibodies are directed towards malondialdehyde (MDA) and copper-oxidized LDL⁸⁷. These antibodies proved to be exactly similar to those produced by natural occurring T15 B-1 cell clones and all recognize the phosphorylcholine (PC) antigen on oxLDL⁹⁰, but also on apoptotic cells and *Streptococcus pneumoniae*, which share molecular mimicry^{91, 92}.

These antibodies are suggested to block the oxLDL-uptake by scavenger receptor-bearing macrophages and block foam cell and atherosclerotic lesion formation,

but could also serve as risk markers for atherosclerotic and restenotic lesion development. Several studies have reported increased plasma titers of IgG anti-oxLDL antibodies in patients with angiographically verified coronary artery disease and with acute myocardial infarction⁹³⁻⁹⁵. Many studies found that low levels of IgM anti-oxLDL antibodies are associated with increased atherosclerosis in hypertensive patients and low levels of IgM anti-PC antibodies with acute myocardial infarction, ischemic stroke and cardiovascular disease in general in both the general population and patients with either hypertension or SLE⁹³⁻⁹⁶. Therefore, this could also hold true for restenosis due to accelerated atherosclerosis development and the severity of lesion development. In general, these studies have identified anti-oxLDL and specifically anti-PC antibodies as biomarkers for cardiovascular disease monitoring with potentially high additive value to current diagnostic strategies.

Microparticles

Thrombocytes, monocytes and those cellular types lining the arterial wall including endothelial cells and SMCs have been shown to vesiculate and release membrane-shed microparticles in response to cellular activation and apoptosis such as occur during the development of atherosclerotic and restenotic lesions^{97, 98}. Membrane integrity is largely controlled by intracellular calcium and caspase homeostasis⁹⁹. Disorganization of the cytoskeleton enables blebbing to occur and disruption of the membrane phospholipid symmetry supports PS externalization⁹⁹. These PS-containing microparticles have been implicated in the development, progression and complications of atherosclerotic lesions and patients suffering from atherosclerotic or restenotic cardiovascular disease display high levels of circulating microparticles and since these microparticles are absent in healthy individuals, their circulating levels prove to allow excellent follow-up of lesion progression and serve as surrogate markers for vascular function⁹⁹.

Specifically endothelium-derived microparticles, but not those originating from other cellular types, have been shown to bear high prognostic value in the risk assessment of mortality and major adverse cardiovascular events in patients with coronary artery disease, but also pulmonary hypertension and end-stage renal failure⁹⁸.

What can we learn from the lesion itself for selecting novel biomarkers?

In an ideal situation we would like to extract our biomarkers directly out of the lesion since this area previously gave problems and here postinterventional remodeling will start again.

Previously detectable CRP levels in the arterial intima were found preceding the appearance of monocytes. Furthermore, CRP had actually chemotactic capacities by direct influence on monocyte recruitment both in vitro as in vivo¹⁰⁰. Another study showed that immunoreactivity to CRP was localized to macrophages, SMCs and necrotic areas. Moreover, the immunoreactivity to CRP in coronary atheromatous plaque increases in culprit lesions of unstable angina and it affects restenosis¹⁰¹. This may indicate that local CRP levels are much more specific to study while the role of circulating CRP and the relation with post-interventional remodeling may still be difficult to assess since it may be upregulated in multiple ways even independently

of the interventional procedure. Another factor of which its plaque levels were more than 70 times higher in plaques than in plasma is oxLDL in patients undergoing carotid endarterectomy¹⁰². The same authors also found differences in the oxLDL amount in macrophages rich plaques versus macrophage poor plaques. Interestingly plasma oxLDL levels were only significantly different between control patients and patients with macrophage-rich plaques which may indicate that when studying only oxLDL on the plasma level will not discriminate patients without or patients with a macrophage-poor plaque and may be more helpful in determination of plaque vulnerability than just plaque formation or progression¹⁰². Bamberg and co-workers showed that different biomarkers of inflammation, vascular remodeling, oxidation, and lipoprotein metabolism maybe associated with different patterns of coronary atherosclerosis as quantified by coronary CT angiography¹⁰³. So lesion phenotype may be very important for the selection of proper novel biomarkers. Only recently a novel study was conducted that uses the knowledge of specific lesions to study the disease process and use it as a predictor of future restenosis and or atherosclerosis occurrence even at other sites than the initial lesion. This Athero-Express study was the first study to provide prospective evidence that plaque composition may predict the risk of restenosis after endarterectomy. Here they found associations for non-vulnerable plaque phenotype to be more prone to develop restenosis¹⁰⁴. The Athero-Express biobank was also used for a proteomics search approach to identify local biomarkers (selected proteins that have been identified earlier in experimental set-ups with any cardiovascular phenotype but not necessarily with atherosclerosis, osteopontin (OPN) and Macrophage migration inhibitory factor (MIF)) in the atherosclerotic plaque to predict atherosclerotic plaque development in other vascular beds. The authors collected plaques from carotids as well as plaques from femoral arteries and in both cases they found plaque osteopontin (OPN) levels highly predictive for secondary atherosclerotic development. Furthermore, plaque MIF levels were strongly associated with secondary cardiovascular events and showed that the concept not only applies for OPN¹⁰⁵. Although beyond the scope of this review, the field of proteomic research is evolving and could contribute substantially to the discovery of new biomarkers in post-interventional restenosis and accelerated atherosclerosis.

Most studies are of limited value for the risk stratification of individual patients with the current available biomarkers²⁵ and are therefore playing a very little role in the prediction of restenosis and decision-making for its exploration and treatment. Furthermore, in many clinical centers it is not possible yet to sample and extract tissue to select for biomarkers patient specifically however combining results of these kind of studies on plaque development and progression together with increased specific knowledge on the complex pathways extracted from experimental research may help us in understanding not only the pathophysiological process but also to select novel biomarkers. They probably will contribute largely to our knowledge and selection of novel biomarkers and may find new correlations between local and circulating levels of biomarkers and post-interventional remodeling and accelerated atherosclerosis. In addition these local studies may even come up with novel biomarkers inside the plaque that can not be detected in plasma due to their low plasma levels, incapacity of being released outside the plaque or just being plaque specific.

Conclusion

Recently published studies have demonstrated that both lowered and elevated concentrations of local arterial and circulating biomarkers are associated with cardiovascular risk profiles and specifically post-interventional vascular remodeling due to accelerated atherosclerosis development. These associations are independent of traditional risk factors and could serve as helpful tools for risk stratification or diagnostic assessment of patients eligible for intensified treatment for clinicians performing target lesion revascularization interventions. Improved assays have identified not only circulating biomarkers, but also cellular-expressed receptors, co-factors and microparticles that all directly causally involved in disease progress, but also indirectly as biomarkers of inflammatory status and vascular function. Provided these findings are replicated in other studies, the combined power of current diagnostic strategies with the latest tools and multiple biological risk markers could contribute significantly to the optimization of patient selection and future individual tailor-made treatment.

Executive summary

Introduction

- Coronary heart disease remains the leading cause of death and is caused by atherosclerosis, a chronic inflammatory disease

Underlying causes of restenosis

- Post-PCI restenosis is determined by biological, arterial, stent and technical factors

Inflammation status as biomarker

- Biomarkers can be divided into local, circulating and circulating cell-bound markers and are most valuable when causally related to disease progression

Circulating biomarkers

- Circulating markers and ligands of the innate immune system such as fibronectin, inflammatory cytokines, annexin A5 and natural antibodies towards oxidized LDL cholesterol and HMGB-1 can be highly predictive
- Inflammatory receptors on circulating leukocytes such as TLRs and scavenger receptors, but also microparticles are directly implicated in and strongly indicative of atherosclerotic vascular remodeling

What can we learn from the lesion itself for selecting novel biomarkers?

- Biobanks containing mRNA and protein profiles from numerous atherosclerotic plaques are highly valuable for local biomarker screening

Conclusion

- Biomarkers of inflammation status possess the highest predictive value for accelerated atherosclerosis disease progression, especially when combined and in addition to current diagnostic strategies

Future perspective

The insight into the development of atherosclerosis and post-PCI restenosis has developed very quickly over the past decade. Ever since, atherosclerosis is primarily

viewed as a chronic inflammatory disease due to a dysfunctional immune response towards the arterial wall. To this end, the focus on atherosclerotic biomarkers has shifted from traditional markers that serve as risk factors, such as hypercholesterolemia, towards markers of systemic inflammation (e.g. C-reactive protein) and arterial dysfunction. The important notion remains that causal factors are additionally powerful predictors of disease progression and the same would apply for inflammatory markers. The field of diagnostic and treatment-evaluation markers will shift in the same direction, guided by new insights, and rely heavily on the additional value of new biomarkers to the current diagnostic strategies. Epidemiologic assessment of additional value from combining biomarkers is a powerful tool to discover new biomarkers entities for the development of highly specific assays, specifically for genetic biomarkers such as polymorphisms that are associated with disease risk.

The field of biomarkers for accelerated atherosclerosis and post-interventional vascular remodeling has changed due to the introduction of drug-eluting stents. These stents have rendered various markers of little use, since they closely followed the inflammatory reaction towards BMS placement and are currently prevented by adequate local drug release. Their usefulness could be further compromised in future due to the ever-increasing application of drug-eluting balloons. Nevertheless, new inflammatory factors such as intraplaque and circulating proteins, natural antibodies, microparticles and cellular receptor expression could prove to be of highly-specific and diagnostic value. Furthermore, application of such screening assays would allow for optimal treatment evaluation such as occurred in the past with the introduction of cholesterol-lowering statin therapy.

Development and application of future biomarkers requires clinical validation, which remains a time-consuming and expansive entity, and this uncertainty is inherently (most notably on safety issues) present at the final stages of drug validation, limiting future biomarker development. In spite of this, investigations continue to proceed and will improve diagnostic and treatment accuracy of post-interventional atherosclerotic vascular remodeling.

Reference List

1. Niccoli G, Montone RA, Ferrante G, Crea F: The evolving role of inflammatory biomarkers in risk assessment after stent implantation. *J. Am. Coll. Cardiol.* 56, 1783-1793 (2010).
2. Wang TJ, Gona P, Larson MG et al. : Preprocedural C-reactive protein levels and cardiovascular events after coronary stent implantation. *N. Engl. J. Med.* 355, 2631-2639 (2006).
3. Dahlof B: Cardiovascular disease risk factors: epidemiology and risk assessment. *Am. J. Cardiol.* 105, 3A-9A (2010).
4. Andersson J, Libby P, Hansson GK: Adaptive immunity and atherosclerosis. *Clin. Immunol.* 134, 33-46 (2010).
5. Hansson GK: Inflammation, atherosclerosis, and coronary artery disease. *N. Engl. J. Med.* 352, 1685-1695 (2005).
6. Libby P, Ridker PM, Hansson GK: Progress and challenges in translating the biology of atherosclerosis. *Nature* 473, 317-325 (2011).
This review describes current immunological insights in the field of experimental and clinical atherosclerosis research.
7. Tabas I: Apoptosis and efferocytosis in mouse models of atherosclerosis. *Curr. Drug Targets.* 8, 1288-1296 (2007).
8. Libby P, Ridker PM, Hansson GK: Inflammation in atherosclerosis: from pathophysiology to practice. *J. Am. Coll. Cardiol.* 54, 2129-2138 (2009).
9. van der Hoeven BL, Pires NM, Warda HM, et al : Inflammation in atherosclerosis: from pathophysiology to practice. *Int. J. Cardiol.* 99, 9-17 (2005).
10. Farooq V, Gogas BD, Serruys PW: Restenosis: delineating the numerous causes of drug-eluting stent restenosis. *Circ. Cardiovasc. Interv.* 4, 195-205 (2011).
11. Garg S, Serruys PW: Coronary stents: current status. *J. Am. Coll. Cardiol.* 56, S1-42 (2010).
12. Dangas GD, Claessen BE, Caixeta A, Sanidas EA, Mintz GS, Mehran R: In-stent restenosis in the drug-eluting stent era. *J. Am. Coll. Cardiol.* 56, 1897-1907 (2010).
13. Weintraub WS: The pathophysiology and burden of restenosis. *Am. J. Cardiol.* 100, 3K-9K (2007).
14. Pires NM, Jukema JW, Daemen MJ, Quax PH: Drug-eluting stents studies in mice: do we need atherosclerosis to study restenosis? *Vascul. Pharmacol.* 44, 257-264 (2006).
15. Newby AC: Matrix metalloproteinases regulate migration, proliferation, and death of vascular smooth muscle cells by degrading matrix and non-matrix substrates. *Cardiovasc. Res.* 69, 614-624 (2006).
16. van Hinsbergh VWM, Engelse MA, Quax PHA: Pericellular proteases in angiogenesis and vasculogenesis. *Arterioscler. Thromb. Vasc. Biol.* 26, 716-728 (2006).
17. Jukema JW, Verschuren JJ, Ahmed TA, Quax PHA: Restenosis after PCI. Part 1: pathophysiology and risk factors. *Nat Rev Cardiol.* 9, 53-62 (2011)
18. Jukema JW, Ahmed TA, Verschuren JJ, Quax PHA: Restenosis after PCI. Part 2: prevention and therapy. *Nat Rev Cardiol.* (2011) Oct 11. epub ahead doi: 10.1038
19. Vasan RS: Biomarkers of cardiovascular disease: molecular basis and practical considerations. *Circulation* 113, 2335-2362 (2006).
This review provides an overview of the molecular basis of biomarker discovery and selection and the practical considerations that are a prerequisite to their clinical use.
20. Sukhija R, Fahdi I, Garza L, et al : Inflammatory markers, angiographic severity of coronary artery disease, and patient outcome. *Am. J. Cardiol.* 99, 879-884 (2007).
21. Walter DH, Fichtlscherer S, Sellwig M, et al: Preprocedural C-reactive protein levels and cardiovascular events after coronary stent implantation. *J. Am. Coll. Cardiol.* 37, 839-846 (2001).
22. Ferrante G, Niccoli G, Biasucci LM, et al: Association between C-reactive protein and angiographic restenosis after bare metal stents: an updated and comprehensive meta-analysis of 2747 patients. *Cardiovasc. Revasc. Med.* 9, 156-165 (2008).
23. Walter DH, Fichtlscherer S, Britten MB, et al: Statin therapy, inflammation and recurrent coronary events in patients following coronary stent implantation. *J. Am. Coll. Cardiol.* 38, 2006-2012 (2001).
24. Aronson D: Inflammatory markers: linking unstable plaques to coronary event, an interventional perspective. *Int. J. Cardiovasc. Intervent.* 6, 110-118 (2004).
25. Ware JH: The limitations of risk factors as prognostic tools. *N. Engl. J. Med.* 355, 2615-2617

- (2006).
26. Kawai T, Akira S: The role of pattern-recognition receptors in innate immunity: update on Toll-like receptors. *Nat. Immunol.* 11, 373-384 (2010).
This review describes the recent advances that have been made by research into the role of TLR biology in host defense and disease.
27. Miyake K: Innate immune sensing of pathogens and danger signals by cell surface Toll-like receptors. *Semin. Immunol.* 19, 3-10 (2007).
This review describes how TLRs can recognize not only exogenous ligands but also endogenous danger signals.
28. Boersma HH, Kietselaer BL, Stolk LM, et al: Past, present, and future of annexin A5: from protein discovery to clinical applications. *J. Nucl. Med.* 46, 2035-2050 (2005).
29. Cederholm A, Frostegard J: Annexin A5 as a novel player in prevention of atherothrombosis in SLE and in the general population. *Ann. N. Y. Acad. Sci.* 1108, 96-103 (2007).
30. van Genderen HO, Kenis H, Hofstra L, Narula J, Reutelingsperger CP: Extracellular annexin A5: functions of phosphatidylserine-binding and two-dimensional crystallization. *Biochim. Biophys. Acta* 1783, 953-963 (2008).
A clear overview of the important functions of extracellular annexin A5 in the field of cellular and vascular biology.
31. Cederholm A, Frostegard J: Annexin A5 multitasking: a potentially novel antiatherothrombotic agent? *Drug News Perspect.* 20, 321-326 (2007).
32. Cederholm A, Frostegard J: Annexin A5 in cardiovascular disease and systemic lupus erythematosus. *Immunobiology* 210, 761-768 (2005).
33. Ewing MM, de Vries MR, Nordzell M, et al: Annexin A5 therapy attenuates vascular inflammation and remodeling and improves endothelial function in mice. *Arterioscler. Thromb. Vasc. Biol.* 31, 95-101 (2011).
34. van Tits LJ, van Heerde WL, van der Vleuten GM, et al: Plasma annexin A5 level relates inversely to the severity of coronary stenosis. *Biochem. Biophys. Res. Commun.* 356, 674-680 (2007).
35. Hofstra L, Heymans S: Annexin A5 and the failing heart; lost or found in translation? *Eur. Heart J.* 28, 2695-2696 (2007).
36. Michelsen KS, Wong MH, Shah PK, et al: Lack of Toll-like receptor 4 or myeloid differentiation factor 88 reduces atherosclerosis and alters plaque phenotype in mice deficient in apolipoprotein E. *Proc. Natl. Acad. Sci. U. S. A* 101, 10679-10684 (2004).
37. Hansson GK, Hermansson A: The immune system in atherosclerosis. *Nat. Immunol.* 12, 204-212 (2011).
38. Hansson GK, Lundberg AM: Toll in the vessel wall--for better or worse? *Proc. Natl. Acad. Sci. U. S. A* 108, 2637-2638 (2011).
39. Ionita MG, Arslan F, de Kleijn DP, Pasterkamp G: Endogenous inflammatory molecules engage Toll-like receptors in cardiovascular disease. *J. Innate. Immun.* 2, 307-315 (2010).
40. Andonegui G, Kerfoot SM, McNagny K, Ebbert KV, Patel KD, Kubes P: Platelets express functional Toll-like receptor-4. *Blood* 106, 2417-2423 (2005).
41. Hollestelle SC, de Vries MR, van Keulen JK et al: Toll-like receptor 4 is involved in outward arterial remodeling. *Circulation* 109, 393-398 (2004).
42. Karper JC, de Vries MR, van den Brand BT et al: Toll-like receptor 4 is involved in human and mouse vein graft remodeling, and local gene silencing reduces vein graft disease in hypercholesterolemic APOE*3Leiden mice. *Arterioscler. Thromb. Vasc. Biol.* 31, 1033-1040 (2011).
43. Vink A, Schoneveld AH, van der Meer JJ et al: In vivo evidence for a role of toll-like receptor 4 in the development of intimal lesions. *Circulation* 106, 1985-1990 (2002).
44. Stewart CR, Stuart LM, Wilkinson K et al: CD36 ligands promote sterile inflammation through assembly of a Toll-like receptor 4 and 6 heterodimer. *Nat. Immunol.* 11, 155-161 (2010).
45. Park JS, Svetkauskaite D, He Q et al: Involvement of toll-like receptors 2 and 4 in cellular activation by high mobility group box 1 protein. *J. Biol. Chem.* 279, 7370-7377 (2004).
46. Park JS, Gamboni-Robertson F, He Q et al: High mobility group box 1 protein interacts with multiple Toll-like receptors. *Am. J. Physiol Cell Physiol* 290, C917-C924 (2006).
47. Yu M, Wang H, Ding A et al: HMGB1 signals through toll-like receptor (TLR) 4 and TLR2. *Shock* 26, 174-179 (2006).
48. Gondokaryono SP, Ushio H, Niyonsaba F et al: The extra domain A of fibronectin stimulates murine mast cells via toll-like receptor 4. *J. Leukoc. Biol.* 82, 657-665 (2007).

49. Lotze MT, Tracey KJ: High-mobility group box 1 protein (HMGB1): nuclear weapon in the immune arsenal. *Nat. Rev. Immunol.* 5, 331-342 (2005).
50. Abraham E, Arcaroli J, Carmody A, Wang H, Tracey KJ: HMG-1 as a mediator of acute lung inflammation. *J. Immunol.* 165, 2950-2954 (2000).
51. Wang H, Bloom O, Zhang M et al: HMG-1 as a late mediator of endotoxin lethality in mice. *Science* 285, 248-251 (1999).
52. Kalinina N: Increased expression of the DNA-binding cytokine HMGB1 in human atherosclerotic lesions: role of activated macrophages and cytokines. *Arteriosclerosis, thrombosis, and vascular biology* 24, 2320-2325 (2004).
53. Kohno T, Anzai T, Naito K et al: Role of high-mobility group box 1 protein in post-infarction healing process and left ventricular remodelling. *Cardiovasc. Res.* 81, 565-573 (2009).
54. Kohno T, Anzai T, Shimizu H et al: Impact of serum high-mobility group box 1 protein elevation on oxygenation impairment after thoracic aortic aneurysm repair. *Heart Vessels* 26, 306-312 (2011).
55. Leelahavanichkul A, Huang Y, Hu X et al: Chronic kidney disease worsens sepsis and sepsis-induced acute kidney injury by releasing High Mobility Group Box Protein-1. *Kidney Int* (2011).
56. Urbonaviciute V, Voll RE: HMGB1 represents a potential marker of disease activity and novel therapeutic target in SLE. *J. Intern. Med.* (2011).
57. Ito T, Kawahara K, Nakamura T et al: High-mobility group box 1 protein promotes development of microvascular thrombosis in rats. *J. Thromb. Haemost.* 5, 109-116 (2007).
58. Okamura Y, Watari M, Jerud ES et al: The extra domain A of fibronectin activates Toll-like receptor 4. *J. Biol. Chem.* 276, 10229-10233 (2001).
59. Tan MH, Sun Z, Opitz SL et al: Deletion of the alternatively spliced fibronectin EIIIA domain in mice reduces atherosclerosis. *Blood* 104, 11-18 (2004).
60. Lasarte JJ, Casares N, Gorraiz M et al: The extra domain A from fibronectin targets antigens to TLR4-expressing cells and induces cytotoxic T cell responses in vivo. *J. Immunol.* 178, 748-756 (2007).
61. Arslan F, Smeets MB, Riem Vis PW et al: Lack of fibronectin-EDA promotes survival and prevents adverse remodeling and heart function deterioration after myocardial infarction. *Circ. Res.* 108, 582-592 (2011).
62. Babaev VR, Porro F, Linton MF, Fazio S, Baralle FE, Muro AF: Absence of regulated splicing of fibronectin EDA exon reduces atherosclerosis in mice. *Atherosclerosis* 197, 534-540 (2008).
63. Takaoka M, Uemura S, Kawata H et al: Inflammatory response to acute myocardial infarction augments neointimal hyperplasia after vascular injury in a remote artery. *Arterioscler. Thromb. Vasc. Biol.* 26, 2083-2089 (2006).
64. Krasinski K, Spyridopoulos I, Kearney M, Losordo DW: In vivo blockade of tumor necrosis factor- α accelerates functional endothelial recovery after balloon angioplasty. *Circulation* 104, 1754-1756 (2001).
65. Rectenwald JE, Moldawer LL, Huber TS, Seeger JM, Ozaki CK: Direct evidence for cytokine involvement in neointimal hyperplasia. *Circulation* 102, 1697-1702 (2000).
66. Monraats PS, Pires NM, Schepers A et al: Tumor necrosis factor- α plays an important role in restenosis development. *FASEB J.* 19, 1998-2004 (2005).
67. Parmar JH, Aslam M, Standfield NJ: Percutaneous transluminal angioplasty of lower limb arteries causes a systemic inflammatory response. *Ann. Vasc. Surg.* 23, 569-576 (2009).
68. Kubica J, Kozinski M, Krzewina-Kowalska A et al: Combined periprocedural evaluation of CRP and TNF- α enhances the prediction of clinical restenosis and major adverse cardiac events in patients undergoing percutaneous coronary interventions. *Int. J. Mol. Med.* 16, 173-180 (2005).
69. Rogers C, Welt FG, Karnovsky MJ, Edelman ER: Monocyte recruitment and neointimal hyperplasia in rabbits. Coupled inhibitory effects of heparin. *Arterioscler. Thromb. Vasc. Biol.* 16, 1312-1318 (1996).
70. Egashira K, Zhao Q, Kataoka C et al: Importance of monocyte chemoattractant protein-1 pathway in neointimal hyperplasia after periarterial injury in mice and monkeys. *Circ. Res.* 90, 1167-1172 (2002).
71. Roque M, Kim WJ, Gazdoin M et al: CCR2 deficiency decreases intimal hyperplasia after arterial injury. *Arterioscler. Thromb. Vasc. Biol.* 22, 554-559 (2002).
72. Schepers A, Eefting D, Bonta PI et al: Anti-MCP-1 gene therapy inhibits vascular smooth muscle cells proliferation and attenuates vein graft thickening both in vitro and in vivo. *Arterioscler. Thromb. Vasc. Biol.* 26, 2063-2069 (2006).

73. Korybalska K, Pyda M, Grajek S, Lanocha M, Breborowicz A, Witowski J: Serum profiles of monocyte chemoattractant protein-1 as a biomarker for patients recovering from myocardial infarction. *Clin. Res. Cardiol.* 99, 315-322 (2010).
74. de Lemos JA, Morrow DA, Sabatine MS et al: *Circulation* 107, 690-695 (2003).
75. Sako H, Miura S, Iwata A et al: Changes in CCR2 chemokine receptor expression and plasma MCP-1 concentration after the implantation of bare metal stents versus sirolimus-eluting stents in patients with stable angina. *Intern. Med.* 47, 7-13 (2008).
76. Oshima S, Ogawa H, Hokimoto S et al: Plasma monocyte chemoattractant protein-1 antigen levels and the risk of restenosis after coronary stent implantation. *Jpn. Circ. J.* 65, 261-264 (2001).
77. Eefting D, Schepers A, de Vries MR et al: The effect of interleukin-10 knock-out and overexpression on neointima formation in hypercholesterolemic APOE*3-Leiden mice. *Atherosclerosis* 193, 335-342 (2007).
78. Feldman LJ, Aguirre L, Ziol M et al: Interleukin-10 inhibits intimal hyperplasia after angioplasty or stent implantation in hypercholesterolemic rabbits. *Circulation* 101, 908-916 (2000).
79. Monraats PS, Kurreeman FA, Pons D et al: Interleukin 10: a new risk marker for the development of restenosis after percutaneous coronary intervention. *Genes Immun.* 8, 44-50 (2007).
80. Zurakowski A, Wojakowski W, Dzielski T et al: Plasma levels of C-reactive protein and interleukin-10 predict late coronary in-stent restenosis 6 months after elective stenting. *Kardiol. Pol.* 67, 623-630 (2009).
81. Hong SJ, Kim ST, Kim TJ et al: Cellular and molecular changes associated with inhibitory effect of pioglitazone on neointimal growth in patients with type 2 diabetes after zotarolimus-eluting stent implantation. *Arterioscler. Thromb. Vasc. Biol.* 30, 2655-2665 (2010).
82. Schober A, Manka D, von Hundelshausen P et al: Deposition of platelet RANTES triggering monocyte recruitment requires P-selectin and is involved in neointima formation after arterial injury. *Circulation* 106, 1523-1529 (2002).
83. Inami N, Nomura S, Manabe K, Kimura Y, Iwasaka T: Platelet-derived chemokine RANTES may be a sign of restenosis after percutaneous coronary intervention in patients with stable angina pectoris. *Platelets* 17, 565-570 (2006).
84. Satoh D, Inami N, Shimazu T et al: Soluble TRAIL prevents RANTES-dependent restenosis after percutaneous coronary intervention in patients with coronary artery disease. *Journal of thrombosis and thrombolysis* 29, 471-476 (2010).
85. Vogiatzi K, Voudris V, Apostolakis S et al: Genetic diversity of RANTES gene promoter and susceptibility to coronary artery disease and restenosis after percutaneous coronary intervention. *Thrombosis research* 124, 84-89 (2009).
86. Hartvigsen K, Chou MY, Hansen LF et al: The role of innate immunity in atherogenesis. *J. Lipid Res.* 50 Suppl, S388-S393 (2009).
87. Nilsson J, Nordin FG, Schioppa A, Shah PK, Jansson B, Carlsson R: Oxidized LDL antibodies in treatment and risk assessment of atherosclerosis and associated cardiovascular disease. *Curr. Pharm. Des* 13, 1021-1030 (2007).
88. de Faire U, Frostegard J: Natural antibodies against phosphorylcholine in cardiovascular disease. *Ann. N. Y. Acad. Sci.* 1173, 292-300 (2009).
89. Frantz S, Ertl G, Bauersachs J: Mechanisms of disease: Toll-like receptors in cardiovascular disease. *Nat. Clin. Pract. Cardiovasc. Med.* 4, 444-454 (2007).
90. Amabile N, Rautou PE, Tedgui A, Boulanger CM: Microparticles: key protagonists in cardiovascular disorders *Semin. Thromb. Hemost.* 36, 907-916 (2010).
91. Chou MY, Fogelstrand L, Hartvigsen K et al: Oxidation-specific epitopes are dominant targets of innate natural antibodies in mice and humans. *J. Clin. Invest* 119, 1335-1349 (2009).
92. Binder CJ, Horkko S, Dewan A et al: Pneumococcal vaccination decreases atherosclerotic lesion formation: molecular mimicry between *Streptococcus pneumoniae* and oxidized LDL. *Nat. Med.* 9, 736-743 (2003).
This study demonstrates the vital molecular mimicry between oxLDL and pathogens that are recognized by the innate immune system in atherosclerosis development.
93. Fiskesund R, Stegmayr B, Hallmans G et al: Low levels of antibodies against phosphorylcholine predict development of stroke in a population-based study from northern Sweden. *Stroke* 41, 607-612 (2010).
94. Frostegard J: Low level natural antibodies against phosphorylcholine: a novel risk marker and potential mechanism in atherosclerosis and cardiovascular disease *Clin. Immunol.* 134, 47-54 (2010).

95. Su J, Georgiades A, Wu R, Thulin T, de Faire U, Frostegard J: Antibodies of IgM subclass to phosphorylcholine and oxidized LDL are protective factors for atherosclerosis in patients with hypertension. *Atherosclerosis* 188, 160-166 (2006).
96. de Faire U, Su J, Hua X, Frostegard A et al: Low levels of IgM antibodies to phosphorylcholine predict cardiovascular disease in 60-year old men: effects on uptake of oxidized LDL in macrophages as a potential mechanism. *J. Autoimmun.* 34, 73-79 (2010).
97. Leroyer AS, Tedgui A, Boulanger CM: Role of microparticles in atherothrombosis *J. Intern. Med.* 263, 528-537 (2008).
98. Dignat-George F, Boulanger CM: The many faces of endothelial microparticles *Arterioscler. Thromb. Vasc. Biol.* 31, 27-33 (2011).
99. Rautou PE, Vion AC, Amabile N et al: Microparticles, vascular function, and atherothrombosis. *Circ. Res.* 109, 593-606 (2011).
100. Torzewski M, Rist C, Mortensen RF et al: C-reactive protein in the arterial intima: role of C-reactive protein receptor-dependent monocyte recruitment in atherogenesis. *Arterioscler. Thromb. Vasc. Biol.* 20, 2094-2099 (2000).
101. Ishikawa T, Hatakeyama K, Imamura T et al: Involvement of C-reactive protein obtained by directional coronary atherectomy in plaque instability and developing restenosis in patients with stable or unstable angina pectoris. *Am. J. Cardiol.* 91, 287-292 (2003).
102. Nishi K, Itabe H, Uno, M et al: Oxidized LDL in carotid plaques and plasma associates with plaque instability. *Arterioscler. Thromb. Vasc. Biol.* 22, 1649-1654 (2002).
103. Bamberg F, Truong QA, Koenig W et al: Differential associations between blood biomarkers of inflammation, oxidation, and lipid metabolism with varying forms of coronary atherosclerotic plaque as quantified by coronary CT angiography. *Int. J. Cardiovasc. Imaging* (2011).
104. Hellings WE, Moll FL, de Vries JP et al: Atherosclerotic plaque composition and occurrence of restenosis after carotid endarterectomy. *JAMA* 299, 547-554 (2008).
105. de Kleijn DP, Moll FL, Hellings WE et al: Local atherosclerotic plaques are a source of prognostic biomarkers for adverse cardiovascular events. *Arterioscler. Thromb. Vasc. Biol.* 30, 612-619 (2010).

Chapter 3

Small Animal Models to Study Restenosis and Effects of (Local) Drug Therapy

M.M. Ewing^{1,2,3*}, J.C. Karper^{2,3*}, M.R. de Vries^{2,3}, J.W. Jukema^{1,3}, P.H.A. Quax^{2,3}

1 Dept. of Cardiology, Leiden University Medical Center (LUMC), Leiden, The Netherlands

2 Dept. of Surgery, LUMC, Leiden, The Netherlands

3 Einthoven Laboratory for Experimental Vascular Medicine, LUMC, Leiden, The Netherlands

* Both authors contributed equally

Abstract

In-stent restenosis remains the major drawback of coronary interventions and is a highly complex process, initiated by the induction of vascular injury and stent deployment, ultimately leading to negative vascular remodeling and reoccurrence of symptoms. Development, testing and validation of new therapies strongly depends on the availability of animal models that closely mimic human restenotic pathophysiology. Moreover, for a better understanding of the pathophysiology of the restenosis process adequate animal models mimicking the human restenosis process are essential.

Here, we review various animal models, predominately humanized mouse models, currently used to study the pathophysiology of restenosis. Larger animal models such as pigs and rabbits that are used for testing new therapeutic strategies such as new drug-eluting stents, will not be discussed in this chapter.

We will discuss the involvement of inflammatory and immune modulatory factors in the development and progression of restenosis. Furthermore, we will discuss in detail several new therapeutic options based on modulation of their anti-proliferative, anti-inflammatory or proteinase-interference abilities.

We can conclude highly-reproducible animal models for post-interventional vascular remodeling remain essential for the development of future anti-restenotic therapies.

Introduction

Pathophysiology of Restenosis in Humans and Animals

Restenosis is defined angiographically in patients when neointimal tissue comprises over 50% of the luminal surface at the site of intervention of the affected artery. Restenosis is characterized by acute elastic recoil, negative remodeling and intimal hyperplasia due to inflammation, deposition of granulation tissue and extracellular matrix remodeling. Intracoronary stenting has virtually eliminated elastic recoil and negative remodeling. However, after balloon angioplasty and stent placement neointimal formation still occurs due to de-endothelization and injury of the vessel wall including the atherosclerotic plaque.

Together, these effects lead to activation of the remaining endothelium, platelet adhesion and subsequent activation, fibrin formation and the expression of adhesion molecules, leukocyte adherence and infiltration. Adhered leukocytes release an array of inflammatory cytokines, chemokines, proteases such as matrix metalloproteinases and growth factors which not only promote inflammation, but also cause medial smooth muscle cell migration and proliferation, matrix degradation, local proteoglycan deposition and subsequent extracellular matrix remodeling. Under hypercholesterolemic conditions this is accompanied by influx and accumulation of low-density lipoprotein (LDL) cholesterol in the vessel wall. This will be taken up by macrophages, that become foam cells and initiate a process of accelerated atherosclerosis in these vessel segments¹. Patients receive platelet-inhibitors throughout interventional procedures to prevent arterial thrombosis and end-organ ischemia due to thrombotic occlusion of the affected vessel. Furthermore, this therapy partly prevents the initial pathophysiological events that eventually lead to restenosis development. Nonetheless, in patients limited local inflammatory processes are related to the healing of the vascular injury triggered by mechanical dilation, stent deployment and the continuous presence of stent struts against the arterial wall and their exposure to flowing blood^{2, 3}. However, uncontrolled inflammatory processes may induce intimal hyperplasia.

Intravascular injury to diseased vessels with a hypercholesterolemic background is common in patients, but severely difficult to reproduce in healthy vessels of mainly young animals with a normocholesterolemic phenotype. Therefore, transgenic mouse models with a pro-atherosclerotic or hypercholesterolemic phenotype have attracted attention as humanized mouse models for mechanistic and pathophysiological restenosis research.

Animal Models for Restenosis and Vascular Remodeling

Various animal models, mainly in mice, are currently available to mimic human restenosis, extensively based on perivascular injury, aimed to induce local coagulation and subsequent inflammation, leading to accelerated atherosclerosis formation.

Balloon angioplasty of rat carotid arteries

A model of balloon-induced injury to the carotid artery in rats was described in 1983 by Clowes et al.⁴ and used many studies there after, amongst others by Ohlstein et al.⁵, in which an arterial embolectomy catheter is inserted into the common carotid artery and a balloon is inflated and drawn along the vessel wall to induce mechanical

injury. Afterwards, the external carotid artery is ligated. This leads to severe SMC migration and proliferation and intimal thickening.

Common carotid artery ligation in mice

Neointimal formation can be elicited by completely ligating the common carotid artery just proximal to the carotid bifurcation to disrupt blood flow as has been described by Kumar et al.⁶ and since then has frequently been used by several groups. After 4 weeks, intimal thickening occurs and consists of both SMCs and leukocytes, indicating the pivotal role of inflammation in the formation of neointimal tissue. The model is hampered by its reproducibility, since morphometric analysis is very critical. The degree of the intimal hyperplasia depends on the position the analyzed section in regard to the point of ligation.

Mouse model of femoral artery denudation injury

Femoral artery transluminal injury can be induced by passage of a 0.25-mm diameter angioplasty guide wire in mice⁷. Four weeks after injury, neointima formation can be analyzed and consist predominately of migrated and proliferated SMCs, although inflammatory cells can already be observed early after injury.

Perivascular electrocoagulation injury

Electrocoagulation-induced injury to the femoral artery of mice was introduced in 1997 by Carmeliet et al.⁸, leading to loss of all endothelial and medial smooth muscle cells (SMCs) and formation of a mural non-occlusive platelet-rich thrombus. This leads to inflammatory cell recruitment and SMC migration and proliferation, eventually leading to intimal thickening.

Photochemical intravascular injury

Photochemical endothelial injury to the femoral artery of mice injected with rose Bengal solution using transluminal green light has been used by Kikuchi et al.⁹ in 1998 to induce a local thrombus formation, followed by endothelial denudation and medial SMC apoptosis and eventually intimal thickening. Unfortunately, the reproducibility of this model remains rather low.

Perivascular chemical injury

Chemical perivascular injury to the carotid artery of dyslipidemic mice using a filter paper saturated with a 10% ferric chloride solution was used by Zhu et al.¹⁰ to induce formation of an occlusive platelet-rich thrombus due to endothelial cell loss and medial SMC necrosis, triggering inflammatory cell recruitment and SMC migration and proliferation. Eventually, this promotes intimal thickening.

Inter-arterial venous engraftment

Accelerated atherosclerosis and vascular remodeling also appear in engrafted vascular segments, which are performed frequently to bypass occluded arterial segments in patients. Although bypass models do not mimic the pathophysiology of restenosis completely, they can be used excellently to study various aspects of restenotic disease. Models have been developed for several animal species. Only relatively recently have mouse models for vein graft disease become available, de-

veloped by Xu et al.⁷, most often based on the model described by Lardenoye et al.¹¹, in which a venous interposition is made within the carotid artery of a mouse. For this, an inferior caval vein is harvested from littermate donor mice and preserved in a 0.9% NaCl solution containing 100U of heparin at 4°C, to prevent thrombosis. Afterwards, the carotid artery is dissected free from its surroundings, ligated twice and cut between the two 8.0 silk ligatures. Clamps are placed proximally and distally from the ligatures to allow haemostatic control to the surgeon throughout the procedure, leaving free arterial ends over which a cuff can be placed. Next, the free arterial ends are everted over the cuffs and ligated with an 8.0 silk ligature, after which the harvested inferior caval vein is interpositioned between the ends of the artery. The connections are ligated together with an 8.0 silk suture and visible pulsations confirm successful engraftment.

When performed in hypercholesterolemic mice, concentric lesions are formed within 4 weeks and are friable, with extracellular lipid deposition and foam cell accumulation, underneath a poorly developed or absent fibrous cap. This morphology highly resembles the morphology observed in arterially-engrafted veins in patients. All aspects of rapid post-interventional vascular remodeling and accelerated atherosclerosis development are present in this very reproducible animal model.

Intravascular balloon dilatation injury

Intravascular injury models resembling invasive coronary procedures have been developed recently, but remain technically very demanding.

Kwak et al.¹² described a mouse model in which intravascular carotid balloon distension injury is performed, which a balloon catheter was introduced through an arteriotomy on the proximal external carotid artery and advanced into the common carotid artery and subsequently distended to induce controlled vessel wall distension. In this elegant model, distention could be matched to the animal's weight and the balloon was expanded using a water-filled inflation device. Vessel wall damage led to endothelial denudation, followed by leukocyte recruitment and medial SMC activation, leading to intimal thickening and luminal stenosis. Although this model is technically difficult to perform, vascular injury highly resembles the human situation and leads to a similar pathophysiological vessel wall response.

Inter-arterial stented-arterial engraftment

Ali et al.¹³ have taken intravascular stenting in mouse models a step further, which they reported in 2007. Donor mice receiving aspirin underwent stenting using a stainless-steel stent crimped onto an angioplasty balloon catheter, which was guided into place retrograde through the thoracic aorta, leaving the balloon and stent in the descending thoracic aorta. The balloon was inflated for 30 seconds until 8 times atmospheric pressure to induce stent deployment. Next, the stented-aorta was removed and kept in heparinised PBS solution, before being engrafted within the ligated carotid artery of a hypercholesterolemic recipient mouse, similarly to the vein graft procedure. After 28 days, intimal thickening was significantly increased in the stented arterial graft, when compared to the aorta and balloon-inflated aortic grafts. Lesions consisted predominately of SMCs, macrophages and foam cells, similarly to human coronary lesions after interventions.

Perivascular femoral arterial cuff placement

Already in 1989, it was shown by Booth et al.¹⁴ that placement of a perivascular non-constrictive plastic cuff around the common carotid artery of hypercholesterolemic rabbits results in intimal thickening based on SMC migration and proliferation, cholesterol deposition and foam cell formation as seen in human restenotic lesions. This is due to mechanical vascular damage and an inflammatory response evoked by the cuff. There was no need for endothelial cell damage and the formation of a transient occlusive thrombus in this model.

When this attractive model was downscaled to mice¹⁵, this offered the unique opportunity to employ a mechanically-induced inflammatory-based restenosis model in an animal species of which an enormous range of strains with genetic variations existed, including atherosclerosis prone transgenic strains.

Since like the human genome, the murine genome has currently been completely mapped and multiple humanized-mouse models have been developed, this has allowed researchers to investigate the role of specific genotypic and general phenotypic traits in restenosis development. The aim was to identify pathophysiological changes leading to restenosis and accelerated atherosclerosis development, and subsequently identify key targets for prevention and treatment of restenosis in patients in a clinical setting.

The technical procedure of perivascular cuff placement¹⁵ is described in detail in the next section. Before surgery, mice are anaesthetized with an intraperitoneal injection with a combination of 5 mg/kg Midazolam (Roche, Basel, Switzerland), 0.5 mg/kg Medetomidine (Orion, Helsinki, Finland) and 0.05 mg/kg Fentanyl (Janssen, Geel, Belgium). This combination of anesthetics gives complete narcosis, lasting minimally one hour and can be antagonized using Antisedan 2.5 mg/kg (Orion), Anexate 0.5 mg/kg (Roche) and Buprenorphine 0.08 mg/kg (Schering-Plough, Kenilworth, NJ, USA).

A microscope with 10-15x total magnification is used during the microsurgery procedures (Olympus SZX9 microscope). Basic instruments required are a blunt micro forceps (length: 10.5cm, height: 0.3mm, Medicon Instruments, Tuttlingen, Germany), a sharp micro forceps (length: 10.5cm, height: 0.3mm, Medicon Instruments), a micro scissor (length: 12.5cm, height: 10mm, Medicon Instruments) and a micro needle holder (length: 18.5cm, Medicon Instruments).

A longitudinal incision is made at the internal side of the thigh and the femoral artery is dissected from the femoral nerve and vein. The femoral artery is looped twice with a ligature (USP: 6/0, Metric: 0.7., Silkam natural silk, B. Braun, Melsungen, Germany) and a non-constrictive fine bore polyethylene tubing (0.40mm inner diameter, 0.80mm outer diameter, Portex, Kent, UK) is cut 2.0mm length and longitudinally opened and sleeved loosely around the femoral artery. The cuff is closed with two 6/0 ligature knots in the extremities of the cuff. Finally, the skin incision is closed with a running suture (USP: 6/0, Metric: 0.7., Silkam silk, B. Braun). After surgery, animals are placed in a clean cage on top of a heating pad for four hours. A schematic representation and photomicrograph of the femoral arterial cuff placement are shown in figure 1.

For histological analysis, animals are typically sacrificed 2-3 weeks after cuff placement. After anesthesia, the thorax is opened and a mild pressure-perfusion (100 mmHg) with 4% formaldehyde in 0.9% NaCl is performed for 5 minutes by cardiac

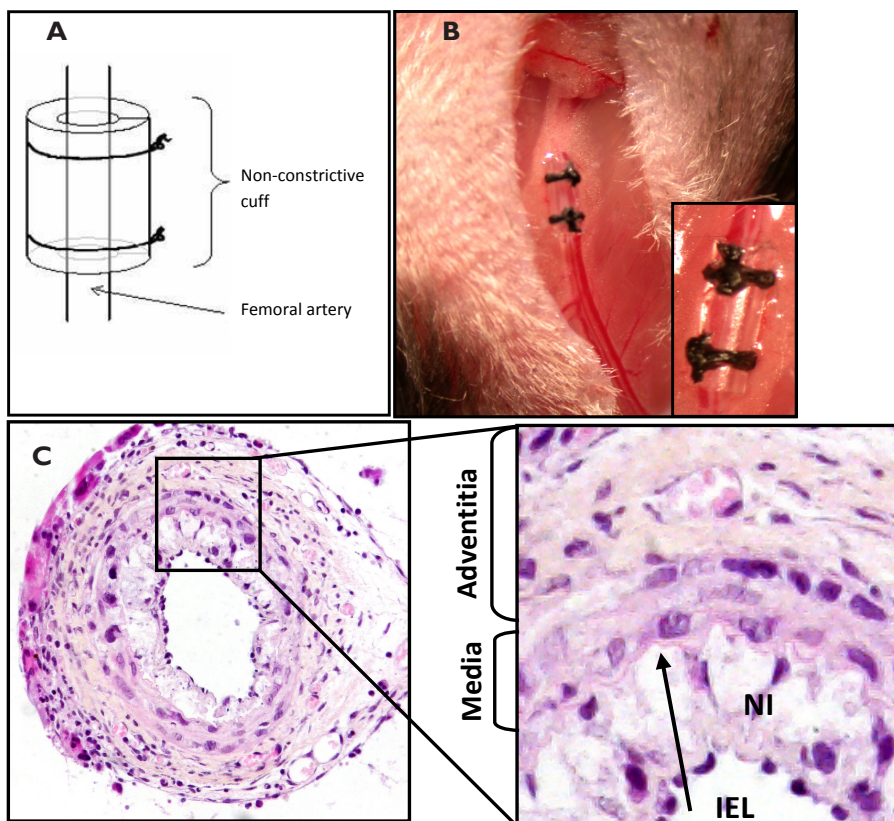


Figure 1. Schematic representation of non-constrictive cuff placed loosely around a murine femoral artery, held in place by two ligatures (A) and a photomicrograph (B) of a positioned cuff in vivo. (C) Photomicrograph of the restenosis lesion in the cuffed femoral artery in the mouse. Indicated are the internal elastic lamina (IEL) and the neointima (NI) formed within the vessel wall.

puncture. After perfusion, a longitudinal incision is made in the internal side of the thigh and the cuffed femoral artery is harvested as a whole and fixed overnight in 4% formaldehyde.

Preclinical application of drug-eluting stents and balloons

Intracoronary stenting decreased restenosis rates by preventing elastic recoil and negative remodeling, although in-stent restenosis due to neointimal proliferation remains the major limiting factor of the success rate for coronary interventions as treatment for coronary artery disease. Drug-eluting stents with a polymer coating have been developed which are loaded with various types of drugs designed to prevent in-stent restenosis. These drugs, some originally used as chemotherapeutic agents, against transplant rejection or as immunosuppressive drugs, tend to prevent the local inflammatory reaction, SMC proliferation and migration or promote local healing due to a slow local release. Drug-eluting balloons are coated with similar drugs, but are designed to deliver the drug only for a very short period of time whilst the balloon is left inflated, to prevent

solely the initial local responses to balloon inflation and vessel wall distention.

Limited (post-mortem) pathological data is available from stented human coronary arteries, since histology is usually not readily available. All in vitro and in vivo effects of new drug-eluting stents should be evaluated for safety and efficiency before being applied in human studies. Preclinical animal studies can also provide insight in the method-of-action, dose-response and side-effects of these new stents. Additionally, they can be used for investigation into specific genes involved in restenosis development. Genes of interest can be found in large prospective follow up studies, such as the GENDER study¹⁶, in which the association between gene polymorphisms and clinical outcome can be studied. Additionally, these highly-reproducible models can be used to screen candidate compounds, without the need for expensive, large, long-lasting and time-consuming clinical trials.

Drug-eluting stents can be mimicked in mice by placement of a perivascular non-constrictive drug-eluting cuff¹⁷, comprised of a poly(ϵ -caprolactone) (PCL) polymer and non-toxic polyethylene glycol, loaded with the candidate drug, shown in figure 2. This polymer cuff allows encapsulation and local sustained release of compounds over a longer period of time. Depending on the ratio between PCL and polyethylene glycol, the duration of drug-release can be extended up until 21 days after cuff placement, to allow local vessel wall drug-exposure throughout the entire study period, even in non-hypercholesterolemic mice which develop restenotic lesions relatively slowly.

An alternative for local delivery of active compounds to the mouse vessel wall is the use of local administration of the compound dissolved in pluronic gel or gelatin in and around the cuff. This allows short period of delivery of compounds locally in the murine cuff model as the gelatin or the pluronic gel will degrade in a short period of time. The set-up of this local application of pluronic gel in the cuff is shown in figure 3. In patients, drug-eluting stents release the drug intraluminally, whilst in this model drugs are released from the adventitial side of the vessel wall. However, the vessel wall in the mouse is smaller, therefore penetration of the compound will be efficient, although applied via the adventitia. Nonetheless, this drug-eluting PCL cuff is certainly an extremely useful and practical tool to evaluate the effects of new candidate anti-restenotic drugs on local vessel wall pathology and intimal thickening as part of post-interventional vascular remodeling.

Suitable mouse strains

Contrary to patients, wild-type mouse strains have low levels of pro-atherosclerotic low-density-lipoprotein and high plasma levels of anti-atherosclerotic high-density lipoprotein and therefore do not readily develop native atherosclerosis. Inbred mice used for studies into accelerated atherosclerosis and restenosis tend to respond to restenotic stimuli by displaying either a type 1 or type 2 helper T cell (Th1 or Th2) response. The Th1 response, typical of the C57BL/6 mouse strain, leads to macrophage differentiation into proatherogenic M1 macrophages and production of inflammatory cytokines and chemokines, which promote lesion formation¹⁸. The Th2 response, typical of the BALB/C mouse strain, promotes the differentiation of macrophages into anti-inflammatory M2 macrophages, which produce anti-inflammatory and anti-atherogenic cytokines, eventually leading to a healing response within the damaged vessel wall. For this reason, mouse strains with a C57BL/6 background

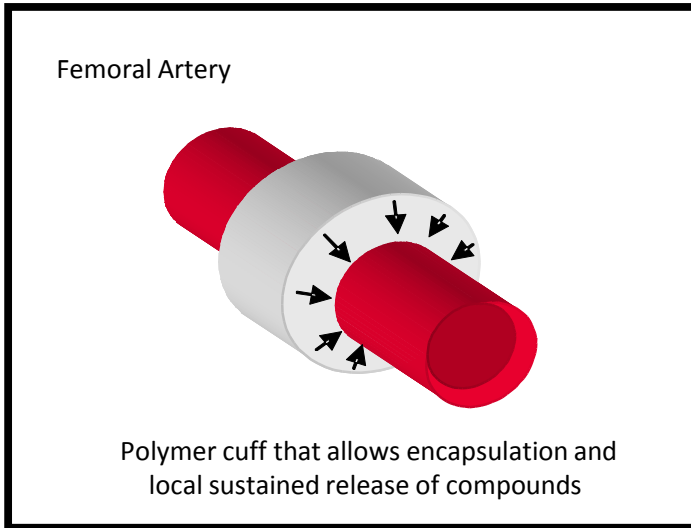


Figure 2. Schematic representation of a drug-eluting femoral arterial cuff and method-of-action.

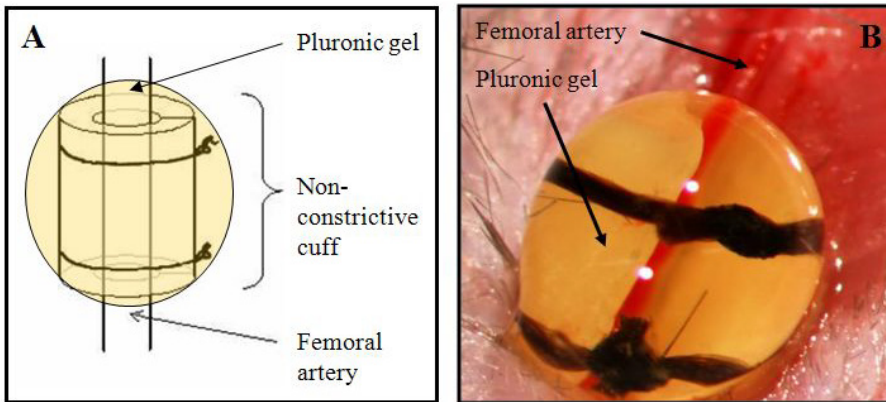


Figure 3. Schematic representation of non-constrictive cuff around a murine femoral artery, covered by hardened pluronic gel (A). Photomicrograph cuff in vivo, with hardened (40%) pluronic gel applied to the cuffed vessel segment, loaded with an anti-restenotic drug (yellow) (B).

a favored for studying pathophysiological changes leading to restenosis. When the perivascular non-constrictive cuff procedure is performed in this mouse strain¹⁹, concentric lesions develop within 21 days after surgery and typically consist of collagen and α -actin positive SMCs.

Dyslipidemic mouse strains

Intravascular injury by balloon inflation and stent placement in diseased human vessels in hypercholesterolemic patients can be mimicked by cuff placement in hypercholesterolemic knock-out or transgenic mouse strains.

Apolipoprotein (Apo) E is an important part of circulating very (V) LDL and LDL cholesterol and acts as a ligand for the LRL-R, thus leading to uptake of proathero-

sclerotic cholesterol from the circulation. Genetic ApoE deficiency therefore leads to hypercholesterolemia due to insufficient LDL-receptor(R)-mediated VLDL and LDL clearance, especially when fed a high-cholesterol diet, and spontaneous atherosclerotic and interventional-induced lesion formation. Drawbacks of this mouse strain are plasma cholesterol levels that are mainly determined by the VLDL fraction, that exceed by far any physiological level and that all other atheroprotective (anti-inflammatory, anti-platelet and anti-proliferative) properties of ApoE are lost²⁰.

Patients with familial hypercholesterolemia display mutations in the LDL-R gene, leading to insufficient LDL clearance and dyslipidemia. Similarly, LDL-R knockout mice develop mild hypercholesterolemia, which increases strongly when fed a high-cholesterol diet. Since cholesterol elevation is mainly determined by the LDL fraction and spontaneous atherosclerotic lesions develop more slowly than in ApoE knockout mice, this is classified as a more moderate model. Nonetheless, both mouse strains can be used to study post-interventional restenosis development²⁰.

Mutations in the ApoE3 gene are associated with dysbetaproteinemia in patients. One of these mutations is the ApoE3Leiden mutation²¹. By introducing an ApoE3 and ApoC1 gene construct in the C57BL/6 mice, the transgenic ApoE3*Leiden mouse strain was generated²². Since the animals still express endogenous ApoE proteins, contrary to the ApoE knockout animals, the uptake of ApoE-containing lipoproteins is merely reduced and not completely inhibited. Animals have diet-induced increased plasma cholesterol concentrations, mainly in VLDL and LDL fractions. They are very responsive to high-cholesterol feeding. Desired plasma cholesterol concentrations can be obtained by varying dietary cholesterol content. Additionally, since both ApoE and LDL-R are still present, plasma cholesterol levels are subject to modulation by lipid-lowering drugs that influence endogenous chylomicron and VLDL production and indirectly affect LDL-R expression, such as statins. Restenotic lesions after cuff placement develop moderately and consist predominately of SMCs, foam cells and extracellular matrix formation, very similar to human lesions¹⁵.

New mechanistic and therapeutic insights

Agents currently used or under investigation to prevent and treat restenosis can be divided between either drugs with cytotoxic/anti-proliferative and anti-inflammatory effects or drugs that target proteolytic systems. Here we give an overview how animal models may contribute to gain further insight into the mechanism of restenosis and to test new therapeutic strategies.

Proliferation

Rapamycin (sirolimus)

Immunosuppressive drugs like rapamycin are currently widely used in drug-eluting stents to prevent the development of in-stent restenosis. Rapamycin is a macrolide antibiotic drug with anti-proliferative and immunosuppressive effects that targets protein translation, resulting in a G1 arrest of the cell cycle which is known to inhibit vascular SMC proliferation and migration in vitro by inhibiting DNA synthesis and cell growth²³⁻²⁵. Rapamycin has been shown to effectively inhibit the arterial proliferative response after PCTA in a porcine restenosis model, without toxicity in low

doses. Local rapamycin application in the murine cuff model was performed using a rapamycin-eluting cuff and it was observed that locally released rapamycin led to an inhibition of neointima formation by $75\pm 6\%$ for all tested concentrations. Experiments demonstrated that perivascular sustained release was restricted to the cuffed vessel segment, with no systemic adverse effects. Moreover, when applying the rapamycin eluting cuff to a diseased atherosclerotic vessel segment in ApoE3Leiden mice, no progression of the atherosclerotic lesion development could be observed, nor any systemic side effects

Paclitaxel

Paclitaxel belongs to the taxanes, which are potent anti-proliferatives widely used to treat patients suffering from cancer. It leads to polymerization of the α - and β -units of tubulin and thus stabilizes microtubules, which are necessary for the G2 transition of a dividing cell into the M phase. Paclitaxel causes almost complete inhibition of cell growth and SMC proliferation and migration by targeting cytoskeleton structure. SMC proliferation and migration are both induced by balloon inflation and stent placement during interventional procedures. In a murine femoral arterial cuff model, drug-eluting cuffs containing high paclitaxel concentrations (1–5%) have been shown to reduce intimal thickening by $76\pm 2\%$. When placing the paclitaxel eluting cuff in hypercholesterolemic mice or even over an existing atherosclerotic lesion in mice, dose dependent negative side effects were observed. High dosage of paclitaxel significantly increased apoptosis (also in the media), disruption of the elastic laminae and decrease medial and intimal smooth muscle cell as well as collagen content. These findings show elegantly the added value of testing drug eluting devices in atherosclerotic animal model. Many clinical trials²⁶⁻²⁸ have investigated the effectiveness of (non) polymer-based paclitaxel-eluting stents and have shown to be very effective in the prevention of restenosis development, however, negative effects on the vascular pathology were not detected, emphasizing that the femoral arterial cuff model is of high predictive value in the screening for new candidate drugs for efficacy and local adverse side effects.

Inflammation

Although neointima formation is characterized by proliferation and migration of smooth muscle cells (SMC) and extracellular matrix turnover it is now broadly accepted that these processes are triggered by inflammatory activation of the vessel wall¹⁶. Evidence that inflammation is the initial trigger for vascular remodeling has accumulated over the past years and the role of various cytokines and chemokines as pro-inflammatory factors as well as immune modulation in general has been the focus of many studies on vascular remodeling and restenoses. In the next section we would like to illustrate this with a couple of representative examples. Starting with the description of the effects of the general anti-inflammatory factor dexamethason, we will further zoom in on the effects of specific cytokines (TNF α , IL10), chemokines (MCP-1) and the role of the innate immune system (complement, toll-like receptors) on restenosis in the mouse models.

Dexamethason

Dexamethason is a corticosteroid with strong glucocorticoid properties and is widely

used as a broad anti-inflammatory and immunosuppressant drug. Prolonged systemic delivery is associated with multiple side effects in humans and animals. These effects could be abolished by local delivery using a drug-eluting cuff (DEC), mimicking the potential effect of drug eluting stents. Local delivery of dexamethason via DEC delivery inhibited neointima formation drastically without systemic side effects, indicating a beneficial effect of local suppression of inflammation over systemic delivery as was tested by applying dexamethason via the drinking water in the same model. However pathobiological examination of the murine arteries revealed a dose-dependent medial atrophy, a reduction in vascular smooth muscle cells and collagen content, an increase in apoptotic cell count and disruption of the internal elastic lamina²⁹. Short term systemic delivery in a model for vein graft remodeling showed a reduction in intimal hyperplasia formation without serious side effects probably due to the short period of delivery³⁰. These results not only emphasize the importance of the immune system and the role of inflammation in restenosis more specifically and systematically, but also show that the use of small (hypercholesterolemic) animal models does have predictive value in regard to negative side effects on vascular pathology after local drug application.

Innate immunity

Innate immunity is very important in triggering inflammation and can be divided into a humoral and a cellular component. It comprises multiple cell types, receptors and mechanisms such as the Complement system and Toll like receptors (TLRs) that are very important in host defense. The innate immune system is considered to be highly involved in regulation of intimal hyperplasia and atherogenesis. This could very elegantly be demonstrated using specific mouse models in combination with cuff placement or vein grafting as described in the section below.

Complement

The complement system comprises the humoral mechanism of the innate immune system. C3 cleavage plays a central role in the complex regulation of complement activation and can be initiated via the classical, alternative or the lectin pathway. The role of complement was studied in the model of vein graft restenosis combined with accelerated atherosclerosis in the ApoE3*Leiden mouse. The expression of complement components C1q, C3, and the regulatory proteins CD59 and complement receptor-related gene γ (Crry) could be detected on the protein and mRNA level in the grafts. A reduction in vein graft thickening and intimal hyperplasia was accomplished after interference with C3 activation by systemic administration of either Cobra Venom Factor or Crry-Ig protein. The latter was associated with a reduced number of inflammatory cells in the vessel wall³¹, indicating that blocking the central factor in the complement activation cascade, C3, results in a profound reduction of vascular remodeling. This underscores a role of the innate immune system in restenosis related vascular remodeling.

Toll-like Receptors

TLRs are membrane bound receptors located on a variety of immune and non-immune cells including macrophages, endothelium and SMCs. Cell stress and tissue damage may cause a release of Damage Associated Molecular Patterns (DAMPs)

that function as endogenous TLR ligands. Balloon inflation and stent placement or bypass grafting lead to injury to the vessel wall and may cause up regulation of DAMPs such as Heat Shock Protein 60 (HSP60), Fibronectin-EDA, Tenascin C and Biglycan. HSP60 binds directly to TLR2 or TLR4 thereby initiating proliferation of VSMC³². In response to peri-adventitial cuff induced injury TLR4 expression is up regulated in the vessel wall during at least 7 days (unpublished data). A causal role for TLR4 in restenosis was demonstrated by a reduced cuff induced neointima formation in TLR4 deficient mice³³. Moreover, local adventitial TLR4 activation by LPS application strongly augmented neointima formation in both mouse models, so with and without involvement of accelerated atherosclerosis³⁴. The same method was used to stimulate TLR2 with Pam3Cys and resulted in an increase in neointima formation in C57/B6 mice and in APOE^{-/-} mice that develop atherosclerotic lesions³⁵. We believe that the release upon vascular injury of specific DAMPs as endogenous TLR ligands is one of the earliest triggers in vascular remodeling in restenosis and there are convinced that the TLR signaling pathway has a crucial function in the restenosis process. This is supported by the SNPs found in the TLR4 gene that correlate with an increased risk for cardiovascular event and/or restenosis after an initial PCI³⁶⁻³⁸.

Cytokines

Activation of the immune system results in secretion of multiple pro and anti-inflammatory cytokines. These cytokines can be seen as hormones of the immune system that communicate, can attract and activate different cell types importantly involved in restenosis and atherosclerosis like SMC and macrophages. A disturbance in the cytokine balance, locally or systemically, alters the inflammatory status thereby mediating inflammatory processes. Since many cytokines have their role in multiple inflammatory reactions it is important to know whether they are involved, can be a therapeutic target or may function as biomarker for the process of restenosis.

TNF α

Tumor Necrosis Factor alpha (TNF α) is a cytokine that regulates immune cells and promotes the inflammatory response. It is produced by many cells including endothelial cells, VSMCs and macrophages. The GENDER project systematically genotyped for six polymorphisms in the TNF α gene and found associations with an increased clinical and angiographic risk for restenosis in humans³⁹. In a rat balloon-injury model blockade of the TNF α caused a reduction in neointima formation via acceleration of endothelium repair⁴⁰. In mice, after common carotid artery (CCA) ligation, TNF α mRNA expression was found in intimal lesions itself. Application of the same model in knockout mice showed a decrease in lesion size⁴¹. After peri-adventitial cuff placement TNF α mRNA is rapidly up regulated to levels 4000 times to original mRNA levels and deficiency of TNF α in a murine study of restenosis with accelerated atherosclerosis, performed in ApoE*3-Leiden-TNFalpha knockout mice, caused a marked reduction in neointima formation. Interestingly, the use of a DEC for local delivery of thalidomide as a potent TNFalpha biosynthesis inhibitor demonstrated a powerful reduction of the neointima formation after cuff placement to levels similar to those observed in the ApoE*3-Leiden-TNFalpha knockout model³⁹. TNFalpha is clearly an important cytokine in the inflammatory process that take place in the

vessel wall during restenosis and its role can be studied in detail using the specific mouse models for restenosis, cuff and drug eluting cuff placement.

CCR2/MCP1

The chemokine Monocyte Chemoattractant Protein1 (MCP1) or CCL2 is a cytokine that is capable of attracting immune cell types like monocytes that are known to infiltrate the vessel wall as a one of the first in neointima formation. Furthermore MCP1 influences SMC proliferation and is expressed in various stages of vascular remodeling. MCP1 binds to its receptor CC chemokine receptor 2 (CCR2) that belongs to the family of G-coupled receptors. Femoral artery transluminal injury by passage of a 0.25-mm diameter angioplasty guide wire was done in a CCR2^{-/-} mice⁷. Four weeks after injury, CCR2^{-/-} mice showed a 61.4% reduction in neointima formation and a 62% reduction in intima/media ratio. The effects of MCP1 in vivo were studied in the murine vein graft model as well as in the femoral cuff model. Systemic overexpression of a dominant negative form of MCP-1, 7ND-MCP, by electroporation of a plasmid into the calf muscle resulted in circulating levels of this MCP-1 inhibitor that were sufficient to decrease intimal hyperplasia significantly, both in the cuff model⁴² as well as in the vein graft model⁴³.

In addition, in the mouse vein graft restenosis model perivascular local vector application for lentiviral shRNA targeting CCR2 reduced intimal hyperplasia in the vein grafts by approximately 50%⁴⁴. These studies demonstrate the role of these models in evaluation of experimental therapeutic strategies.

Interleukin-10

Interleukin-10 (IL-10) is one of the most prominent anti-inflammatory cytokines and functions pleiotropic. It may suppress antigen presentation and is capable of inhibiting pro-inflammatory cytokine production. These capacities make IL-10 a very attractive candidate for anti restenotic and anti atherosclerotic therapy. Three polymorphisms significantly increased the risk of restenosis in patients and demonstrate that IL-10 is associated with restenosis. This set interest for anti-inflammatory genes to be involved in the development of restenosis⁴⁵. The functional role of IL-10 in restenosis was assessed by Feldman et al.⁴⁶ and showed beneficial effects of recombinant human IL-10 after balloon angioplasty or stenting in hypercholesterolemic rabbits. Per-adventitial cuff placement in hypercholesterolemic APOE*3-Leiden-IL-10^{-/-} mice (hypercholesterolemic mice deficient for IL-10) resulted in an increased neointima formation indicating a protective role for IL-10 in a murine model for restenosis and accelerated atherosclerosis⁴⁷. Electroporation of an IL-10 plasmid into the calf muscle resulted in IL-10 overexpression in ApoE3*Leiden mice and caused a reduction in cholesterol and neointima formation two weeks after cuff placement, underscoring the therapeutic potential of IL-10 in restenosis.

Protease Inhibition in Restenosis

Proteases of the Matrix metalloproteinase (MMP) system and of the plasminogen activator system are thought to play an important role in the matrix degradation and smooth muscle cell migration during vascular remodeling and are upregulated after coronary angioplasty⁴⁸. Studies in mice showed a decreased neointima formation in MMP2^{-/-}, MMP9^{-/-} mice and augmented neointima formation in TIMP1^{-/-} mice⁴⁹⁻⁵¹. By

use of the electrocoagulation vascular injury model Lijnen et al.⁵² studied whether the plasminogen activation system, a system that also may activate the MMP system, and the MMP system itself play a role in neointima formation using knockout mice. Neointima formation was reduced in urokinase-type plasminogen activator knockout (uPA^{-/-}) and Plasminogen (Plg) knockouts (Plg^{-/-}) but no effect was seen in the tissue-type Plg activator knockout (tPA^{-/-}) mice.

To study the therapeutic potential of these findings a hybrid protein consisting of the receptor-binding amino-terminal fragment of uPA (ATF), linked to the potent protease inhibitor bovine pancreas trypsin inhibitor (BPTI) was constructed and cloned into an adenoviral vector⁵³. Mice were infected with the combined ATF.BPTI vector or single vectors for ATF or BPTI and cuffs were placed around the femoral arteries to induce neointima formation. Only the ATF.BPTI showed a strong inhibition of neointima formation by selective binding to the uPA receptor and inhibiting plasmin activity⁵⁴. Infection with the same vector in a balloon injury model also showed significant inhibition of neointima formation in rats⁵⁵ as well as in mice after cuff placement⁵³. In 2002 a novel hybrid protein consisting of the tissue inhibitor of metalloproteinase-1 (TIMP-1) domain, as MMP inhibitor, linked to ATF (TIMP-1.ATF) was constructed. By binding to the u-PA receptor this protein blocks binding of u-PA and attaches TIMP-1 directly to the cell surface. This construct was able to inhibit SMC migration and neointima formation *in vitro*⁵⁶. *In vivo* intimal hyperplasia combined with accelerated atherosclerosis was studied in murine vein grafts. Plasmids encoding ATF, TIMP-1, TIMP-1.ATF, were injected and electroporated (non-viral gene transfer) in both calf muscles of hypercholesterolemic ApoE*3Leiden mice. Although all constructs reduced vein graft thickening compared with the controls, the luminal area was best preserved in the TIMP-1.ATF-treated mice⁵⁷.

Finally a non-viral expression vector encoding the hybrid protein TIMP-1.ATF.BPTI (TAB) was constructed and validated. After four weeks, vein graft thickening was significantly inhibited in mice treated with the single domains TIMP-1, ATF or BPTI. In the TAB treated mice vein graft thickening was reduced and was also significantly stronger as compared to the individual domains⁵⁸.

Conclusions

For restenosis research animal models are definitely essential for testing new anti-restenosis devices, such as new drug eluting stent, as well as for unraveling the underlying pathophysiological mechanism and identifying new therapeutic targets. It is important to work with models that mimic the human situation as good as possible, either in vascular anatomical aspects (size, diameter, wall thickness) or disease stage related aspects (hypercholesterolemia, vessel with atherosclerotic lesions).

In the current chapter we have focused on the later group of animal models, those humanized models that have the best predictive value for the pathophysiological process in the development of restenosis, intimal hyperplasia and accelerated atherosclerosis in the lesions. Various vascular interventions in transgenic mouse models have been described, with a strong focus on the mouse femoral artery cuff model and these mouse models have proven to be technically suitable for the study into restenosis development.

Next, to study effects of (local) drug therapy, animals should be susceptible to the

treatment of interest, have similar metabolic levels, coagulatory phenotype and react in a human-like fashion. The use of humanized (transgenic) animal models has extensively increased the similarity between human and animal lesions and the translation of new therapies into in the clinical setting.

Mechanistic and pathophysiological studies have shown that local vessel wall inflammation, proliferation and proteolysis play important roles in the post-interventional vascular remodeling, both in humans and in the animal models used.

In addition, these animal models are extremely suitable to identify new potential therapeutic targets to prevent restenosis and test new experimental strategies for therapy, e.g. based on systemic or local gene delivery of inhibitory factors (anti-proliferative, anti-inflammatory or anti-proteolytic). These studies clearly demonstrate the importance and value of animal models for clinical medicine.

We can conclude that highly-reproducible animal models for post-interventional vascular remodeling remain essential for studying the process of restenosis and the development of future anti-restenotic therapies.

REFERENCES

1. Pires NM, Jukema JW, Daemen MJ, Quax PH. Drug-eluting stents studies in mice: do we need atherosclerosis to study restenosis? *Vascul Pharmacol* 2006;44(5):257-64.
2. Landau C, Lange RA, Hillis LD. Percutaneous transluminal coronary angioplasty. *N Engl J Med* 1994;330(14):981-93.
3. Mehilli J, Kastrati A, Bollwein H, Dibra A, Schuhlen H, Dirschinger J, Schomig A. Gender and restenosis after coronary artery stenting. *Eur Heart J* 2003;24(16):1523-30.
4. Clowes AW, Reidy MA, Clowes MM. Mechanisms of stenosis after arterial injury. *Lab Invest* 1983;49(2):208-15.
5. Ohlstein EH, Douglas SA, Sung CP, Yue TL, Loudon C, Arleth A, Poste G, Ruffolo RR, Jr., Feuerstein GZ. Carvedilol, a cardiovascular drug, prevents vascular smooth muscle cell proliferation, migration, and neointimal formation following vascular injury. *Proc Natl Acad Sci U S A* 1993;90(13):6189-93.
6. Kumar A, Lindner V. Remodeling with neointima formation in the mouse carotid artery after cessation of blood flow. *Arterioscler Thromb Vasc Biol* 1997;17(10):2238-44.
7. Roque M, Kim WJ, Gazdoin M, Malik A, Reis ED, Fallon JT, Badimon JJ, Charo IF, Taubman MB. CCR2 deficiency decreases intimal hyperplasia after arterial injury. *Arterioscler Thromb Vasc Biol* 2002;22(4):554-9.
8. Carmeliet P, Moons L, Stassen JM, De MM, Bouche A, van den Oord JJ, Kockx M, Collen D. Vascular wound healing and neointima formation induced by perivascular electric injury in mice. *Am J Pathol* 1997;150(2):761-76.
9. Kikuchi S, Umemura K, Kondo K, Saniabadi AR, Nakashima M. Photochemically induced endothelial injury in the mouse as a screening model for inhibitors of vascular intimal thickening. *Arterioscler Thromb Vasc Biol* 1998;18(7):1069-78.
10. Zhu Y, Farrehi PM, Fay WP. Plasminogen activator inhibitor type 1 enhances neointima formation after oxidative vascular injury in atherosclerosis-prone mice. *Circulation* 2001;103(25):3105-10.
11. Lardenoye JH, de Vries MR, Lowik CW, Xu Q, Dhore CR, Cleutjens JP, van Hinsbergh VW, van Bockel JH, Quax PH. Accelerated atherosclerosis and calcification in vein grafts: a study in APOE*3 Leiden transgenic mice. *Circ Res* 2002;91(7):577-84.
12. Kwak BR, Veillard N, Pelli G, Mulhaupt F, James RW, Chanson M, Mach F. Reduced connexin43 expression inhibits atherosclerotic lesion formation in low-density lipoprotein receptor-deficient mice. *Circulation* 2003;107(7):1033-9.
13. Ali ZA, Alp NJ, Lupton H, Arnold N, Bannister T, Hu Y, Mussa S, Wheatcroft M, Greaves DR, Gunn J, Channon KM. Increased in-stent stenosis in ApoE knockout mice: insights from a novel mouse model of balloon angioplasty and stenting. *Arterioscler Thromb Vasc Biol* 2007;27(4):833-40.
14. Booth RF, Martin JF, Honey AC, Hassall DG, Beesley JE, Moncada S. Rapid development of atherosclerotic lesions in the rabbit carotid artery induced by perivascular manipulation. *Atherosclerosis* 1989;76(2-3):257-68.
15. Lardenoye JH, Delsing DJ, de Vries MR, Deckers MM, Princen HM, Havekes LM, van Hinsbergh VW, van Bockel JH, Quax PH. Accelerated atherosclerosis by placement of a perivascular cuff and a cholesterol-rich diet in ApoE*3Leiden transgenic mice. *Circ Res* 2000;87(3):248-53.
16. Monraats PS, Pires NM, Agema WR, Zwinderman AH, Schepers A, de Maat MP, Doevendans PA, de Winter RJ, Tio RA, Waltenberger J, Frants RR, Quax PH, van Vlijmen BJ, Atsma DE, van der Laarse A, van der Wall EE, Jukema JW. Genetic inflammatory factors predict restenosis after percutaneous coronary interventions. *Circulation* 2005;112(16):2417-25.
17. Pires NM, van der Hoeven BL, de Vries MR, Havekes LM, van Vlijmen BJ, Hennink WE, Quax PH, Jukema JW. Local perivascular delivery of anti-restenotic agents from a drug-eluting poly(epsilon-caprolactone) stent cuff. *Biomaterials* 2005;26(26):5386-94.
18. Hansson GK. Inflammation, atherosclerosis, and coronary artery disease. *N Engl J Med* 2005;352(16):1685-95.
19. Krom YD, Pires NM, Jukema JW, de Vries MR, Frants RR, Havekes LM, van Dijk KW, Quax PH. Inhibition of neointima formation by local delivery of estrogen receptor alpha and beta specific agonists. *Cardiovasc Res* 2007;73(1):217-26.
20. Zadelaar S, Kleemann R, Verschuren L, de Vries-Van der Weij, van der Hoorn J, Princen

- HM, Kooistra T. Mouse models for atherosclerosis and pharmaceutical modifiers. *Arterioscler Thromb Vasc Biol* 2007;27(8):1706-21.
21. Havekes L, de WE, Leuven JG, Klasen E, Utermann G, Weber W, Beisiegel U. Apolipoprotein E3-Leiden. A new variant of human apolipoprotein E associated with familial type III hyperlipoproteinemia. *Hum Genet* 1986;73(2):157-63.
22. van den Maagdenberg AM, de KP, Stalenhoef AF, Gevers Leuven JA, Havekes LM, Frants RR. Apolipoprotein E*3-Leiden allele results from a partial gene duplication in exon 4. *Biochem Biophys Res Commun* 1989;165(2):851-7.
23. Gallo R, Padurean A, Jayaraman T, Marx S, Roque M, Adelman S, Chesebro J, Fallon J, Fuster V, Marks A, Badimon JJ. Inhibition of intimal thickening after balloon angioplasty in porcine coronary arteries by targeting regulators of the cell cycle. *Circulation* 1999;99(16):2164-70.
24. Marx SO, Jayaraman T, Go LO, Marks AR. Rapamycin-FKBP inhibits cell cycle regulators of proliferation in vascular smooth muscle cells. *Circ Res* 1995;76(3):412-7.
25. Poon M, Marx SO, Gallo R, Badimon JJ, Taubman MB, Marks AR. Rapamycin inhibits vascular smooth muscle cell migration. *J Clin Invest* 1996;98(10):2277-83.
26. Gershlick A, De S, I, Chevalier B, Stephens-Lloyd A, Camenzind E, Vrints C, Reifart N, Missault L, Goy JJ, Brinker JA, Raizner AE, Urban P, Heldman AW. Inhibition of restenosis with a paclitaxel-eluting, polymer-free coronary stent: the European evaluation of paclitaxel Eluting Stent (ELUTES) trial. *Circulation* 2004;109(4):487-93.
27. Grube E, Silber S, Hauptmann KE, Mueller R, Buellesfeld L, Gerckens U, Russell ME. TAXUS I: six- and twelve-month results from a randomized, double-blind trial on a slow-release paclitaxel-eluting stent for de novo coronary lesions. *Circulation* 2003;107(1):38-42.
28. Park SJ, Shim WH, Ho DS, Raizner AE, Park SW, Hong MK, Lee CW, Choi D, Jang Y, Lam R, Weissman NJ, Mintz GS. A paclitaxel-eluting stent for the prevention of coronary restenosis. *N Engl J Med* 2003;348(16):1537-45.
29. Pires NM, Schepers A, van der Hoeven BL, de Vries MR, Boesten LS, Jukema JW, Quax PH. Histopathologic alterations following local delivery of dexamethasone to inhibit restenosis in murine arteries. *Cardiovasc Res* 2005;68(3):415-24.
30. Schepers A, Pires NM, Eefting D, de Vries MR, van Bockel JH, Quax PH. Short-term dexamethasone treatment inhibits vein graft thickening in hypercholesterolemic ApoE3Leiden transgenic mice. *J Vasc Surg* 2006;43(4):809-15.
31. Schepers A, de Vries MR, van Leuven CJ, Grimbergen JM, Holers VM, Daha MR, van Bockel JH, Quax PH. Inhibition of complement component C3 reduces vein graft atherosclerosis in apolipoprotein E3-Leiden transgenic mice. *Circulation* 2006;114(25):2831-8.
32. de Graaf R, Kloppenburg G, Kitslaar PJ, Bruggeman CA, Stassen F. Human heat shock protein 60 stimulates vascular smooth muscle cell proliferation through Toll-like receptors 2 and 4. *Microbes Infect* 2006;8(7):1859-65.
33. Vink A, Schoneveld AH, van der Meer JJ, Van Middelaar BJ, Sluijter JP, Smeets MB, Quax PH, Lim SK, Borst C, Pasterkamp G, de Kleijn DP. In vivo evidence for a role of toll-like receptor 4 in the development of intimal lesions. *Circulation* 2002;106(15):1985-90.
34. Hollestelle SC, de Vries MR, van Keulen JK, Schoneveld AH, Vink A, Strijder CF, Van Middelaar BJ, Pasterkamp G, Quax PH, de Kleijn DP. Toll-like receptor 4 is involved in outward arterial remodeling. *Circulation* 2004;109(3):393-8.
35. Schoneveld AH, Oude Nijhuis MM, van MB, Laman JD, de Kleijn DP, Pasterkamp G. Toll-like receptor 2 stimulation induces intimal hyperplasia and atherosclerotic lesion development. *Cardiovasc Res* 2005;66(1):162-9.
36. Boekholdt SM, Agema WR, Peters RJ, Zwiderman AH, van der Wall EE, Reitsma PH, Kastelein JJ, Jukema JW. Variants of toll-like receptor 4 modify the efficacy of statin therapy and the risk of cardiovascular events. *Circulation* 2003;107(19):2416-21.
37. Hamann L, Gomma A, Schroder NW, Stamme C, Glaeser C, Schulz S, Gross M, Anker SD, Fox K, Schumann RR. A frequent toll-like receptor (TLR)-2 polymorphism is a risk factor for coronary restenosis. *J Mol Med* 2005;83(6):478-85.
38. Kiechl S, Lorenz E, Reindl M, Wiedermann CJ, Oberhollenzer F, Bonora E, Willeit J, Schwartz DA. Toll-like receptor 4 polymorphisms and atherogenesis. *N Engl J Med* 2002;347(3):185-92.
39. Monraats PS, Pires NM, Schepers A, Agema WR, Boesten LS, de Vries MR, Zwiderman AH, de Maat MP, Doevendans PA, de Winter RJ, Tio RA, Waltenberger J, 't Hart LM, Frants RR, Quax PH, van Vlijmen BJ, Havekes LM, van der Laarse A, van der Wall EE, Jukema JW. Tumor necrosis factor-alpha plays an important role in restenosis development. *FASEB J* 2005;19(14):1998-2004.

40. Krasinski K, Spyridopoulos I, Kearney M, Losordo DW. In vivo blockade of tumor necrosis factor- α accelerates functional endothelial recovery after balloon angioplasty. *Circulation* 2001;104(15):1754-6.
41. Rectenwald JE, Moldawer LL, Huber TS, Seeger JM, Ozaki CK. Direct evidence for cytokine involvement in neointimal hyperplasia. *Circulation* 2000;102(14):1697-702.
42. Egashira K, Zhao Q, Kataoka C, Ohtani K, Usui M, Charo IF, Nishida K, Inoue S, Katoh M, Ichiki T, Takeshita A. Importance of monocyte chemoattractant protein-1 pathway in neointimal hyperplasia after periarterial injury in mice and monkeys. *Circ Res* 2002;90(11):1167-72.
43. Schepers A, Eefting D, Bonta PI, Grimbergen JM, de Vries MR, van W, V, de Vries CJ, Egashira K, van Bockel JH, Quax PH. Anti-MCP-1 gene therapy inhibits vascular smooth muscle cells proliferation and attenuates vein graft thickening both in vitro and in vivo. *Arterioscler Thromb Vasc Biol* 2006;26(9):2063-9.
44. Eefting D, Bot I, de Vries MR, Schepers A, van Bockel JH, van Berkel TJ, Biessen EA, Quax PH. Local lentiviral short hairpin RNA silencing of CCR2 inhibits vein graft thickening in hypercholesterolemic apolipoprotein E3-Leiden mice. *J Vasc Surg* 2009;50(1):152-60.
45. Monraats PS, Kurreeman FA, Pons D, Sewgobind VD, de Vries FR, Zwinderman AH, de Maat MP, Doevendans PA, de Winter RJ, Tio RA, Waltenberger J, Huizinga TW, Eefting D, Quax PH, Frants RR, van der Laarse A, van der Wall EE, Jukema JW. Interleukin 10: a new risk marker for the development of restenosis after percutaneous coronary intervention. *Genes Immunity* 2007;8(1):44-50.
46. Feldman LJ, Aguirre L, Ziol M, Bridou JP, Nevo N, Michel JB, Steg PG. Interleukin-10 inhibits intimal hyperplasia after angioplasty or stent implantation in hypercholesterolemic rabbits. *Circulation* 2000;101(8):908-16.
47. Eefting D, Schepers A, de Vries MR, Pires NM, Grimbergen JM, Lagerweij T, Nagelkerken LM, Monraats PS, Jukema JW, van Bockel JH, Quax PH. The effect of interleukin-10 knock-out and overexpression on neointima formation in hypercholesterolemic APOE*3-Leiden mice. *Atherosclerosis* 2007;193(2):335-42.
48. Hojo Y, Ikeda U, Katsuki T, Mizuno O, Fujikawa H, Shimada K. Matrix metalloproteinase expression in the coronary circulation induced by coronary angioplasty. *Atherosclerosis* 2002;161(1):185-92.
49. Galis ZS, Johnson C, Godin D, Magid R, Shipley JM, Senior RM, Ivan E. Targeted disruption of the matrix metalloproteinase-9 gene impairs smooth muscle cell migration and geometrical arterial remodeling. *Circ Res* 2002;91(9):852-9.
50. Johnson C, Galis ZS. Matrix metalloproteinase-2 and -9 differentially regulate smooth muscle cell migration and cell-mediated collagen organization. *Arterioscler Thromb Vasc Biol* 2004;24(1):54-60.
51. Lijnen HR, Soloway P, Collen D. Tissue inhibitor of matrix metalloproteinases-1 impairs arterial neointima formation after vascular injury in mice. *Circ Res* 1999;85(12):1186-91.
52. Lijnen HR, Van HB, Lupu F, Moons L, Carmeliet P, Collen D. Function of the plasminogen/plasmin and matrix metalloproteinase systems after vascular injury in mice with targeted inactivation of fibrinolytic system genes. *Arterioscler Thromb Vasc Biol* 1998;18(7):1035-45.
53. Quax PH, Lamfers ML, Lardenoye JH, Grimbergen JM, de Vries MR, Slomp J, de Ruiten MC, Kockx MM, Verheijen JH, van Hinsbergh VW. Adenoviral expression of a urokinase receptor-targeted protease inhibitor inhibits neointima formation in murine and human blood vessels. *Circulation* 2001;103(4):562-9.
54. Lamfers ML, Wijnberg MJ, Grimbergen JM, Huisman LG, Aalders MC, Cohen FN, Verheijen JH, van Hinsbergh VW, Quax PH. Adenoviral gene transfer of a u-PA receptor-binding plasmin inhibitor and green fluorescent protein: inhibition of migration and visualization of expression. *Thromb Haemost* 2000;84(3):460-7.
55. Lamfers ML, Lardenoye JH, de Vries MR, Aalders MC, Engelse MA, Grimbergen JM, van Hinsbergh VW, Quax PH. In vivo suppression of restenosis in balloon-injured rat carotid artery by adenovirus-mediated gene transfer of the cell surface-directed plasmin inhibitor ATF.BPTI. *Gene Ther* 2001;8(7):534-41.
56. Lamfers ML, Grimbergen JM, Aalders MC, Havenga MJ, de Vries MR, Huisman LG, van Hinsbergh VW, Quax PH. Gene transfer of the urokinase-type plasminogen activator receptor-targeted matrix metalloproteinase inhibitor TIMP-1.ATF suppresses neointima formation more efficiently than tissue inhibitor of metalloproteinase-1. *Circ Res* 2002;91(10):945-52.
57. Eefting D, de Vries MR, Grimbergen JM, Karper JC, van Bockel JH, Quax PH. In vivo suppression of vein graft disease by nonviral, electroporation-mediated, gene transfer of tissue inhibitor

- of metalloproteinase-1 linked to the amino terminal fragment of urokinase (TIMP-1.ATF), a cell-surface directed matrix metalloproteinase inhibitor. *J Vasc Surg* 2010;51(2):429-37.
58. Eefting D, Seghers L, Grimbergen JM, de Vries MR, de Boer HC, Lardenoye JW, Jukema JW, van Bockel JH, Quax PH. A novel urokinase receptor-targeted inhibitor for plasmin and matrix metalloproteinases suppresses vein graft disease. *Cardiovasc Res* 2010.

Chapter 4

Annexin A5 Therapy Attenuates Vascular Inflammation and Remodeling and Improves Endothelial Function in Mice

M.M. Ewing^{1,2,3*}, M.R. de Vries^{2,3*}, M. Nordzell⁴, K. Pettersson⁴, H.C. de Boer^{3,5}, A.J. van Zonneveld^{3,5}, J. Frostegård^{6#}, J.W. Jukema^{1, 3#}, P.H.A. Quax^{2,3#}

1 Dept. of Cardiology, Leiden University Medical Center (LUMC), Leiden, The Netherlands

2 Dept. of Surgery, LUMC, Leiden, The Netherlands

3 Einthoven Laboratory for Experimental Vascular Medicine, LUMC, Leiden, The Netherlands

4 Athera Biotechnologies, Stockholm, Sweden

5 Dept. of Nephrology, LUMC, Leiden, The Netherlands

6 Dept. of Medicine, Karolinska University Hospital Huddinge and Karolinska Institutet, Stockholm, Sweden

* Both authors contributed equally

These authors share the senior authorship

Abstract

Objective Annexin A5 (AnxA5) has antithrombotic, anti-apoptotic and anti-inflammatory properties; we investigated its effectiveness against vascular inflammation, remodeling and dysfunction in accelerated atherosclerosis.

Methods and Results AnxA5 (1 mg/kg/d or vehicle) was investigated in vascular injury models in hypercholesterolemic ApoE3*Leiden mice. AnxA5 treatment reduced adhesion and infiltration of leucocytes by 71-69% ($p=0.015$, $p=0.031$) and macrophages by 51-87% ($p=0.014$, $p=0.018$), as well as MCP-1 and TNF- α expression in a femoral artery inflammation model (perivascular cuff for 3d), indicating reduced vascular inflammation. In a vein graft model, 28d AnxA5 treatment reduced vein graft thickening (48%, $p=0.006$) and leukocyte infiltration (46%, $p=0.003$). In these mice, reduced plasma concentrations of IFN γ (-72%, $p=0.040$), G-CSF (-41%, $p=0.010$) and MIP1 β (-66%, $p=0.020$) were measured, indicating reduced systemic inflammation. An in vitro endothelial cell model shows the importance of AnxA5's anticoagulant properties in reducing vascular inflammation.

Endothelium-mediated dilatation in hypercholesterolemic ApoE $^{-/-}$ mice was improved by 3d anxA5 treatment, shown by improved systolic and diastolic blood pressure reductions in response to metacholine, which could be abolished by L-NAME, indicating nitric oxide involvement.

Conclusions AnxA5 reduced local vascular and systemic inflammation, vascular remodeling and improved vascular function, indicating a therapeutic potential against atherosclerotic cardiovascular diseases.

Introduction

Accelerated atherosclerosis is one of the key features leading to vein graft failure next to acute thrombosis and occlusive vein graft thickening and is initiated by endothelial dysfunction, accompanied by an inflammatory activation of endothelial cells and smooth muscle cells (SMCs)^{1, 2}. This activation promotes adhesion of activated platelets and leukocytes and increases endothelial permeability, after which low-density lipoprotein (LDL) cholesterol accumulates in the vessel wall and is taken up by macrophages, which become foam cells^{3, 4}. Leukocytes produce pro-inflammatory cytokines such as monocyte chemoattractant protein (MCP)-1, tumor necrosis factor- α (TNF α) and interferon- γ (IFN γ). Leukocytes and cytokine expression are also observed in murine vein grafts^{3, 5}. IFN γ can activate macrophages and stimulate apoptosis, leading to plaque instability which can result in plaque disruption and thrombosis^{6, 7}.

Viable cells expose phosphatidylcholine and sphingomyelin on their outer cell membrane leaflet and express phosphatidylserine (PS) on their inner membrane leaflet. The annexins are a family of phospholipid-binding proteins and annexin A5 (AnxA5) binds to PS. AnxA5 was originally identified as an anticoagulant and antithrombotic protein⁸⁻¹¹, but is now known to have several other additional properties^{12, 13}. PS is highly polarised to the inner cell membrane in normal cells, but is externalized in the early phase of apoptosis and inflammatory cell activation. AnxA5 binds reversibly, specifically and with high affinity to these cells, as well as to aged erythrocytes, endothelial microparticles (EMP), activated platelets and oxidized (ox) LDL cholesterol, and is present in high concentrations in atherosclerotic plaques. The annexins are thought mainly to act on intracellular mechanisms, but AnxA5 also has extracellular functions¹³⁻¹⁶.

Plasma levels of AnxA5 are reported to be inversely related to the severity of coronary stenosis and are an indication of the extent of atherosclerotic plaques¹⁷, to be elevated in hypertensives with systolic dysfunction¹⁸ and following acute myocardial infarction¹⁹. AnxA5 also has anti-inflammatory effects, e.g. by association with the IFN γ receptor and prevention of inflammatory cellular responses to secreted IFN γ . Atherosclerosis is associated with a reduced capacity of the endothelium to produce vasodilating substances upon stimulation, such as nitric oxide (NO). A reduction in endothelium-mediated dilatation (EMD) is a risk factor for premature cardiovascular disease and is associated with increased atherosclerosis development²⁰. Binding of AnxA5 to PS may prevent PS-mediated platelet and leukocyte adhesion and affect the level of systemic inflammation and circulating cytokines, resulting in improved local and systemic endothelial function.

The binding to oxLDL cholesterol, to apoptotic cells and the potential inhibitory effect on inflammation in combination with its antithrombotic effects make AnxA5 a promising therapeutic agent against atherosclerosis. By using three mouse models for accelerated atherosclerosis development that share a common basis of endothelial cell activation, followed by local vascular wall inflammation, eventually leading to vascular remodeling, the aim of the present study was to investigate if AnxA5 is therapeutically effective against vascular dysfunction, inflammation and remodeling, all of which are important hallmarks of cardiovascular disease.

Materials and Methods

We performed an *in vivo* intervention study in which Western-type diet fed ApoE3*Leiden mice were injected intraperitoneally daily with 1 mg/kg AnxA5 or vehicle only and underwent femoral arterial cuff placement or vein graft surgery. In these vascular segments, inflammatory cell adhesion, infiltration, intimal thickening and lesion composition were assessed using histology, morphometry, and immunohistochemistry. Plasma AnxA5 and cytokine concentrations were determined using ELISA and a multiplex biometric immunoassay. For *in vitro* studies, TNF α -activated HUVEC, incubated with and without AnxA5, underwent whole blood perfusion, allowing assessment of platelet adhesion, aggregation and leukocyte adherence. Western-type diet fed ApoE $^{-/-}$ mice, receiving 3d AnxA5 treatment or vehicle only, were used for endothelial function assessment, performed by stimulating vasodilatation and aortic blood pressure measurements. All materials and methods are detailed in the supplement (available online at <http://atvb.ahajournals.org>).

Results

Annexin A5 effects

AnxA5 treatment did not affect body weight, total plasma cholesterol or triglyceride concentrations. In the ApoE $^{-/-}$ mice, human AnxA5 plasma concentration, measured with ELISA, was 35.3 ± 1.5 ng/ml 1h after 1mg/kg injection and fell to 3.2 ± 1.1 ng/ml 6h after injection, which is within the normal range in man (see online figures for plasma concentrations). In mice receiving AnxA5 no bleeding complications occurred and there was one case of vein graft thrombosis (in n=10 mice) leading to loss of graft patency after 28d, compared to three cases of graft thrombosis in mice receiving vehicle only (n=10), this was statistically not significantly different (vehicle: 3/10 cases, annexin A5: 1/10 cases, $p=0.582$).

Annexin A5 has systemic anti-inflammatory effects

To monitor effects of AnxA5 on systemic inflammation, plasma concentration of a set of cytokines and chemokines were defined before surgery, 3d after cuff placement and 28d after vein graft surgery, respectively, using a multiplex BioRad Luminex analysis. Before surgery, no statistical differences were observed. After 3d, plasma concentrations of inflammatory cytokines were increased in all groups due to the inflammatory response evoked by cuff placement. However, at 28d after vein graft surgery AnxA5 treatment significantly reduced the plasma concentration of G-CSF by 40.8% ($p=0.010$), of IFN γ by 72.2% ($p=0.040$) and of MIP-1 β /CCL4 by 66.1% ($p=0.020$), when compared to vehicle. In addition, AnxA5 treatment gave a trend towards reduction of the plasma levels of the cytokines IL-12 (p40) ($p=0.120$) and MIP-1 α /CCL3 ($p=0.160$), shown in table 1. The total dataset is represented in table 1 in the online data supplement.

Annexin A5 reduces inflammatory cell recruitment after vascular injury

AnxA5 treatment reduced the percentage of femoral arterial endothelial adhesion of leukocytes by 71.3% (vehicle: $34.2 \pm 3.0\%$, AnxA5: $9.7 \pm 8.9\%$ of the sum of endothe

	Vehicle	Annexin A5
Cell type surface (% area)		
Macrophages	35.6±7.7%	32.5±7.4%
Smooth muscle cells	23.0±4.0%	28.4±3.6%
Collagen	35.8±5.5%	45.7±5.0%
Number of cells		
Leukocytes	53.1±6.1	28.8±2.3*
Apoptotic cells	6.2±2.2	4.3±0.8
Plasma cytokine concentration (pg/ml)		
Interferon γ	7.9±2.5	2.2±0.7*
G-CSF	14.2±2.6	8.4±1.0*
MIP-1 β /CCL4	22.1±10.3	7.5±0.9*

Table 1. Percentage of cell type area out of total vein graft wall area, total cell numbers per vein graft wall cross-section and plasma cytokine concentration (pg/ml) in ApoE3*Leiden mice 28d after surgery and vehicle only or AnxA5 treatment (mean±SEM, n=10).

lial and intimal cells, $p=0.015$) and of macrophages by 51.4% (vehicle: 24.5±3.5%, AnxA5: 11.9±2.3%, $p=0.014$) after 3d compared to controls. Furthermore, within the media the percentage of leukocytes out of all cells in the media was reduced by 69.0% (vehicle: 19.6±4.6%, AnxA5: 6.1±2.6%, $p=0.031$) and that of macrophages by 87.3% (vehicle: 14.2±5.5%, AnxA5: 1.8±0.9% $p=0.018$). At this time point foam cells, recognisable by positive macrophage staining, intracellular lipid deposition and cell swelling, could not be detected.

Although plasma levels of MCP-1 and TNF α were not affected by AnxA5 treatment in the femoral artery cuff experiment, the arteries were stained for cells expressing MCP-1 and TNF α to investigate if AnxA5 reduced local vascular inflammation. It was found that AnxA5 treatment reduced the percentage of adherent and endothelial cells expressing MCP-1 by 31.0% (vehicle: 49.1±2.2%, AnxA5: 33.9±3.1%, $p=0.003$) and that of TNF α by 42.7% (vehicle: 39.6±8.0%, AnxA5: 22.7±2.2%, $p=0.049$) after 3d. Additionally, the percentage of cells in the media expressing MCP-1 dropped by 52.7% (vehicle: 31.1±1.8%, AnxA5: 14.7±2.8%, $p=0.001$), although no relative difference was observed for medial cells expressing TNF α (vehicle: 21.2±6.2%, AnxA5: 12.9±2.9%, $p=0.335$) at this time point. The data, including photomicrographs, is shown in figure 1. A complete overview of all data is shown in table 2 of the online data supplement.

Annexin A5 reduces vascular remodeling and preserves vein graft patency

To investigate the therapeutic effectiveness of AnxA5 against vascular remodeling, vein graft thickening, measured as the area between the lumen and adventitia in cross-sections, was quantified after 28d. This revealed that AnxA5 significantly reduced vein graft thickening by 48.0% (vehicle: 0.25±0.05mm², AnxA5: 0.13±0.01mm², $p=0.006$), thus preserving graft patency, shown in figure 2. Although in the controls AnxA5 could be detected by immunohistochemistry, the staining in the vessel wall of the mice injected with human AnxA5 was much more intense. This suggests accumulation of human AnxA5 in the vein graft wall, although one should be careful with

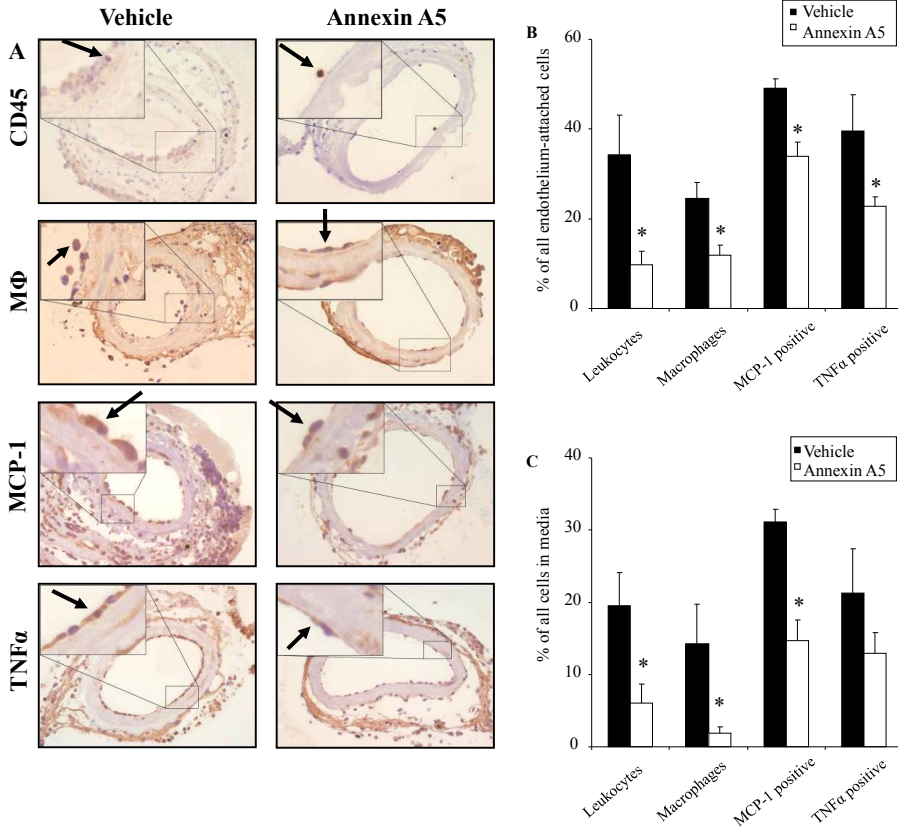


Figure 1. Panel A: representative cross-sections of cuffed-femoral arteries of ApoE3*Leiden mice treated with vehicle or AnxA5, 3d after cuff placement (leukocyte, macrophage, MCP-1 and TNF α staining, magnification 400x, arrows in inserts indicate positive staining). Panels B and C: quantification of cell types in cuffed femoral arteries attaching to the endothelium (panel B) or within the media (panel C), expressed as the percentage of all cells adhering to the endothelium or in the media, in vehicle and AnxA5 treated mice (mean \pm SEM, n=10).

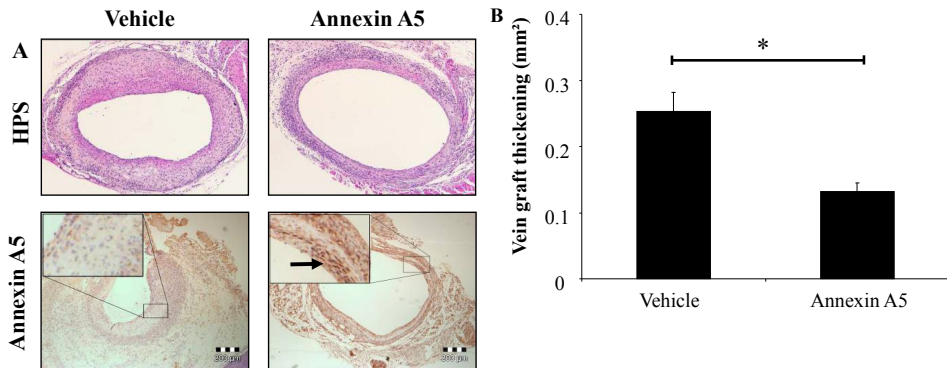


Figure 2. Effect of AnxA5 treatment on vein graft thickening in ApoE3*Leiden mice treated with vehicle or AnxA5, 28d after surgery. Panel A: representative cross-sections of vein grafts, (HPS and AnxA5 staining, magnification 80x, arrows in insert indicates positive staining). Panel B: quantification of vein graft thickening, expressed as mm² thickening in vehicle and AnxA5 treated mice (mean \pm SEM, n=10).

quantification of this immunohistochemistry data.

In order to identify if AnxA5 therapy altered atherosclerotic plaque composition, the presence of several important cell types and extracellular matrix was quantified, shown in table 1. AnxA5 treatment reduced the number of leukocytes in the vein graft wall per cross-section by 46% (vehicle: 53.1 ± 6.1 cells, AnxA5: 28.8 ± 2.3 cells, $p=0.003$). However, despite reduced wall thickening, there was no difference observed in contribution of cell types and collagen to the build-up of the vessel wall, observed in macrophage area (from total wall area) (vehicle: $35.6 \pm 7.7\%$, AnxA5: $32.5 \pm 7.4\%$, $p=0.723$), SMC area (vehicle: $23.0 \pm 4.0\%$, AnxA5: $28.4 \pm 3.6\%$, $p=0.289$) or collagen area (vehicle: $35.8 \pm 5.5\%$, AnxA5: $45.7 \pm 5.0\%$, $p=0.289$) between mice receiving daily AnxA5 or vehicle.

In order to evaluate the therapeutic effects of AnxA5 on plaque stability, apoptotic cell numbers and signs of plaque disruptions, characteristic for vein grafts, were quantified. AnxA5 treatment did not affect vein graft apoptotic cells numbers per cross-section (vehicle: 6.2 ± 2.2 cells, AnxA5: 4.3 ± 0.8 cells, $p=0.796$) after 28d, shown in table 1. Analysis of plaque morphology revealed the presence of disruption features and it was found that AnxA5 therapy did reduce the number, length and severity of endothelial erosions with fibrinogen lining the vessel wall (vehicle: 3/6 cases, AnxA5: 2/9 cases) and therefore characteristically distinct from post-mortem artifacts, leaky vessel formation with intramural erythrocytes (vehicle: 3/6 cases, AnxA5: 0/9 cases) and of severe plaque disruptions with erythrocytes and thrombi in a subendothelial space (vehicle: 1/6 cases, AnxA5: 0/9 cases), shown in figure 3. Although no firm conclusions about the possible protective functions of AnxA5 on plaque stability can be drawn from these observations, the reported features are important to the plaque and vessel wall morphology and are known to be associated with increased plaque instability in human (coronary) atherosclerotic lesions.

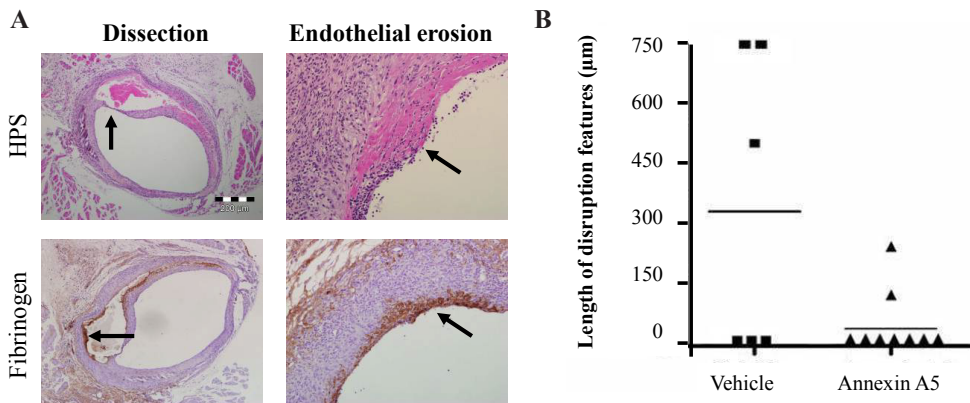


Figure 3. Panel A: representative cross-sections of spontaneous plaque disruption features in vein grafts of ApoE3*Leiden mice after 28d (HPS and fibrinogen staining, magnification 80x, arrows in inserts indicate features). Panel B: quantification of length (in μm) and number of plaque instability features (total of endothelial erosions, leaky vessel formation and plaque disruptions) in vehicle and AnxA5 treated mice (mean \pm SEM, n=10).

Annexin A5 reduced endothelial-platelet and leukocyte-endothelial adhesion

To investigate how AnxA5 led to a reduction of endothelial-leukocyte adhesion in injured vascular segments, human umbilical vein endothelial cells (HUVEC) were

stimulated with TNF α for 4h to induce endothelial cell activation in the presence and absence of AnxA5. AnxA5 (0.75 μ g/mL) was added to HUVEC during TNF α -stimulation (4 hrs) and added to the whole blood prior (5 min) and during the perfusion. AnxA5 inhibited leukocyte adhesion by 58.8% (TNF α only: 47.8 \pm 16.5 leukocytes / microscopic field, TNF α + AnxA5: 19.7 \pm 11.4 leukocytes / microscopic field, n=25 frames, p<0.001) and platelet adhesion area by 48.6% (TNF α only: 21.7 \pm 7.8% coverage, TNF α + AnxA5: 11.1 \pm 6.6% coverage, n=25 frames, p<0.001), shown in figure 4.

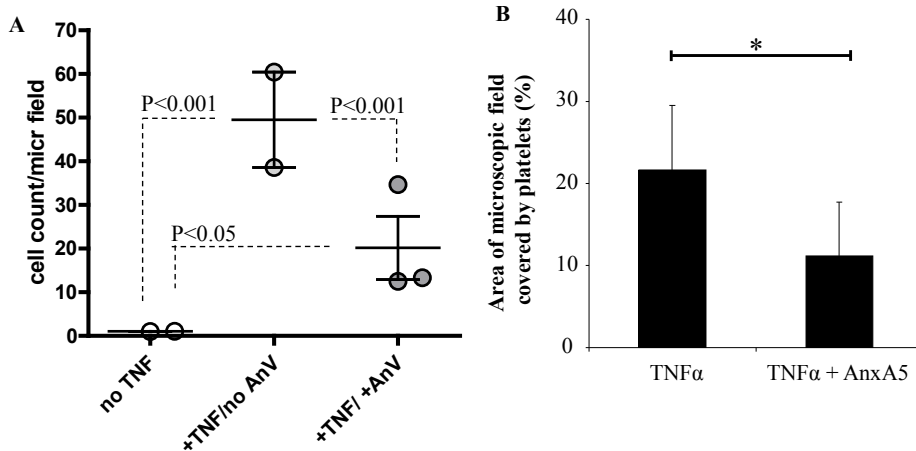


Figure 4. Whole blood was perfused over non-stimulated HUVEC or over TNF α -stimulated HUVEC in the presence of AnxA5 (0.75 μ g/mL) with LMWH-anticoagulated whole blood for 10 minutes at 1 dyne/cm². After each perfusion, 25 images were made to quantify adhered leukocytes per microscopic field (Panel A). Panel B: in the presence of AnxA5, less platelet-adherence (area of microscopic field covered) aggregation are observed.

Non-stimulated HUVEC hardly supported adhesion of platelets and leukocytes, indicating that TNF α -induced tissue factor- and PS-expression was necessary for binding under flow of both platelets and leukocytes.

Annexin A5 improves endothelial function

To test the effect of AnxA5 on vascular function, endothelial dysfunction was induced by feeding ApoE^{-/-} mice a Western-type diet for 16 to 17 weeks and was quantified by measuring the reduction of metacholine-induced NO-mediated vasodilatation. After this period, mice were given IP injections with 1mg/kg AnxA5 once daily for 3d. Mice were then anaesthetized and blood pressure measurements began. There were no differences in heart rate and systolic or diastolic blood pressure between groups receiving vehicle or AnxA5 at baseline.

In normal, non-atherosclerotic mice, 3 μ g/kg of metacholine lead to a transient reduction in blood pressure, the response was maximal after 1-3min and then returned towards baseline after approximately 5min. This effect was blunted in ApoE^{-/-} mice on a Western-type diet. However, AnxA5 treatment restored EMD, leading to a larger systolic blood pressure reduction (vehicle: -5.0mmHg, AnxA5: -22.3mmHg, p=0.027) and diastolic blood pressure reduction (vehicle: -0.8mmHg, AnxA5: -11.0mmHg, p=0.029) in the treated animals, shown in figure 5.

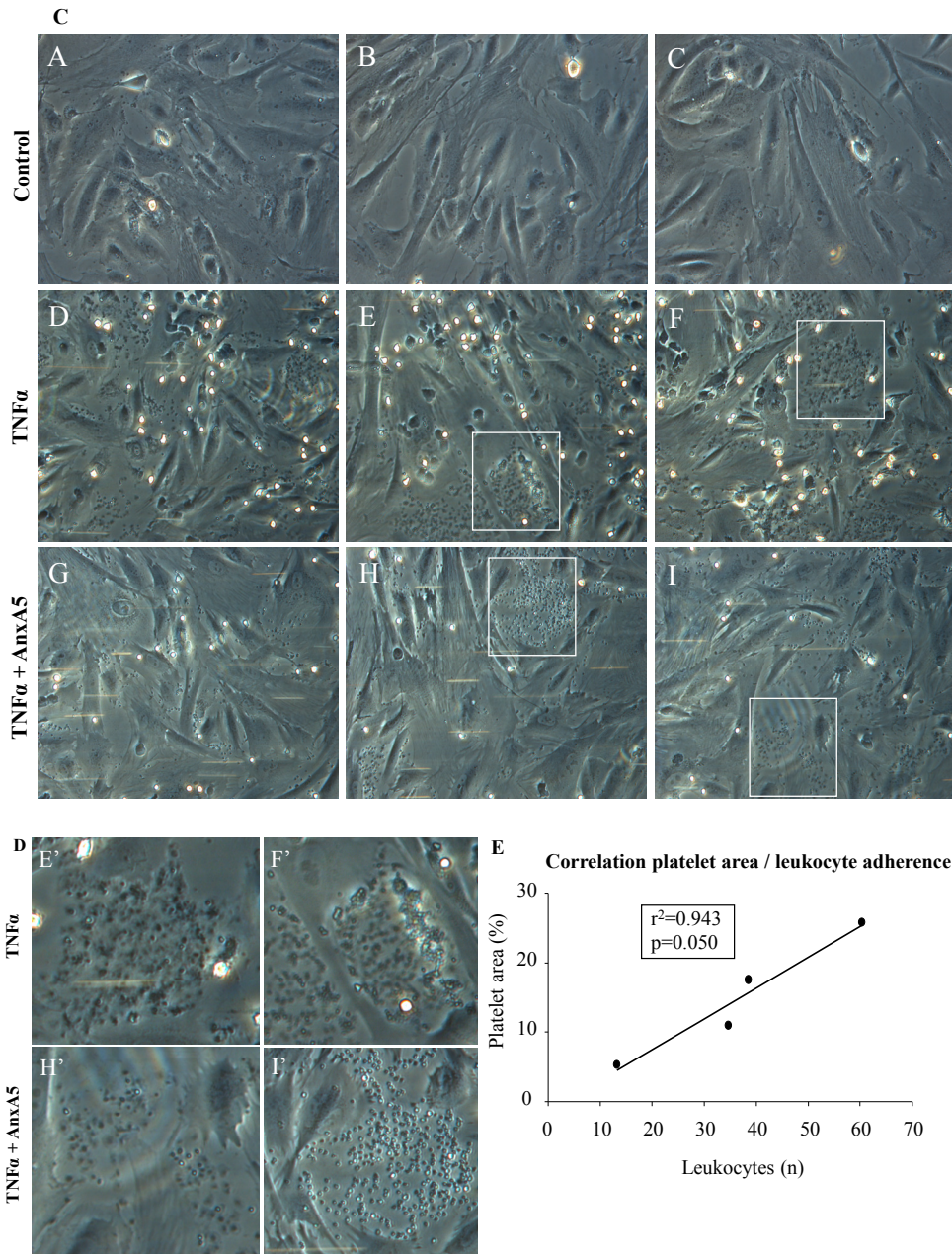


Figure 4. Whole blood was perfused over non-stimulated HUVEC or over TNF α -stimulated HUVEC in the presence of AnxA5 (0.75 μ g/mL) with LMWH-anticoagulated whole blood for 10 minutes at 1 dyne/cm 2 . Panel C: three representative micrographs are shown of cell-adhesion to non-stimulated HUVEC (A, B and C), TNF α -stimulated HUVEC (D, E and F) and TNF α and AnxA5-stimulated HUVEC. The rectangles in panels E, F, H and I are magnified (panel D) and quantified (panel B) to show that platelet morphology is changed after AnxA5 treatment. Panel E: significant correlation exists between area of platelet adherence and leukocyte binding (all conditions, n=4, $r^2=0.943$, $p=0.050$).

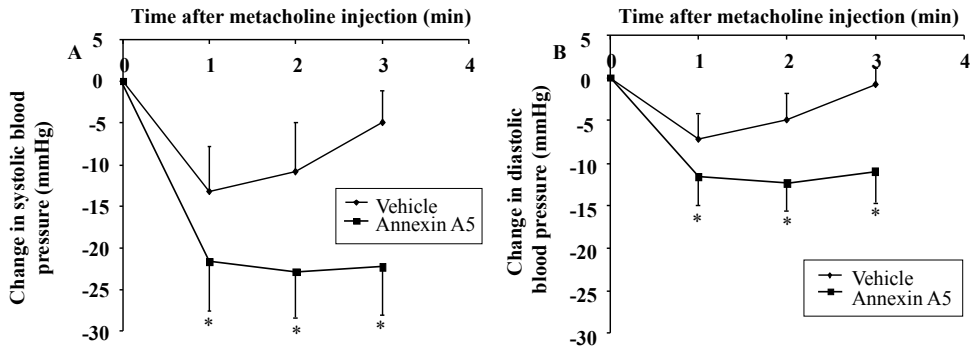


Figure 5. Effect of 3d AnxA5 treatment on impaired endothelial function in ApoE^{-/-} mice, quantified as change in aortic systolic (panel A) and diastolic (panel B) blood pressure (mmHg) in time after IP injection of metacholine to induce vasodilatation (mean±SEM, n=10).

Blood pressures are reported in table 3 in the online data supplement. The reduction in systolic pressure was the largest, thus pulse pressure was reduced during EMD. Metacholine injection did not lead to changes in heart rate (vehicle: -1.5 beats per minute (bpm), AnxA5: -8.5bpm, $p=0.379$).

Injection of 50mg/kg L-NAME resulted in similar increases in systolic (vehicle: +27.6mmHg, AnxA5: +29.7mmHg, $p=0.518$) and diastolic (vehicle: +15.6mmHg, AnxA5: +18.0mmHg, $p=0.350$) blood pressure in both groups, accompanied by an equal reduction in heart rate (vehicle: -40.0bpm, AnxA5: -37.8bpm, $p=0.833$). Subsequent IP injection of metacholine following L-NAME injection did not result in a significant change in heart rate (vehicle: -17.9bpm, AnxA5: -21.0bpm, $p=0.559$) or systolic (vehicle: -5.1mmHg, AnxA5: +1.0mmHg, $p=0.060$) and diastolic (vehicle: -1.3mmHg, AnxA5: +2.2mmHg, $p=0.071$) blood pressure in either group (online supplements, table 2), indicating that AnxA5 could affect vascular function through improved NO-signaling.

Discussion

Our study shows a therapeutic role for AnxA5 against vascular inflammation, remodeling and dysfunction, in mouse models for accelerated atherosclerosis development. It was demonstrated that injection of human AnxA5 had no adverse effects, resulted in a marked reduction in circulating plasma concentrations of IFN γ , G-CSF and MIP-1 β /CCL4, early inflammatory cell recruitment, adhesion and infiltration in the vessel wall after vascular injury, eventually leading to decreased vein graft thickening with less plaque instability features. Furthermore, AnxA5 improved endothelial dysfunction by acting on NO-signaling. This study extends the role of AnxA5 as a regulator of inflammatory processes, and demonstrates its potential therapeutic use in inflammation-associated vascular disease in addition to its known functions in anticoagulation and its use as a marker of apoptosis.

Although these data can be of clinical significance and could potentially lead to new therapeutic strategies, at this point we do not have the complete insight in the underlying mechanism of how AnxA5 affects vessel wall pathology. It was previously

shown that AnxA5 could affect immune reactions on a systemic level. The injection of PS-exposing cells induced a delayed-type hypersensitivity reaction, which was critically affected by AnxA5²¹. This suggested that the PS receptor can act as a switch for immune reactions and AnxA5 will interfere with this function²². In vitro investigation using TNF α -stimulated HUVEC clearly indicated the importance of the anti-coagulant effects of AnxA5 in its ability to reduce leukocyte adhesion to activated endothelium, since platelet adherence is known to be essential for subsequent leukocyte adhesion.

A multiplex analysis of plasma cytokine levels revealed that the raise in levels of circulating cytokines observed 3d after femoral cuff implantation was not affected by AnxA5. However, prolonged exposure to AnxA5 reduced plasma levels of G-CSF, MIP-1 β /CCL4 and IFN γ and certainly did have a systemic immunomodulatory effect. IFN γ production by inflammatory cells leads to improved antigen presentation and increases atherogenesis. In ApoE^{-/-} mice lacking IFN γ or its receptor, atherogenesis was inhibited^{3, 23}. In vitro research has shown that AnxA5 can prevent cellular responses to secreted IFN γ and these data suggest that AnxA5 influences the IFN γ production by circulating cells involved in the early inflammatory processes during atherosclerotic lesion formation and vascular remodeling³⁻⁵.

Leukocyte, and specifically monocyte, adhesion, differentiation and activation is a key component in the onset and progression of atherosclerosis and post-interventional accelerated atherosclerosis³. To investigate effects of AnxA5 on local vascular inflammation, the ApoE3*Leiden femoral artery cuff model²⁴, characterized by inflammatory cell adhesion and infiltration in the vessel wall early after surgery, was used. Not only did AnxA5 reduce endothelial-adhesion and medial infiltration of both leukocytes and macrophages, it was also found that early local expression of the key inflammatory cytokines MCP-1 and TNF α was reduced^{25, 26}. However, this local reduction of MCP-1 and TNF α levels was not reflected by an alteration of plasma levels after 3d, nor after prolonged AnxA5 exposure. Taken together, these findings suggest that AnxA5 can be used therapeutically to reduce local inflammatory responses after vascular injury. The exact mechanism by which AnxA5 led to these effects was not elucidated, but it has been shown that this is probably due to local AnxA5 binding to activated cells. AnxA5 reduces local adherence of platelets, especially their activation and subsequently adherence of leukocytes (figure 4), ultimately preventing their deleterious inflammatory effects.

To investigate if the reduced early vascular inflammation by AnxA5 could be extended to a beneficial clinical therapeutic effect on accelerated atherosclerosis in general, AnxA5 was studied additionally in an model for vein graft pathology²⁷. Here, accelerated atherosclerosis forms due to vascular damage, endothelial cell loss and a pulsatile arterial pressure, similarly to human venous bypass graft disease in which rapid foam cells formation, intimal thickening, apoptotic cell exposure and plaque instability features are observed, processes that lead to loss of graft patency. AnxA5 treatment significantly reduced vein graft thickening after 28d by 48%, as well as leukocyte infiltration in the vein graft wall by 46%. Although AnxA5 did not alter plaque content, it nonetheless preserved graft patency greatly.

Complications of atherosclerosis are either the result of reduced blood flow due to luminal narrowing or from acute vessel occlusion due to rupture of the atherosclerotic plaque. Apoptosis is associated with decreased plaque stability and although AnxA5

can affect apoptosis¹³, no differences in apoptotic cell numbers detected with TUNEL staining were observed at 28d after surgery. Since apoptosis is known to occur predominantly within 14d after surgery in this model²⁸, effects on apoptosis by AnxA5 on earlier time points cannot be ruled out. Despite no change in apoptotic cells numbers after 28d by AnxA5 treatment, it did reduce vessel plaque instability features such as endothelial erosion, leaky vessel formation and severe plaque disruption in addition to vessel wall thickening, indicating that AnxA5 treatment is effective against both vascular inflammation and (the complications of) vascular remodeling.

Improvement of endothelial function is an important therapeutic goal in vascular diseases. In our study, short-term AnxA5 treatment improved EMD in response to metacholine injection to induce vasodilatation, displayed by a larger and longer-lasting reduction of systolic and diastolic blood pressure in ApoE^{-/-} mice with impaired endothelial function. This larger blood pressure reduction was blunted by L-NAME administration prior to the metacholine injection, indicating this effect was mediated via NO. Since this is important for the central arterial compartment compliance²⁹, a large reduction of systolic blood pressure after AnxA5 treatment is suggestive for a positive effect on the endothelium in conduit arteries, often early affected by native atherosclerosis in humans^{3, 4}. Both acute and chronic inflammation is known to hamper EMD, so the effects of AnxA5 on endothelial function could be a result of a reduced inflammatory burden (figures 1 and 2), but also from other mechanisms. For example, endothelial cells can release EMP which in turn can trigger endothelial cytokine release and leukocyte adhesion. AnxA5 can shield EMP through PS-binding and prevent their endothelial cell activation. Thus, although effectiveness was shown, the exact mechanism by which AnxA5 improved deteriorated endothelial function *in vivo* is not yet clear and awaits further research.

In normal humans, plasma AnxA5 concentration is normally well below 10 ng/ml, and is elevated in certain diseases¹⁷⁻¹⁹. In our experiments, 1mg AnxA5/kg/d only transiently elevated plasma AnxA5 above these levels (figure 1 online supplement). In spite of this, profound treatment effects were observed. This is probably explained by a rapid and strong binding to its target tissue, acting long after free AnxA5 is cleared from plasma. Clearance of AnxA5 is much slower from tissue compartments than from plasma, which is why it is useful as an apoptosis marker *in vivo*³⁰.

AnxA5 is already used safely in patients as a diagnostic tool for atherosclerosis¹⁴. Since the present study shows pronounced anti-inflammatory and anti-atherogenic effects of AnxA5 *in vivo* on accelerated atherosclerosis associated with post-interventional vascular remodeling and vein graft disease, as well as atherosclerosis-associated vascular dysfunction, it also indicates a possible therapeutic role for AnxA5 in the prevention of accelerated atherosclerosis after vascular surgery and coronary interventions.

Reference List

1. Schepers A, de Vries MR, van Leuven CJ, Grimbergen JM, Holers VM, Daha MR, van Bockel JH, Quax PH. Inhibition of complement component C3 reduces vein graft atherosclerosis in apolipoprotein E3-Leiden transgenic mice. *Circulation* 2006;114:2831-2838.
2. Motwani JG, Topol EJ. Aortocoronary saphenous vein graft disease: pathogenesis, predisposition, and prevention. *Circulation* 1998;97:916-931.
3. Hansson GK. Inflammation, atherosclerosis, and coronary artery disease. *N Engl J Med* 2005;352:1685-1695.
4. Ross R. Atherosclerosis--an inflammatory disease. *N Engl J Med* 1999;340:115-126.
5. Leon C, Nandan D, Lopez M, Moeenrezakhanlou A, Reiner NE. Annexin V associates with the IFN-gamma receptor and regulates IFN-gamma signaling. *J Immunol* 2006;176:5934-5942.
6. Yan ZQ, Hansson GK. Innate immunity, macrophage activation, and atherosclerosis. *Immunol Rev* 2007;219:187-203.
7. Virmani R, Kolodgie FD, Burke AP, Farb A, Schwartz SM. Lessons from sudden coronary death: a comprehensive morphological classification scheme for atherosclerotic lesions. *Arterioscler Thromb Vasc Biol* 2000;20:1262-1275.
8. Andree HA, Stuart MC, Hermens WT, Reutelingsperger CP, Hemker HC, Frederik PM, Willems GM. Clustering of lipid-bound annexin V may explain its anticoagulant effect. *J Biol Chem* 1992;267:17907-17912.
9. Chen HH, Vicente CP, He L, Tollefsen DM, Wun TC. Fusion proteins comprising annexin V and Kunitz protease inhibitors are highly potent thrombogenic site-directed anticoagulants. *Blood* 2005;105:3902-3909.
10. Thiagarajan P, Benedict CR. Inhibition of arterial thrombosis by recombinant annexin V in a rabbit carotid artery injury model. *Circulation* 1997;96:2339-2347.
11. van Heerde WL, Sakariassen KS, Hemker HC, Sixma JJ, Reutelingsperger CP, De Groot PG. Annexin V inhibits the procoagulant activity of matrices of TNF-stimulated endothelium under blood flow conditions. *Arterioscler Thromb* 1994;14:824-830.
12. Kenis H, Hofstra L, Reutelingsperger CP. Annexin A5: shifting from a diagnostic towards a therapeutic realm. *Cell Mol Life Sci* 2007;64:2859-2862.
13. van Genderen HO, Kenis H, Hofstra L, Narula J, Reutelingsperger CP. Extracellular annexin A5: functions of phosphatidylserine-binding and two-dimensional crystallization. *Biochim Biophys Acta* 2008;1783:953-963.
14. Boersma HH, Kietselaer BL, Stolk LM, Bennaghmouch A, Hofstra L, Narula J, Heidendal GA, Reutelingsperger CP. Past, present, and future of annexin A5: from protein discovery to clinical applications. *J Nucl Med* 2005;46:2035-2050.
15. Leroyer AS, Tedgui A, Boulanger CM. Role of microparticles in atherothrombosis. *J Intern Med* 2008;263:528-537.
16. Cederholm A, Frostegard J. Annexin A5 as a novel player in prevention of atherothrombosis in SLE and in the general population. *Ann N Y Acad Sci* 2007;1108:96-103.
17. van Tits LJ, van Heerde WL, van der Vleuten GM, de Graaf J, Grobbee DE, van de Vijver LP, Stalenhoef AF, Princen HM. Plasma annexin A5 level relates inversely to the severity of coronary stenosis. *Biochem Biophys Res Commun* 2007 ;356:674-680.
18. Ravassa S, Gonzalez A, Lopez B, Beaumont J, Querejeta R, Larman M, Diez J. Upregulation of myocardial Annexin A5 in hypertensive heart disease: association with systolic dysfunction. *Eur Heart J* 2007;28:2785-2791.
19. Peetz D, Hafner G, Blankenberg S, Peivandi AA, Schweigert R, Brunner K, Dahm M, Rupprecht HJ, Mockel M. Annexin V does not represent a diagnostic alternative to myoglobin for early detection of myocardial infarction. *Clin Lab* 2002;48:517-523.
20. Landmesser U, Hornig B, Drexler H. Endothelial function: a critical determinant in atherosclerosis? *Circulation* 2004;109(21 Suppl 1):II27-II33.
21. Frey B, Munoz LE, Pausch F, Sieber R, Franz S, Brachvogel B, Poschl E, Schneider H, Rodel F, Sauer R, Fietkau R, Herrmann M, Gaipal US. The immune reaction against allogeneic necrotic cells is reduced in Annexin A5 knock out mice whose macrophages display an anti-inflammatory phenotype. *J Cell Mol Med* 2009;13:1391-1399.
22. Henson PM, Bratton DL, Fadok VA. The phosphatidylserine receptor: a crucial molecular switch? *Nat Rev Mol Cell Biol* 2001;2:627-633.
23. Whitman SC, Ravisankar P, Daugherty A. IFN-gamma deficiency exerts gender-specific effects

- on atherogenesis in apolipoprotein E^{-/-} mice. *J Interferon Cytokine Res* 2002;22:661-670.
24. Lardenoye JH, Delsing DJ, de Vries MR, Deckers MM, Princen HM, Havekes LM, van Hinsbergh VW, van Bockel JH, Quax PH. Accelerated atherosclerosis by placement of a perivascular cuff and a cholesterol-rich diet in ApoE^{*3}Leiden transgenic mice. *Circ Res* 2000;7:248-53.
 25. Monraats PS, Pires NM, Schepers A, Agema WR, Boesten LS, de Vries MR, Zwinderman AH, de Maat MP, Doevendans PA, de Winter RJ, Tio RA, Waltenberger J, 't Hart LM, Frants RR, Quax PH, van Vlijmen BJ, Havekes LM, van der LA, van der Wall EE, Jukema JW. Tumor necrosis factor-alpha plays an important role in restenosis development. *FASEB J* 2005;19:1998-2004.
 26. Schepers A, Eefting D, Bonta PI, Grimbergen JM, de Vries MR, van W, V, de Vries CJ, Egashira K, van Bockel JH, Quax PH. Anti-MCP-1 gene therapy inhibits vascular smooth muscle cells proliferation and attenuates vein graft thickening both in vitro and in vivo. *Arterioscler Thromb Vasc Biol* 2006;26:2063-2069.
 27. Heeneman S, Lutgens E, Schapira KB, Daemen MJ, Biessen EA. Control of atherosclerotic plaque vulnerability: insights from transgenic mice. *Front Biosci* 2008;13:6289-6313.
 28. Lardenoye JH, de Vries MR, Grimbergen JM, Havekes LM, Knaapen MW, Kockx MM, van Hinsbergh VW, van Bockel JH, Quax PH. Inhibition of accelerated atherosclerosis in vein grafts by placement of external stent in apoE^{*3}-Leiden transgenic mice. *Arterioscler Thromb Vasc Biol* 2002 22:1433-1438.
 29. Sugawara J, Komine H, Hayashi K, Yoshizawa M, Yokoi T, Otsuki T, Shimojo N, Miyauchi T, Maeda S, Tanaka H. Effect of systemic nitric oxide synthase inhibition on arterial stiffness in humans. *Hypertens Res* 2007;30:411-415.
 30. Kemerink GJ, Liu X, Kieffer D, Ceyskens S, Mortelmans L, Verbruggen AM, Steinmetz ND, Vanderheyden JL, Green AM, Verbeke K. Safety, biodistribution, and dosimetry of 99mTc-HYNIC-annexin V, a novel human recombinant annexin V for human application. *J Nucl Med* 2003;44:947-952.

Supplement Material

Mice

All experiments were approved by the Institutional Committees for Animal Welfare. Transgenic male ApoE*3-Leiden mice (bred in our own laboratory), backcrossed for more than 20 generations on a C57BL/6J background and male ApoE^{-/-} mice (Taconics, Lille Skensved, Denmark), aged 10-12 weeks at the start of a dietary run-in period, were used for this experiment.

Diets

Transgenic male ApoE*3-Leiden mice were fed a Western-type diet containing 1% cholesterol and 0.05% cholate to induce hypercholesterolemia (AB Diets, Woerden, The Netherlands). The diet was given three weeks prior to surgery and was continued throughout the experiment. Male ApoE^{-/-} mice, 8-10 weeks old, received a Western-type diet (Harlan Teklad TD.88137) for 16-17 weeks to induce endothelial dysfunction. All animals received food and water ad libitum during the entire experiment.

Femoral artery cuff mouse model

To investigate the effect of annexin A5 on vascular inflammation, ApoE*3-Leiden mice underwent femoral arterial cuff placement¹ after three weeks of diet to induce vascular inflammation. Mice were anesthetized before surgery with a combination of intraperitoneally (IP) injected Midazolam (5mg/kg, Roche, Woerden, The Netherlands), Medetomidine (0.5mg/kg, Orion, Espoo, Finland) and Fentanyl (0.05mg/kg, Janssen, Berchem, Belgium). The right femoral artery was isolated and sheathed with a rigid non-constrictive polyethylene cuff (Portex, Kent, UK, 0.40mm inner diameter, 0.80mm outer diameter and an approximate length of 2.0mm). 3d after cuff placement, mice were anesthetized as before and euthanized.

The thorax was opened and mild pressure-perfusion (100mm Hg) with 3.7% formaldehyde in water (w/v) was performed for 5min by cardiac puncture in the left ventricle. After perfusion, the cuffed femoral artery was harvested, fixed overnight in 3.7% formaldehyde in water (w/v) and paraffin-embedded. Serial cross-sections (5µm thick) were taken from the entire length of the artery for analysis.

Mice received daily IP injections with 1mg/kg human recombinant annexin A5 (Bender Medsystems cat.no. BMS306/50mg. lot no.24926000) in a volume of 150µl, using 150µl 0.9% w/v NaCl (vehicle), injected IP daily as control.

Carotid vein graft model for accelerated atherosclerosis

To study the effect of annexin A5 on vascular remodeling, vein graft surgery² was done in ApoE*3-Leiden mice after three weeks of diet and performed by one surgeon, to exclude the possibility of inter-group variation due to different surgical skills. Mice were anesthetized and the right common carotid artery was dissected free from its surroundings from the bifurcation at the distal end towards the proximal end. The vessel was ligated twice with an 8.0 silk ligature and dissected between the middle ties. A cuff was placed over both ends after which these were everted over the cuffs and ligated with an 8.0 silk ligature. Littermates were used as donor for the inferior caval vein. The carefully harvested inferior caval vein was temporarily preserved in a

0.9% NaCl solution, containing 100U/ml of heparin and was interpositioned between the ends of the artery. The connections were ligated together with an 8.0 silk suture. Pulsations confirmed successful engraftment. Mice were sacrificed 28d after vein grafting as described before. Daily annexin A5 and vehicle treatments were as described above. Blood samples were taken from the tail vein for plasma annexin A5 analysis at 1, 3 and 6h after administration.

Biochemical analysis

Total plasma cholesterol (Boehringer Mannheim GmbH, kit 236691) and triglyceride (Sigma Diagnostics, kit 337-B) concentrations were measured enzymatically.

Annexin A5 plasma concentration was determined using a human annexin A5 ELISA kit (Bender MedSystems Products, Vienna, Austria).

To investigate effects of annexin A5 on systemic inflammation, a multiplex biometric immunoassay was used for cytokine and chemokine measurements according to the manufacturer's instructions (Bio-Plex™ Mouse Cytokine 23-Plex Panel; Bio-Rad., Hercules, CA, USA). The plasma concentrations of eotaxin, granulocyte colony stimulating factor (G-CSF), granulocyte-monocyte colony stimulating factor (GM-CSF), IFN γ , interleukin (IL)-1 α , IL-1 β , IL-2, IL-3, IL-4, IL-5, IL-6, IL-9, IL-10, IL-12 (p40), IL-12(p70), IL-13, IL-17, keratinocyte chemoattractant (KC), MCP-1/CCL2, MIP-1 α / CCL3, MIP-1 β /CCL4, RANTES and TNF α were measured. Bio-Plex™ mouse cytokine standard values were provided by Bio-Rad Laboratories. Cytokine levels were determined using a Liquichip-200 multiplex array reader with Luminex x MAP™ technology (Bio-Rad Laboratories). The analyte concentration was calculated using software provided by the manufacturer (Bio-Plex Manager Software).

Quantification of cuffed femoral artery and vein graft lesions

At time of sacrifice, vessels were harvested after 5min in vivo perfusion-fixation with formaldehyde (4%), fixated overnight and embedded in paraffin. Immunohistochemical (IHC) staining was performed using positive and negative tissue-specific controls as indicated by the antibody manufacturer. All samples were stained with hematoxylin-phloxine-saffron (HPS) and specific vessel wall cellular composition was visualized using antibodies against leukocytes (anti-CD45 antibodies 1:200, Pharmingen, San Diego, CA, USA) and monocytes and macrophages (AIA 31240 1:3000, Accurate Chemical, Westbury, NY, USA). To evaluate if annexin A5 could affect the degree of inflammation within the arterial wall, cells expressing cytokines known to be important in the restenotic process were quantified using antibodies against TNF α (anti-TNF α 1:200, BioLegend, San Diego, CA, USA) and MCP-1 (anti-MCP-1 1:100, Santa Cruz Biotechnology, Santa Cruz, CA, USA). The number of leukocytes, macrophages, foam cells and cells expressing MCP-1 and TNF α attached to the endothelium or in the media of the femoral arteries was quantified and is displayed as a percentage of the total number of present cells. All quantification in this study was performed on six equally spaced (150 μ m distance) serial stained perpendicular cross-sections throughout the entire length of the vessel and was performed by blinded observers.

Vein grafts were stained for collagen (Sirius Red staining) and with antibodies against vascular SMCs (α -SM-actin 1:800, Dako, Enschede, The Netherlands), annexin A5 (anti-annexin V 1:100, Biovision, Mountain View, CA, USA), fibrinogen and

fibrin (anti-fibrinogen and fibrin, 1:400³) and apoptotic cells (TUNEL staining, Roche, Applied Sciences, Almere, The Netherlands). The area containing SMCs, collagen, macrophages and foam cells in vein grafts was quantified using computer-assisted morphometric analysis (Qwin, Leica) and is expressed as a percentage of the total cross-sectional vein graft area. Since there are only a few cell layers within the media of murine veins and no clear morphological border exists between the media and neointima, the region between lumen and adventitia was used to define lesion area and vein graft thickening. To determine the therapeutic effect of annexin A5 on plaque instability features in vein grafts, the absolute number of apoptotic cells and leukocytes and signs of plaque erosion (endothelial disruption and fibrinogen deposition), leaky vessels (erythrocytes within newly formed vessels in the vessel wall) or plaque dissection (erythrocytes in a subendothelial space) were counted.

Effects of annexin A5 on endothelial-platelet and endothelial-leukocyte interaction using an ex vivo vascular injury perfusion model

To investigate if annexin A5 affects platelet-endothelium or leukocyte-endothelium interactions, human umbilical vein endothelial cells (HUVEC), isolated from umbilical cord according to the method of Jaffe et al⁴, were cultured on gelatin-coated glass coverslips in endothelial specific medium (EGM-2, Clonetics, Lonza Verviers, S.p.r.l., Verviers, Belgium) supplemented with growth factors and cytokines. At confluence, HUVEC from passage 2 or 3 were stimulated for 4 hours with tumor necrosis factor- α (TNF α , 10 ng/mL, Boehringer, Ingelheim, Alkmaar, The Netherlands) to activate the endothelial cells and thus induce expression of TF and PS, in the presence or absence of annexin A5 (0.75 μ g/ml, AbD Serotec, Düsseldorf, Germany). Non-stimulated HUVEC kept in EGM-2 medium were used as negative control. After TNF-stimulation, HUVEC were washed and kept in EGM-2 medium.

To evaluate the effect of annexin A5 on the adhesion of leukocytes, low-molecular weight heparin (LMWH-Pfizer, Capelle a/d IJssel, The Netherlands)-anticoagulated whole blood perfusions were performed, obtained from aspirin-free donors. Perfusions were performed for 10 minutes at 1 dyne/cm² according to de Boer et al⁵. When HUVEC were treated with annexin A5 during TNF α -stimulation, whole blood was also pre-incubated with annexin A5 for 5 min prior to the perfusion and during the perfusion, to inhibit PS, generated during flow. Non-bound blood components were removed by washing with HEPES buffer (20 mmol/L HEPES, 132 mmol/L NaCl, 6 mmol/L KCl, 1 mmol/L MgSO₄, 1.2 mmol/L KH₂PO₄, 5 mmol/L glucose, 1.0 mmol/L CaCl₂, 0.5% human serum albumin [CeAlb, Sanquin, Amsterdam, The Netherlands], pH 7.4). All perfusions were performed in duplicate/ triplicate runs. Afterwards, at least 25 photomicrographs were taken (Leica DMI-6000) per perfusion, allowing quantification of leukocyte adhesion to the endothelium.

Assessment of vascular function through endothelium-mediated dilatation

To determine therapeutic effects of annexin A5 on vascular function, EMD was evaluated in ApoE^{-/-} mice after 16-17 weeks on a Western-type diet. Mice were treated with annexin A5 or vehicle as described above once daily for three days. Afterwards, mice were anaesthetized with Isofluran (Isoba®vet, Schering-Plough Animal Health, Denmark, 4.5% for induction and 1.5-2% for maintenance). A high fidelity pressure transducer (Samba Sensor preclin 420LP, Västra Frölunda, Sweden) was introdu-

ced into the left common carotid artery and transferred into the aortic arch. The Samba sensor was connected to a Samba 3200 unit, with 1000Hz as sample rate. Data was acquired in Powerlab (AD Instrument, v5) at 2KHz. Mice were allowed to stabilize for 15min after surgery.

Blood pressure measurements were performed at basal level and after IP injection of 3µg/kg metacholine to stimulate endothelial NO-release and vasodilatation (Acetyl-β-methylcholine-chloride, 98%, Sigma-Aldrich, Stockholm, Sweden). The blood pressure was measured for up to 5min. When baseline pressure was again established, IP injection of 50mg/kg (10µl/g) Nw-Nitro-L-Arginine-methyl-ester-hydrochloride 98% (L-NAME), a NO-synthase inhibitor, (Sigma-Aldrich) was given. Blood pressure was then measured until a new plateau was reached (12-15min), after which an additional IP injection of 3µg/kg metacholine was given and blood pressure was measured again for 5min.

Statistical analysis

All data are presented as mean±standard error of the mean (SEM), unless otherwise indicated. Overall comparisons between data from groups were performed using the Kruskal-Wallis test. If a significant difference was found, groups were compared using a Mann-Whitney sum test. For the evaluation of cases of vein graft thrombosis, the Fisher's exact test was used (incidences in both groups were $n < 5$). Comparison of endothelial-leukocyte adhesion between various groups was performed using a 2-way ANOVA group analysis with Bonferroni posttest. All statistical analyses were performed with SPSS 14.0 software for Windows. P-values ≤ 0.05 were regarded as statistically significant and are indicated with an asterisk (*).

Reference list

1. Lardenoye JH, Delsing DJ, de Vries MR, Deckers MM, Princen HM, Havekes LM, van Hinsbergh VW, van Bockel JH, Quax PH. Accelerated atherosclerosis by placement of a perivascular cuff and a cholesterol-rich diet in ApoE*3Leiden transgenic mice. *Circ Res* 2000;87:248-53.
2. Lardenoye JH, de Vries MR, Lowik CW, Xu Q, Dhore CR, Cleutjens JP, van Hinsbergh VW, van Bockel JH, Quax PH. Accelerated atherosclerosis and calcification in vein grafts: a study in APOE*3 Leiden transgenic mice. *Circ Res* 2002;91:577-84.
3. Koopman J, Maas A, Rezaee F, Havekes L, Verheijen J, Gijbels M, Haverkate F. Fibrinogen and atherosclerosis: a study in transgenic mice. *Fibrinol Proteol* 1997;11(Suppl 1):19-21.
4. Jaffe EA, Nachman RL, Becker CG, Minick CR. Culture of human endothelial cells derived from umbilical veins. Identification by morphologic and immunologic criteria. *J Clin Invest* 1973;52:2745-56.
5. de Boer HC, Verseyden C, Ulfman LH, Zwaginga JJ, Bot I, Biessen EA, Rabelink TJ, van Zonneveld AJ. Fibrin and activated platelets cooperatively guide stem cells to a vascular injury and promote differentiation towards an endothelial cell phenotype. *Arterioscler Thromb Vasc Biol* 2006;26:1653-9.

Supplemental figures

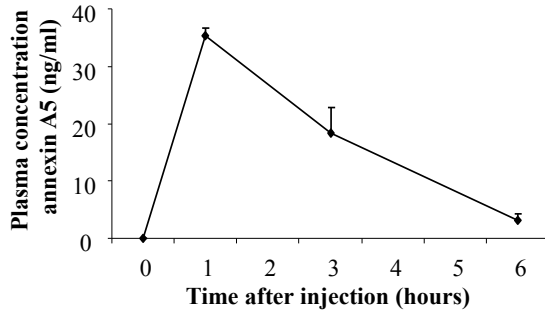


Figure I. Plasma concentration (ng/ml) of circulating human AnxA5 in ApoE3*Leiden mice after IP injection of 1mg/kg/d AnxA5, detected by ELISA, in time (mean±SEM, n=3).

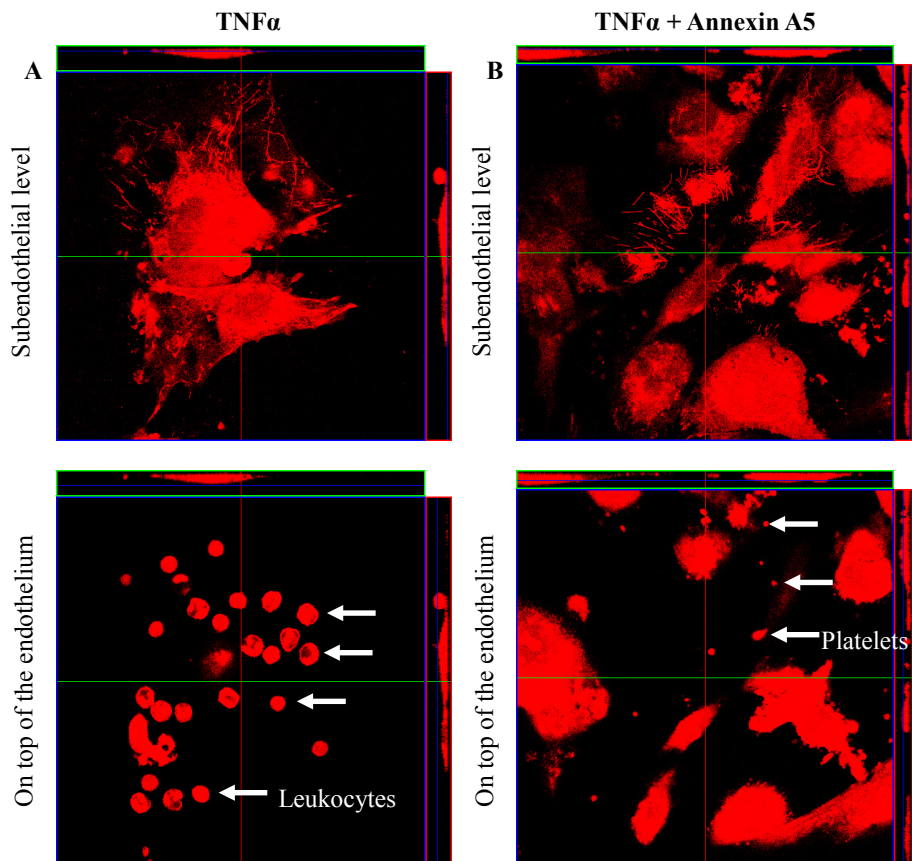


Figure II. Representative photomicrographs of cultured HUVECS, 4h after stimulation with TNF α with and without anxA5, taken using confocal laser scanning microscopy (original magnification 40x), in a three-dimensional area (1 and 8 μ m cell height). Note the presence of platelets and fibrin at the endothelial cell level, with the presence of adhered leukocytes (n=21 in TNF α group, n=2 in the TNF α + AnxA5 group), restricted to the endothelial cell surface in the TNF α only group.

Cytokine (pg/ml)	Vehicle	Annexin A5
Eotaxin	76.5±38.7	118.5±24.2
G-CSF	14.2±2.6	8.4±1.0*
GM-CSF	9.9±4.4	3.3±1.2
Interferon γ	7.9±2.5	2.2±0.7*
IL-10	9.6±2.0	10.0±1.3
IL-12 (p40)	78.7±19.9	53.2±5.8
IL-12 (p70)	2.3±0.6	1.7±0.4
IL-13	56.1±18.2	102.3±21.3
IL-17	44.3±8.8	36.1±9.6
IL-1 α	0.8±0.4	1.5±0.5
IL-1 β	39.1±21.2	17.8±2.5
IL-2	13.6±3.6	14.2±2.6
IL-3	0.3±0.3	0.0±0.0 [†]
IL-4	0.0±0.0 [†]	0.0±0.0 [†]
IL-5	2.9±1.7	1.3±0.5
IL-6	17.0±14.5	1.1±0.6
IL-9	74.4±21.8	102.4±13.8
KC	22.2±3.5	28.3±3.5
MCP-1	46.6±7.1	43.9±5.5
MIP-1 α /CCL3	21.9±6.2	10.9±3.6
MIP-1 β /CCL4	22.1±10.3	7.5±0.9*
RANTES	3.6±0.7	3.3±0.5
TNF α	204.2±48.2	158.4±37.3

Table 1. Plasma cytokine concentration (pg/ml), determined using a multiplex biometric immunoassay in ApoE3*Leiden mice, 3 and 28 days after (femoral arterial cuff or vein graft) surgery and vehicle only or (1mg/kg/d) anxA5 treatment (mean±SEM, n=10). * p<0.05, † not detectable.

	Attached cells to endothelium		Cells in medial layer	
	Vehicle	AnxA5	Vehicle	AnxA5
Macrophages	24.5±3.5%	11.9±2.3%*	14.2±5.5%	1.8±0.9%*
Leukocytes	34.2±8.9%	9.7±3.0%*	19.6±4.6%	6.1±2.6%*
Cells expressing MCP-1	49.1±2.2%	33.9±3.1%*	31.1±1.8%	14.7±2.8%*
Cells expressing TNF α	39.6±8.0%	22.7±2.2%*	21.2±6.2%	12.9±2.9%

Table II. Quantification of inflammatory cell recruitment to the site of vascular injury in ApoE3*Leiden mice, 3d after femoral arterial cuff placement and treatment with vehicle or anxA5. Inflammatory cell types, expressed as a percentage of all cells present (stained with hematoxylin) in the arterial wall (mean±SEM, n=10).

	Systolic pressure (mmHg)		Diastolic pressure (mmHg)	
	Vehicle	Annexin A5	Vehicle	Annexin A5
Basal level	133.7±5.8	129.9±5.7	92.7±6.1	88.1±3.4
Metacholine	128.7±5.1	107.6±6.6*	91.9±5.5	77.1±5.1*
L-NAME	161.3±14.2	159.6±6.5	108.3±9.1	106.1±3.9
L-NAME + metacholine	155.9±11.8	160.6±8.3	107.0±7.8	108.3±9.4

Table III. Systolic and diastolic aortic blood pressure (mmHg) in ApoE^{-/-} mice with endothelial dysfunction and 3d treatment with vehicle or annexin A5, shown at basal level, 3min after metacholine injection, after L-NAME injection and after a combination of L-NAME with subsequent metacholine injection (mean±SEM, n=10).

Chapter 5

Annexin A5 prevents post-interventional accelerated atherosclerosis development in a dose-dependent fashion in mice

M.M. Ewing^{1,2,3}, J.C. Karper^{2,3}, M.L. Sampietro^{4,5}, M.R. de Vries^{2,3}, K. Pettersson⁶, J.W. Jukema^{1,3}, P.H.A. Quax^{2,3}

1 Dept. of Cardiology, Leiden University Medical Center (LUMC), Leiden, The Netherlands

2 Dept. of Surgery, LUMC, Leiden, The Netherlands

3 Einthoven Laboratory for Experimental Vascular Medicine, LUMC, Leiden, The Netherlands

4 Dept. of Human Genetics, LUMC, Leiden, The Netherlands

5 Interuniversity Cardiology Institute of the Netherlands (ICIN), Utrecht, The Netherlands

6 Athera Biotechnologies, Stockholm, Sweden

Abstract

Background Activated cells in atherosclerotic lesions expose phosphatidylserine (PS) on their surface. Annexin A5 (AnxA5) binds to PS and is used for imaging atherosclerotic lesions. Recently, AnxA5 was shown to inhibit vascular inflammatory processes after vein grafting. Here, we report a therapeutic role for AnxA5 in post-interventional vascular remodeling in a mouse model mimicking percutaneous coronary intervention (PCI).

Methods and Results Associations between the rs4833229 (OR=1.29 (CI 95%), $p_{\text{allelic}}=0.011$) and rs6830321 (OR=1.35 (CI 95%), $p_{\text{allelic}}=0.003$) SNPs in the AnxA5 gene and increased restenosis-risk in patients undergoing PCI were found in the GENDER study. To evaluate AnxA5 effects on post-interventional vascular remodeling and accelerated atherosclerosis development in vivo, hypercholesterolemic ApoE^{-/-} mice underwent femoral arterial cuff placement to induce intimal thickening. Dose-dependent effects were investigated after 3 days (effects on inflammation and leukocyte recruitment) or 14 days (effects on remodeling) after cuff placement. Systemically administered AnxA5 in doses of 0.1, 0.3 and 1.0 mg/kg compared to vehicle reduced early leukocyte and macrophage adherence up to 48.3% ($p=0.001$) and diminished atherosclerosis development by 71.2% ($p=0.012$) with a reduction in macrophage/foam cell presence. Moreover, it reduced the expression of the endoplasmic reticulum stress marker GRP78/BiP, indicating lower inflammatory activity of the cells present.

Conclusions AnxA5 SNPs could serve as markers for restenosis after PCI and AnxA5 therapeutically prevents vascular remodeling in a dose-dependent fashion, together indicating clinical potential for AnxA5 against post-interventional remodeling.

Introduction

Post-interventional vascular remodeling and accelerated atherosclerosis development are important complications of revascularization strategies and limit treatment success rate¹. These features are elicited by endothelial and atherosclerotic plaque injury, triggering inflammatory activation and leukocyte recruitment to the injured arterial segment. These cells are the driving factors behind smooth muscle cell (SMC) proliferation and extracellular matrix deposition leading to intimal hyperplasia. Sub-endothelial retention and oxidation of low-density lipoprotein (LDL) cholesterol is central to the initial lesion formation in both native atherosclerosis and restenosis development^{2,3}. Recently, it was postulated that endoplasmic reticulum (ER) stress, leading to the unfolded protein response (UPR), is involved in the regulation of inflammation in activated vascular cells and the link between UPR and arterial inflammation is emerging as an important factor in (accelerated) atherosclerosis development⁴⁻⁷.

AnxA5 is a member of the annexin family of proteins that calcium-dependently bind to negatively-charged phospholipid surfaces and was originally discovered as an anticoagulant and antithrombotic protein⁸⁻¹¹ and has been shown to inhibit the prothrombinase complex¹² and to down-regulate the surface expression of tissue factor¹³. It is now known to have anti-inflammatory and anti-atherosclerotic properties^{14,15} and to regulate interferon γ signalling¹⁶. Viable cells express phosphatidylserine (PS) on their inner cellular membrane leaflet. When PS is externalized, it serves as an 'eat-me' signal. Annexin A5 (AnxA5) binds reversibly, specifically and with high affinity to PS¹⁵. PS becomes externalized during apoptosis, which makes AnxA5 a powerful tool to detect apoptosis (and atherosclerosis) both *in vitro* and *in vivo*¹⁷. PS is expressed in native atherosclerosis and after revascularisation procedures, and circulating AnxA5 binds with high affinity to these cells, and is therefore present in high concentrations in atherosclerotic plaques and injured vascular segments. PS externalization is normally thought to be associated to apoptosis, but can also be externalized in a controlled and reversible way in non-apoptotic cells^{18,19}.

Plasma levels of AnxA5 are inversely related to the severity of coronary stenosis and are indicative of the extent of atherosclerotic plaques²⁰, but are also elevated in subjects with left ventricular hypertrophy and following myocardial infarction^{21,22}. It was recently shown that systemically administered AnxA5 can prevent vein graft disease and vascular inflammation²³ and that the dimer of annexin A5, diannexin, can protect against renal ischemia-reperfusion injury and inflammatory cell infiltration into transplanted islet grafts^{24,25}. Patients with hypercholesterolemia and previous coronary heart disease (CHD) undergoing PCI for atherosclerosis are most at risk for inflammatory-driven post-interventional restenosis development. The risk for development of restenosis may partially be determined by genetic factors. It has been shown that genetic variations in genes encoding inflammatory factors (SNPs) can predict the risk for restenosis after percutaneous coronary intervention (PCI)²⁶. The effects of genetic variation in the AnxA5 gene on clinical restenosis after PCI or cardiovascular disease progression have thus far not been elucidated.

In the present study we investigated the association between AnxA5 SNPs and restenosis-risk in patients undergoing PCI, followed by *in vivo* evaluation of the therapeutic effectiveness of AnxA5 in a humanized mouse model for post-interventional

vascular remodeling using ApoE3*Leiden mice. Our findings point to a potential diagnostic and therapeutic clinical role for AnxA5 against post-PCI vascular remodeling.

Materials and Methods

Association between single nucleotide polymorphisms (SNPs) in the AnxA5 gene, extracted from the GENDER genome wide association study (GWAS) dataset²⁷ and restenosis-risk following PCI was investigated.

We performed *in vivo* intervention studies in which hypercholesterolemic ApoE^{-/-} mice on a Western-type diet were subjected to femoral artery cuff placement to induce vascular injury and remodeling²⁸. Cuff placement leads to a localized vascular inflammation, which in turn produces concentric intimal lesions that can affect vessel patency. The lesions consist of SMCs, connective tissue and infiltrated leukocytes such as macrophages / foam cells and are strongly inflammation-dependent²⁹. In these vascular segments, inflammatory cell adhesion, infiltration, intimal thickening and lesion composition were assessed using histology, morphometry and immunohistochemistry (IHC), as described previously²⁹. Treatment with vehicle, 0.1, 0.3 and 1.0 mg/kg AnxA5 was given to operated ApoE^{-/-} mice. A three day protocol was used to evaluate effects on leukocyte recruitment, and a 14 day protocol to evaluate effects on vascular remodeling. All materials and methods are described in detail in the supplemental material.

Results

Annexin A5 SNP as risk marker for clinical restenosis

AnxA5 plasma levels are linked to the severity of coronary stenosis and AnxA5 is a marker of cardiovascular disease progress. These data indicate a potential role of AnxA5 in (post-interventional) accelerated atherosclerosis development. Therefore we investigated the association between AnxA5 SNPs and restenosis risk in patients undergoing PCI enrolled in the GENDER study, composed of 866 patients (295 cases that developed restenosis following PCI and 571 controls that did not develop restenosis). Clinical outcome was linked to genetic data obtained through a genome-wide association analysis.

The allelic association test identified two SNPs, rs4833229 and rs6830321, which are significantly associated with restenosis risk after PCI (fig 1A). Both SNPs increased the risk for restenosis (rs4833229, odds ratio (OR) =1.29, (95% confidence interval (CI) 1.06-1.58), *p*-value=0.011 and rs6830321, OR=1.35 (95% CI 1.10-1.64), *p*-value=0.003), even after adjustment for clinical risk factors, such as total occlusion, diabetes, smoking and residual stenosis (table 1). The minor allele frequencies for cases and controls from the GENDER population are 0.481 and 0.418 for rs4833229 and 0.510 and 0.436 for rs6830321 respectively, indicating they are present in a large proportion of the population. The AnxA5 gene linkage disequilibrium (LD) plot shows that rs4833229 and rs6830321 are in high LD ($r^2=0.91$, fig 1B). Haplotype analysis in the gene showed similar association results with restenosis as found in the single SNP analysis (haplotype ACAGTTGTT, frequency: 0.427, OR=1.275,

$p=0.018$). These data link AnxA5 SNPs to restenosis-risk after PCI and suggest that AnxA5 genotype functions as risk marker for restenosis. We therefore further explored AnxA5's therapeutic potential using an in vivo model for restenosis and intimal hyperplasia.

SNP	Base Position	Minor / major allele	MAF cases / controls	OR (95% CI)	p value
rs2306420	122810925	T/C	0.283 / 0.309	0.88 (0.71-1.10)	0.2622
rs4833229	122820114	A/G	0.481 / 0.418	1.29 (1.06-1.58)	0.0114
rs1480287	122821231	A/G	0.481 / 0.215	0.81 (0.63-1.04)	0.0954
rs17449954	122827178	C/T	0.181 / 0.067	0.86 (0.57-1.30)	0.4705
rs6534309	122829379	C/T	0.058 / 0.108	0.75 (0.53-1.06)	0.1040
rs6857766	122830735	A/G	0.083 / 0.230	0.79 (0.62-1.01)	0.0636
rs6830321	122834205	T/C	0.510 / 0.436	1.35 (1.10-1.64)	0.0034
rs2306416	122837138	CT	0.139 / 0.145	0.96 (0.72-1.27)	0.7564

Table 1. Association between restenosis risk and SNPs in the ANXA5 gene.

Allelic association results for 8 SNPs included in the annexin A5 gene in the GENDER study. Positions are based on hg18 build. Abbreviations: Chr: Chromosome, MAF: Minor Allele Frequency. ORs are computed for the minor allele from the two by two allele contingency table. Significant association was observed for SNPs rs4833229 and rs6830321 and restenosis-risk with SNPs displaying high linkage.

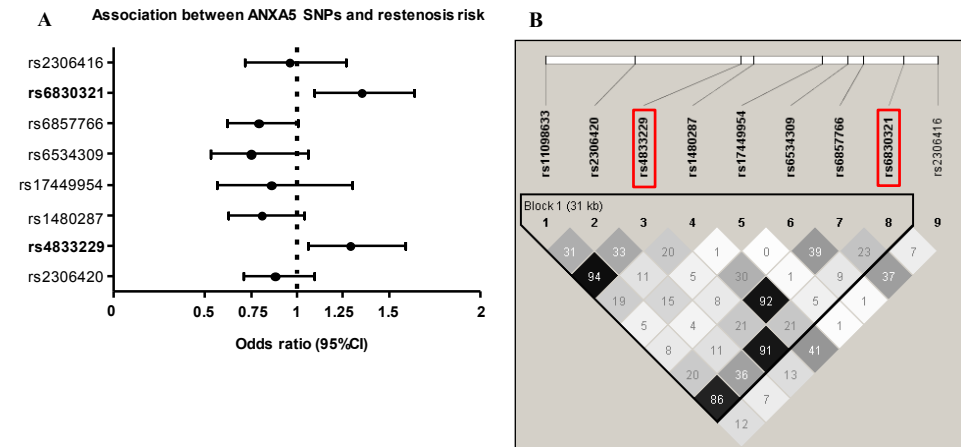


Figure 1. AnxA5 is a genetic risk marker for clinical restenosis after PCI. Association results for the allelic test for eight SNPs in the ANXA5 gene (A). LD plot shows that rs4833229 and rs6830321 SNPs are in high LD ($r^2 = 0.91$) (B).

Annexin A5 dose-dependently prevents leukocyte recruitment after vascular injury

Effects of AnxA5 on leukocyte recruitment to injured arterial segments was investigated in the femoral artery cuff model in ApoE^{-/-} mice receiving daily vehicle or 0.1, 0.3 or 1.0 mg/kg AnxA5 through IP injection. Total plasma cholesterol was not affected by annexin A5 treatment (supplementary table I). Three days after cuff placement there is inflammation in the cuffed arteries, with leukocytes both adherent to the endothelial surface and with cells that have migrated into the media layer (fig 2A). Staining of arterial lesions at this time point revealed that 0.1, 0.3 and 1.0 mg/

kg/d AnxA5-treated animals displayed a reduced percentage of endothelial leukocyte adhesion by 26.7% ($p=0.014$), 34.9% ($p=0.010$) and 48.3% ($p=0.001$) respectively (fig 2B). For monocytes/macrophages, this percentage was reduced by 40.0% ($p=0.029$), 66.9%, ($p=0.001$) and 45.0% ($p=0.037$) respectively (fig 2C).

The percentage leukocyte infiltration into the media was reduced by all AnxA5 treatments by 49.4% ($p=0.008$), 53.3% ($p=0.006$) and 49.9% ($p=0.011$) respectively (fig 2D). The percentage medial macrophages was reduced by 61.2% ($p=0.025$) by 1.0 mg/kg AnxA5, the other dosages did not significantly affect monocyte/macrophage extravasation (fig 2E). Together, these data indicate an important role for AnxA5 in low dosages in the prevention of leukocyte recruitment to injured arterial segments.

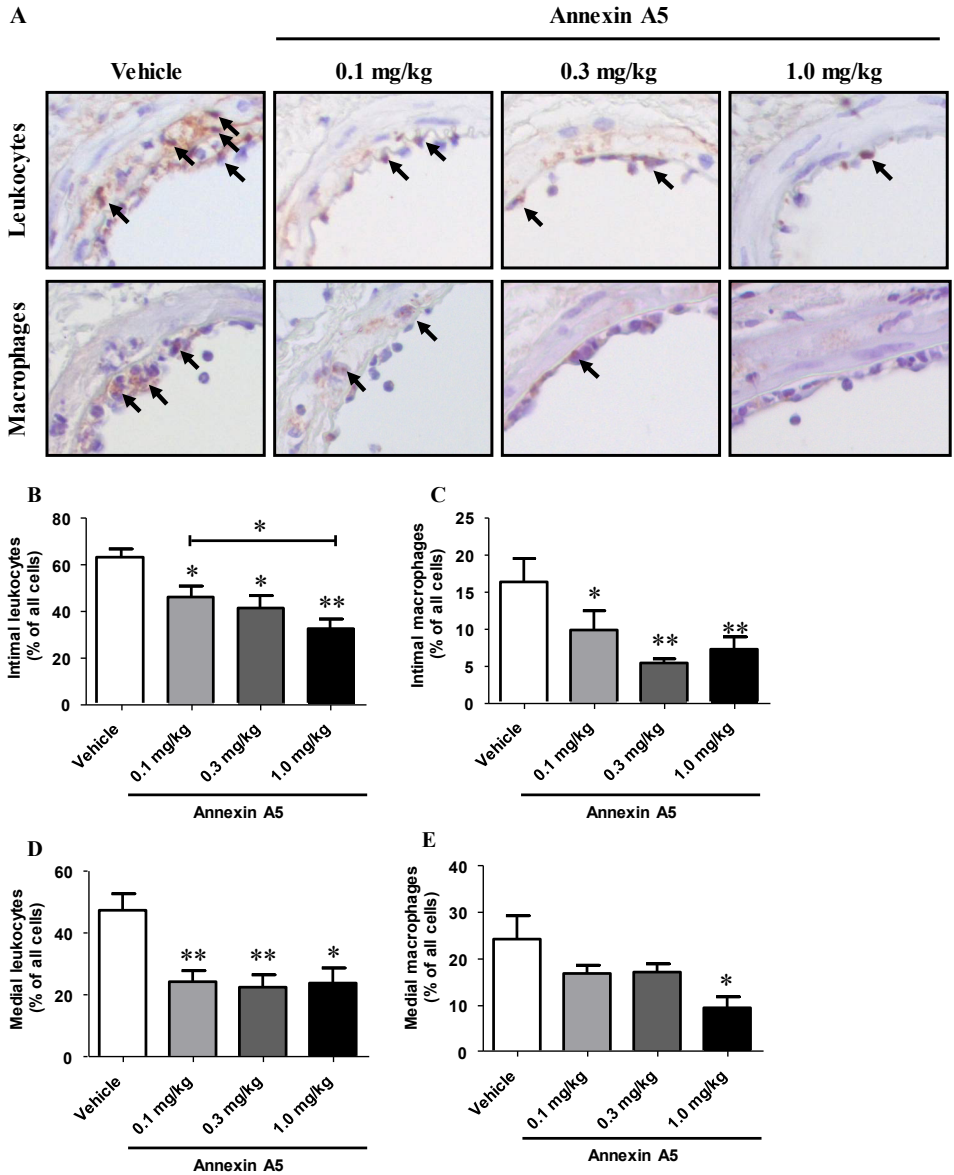
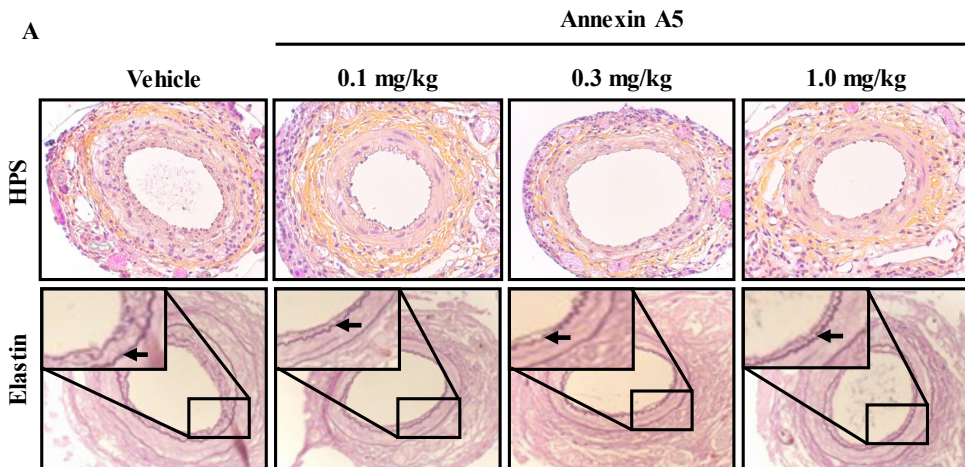


Figure 2. Annexin A5 dose-dependently prevents leukocyte recruitment after vascular injury. Representative cross-sections of cuffed-femoral arteries of ApoE^{-/-} mice treated with vehicle or 0.1, 0.3 or 1.0 mg/kg/d AnxA5 (leukocyte and macrophage staining, magnification 80x, arrows indicate positive staining) after 3d (A). Quantification of intimal adhering leukocytes (B) and macrophages (C) as percentage of all cells within the internal elastic lamina and medial infiltrated leukocytes (D) and macrophages (E) (%). Results indicated as mean±SEM, n=10. * p<0.05, ** p<0.01.

Annexin A5 dose-dependently prevents accelerated atherosclerosis development

The inflammation caused by cuff placement leads to an inflammation driven intimal hyperplasia. Therapeutic effectiveness of AnxA5 on (neo-)intima development was evaluated 14 days after cuff placement. Annexin A5 treatment did not affect plasma total cholesterol concentration (supplementary table I). Accelerated atherosclerotic lesion development was measured on sections stained with HPS and Weigert's elastin (fig 3A). Vehicle-treated animals developed intimal thickening, resulting in luminal stenosis. Quantitative analysis displayed reduced intimal thickening (expressed as μm^2 per cross-section) after 0.1, 0.3 and 1.0 mg/kg AnxA5-treatment by 54.6% (p=0.041), 71.2% (p=0.012) and 66.9% (p=0.009) respectively (fig 3B). Intimal thickening was 38.1% more reduced (p=0.031) by 0.3 compared to 0.1 mg/kg AnxA5. AnxA5 (0.3 and 1.0 mg/kg) also decreased the absolute medial surface area (μm^2) by 30.1% (p=0.012) and 24.1% (p=0.025, fig 3C) and intima / media ratio by 62.3% (p=0.004) and 60.3% (p=0.007, fig 3D), although the lowest dose was ineffective. Furthermore, luminal stenosis (%) was reduced by 58.0% (p=0.001) and 58.8% (p=0.0004, fig 3E), identifying a potent role for AnxA5 in the control of inflammatory post-interventional vascular remodeling. Compared to 0.1 mg/kg, 0.3 mg/kg AnxA5 had increased protective effects on both the intima / media ratio (by 38.5%, p=0.016) and luminal stenosis percentage (by 33.2%, p=0.042). The total vessel wall diameter and luminal areas were both similar in all AnxA5 dosages, except for 1.0 mg/kg, which displayed 27.1% (p=0.043) reduced total vessel area (supplementary fig 1A, B).



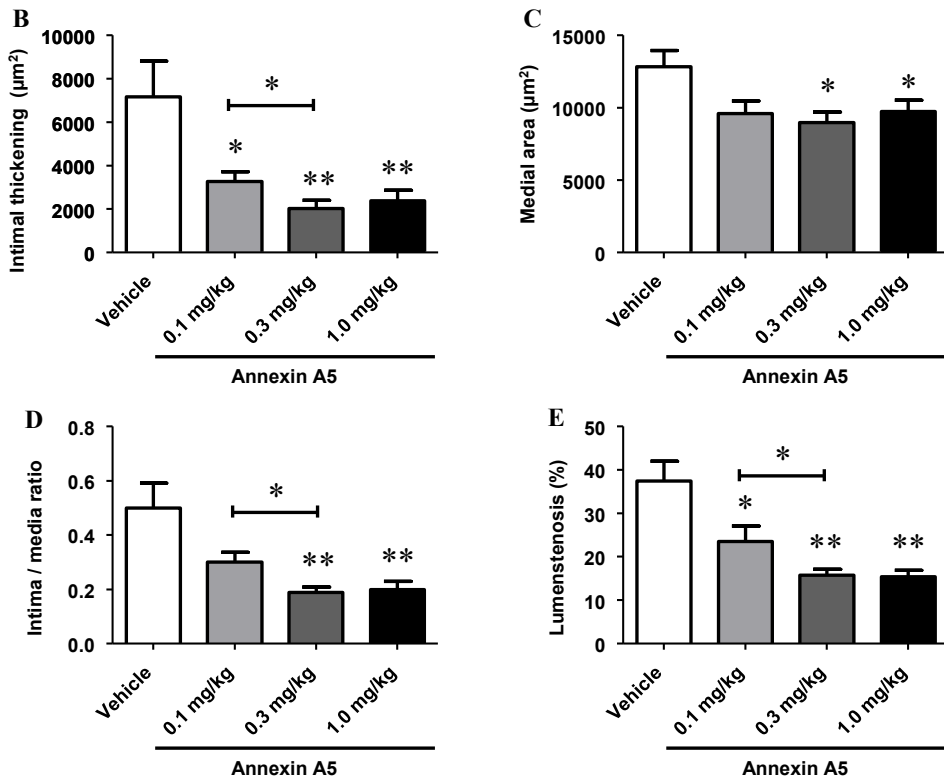


Figure 3. Annexin A5 reduces accelerated atherosclerosis development in a dose-dependent fashion. Representative cross-sections of cuffed arteries of ApoE^{-/-} mice receiving vehicle or 0.1, 0.3 or 1.0 mg/kg AnxA5 (A) after 14d (HPS and Weigert's elastin staining, magnification 40x, arrows indicate internal elastic laminae). Quantification of intimal thickening (μm^2) (B), medial area (μm^2) (C), intima / media ratio (D) and luminal stenosis (%) (E). Results indicated as mean \pm SEM, n=10. * p<0.05, ** p<0.01.

IHC showed profound intravascular macrophages/foam cell areas, which co-localized with AnxA5 (supplementary fig IIA, B) staining at both 3d and 14d after surgery. AnxA5 in all dosages strongly reduced the accumulation of the percentage of macrophages/foam cell area (fig 4A) in the tunica media (fig 4B, p=0.0002, p=0.028 and p=0.0005 respectively) and in the tunica intima (fig 4C, p=0.002, p=0.011 and p=0.002 respectively) after 14d. The 78 kDa glucose regulated protein/BiP (GRP78) is an ER protein and associates permanently with mutant or defective incorrectly folded proteins, preventing their export from the ER lumen. ER stress including up-regulation of GRP78 is present in unstable atherosclerotic lesions. We investigated if annexin A5 affected GRP78 expression in cuffed femoral arteries. AnxA5 in all dosages strongly reduced GRP78 BiP expressing cells in the media (fig 4D) by 50.2% (p=0.006), 66.3% (p=0.0006) and 68.0% (p=0.004) respectively, but not in the intima (fig 4E).

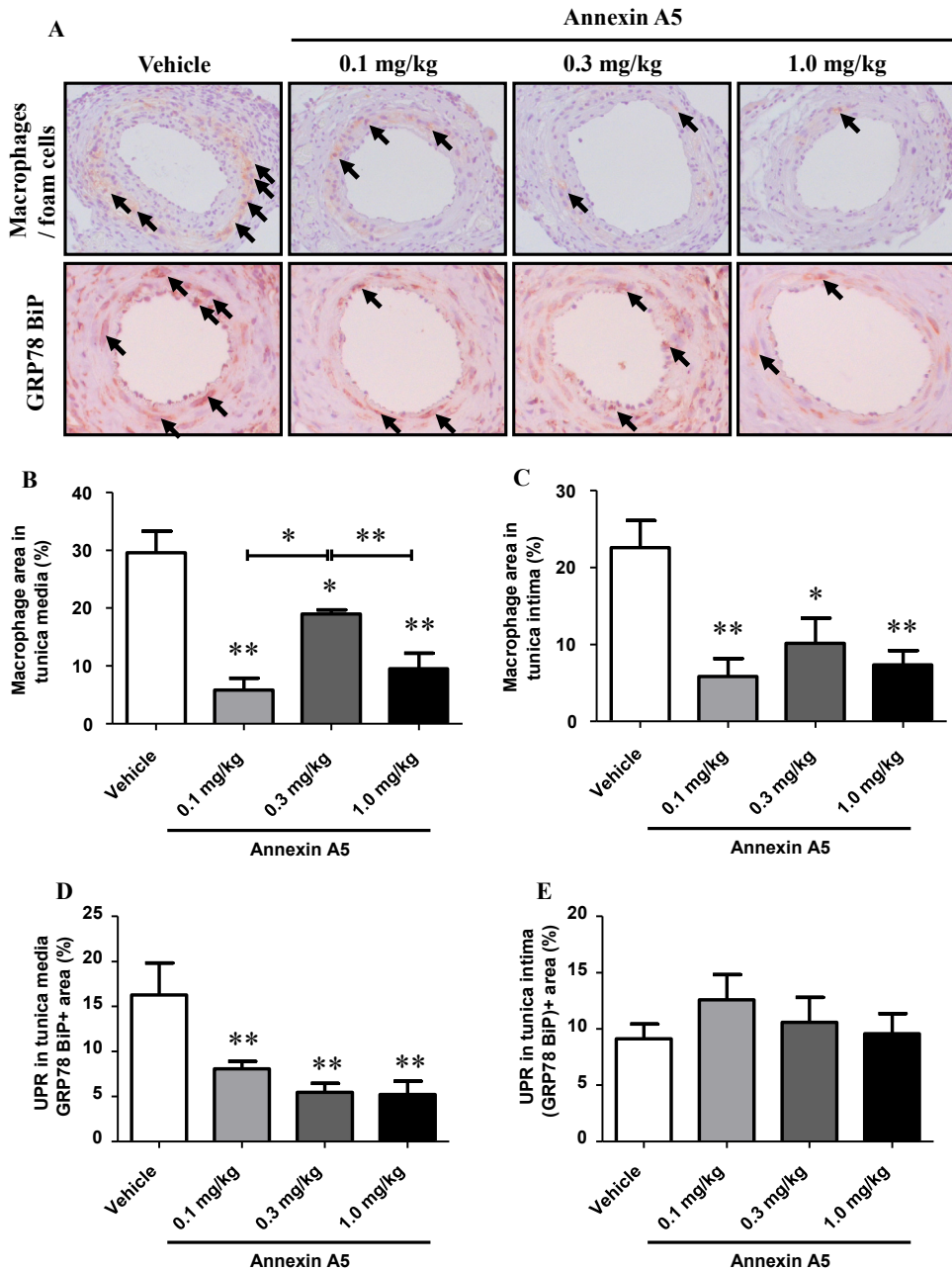


Figure 4. Annexin A5 leads to a less-inflammatory phenotype with reduced intravascular signs of ER-stress. Representative cross-sections of cuffed arteries of ApoE^{-/-} mice receiving vehicle or 0.1, 0.3 or 1.0 mg/kg AnxA5 (A) after 14d (macrophages and GRP78 BiP staining, magnification 40x, arrows indicate positive staining) and quantification of medial (B) and intimal (C) macrophage/foam cell area (%) and medial (D) and intimal (E) GRP78 BiP expression (%). Results indicated as mean±SEM, n=10. * p<0.05, ** p<0.01.

Discussion

This study demonstrates an important therapeutic role for AnxA5 in post-interventional intimal hyperplasia and accelerated atherosclerosis development. Association between AnxA5 SNPs and increased restenosis-risk in patients undergoing PCI was found. Systemic AnxA5 was effective in preventing intimal thickening and could dose-dependently reduce leukocyte and macrophage recruitment to injured arterial segments in ApoE^{-/-} mice in 0.3 and 0.1 mg/kg dosages. Finally, we demonstrate that sustained therapy reduces accelerated atherosclerosis with fewer infiltrated macrophages / foam cells and UPR-expressing cells in the injured arterial wall. Together, these data indicate high diagnostic and therapeutic potential for AnxA5 against post-PCI vascular remodeling.

Association between AnxA5 SNPs and restenosis development were investigated using a large study population that underwent PCI, the GENDER population. It has already been shown in this material that mutations in several genes associated with inflammation were associated to restenosis development²⁴. Our results demonstrate that SNPs rs4833229 and rs6830321 show significant association with increased risk for clinical restenosis (OR 1.29 and 1.35, fig 1A). This genetic variance in addition to plasma levels¹⁹ would allow for excellent stratification of patients that are most at risk for restenosis development, enabling individual tailor-made treatment strategy. Additionally, our results support the notion that genetic programming of not only pro-inflammatory mediators, but also the endogenous anti-inflammatory system exerts a significant role in post-interventional remodeling.

In this study, a perivascular cuff-mediated arterial injury model was applied, which allows for quick and reproducible lesion formation with continuous blood flow in a patent vessel segment, although the perivascular approach rather differs from clinical endovascular injury through balloon inflation and stent deployment during PCI. This perivascular approach could affect the amount of exposure of subendothelial thrombogenic material and thrombosis, which are important targets for AnxA5.

Therapeutic effects were shown to most likely result from local AnxA5 binding to activated cells in the injured vascular segment. Local AnxA5 can reduce adherence of platelets leukocytes and eventually prevent their inflammatory activation, with reduced signs of ER-stress and the UPR within these cells. We found reduced GRP78/BiP expression in the tunica media (fig 4D) but not in the intima (fig 4E) Prolonged intracellular cholesterol storage leads to increased ER stress in cells, which is more likely to occur in foam cells than in early monocyte/macrophages. In this study, such cells should predominantly be found among cells that have migrated towards the tunica media, which in turn may explain the difference between GRP78/BiP expression between the media and intima layers.

The fact that clearance of AnxA5 is much slower from the arterial wall than from plasma³⁰ and accumulates in the injured vascular wall after systemic injection²³, supports the hypothesis that AnxA5 could act anti-inflammatory in levels lower than originally investigated (<1.0 mg/kg). Current results confirm this, with AnxA5 already effective in reducing leukocyte (fig 2B) and macrophage (fig 2C) recruitment and intimal thickening (fig 3B) in dosages 3-10 times lower than previously investigated. This would favour clinical application, where undesired side-effects can be kept to a minimum. In conclusion, this study shows that systemic AnxA5 treatment strongly influences

post-interventional accelerated atherosclerosis development and can dose-dependently prevent vascular remodeling. AnxA5 has previously been successfully applied to diagnose atherosclerotic patients non-invasively¹⁹. These results therefore may have important clinical implications. Immune-mediated interventions directed towards therapeutically controlling the leukocyte recruitment and vascular remodeling process could strongly benefit from systemic AnxA5, which could be applied in an early phase following revascularization or bypass grafting to prevent accelerated atherosclerosis development. AnxA5 SNPs could function as biomarkers in the assessment of restenosis risk in patients undergoing PCI, improving patient screening. Together, these data indicate high clinical potential for AnxA5 against post-interventional remodeling.

Reference List

1. van der Hoeven, B. L., N. M. Pires, H. M. Warda, P. V. Oemrawsingh, B. J. van Vlijmen, P. H. Quax, M. J. Schaliij, E. E. van der Wall, and J. W. Jukema. 2005. Drug-eluting stents: results, promises and problems. *Int. J. Cardiol.* 99: 9-17.
2. Hansson, G. K. 2005. Inflammation, atherosclerosis, and coronary artery disease. *N. Engl. J. Med.* 352: 1685-1695.
3. Ross, R. 1999. Atherosclerosis--an inflammatory disease. *N. Engl. J. Med.* 340: 115-126.
4. Moore, K. J., and I. Tabas. 2011. Macrophages in the pathogenesis of atherosclerosis. *Cell* 145: 341-355.
5. Tabas, I. 2011. Pulling down the plug on atherosclerosis: Finding the culprit in your heart. *Nat. Med.* 17: 791-793.
6. Hotamisligil, G. S. 2010. Endoplasmic reticulum stress and atherosclerosis. *Nat. Med.* 16: 396-399.
7. Tabas, I. 2010. The role of endoplasmic reticulum stress in the progression of atherosclerosis. *Circ. Res.* 107: 839-850.
8. Andree, H. A., M. C. Stuart, W. T. Hermens, C. P. Reutelingsperger, H. C. Hemker, P. M. Frederik, and G. M. Willems. 1992. Clustering of lipid-bound annexin V may explain its anticoagulant effect. *J Biol Chem.* 267: 17907-17912.
9. Thiagarajan, P., and C. R. Benedict. 1997. Inhibition of arterial thrombosis by recombinant annexin V in a rabbit carotid artery injury model. *Circulation* 96: 2339-2347.
10. van Heerde, W. L., K. S. Sakariassen, H. C. Hemker, J. J. Sixma, C. P. Reutelingsperger, and P. G. De Groot. 1994. Annexin V inhibits the procoagulant activity of matrices of TNF-stimulated endothelium under blood flow conditions. *Arterioscler. Thromb.* 14: 824-830.
11. Gerke, V., and S. E. Moss. 2002. Annexins: from structure to function. *Physiol Rev.* 82: 331-371.
12. van Heerde, W. L., S. Poort, 'I. van, V. C. P. Reutelingsperger, and P. G. De Groot. 1994. Binding of recombinant annexin V to endothelial cells: effect of annexin V binding on endothelial-cell-mediated thrombin formation. *Biochem. J* 302 (Pt 1): 305-312.
13. Ravassa, S., A. Bennaghmouch, H. Kenis, T. Lindhout, T. Hackeng, J. Narula, L. Hofstra, and C. Reutelingsperger. 2005. Annexin A5 down-regulates surface expression of tissue factor: a novel mechanism of regulating the membrane receptor repertoire. *J Biol Chem.* 280: 6028-6035.
14. Kenis, H., L. Hofstra, and C. P. Reutelingsperger. 2007. Annexin A5: shifting from a diagnostic towards a therapeutic realm. *Cell Mol. Life Sci.* 64: 2859-2862.
15. van Genderen, H. O., H. Kenis, L. Hofstra, J. Narula, and C. P. Reutelingsperger. 2008. Extracellular annexin A5: functions of phosphatidylserine-binding and two-dimensional crystallization. *Biochim. Acta* 1783: 953-963.
16. Leon, C., D. Nandan, M. Lopez, A. Moenrezakhanlou, and N. E. Reiner. 2006. Annexin V associates with the IFN-gamma receptor and regulates IFN-gamma signaling. *J Immunol.* 176: 5934-5942.
17. Kietselaer, B. L., C. P. Reutelingsperger, G. A. Heidendal, M. J. Daemen, W. H. Mess, L. Hofstra, and J. Narula. 2004. Noninvasive detection of plaque instability with use of radiolabeled annexin A5 in patients with carotid-artery atherosclerosis. *N. Engl. J. Med.* 350: 1472-1473.
18. Balasubramanian, K., B. Mirnikjoo, and A. J. Schroit. 2007. Regulated externalization of phosphatidylserine at the cell surface: implications for apoptosis. *J. Biol. Chem.* 282: 18357-18364.
19. Boersma, H. H., B. L. Kietselaer, L. M. Stolk, A. Bennaghmouch, L. Hofstra, J. Narula, G. A. Heidendal, and C. P. Reutelingsperger. 2005. Past, present, and future of annexin A5: from protein discovery to clinical applications. *J Nucl. Med.* 46: 2035-2050.
20. van Tits, L. J., W. L. van Heerde, G. M. van der Vleuten, J. de Graaf, D. E. Grobbee, L. P. van de Vijver, A. F. Stalenhoef, and H. M. Princen. 2007. Plasma annexin A5 level relates inversely to the severity of coronary stenosis. *Biochem. Biophys. Res. Commun.* 356: 674-680.
21. Ravassa, S., A. Gonzalez, B. Lopez, J. Beaumont, R. Querejeta, M. Larman, and J. Diez. 2007. Upregulation of myocardial Annexin A5 in hypertensive heart disease: association with systolic dysfunction. *Eur. Heart J.* 28: 2785-2791.
22. Peetz, D., G. Hafner, S. Blankenberg, A. A. Peivandi, R. Schweigert, K. Brunner, M. Dahm, H. J. Rupprecht, and M. Mockel. 2002. Annexin V does not represent a diagnostic alternative to myoglobin for early detection of myocardial infarction. *Clin. Lab* 48: 517-523.
23. Ewing, M. M., M. R. de Vries, M. Nordzell, K. Pettersson, H. C. de Boer, A. J. van Zonneveld, J.

- Frostegard, J. W. Jukema, and P. H. Quax. 2010. Annexin A5 Therapy Attenuates Vascular Inflammation and Remodeling and Improves Endothelial Function in Mice. *Arterioscler. Thromb. Vasc. Biol.*
24. Wever, K. E., F. A. Wagener, C. Frielink, O. C. Boerman, G. J. Scheffer, A. Allison, R. Mase-reeuw, and G. A. Rongen. 2011. Diannexin Protects against Renal Ischemia Reperfusion Injury and Targets Phosphatidylserines in Ischemic Tissue. *PLoS. One.* 6: e24276.
25. Cheng, E. Y., V. K. Sharma, C. Chang, R. Ding, A. C. Allison, D. B. Leeser, M. Suthanthiran, and H. Yang. 2010. Diannexin decreases inflammatory cell infiltration into the islet graft, reduces beta-cell apoptosis, and improves early graft function. *Transplantation* 90: 709-716.
26. Monraats, P. S., N. M. Pires, W. R. Agema, A. H. Zwinderman, A. Schepers, M. P. de Maat, P. A. Doevendans, R. J. de Winter, R. A. Tio, J. Waltenberger, R. R. Frants, P. H. Quax, B. J. van Vlijmen, D. E. Atsma, L. A. van der, E. E. van der Wall, and J. W. Jukema. 2005. Genetic inflammatory factors predict restenosis after percutaneous coronary interventions. *Circulation* 112: 2417-2425.
27. Sampietro, M. L., D. Pons, K. P. de, P. E. Slagboom, A. Zwinderman, and J. W. Jukema. 2009. A genome wide association analysis in the GENDER study. *Neth. Heart J.* 17: 262-264.
28. Lardenoye, J. H., D. J. Delsing, M. R. de Vries, M. M. Deckers, H. M. Princen, L. M. Havekes, V. W. van Hinsbergh, J. H. van Bockel, and P. H. Quax. 2000. Accelerated atherosclerosis by placement of a perivascular cuff and a cholesterol-rich diet in ApoE*3Leiden transgenic mice. *Circ. Res.* 87: 248-253.
29. Pires, N. M., A. Schepers, B. L. van der Hoeven, M. R. de Vries, L. S. Boesten, J. W. Jukema, and P. H. Quax. 2005. Histopathologic alterations following local delivery of dexamethasone to inhibit restenosis in murine arteries. *Cardiovasc. Res.* 68: 415-424.
30. Kemerink, G. J., X. Liu, D. Kieffer, S. Ceysens, L. Mortelmans, A. M. Verbruggen, N. D. Steinmetz, J. L. Vanderheyden, A. M. Green, and K. Verbeke. 2003. Safety, biodistribution, and dosimetry of ^{99m}Tc-HYNIC-annexin V, a novel human recombinant annexin V for human application. *J. Nucl. Med.* 44: 947-952.

Online supplements

Materials and Methods

GENDER project

The GENetic DEterminants of Restenosis (GENDER) study was designed to investigate the association between genetic polymorphisms and clinical restenosis¹. In brief, it is a large multicenter prospective follow-up study conducted during 1999-2001 and comprised of patients treated successfully by percutaneous coronary intervention (PCI) for an acute coronary syndrome. Clinical restenosis was established during a nine-month follow-up period for death, myocardial infarction and target vessel revascularization (TVR), which occurred in 9.8% of all patients. Eight Single Nucleotide Polymorphisms (SNPs) included in the AnxA5 gene were extracted from the GENDER genome wide association study (GWAS) dataset² composed of 866 patients (295 cases that developed restenosis following PCI and 571 controls that did not develop restenosis after PCI). The GWAS was conducted using Illumina Human 610-Quad Beadchips (Illumina) and the Infinium II assay, following the manufacturer's instructions. After genotyping, samples and genetic markers were subjected to a stringent quality control protocol, described in detail elsewhere². The open source software PLINK³ was used to perform genetic association analysis. All p values were corrected for multiple testing. For linkage disequilibrium (LD) analyses in terms of r^2 and haplotype block delineation, we used Haploview software⁴.

Mice

All experiments were approved by the Institutional Committee for Animal Welfare of the Leiden University Medical Center (LUMC). ApoE^{-/-} mice, purchased from the Jackson Laboratory (Bar Harbor) on a C57BL/6J background were used for these studies. All animals were 10-12 weeks at the start of a dietary run-in period before surgery. ApoE^{-/-} mice were fed a Western-type diet containing 0.15% cholesterol (Lantmännen Lantbruk, diet R638). The diet was given three weeks prior to surgery and was continued throughout the entire experiment. All animals received food and water ad libitum during the experiment.

Femoral artery cuff mouse model

Mice were subjected to arterial femoral arterial cuff placement to induce intimal thickening and accelerated atherosclerosis development, as described previously⁵⁻⁷. In brief, animals were anesthetized before surgery with a combination of intraperitoneally (IP)-injected Midazolam (5 mg/kg, Roche), Medetomidine (0.5 mg/kg, Orion) and Fentanyl (0.05 mg/kg, Janssen). The right femoral artery was isolated and sheathed with a rigid non-constrictive polyethylene cuff (Portex, 0.40mm inner diameter, 0.80mm outer diameter and an approximate length of 2.0mm).

Animals received vehicle (0.9% sterile NaCl) or AnxA5 (Athera Biotechnologies AB) through IP injection. Three and 14 days after cuff placement, mice were anesthetized as before and euthanized. At sacrifice, blood was drawn in EDTA collection tubes (Sarstedt B.V.) and centrifuged at 6000 r.p.m. for 10 min at 4°C to obtain plasma, which was stored at -20°C. Next, the thorax was opened and mild pressure-

perfusion (100mm Hg) with phosphate-buffered saline for 5 min by cardiac puncture in the left ventricle. After perfusion, the cuffed femoral artery was harvested, fixed in 3.7% formaldehyde in water (w/v) and paraffin-embedded. Serial cross-sections (5 μ m thick) were made from the entire length of the artery for analysis.

Biochemical analysis

Total plasma cholesterol (Roche Diagnostics, kit 1489437) concentration was measured enzymatically before randomization at surgery.

Quantification of cuffed femoral artery lesions

Immunohistochemical (IHC) staining was performed using positive and negative tissue-specific controls as indicated by the antibody manufacturer. Samples were stained with hematoxylin-phloxine-saffron (HPS) and specific vessel wall composition was visualized for elastin (Weigert's elastin staining) and with antibodies against GRP78 BiP (1:200, Abcam, to identify cells displaying signs of UPR), CD45 for leukocytes (1:200, Pharmingen), MAC3 for monocytes/macrophages/foam cells (1:200, BD Biosciences) and anti-annexin V for injected protein accumulation (1:100, Bio-Vision). Using image analysis software (Leica Qwin), total cross-sectional medial area was measured between the external and internal elastic laminae; total cross-sectional intimal area was measured between the endothelial cell monolayer and the internal elastic lamina, as was GRP78 BiP+ surface area. The luminal stenosis is expressed as the percentage of surface area (μ m²) within the internal elastic lamina (comprised of the luminal and neointimal areas) that is taken up by neointimal tissue (in μ m²). The number of leukocytes and monocytes/macrophages attached to the endothelium, within the neointimal tissue or infiltrated in the medial layer of the femoral arteries was quantified and is displayed as a percentage of the total number of present cells. All quantification in this study was performed on six equally spaced (150 μ m distance) serial stained perpendicular cross-sections throughout the entire length of the vessel and was performed by blinded observers.

Statistical analysis

All data are presented as mean \pm standard error of the mean (SEM). Association between clinical outcome and individual SNPs was tested using an allelic association test. Groups were compared using a Mann-Whitney sum test for non-parametric data. Total plasma cholesterol concentrations in time were compared using a Wilcoxon matched pairs test. All statistical analyses were performed with SPSS 17.0 software for Windows or using Prism software. P-values <0.05 were regarded as statistically significant and are indicated with an asterisk (*).

Reference List

1. Monraats, P. S., N. M. Pires, W. R. Agema, A. H. Zwinderman, A. Schepers, M. P. de Maat, P. A. Doevendans, R. J. de Winter, R. A. Tio, J. Waltenberger, R. R. Frants, P. H. Quax, B. J. van Vlijmen, D. E. Atsma, L. A. van der, E. E. van der Wall, and J. W. Jukema. 2005. Genetic inflammatory factors predict restenosis after percutaneous coronary interventions. *Circulation* 112: 2417-2425.
2. Sampietro, M. L., D. Pons, K. P. de, P. E. Slagboom, A. Zwinderman, and J. W. Jukema. 2009. A genome wide association analysis in the GENDER study. *Neth. Heart J.* 17: 262-264.
3. Purcell, S., B. Neale, K. Todd-Brown, L. Thomas, M. A. Ferreira, D. Bender, J. Maller, P. Sklar, P. I. de Bakker, M. J. Daly, and P. C. Sham. 2007. PLINK: a tool set for whole-genome association and population-based linkage analyses. *Am. J. Hum. Genet.* 81: 559-575.
4. Barrett, J. C., B. Fry, J. Maller, and M. J. Daly. 2005. Haploview: analysis and visualization of LD and haplotype maps. *Bioinformatics.* 21: 263-265.
5. Lardenoye, J. H., D. J. Delsing, M. R. de Vries, M. M. Deckers, H. M. Princen, L. M. Havekes, V. W. van Hinsbergh, J. H. van Bockel, and P. H. Quax. 2000. Accelerated atherosclerosis by placement of a perivascular cuff and a cholesterol-rich diet in ApoE*3Leiden transgenic mice. *Circ. Res.* 87: 248-253.
6. Pires, N. M., A. Schepers, B. L. van der Hoeven, M. R. de Vries, L. S. Boesten, J. W. Jukema, and P. H. Quax. 2005. Histopathologic alterations following local delivery of dexamethasone to inhibit restenosis in murine arteries. *Cardiovasc. Res.* 68: 415-424.
7. Ewing, M. M., M. R. de Vries, M. Nordzell, K. Pettersson, H. C. de Boer, A. J. van Zonneveld, J. Frostegard, J. W. Jukema, and P. H. Quax. 2011. Annexin A5 therapy attenuates vascular inflammation and remodeling and improves endothelial function in mice. *Arterioscler. Thromb. Vasc. Biol.* 31: 95-101.

Supplemental figures

Group	Total plasma cholesterol (mmol/L)	
	Surgery	Sacrifice
Early time point (3d)		
Vehicle	19.5±1.3	25.0±0.8
1.0 mg/kg annexin A5	15.4±0.4	19.8±1.6
0.3 mg/kg annexin A5	16.6±0.6	20.0±1.7
0.1 mg/kg annexin A5	19.6±1.8	22.8±2.2
Late time point (14d)		
Vehicle	23.7±2.7	21.1±2.4
1.0 mg/kg annexin A5	18.0±2.7	17.1±2.7
0.3 mg/kg annexin A5	19.9±4.1	19.2±3.3
0.1 mg/kg annexin A5	19.3±1.6	19.8±1.6

Table I. Plasma cholesterol in mice undergoing annexin A5 dose-response investigations. Plasma total cholesterol (mmol/L) of ApoE^{-/-} mice receiving vehicle or annexin A5 (1.0, 0.3 or 0.1 mg/kg/d) through IP injection, measured at surgery or at sacrifice (day 3 or 14). No significant differences were observed (mean±SEM, n=10).

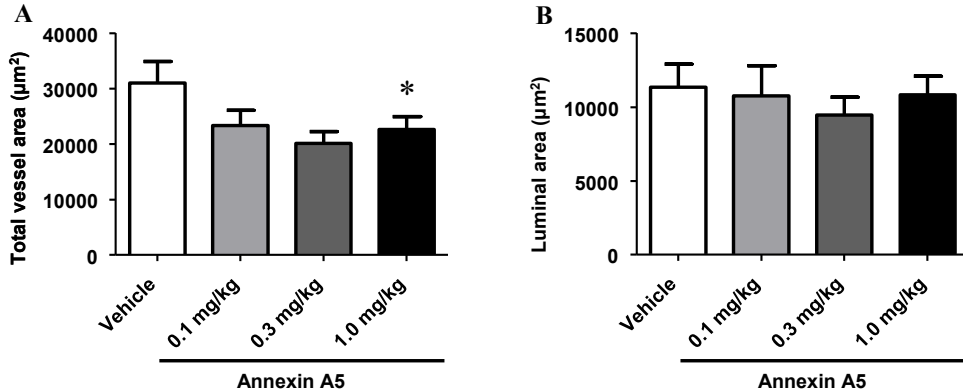


Figure I. Annexin A5 reduces accelerated atherosclerosis development in a dose-dependent fashion. Quantification of total vessel area (µm²) (A) and luminal area (µm²) (B) in ApoE^{-/-} mice receiving vehicle or 0.1, 0.3 or 1.0 mg/kg AnxA5 after 14d. Results indicated as mean±SEM, n=10. * p<0.05, ** p<0.01, n.s. not significant.

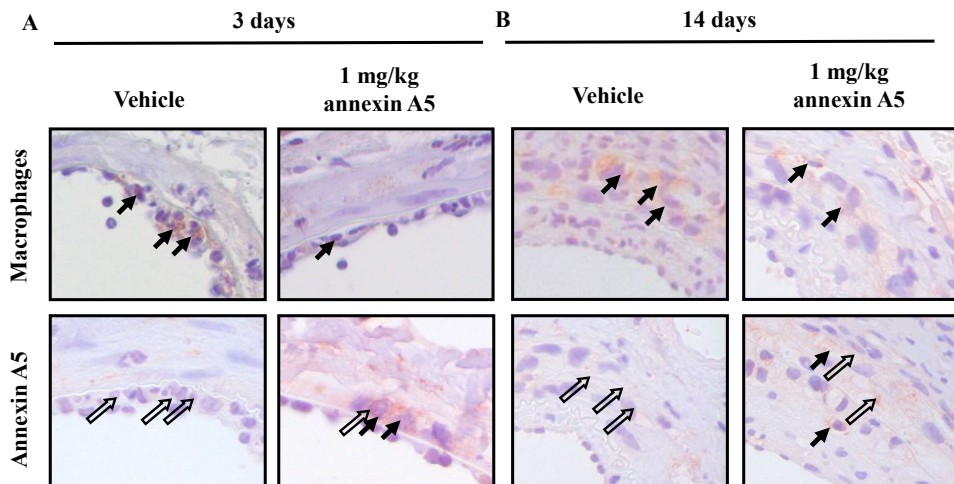


Figure II. Co-localization of injected AnxA5 at macrophage (3d) and macrophage/foam cell (14d) areas after 3d (A) and 14d (B). Representative cross-sections of cuffed arteries of ApoE^{-/-} mice receiving vehicle or 1.0 mg/kg AnxA5 (MAC3 and annexin A5 staining, magnification 80x, closed arrows indicate positive macrophage and AnxA5 staining, open arrows indicate projected macrophages in consecutive slides (5 μ m distance) in annexin A5 stained femoral artery cross-sections to indicate co-localization).

Chapter 6

Optimizing natural occurring IgM antibodies for therapeutic use: inflammatory vascular disease treatment with anti-phosphorylcholine IgG

M.M. Ewing^{1,2,3}, J.C. Karper^{2,3}, M. Nordzell⁴, S.A.P. Karabina⁵, R. Atout⁵, D. Sexton⁶, H. Lettesjö⁷, M.R. de Vries^{2,3}, I. Dahlbom⁴, O. Camber⁴, J. Frostegård⁸, J. Kuiper⁹, E. Ninio⁵, J.W. Jukema^{1,3}, K. Pettersson⁴, P.H.A. Quax^{2,3}

1 Dept. of Cardiology, Leiden University Medical Center (LUMC), Leiden, The Netherlands

2 Dept. of Surgery, LUMC, Leiden, The Netherlands

3 Eindhoven Laboratory for Experimental Vascular Medicine, LUMC, Leiden, The Netherlands

4 Athera Biotechnologies, Stockholm, Sweden

5 INSERM UMRS937, Université Pierre et Marie Curie UPMC-Paris and Faculté de Médecine Pierre et Marie Curie, Paris, France

6 Dyax Corporation, Cambridge, MA, USA

7 Dept. of Women's and Children's Health, Uppsala University Hospital, Uppsala, Sweden

8 Dept. of Medicine, Karolinska University Hospital Huddinge and Karolinska Institutet, Stockholm, Sweden

9 Division of Biopharmaceutics, LACDR, Leiden, The Netherlands

Submitted for publication

Abstract

Background Phosphorylcholine (PC) is an important pro-inflammatory damage associated molecular pattern and natural anti-PC T15 IgM antibodies are both clinical risk markers for cardiovascular diseases and prevent native atherogenesis in mice. For clinical use, however, only IgGs are suitable, but major variability exists in natural anti-PCs IgG effects.

Methods and results Chimeric anti-PC T15 IgG was developed and shown to bind locally to human atherosclerotic tissues. Following immunization of hyperlipidemic ApoE3*Leiden mice undergoing femoral arterial cuff placement to induce vascular inflammation and remodeling, 73.6% reduced atherosclerotic lesion size was observed ($p=0.0003$), with reduced expression of local ER-stress markers and MCP-1 production.

Phage display-library screening led to the development of three fully human monoclonal anti-PC IgG constructs which specifically bound PC and apoptotic cells and prevented both macrophage oxLDL-uptake and their MCP-1 expression in vitro, superiorly to natural anti-PC T15 IgM antibodies. Of these, anti-PC M99-B05 IgG was most effective in vivo by reducing inflammation and atherosclerotic lesion size with 61.4% ($p=0.014$). Germ lining and codon optimization of M99-B05 produced anti-PC X19-A05 IgG, which was as effective as M99-B05 in vivo, even in low dosages.

Conclusions Both chimeric and fully human anti-PC IgGs can prevent post-interventional atherosclerotic lesion formation by inhibiting injury-induced vascular inflammation directly and through reduced macrophage oxLDL-uptake. These could represent a novel strategy for prevention of post-interventional atherosclerotic lesion development.

Introduction

Although treatments for atherosclerosis-induced acute coronary syndromes (ACS) have improved patient outcome greatly in the last decades, there is still much room for improvement, especially for treatment modalities that target increased local vascular inflammatory burden after myocardial infarction¹. In this acute phase, cellular stress and inflammation can lead to the generation of endogenous ligands. These ligands, such as phosphorylcholine (PC), have recently been described as damage associated molecular patterns (DAMPs) that are recognized by the innate immune system². PC is the polar headgroup of the dominating membrane phospholipid phosphatidylcholine. In cellular stress and inflammation as well as during enzymatic and oxidative modification of LDL the fatty acids of phosphatidylcholine, especially the fatty acids in the sn-2 position, are metabolized. Many of these PC containing metabolites (oxPL) have powerful biological effects and are considered important mediators of vascular inflammation. A recent review summarized these effects and concluded that oxPL is a promising therapeutic target³. There are several receptors recognizing PC including proteins, scavenger receptors of phagocytic cells and natural antibodies^{2, 4}. PC recognition has been reported to stimulate a range of responses including endothelial dysfunction, apoptosis, endoplasmatic reticulum (ER)-stress and the unfolded protein response (UPR)^{5, 6}. They all lead to vascular inflammation, eventually responsible for accelerated atherosclerotic lesion formation, often requiring revascularization⁷. Interestingly, there is competition between these receptors and the prototypic natural anti-PC, the murine T15/E06 IgM, is well known to inhibit macrophage binding and uptake of oxLDL through scavenger receptors⁸.

Uptake of oxLDL by vessel wall macrophages is considered as a pro-atherogenic event⁹, while anti-PC has anti-atherosclerotic effects. Immunization leading to high anti-PC levels can prevent native atherosclerosis in mice by inhibition of oxLDL-uptake and inflammatory foam cell formation¹⁰⁻¹². Epidemiological data suggests that IgM anti-PC protects against cardiovascular disease (CVD) development, as low levels of the IgM anti-PC are associated with increased risks for CV events¹³⁻¹⁵. Additionally, ACS patients with low levels of IgM anti-PC have a worse prognosis than patients with higher levels¹⁶. The increased risk was particularly present in the semi-acute phase following ACS, during which there is an elevated systemic inflammatory activity¹⁷. Experimental data shows that the T15/E06 natural antibodies also have profound anti-inflammatory properties unrelated to foam cell formation and enhance clearance of apoptotic cells^{18, 19}. This suggests that they could also be therapeutically effective in the acute injury phase following ACS, during which there is still a high risk for secondary events.

Experimental data has principally been generated using the natural IgM anti-PC. Serum contains anti-PCs of several subclasses²⁰ and not all may be able to block vascular inflammatory processes. Hypertensive patients display an inverse correlation between the progression of carotid artery intima media thickness and IgM anti-PC titers, but not for IgG anti-PCs²¹. While T15 IgM was effective against *Streptococcus* infections in mice, there was major variability in IgG anti-PCs effects²²⁻²⁴. These results indicate that although PC is a chemically defined entity, the presentation of the PC (neo)epitope depends on the local environment and that different IgG anti-PCs may be more specific for the presentation of PC than the natural IgM anti-PC.

IgM antibodies are not suitable for therapeutic use. The aim of this work was to investigate if anti-PC in an IgG format has the potential to block vascular inflammation, and to identify a fully human monoclonal anti-PC that has therapeutic potential. We first generated an anti-PC T15 IgG chimeric antibody that prevented inflammatory vascular disease both *in vitro* and *in vivo*, providing support that anti-PC IgGs are attractive as therapeutic antibodies. We then identified multiple, fully human recombinant anti-PC IgGs by phage-display library screening. These were selected and optimized for their *in vitro* and *in vivo* anti-inflammatory and anti-atherosclerotic effects, with potential to become a new treatment modality against post-interventional vascular remodeling.

Materials and Methods

The materials and methods sections can be found in the online supplements section.

Results

Chimeric anti-PC T15 IgG binds to human atherosclerotic lesions and is effective against vascular inflammation *in vivo*

A chimeric anti-PC T15 IgG antibody was developed, containing the murine T15/E06 variable region and human IgG1 in the constant region, highly specific for PC. Immunohistochemical (IHC) staining with chimeric anti-PC T15 IgG showed strong and specific binding to cells within human aortic atherosclerotic lesions (fig 1a), confirmation of antibody affinity for the target tissue. Next, therapeutic effectiveness of chimeric anti-PC T15 IgG was tested in a well-established mouse model for post-interventional inflammatory vascular disease²⁵. Short term leukocyte recruitment and long-term vascular remodeling were evaluated.

Despite similar plasma total cholesterol concentrations (table 2), chimeric anti-PC T15 IgG (plasma titer 1208 ± 329 $\mu\text{g/ml}$) significantly reduced endothelial-adherence and extravasation of leukocytes (fig 1c) and macrophages (fig 1c) to the injured arterial segments 3d after injury, prior to foam cell development. Furthermore, anti-PC T15 IgG staining displayed strong and specific co-localisation with GRP78 BiP and CHOP expressing cells, suggesting specific binding of T15 IgG to PC-expressing stressed cells within atherosclerotic plaques. Treatment significantly reduced cells displaying ER-stress markers CHOP and GRP78BiP by 73.0% ($p=0.021$, fig 2b) and 54.7% ($p=0.050$, fig 2c) respectively. Together, these results indicate that anti-PC T15 IgG prevents early inflammatory responses, well before the generation of local foam cells²⁶.

Chimeric anti-PC T15 IgG is effective against vascular remodeling *in vivo*

Vascular remodeling was evaluated after 14d treatment (fig 3a) and revealed that despite similar plasma cholesterol levels (table 2), anti-PC T15 IgG significantly prevented intimal thickening by 76.3% ($p=0.0003$, fig 3b) and reduced intima/media ratio by 72.2% ($p=0.000$, fig 3c), luminal stenosis by 60.3% ($p=0.000$, fig 1Ia) and medial thickening by 20.0% ($p=0.050$, fig 1Ib). After 14d, the medial arterial layer displayed a less inflamed phenotype, with a higher proportion of stable SMCs (87.0%,

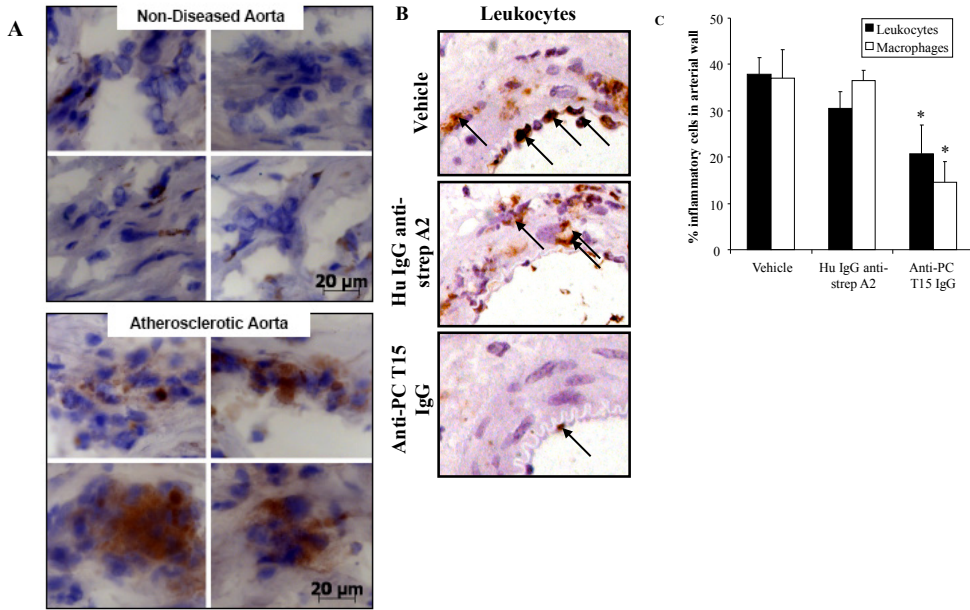


Figure 1 Representative cross-sections of (A) human non-diseased and atherosclerotic aortic tissue (chimeric anti-PC T15 IgG staining, magnification 20x) and of cuffed arteries of ApoE3*Leiden mice receiving vehicle, human anti-streptavidin or anti-PC T15 IgG (B) after 3d (CD45 staining, magnification 80x, arrows indicate leukocytes). Quantification of (C) leukocyte and macrophages (% of total cells). Results indicated as mean±SEM, n=10. * p<0.05.

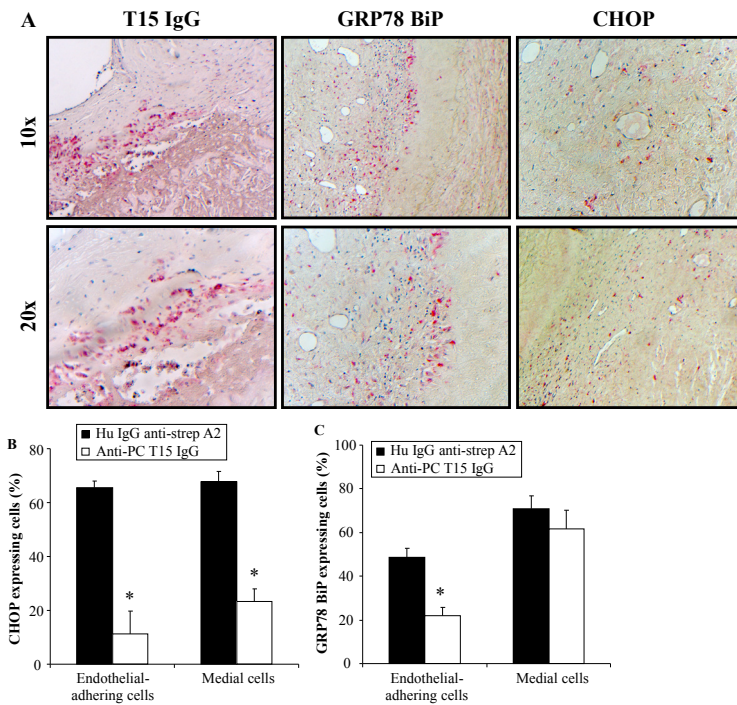
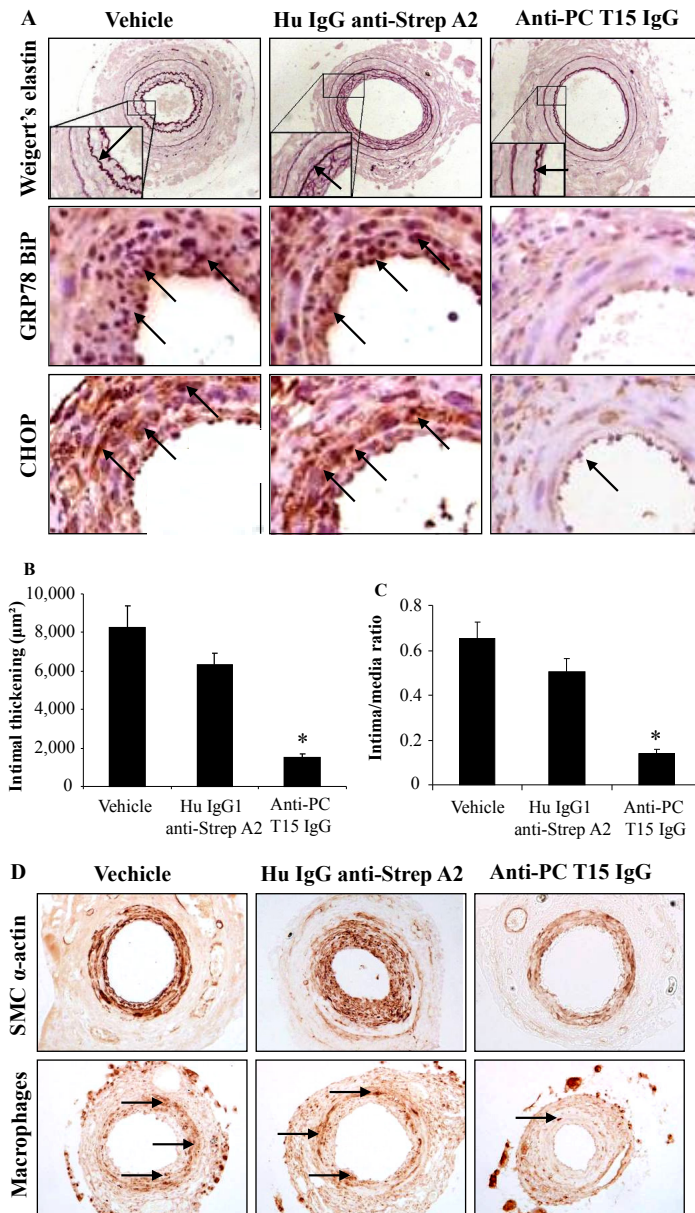


Figure 2 Representative cross-sections of (A) human atherosclerotic coronary arteries (chimeric anti-PC T15 IgG, GRP78 BiP and CHOP staining, magnification 10-20x). Quantification of cuffed arteries of ApoE3*Leiden mice receiving vehicle, human anti-streptavidin or anti-PC T15 IgG after 3d for cells expressing (B) CHOP (% of total cells) and (C) GRP78 BiP (% of total cells). Results indicated as mean±SEM, n=10. * p<0.05.

p=0.016, fig 3e) and 72.2% less macrophages (p=0.000, fig 3f). Anti-PC T15 IgG also reduced leukocyte infiltration in the intima and media by 66.0% (p=0.001, fig 3h) and 74.2% (p=0.002, fig 3i).



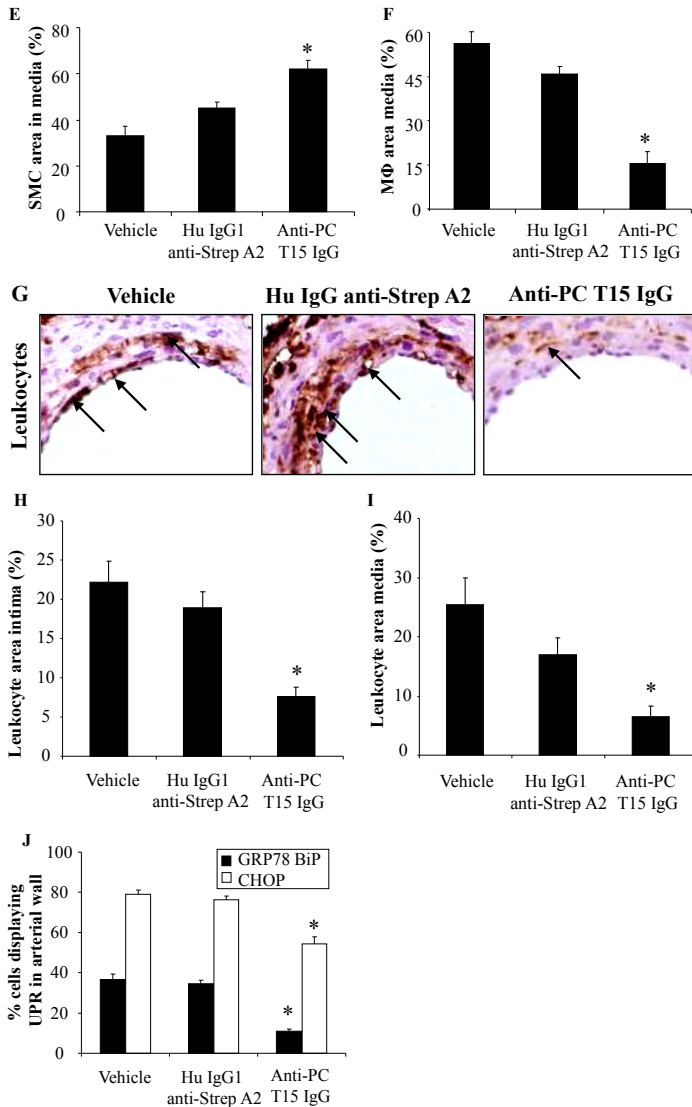


Figure 3 Representative cross-sections of cuffed arteries of ApoE3*Leiden mice receiving vehicle, human anti-streptavidin or anti-PC T15 IgG after 14d (A Weigert's elastin, GRP78 BiP and CHOP staining, D SMC- α actin and MAC3 staining; G CD45 staining; magnification 40-80x). Quantification of (B) intimal thickening (μm^2), (C) intima/media ratio, (E) SMCs in the media (% of total area), (F) macrophages in the media (% of total area), (H) leukocytes in the intima (% of total), (I) leukocytes in the media (% of total) and (J) ER-stressed cells (% of total cells). Results indicated as mean \pm SEM, n=10. * p<0.05.

Furthermore, anti-PC T15 IgG significantly reduced cells displaying ER-stress markers CHOP (absent before injury, fig 1Ic) and GRP78BiP by 31.4% (p=0.0003) and 70.4% (p=0.0003, fig 3j), demonstrating that chimeric anti-PC T15 IgG prevents the inflammatory UPR, involved in inflammatory vascular remodeling.

Unlike murine anti-PC IgM, chimeric anti-PC T15 IgG does not block oxLDL-

uptake by macrophages

Polyclonal IgM and IgG anti-PC obtained from human serum were evaluated to block the uptake of oxLDL particles by macrophages, as the murine T15/E06 IgM natural antibody is known to block this scavenger receptor-mediated uptake¹⁰. As expected, polyclonal anti-PC IgMs showed a dose-dependent (fig IIIa-b) inhibition of Dil-labelled Cu-oxLDL uptake (fig 4a), whereas polyclonal anti-PC IgGs did not (fig 4b). Previously, low concentrations of polyclonal human anti-PC IgG from serum following active immunization was shown to partly inhibit oxLDL-uptake in macrophages¹¹. Similar results were obtained with 20 µg/ml anti-PC IgG, but not with higher concentrations (fig 4c). Cimeric anti-PC T15 IgG also did not prevent Cu-oxLDL uptake by human macrophages (fig 4d).

Unlike IgM, the Fc region of IgG1 bears a highly conserved N-glycosylation site that is essential for Fc receptor-mediated activity by macrophages and could lead to increased antibody-PC complex binding by macrophages and oxLDL-uptake. This possibility was excluded by using both a chimeric anti-PC T15 IgG4 antibody, as IgG4 antibodies are less prone to bind Fc receptors (fig 4d), as well as Fc-receptor blocking anti-CD32 and anti-CD64 antibodies (fig IIIc), through which no blocked oxLDL-uptake was observed. Although effective *in vivo*, at least partly through UPR downregulation, the transfer of the T15/E06 variable region from IgM to IgG format abolished the scavenger receptor blocking effects of chimeric anti-PC T15 IgG.

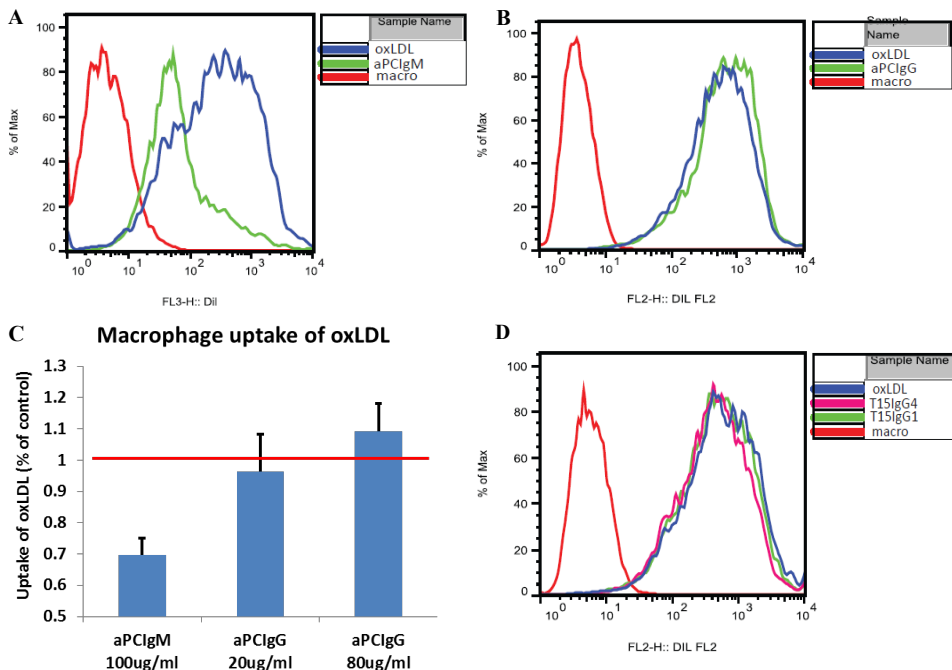


Figure 4 FACS analysis demonstrates that unlike murine anti-PC IgM (A), polyclonal anti-PC IgG does not block oxLDL-uptake by macrophages (B), in both low (20 µg/ml) and high (80 µg/ml) concentrations (C). Both IgG1 and IgG4 antibodies fail to display an inhibiting effect (D), excluding the potential enhanced Fc-receptor-regulated uptake of oxLDL.

Development of monoclonal human anti-PC IgG antibodies

Fully human, monoclonal IgG antibodies against PC were obtained by phage display by panning human Fab fragment displayed libraries²⁷ against either BSA- or ferritin-conjugated PC. Over ten thousand different phage clones were screened by ELISA, which yielded over 1500 positive hits, defined as > 3-fold stronger signal for binding to BSA- or ferritin-conjugated PC compared to streptavidin-coated controls. After DNA sequencing and recombinant reformatting to full length IgG1 51 antibodies with unique amino acid sequences were recovered. Binding specificity was assessed using a Biacore SPR assay to binding to either PC-BSA or a control BSA containing the aminophenol linker that used for the conjugation of PC to BSA, allowing selection of antibodies with likely therapeutic effectiveness, also shown by ELISA (fig 5a). Of these, 27 antibodies with highest signal for binding PC-BSA were investigated for their effects on macrophage oxLDL-uptake. Nine fully human recombinant anti-PC IgG antibodies inhibited oxLDL-uptake similarly or better than polyclonal anti-PC IgM on a weight basis (fig 5b).

These 9 monoclonal IgGs displayed approximately 1000-fold higher binding efficacy to PC than polyclonal IgG anti-PC, as measured in an ELISA (fig 5c). Antibodies M99-B05 and X9-C01, potent inhibitors of oxLDL uptake, were analysed for binding to Cu-oxidized LDL and displayed profound increased binding compared to chimeric anti-PC T15 IgG (fig 5d). The lack of effect of chimeric anti-PC T15 IgG to block oxLDL-uptake is probably explained by the poor binding to oxLDL. The high avidity of the murine IgM T15/E06 to PC compared to IgG isotype probably explains the effectiveness of the IgM isotype anti-PC¹⁸. Antibodies with high apparent affinity for PC and oxLDL were tested for binding to apoptotic Jurkat cells using FACS analysis. Only marginally increased binding to cells considered as early apoptotic (annexin A5+ PI-) compared to normal viable cells was found. Some antibodies, including M99-B05, were found to bind strongly to late apoptotic (annexin A5+ PI+) Jurkat cells (fig 5e-h), while others did not. Four selected antibodies were finally tested for their ability to block oxLDL-induced release of MCP-1 from monocytes and both M99-B05 and X9-C01 effectively blocked this release in a dose-dependent fashion with an IC₅₀ in the 1-3 nM range whilst the other tested antibodies were ineffective (fig 5i). M99-B05 displayed strong and specific binding to human atherosclerotic aortic tissue, unlike HRP streptavidin controls (fig IVa).

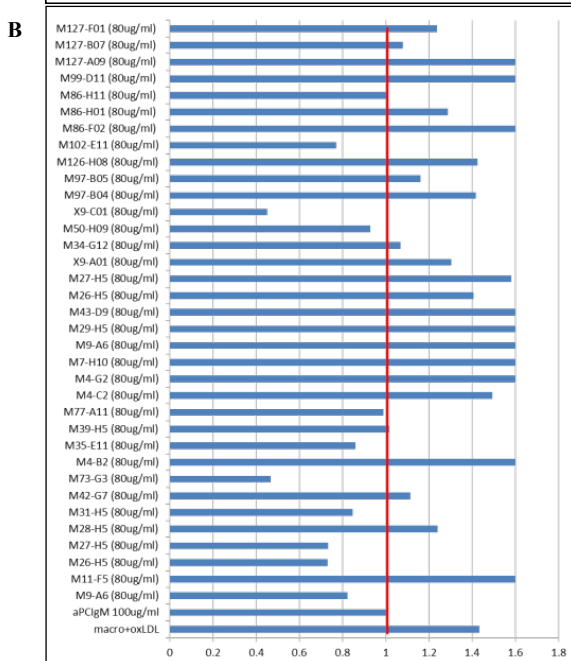
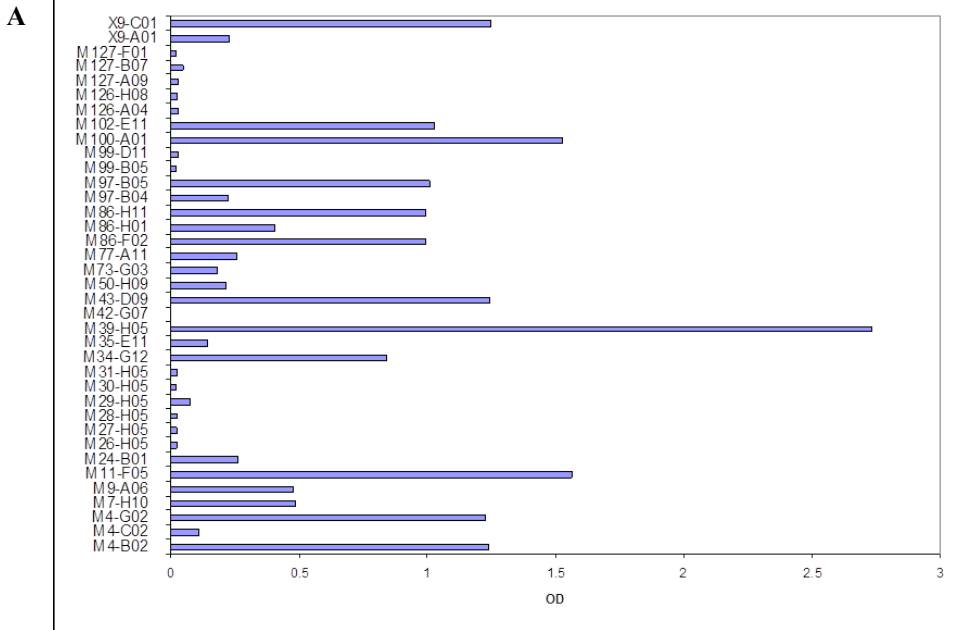
Monoclonal human anti-PC IgGs are effective against vascular inflammation in vivo

The anti-inflammatory properties of X9-C01, M73-G3 and M99-B05 were tested in vivo in the femoral artery cuff mouse model, with chimeric anti-PC T15 IgG, Hu a-strep A2 IgG and sterile water as controls (fig Va). Despite similar plasma lipid concentrations and antibody titers (tables 2, 3), 3d treatment with anti-PC M99-B05 reduced the endothelial-adherence and extravasation of leukocytes by 60.9% (p=0.021), macrophages by 48.9% (p=0.006, fig 6a) and MCP-1 expressing cells by 81.7% (p=0.003, fig 6c), while other antibodies were less effective.

Monoclonal human anti-PC IgG is effective against vascular remodeling in vivo

Despite similar plasma lipid concentrations and antibody titers (table 2, 3), twice weekly immunization with 10mg/kg M99-B05 significantly prevented vascular remo-

deling, with reduced intimal thickening by 61.4% ($p=0.014$, fig 6e), intima/media ratio by 58.3% ($p=0.008$, fig 6f) and outward remodeling by 35.3% ($p=0.039$, fig VIa) after 14d. Luminal stenosis was reduced by 20.7%, although not significantly ($p=0.160$, fig VIb). IHC analysis from human aortic atherosclerotic lesions revealed specific M99-B05 staining (fig 6g) in macrophage-rich areas.



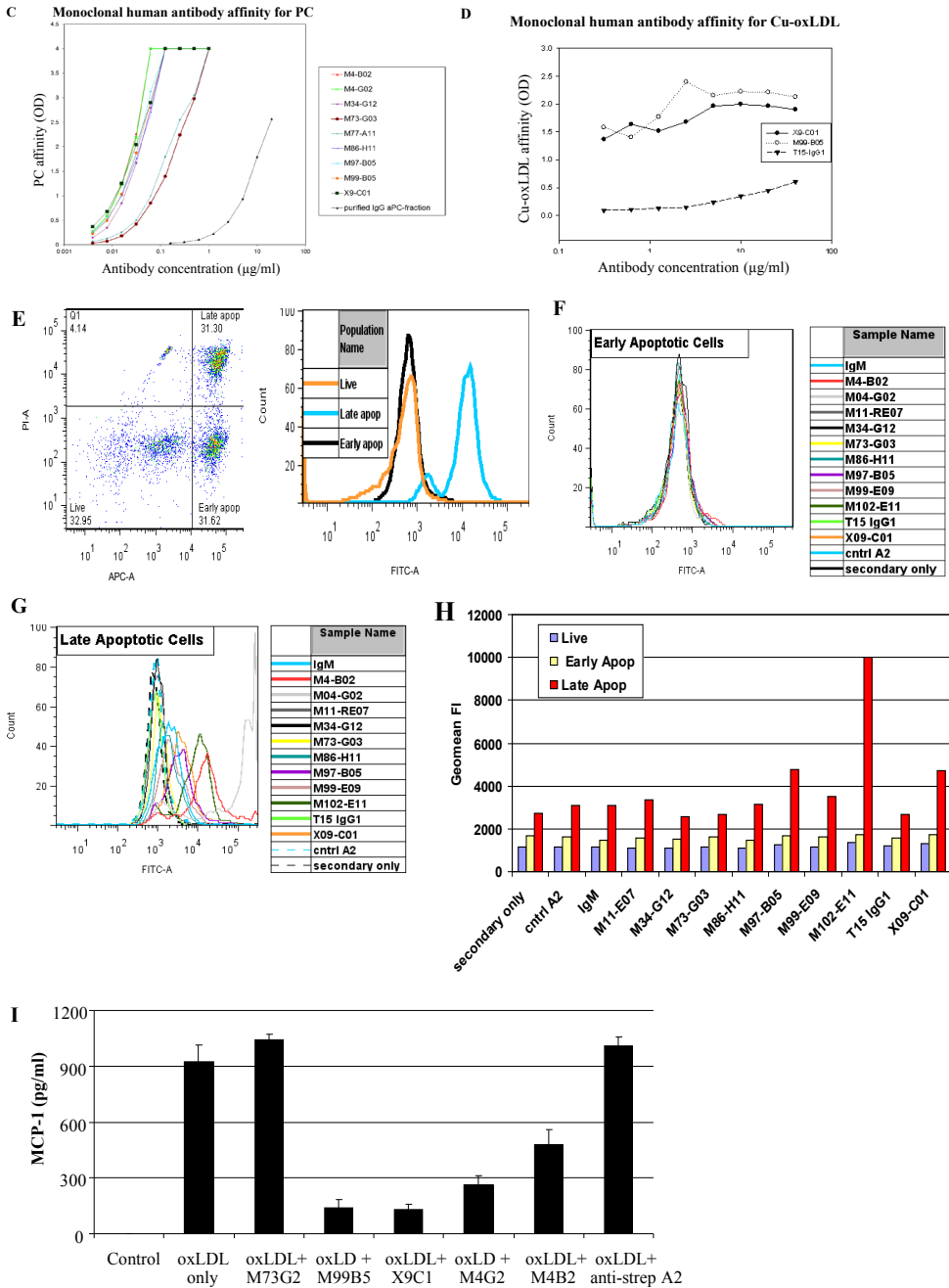


Figure 5 Antibody binding efficacy by 27 clones to BSA-PC (A), inhibitory effects on macrophage oxLDL-uptake of nine selected antibody clones compared to anti-PC IgM (B), and their affinity to PC (C) and oxLDL (D), measured through ELISA (expressed as OD). Of these, 7 antibodies had approximately 1000-fold higher affinity to PC than polyclonal IgG anti-PC. FACS analysis of dot plot showing (E) different cell populations after staurosporine inducing, including live cells (annexin A5-PI-), (F) early apoptotic cells (annexin A5+PI-) and (G) late apoptotic cells (annexin A5+PI+). (H) Mean fluorescent intensity of each cell

population. (I) MCP-1 release assay of human monocytes stimulated with oxLDL alone or in combination with antibody clones (pg/ml) with $IC_{50}=1.8 \pm 0.74$ nM for anti-PC M99B05 IgG.

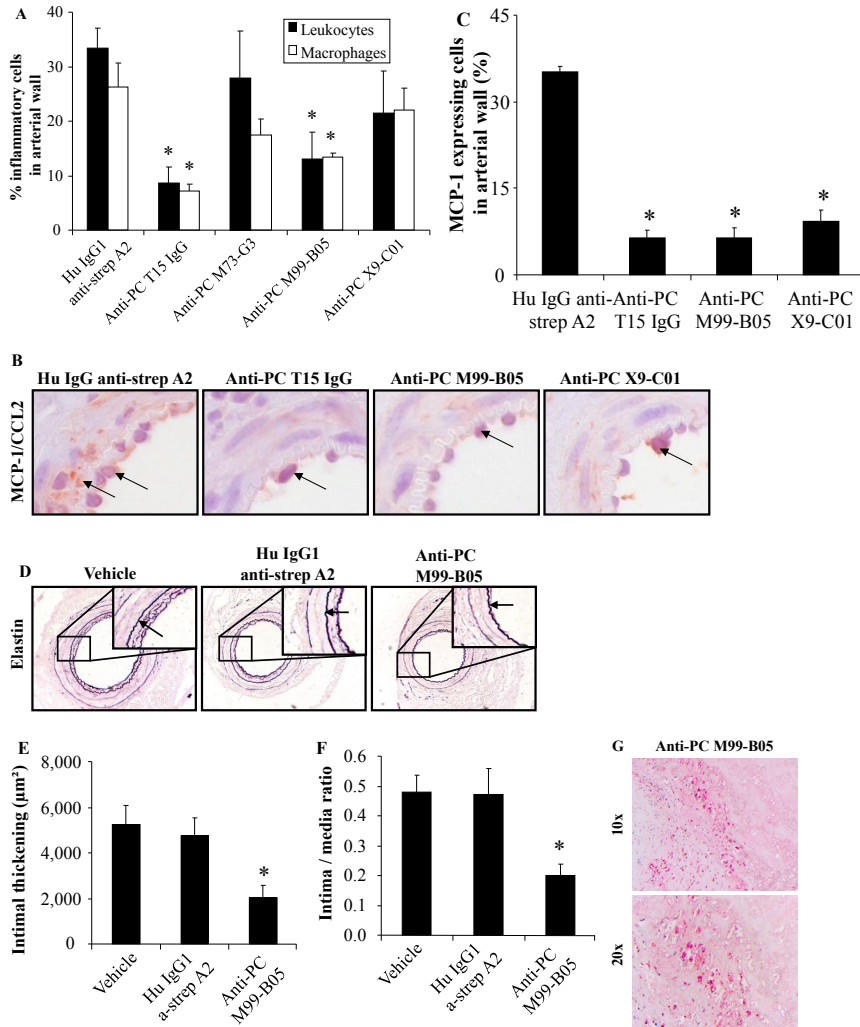


Figure 6 Representative cross-sections of cuffed arteries of ApoE3*Leiden mice receiving human anti-streptavidin, anti-PC T15, M99-B05 or X9-C01 (B) after 3d (MCP-1 staining), (D) 14d (Weigert's elastin staining) or (G) human atherosclerotic coronary artery sections (anti-PC M99-B05 staining, magnification 10-80x). Quantification of after 3d (A) leukocyte and macrophages (% of total cells), and after 14d (C) MCP-1 expressing cells (% of total cells), (E) intimal thickening (μm^2) and (F) intima/media ratio. Results indicated as mean \pm SEM, n=10. * $p < 0.05$.

Optimization of monoclonal human anti-PC M99-B05 into X19-A05

A site-directed mutagenesis study was performed to determine which CDR regions were involved in binding PC, providing insight into the paratope of M99-B05. A 3-D model of M99-B05 was constructed (fig VIIa) together with an amino acid sequence analysis (fig VIIb, c), designed to obtain a full characterization of the antigen-antibody interaction. Western-Blot analysis showed good antibody stability in serum (fig

VIIId, e). Codon optimization produced a series of M99-B05 mutants that had some replacements for potential de-amidation sites constructed. These were tested for the binding to PC (ELISA) and it was observed that some modifications of the M99-B05 antibody negatively affected binding affinity to PC (fig 7a). The mutant X19-A05 was selected as the optimal antibody, as it combines several modifications of M99-B05 while retaining good binding affinity to PC.

X19-A05 anti-PC IgG is effective in vivo in low dosages

Despite similar plasma lipid concentrations and antibody titers (tables 2, 3), 14d treatment with X19-A05 anti-PC in twice weekly 0.5, 2 and 10mg/kg dosages significantly prevented intimal thickening by 40.1% ($p=0.024$), 46.8% ($p=0.014$) and 67.6% ($p=0.000$) respectively, similarly to M99-B05, when compared to Hu a-strep A2 IgG controls (fig 7c), with 10 mg/kg 17.5% more effective ($p=0.031$) than 0.5mg/kg. Versus vehicle, 0.5, 2 and 10m/kg X19-A05 anti-PC reduced reduced the intima / media ratio by 38.9% ($p=0.042$), 39.1% ($p=0.018$) and 56.1% ($p=0.002$, fig VIIIa). In conclusion, the optimized monoclonal X19-A05 anti-PC IgG antibody retained the therapeutic effectiveness of M99-B05 and forms a promising antibody clone for clinical use to prevent post-interventional vascular remodeling.

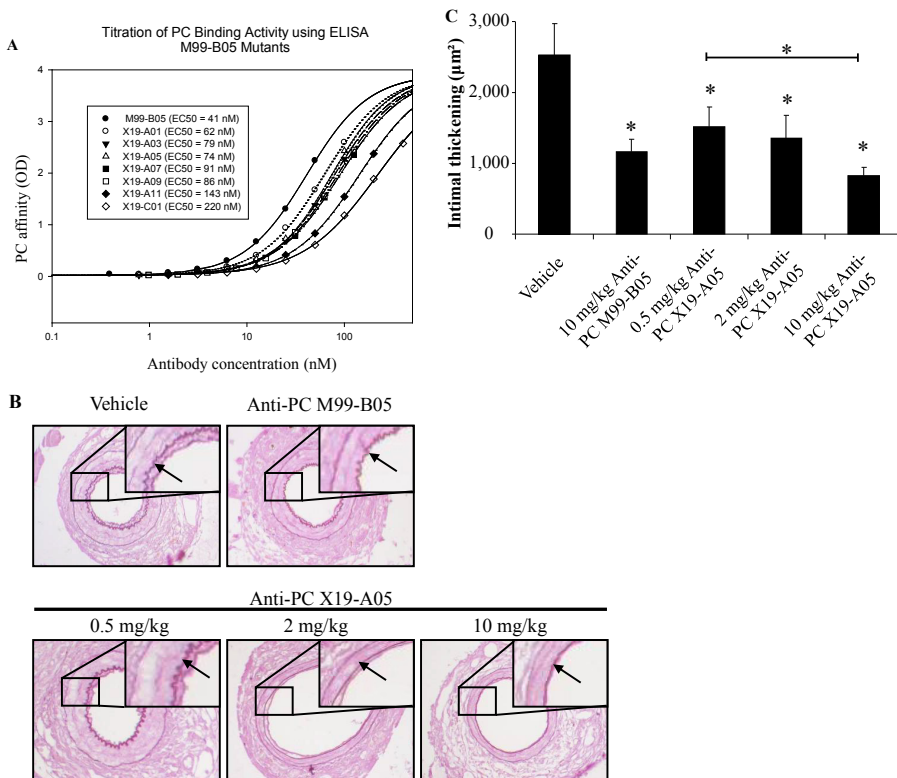


Figure 7 PC-affinity by seven M99-B05 clones, measured by ELISA (expressed as OD) (A). Representative cross-sections (B) of cuffed arteries of ApoE3*Leiden mice receiving human anti-streptavidin, M99-B05 or X19-A05 (0.5, 2, 10mg/kg) after 14d (Weigert's elastin staining, magnification 40x). Quantification of (C) intimal thickening (μm^2). Results indicated as mean \pm SEM, n=10. * $p<0.05$.

Discussion

This study demonstrates for the first time natural anti-PC IgM antibody optimization and therapeutic efficacy of a phage-library display selected monoclonal human anti-PC IgG construct against inflammatory atherosclerotic disease. Passive *in vivo* immunization with chimeric anti-PC T15 IgG prevented inflammatory arterial disease including UPR and atherosclerotic remodeling. Since natural anti-PC IgM antibodies display inhibition of oxLDL-uptake by macrophages and this function was lost by the chimeric anti-PC T15 IgG, monoclonal human anti-PC IgGs were screened for this function. These proved to be effective *in vivo* by profoundly reducing inflammation and atherosclerotic remodeling.

Research into new monoclonal recombinant antibodies is a fast-developing and expanding field and atherosclerotic-related CVDs with high incidence, prevalence and mortality rates¹ are extremely suitable for therapeutic immunization strategies. PC plays a key role as DAMP in the inflammatory reaction in both native atherosclerosis and following vascular intervention strategies. In the latter setting, it has emerged as a promising target for active immunization to prevent vascular remodeling. Until now, successful therapeutic immunization against PC has mostly been on an IgM basis in mice, whilst for clinical application, IgG-based vaccination is preferred²⁸.

Specific chimeric anti-PC T15 IgG binding was observed in human atherosclerotic lesions with distinctive co-localization with regions displaying signs ER stress (fig 1-2a), proving antibody binding to the target tissue. In hyperlipidemic mice, chimeric anti-PC T15 IgG effectively reduced leukocyte and macrophage adherence and extravasation following vascular injury (fig 1c), with notably less MCP-1 expression by adhered and infiltrated leukocytes (fig 1d), clearly showing therapeutic efficacy. Due to hypercholesterolemia, α -actin SMCs display markers of early ER-stress (fig 11b), whilst this progressed to advanced ER-stress and UPR following vascular injury. Defective inflammatory resolution is known lead to the progression of atherosclerotic lesions^{29,30} and by reduction of ER-stress and UPR-induced inflammation, prolonged anti-PC T15 IgG treatment led to retarded occlusive vascular remodeling (fig 3b) and a less inflammatory arterial wall phenotype (fig 3g).

Polyclonal anti-PC IgMs showed an inhibition of oxLDL-uptake by macrophages *in vitro*, whereas polyclonal anti-PC IgGs did not. Similarly, chimeric anti-PC T15 IgG also did not prevent oxLDL-uptake by macrophages *in vitro* (fig 4d), an effect unrelated to Fc receptor-mediated activity in IgG1 antibodies by macrophages, making them unsuitable for clinical use to prevent native atherosclerosis. Post-interventional vascular remodeling however does not primarily result from oxLDL-uptake, but from local cellular (ER) stress and DAMP expression, followed by leukocyte chemotaxis (e.g. through MCP-1) and inflammation. Although this concept supports the chimeric anti-PC T15 IgG effectiveness in the murine vascular injury model, vascular remodeling can be enhanced through oxLDL-uptake by infiltrated macrophages. Since these processes occur simultaneously in the human ACS setting, phage library-display selection was used to screen for monoclonal human anti-PC IgGs that have both anti-inflammatory effects and an ability to block oxLDL-uptake. Recombinant antibody libraries provide a solid basis for the discovery of antibody-based biopharmaceuticals³¹ and are an excellent source of active and well tolerated experimental therapeutics³². IgGs were selected upon their binding capability to PC and apoptotic

cells, as well as their ability to block macrophage oxLDL uptake and MCP-1 expression in vitro (fig 5g). Out of a total 10.660 phage clones, these selection criteria yielded three promising antibody clones, designated M99-B05, X9-C01 and M73-G3.

Only anti-PC M99-B05 significantly reduced leukocyte and macrophage adherence and infiltration in the injured local arterial wall segments (fig 6a), although both M99-B05 and M73-G03 reached high plasma titers, whereas X9-C01 did not. It cannot be excluded that X9-C01 could be effective in similar concentrations, although M73-G3 was clearly ineffective. Despite this, effects of prolonged anti-PC M99-B05 treatment were investigated and displayed reduced vascular thickening, proving its long-term efficacy (fig 6e). In combination with strong local binding to atherosclerotic human arterial segments (fig 6g), this makes the anti-PC M99-B05 clone a promising therapeutic antibody for clinical use.

To increase production efficacy, reduce immunogenicity and increase antibody stability in serum, codon optimization of M99-B05 anti-PC was performed. PC-affinity assays and in vivo application clearly showed preserved PC-affinity and therapeutic efficacy (fig 8b), even in low dosages (2mg/kg/twice weekly).

The limited time period (14d) of antibody exposure was used to minimize the generation of murine anti-human IgG antibodies, although their development cannot be ruled out. Furthermore, despite in vitro and in vivo therapeutic effectiveness, murine results cannot be extrapolated to the human situation automatically. Nevertheless, anti-PC X19-A05 IgG has been shown to be a promising therapeutic tool.

The present findings show that PC is a promising therapeutic target in the prevention of accelerated atherosclerosis development, suitable for passive therapeutic immunization with recombinant monoclonal antibodies. By providing direct control of the patient's immune response with restriction to a single immunogenic epitope, this immunization approach could prove to be an effective treatment modality against CVD in patients.

Reference List

1. Lloyd-Jones D, Adams R, Carnethon M, et al. Heart disease and stroke statistics--2009 update: a report from the American Heart Association Statistics Committee and Stroke Statistics Subcommittee. *Circulation* 2009; 119:480-6.
2. Miller YI, Choi SH, Wiesner P, et al. Oxidation-specific epitopes are danger-associated molecular patterns recognized by pattern recognition receptors of innate immunity. *Circ Res* 2011; 108:235-48.
3. Lee S, Birukov KG, Romanoski CE, Springstead JR, Lusis AJ, Berliner JA. Role of phospholipid oxidation products in atherosclerosis. *Circ Res* 2012; 111:778-99.
4. Binder CJ, Shaw PX, Chang MK, et al. The role of natural antibodies in atherogenesis. *J Lipid Res* 2005; 46:1353-63.
5. Gargalovic PS, Gharavi NM, Clark MJ, et al. The unfolded protein response is an important regulator of inflammatory genes in endothelial cells. *Arterioscler Thromb Vasc Biol* 2006; 26:2490-6.
6. Gora S, Maouche S, Atout R, et al. Phospholipolyzed LDL induces an inflammatory response in endothelial cells through endoplasmic reticulum stress signaling. *FASEB J* 2010; 24:3284-97.
7. Pires NM, Jukema JW, Daemen MJ, Quax PH. Drug-eluting stents studies in mice: do we need atherosclerosis to study restenosis? *Vascul Pharmacol* 2006; 44:257-64.
8. Horkko S, Bird DA, Miller E, et al. Monoclonal autoantibodies specific for oxidized phospholipids or oxidized phospholipid-protein adducts inhibit macrophage uptake of oxidized low-density lipoproteins. *J Clin Invest* 1999; 103:117-28.
9. Marleau S, Harb D, Bujold K, et al. EP 80317, a ligand of the CD36 scavenger receptor, protects apolipoprotein E-deficient mice from developing atherosclerotic lesions. *FASEB J* 2005; 19:1869-71.
10. Binder CJ, Horkko S, Dewan A, et al. Pneumococcal vaccination decreases atherosclerotic lesion formation: molecular mimicry between *Streptococcus pneumoniae* and oxidized LDL. *Nat Med* 2003; 9:736-43.
11. Caligiuri G, Khallou-Laschet J, Vandaele M, et al. Phosphorylcholine-targeting immunization reduces atherosclerosis. *J Am Coll Cardiol* 2007; 50:540-6.
12. Faria-Neto JR, Chyu KY, Li X, et al. Passive immunization with monoclonal IgM antibodies against phosphorylcholine reduces accelerated vein graft atherosclerosis in apolipoprotein E-null mice. *Atherosclerosis* 2006; 189:83-90.
13. de FU, Su J, Hua X, et al. Low levels of IgM antibodies to phosphorylcholine predict cardiovascular disease in 60-year old men: Effects on uptake of oxidized LDL in macrophages as a potential mechanism. *J Autoimmun* 2009.
14. Gronlund H, Hallmans G, Jansson JH, et al. Low levels of IgM antibodies against phosphorylcholine predict development of acute myocardial infarction in a population-based cohort from northern Sweden. *Eur J Cardiovasc Prev Rehabil* 2009; 16:382-6.
15. Sjoberg BG, Su J, Dahlbom I, et al. Low levels of IgM antibodies against phosphorylcholine-A potential risk marker for ischemic stroke in men. *Atherosclerosis* 2009; 203:528-32.
16. Caidahl K, Hartford M, Karlsson T, et al. IgM-phosphorylcholine autoantibodies and outcome in acute coronary syndromes. *Int J Cardiol* 2012.
17. Ridker PM, Cannon CP, Morrow D, et al. C-reactive protein levels and outcomes after statin therapy. *N Engl J Med* 2005; 352:20-8.
18. Chang MK, Binder CJ, Miller YI, et al. Apoptotic cells with oxidation-specific epitopes are immunogenic and proinflammatory. *J Exp Med* 2004; 200:1359-70.
19. Chou MY, Fogelstrand L, Hartvigsen K, et al. Oxidation-specific epitopes are dominant targets of innate natural antibodies in mice and humans. *J Clin Invest* 2009; 119:1335-49.
20. Sampi M, Veneskoski M, Ukkola O, Kesaniemi YA, Horkko S. High plasma immunoglobulin (Ig) A and low IgG antibody titers to oxidized low-density lipoprotein are associated with markers of glucose metabolism. *J Clin Endocrinol Metab* 2010; 95:2467-75.
21. Su J, Georgiades A, Wu R, Thulin T, de FU, Frostegard J. Antibodies of IgM subclass to phosphorylcholine and oxidized LDL are protective factors for atherosclerosis in patients with hypertension. *Atherosclerosis* 2006; 188:160-6.
22. Gearhart PJ, Johnson ND, Douglas R, Hood L. IgG antibodies to phosphorylcholine exhibit more diversity than their IgM counterparts. *Nature* 1981; 291:29-34.
23. Briles DE, Forman C, Hudak S, Clafin JL. Anti-phosphorylcholine antibodies of the T15 idiotype

24. are optimally protective against *Streptococcus pneumoniae*. *J Exp Med* 1982; 156:1177-85.
24. Szu SC, Clarke S, Robbins JB. Protection against pneumococcal infection in mice conferred by phosphocholine-binding antibodies: specificity of the phosphocholine binding and relation to several types. *Infect Immun* 1983; 39:993-9.
25. Ewing MM, de Vries MR, Nordzell M, et al. Annexin A5 therapy attenuates vascular inflammation and remodeling and improves endothelial function in mice. *Arterioscler Thromb Vasc Biol* 2011; 31:95-101.
26. Lardenoye JH, Delsing DJ, de Vries MR, et al. Accelerated atherosclerosis by placement of a perivascular cuff and a cholesterol-rich diet in ApoE*3Leiden transgenic mice. *Circ Res* 2000; 87:248-53.
27. Hoet RM, Cohen EH, Kent RB, et al. Generation of high-affinity human antibodies by combining donor-derived and synthetic complementarity-determining-region diversity. *Nat Biotechnol*. 2005;23:344-8.
28. Beck A, Wurch T, Bailly C, Corvaia N. Strategies and challenges for the next generation of therapeutic antibodies. *Nat Rev Immunol* 2010; 10:345-52.
29. Tabas I. The role of endoplasmic reticulum stress in the progression of atherosclerosis. *Circ Res* 2010; 107:839-50.
30. Tabas I. Macrophage death and defective inflammation resolution in atherosclerosis. *Nat Rev Immunol* 2010; 10:36-46.
31. Hoogenboom HR. Selecting and screening recombinant antibody libraries. *Nat Biotechnol* 2005; 23:1105-16.
32. Lonberg N. Fully human antibodies from transgenic mouse and phage display platforms. *Curr Opin Immunol* 2008; 20:450-9.

Supplemental material

Methods

Cell cultures

Peripheral blood mononuclear cells (PBMCs) were isolated from citrated human blood using Ficoll-Paque PLUS (GE Healthcare) according to the instructions of the manufacturer. Monocytes were resuspended in serum free RPMI 1640 medium at density of 8×10^5 cells/ml and 250 μ L cell suspension was added into wells of a 96-well plate (2×10^5 cells/well). PBMC cells were treated with 2 μ g/mL Ox-LDL (Kalen Biomedical) in the presence or absence of up to 40 nM anti-PC IgG for 40 hours at 37°C, 5% CO₂.

Preparation and characterization of chimeric anti-PC T15 IgG

Anti-PC T15-IgG was constructed by synthesizing the DNA encoding the mouse variable regions and cloning the heavy and light chains into two different IgG expression vectors. To generate an IgG1 chimera the variable regions were cloned into an IgG1 expression vector, pRH1-f-CHO¹, such that the final antibody contains a fully human IgG1 Fc fragment consisting of human CH1, CH2, and CH3 with a mouse variable region. The heavy chain was cloned using the restriction enzymes BstXI and NheI and the light chain is cloned using the restriction enzymes ApalI and AsclI. The resulting T15-IgGs are mouse/human chimeras that contains mouse heavy and light variable regions and a human Fc region. The T15-IgG1 antibody was transiently expressed in 293T (human kidney) cells using FugeneHD (Roche) as the transfection reagent using Corning® CellStack® chambers (6360 cm² cell growth area). After 10 days of expression, the supernatant was harvested and antibody was initially purified using protein A sepharose (MabSelect, GE Healthcare) in which approximately 2.5 L of clarified cell culture media was applied (2 mL/min) over a 4.2 mL column equilibrated in PBS, washed with PBS containing an additional 0.4 M NaCl, and eluted with 50 mM Sodium Citrate, pH: 3.2. The pH of the eluted protein was adjusted to 5.0 and applied to a Poros HS (Applied Biosystems) ion exchange column (4.0 mL bed volume) at 2 mL/min equilibrated in 50 mM NaAcetate, pH: 5.0 and eluted with a linear gradient over 10 column volumes to 50 mM NaAcetate, 0.5 M NaCl, pH: 5.0. Eluted antibodies were buffer exchanged into Antibody Formulation Buffer (0.1 M citrate-phosphate, 50 mM NaCl, 0.01% Tween-80, 2% Trehalose, pH 6.0). Antibody concentrations were determined on purified samples by absorbance at 280 nm (1 mg/mL = 1.4 O.D.).

Mice

All animal experiments were approved by the Institutional Committee for Animal Welfare of the Leiden University Medical Center (LUMC). Transgenic male C57BL/6 ApoE*3-Leiden mice (bred in our own laboratory), aged 10-12 weeks at the start of a dietary run-in period, were used for this experiment.

Diets

Animals were fed a cholesterol-rich high-fat diet to induce hypercholesterolemia

containing 0.05% cholate (to improve intestinal cholesterol uptake and suppress bile acid synthesis, both leading to increased plasma cholesterol levels) and 1% cholesterol (as well as 20% casein, 1% choline chloride, 0.2% methionine, 15% cocoa butter, 40.5% sucrose, 10% cornstarch, 1% corn oil, 5.1% cellulose and 5.1% mineral mixture) (AB Diets). They received the diet three weeks prior to surgery and the diet was continued throughout the entire experiment. All animals received food and water ad libitum during the entire experiment.

Route of administration and treatment protocol

For all experiments, mice received intraperitoneal injections with antibody solutions (Dyax Corporation) in a volume of 100 μ l, using 100 μ l sterile 0.9% w/v NaCl (vehicle) as control, injected at the time of surgery (3 days) or twice weekly (14 days).

Vascular injury and accelerated atherosclerosis model²

After three weeks of diet, mice were anesthetized before surgery with a combination of Midazolam (5 mg/kg, Roche), Medetomidine (0.5 mg/kg, Orion) and Fentanyl (0.05 mg/kg, Janssen) through intraperitoneal injection. The right femoral artery was isolated and sheathed with a rigid non-constrictive polyethylene cuff (Portex) with 0.40 mm inner diameter, 0.80 mm outer diameter and an approximate length of 2.0 mm). Mice were sacrificed 3 or 14 days after cuff placement. For this, mice were anesthetized as before and euthanized.

The thorax was opened and mild pressure-perfusion (100mm Hg) with 3.7% formaldehyde in water (w/v) was performed for 5min by cardiac puncture in the left ventricle. After perfusion, the cuffed femoral artery was harvested, fixed overnight in 3.7% formaldehyde in water (w/v) and paraffin-embedded. Serial cross-sections (5 μ m thick) were taken from the entire length of the artery for histological analysis.

Immunoassays

After three weeks of diet (one day before surgery) and at the time of euthanasia, EDTA plasma samples were taken from the tail vein to determine total plasma cholesterol. Total plasma cholesterol (Boehringer Mannheim GmbH, kit 236691) concentration was measured enzymatically. Before surgery, mice were randomized in groups based on their total plasma cholesterol level. Enzyme-linked immuno sorbent assays (ELISA) were used to determine antibody titers. MCP-1 in cell supernatant was detected using the MCP-1 ELISA kit (R&D Systems), according to the manufacturer's instructions.

Vascular lesion quantification

The number of leukocytes, macrophages and cells expressing MCP-1, GRP78 BiP and CHOP attached to the endothelium or in the media of the femoral arteries was quantified and is displayed as a percentage of the total number of present cells. All quantification in this study was performed on six equally spaced (150 μ m distance) serial stained perpendicular cross-sections throughout the entire length of the vessel and was performed by blinded observers. Using image analysis software (Leica Qwin), the area containing SMCs and macrophages grafts was quantified morphometrically and is expressed as a percentage of the total cross-sectional vessel wall layer area. Additionally, total cross-sectional medial area was measured between

the external and internal elastic lamina and total cross-sectional intimal area was measured between the lumen and the internal elastic lamina.

Immunohistochemical stainings

Murine samples

All samples were stained with hematoxylin-phloxine-saffron (HPS). Weigert's elastin stain was used to visualize elastic laminae. Vessel wall sections undergoing immunological staining were pre-treated with a peroxidase block to decrease background staining due to endogenous peroxidase and with a concentrated solution of bovine serum albumin to block the adsorption of other proteins to non-specific binding sites on the vessel wall. Afterwards the primary antibody was added to the sections, left overnight and washed before the second antibody, specific to the primary antibody, was applied. After rinsing, an Avidin-Biotinylated enzyme complex was added to increase the sensitivity of the later to be added peroxidase Nova Red substrate, used as chromogen for colour development. Leukocytes were detected with the use of anti-CD45 antibodies (dilution 1:200, Pharmingen). Smooth muscle cells were stained with the use of anti-smooth muscle α -actin antibodies (dilution 1:800, Dako) and macrophages were detected with MAC3 staining (dilution 1:200, Pharmingen). MCP-1 expression was determined with the use of anti-mouse MCP-1 antibodies (dilution 1:300, Santa Cruz Biotechnology). The presence of ER stress and UPR was evaluated with antibodies against GRP78 BiP (GRP78 BiP, dilution 1:200, Abcam) and against CHOP (GADD153, dilution 1:200, Abcam).

Human aortic samples

The Tissue MicroArrays (TMA) included 20 aortic samples with atherosclerotic plaques from different individuals. The classification of the lesions was performed according to Stary³. For each lesion three representative areas were selected from hematoxylin- and eosin-stained sections of a donor block. Core cylinders (diameter: 0.6 mm) were punched and deposited into a recipient paraffin block using a specific arraying device (Beecher Instruments, Alphelys ring, MD)⁴. 5 μ m TMA sections were used for IHC analyses using digital slides (magnification 40) of each TMA spot which were acquired using Aperio ScanScope CS-US.

IHC was performed by using standard protocols with the following commercial primary antibodies directed against: CD68 (Dako; 1:500), alpha AML (Dako; 1:500), CD34 (Dako; 1:100), GRP78 (Abcam; 1:100) and ATF3 (Santa Cruz Biotechnology; 1:200) and noncommercial primary antibodies T15 (1:500) and M99 (1:50000). Briefly, IHC was performed on 5- μ m sections of TMA blocks. Deparaffinized and rehydrated sections were incubated for 30 min at room temperature with primary antibodies, washed, and incubated for 30 minutes with a Multilink kit (Biosys) for polyclonal antibodies and ABC Vector kit (Biosys) for monoclonal antibodies. After washing, the alkaline phosphatase/anti-alkaline phosphatase complexes and Fast Red TR substrate (Dako) or Ultravision LP detection System HRP DAB (MICROM) were added. Slides were counterstained with aqueous hematoxylin and mounted with Immunomount (Shandon).

Phage display selections

Phage display selections were performed using PC conjugated to bovine serum albumin (BSA) and to transferrin (Isosep AB) through a para-aminophenol linker using

isothiocyanate reaction chemistry. PC-BSA was produced at molar PC/BSA ratios of 1.4, 2.9, 5.7, and 22 mol PC/mol BSA. PC-transferrin was similarly prepared to contain 52 mol PC/mol transferrin. BSA was also reacted with just the para-aminophenol linker to serve as a reagent to remove antibody binders to the linker group from selected antibodies. PC modified BSA, PC modified transferrin, and linker modified BSA were biotinylated using EZ Link NHS-PEG4-Biotin (Pierce) to give molar incorporation ratios between 2 and 8 mol biotin per mol protein. Free biotinylation reagent was removed by dialysis against phosphate buffered saline (137 mM NaCl, 2.7 mM KCl, 4.3 mM Na₂HPO₄, 1.47 mM KH₂PO₄, pH 7.4). Biotinylation incorporation was determined using the 2-(4'-hydroxyazobenzene) benzoic acid (HABA) method according to the manufacturer (Pierce).

Phage display selections were performed using previously described antibody phage display procedures⁴ and antibody phage display libraries that combine natural and synthetic diversity⁵. Selections were initiated by first depleting the library of antibody binders to BSA, transferrin or the linker by incubating the library with the biotinylated depletion proteins immobilized on streptavidin coated magnetic beads (Invitrogen). The supernatant from the depletion step was then titered and incubated with biotinylated PC-protein conjugates that were immobilized on streptavidin coated magnetic beads (input titer in first round $\sim 2 \times 10^{12}$ pfu). Selection strategies alternated between panning on biotinylated PC-BSA in one round with panning on biotinylated PC-transferrin in the next round. Alternative selection strategies involved selecting on the same biotinylated PC-modified protein in each round. Prior to exposing the amplified phage from each selection round the phage were depleted using the biotinylated carrier protein in the absence of PC. In the case of selections on PC-BSA, the phage particles were first depleted with biotinylated BSA that contained the para-aminophenol linker molecule used to couple PC to BSA. Phage outputs after between 2 to 4 rounds of selection were isolated as individual phage isolates and screened for PC binding by phage ELISA.

Individual phage isolates were picked as colonies, grown overnight and the supernatant used in an ELISA to detect binding to biotinylated PC-BSA or biotinylated PC-transferrin immobilized on streptavidin coated plates as previously described using HRP-labeled anti-M13 and TMB substrate². ELISA positive hits were identified as having a target signal over background ratio greater than 3, where the target signal is the absorbance observed with target PC-BSA and PC-transferrin and the background is the signal observed with linker-BSA or transferrin, respectively. A total of 10560 phage clones was screened by ELISA to yield 1511 ELISA positive hits, which were subsequently found by DNA sequencing (Applied Biosystems 3730) to consist of 54 different antibody sequences.

IgG reformatting, expression and purification

The 54 different anti-PC antibodies were converted by batch sub-cloning the Fab fragments displayed on gene III of M13 phage into the pBRH1-f vector for the transient expression of fully human IgG1 (f-allotype) in 293T cells as previously described⁴. A total of 49 out of the 54 unique anti-PC antibodies were successfully recovered after batch sub-cloning and DNA sequencing as full length IgG1 antibodies. The remaining 5 antibodies were not recovered by DNA sequencing and were not pursued further.

DNA for each of the 49 IgGs was prepared from *E. coli* (DH5 α) using plasmid purification kits (Qiagen) and transfected into human kidney 293T cells to transiently generate IgG after a 10 day media harvest in a T175 flask. Purified IgG was recovered after a single step protein A sepharose (MabSelect, GE Healthcare) for 41 IgGs; the remaining 8 antibodies were either poorly expressed or not well purified and were consequently not pursued further. The 41 IgGs purified by protein A sepharose chromatography were used for *in vitro* binding studies (SPR and ELISA analysis). The IgGs with superior *in vitro* binding properties were produced in larger quantities for testing in *in vivo* animal as well as *in vitro* cell culture experiments and purified using both protein A sepharose and ion exchange chromatography as described above for the T15-IgG.

SPR analysis

IgGs were screened for binding to PC using a surface plasmon resonance (SPR) biosensor (Biacore 3000). Aminophenylphosphorylcholine (Biosearch Technologies) was coupled through the free amine group to one flow cell of a CM5 chip to a density of 120 RU. To another flow cell of the same CM5 chip the counter screen reagent 4-aminophenyl phosphate (Gold Biotechnology) was amine coupled to a density of approximately 120 RU. PC-KLH (Biosearch Technologies) and PC-BSA were also coupled to separate flow cells of a CM5 chip. Using these surfaces with PC immobilized in different contexts, the antibodies were injected at 100 nM at 50 μ L/min and binding sensorgrams were obtained. Binding was assessed by recording the signal at the end of the injection.

Antibody binding assays

Oxidized LDL (5 μ g) was coated on the surface of a 384-well ELISA in PBS by overnight incubation at 4°C. The plate was blocked with 2% BSA and washed 5 times with PBST before 50 μ L of the antibody at different concentrations was added. Unbound antibody was removed by washing with PBST and bound antibody was detected using a 1:5000 dilution of HRP labeled goat anti-human IgG, Fc- γ specific secondary antibody with a TMB colorimetric substrate.

Apoptotic cell binding assays

Jurkat T cells (ATCC) were cultured in RPMI 1640 media supplemented with 10% FBS, penicillin (100 U/mL) and streptomycin (100 μ g/mL). Cells were harvested by centrifugation, washed with ice-cold PBS and aliquoted into wells of a 96-well plate. Cells were blocked with 5% BSA in PBS at 4°C for 30 minutes prior to incubation with anti-PC antibodies at a concentration of 20 μ g/mL in PBS containing 5% BSA at 4°C for an additional 30 minutes. A recombinant human IgG1 (A2) with a binding specificity towards streptavidin was used as an isotype control. After washing with PBS containing 5% BSA, cells were incubated with the secondary antibody (FITC-conjugated goat anti-human IgA, IgG, or IgM, Thermo) at a dilution of 1:50 in PBS containing 5% BSA. Prior to washing the cells, 5 μ L of APC- annexin V antibody (BD Biosciences) was added. After the cells were washed, they were resuspended cells in PBS with 5% BSA and 1 μ L of 1 mg/mL propidium iodide per sample. Cells were analyzed by flow cytometry using the LSRII instrument from BD Biosciences.

Construction of germline and stability mutants of anti-PC M99-B05 IgG

The amino acid sequence of the M99-B05 anti-PC IgG was inspected in order to identify potential amino acid substitutions that could reduce potential immunogenicity of the antibody in human and avoid susceptible amino acid modification that may occur during antibody expression and purification. Substitutions that could make the antibody less immunogenic were identified by aligning the amino acid sequence of M99-B05 with the most closely related germline antibody sequence from the Kabat database. The heavy chain of M99-B03 was compared to the VH3-23, JH3 heavy chain and the light chains were compared to the VK4-B3, JK1 light chain germline sequence. The variant X19-A05 incorporates a total of 9 mutations that include germline substitutions as well as substitution to remove potential deamidation sites. The X19-A05 was transiently expressed and purified as described above for antibodies to be tested in in vivo experiments.

Statistical analysis

All data are presented as mean \pm standard error of the mean (SEM), unless otherwise indicated. Overall comparisons between data from groups were performed using the Kruskal-Wallis test. If a significant difference was found, groups were compared using a Mann-Whitney sum test. All statistical analyses were performed with SPSS 16.0 software for Windows. P-values less than 0.05 were regarded as to be statistically significant and are indicated with an asterisk (*).

Reference List

1. Jostock T, Vanhove M, Brepoels E, et al. Rapid generation of functional human IgG antibodies derived from Fab-on-phage display libraries. *J Immunol Methods* 2004; 289:65-80.
2. Ewing MM, de Vries MR, Nordzell M, et al. Annexin A5 therapy attenuates vascular inflammation and remodeling and improves endothelial function in mice. *Arterioscler Thromb Vasc Biol* 2011; 31:95-101.
3. Stary, H. C., Chandler, B. A., Glagov, S., et al. A definition of initial, Fatty Streak, and Intermediate Lesion of Atherosclerosis. *Arterioscler Thromb* 1994;14:840-56.
4. Richter, J., Wagner, U., Kononen, J., et al. High-throughput tissue microarray analysis of cyclin E gene amplification and overexpression in urinary bladder cancer. *Am J Pathol* 2000;157:787-94.
5. Buckler DR, Park A, Viswanathan M, Hoet RM, Ladner RC. Screening isolates from antibody phage-display libraries. *Drug Discov Today* 2008; 13:318-24.
6. Hoet RM, Cohen EH, Kent RB, et al. Generation of high-affinity human antibodies by combining donor-derived and synthetic complementarity-determining-region diversity. *Nat Biotechnol* 2005; 23:344-8.

Supplemental figures

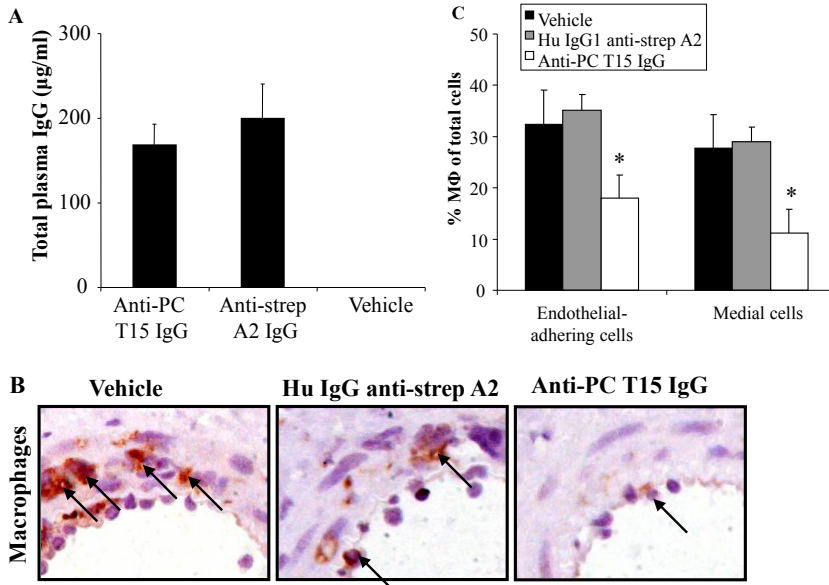


Figure I (A) Total plasma antibody IgG concentration (µg/ml) of ApoE3*Leiden mice receiving vehicle, human anti-streptavidin or anti-PC T15 IgG after 3d. (B) Representative cross-sections (MAC3 staining, magnification 80x). (C) Quantification of macrophages in the intima and media (% of all cells). Results indicated as mean±SEM, n=10. * p<0.05.

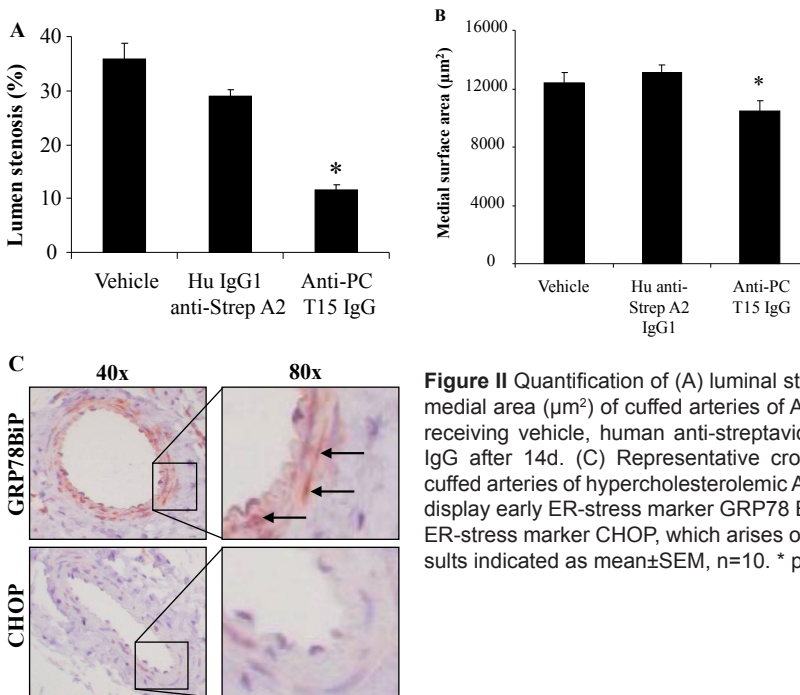


Figure II Quantification of (A) luminal stenosis (%) and (B) medial area (µm²) of cuffed arteries of ApoE3*Leiden mice receiving vehicle, human anti-streptavidin or anti-PC T15 IgG after 14d. (C) Representative cross-sections of uncuffed arteries of hypercholesterolemic ApoE3*Leiden mice display early ER-stress marker GRP78 BiP, but not the late ER-stress marker CHOP, which arises only after injury. Results indicated as mean±SEM, n=10. * p<0.05.

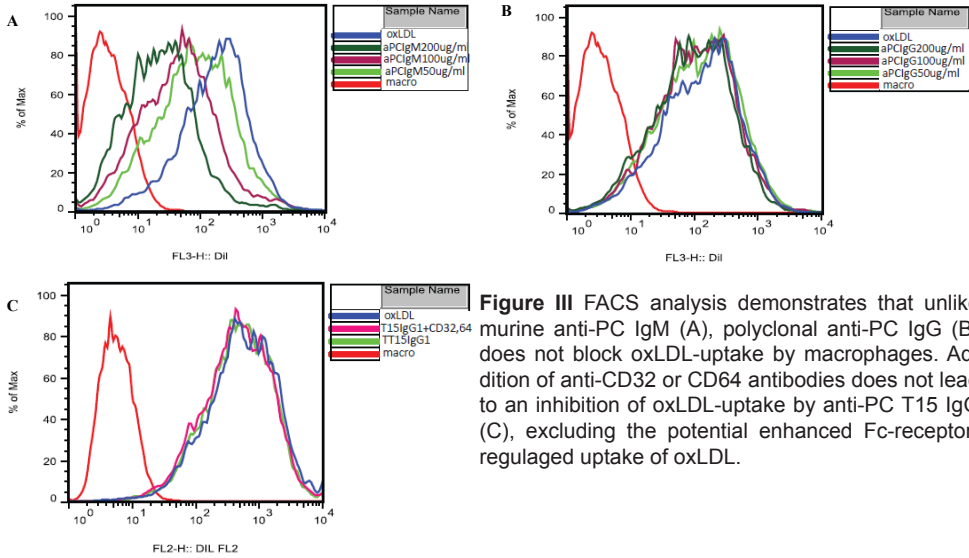
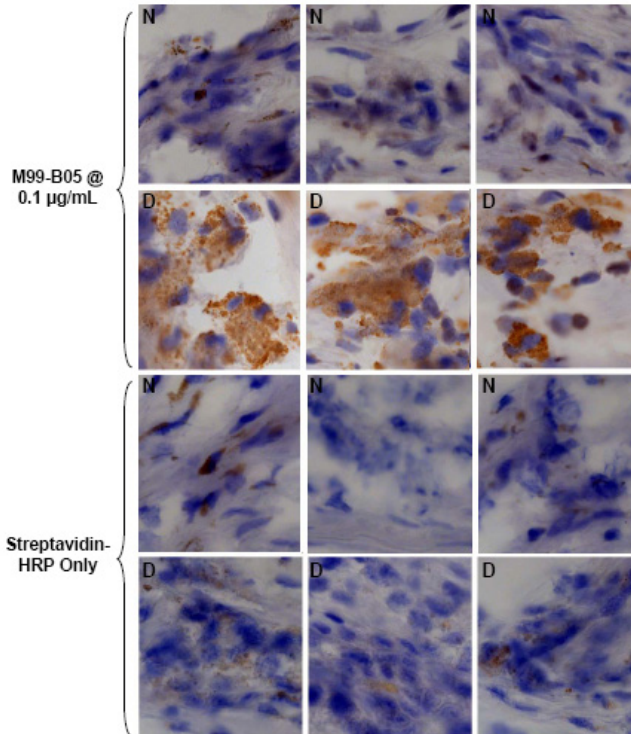


Figure III FACS analysis demonstrates that unlike murine anti-PC IgM (A), polyclonal anti-PC IgG (B) does not block oxLDL-uptake by macrophages. Addition of anti-CD32 or CD64 antibodies does not lead to an inhibition of oxLDL-uptake by anti-PC T15 IgG (C), excluding the potential enhanced Fc-receptor-regulated uptake of oxLDL.

A

Immunohistochemistry Staining of Phosphorylcholine in Human Non-Diseased and Atherosclerotic Aorta



N= Non-Diseased Aorta; D= Atherosclerotic Aorta

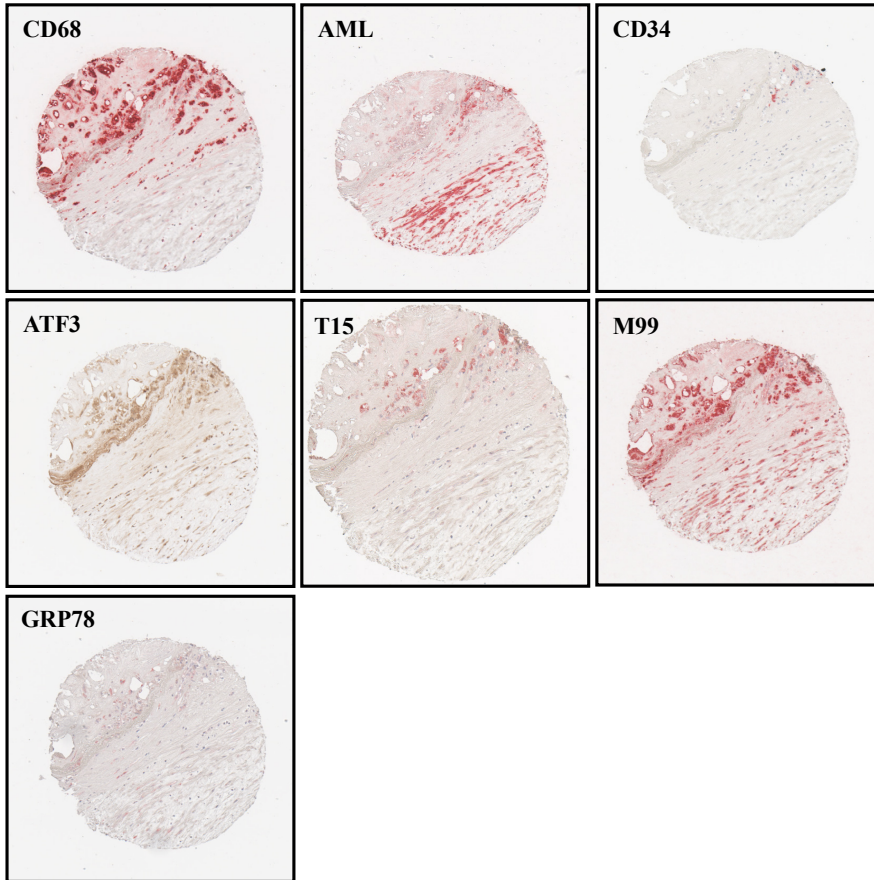
B

Figure IV Representative cross-sections of (A) human non-diseased and atherosclerotic aortic tissue (anti-PC M99B05 and HRP streptavidin staining, magnification 20x) and (B) IHC studies on the serial sections of TMA of human aortic fibroatheromatous plaques (original magnification 100x). The representative sections are shown: CD68 staining is specific for monocyte/macrophages and foam cells of monocyte origin, alpha AML staining is specific for smooth muscle cells and CD34 staining is specific for endothelial cell. T15 and M99 stainings correspond to PC.

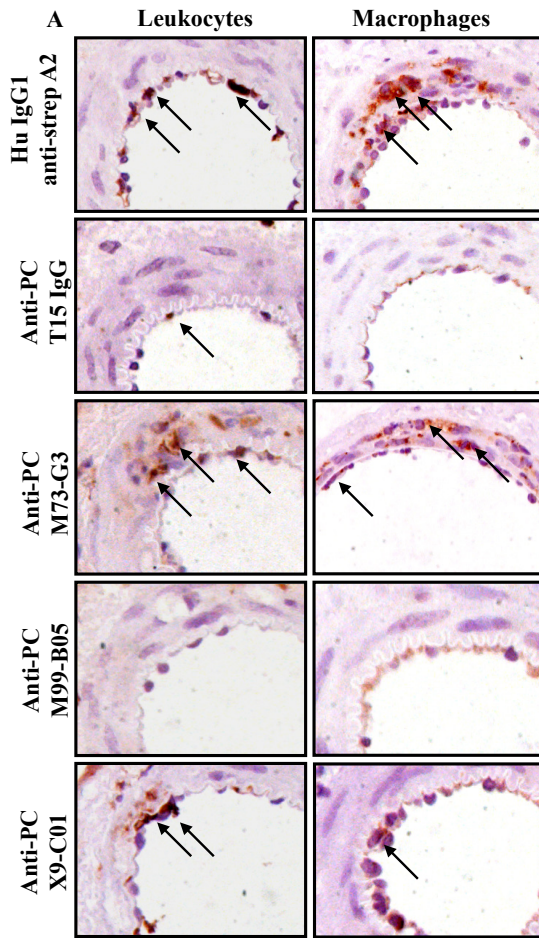


Figure V (A) Representative cross-sections of cuffed arteries of ApoE3*Leiden mice receiving human anti-streptavidin, anti-PC T15 IgG, anti-PC M73-G3, anti-PC M99-B05 or anti-PC X9-C01 after 3d (MAC3 and CD45 staining, magnification 40x, arrows indicate leukocytes and macrophages).

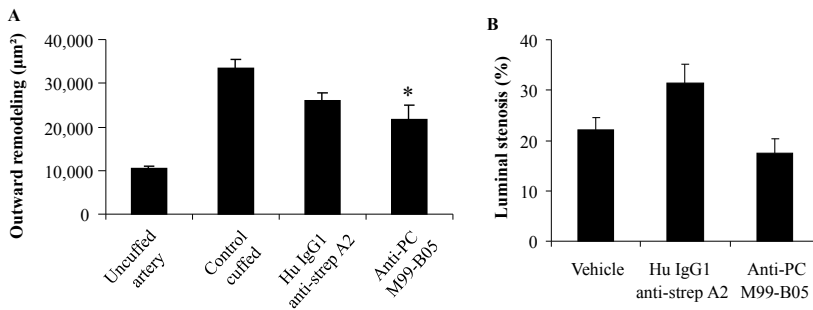
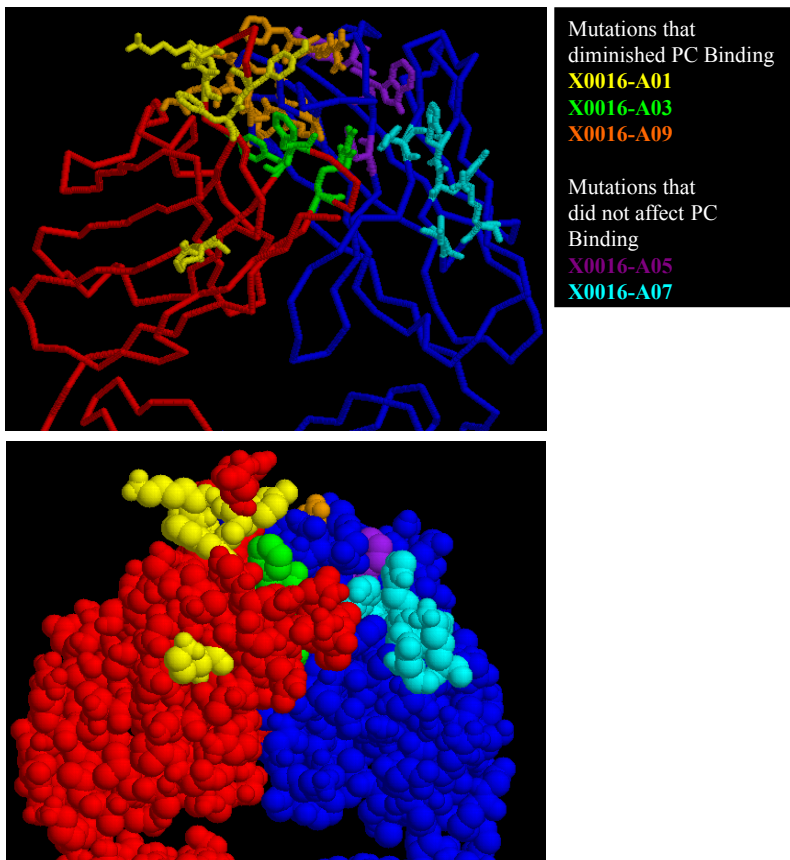


Figure VI Quantification of (A) outward remodeling (μm^2) and (B) lumen stenosis (%) of ApoE3*Leiden mice receiving vehicle, human anti-streptavidin or anti-PC M99-B05 after 14d. Results indicated as mean \pm SEM, n=10. * p<0.05.

A 3-D model of M99-B05**B****M99-B05 Heavy Chain Sequences**

M99-B05 EVQLLESGGGLVQPGGSLRLSCAASGFT-SGYWMHWVRQAPGKGLEWVSY
M99-B05 ISPSGGGTHYADSVKGRFTISRDNKNTLYQMNSLRAEDTAVYYCARVR
M99-B05 FRVCSNGVCRPTAYDAFDIWGQGTAVTVSS

C**M99-B05 Light Chain Sequences**

M99-B05 QDIQMTQSPDLSAVSLGERATINCKSSQSVFYNSNKKNYLAWYQQKAGQPP
M99-B05 KLLIHWASTRESGVPDRFSGSGSGTDFLTISNLAEDVALYQCQQYFNA
M99-B05 PRTFGQGTKVEIK

Figure VII (A) A 3-D model of M99-B05 was constructed by grafting the antibody sequence onto existing structures of similar antibodies. From the above information on which mutations disrupted PC binding it was able to obtain approximations from the model on where the PC antigen may be binding. Analysis suggests that M99-B05 binds PC through an antibody structure that involves multiple CDRs at the interface between the light and heavy chains. The light chain is shown in red and the heavy chain is shown in blue. (B) Heavy chain sequence optimization of M99-B05. (C) Light chain sequence optimization of M99-B05.

Antibody stability in human serum

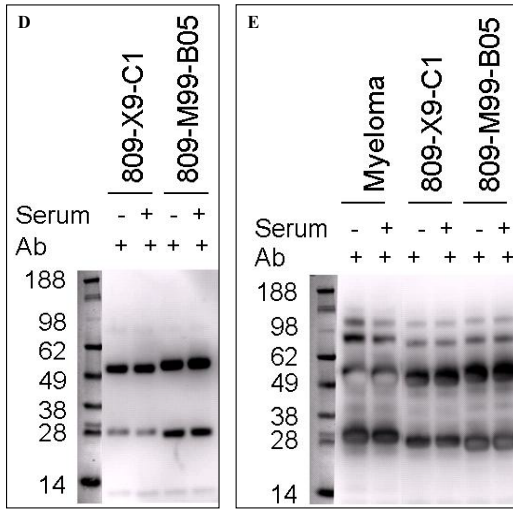


Figure VII Western blot analysis with HRP-conjugated goat anti-human IgG (D) or HRP-conjugated streptavidin (E). Both antibodies are stable in serum under the tested conditions, as evidenced by the lack of degradation in the band intensity of the heavy chain (band above the 49kDa marker) and the light chain (band near the 28 kDa marker). Ab Antibody.

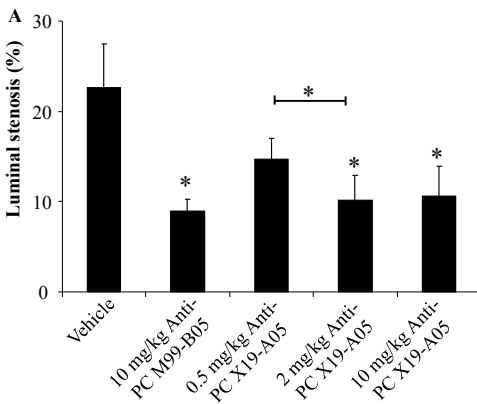


Figure VIII Quantification of (A) luminal stenosis (%) of ApoE3*Leiden mice receiving vehicle, 10mg/kg anti-PC M99-B05 or 0.5, 2 or 10mg/kg X19-A05 after 14d. Results indicated as mean±SEM, n=10. * p<0.05.

Quantification of arterial wall phenotype

Group	Leukocyte area (%)		Macrophage area (%)		SMC area (%)	
	Intima	Media	Intima	Media	Intima	Media
Vehicle	22.3±2.7	25.4±4.5	44.3±5.9	54.9±6.1	34.0±4.2	33.1±4.1
Hu IgG1 anti-strep A2	18.9±2.1	17.0±2.8	36.9±4.4	45.0±3.2	41.4±3.7	45.1±2.6
Anti-PC T15 IgG	7.5±1.2*	6.5±1.8*	11.3±2.0*	15.3±3.1*	35.8±3.9	61.8±3.8*

Table I Quantification of arterial wall phenotype.

Quantification of leukocyte area (%), macrophage area (%) and SMC area (%) in the tunica intima and media of the cuffed femoral artery of ApoE3*Leiden mice receiving vehicle, human anti-streptavidin or anti-PC T15 IgG after 14d. Results indicated as mean±SEM, n=10. * p<0.05.

Total plasma cholesterol (mmol/L)

Group	Surgery	Sacrifice
10 mg/kg Anti-PC IgG	13.3±2.5	18.7±1.4
10 mg/kg Hu IgG1 anti-strep A2	11.1±0.9	13.8±0.6
Vehicle	10.8±1.0	19.2±1.4
10 mg/kg Anti-PC M73-G3	9.9±2.0	12.4±2.4
10 mg/kg Anti-PC M99-B05	9.1±1.8	9.5±1.8
10 mg/kg Anti-PC X9-C01	9.0±1.5	12.5±2.2
10 mg/kg anti-PC T15 IgG	8.3±1.4	10.6±1.8
10 mg/kg Hu IgG1 anti-strep A2	10.5±2.0	13.3±2.3
Vehicle	14.4±2.4	12.4±2.3
10 mg/kg Hu IgG1 anti-strep A2	12.5±1.6	11.4±2.4
10 mg/kg Anti-PC M99-B05	9.9±1.1	10.6±1.2
10 mg/kg Anti-PC X19-A05	11.0±1.0	9.9±1.0
2 mg/kg Anti-PC X19-A05	9.7±0.8	8.3±0.3
0.5 mg/kg Anti-PC X19-A05	10.4±0.8	10.5±0.5
10 mg/kg Anti-PC M99-B05	9.5±0.7	8.4±0.5
10 mg/kg Hu IgG1 anti-strep A2	11.2±1.0	10.8±2.2

Table 2 Plasma cholesterol concentrations.

Plasma total cholesterol (mmol/L) of ApoE3*Leiden mice receiving vehicle, human anti-streptavidin, anti-PC T15 IgG, anti-PC M73-G3, anti-PC M99-B05, anti-PC X9-C01 or X19-A05, measured at surgery or at sacrifice (day 3 or 14). Results indicated as mean±SEM, n=10. No statistical significant differences were observed.

Plasma antibody concentrations

Group	Total IgG ($\mu\text{g/ml}$)	Anti-PC IgG ($\mu\text{g/ml}$)
10 mg/kg Anti-PC IgG	169 \pm 76.0	1208 \pm 329
10 mg/kg Hu IgG1 anti-strep A2	200 \pm 131	0.8 \pm 0.3
Vehicle	0.4 \pm 0.1	0.5 \pm 0.1
10 mg/kg Anti-PC M73-G3	58.3 \pm 6.3	n.d.
10 mg/kg Anti-PC M99-B05	54.6 \pm 11.4	n.d.
10 mg/kg Anti-PC X9-C01	3.5 \pm 0.6	n.d.
10 mg/kg anti-PC T15 IgG	103 \pm 25.6	n.d.
10 mg/kg Hu IgG1 anti-strep A2	70.9 \pm 14.0	n.d.
Vehicle	0.4 \pm 1.0	0.3 \pm 0.2
10 mg/kg Hu IgG1 anti-strep A2	142 \pm 76.4	0.2 \pm 0.0
10 mg/kg Anti-PC M99-B05	49.1 \pm 99.4	65.6 \pm 47.4
10 mg/kg Anti-PC X19-A05	42.2 \pm 23.8	9.9 \pm 1.0
2 mg/kg Anti-PC X19-A05	3.3 \pm 6.6	8.3 \pm 0.3
0.5 mg/kg Anti-PC X19-A05	2.9 \pm 2.5	10.5 \pm 0.5
10 mg/kg Anti-PC M99-B05	12.8 \pm 15.1	8.4 \pm 0.5
10 mg/kg Hu IgG1 anti-strep A2	155 \pm 33.5	10.8 \pm 2.2

Table 3 Plasma antibody titers.

Plasma total IgG ($\mu\text{g/ml}$) and anti-PC IgG ($\mu\text{g/ml}$) antibody concentration in ApoE3*Leiden mice receiving vehicle, human anti-streptavidin, anti-PC T15 IgG, anti-PC M73-G3, anti-PC M99-B05, anti-PC X9-C01 or X19-A05, measured at surgery or at sacrifice (day 3 or 14). Results indicated as mean \pm SEM, n=10. Between groups, no statistical significant differences were observed. n.d. not determined.

Chapter 7

Blocking Toll-Like Receptors 7 and 9 Reduces Postinterventional Remodeling via Reduced Macrophage Activation, Foam Cell Formation, and Migration

J.C Karper^{1,2}, M.M. Ewing^{1,2,3}, K.L.L. Habets⁴, M.R de Vries^{1,2}, H.A.B Peters^{1,2}, A.M. van Oeveren-Rietdijk^{2,5}, H.C. de Boer^{2,5}, J.F Hamming¹, J. Kuiper⁴, E.R. Kandimalla⁶, N. La Monica⁶, J.W. Jukema^{2,3}, P.H.A. Quax^{1,2}

1 Dept. of Surgery, Leiden University Medical Center (LUMC), Leiden, The Netherlands

2 Eindhoven Laboratory for Experimental Vascular Medicine, LUMC, Leiden, The Netherlands

3 Department of Cardiology, LUMC, Leiden, The Netherlands

4 Department of Biopharmaceutics, Leiden University, Leiden, The Netherlands

5 Department of Nephrology, LUMC, Leiden, The Netherlands

6 Idera Pharmaceuticals, Boston, Massachusetts, USA

Abstract

Objective The role of toll-like receptors (TLRs) in vascular remodeling is well established. However, the involvement of the endosomal TLRs is unknown. Here, we study the effect of combined blocking of TLR7 and TLR9 on postinterventional remodeling and accelerated atherosclerosis.

Methods and Results In hypercholesterolemic apolipoprotein E*3-Leiden mice, femoral artery cuff placement led to strong increase of TLR7 and TLR9 presence demonstrated by immunohistochemistry. Blocking TLR7/9 with a dual antagonist in vivo reduced neointimal thickening and foam cell accumulation 14 days after surgery by 65.6% ($P=0.0079$). Intima/media ratio was reduced by 64.5% and luminal stenosis by 62.8%. The TLR7/9 antagonist reduced the arterial wall inflammation, with reduced macrophage infiltration, decreased cytoplasmic high-mobility group box 1 expression, and altered serum interleukin-10 levels. Stimulation of cultured macrophages with TLR7 and TLR9 ligands enhanced tumor necrosis factor- α expression, which is decreased by TLR7/9 antagonist coadministration. Additionally, the antagonist abolished the TLR7/9-enhanced low-density lipoprotein uptake. The antagonist also reduced oxidized low-density lipoprotein-induced foam cell formation, most likely not via decreased influx but via increased efflux, because CD36 expression was unchanged whereas interleukin-10 levels were higher (36.1 ± 22.3 pg/mL versus 128.9 ± 6.6 pg/mL; $P=0.008$).

Conclusion Blocking TLR7 and TLR9 reduced postinterventional vascular remodeling and foam cell accumulation indicating TLR7 and TLR9 as novel therapeutic targets.

Introduction

Postinterventional remodeling is a critical determinant of long-term efficacy of percutaneous coronary interventions. Restenosis is characterized by acute elastic recoil and intimal hyperplasia attributable to inflammation, smooth muscle cell (SMC) proliferation, and extracellular matrix turnover.¹ Under hypercholesterolemic conditions, this is accompanied by influx and accumulation of low-density lipoprotein (LDL) cholesterol in the vessel wall that becomes oxidized and taken up by macrophages. Thereby these macrophages become foam cells and initiate a process of accelerated atherosclerosis.² Previously, we and others described an important causal role for extracellular toll-like receptors (TLRs) in postinterventional remodeling. It has been shown that TLR4 and the MyD88-dependent pathway play an important role in restenosis and postinterventional accelerated atherosclerosis.³⁻⁶ Similarly, a crucial role for TLR2 has been described.⁷

TLRs, as part of the innate immune system, are pattern recognition receptors known to recognize exogenous ligands that originate from bacteria or viruses as well as endogenous ligands. These endogenous ligands may be released after tissue damage or cell stress, processes that may be initiated by percutaneous coronary interventions. MyD88-dependent signaling is the dominant activation pathway of TLR signaling leading to nuclear factor- κ B activation and upregulation of several proinflammatory cytokines. Because TLR2 and TLR4 are known to be expressed on the cell surface of vascular cells and activated in vascular disease processes via damage-associated molecular patterns as endogenous ligands, such as heat shock proteins, fibronectin containing extradomain A, tenascin-C, and high-mobility group box 1 (HMGB1),⁸⁻¹¹ research in the cardiovascular field mainly focused on TLR2 and TLR4. Little is known about the role of endosomal TLRs that are mostly studied for their recognition of viral/bacterial DNA and RNA fragments, and were originally considered absent in the healthy arterial vessel wall.¹² Activation of endosomal TLRs like TLR7 and TLR9 may lead to upregulation of interferon- α (IFN- α), interleukin-6 (IL-6), IL-12, or tumor necrosis factor- α (TNF- α) by innate immune cells (eg, macrophages). Recently, increased TLR7 mRNA was found in atheroma of human carotids.¹³ Moreover, TLR9 was also found in human atherosclerotic plaques,¹⁴ and arterial cells were responsive to TLR9 ligand.¹⁵ Interestingly, it has been suggested that these receptors may also recognize self-DNA/RNA that is exposed after cell stress and damage causing a sterile inflammatory reaction.¹⁶⁻¹⁹ TLR7 and TLR9 have also been shown to recognize immune complexes containing selfnucleic acids in autoimmune diseases.^{16,20} Percutaneous coronary interventions are considered to cause severe damage to the endothelium allowing influx of lipids and inflammatory cells into the vessel wall. Concurrently, deeper layers in the vessel wall experience severe stress, and cellular death at the place of intervention may cause a release of self-RNA/DNA or proteins that enhance the direct recognition of nucleic acids by intracellular TLRs or binding of these nucleic acids to intracellular TLR signaling regulators such as HMGB1.²¹ Most interestingly, activation of TLR9 is also reported to increase the secretion of HMGB1, the endogenous ligand for TLR4.²² Recently, we have identified a novel class of oligonucleotidebased compounds that act as dual antagonists of TLR7 and TLR9, and inhibit immune responses mediated through these receptors.^{23,24} In the present study, we focus on the therapeutic poten-

tial of targeting TLR7 and TLR9 to reduce postinterventional remodeling by preventing neointima formation and accelerated atherosclerosis. We illustrate the presence and upregulation of TLR7 and TLR9 and their colocalization with macrophages/foam cells in a murine model for neointima formation and accelerated atherosclerosis. A causal role of the TLR7/9 was studied in a murine model for postinterventional vascular remodeling in hypercholesterolemic apolipoprotein E*3-Leiden (apoE*3-Leiden) mice by the use of the TLR7/9 antagonist. Furthermore, we studied activation and antagonism of TLR7 and TLR9 on cultured macrophages and on foam cell formation using a novel TLR7/9 dual antagonist.

Materials and Methods

A detailed description of all materials and methods used is available in the online-only Data Supplement. In brief, nonconstricted polyethylene cuffs were placed around the femoral arteries as a well-established model for neointima formation and accelerated atherosclerosis in hypercholesterolemic apoE3-Leiden mice. Immunohistochemistry for TLR7 and TLR9 was performed on paraffin-embedded sections of cuffed arteries of hypercholesterolemic apoE3-Leiden mice at $t=0$ and $t=14$. A TLR7/TLR9 dual antagonist was synthesized, and specificity was determined. We studied its effect on neointima formation and accelerated atherosclerosis in hypercholesterolemic apoE*3-Leiden mice after femoral arterial cuff placement by injecting the antagonist biweekly to get sufficient TLR7/9 blockade. Intimal lesions were analyzed for CD45, MAC3, and HMGB1 by immunohistochemistry. The antagonist was used to study the effect of blocking of TLR7/9 on macrophage activation and lipid accumulation in macrophages. Cytokine levels of TNF- α , IFN- γ -induced protein 10, IL-6, IL-12, and IL-10 were quantified by ELISA.

Results

Arterial Injury Leads to TLR7 and TLR9 Presence in the Vessel Wall

Little is known about the presence of TLR7 and TLR9 in the vessel wall after surgical intervention. Using immunohistochemical analysis, we explored whether TLR7 and TLR9 are expressed in cuffed remodeled arteries with neointimal lesions after 14 days and in noncuffed arteries of hypercholesterolemic apoE*3-Leiden mice, because TLR expression may differ among different arterial segments and also in response to vessel damage.^{12,13} Cuff placement for 14 days provoked severe neointimal thickening, and showed the presence of TLR7/9 profoundly in the tunica media of these arterial segments. Presence of either TLR7 or TLR9 could not be observed in noncuffed femoral arteries (Figure 1A–1D). Lesions in cuffed arteries of wild-type mice on a chow diet that consist dominantly of vascular SMCs were also negative for TLR7 and TLR9 (Figure 1A and 1B in the online-only Data Supplement). Negative controls showed no staining (Figure 1C in the online-only Data Supplement). The area with positive staining for both TLRs contained many macrophages, whereas in mice with normal cholesterol these lesions hardly show any of these cells. (Figure 1D and 1E in the online-only Data Supplement).

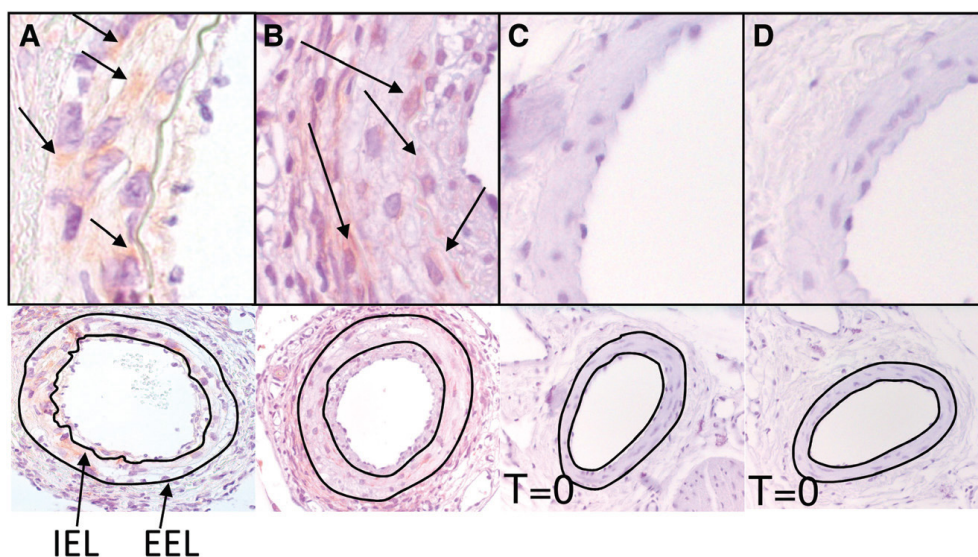


Figure 1. Toll-like receptor (TLR) expression in injured femoral artery lesions of hypercholesterolemic apolipoprotein E*3-Leiden (apoE3*3-Leiden) mice. TLR7 expression (A) and TLR9 expression on femoral arteries with neointima 14 days after cuff placement (B). Noncuffed femoral arteries stained for TLR7 (C) and TLR9 (D). EEL indicates external elastic lamina; IEL, internal elastic lamina.

Inhibition of TLR7- and TLR9-Mediated Immune Responses by Antagonist

Splenocytes were cultured with 0.01 to 10 $\mu\text{g}/\text{mL}$ of the dual TLR7/9 antagonist in combination with TLR3, TLR4, TLR7, or TLR9 agonist. The antagonist showed a dose-dependent reduced production of TNF, IL-6, and IFN- γ -induced protein 10 on either TLR7 or TLR9 activation. Activation of TLR4, the most robust signaling TLR, was not affected. Also cytokine production via activation of intracellular TLR3, which recognizes double-stranded RNA, was not affected by the antagonist (Figure IIA–IID in the online-only Data Supplement). Culturing of splenocytes with the antagonist alone did not induce cytokine production (not shown). Administration of either TLR7 or TLR9 agonists alone to mice resulted in elevated inflammation indicated by increased levels of serum IL-12. Mice administered with antagonist before TLR7 or TLR9 agonist administration displayed lower levels of serum IL-12. TLR7/9 antagonist alone did not induce IL-12 expression, suggesting it does not induce immune responses. At the dose used, antagonist showed $\approx 64\%$ and 85% inhibition of TLR9 and TLR7 agonist-induced IL-12 in mice, respectively. (Figure III in the online-only Data Supplement). Control oligo showed no inhibition of either TLR7- or TLR9-mediated immune response in mice (Figure 2).

TLR7/9 Antagonist Reduced Neointima Formation and Accelerated Atherosclerosis

After detecting TLR7 and TLR9 presence in remodeled arteries, we focused on vascular remodeling. By *in vivo* administration of the antagonist, the causal involvement of TLR7/9 activation in intimal hyperplasia and accelerated atherosclerosis was assessed in hypercholesterolemic apoE*3-Leiden mice that underwent femoral arterial cuff placement, a widely applied model for restenosis. These mice were fed a Wes

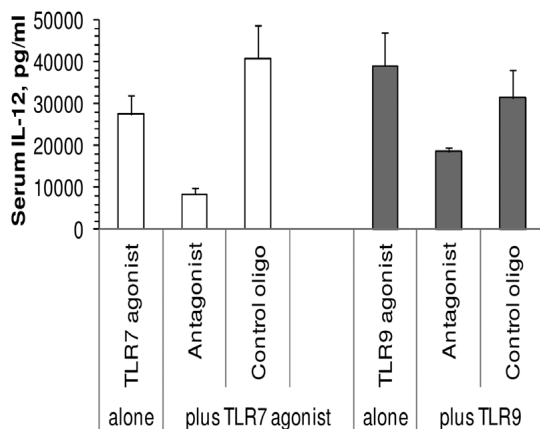


Figure 2. Antagonist or control oligo was injected at 5 mg/kg, s.c. in the left flank of 6- to 8-week-old female C57BL/6 mice ($n=2$ /group). RNA-based toll-like receptor 7 (TLR7) agonist at 10 mg/kg, s.c. or TLR9 agonist at 0.25 mg/kg, s.c. was injected 48 hours later in the right flank. Two hours post-TLR agonist administration, blood was collected, and serum interleukin-12 (IL-12) level was determined by ELISA. TLR7 or TLR9 agonist alone was used as a positive control. Data shown are representative of at least 2 independent experiments.

tern-type diet, starting 3 weeks before surgery to induce hypercholesterolemia, and are well known to develop intimal lesions attributable to neointima formation and accelerated atherosclerosis. No significant difference in plasma total cholesterol levels was detected before surgery (control 9.3 ± 0.60 mmol/L; TLR7/9 antagonist 9.0 ± 0.46 mmol/L), nor had antagonist-treated mice significant altered cholesterol levels compared with control mice after 14 days at euthanizing (control 8.4 ± 0.4 mmol/L; TLR7/9 antagonist 7.7 ± 0.8 mmol/L). Hematoxylin-phloxine-saffron-stained sections were used to study vessel wall composition and showed a profound neointima formation with foam cell formation, which was clearly reduced in the antagonist-treated group. After quantification, we observed reduction in neointima formation of 66% ($n=9$ versus $n=7$; 5838 ± 1158 μm^2 versus 2008 ± 223 μm^2 ; $P=0.0079$), a beneficial intima/media ratio (0.473 ± 0.09 μm^2 versus 0.168 ± 0.018 μm^2 ; $P=0.0021$), and a reduction in percentage of lumen stenosis of 64% ($33.9 \pm 6.6\%$ versus $12.5 \pm 2.9\%$; $P=0.0021$) after administration of antagonist biweekly. No differences in total vessel wall area or media area were found (Figure 3A–3G). In addition, we found a difference in IL-10 serum levels that were significantly higher in the antagonist-treated mice 14 days after cuff placement (0.43 versus 15.46 pg/mL; $P=0.0003$; Figure IV in the online only Data Supplement). At euthanizing, the antagonist-treated mice had a higher number of circulating Ly6Clow monocytes compared with PBS-treated controls (Figure V in the online-only Data Supplement). In the lesions of the antagonist-treated mice, a reduced number of macrophages (MAC3-positive cells) was observed (Figure 3). This difference may be attributable to reduced infiltration of the vessel wall by the circulating monocytes because the expression of adhesion molecule CD11b was decreased on the cells of the antagonist-treated mice (Figure 3H). Nonspecific oligonucleotide administration not only had no effect on the number of circulating (Ly6Clow) monocytes or CD11b expression compared with PBS treatment, it also did not affect neointima formation (Figure 3I and 3J).

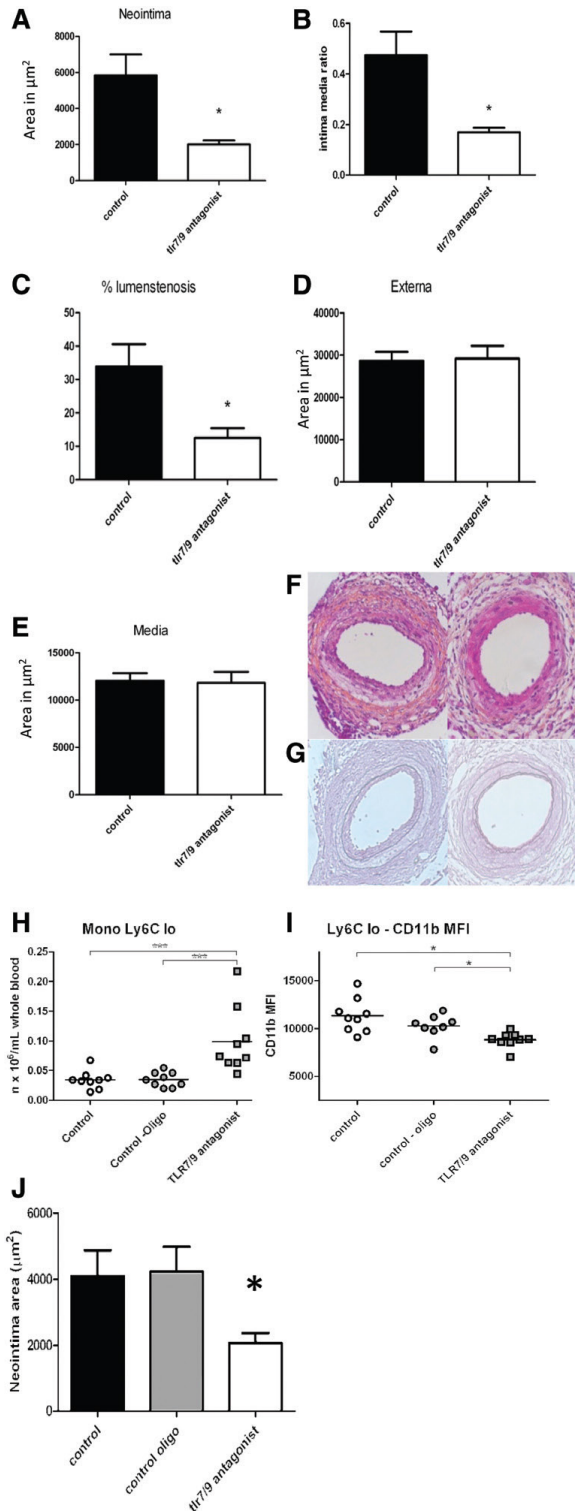


Figure 3. Restenosis with accelerated atherosclerosis was initiated via cuff placement around the femoral artery in hypercholesterolemic apolipoprotein E*3-Leiden (apoE*3-Leiden) mice. Areas of femoral arteries were quantified by using 6 sections

per vessel of each mouse. A mean of these 6 sections was used as the outcome of arterial remodeling per mouse. Outcomes of

analysis are expressed in μm^2 (mean \pm SEM). Mice treated with the antagonist showed a significant reduction in neointima formation compared with controls (A). Antagonist-treated mice also showed a decrease in percentage of lumen stenosis (B) and a beneficial intima/media ratio (C). Neither total vessel wall area nor media area were altered (D and E). Representative hematoxylin-phloxine-saffron (HPS; F) and Weigert elastin (G) stained cross sections of control mice and antagonist-treated mice 14 days after cuff placement. Number of circulating Ly6C^{low} monocytes (corrected for total white blood cell count; H). Expression of adhesion molecule CD11b on Ly6C^{low} monocytes (I). Neointima formation of cuffed mice treated with PBS, control oligo, and toll-like receptors 7 and 9 (TLR7/9) antagonist (J). *P<0.05. Statistical analysis was performed by use of a nonparametric Mann-Whitney test, *P<0.05. MFI indicates mean fluorescence intensity.

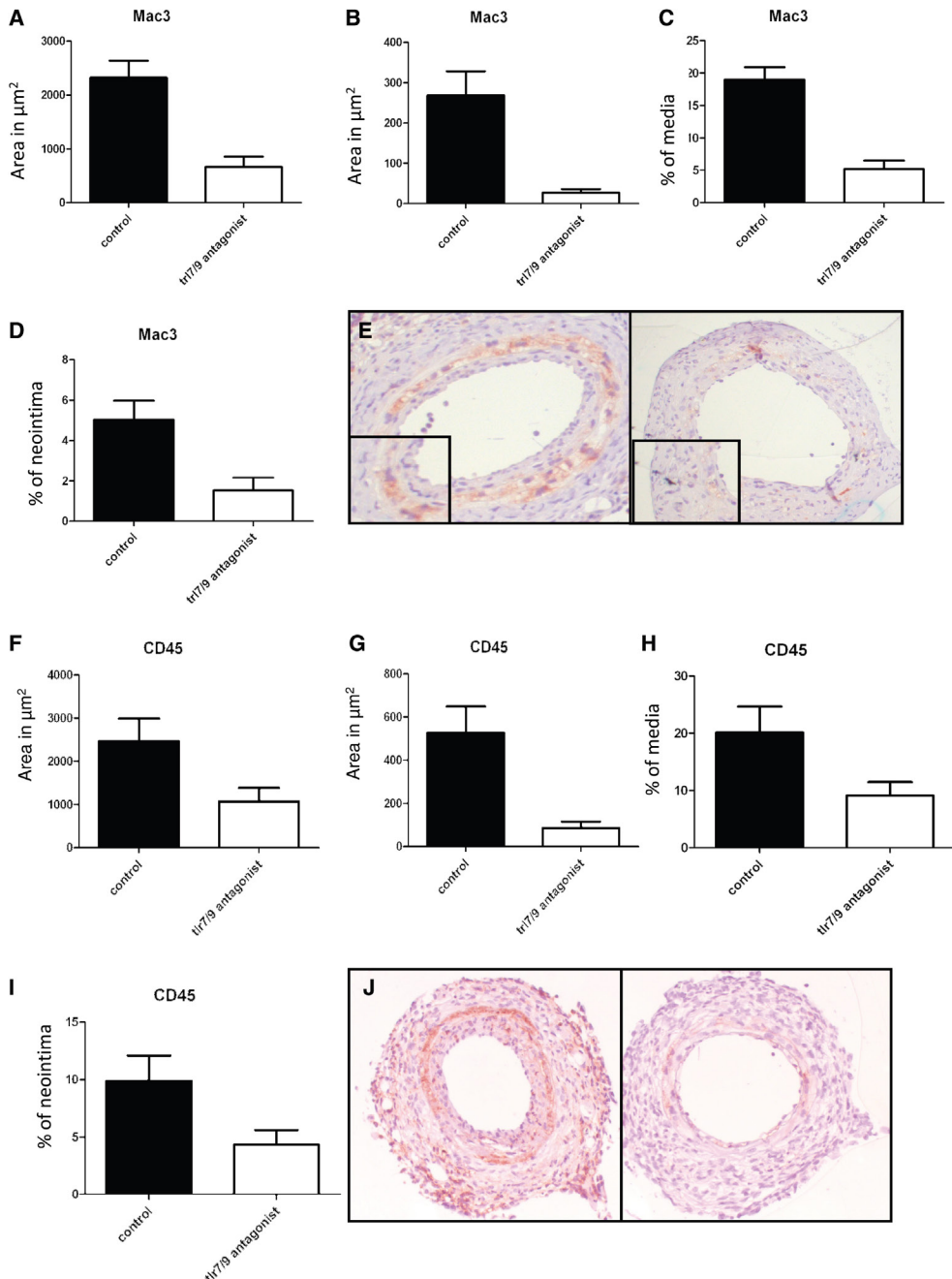


Figure 4. Lesion composition after treatment with toll-like receptors 7 and 9 (TLR7/9) antagonist in hypercholesterolemic apolipoprotein E*3-Leiden (apoE*3-Leiden) mice. Sections were stained for MAC3 and CD45. Positive staining in areas of femoral arteries was quantified by using 6 sequential sections per artery of each mouse. A mean of positive staining of these 6 sections was used as the outcome of positive immunostaining per mouse. Outcomes of analysis are expressed in μm^2 (mean \pm SEM) and percentage of area of either media or neointima. Macrophage infiltration was significantly reduced in the antagonist-treated group compared with the controls in both neointima (A) as well as media (B). Percentage of positive staining for MAC3 was reduced in this group in both media (C) and neointima (D). Representative

pictures of control mice and antagonist-treated mice (E). Leukocyte infiltration in the antagonist-treated group compared with the controls in media (F) as well as neointima (G). Percentage of positive staining for CD45 in the media (H) and neointima (I). Representative pictures of CD45 stained sections of control mice and antagonist-treated mice (J). Statistical analysis was performed with a nonparametric Mann-Whitney test, * $P < 0.05$.

TLR7/9 Blockade Reduced Macrophage/Foam Cell-Positive Area

As stated above, we observed a significant reduced MAC3-positive area. This was the case in both media ($2445 \pm 327 \mu\text{m}^2$ versus $661 \pm 199 \mu\text{m}^2$; $P = 0.002$) as well as neointima ($268 \pm 59 \mu\text{m}^2$ versus $26 \pm 9 \mu\text{m}^2$; $P = 0.003$), indicating less infiltration of macrophages that are importantly involved in the remodeling process. The percentage of positive area was also significantly reduced indicating a reduction of positive cells per μm^2 in both media as well as in the formed neointima. We also checked whether the effects observed in vivo could be related to the accumulation of total leukocytes in the lesions. Therefore, we quantified the area of the vessel segments that was positive of CD45, a pan-leukocyte marker. Vessels of the antagonist-treated mice showed a trend toward a reduced CD45-positive area which was significant in the neointima (Figure 4A–4J).

TLR7/9 Blockade Reduced Cytoplasmic HMGB1

Layers in the vessel wall undergo severe stress on intervention. Together with our finding of a significant decrease in macrophages, we searched for the presence of cytoplasmic or extracellular HMGB1 that is a marker of cell stress and macrophage activation. HMGB1 can be directly upregulated by TLR9 activation and is an important TLR7/9 signaling regulator and an endogenous TLR2/4 ligand. Kalinina et al previously showed that HMGB1 could be detected in atherosclerotic plaques. Furthermore, the authors showed that this was dominant in macrophages, and that in these macrophages there was a marked increase of HMGB1 in the cytoplasm.²⁵ Therefore, we performed analysis for the presence of cytoplasmic HMGB1 in the arterial wall. Because TLR7/9 was predominately expressed in the tunica media, where most macrophages/foam cells were present, the media area of the vessel segments that was positive for HMGB1 outside the nucleus was quantified. We found a significant decrease in the percentage of positive cytoplasmic HMGB1 in the media area of mice treated with antagonist ($12.97 \pm 1.03\%$ versus $7.80 \pm 1.28\%$; $P = 0.011$; Figure 5A–5C). This is of special interest, because HMGB1 release is increased on TLR7/9 activation, regulates TLR7/9 signaling, and is known to function as an endogenous ligand for TLR2 and TLR4 (Figure 5A–5C).

TLR7/9 Blockade Reduced Macrophage Proinflammatory Cytokine Production on TLR7/9 Activation

Macrophage activation and foam cell accumulation play a crucial role in lesion formation and accelerated atherosclerosis development after cuff placement. Because we found less macrophages and HMGB1 after blocking TLR7/9, we studied the effects of modulation of the TLR7/9 signaling in cultured bone marrow–derived macrophages. Bone marrow–derived macrophages were cultured for 7 days, and then stimulated with either TLR7 ligand imiquimod, TLR9 ligand C-phosphate-G (CpG)-oligodeoxynucleotide, or a combination of both for 24 hours. Activation was monitored by analysis of TNF- α expression, a key proinflammatory cytokine also known to

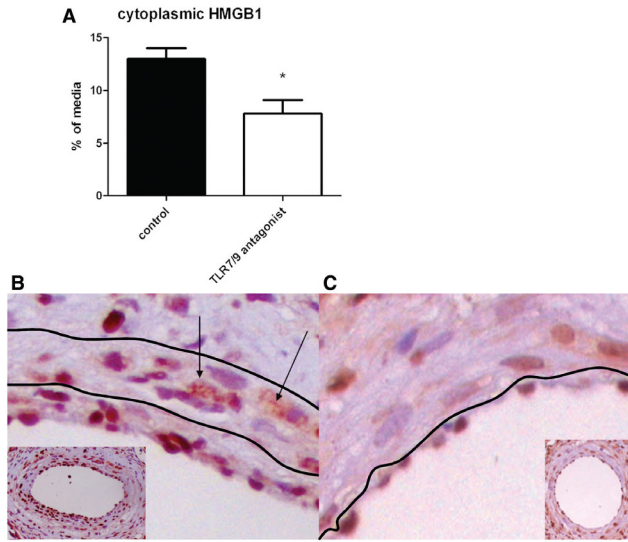


Figure 5. Presence of cytoplasmic highmobility group box 1 (HMGB1) in the injured vessel wall of hypercholesterolemic apolipoprotein E*3-Leiden (apoE3*Leiden) mice 14 days after surgery. Sections were stained for HMGB1. Positive staining in areas of femoral arteries was quantified by using 6 sequential sections per artery of each mouse. A mean of positive staining of these 6 sections was used as the outcome of positive immunostaining per mouse. Outcome of cytoplasmic HMGB1 analysis in percentage (mean±SEM) of area of media (A). Representative pictures of HMGB1 staining in control mice (B) and antagonist-treated mice (C). Statistical analysis was performed with a nonparametric Mann-Whitney test, *P<0.05. TLR7/9 indicates toll-like receptors 7 and 9.

be regulated *in vivo* after cuff placement.²⁶ Coadministration of TLR7/9 ligands with the antagonist caused a significant reduction in the production of TNF- α , whereas lipopolysaccharide-induced production of TNF- α was not altered by the antagonist (Figure 6A).

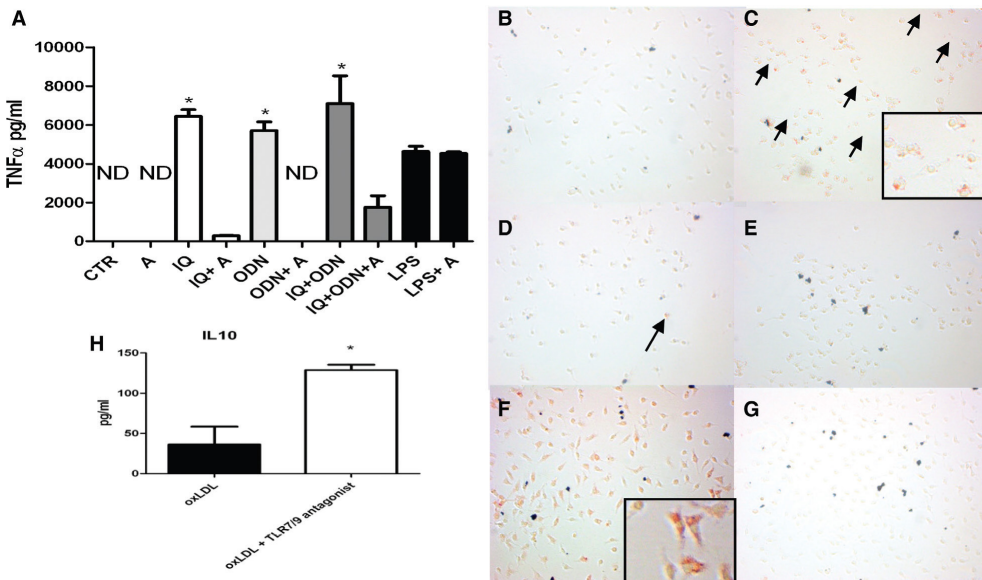


Figure 6. Bone marrow–derived macrophages cultured with imiquimod (IQ) as a ligand for toll-like receptor 7 (TLR7), C-phosphate-G–oligodeoxynucleotide (CpG-ODN) as a ligand for TLR9 or TLR7/9 antagonist for 24 hours. IQ and CpG induced macrophage activation. Use of the TLR7/9 antagonist caused a decrease in tumor necrosis factor- α (TNF- α) production. TLR4- (lipopolysaccharide, [LPS]) induced activation was not altered by the antagonist. A, Foam cell formation was studied on cultured macrophages in the presence of empty medium, native low-density lipoprotein (LDL), IQ, IQ+LDL, and IQ+LDL+antagonist. All wells were screened for positive Oil Red O (ORO) staining, and representative pictures are shown. Macrophages with native LDL showed no lipid uptake after staining with ORO (B). Positive staining in the presence IQ with native LDL (C), IQ+LDL+antagonist (D), and IQ (E). Foam cell formation independent of direct TLR activation was studied on cultured macrophages in the presence of oxidized LDL (oxLDL) or oxLDL+antagonist. All wells were screened for positive ORO staining, and representative pictures are shown. Macrophages with oxLDL showed lipid uptake after staining with ORO (F) but only a few positive spots in the presence of TLR7/9 antagonist (G). Analysis by ELISA showed a significant difference in interleukin-10 (IL-10) levels in the presence of TLR7/9 antagonist (H). Student t test was used for statistical analysis, * $P < 0.05$. CTR indicates control.

TLR7/9 Blockade Reduced Foam Cell Formation by Macrophages

Additionally to the direct effect of proinflammatory cytokine excretion by macrophages, we looked into the effect on lipid accumulation by macrophages because both processes are important in postinterventional remodeling. Because macrophage-induced cytokine production and foam cell formation are major contributors to neointima formation and accelerated atherosclerosis, we studied whether TLR7 activation in combination with native LDL could induce lipid uptake by macrophages as was shown previously for TLR9. Reduced TLR9 activation was previously described to be important in foam cell formation via oxidation of native LDL-cholesterol that normally is not capable of causing foam cell formation.²⁷ Furthermore, we were interested in whether our antagonist could block this process efficiently like it did on inflammation with only the agonists. Presence of native LDL with TLR7 stimulation alone caused lipid accumulation shown by positive Oil Red O staining in the macrophages whereas native LDL-cholesterol alone showed no staining at all (Figure 6A and 6B). The use of antagonist showed a clear reduction in lipid uptake, and thus foam cell formation indicated less intracellular Oil Red O staining in the fixed macrophages (Figure 6B–6E). TLR9 activation and blockade in the presence of LDL gave the same results, and was described previously^{27,28} (data not shown). Foam cells, formed by oxidized LDL (oxLDL) uptake of macrophages, die of releasing lipids, intracellular molecules, and necrotic debris which can further activate the remaining macrophages via endosomal receptors like TLR7/TLR9.²⁹ Therefore, we cultured macrophages in the presence of oxLDL cholesterol (Figure 6F) to check whether the antagonist also could influence this lipid accumulation if we combined oxLDL administration with the antagonist. Oil Red O staining was found in the oxLDL-treated macrophages, whereas in combination with the antagonist showed only a few slightly positive cells (Figure 6F and 6G). To see whether this effect was dependent on influx or efflux of lipids, we analyzed expression of scavenger receptor CD36 and IL-10 production. CD36 scavenger receptor expression was not different (positive CD36 macrophages; control 41.48% versus antagonist 41.32%; Figure V in the online-only Data Supplement), however we noticed significant change in IL-10 levels (Figure 6G) indicating effects on lipid efflux whereas IL-10 enhances lipid efflux via the peroxisome proliferator-activated receptor- γ -liver X receptor-ATP-binding cassette subfamily A member 1/ATP-binding cassette subfamily G member 1 pathway.³⁰

Discussion

The present study describes the role of a novel TLR7/9 dual antagonist in restenosis and accelerated atherosclerosis in mice. Individual presence of both TLR7 and TLR9 was noticed in femoral arteries of hypercholesterolemic apoE*3-Leiden mice with neointimal lesions and accelerated atherosclerosis after 14 days. These have to be infiltrating cells (eg, macrophages), whereas normal arteries or arterial lesion from normal mice that consist dominantly of vascular SMC stained negative for both TLRs and macrophages. In vivo administration of antagonist showed a significant reduction in neointima formation with a beneficial intima/media ratio in hypercholesterolemic apoE*3-Leiden mice. Moreover, blockade of TLR7/9 signaling led to a reduction in CD45- and MAC3-positive cells in both media as well as in the neointimal lesions, and we notice a decrease in cytoplasmic HMGB1 indicating a decrease in cellular stress and a difference in serum IL-10. In vitro, macrophages showed a significant increase in TNF- α production on TLR7 or TLR9 activation that was reduced after receiving TLR7/9 dual antagonist. Administration with TLR7 ligand imiquimod or TLR9 agonist CpG caused lipid accumulation in macrophages that could be sufficiently blocked by the antagonist. Moreover, oxLDL-induced foam cell formation was inhibited by antagonist, possibly via upregulation of IL-10.

Previously, we and others described involvement of TLR2 and TLR4 in postinterventional neointima formation.^{3,6,7} Recently, a protective role for intracellular receptor TLR3, important in recognition of double-stranded RNA, was found in vascular remodeling.³¹ Neointima formation attributable to postinterventional remodeling is strongly mediated by local activation and physiological changes, such as increased wall stress, cell damage, and inflammation. In the present study, we were able to notice the presence of TLR7 and TLR9 in the postinterventional remodeled arteries whereas noncuffed vessels show no presence of these TLRs at all. This can probably be related to leukocytes that express these TLRs and infiltrate the vessel wall as a result of the damage of the intervention such as macrophages, and start to clear apoptotic cells and infiltrated lipids. The level of TLR expression may vary among different vessel specimens and may be influenced by these changes.¹² Other studies in addition to the present showed TLR7 expression in atheroma of carotids¹³ and TLR9 presence in human atherosclerotic plaques¹⁴ that may be activated via unmethylated CpG motifs from bacteria.³² Furthermore, DNA from 17 different bacterial genera that can activate TLR9 was found in atherosclerotic carotids,¹⁵ together indicating a possibly important contribution of these pattern recognition receptors to vascular remodeling.

Blocking TLR7/9 signaling by antagonist strongly inhibited neointima formation thereby reducing the percentage of lumen stenosis. Neointima formation is strongly mediated by SMC proliferation/migration and macrophage activation and lipid uptake. Because TLR7/9 presence could not be detected in undamaged arteries, it is unlikely that there is a direct activation of SMC. However, indirect activation of SMC is still possible via cytokines produced by leukocytes which express these TLRs. Our results may be explained, at least in part, by the difference in IL-10 production. On the other hand, TLR7 and TLR9 stimulation by their ligands causes a strong increase in the upregulation of TNF- α , which is important in postinterventional vascular remodeling, indicating a direct influence of TLR7/9 activation on inflammation. This

response was nicely blocked by the antagonist in macrophages. Furthermore, we observed lower levels of HMGB1 in the cytoplasm after cuff placement in the antagonist-treated mice, thereby reducing its effect via direct activation of TLR2/4 and activation of intracellular TLRs via its binding to their nucleic acid ligands.^{21,33} Moreover, there were significantly fewer numbers of macrophages/foam cells present in media as well as neointima.

Activation of TLR7/9 leads to nuclear factor-kappaB–mediated upregulation of proinflammatory cytokines. Furthermore, it is known that TLR9 activation causes release of nuclear HMGB1 that may become available in the cytoplasm or even outside the cell, where it is known to act as TLR2 and TLR4 ligand and was seen in macrophages in atherosclerotic plaques.^{22,25,33,34} Not only can this release be initiated on cell stress but also on activated macrophages that are capable of releasing HMGB1.^{34,35} Previously, we were able to detect HMGB1 in remodeled vein grafts in and outside the nucleus.⁴ On cuff placement, we noticed the presence of HMGB1 in the cytoplasm as well. Others previously showed that CpG-oligodeoxynucleotide stimulates macrophages to secrete HMGB1, and extracellular HMGB1 is known to accelerate the delivery of CpG-oligodeoxynucleotides to its receptor, leading to a TLR9-dependent enhancement of IL-6, IL-12, and TNF- α .²² Interestingly, HMGB1 is also known as a regulator of TLR7/9 signaling itself because the absence of HMGBs also severely impairs the activation of TLR3, TLR7, and TLR9 by their cognate nucleic acids.²¹ Therefore, these intracellular TLRs are thought to play a very important role in autoimmune and other inflammatory diseases.^{20,21} Our data confirm causal involvement of TLR7 and TLR9 in vascular-related diseases, and development of a novel TLR7/9 dual antagonist may have important implications for understanding and treatment of exacerbation periods of other inflammatory diseases such as rheumatoid arthritis and after vascular interventions that cause direct vessel damage.

Blocking TLR7/9 signaling leads to a reduction in inflammation and reduced lipid accumulation. The role for TLR7/9 may therefore indicate regulation of cell stress and thereby providing activation of macrophages to start scavenging lipids, dying cells, and attracting more leukocytes to the inflammatory hazard. Our results confirm macrophage activation via TLR7/9 ligands and show a decrease of the presence of macrophages in the vessel wall after cuff placement in the TLR7/9 antagonist-treated mice.

Several studies have demonstrated the effect of intracellular TLR activation on lipid uptake.^{27,28,36,37} Both TLR7 and TLR9 agonists cause upregulation of adipocyte differentiation-related protein that is involved in lipid droplet formation in macrophages.³⁸ TLR9 was previously described to be involved in foam cell formation via upregulation of nicotinamide adenine dinucleotide phosphate oxidase 1, lectin-type oxLDL receptor 1, and perilipin 3.^{27,28} This foam cell formation was nuclear factor-kappaB– and IFN regulatory factor 7–dependent, and can be countered via liver X receptor activation.³⁷ Both nuclear factor-kappaB and IFN regulatory factor 7 are also important mediators of TLR7 signaling, and additionally we show that TLR7 stimulation in the presence of LDL leads to lipid uptake in macrophages. Our data show that blocking of TLR7 receptor results in no lipid uptake in macrophages that receive only LDL. Interestingly, the antagonist was capable of decreasing lipid accumulation of oxLDL in macrophages probably via IL-10. This might be attributable to altered efflux of lipids rather than decreased influx because CD36 expression is not altered whereas

IL-10, like *in vivo*, is upregulated. Macrophage IL-10 is known to enhance the efflux of cholesterol.³⁰ Different mechanisms, directly related to TLR signaling, can be involved in changing IL-10 levels. Martin et al.³⁹ showed that glycogen synthase kinase 3 can differentially regulate TLR-mediated cytokine production. In the normal TLR activation situation, there is little phosphatidylinositol 3-kinase stimulation, and glycogen synthase kinase 3 primarily remains constitutively active promoting the expression of IL-12. Alternative situations, with different pathogenic stimuli or blocking antagonists (small molecule inhibitors, RNA inhibitors), can lead to TLR-dependent activation of phosphatidylinositol 3-kinase and thereby inhibition of glycogen synthase kinase 3 that causes a decrease in IL-12 production and an increase in IL-10 production. Woodgett and Ohashi⁴⁰ have provided a nice overview about this glycogen synthase kinase 3 in TLR signaling. Alternatively, it was previously described that TLR4 activation can cause an increase of HMGB1 in macrophages, and that this HMGB1 is capable of reducing IL-10 levels.⁴¹ OxLDL triggers inflammatory signaling through a heterodimer of TLR 4 and TLR6. Assembly of this newly identified heterodimer is regulated by signals from the scavenger receptor CD36.⁴² Foam cells die of releasing lipids, intracellular molecules, and necrotic debris which can further activate the remaining macrophages via endosomal receptors like TLR7/TLR9.²⁹ Although HMGB1 can also be upregulated via TLR9 activation and it further enhances TLR7/9 activation, this might be a mechanism that causes the differences seen in IL-10 levels. Previously, it was already shown on regulatory T cells that additional TLR9 activation could inhibit IL-10 synthesis.⁴³ Further studies are needed to fully elucidate the mechanisms causing differences in IL-10 levels in relation to TLR signaling and blockade.

In summary, we observed upregulation of TLR7/9 expression during arterial restenosis and reduced macrophage activation and foam cell formation after TLR7/9 blockade, which was accompanied with increase in IL-10 production. Additional blocking of TLR7/9 leads to a reduction in neointima formation, increased IL-10 production, reduced macrophage presence in the lesions as well as less HMGB1 release, indicating the important role of TLR7 and TLR9 in postinterventional remodeling via reducing inflammation as well as lipid accumulation, thereby making it an interesting therapeutic target to reduce restenosis and accelerated atherosclerosis after vascular intervention.

References

1. Pires NM, Jukema JW, Daemen MJ, Quax PH. Drug-eluting stents studies in mice: do we need atherosclerosis to study restenosis? *Vascul Pharmacol.* 2006;44:257–264.
2. Lardenoye JH, Delsing DJ, de Vries MR, Deckers MM, Princen HM, Havekes LM, van Hinsbergh VW, van Bockel JH, Quax PH. Accelerated atherosclerosis by placement of a perivascular cuff and a cholesterol-rich diet in ApoE*3Leiden transgenic mice. *Circ Res.* 2000;87:248–253.
3. Hollestelle SC, De Vries MR, Van Keulen JK, Schoneveld AH, Vink A, Strijder CF, Van Middelaar BJ, Pasterkamp G, Quax PH, De Kleijn DP. Toll-like receptor 4 is involved in outward arterial remodeling. *Circulation.* 2004;109:393–398.
4. Karper JC, de Vries MR, van den Brand BT, Hoefler IE, Fischer JW, Jukema JW, Niessen HW, Quax PH. Toll-like receptor 4 is involved in human and mouse vein graft remodeling, and local gene silencing reduces vein graft disease in hypercholesterolemic APOE*3Leiden mice. *Arterioscler Thromb Vasc Biol.* 2011;31:1033–1040.
5. Michelsen KS, Wong MH, Shah PK, Zhang W, Yano J, Doherty TM, Akira S, Rajavashisth TB, Arditi M. Lack of Toll-like receptor 4 or myeloid differentiation factor 88 reduces atherosclerosis and alters plaque phenotype in mice deficient in apolipoprotein E. *Proc Natl Acad Sci USA.* 2004;101:10679–10684.
6. Vink A, Schoneveld AH, van der Meer JJ, van Middelaar BJ, Sluijter JP, Smeets MB, Quax PH, Lim SK, Borst C, Pasterkamp G, de Kleijn DP. In vivo evidence for a role of toll-like receptor 4 in the development of intimal lesions. *Circulation.* 2002;106:1985–1990.
7. Schoneveld AH, Oude Nijhuis MM, van Middelaar B, Laman JD, de Kleijn DP, Pasterkamp G. Toll-like receptor 2 stimulation induces intimal hyperplasia and atherosclerotic lesion development. *Cardiovasc Res.* 2005;66:162–169.
8. Arslan F, Smeets MB, Riem Vis PW, Karper JC, Quax PH, Bongartz LG, Peters JH, Hoefler IE, Doevendans PA, Pasterkamp G, de Kleijn DP. Lack of fibronectin-EDA promotes survival and prevents adverse remodeling and heart function deterioration after myocardial infarction. *Circ Res.* 2011;108:582–592.
9. Hochleitner BW, Hochleitner EO, Obrist P, Eberl T, Amberger A, Xu Q, Margreiter R, Wick G. Fluid shear stress induces heat shock protein 60 expression in endothelial cells in vitro and in vivo. *Arterioscler Thromb Vasc Biol.* 2000;20:617–623.
10. Li W, Sama AE, Wang H. Role of HMGB1 in cardiovascular diseases. *Curr Opin Pharmacol.* 2006;6:130–135.
11. Midwood K, Sacre S, Piccinini AM, Inglis J, Trebaul A, Chan E, Drexler S, Sofat N, Kashiwagi M, Orend G, Brennan F, Foxwell B. Tenascin-C is an endogenous activator of Toll-like receptor 4 that is essential for maintaining inflammation in arthritic joint disease. *Nat Med.* 2009;15:774–780.
12. Pryshchep O, Ma-Krupa W, Younge BR, Goronzy JJ, Weyand CM. Vessel-specific Toll-like receptor profiles in human medium and large arteries. *Circulation.* 2008;118:1276–1284.
13. Edfeldt K, Swedenborg J, Hansson GK, Yan ZQ. Expression of tolllike receptors in human atherosclerotic lesions: a possible pathway for plaque activation. *Circulation.* 2002;105:1158–1161.
14. Niessner A, Sato K, Chaikof EL, Colmegna I, Goronzy JJ, Weyand CM. Pathogen-sensing plasmacytoid dendritic cells stimulate cytotoxic T-cell function in the atherosclerotic plaque through interferon-alpha. *Circulation.* 2006;114:2482–2489.
15. Erridge C, Burdess A, Jackson AJ, Murray C, Riggio M, Lappin D, Milligan S, Spickett CM, Webb DJ. Vascular cell responsiveness to Toll-like receptor ligands in carotid atheroma. *Eur J Clin Invest.* 2008;38:713–720.
16. Boulé MW, Broughton C, Mackay F, Akira S, Marshak-Rothstein A, Rifkin IR. Toll-like receptor 9-dependent and -independent dendritic cell activation by chromatin-immunoglobulin G complexes. *J Exp Med.* 2004;199:1631–1640.
17. Kawai T, Akira S. The role of pattern-recognition receptors in innate immunity: update on Toll-like receptors. *Nat Immunol.* 2010;11:373–384.
18. Means TK, Latz E, Hayashi F, Murali MR, Golenbock DT, Luster AD. Human lupus autoantibody-DNA complexes activate DCs through cooperation of CD32 and TLR9. *J Clin Invest.* 2005;115:407–417.
19. Uccellini MB, Busconi L, Green NM, Busto P, Christensen SR, Shlomchik MJ, Marshak-Rothstein A, Viglianti GA. Autoreactive B cells discriminate CpG-rich and CpG-poor DNA and

- this response is modulated by IFN- α . *J Immunol.* 2008;181:5875–5884.
20. Krieg AM, Vollmer J. Toll-like receptors 7, 8, and 9: linking innate immunity to autoimmunity. *Immunol Rev.* 2007;220:251–269.
 21. Yanai H, Ban T, Wang Z, Choi MK, Kawamura T, Negishi H, Nakasato M, Lu Y, Hangai S, Koshiba R, Savitsky D, Ronfani L, Akira S, Bianchi ME, Honda K, Tamura T, Kodama T, Taniguchi T. HMGB proteins function as universal sentinels for nucleic-acid-mediated innate immune responses. *Nature.* 2009;462:99–103.
 22. Ivanov S, Dragoi AM, Wang X, Dallacosta C, Louten J, Musco G, Sitia G, Yap GS, Wan Y, Biron CA, Bianchi ME, Wang H, Chu WM. A novel role for HMGB1 in TLR9-mediated inflammatory responses to CpGDNA. *Blood.* 2007;110:1970–1981.
 23. Wang D, Bhagat L, Yu D, Zhu FG, Tang JX, Kandimalla ER, Agrawal S. Oligodeoxyribonucleotide-based antagonists for toll-like receptors 7 and 9. *J Med Chem.* 2009;52:551–558.
 24. Yu D, Wang D, Zhu FG, Bhagat L, Dai M, Kandimalla ER, Agrawal S. Modifications incorporated in CpG motifs of oligodeoxynucleotides lead to antagonist activity of toll-like receptors 7 and 9. *J Med Chem.* 2009;52:5108–5114.
 25. Kalinina N, Agrotis A, Antropova Y, DiVitto G, Kanellakis P, Kostolias G, Ilyinskaya O, Tararak E, Bobik A. Increased expression of the DNAbinding cytokine HMGB1 in human atherosclerotic lesions: role of activated macrophages and cytokines. *Arterioscler Thromb Vasc Biol.* 2004;24:2320–2325.
 26. Monraats PS, Pires NM, Schepers A, Agema WR, Boesten LS, de Vries MR, Zwinderman AH, de Maat MP, Doevendans PA, de Winter RJ, Tio RA, Waltenberger J, 't Hart LM, Frants RR, Quax PH, van Vlijmen BJ, Havekes LM, van der Laarse A, van der Wall EE, Jukema JW. Tumor necrosis factor- α plays an important role in restenosis development. *FASEB J.* 2005;19:1998–2004.
 27. Lee JG, Lim EJ, Park DW, Lee SH, Kim JR, Baek SH. A combination of Lox-1 and Nox1 regulates TLR9-mediated foam cell formation. *Cell Signal.* 2008;20:2266–2275.
 28. Gu JQ, Wang DF, Yan XG, Zhong WL, Zhang J, Fan B, Ikuyama S. A Toll-like receptor 9-mediated pathway stimulates perilipin 3 (TIP47) expression and induces lipid accumulation in macrophages. *Am J Physiol Endocrinol Metab.* 2010;299:E593–E600.
 29. Huang Q, Pope RM. Toll-like receptor signaling: a potential link among rheumatoid arthritis, systemic lupus, and atherosclerosis. *J Leukoc Biol.* 2010;88:253–262.
 30. Han X, Kitamoto S, Wang H, Boisvert WA. Interleukin-10 overexpression in macrophages suppresses atherosclerosis in hyperlipidemic mice. *FASEB J.* 2010;24:2869–2880.
 31. Cole JE, Navin TJ, Cross AJ, Goddard ME, Alexopoulou L, Mitra AT, Davies AH, Flavell RA, Feldmann M, Monaco C. Unexpected protective role for Toll-like receptor 3 in the arterial wall. *Proc Natl Acad Sci USA.* 2011;108:2372–2377.
 32. Chen WH, Kang TJ, Bhattacharjee AK, Cross AS. Intranasal administration of a detoxified endotoxin vaccine protects mice against heterologous Gram-negative bacterial pneumonia. *Innate Immun.* 2008;14:269–278.
 33. Park JS, Svetkauskaite D, He Q, Kim JY, Strassheim D, Ishizaka A, Abraham E. Involvement of toll-like receptors 2 and 4 in cellular activation by high mobility group box 1 protein. *J Biol Chem.* 2004;279:7370–7377.
 34. Lotze MT, Tracey KJ. High-mobility group box 1 protein (HMGB1): nuclear weapon in the immune arsenal. *Nat Rev Immunol.* 2005;5:331–342.
 35. Wang H, Bloom O, Zhang M, Vishnubhakat JM, Ombrellino M, Che J, Frazier A, Yang H, Ivanova S, Borovikova L, Manogue KR, Faist E, Abraham E, Andersson J, Andersson U, Molina PE, Abumrad NN, Sama A, Tracey KJ. HMG-1 as a late mediator of endotoxin lethality in mice. *Science.* 1999;285:248–251.
 36. Chen S, Sorrentino R, Shimada K, Bulut Y, Doherty TM, Crother TR, Arditi M. Chlamydia pneumoniae-induced foam cell formation requires MyD88-dependent and -independent signaling and is reciprocally modulated by liver X receptor activation. *J Immunol.* 2008;181:7186–7193.
 37. Sorrentino R, Morello S, Chen S, Bonavita E, Pinto A. The activation of liver X receptors inhibits toll-like receptor-9-induced foam cell formation. *J Cell Physiol.* 2010;223:158–167.
 38. Feingold KR, Kazemi MR, Magra AL, McDonald CM, Chui LG, Shigenaga JK, Patzek SM, Chan ZW, Lontos C, Grunfeld C. ADRP/ADFP and Mal1 expression are increased in macrophages treated with TLR agonists. *Atherosclerosis.* 2010;209:81–88.
 39. Martin M, Rehani K, Jope RS, Michalek SM. Toll-like receptor-mediated cytokine production is differentially regulated by glycogen synthase kinase 3. *Nat Immunol.* 2005;6:777–784.
 40. Woodgett JR, Ohashi PS. GSK3: an in-Toll-erant protein kinase? *Nat Immunol.* 2005;6:751–

-
- 752.
41. El Gazzar M. HMGB1 modulates inflammatory responses in LPS-activated macrophages. *Inflamm Res.* 2007;56:162–167.
 42. Stewart CR, Stuart LM, Wilkinson K, van Gils JM, Deng J, Halle A, Rayner KJ, Boyer L, Zhong R, Frazier WA, Lacy-Hulbert A, El Khoury J, Golenbock DT, Moore KJ. CD36 ligands promote sterile inflammation through assembly of a Toll-like receptor 4 and 6 heterodimer. *Nat Immunol.* 2010;11:155–161.
 43. Urry Z, Xystrakis E, Richards DF, McDonald J, Sattar Z, Cousins DJ, Corrigan CJ, Hickman E, Brown Z, Hawrylowicz CM. Ligation of TLR9 induced on human IL-10-secreting Tregs by 1 α ,25-dihydroxyvitamin D₃ abrogates regulatory function. *J Clin Invest.* 2009;119: 387–398.

Supplements

Material and Methods

Animals

All animal experiments were approved by the animal welfare committee of our institute and are performed according to the regulatory guidelines. Ten week old male hypercholesterolemic APOE*3Leiden mice bred in our laboratory were used as previously described elsewhere.¹ Mice were fed a Western-type diet starting three weeks before surgery that was continued throughout the entire experiment. Mice were allocated randomly to different treatment groups. Cholesterol levels were measured one day before surgery and at sacrifice. All mice received water and food ad libitum.

Murine model for neointima formation

Non-constricted polyethylene cuffs were placed around the femoral arteries as a well-established model for neointima formation and accelerated atherosclerosis.¹ Mice were sacrificed 14 days after cuff placement. All mice received a subcutaneous (s.c) injection with either 200µl sterile water (n=9) or 200µl TLR7/9 antagonist (n=7) (15mg/kg dissolved in sterile water) for sufficient blocking of TLR7/9 continuously without infectious complications. The first injection was administered directly after cuff placement and injections were repeated 4 times (schedule of two injection per week) until sacrifice of the mice.

Antagonist activity for TLR7 and TLR9 was assessed in six-to-eight-week-old female C57BL/6 mice obtained from Charles River Labs, (Wilmington, MA). Experimental procedures were performed according to the approved protocols and guidelines of the Institutional Animal Care and Use Committee of Idera Pharmaceuticals. Mice (n=2) were injected subcutaneously (s.c.) with 5 mg/kg antagonist. This was followed twenty-four hours later by 0.25 mg/kg TLR9 agonist 2 or 10 mg/kg of an RNA-based TLR7 agonist.³ Two hours post agonist administration, blood was collected by retro-orbital bleeding.

Morphological Quantification

At sacrifice blood was taken for cholesterol measurement and perfusion/fixation was done at 100mmHg with 4% formaldehyde via the left ventricle. Paraffin-embedded cross-sections were stained with either Weigert's Elastin stain or Hematoxylin-Phloxine-Saphrane (HPS) to visualize overall morphology. Six sections (5 µm thick) equally spaced throughout the cuffed segment were used to quantify intimal lesions, media and total vessel size using image analysis software for morphometric analysis (Qwin, Leica, Germany).

Cell cultures and reagents

Macrophages were derived from bone marrow from tibia and femur and seeded at a density of 250.000 cells/well in 6-wells plates and cultured for 7 days in RPMI Gluta-Max (Gibco) supplemented with 100U/ml penicillin/streptavidin, 25% Fetal Calf Serum (FCS) and 20µg/ml M-CSF (Myltec Biotechnologies) as described previously.⁴ Cells were cultured in the presence of the TLR7 agonist imiquimod (5µg/ml, Invivo-

gen), the TLR9 agonist ODN-CpG (10µg/ml, Invivogen), oxLDL 50µg/ml or native LDL 50µg/ml (Myltec Biotechnologies) and TLR7/9 antagonist (10µg/ml antagonist, Idera Pharmaceuticals). All analysis was done on triplicate wells each in three independent experiments.

C57BL/6 spleen cells (1×10^6 cells/ml) were cultured with 0.01 to 10 µg/ml of a TLR7/9 antagonist in combination with 1 µg/ml of a TLR9 agonist (DNA), 200µg/ml of a TLR7 (sRNA) agonist or 50 µg/ml of a TLR4 agonist (LPS) or 1µg/ml TLR3 agonist (Poly I:C). As controls, spleen cells were cultured with medium alone, TLR9, 7, 4 or 3 agonist alone, or highest dose (10 µg/ml) of the TLR7/9 antagonist alone. After 24 hours, culture supernatants were collected and induction of selected cytokines and chemokines was assessed. All analysis was done on triplicate wells each in three independent experiments.

FACS analysis

Circulating monocytes were stained with anti-mouse CD11b (Biolegend 101224) and Ly6C (Bioconnect MCA2389A488). BMD Macrophages (non-stimulated, antagonist, oxLDL or oxLDL+antagonist, 24h) were stained anti-mouse CD36-PE, clone 72-1, isotype Rat IgG2a (Ebioscience) and analyzed by FACS (BDcalibur).

TLR7/9 antagonist

TLR7 and TLR9 antagonist (5'-TGUCG*TTCT-X-TCTTG*CUGT-5'; wherein, G/U are 2'-O-methyl-ribonucleotides, G* is 7-deaza-dG, and X is glycerol linker) was synthesized at Idera Pharmaceuticals on solid support on an automated DNA/RNA synthesizer with phosphorothioate backbone, purified by HPLC, and analyzed. The purity of full-length antagonist was over 93% with the material balance comprised of oligonucleotides shorter than the full-length product (n-1 and n-2) as determined by anion-exchange HPLC, capillary gel electrophoresis and/or denaturing polyacrylamide gel electrophoresis. Sequence integrity was confirmed by MALDI-TOF mass spectral analysis. Antagonist contained less than 0.2 EU/ml of endotoxin, as determined by the Limulus assay (Bio-Whittaker). A novel control oligo was created with similar chemical modulations in the backbone as in our antagonist since these modifications are crucial to the functional activities of the antagonist. The following sequence was used as a control oligo=: 5'-CACCCAAGACAGCAGAAAG-3'; It is a phosphorothioate oligodeoxynucleotide with 2'-O-methyl-ribonucleotides at each end (nucleotides shown in bold).

Assessment of foam cell formation

Foam cell formation was assessed in macrophages that were either stimulated with native LDL 50µg/ml or oxLDL 50µg/ml (Myltec Biotechnologies). Incubation with native LDL was used to study the effect of TLR7 and TLR9 agonists (IQ, and ODN CpG) on lipid accumulation in macrophages, whereas oxLDL was used under conditions where effects the antagonist are studied. Oil-red-O staining of macrophages was used to identify foam cells. Cells were washed with PBS, fixed in 4%formaldehyde and pretreated with 60% isopropanol followed by staining with 1% Oil-Red-O solution (Sigma Aldrich). Cells were washed with 60% isopropanol followed by three times washing with PBS and examined by light microscopy. Foam cell designation required positive Oil-Red-O staining. Each condition was tested in triplicate.

ELISA assays

ELISA assays were performed with cell free supernatant using commercial available kits following the instructions of the manufacturer for TNF α , IL6, IL-10 (BD Biosciences) and IP-10 (Ebioscience).

Immunohistochemistry

Paraffin-embedded sections (5 μ m thick) were stained with antibodies against TLR7 (AbD serotec), TLR9 (AbD serotec), CD45 (BD Biosciences), Mac3 (BD Biosciences), HMGB1 (Abcam, Cambridge, United Kingdom) followed by the appropriate secondary antibody (Donkey anti Rabbit, GE Healthcare) (Goat anti Rat, Jackson labs) and incubated with AB complex (Vector laboratories) and were visualized with Novared (Vector laboratories). Slides were counterstained with haematoxylin.

To confirm the specificity of the IHC staining, parallel sections were incubated with 1% PBS/BSA alone without adding the primary antibody or with Rabbit IgG or Rat IgG controls or staining without 1st antibody or staining without the 2nd antibody. Sections were incubated with the secondary antibody, AB complex and were visualized with Novared. Controls were all negative.

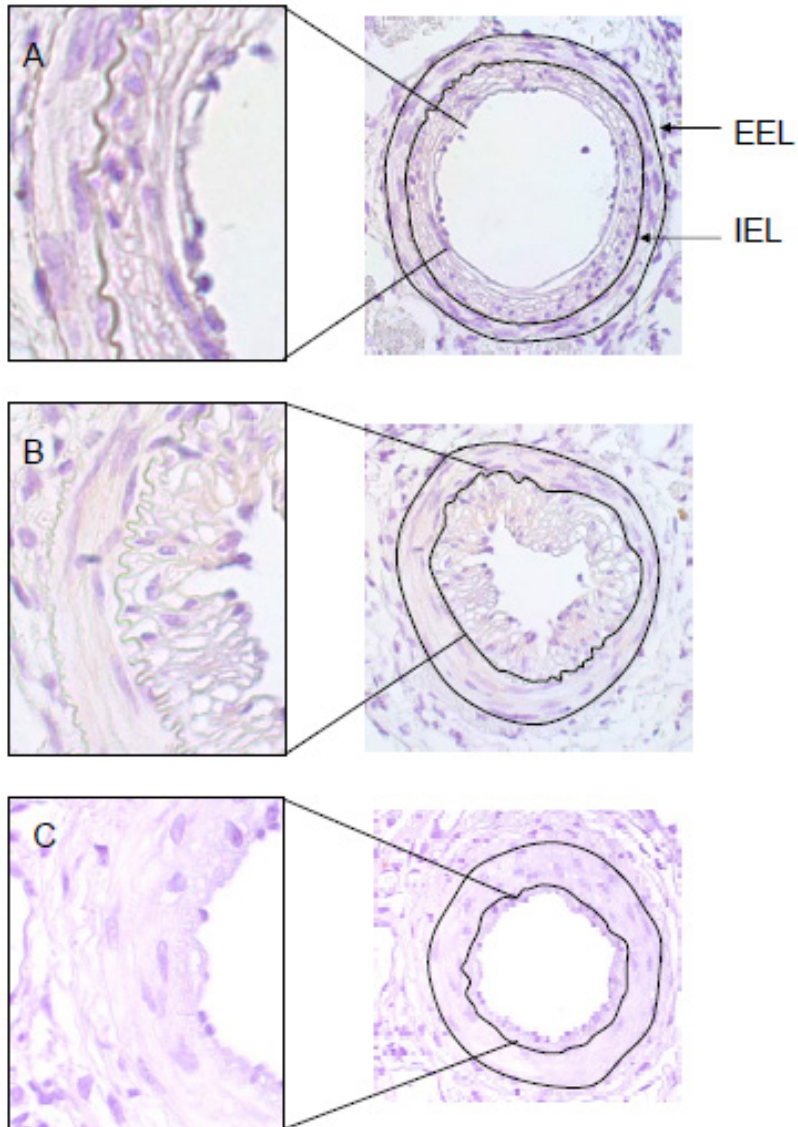
Statistics

For to the animal experiments, values are presented as mean \pm standard error of the mean (SEM). Statistical significance was calculated in SPSS for Windows 17.0. Differences between groups were determined using a non-parametric Mann-Whitney test. In vitro assays are presented as mean \pm standard error of the mean (SEM) and were statistically analyzed with a students T test.

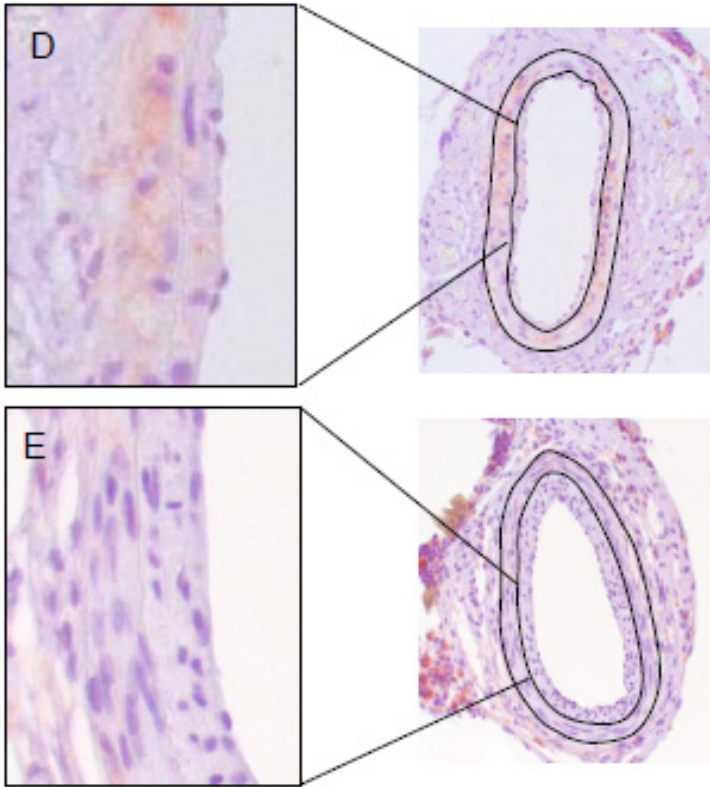
References

1. Lardenoye JH, Delsing DJ, De Vries MR, Deckers MM, Princen HM, Havekes LM, van Hinsbergh VW, van Bockel JH, Quax PH. Accelerated atherosclerosis by placement of a perivascular cuff and a cholesterol-rich diet in ApoE*3Leiden transgenic mice. *Circ Res* 2000;87:248-253.
2. Yu D, Wang D, Zhu FG, Bhagat L, Dai M, Kandimalla ER, Agrawal S. Modifications incorporated in CpG motifs of oligodeoxynucleotides lead to antagonist activity of toll-like receptors 7 and 9. *J Med Chem* 2009;52:5108-5114.
3. Kalinina N, Agrotis A, Antropova Y, DiVitto G, Kanellakis P, Kostolias G, Ilyinskaya O, Tararak E, Bobik A. Increased expression of the DNA-binding cytokine HMGB1 in human atherosclerotic lesions: role of activated macrophages and cytokines. *Arterioscler Thromb Vasc Biol* 2004;24:2320-2325.
4. Monraats PS, Pires NM, Schepers A, Agema WR, Boesten LS, De Vries MR, Zwinderman AH, de Maat MP, Doevendans PA, de Winter RJ, Tio RA, Waltenberger J, 't Hart LM, Frants RR, Quax PH, van Vlijmen BJ, Havekes LM, van der Laarse A, van der Wall EE, Jukema JW. Tumor necrosis factor-alpha plays an important role in restenosis development. *FASEB J* 2005;19:1998-2004.

Supplemental figures

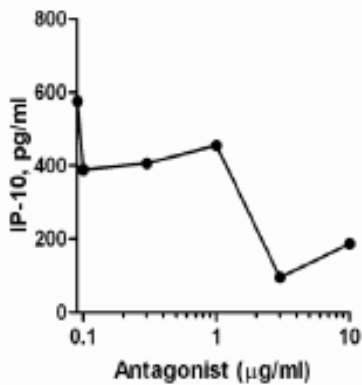
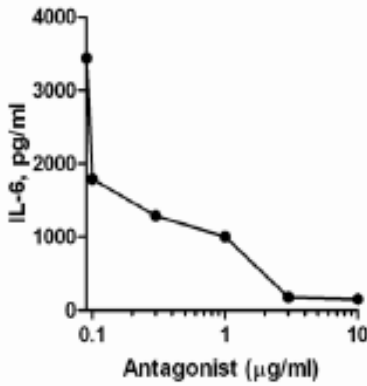
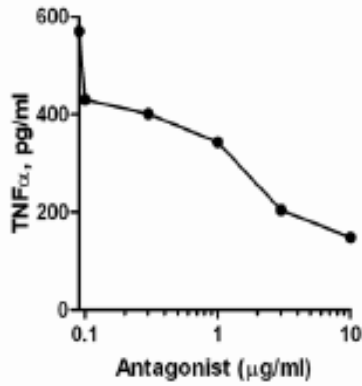


Supplemental figure 1: TLR7 staining on arterial lesion of wild type mice (A). TLR9 staining on arterial lesion of wild type mice (B). Example of negative control (C), Macrophage staining in lesions of hypercholesterolemic mice (D) and in wild type mice (E). N= 4 mice per staining; at least 6 sections per mouse were stained for either TLR7 or TLR9. IEL= Internal Elastic Lamina. EEL= External Elastic Lamina

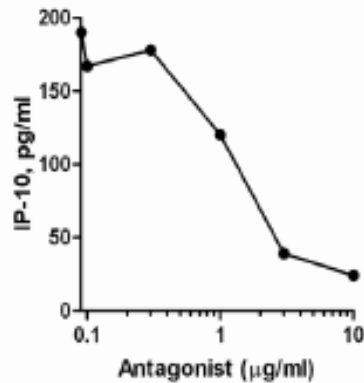
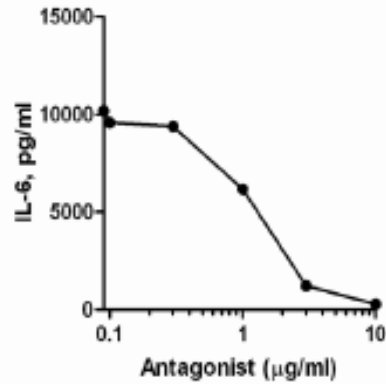
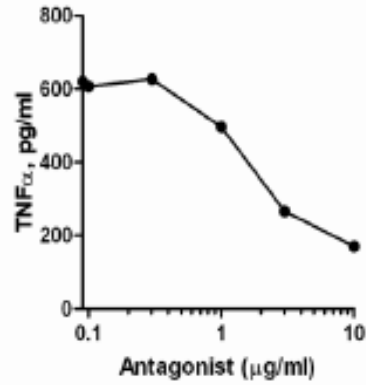


Supplemental figure I: TLR7 staining on arterial lesion of wild type mice (A). TLR9 staining on arterial lesion of wild type mice (B). Example of negative control (C), Macrophage staining in lesions of hypercholesterolemic mice (D) and in wild type mice (E). N= 4 mice per staining; at least 6 sections per mouse were stained for either TLR7 or TLR9. IEL= Internal Elastic Lamina. EEL= External Elastic Lamina

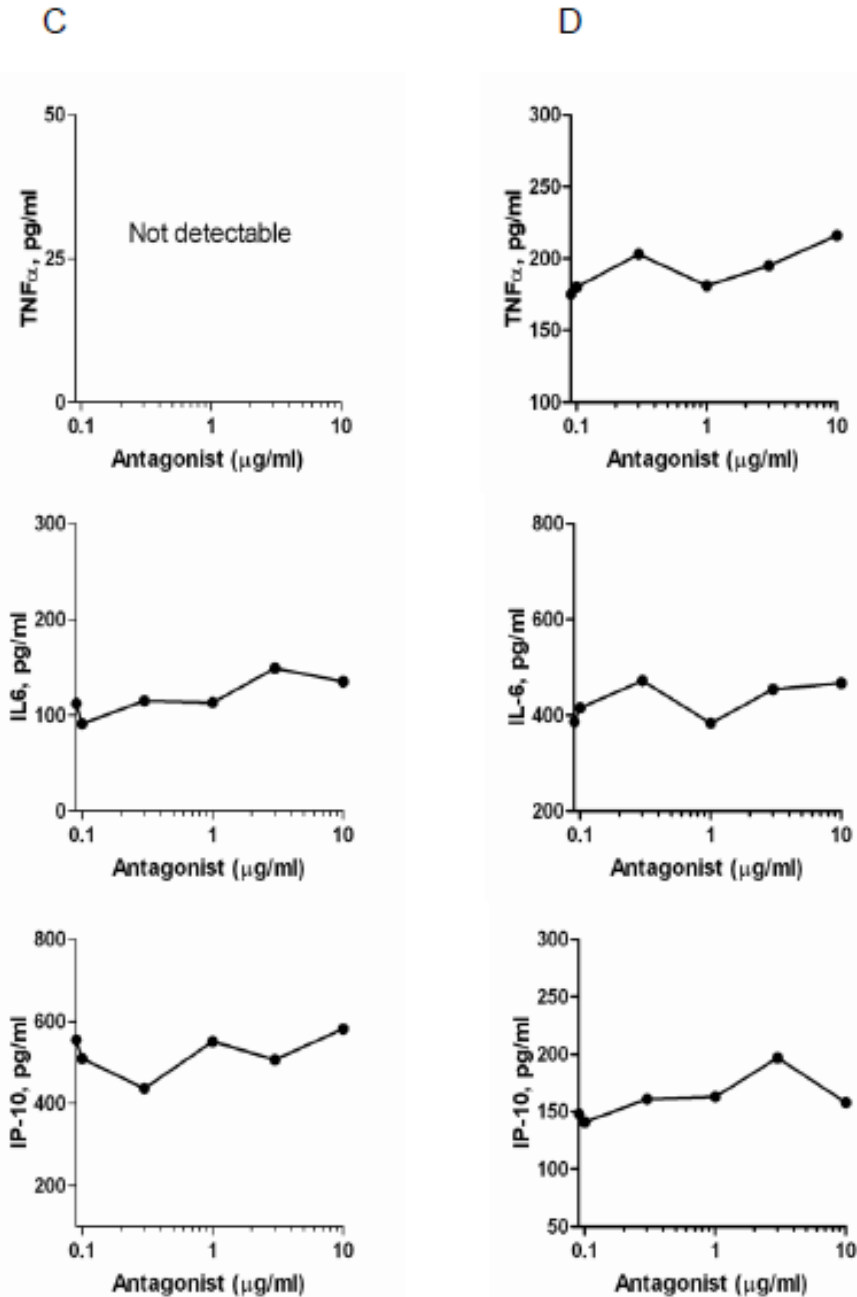
A



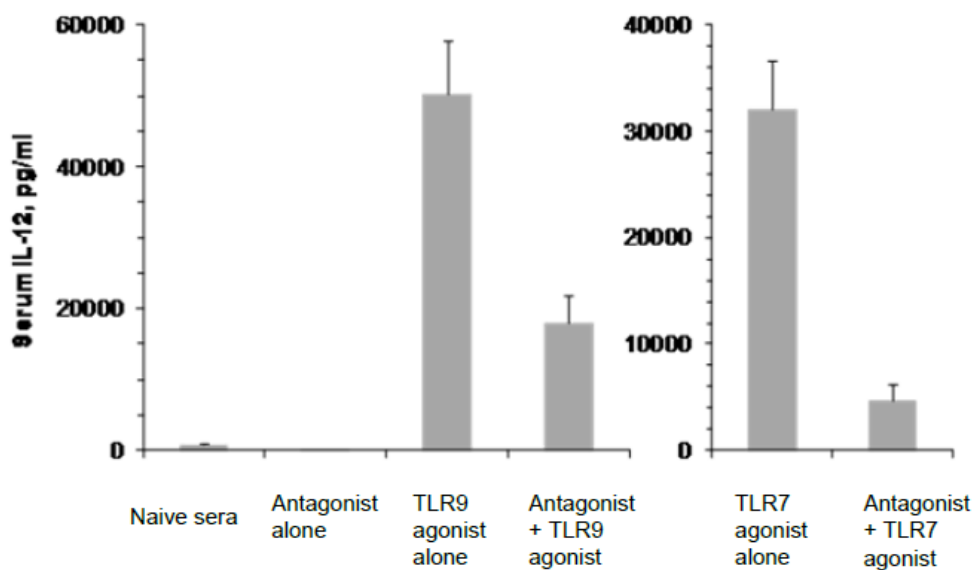
B



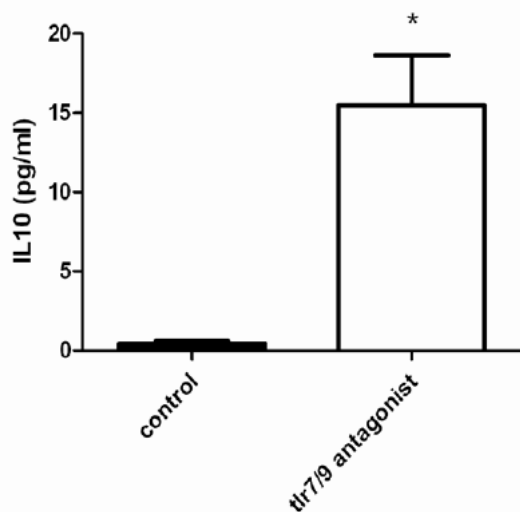
Supplemental figure II: Effect of antagonist on different TLR stimuli. Cytokine production of TNF α , IL6 and IP-10 upon TLR activation in the presence of 0.01 to 10 $\mu\text{g/ml}$ of the TLR7/9 antagonist. TLR7 agonist IQ+ TLR7/9 antagonist (A), TLR9 agonist ODN-CpG + TLR7/9 antagonist (B), TLR3 agonist PolyI:C + TLR7/9 antagonist (C), TLR4 agonist LPS + TLR7/9 antagonist (D). Data shown is 1 representative experiment out of 3 independent experiments.



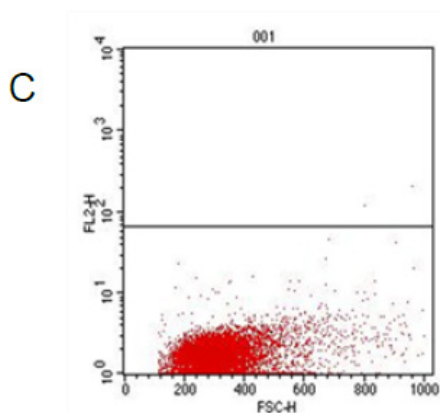
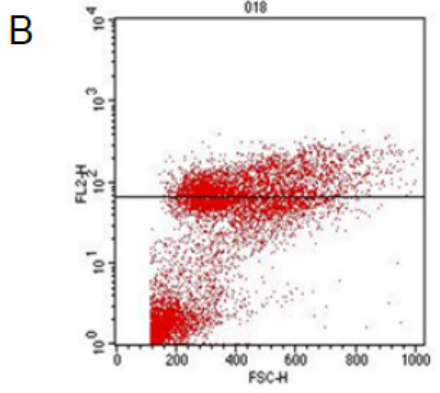
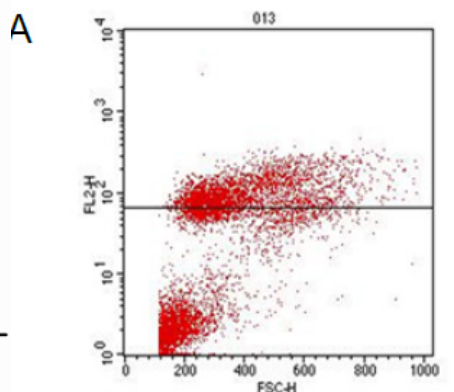
Supplemental figure II: Effect of antagonist on different TLR stimuli. Cytokine production of TNF α , IL6 and IP-10 upon TLR activation in the presence of 0.01 to 10 $\mu\text{g/ml}$ of the TLR7/9 antagonist. TLR7 agonist IQ+ TLR7/9 antagonist (A), TLR9 agonist ODN-CpG + TLR7/9 antagonist (B), TLR3 agonist PolyI:C + TLR7/9 antagonist (C), TLR4 agonist LPS + TLR7/9 antagonist (D). Data shown is 1 representative experiment out of 3 independent experiments.



Supplemental figure III: Inhibition of TLR9 and TLR7 agonist induced IL-12 by dual antagonist of TLR7/9 in C57BL/6 mice. Mice (n=2/group) were injected s.c. with 5 mg/kg of antagonist in the left flank and 24 hr later 0.25 mg/kg of TLR9 agonist or 10 mg/kg of TLR7 agonist s.c. in the right flank. Two hours after agonist administration, blood was collected and serum IL-12 levels were measured by ELISA.



Supplemental figure IV: Plasma IL10 levels in hypercholesterolemic ApoE3Leiden mice treated with or without TLR7/9 antagonist 14 days after cuff placement. Statistical analysis was performed by use of a non-parametric Mann-Whitney test, * = $P < 0.05$.



Supplemental figure V: FACS analysis of CD36 expression on oxDL stimulated macrophages. CD36 expression on macrophages stimulated for 24h with either oxDL (A) and or with oxDL in the presence of TLR7/9 antagonist (B) Isotype Control (C).

Chapter 8

T-cell co-stimulation by CD28- CD80/86 and its negative regulator CTLA-4 strongly influence accelerated atherosclerosis development

MM Ewing^{1,2,3}, JC Karper^{2,3}, S Abdul^{2,3}, RCM de Jong^{2,3}, HAB Peters^{2,3},
MR de Vries^{2,3}, A Redeker⁴, J Kuiper⁵, RE Toes⁶, R Arens⁴, JW Juke-
ma^{1,3}, PHA Quax^{2,3}

1 Dept. of Cardiology, Leiden University Medical Center (LUMC), Leiden, The Netherlands

2 Dept. of Surgery, LUMC, Leiden, The Netherlands

3 Einthoven Laboratory for Experimental Vascular Medicine, LUMC, Leiden, The Netherlands

4 Dept. of Immunohematology and Blood Transfusion, LUMC, Leiden, The Netherlands

5 Dept. of Biopharmaceutics, Leiden University, Leiden, The Netherlands

6 Dept. of Rheumatology, LUMC, Leiden, The Netherlands

Abstract

Objective T-cells are central to the immune response responsible for native atherosclerosis. The objective of this study is to investigate T-cell contribution to post-interventional accelerated atherosclerosis development, as well as the role of the CD28-CD80/86 co-stimulatory and Cytotoxic T-Lymphocyte Antigen (CTLA)-4 co-inhibitory pathways controlling T-cell activation status in this process.

Methods and Results The role of T-cells and the CD28-CD80/86 co-stimulatory and CTLA-4 co-inhibitory pathways were investigated in a femoral artery cuff mouse model for post-interventional remodeling, with notable intravascular CTLA-4+ T-cell infiltration. Reduced intimal lesions developed in CD4^{-/-} and CD80^{-/-}CD86^{-/-} mice compared to normal C57Bl/6J controls. Systemic abatacept-treatment, a soluble CTLA-4Ig fusion protein that prevents CD28-CD80/86 co-stimulatory T-cell activation, prevented intimal thickening by 58.5% (p=0.029).

Next, hypercholesterolemic ApoE3*Leiden mice received abatacept-treatment which reduced accelerated atherosclerosis development by 78.1% (p=0.040) and prevented CD4 T-cell activation, indicated by reduced splenic fractions of activated KLRG1+, PD1+, CD69+ and CTLA-4+ T-cells. This correlated with reduced plasma interferon- γ and elevated interleukin-10 levels. The role of CTLA-4 was confirmed using CTLA-4 blocking antibodies, which strongly increased vascular lesion size by 66.7% (p=0.008), compared to isotype-treated controls.

Conclusions T-cell CD28-CD80/86 co-stimulation is vital for post-interventional accelerated atherosclerosis development and is regulated by CTLA-4 co-inhibition, indicating promising clinical potential for prevention of post-interventional remodeling by abatacept.

Introduction

Atherosclerosis is a chronic inflammatory disease in which endothelial dysfunction leads to retention of oxidized low-density lipoprotein (oxLDL) cholesterol particles, attracting leukocytes and leading to a local inflammatory response¹⁻³. T-cell subsets have been shown to play a vital role in this process^{4,5}. Unlike native atherosclerosis, their contribution to post-interventional remodeling and accelerated atherosclerosis development remains uninvestigated. Although local intimal hyperplasia consist predominately of smooth muscle cells (SMCs) and connective tissue⁶, platelet and leukocyte (e.g. T-cells) adherence and activation have been shown to be driving factors behind this overshooting inflammatory healing response, leading to re-occlusion⁷.

T-cell responses to immunogenic (neo) antigens such as oxLDL cholesterol are regulated by antigen recognition signals provided by peptide-MHC antigen complexes on antigen-presenting cells (APCs) that bind to the T-cell antigen receptor (TCR), which operates in concert with co-stimulatory signals. The dominant co-stimulatory receptor CD28 is constitutively expressed on resting T-cells, whereas Cytotoxic T-lymphocyte antigen (CTLA)-4 is a co-inhibitory receptor expressed on activated T-cells^{8,9}. Their ligands CD80 and CD86 are upregulated upon activation and predominantly expressed on dendritic cells, B cells, and monocytes/macrophages. CTLA-4 is homologous to CD28 and binds CD80-CD86 with much higher affinity than CD28¹⁰. During an ongoing immune response, CTLA-4 is upregulated and outcompetes CD28 leading to inhibition of T-cell proliferation and reduction of interleukin (IL)-2 production¹¹. The importance of the CD28/CTLA-4 pathways has become evident by generating mice genetically deficient in CTLA-4, which develop fatal lymphoproliferative disease with progressive T-cell accumulation in peripheral lymphoid and solid organs^{12,13}.

Upon stimulation, CD4+ T helper 1 (Th1) effector cells upregulate CD40 ligand and produce interferon (IFN)- γ , responsible for pro-atherogenic cellular chemotaxis and macrophage activation³, leading to inflammation. Blocking of CD28-CD80/86 mediated co-stimulation by CTLA-4 domain-containing Ig fusion proteins (abatacept), capable of binding CD80/86 with high-affinity can downregulate T-cell proliferation¹⁴ and production of tumor necrosis factor (TNF)- α , IL-2 and IFN- γ in vitro¹⁵. Abatacept displays little immunogenicity, with <3% of patients developing an antibody response towards abatacept¹⁶ and is used to treat rheumatoid arthritis (RA) patients¹⁷⁻¹⁹. Although the T-cell^{20,21} and CD28-CD80/CD86 co-stimulation^{5,22} roles have been demonstrated in native atherosclerosis, their contribution to post-interventional remodeling and accelerated atherosclerosis development is unknown, as is the role of CTLA-4. We hypothesized that the CD28-CD80/86 pathway is instrumental in post-interventional T-cell-regulated arterial inflammation and that the co-inhibitory CTLA-4 pathway downregulates these T-cell responses limiting inflammatory-induced intimal thickening.

In the present study, we studied the role of CD4 T-cells and co-stimulatory cellular activation in post-interventional remodeling in both CD4^{-/-} and CD80^{-/-}CD86^{-/-} mice using a well-established mouse model^{7,23}. CTLA-4 contribution to this process is investigated by treating operated C57Bl/6 mice with abatacept. Next, CTLA-4 co-inhibition effects are investigated by studying post-interventional accelerated atherosclerosis development in hypercholesterolemic ApoE3*Leiden mice after both aba-

tacept treatment and systemic CTLA-4 antibody blockade. Our results demonstrate that CD4 T-cells promote post-interventional atherosclerosis in a CD28-CD80/CD86-dependent fashion and that CD4 T-cell CTLA-4 co-inhibition regulates accelerated atherosclerosis development and bears high potential for prevention of post-revascularization vascular remodeling.

Methods

The authors of this manuscript have certified that they comply with the Principles of Ethical Publishing in the International Journal of Cardiology²⁴.

Femoral arterial cuff mouse model

All experiments were approved by the Institutional Committee for Animal Welfare of the Leiden University Medical Center and the investigations are in conformation with the Guide for the Care and Use of Laboratory Animals published by the US National Institutes of Health (NIH Publication No. 85-23, revised 1996). We performed multiple *in vivo* studies in which wildtype (C57Bl/6) control, CD4^{-/-} and CD80^{-/-}CD86^{-/-} mice were subjected to femoral artery cuff placement to induce vascular injury and remodeling^{7, 23}. Both during surgery and sacrifice, mice were anesthetized with a combination of IP injected Midazolam (5 mg/kg, Roche), Medetomidine (0.5 mg/kg, Orion) and Fentanyl (0.05 mg/kg, Janssen). This surgery produces concentric intimal lesions that affect vessel patency and consist predominately of SMCs and connective tissue and is strongly inflammation-dependent⁶.

Abatacept treatment

Treatment with 10 mg/kg abatacept at the time of surgery through intraperitoneal injection, similarly to that used in clinical treatment of RA and in earlier murine studies was given to evaluate the role of the CD28-CD80/CD86 co-stimulatory pathway in this process.

Vascular wall lesion analysis

In these vascular segments, inflammatory cell adhesion, infiltration, intimal thickening and lesion composition were assessed using histology, morphometry and immunohistochemistry (IHC), as described previously²³. Samples were stained with hematoxylin-phloxine-saffron and specific vessel wall composition was visualized for elastin, collagen and with antibodies against leukocytes, macrophages, vascular SMCs, CD3 and CD4 T-cells, matrix metalloproteinase-9 and CTLA-4. This analysis was repeated in operated hypercholesterolemic ApoE3*Leiden mice to assess accelerated atherosclerotic lesion phenotype.

Flow cytometry

Leukocyte subsets were characterized using flow cytometry in spleen and draining inguinal lymph nodes²⁵. These were harvested and single-cell suspensions were prepared by mincing the tissue through a 70- μ m cell strainer. For cell surface staining, cells were resuspended in staining buffer and incubated with fluorescent conjugated antibodies. After washing and resuspension in staining buffer, cells were acquired using a BD LSRII flow cytometer and data was analyzed using FlowJo software.

Cells were stained with fluorochrome-conjugated monoclonal antibodies specific for CD3, CD4, CD44, CD25, CD62L CD69, CD127, CTLA-4, and KLRG1 and staining for intracellular FoxP3 was performed using the FoxP3 staining set. 7-AAD was used to exclude dead cells.

Biochemical analysis

Plasma IFN- γ and IL-10 levels were determined using ELISA were performed according to the manufacturer's instructions and total plasma cholesterol was measured enzymatically.

Functional CTLA-blockade

CTLA-4 co-inhibition effects on accelerated atherosclerosis development was confirmed using anti-CTLA-4 blocking antibodies¹¹. Anti-murine CTLA-4 IgG antibodies used in this study were isolated from supernatants from the 9H10 hybridoma line. Antibody concentration was performed using an artificial kidney and the concentrated antibodies were protein G-purified. CTLA-4 blockade in ApoE3*Leiden mice was induced by injecting animals IP with 200 μ g of anti-mouse CTLA-4 or control IgG once every 2 days, starting at the time of surgery. All materials and methods are described in detail in the supplemental material.

Results

CD4 T-cells and CD80/86 mediated-co-stimulation are critically involved in post-interventional vascular remodeling

To investigate the contribution of CD4 T-cells and the CD28/CTLA-4-CD80/86 pathways to vascular remodeling, we placed femoral artery cuffs in control, CD4^{-/-} and CD80^{-/-}CD86^{-/-} mice and animals receiving abatacept-treatment. Murine body weights were similar at surgery and sacrifice (table 1). 21d after surgery lesions were stained with hematoxylin-phloxine-saffron (HPS) to visualize overall vascular wall morphology (fig 1A), and revealed that untreated animals, compared to CD4^{-/-}, CD80^{-/-}CD86^{-/-} and abatacept-treated mice, developed concentric intimal thickening leading to luminal stenosis. Weigert's elastin staining was performed to allow morphometric analysis using the elastic laminae to assess vessel layer surface area and remodeling. Analysis showed that intimal thickening was reduced by 72.1% ($p=0.006$) in CD4^{-/-} mice, by 64.2% ($p=0.015$) in CD80^{-/-}CD86^{-/-} mice and by 58.5% ($p=0.029$) in abatacept-treated animals compared to controls (fig 1B).

Since the total surface area (μm^2) of the media was similar in all groups (fig 1B), absence of CD4 T-cells and CD80/86 co-stimulatory molecules and abatacept-treatment led to reduced intima / media ratio with respectively 70.0% ($p=0.011$), 66.4% ($p=0.005$) and 55.3% ($p=0.047$, fig 1C). Additionally, the percentage luminal stenosis was reduced in these groups by 48.7% ($p=0.042$), 47.7% ($p=0.031$) and 49.9% ($p=0.036$) respectively (fig 1D). These results indicate a reduced inflammatory-driven remodeling process the injured arterial segments. The total vessel and luminal areas (μm^2) were not different between all groups (fig 1A,C). These data indicate an important role of CD4 T-cells and the CD28/CTLA-4-CD80/CD86 co-stimulatory axis in post-interventional vascular remodeling.

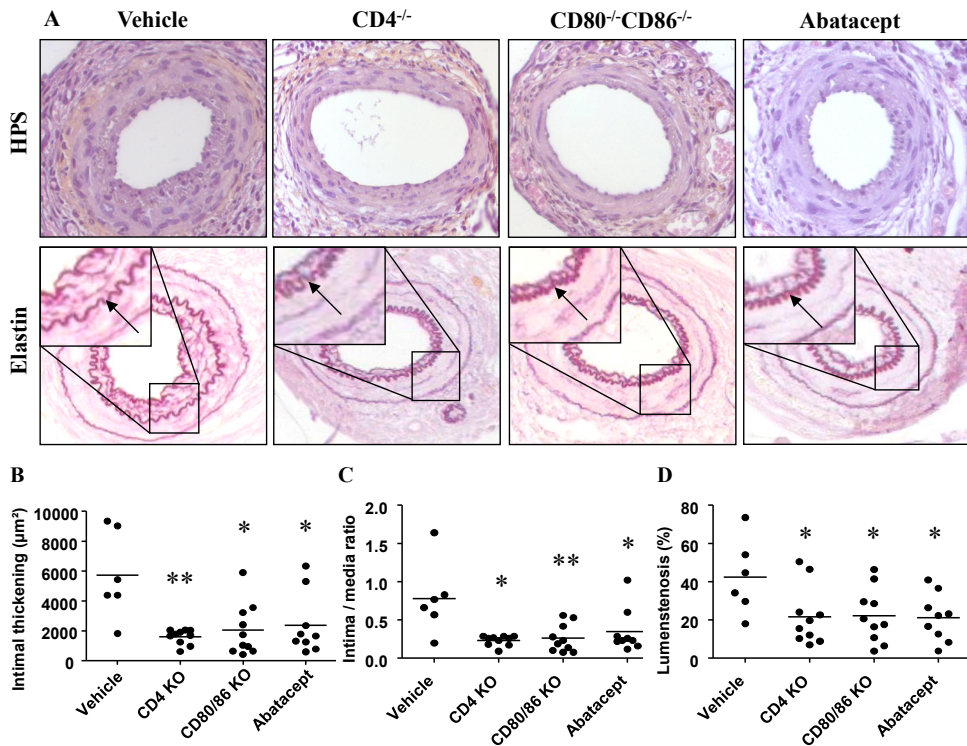


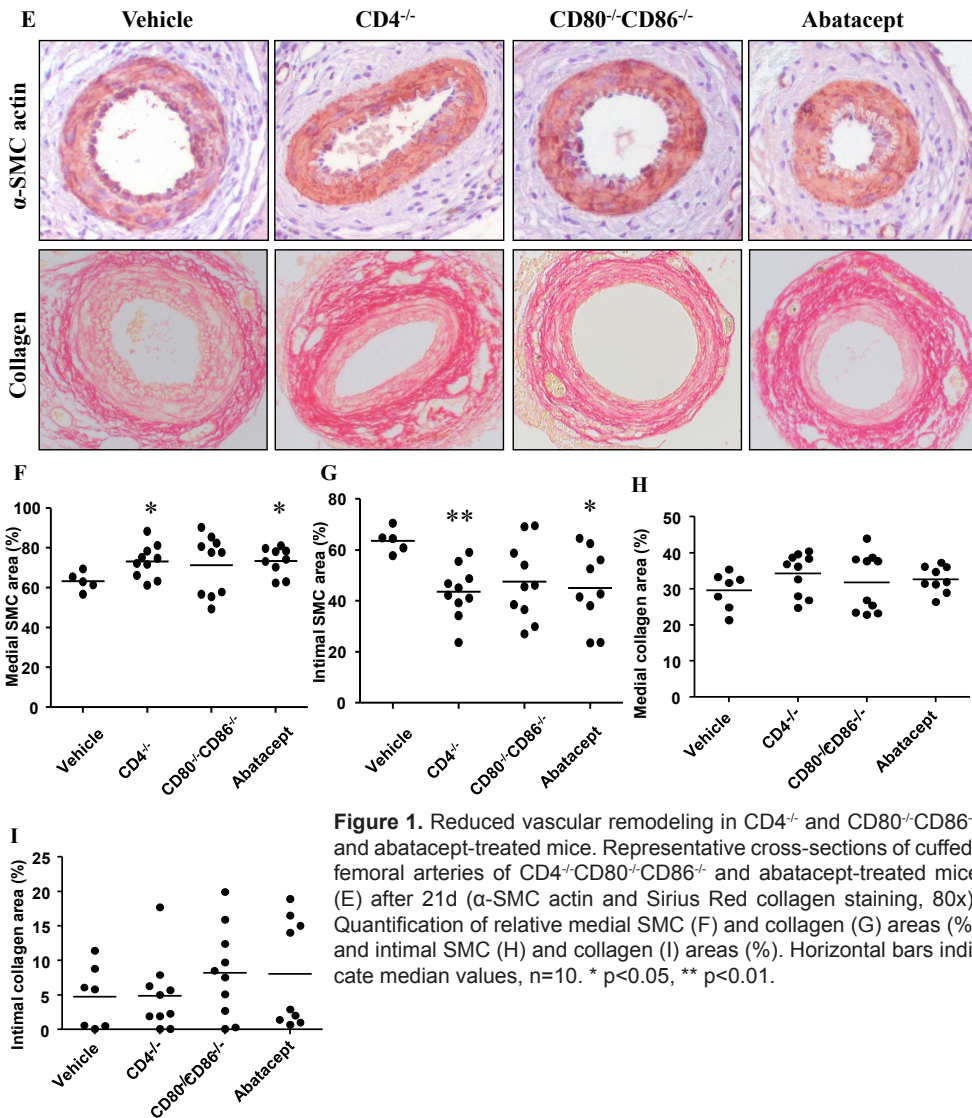
Figure 1. Reduced vascular remodeling in $\text{CD4}^{-/-}$ and $\text{CD80}^{-/-}\text{CD86}^{-/-}$ and abatacept-treated mice. Representative cross-sections of cuffed-femoral arteries of $\text{CD4}^{-/-}\text{CD80}^{-/-}\text{CD86}^{-/-}$ and abatacept-treated mice (A) after 21 d (hematoxylin-phloxine-saffron (HPS) and Weigert's elastin staining, 80x, arrows indicate internal elastic laminae). Quantification of intimal thickening (μm^2) (B), intima / media ratio (C) and luminal stenosis (%) (D). Horizontal bars indicate median values, $n=10$. * $p<0.05$, ** $p<0.01$.

$\text{CD4}^{-/-}$, $\text{CD80}^{-/-}\text{CD86}^{-/-}$ and abatacept-treated mice display an altered lesion composition during post-interventional vascular remodeling

Lesion composition was analyzed using IHC, which showed larger relative areas (to the total vessel layer surface area) of α -SMC actin in the media by 15.8% ($p=0.028$) in $\text{CD4}^{-/-}$ and 16.1% ($p=0.028$) in abatacept-treated mice (fig 1E), whilst α -SMC actin+ relative area in the intima was significantly decreased compared to controls by 31.6% ($p=0.001$) and 29.3% ($p=0.019$) respectively (fig 1G). Both medial (fig 1H) and intimal (fig 1I) relative collagen areas (%) were similar between groups, reflecting absolute α -SMC actin+ and collagen areas (μm^2) in the media (fig 1I A,C). Total α -actin+ SMC area (μm^2) in the intima was only reduced in $\text{CD4}^{-/-}$ mice by 59.7% ($p=0.008$) whilst collagen area (μm^2) remained unchanged (fig 1I B,D) with limited CD45 leukocyte and CD4 T-cell infiltration in the vascular layers in control sections (fig 1I E), indicating an indirect but clear effect of CD4 T-cells upon vascular SMC proliferation and migration.

Abatacept prevents accelerated atherosclerosis

The contribution of the CD28-CD80/CD86 co-stimulatory pathway to accelerated atherosclerosis development was tested in a preclinical model of accelerated athero



sclerosis development in Western-type diet-fed hypercholesterolemic ApoE3*Leiden mice using abatacept as therapeutic intervention strategy. Plasma cholesterol concentrations (12.1 ± 3.1 mmol/L) were similar in all groups throughout this study (table 2). Vehicle and abatacept-treated ApoE3*Leiden mice were sacrificed 14d after arterial cuff placement and accelerated atherosclerotic lesions were stained with HPS to visualize overall vascular morphology (fig 2A). This revealed that vehicle-treated animals developed concentric intimal thickening and luminal stenosis, consisting of connective tissue with profound cellular infiltration which was absent in abatacept-treated mice. Quantitative analysis of cuffed arteries stained with Weigert's elastin identified reduced intimal thickening after abatacept treatment with 78.1% ($p=0.040$, fig 2B). Abatacept also decreased absolute medial surface area (μm^2) by 22.9%

($p=0.040$, fig 2C), and intima / media ratio by 69.5% ($p=0.037$, fig 2D). Furthermore, luminal stenosis percentage was reduced by 48.2% ($p=0.021$, fig 2E), identifying a potent role for CTLA-4 co-inhibition controlling inflammatory post-interventional vascular remodeling. The total vessel and luminal areas (μm^2) were similar in the abatacept-treated group, although a trend towards reduced total vessel area by 34.6% was observed ($p=0.094$) (fig IIIA, B).

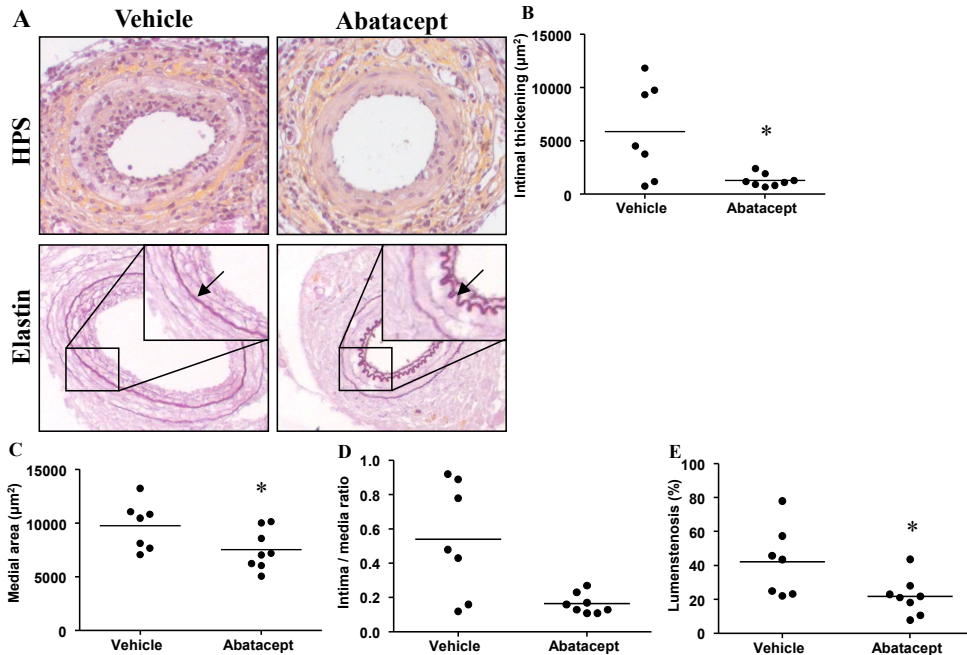


Figure 2. Abatacept prevents accelerated atherosclerosis in hypercholesterolemic mice. Representative cross-sections of cuffed-femoral arteries of hypercholesterolemic ApoE3*Leiden mice following vehicle or abatacept-treatment (A) after 14d (HPS and Weigert's elastin staining, 80x, arrows in inserts indicate internal elastic laminae). Quantification of intimal thickening (μm^2) (B), medial area (μm^2) (C), intima / media ratio (D) and luminal stenosis (%) (E). Horizontal bars indicate median values, $n=10$. * $p < 0.05$.

Abatacept positively affects accelerated atherosclerotic lesion composition

Lesion composition was analyzed using IHC to allow arterial wall inflammatory phenotype assessment (fig 3A). Abatacept-treatment produced an altered lesion composition with a reduced inflammatory phenotype. Abatacept reduced leukocyte and macrophage/foam cell fractions (% of all cells) in the media by 64.0% ($p=0.043$, fig 3B) and 72.1% respectively ($p=0.003$, fig 3D) and intima by 73.9% ($p=0.009$, fig 3C) and 30.5% ($p=0.048$, fig 3E), respectively. Abatacept-treatment also led to a comparable medial ($p=0.602$, fig 3F) and 29.8% ($p=0.042$, fig 3G) increased intimal α -SMC actin surface area (%), although absolute intimal SMC area (μm^2) was not increased ($p=0.743$, fig IVA), similarly to the tunica media ($p=0.888$, fig IVB). Whereas limited CD3 T-cells and matrix metalloproteinase-9 expressing cells could be detected in the tunica intima (fig 3H, I), corresponding with a similar collagen quantity in the intima, abatacept reduced these cells in the tunica adventitia by 65.9% ($p < 0.0001$, fig 3J) and 64.7% ($p < 0.0001$, fig 3K) respectively.

T-cell CTLA-4 and CD4 co-localized expression was identified using IHC in the in-

jured arterial segments of vehicle-treated ApoE3*Leiden mice and was absent in uninjured arteries, but occurred 3d after surgery and could still be observed 14d after injury, indicating continuing local arterial T-cell activation throughout the remodeling process and accelerated atherosclerosis development (fig 3L).

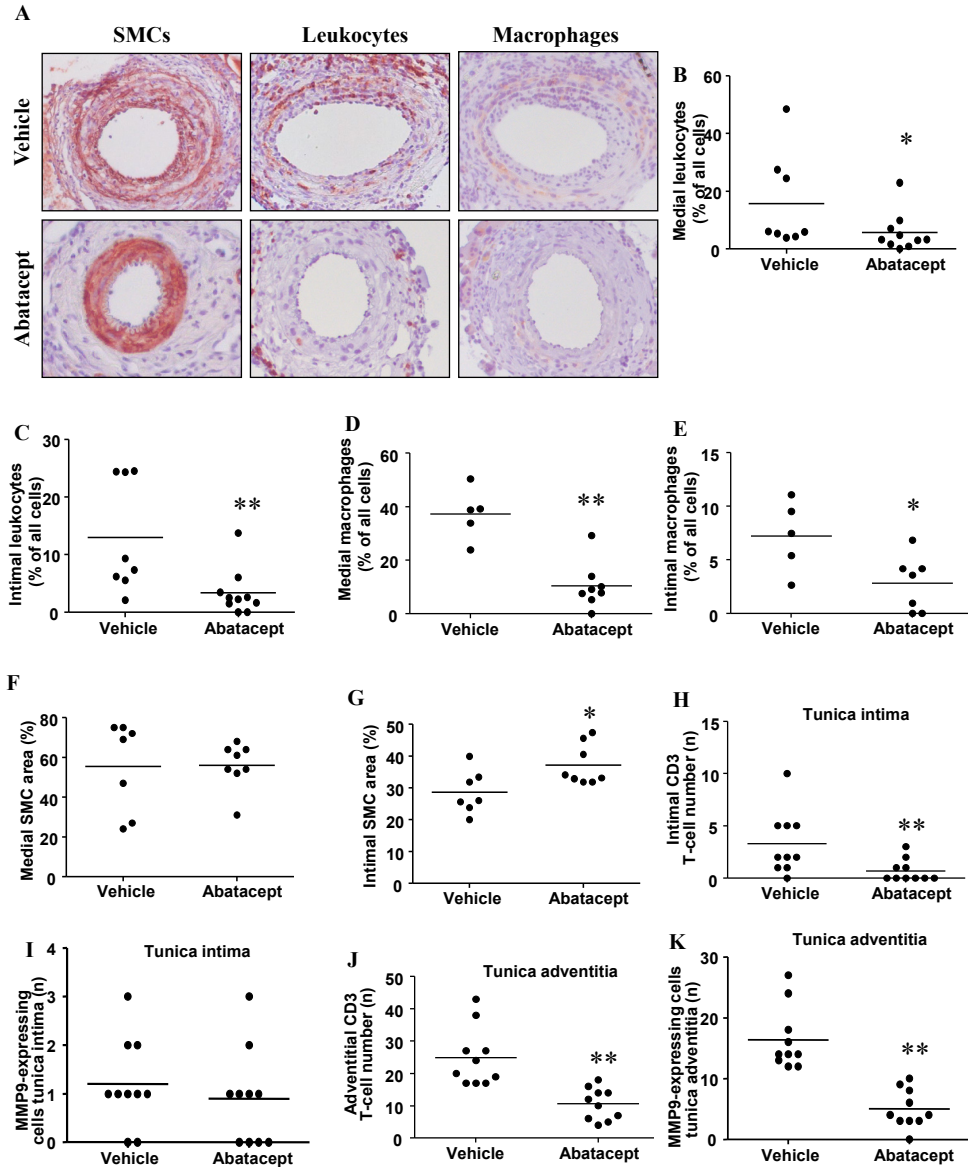


Figure 3. Abatacept positively affects accelerated atherosclerotic lesion composition. Representative cross-sections of cuffed-femoral arteries of ApoE3*Leiden mice following vehicle or abatacept-treatment (A) after 14d (leukocyte, macrophage and α -SMC actin staining, 80x). Quantification of relative medial leukocyte (B), macrophage (D) and SMC (F) areas (%) and intimal leukocyte (C), macrophage (E) and SMC (G) areas (%) and intimal CD3 (n) (H) and MMP-9 (n) (I), as well as adventitial CD3 (n) (J) and MMP-9 cells (n) (K). Horizontal bars indicate median values, n=10. * p<0.05, ** p<0.01.

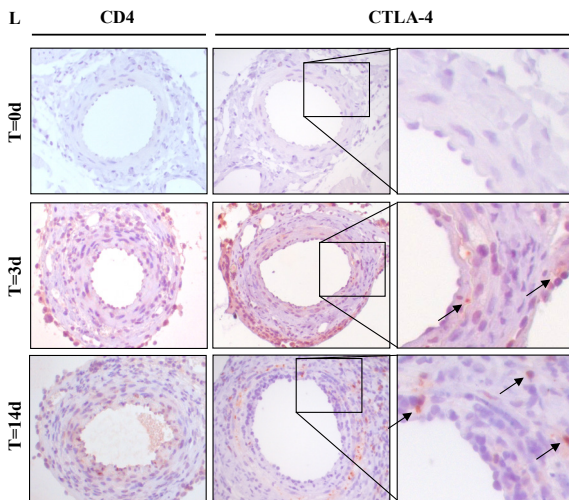


Figure 3. Abatacept positively affects accelerated atherosclerotic lesion composition. (L) T-cell CTLA-4 and CD4 expression throughout the vessel wall of ApoE3*Leiden mice in time before and 3d and 14d after surgery (CTLA-4 and CD4 staining, 80x, arrows in inserts indicate positive staining).

Abatacept prevents systemic CD4 T-cell activation during accelerated atherosclerosis

To examine the role of CTLA-4 co-inhibition upon T-cell activation involved in accelerated atherosclerosis development, CD4 T-cell numbers and T-cell activation status were assessed. The markers Killer cell lectin-like receptor subfamily G member (KLRG)-1, Programmed Death (PD)-1, CD69 and CTLA-4 were used to analyze T-cell activation in the splenic reservoir and draining inguinal lymph nodes of mice 14d after surgery.

Absolute CD4 ($p=0.557$, fig 4A) splenic T-cell numbers were similar in vehicle and abatacept-treated mice, as were total splenic cell contents (absolute cells) and percentages CD4 T-cell fractions (fig VA,B). Abatacept reduced splenic CD4 T-cells fractions expressing CD69 by 61.9% ($p=0.008$, fig 4B), PD1 by 49.4% ($p=0.041$, fig 4C), KLRG1 by 47.4% ($p=0.032$, fig 4E), and CTLA-4 by 47.0% ($p=0.016$, fig 4F). These data indicate that abatacept strongly and consistently prevented systemic CD4 T-cell activation, thereby reducing accelerated atherosclerotic lesion formation. In contrast to the reduced severity of inflammatory vascular remodeling, co-inhibition with abatacept treatment also reduced fractions of CD4+CD25+FoxP3+ regulatory T-cells by 33.3% ($p=0.016$, fig 4H) in the spleen. No significant differences in the percentages of naive (CD62L+ CD44-), central-memory (CD62L+ CD44+) or effector-memory (CD62L- CD44+) CD4 T-cell populations were observed ($p>0.05$, fig VC-F). Contrary to significant reduction of activated CD4 T-cells in the spleen after abatacept-treatment, no evidence of T-cell activation in draining inguinal lymph nodes could be found (fig VIA-G), despite adequate cell number isolation for analysis.

Abatacept affects systemic cytokine levels during accelerated atherosclerosis

Contribution of activated T-cell fractions to vascular remodeling severity is supported by the positive correlation ($R^2=0.61$, $p=0.002$) between KLRG1+ CD4+ T-cells (%)

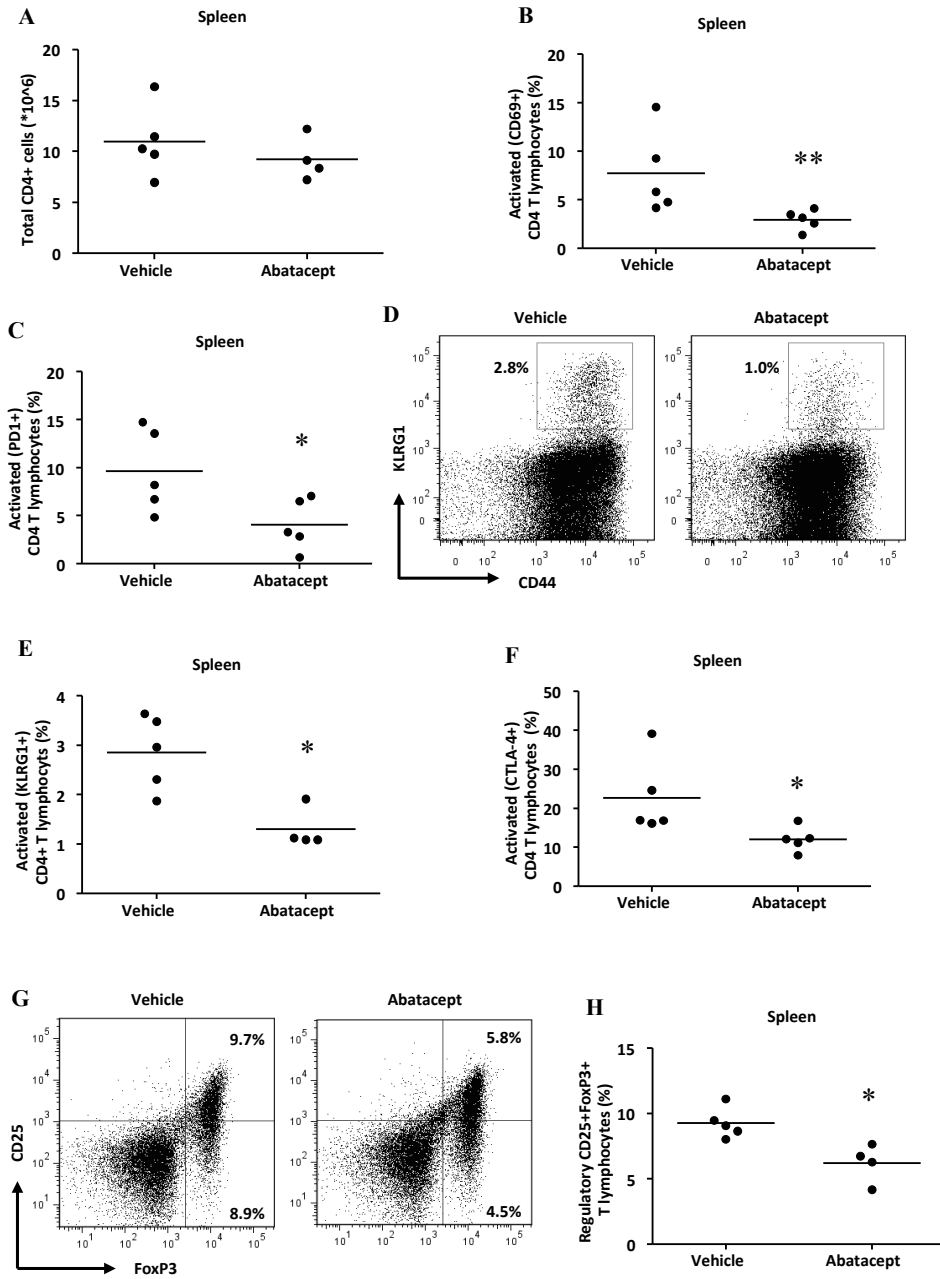


Figure 4. Abatacept prevents systemic CD4 T-cell activation in ApoE3*Leiden mice. Abatacept did not affect total CD4 splenic T-cell count (absolute cells) 14d after surgery (A). T-cells were analyzed using multiparametric flow cytometry and gated for 7AAD-, CD3+ and CD4+ markers and subsequently for either KLRG1+, PD1+, CD69+, CTLA-4+ or CD25+ and FoxP3+ expression and are displayed in dot plots (D and G). Abatacept reduced CD69+ (B), PD1+ (C), KLRG1+ (E) and CTLA-4+ (F) activated CD4 T-cell fractions (%), together with CD25+FoxP3+ regulatory (H) CD4 T-cell fractions (%). Horizontal bars indicate median values, n=5. * p<0.05, ** p<0.01.

and intimal thickening (μm^2) (fig 5A). Interestingly, the ratio between regulatory and effector helper T-cells remained unchanged in treated animals (fig 5B). Affected systemic CD4 T-cell activation in abatacept-treated mice was investigated by IFN- γ and IL-10 measurements in plasma at 14d. Hypercholesterolemic control animals contained an elevated plasma concentration IFN- γ of 43.2 ± 12.1 pg/ml, while abatacept-treatment reduced the IFN- γ concentration to non-detectable levels ($p=0.00023$, fig 5C) after vascular injury. In contrast, plasma IL-10 was significantly elevated from 4.5 ± 2.0 pg/ml in controls to 23.7 ± 7.1 pg/ml ($p=0.012$, fig 5D) in abatacept-treated mice. Together, these cytokines indicate that abatacept reduced systemic inflammation.

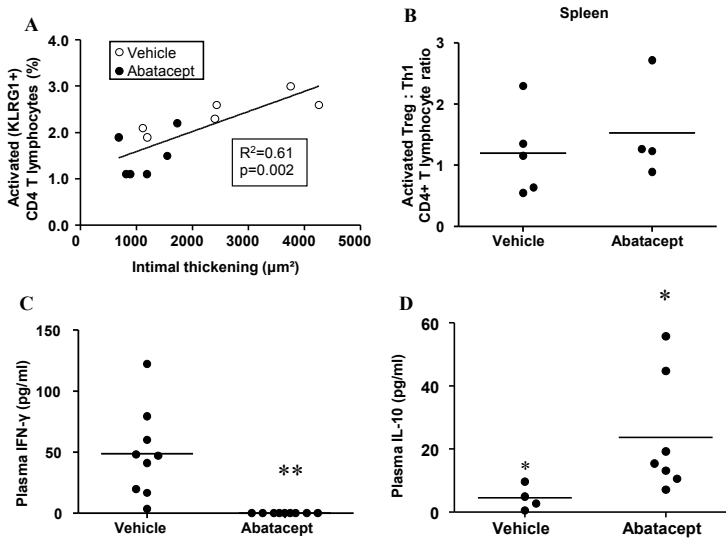


Figure 5. Profound CD4 T-cell contribution to post-interventional accelerated atherosclerosis development. (A) Positive correlation between KLRG1+ CD4 T-cell fractions (%) and intimal thickening (μm^2) ($n=6$). Abatacept did not affect CD4 regulatory T-cell: effector T-cell ratio (B). Plasma IFN γ (pg/ml) was reduced after 14d following abatacept-treatment (C), whilst plasma IL-10 (pg/ml) was upregulated (D). Horizontal bars indicate median values, $n=10$. n.d. non-detectable. * $p<0.05$, ** $p<0.01$.

CTLA-4 blockade exacerbates accelerated atherosclerosis development

To confirm the anti-inflammatory role of CTLA-4 co-inhibition in accelerated atherosclerotic lesion development, we analyzed injured femoral lesions of mice undergoing CTLA-4 blockade using antibodies. HPS staining (fig 6A) revealed that CTLA-4 blocking provoked increased accelerated atherosclerosis development and decreased luminal patency. Weigert's elastin staining and morphometric vessel wall analysis confirmed increased intimal thickening by 66.7% compared to control mice receiving non-specific anti- β gal IgG ($p=0.008$, fig 6B). Due to a comparable medial area between groups, the intima / media ratio was increased by 69.3% ($p=0.010$, fig 6C). Finally, CTLA-4 blockade increased relative luminal stenosis by 86.3% ($p=0.004$, fig 6D) and compromised absolute luminal area by 56.9% ($p=0.010$, fig 6E). Total vessel and medial areas (μm^2) were both not different between groups (fig VIIA,B). Together, these results indicate a strong increase of inflammatory induced post-interventional vascular remodeling during functional blockade of CTLA-4 func-

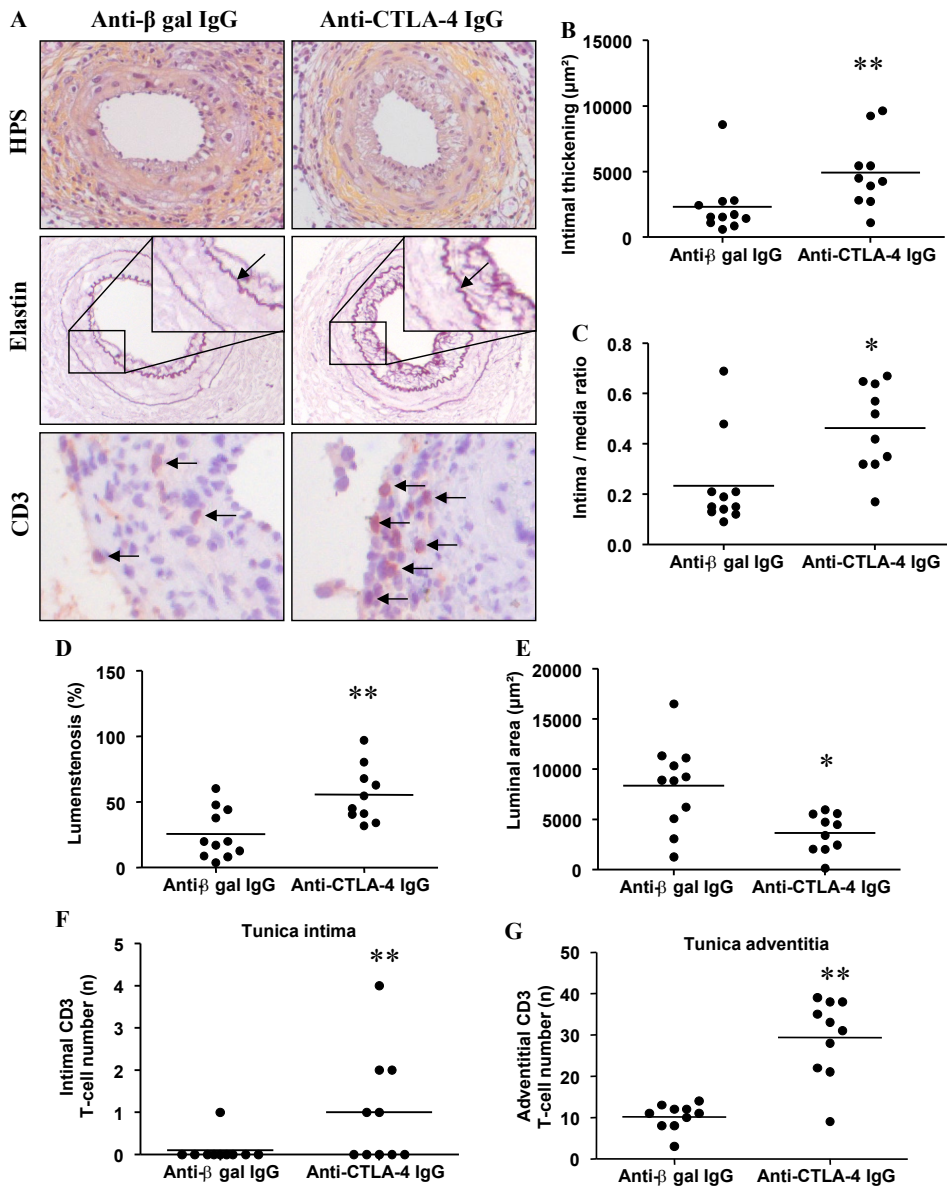


Figure 6. CTLA-4 blockade exacerbates accelerated atherosclerosis development. Representative cross-sections of cuffed-femoral arteries of hypercholesterolemic ApoE3*Leiden mice following isotype antibody or anti-CTLA-4 IgG-treatment (A) after 14d (HPS, Weigert's elastin and CD3 staining, 80-160x, arrows in inserts indicate internal elastic laminae and CD3+ T-cells). Quantification of intimal thickening (μm^2) (B), intima / media ratio (C), luminal stenosis (%) (D) and luminal area (μm^2) (E). Quantification of intimal CD3 (n) (F) and adventitial CD3 (n) (G) cells. Horizontal bars indicate median values, n=10. * $p < 0.05$, ** $p < 0.01$.

Accelerated atherosclerotic lesion phenotype is preserved during CTLA-4 blockade

Lesion composition was analyzed using IHC to assess arterial wall inflammatory

phenotype (fig VIII A). Although CTLA-4 blockade enhanced accelerated atherosclerosis development, no lesion composition differences were observed compared to controls. There were similar leukocyte and macrophage/foam cell fractions (% of all cells) in the media ($p=0.414$, fig VIII B; $p=0.097$, fig VIII D, respectively) and intima ($p=0.142$, fig VIII C; $p=0.769$, fig VIII E, respectively). CTLA-4 blockade also led to a comparable medial ($p=0.728$, fig VIII F) and intimal ($p=0.258$, fig VIII G) α -SMC actin surface areas (%). IHC revealed that functional CTLA-4 blockade led to a significant increase of CD3⁺ T-cells (n) in both the tunica intima by 200.0% ($p=0.0001$, fig 6 F) and in the tunica adventitia by 241.4% ($p=0.0003$, fig 6 G) compared to controls.

Discussion

This study demonstrates an important role for T-cell co-stimulation by CD28-CD80/CD86 and the negative regulator CTLA-4 in post-interventional intimal hyperplasia and accelerated atherosclerosis development. We show that CD4^{-/-} and CD80^{-/-}CD86^{-/-} mice develop significantly smaller SMC-rich lesions following vascular injury and that infiltrated T-cells express CTLA-4 early after surgery. Therapeutic inhibition of CD28-CD80/86 function by abatacept significantly prevented accelerated atherosclerosis development in hypercholesterolemic ApoE3*Leiden mice together with reduced IFN- γ plasma concentration (fig 5 C), probably due to reduced CD4 T-cell activation. The role of CTLA-4 co-inhibition was confirmed using blocking antibodies which led to profound increased vascular lesion size.

The role of CD4 T-cells and CD80/86-mediated co-stimulation during native atherosclerosis development^{26, 27} has been investigated, but their contribution to post-interventional vascular remodeling remained until this study unknown. In ApoE^{-/-} mice, T-cells have been shown to be important in early native atherosclerotic lesion progression, but not its initiation^{27, 28}. We provide evidence for activated CD4 T-cell involvement in the early stage of vascular remodeling following intervention. As of yet, it remains to be investigated towards which antigen the T-cell response is raised. Nevertheless, this form of accelerated atherosclerosis develops within months and in a localized area, opening the perspective for (local) T-cell-directed treatment directly after percutaneous coronary interventions.

CTLA-4 is expressed on activated effector T-cells and constitutively on regulatory T-cells, while both CD80 and CD86 are primarily expressed on activated dendritic cells, B cells, monocytes/macrophages, which play an important role in native atherosclerosis development⁴. T-cell-mediated immune responses are initiated in lymphoid tissues where they are activated by APCs presenting two concomitant signals: an antigenic signal provoked by specific MHC-antigen peptide complexes that bind to the TCR and a co-stimulatory signal induced by CD80 and CD86 molecules that interact with CD28 expressed on all T-cells. Together, TCR and CD28 signals lead to an inflammatory and pro-atherogenic response. We show that abatacept-treatment was able to prevent this systemic activation by reducing the number of activated CD4 T-cells fractions in the spleen as evidenced by the activation markers KLRG1, PD1, CD69 and CTLA-4. Since vascular injury occurs locally, profound T-cell activation was expected to occur in draining lymph nodes. However, only low fractions of activated T-cells were identified in these lymph nodes (fig VIA-G) whilst analysis of splenic T-cell fractions revealed significant activation (fig 4A-F). We cannot exclude

effects of abatacept in other lymph nodes, but these are unlikely to supersede the effects in the analyzed primary draining lymph nodes.

Although abatacept effects on accelerated atherosclerosis are mediated through systemically reduced T-cell activation, it is not clear to which extent effects on specific T-cell subsets contributed to the lesion development. Buono et al.²² showed that CD80^{-/-}CD86^{-/-}LDL-receptor (r)^{-/-} mice developed decreased atherosclerotic lesions compared to LDL-r^{-/-} mice through reduced CD4 Th1 cell activation by CD80/86 on APCs. Unlike activated effector T-cells, regulatory CD25⁺ FoxP3⁺ T-cells constitutively express CTLA-4²⁹ and this is essential for their suppressive function^{30, 31}. Ait-Oufella et al.⁵ demonstrated the vital role of regulatory T-cells in native atherosclerosis development, using irradiated LDL-r^{-/-} mice receiving reconstituted bone-marrow from CD80^{-/-}CD86^{-/-} mice which developed increased atherosclerotic lesions through strongly reduced splenic fractions of regulatory CD25⁺FoxP3⁺ T-cells. Therefore, it is possible that abatacept, may have inhibitory effects on accelerated atherosclerosis development through regulatory T-cell activation status modulation. However, Platt et al. showed that abatacept prevented effector T-cell activation, although effects on regulatory T-cell status in this murine arthritis model were not studied¹⁴.

This study shows reduced fractions of both activated Th1 and regulatory T-cells in hypercholesterolemic ApoE3*Leiden mice receiving abatacept. Since the Th1: regulatory T-cell ratio remained unchanged (fig 5B), this strongly suggests that therapeutic effects of abatacept can primarily be attributed to directly reduced activation of Th1 T-cells and not to Th1 suppression through regulatory T-cells, reflected by an elevated concentration of IL-10 (fig 5D) in plasma (baseline 14.4±2.3 pg/ml)²³ and reduced concentration of IFN-γ (fig 5C) (baseline 9.8±4.6 pg/ml)²³, similarly to that observed following IL-12 vaccination by Hauer et al. which downregulated the Th1 immune response and led to attenuation of native atherosclerosis development³².

These findings are based upon results from animal studies and cannot be automatically extrapolated to the clinical situation. However, they do provide further insight into the role of T-cell co-stimulatory pathways when viewed in the light of recent exiting data by Dumitriu et al.³³ concerning the role of CD28^{-/-} activated T-cells and regulatory T-cells during acute coronary syndromes (ACS) in humans, as well as carotid stenosis³⁴, unstable angina^{35, 36} and atherosclerosis development in both humans³⁷ and animals in general³⁸. The function relevance of CTLA-4 expression for human peripheral T-cell has previously been shown by Hoff et al.³⁹ and Yi-qun et al.⁴⁰, in which CTLA-4 blockade was found to both determine CD28null T-cell and memory T-cell longevity and responsiveness (e.g. IL-2 production). The potential of co-stimulatory-based T-cell-directed intervention strategies in the clinical situation is further enhanced by the findings of Bluestone et al.⁴¹ and Kőrmendy et al.⁴², in which functional CTLA-4 blockade functionally affected circulating regulatory T-cells in patients undergoing kidney transplantation and peripheral Th cells in rheumatoid arthritis patients. This study demonstrated the effectiveness of modulation of co-stimulatory receptors against post-interventional atherosclerotic vascular remodeling in mice, thus greatly enhancing the potential of a similar therapeutic approach to improve the survival of ACS patients.

In conclusion, this study shows that T-cell co-stimulation through the CD28-CD80/86 pathway plays a vital role in post-interventional accelerated atherosclerosis development and is strongly negatively regulated by CTLA-4 co-inhibition. These results

may have important clinical implications. Immune-mediated interventions directed towards therapeutically controlling the inflammatory T-cell response such as abatacept are widely applied in other immune (e.g. rheumatoid) disorders and could now be used in an early phase following interventions such as revascularization or bypass grafting procedures in patients to prevent subsequent vascular remodeling. This application could be accelerated by the availability of abatacept as a currently clinically approved T-cell specific therapeutic agent.

Reference List

1. Ross R. Atherosclerosis--an inflammatory disease. *N Engl J Med* 1999;340:115-26.
2. Hansson GK, Hermansson A. The immune system in atherosclerosis. *Nat Immunol* 2011;12:204-12.
3. Hansson GK. Inflammation, atherosclerosis, and coronary artery disease. *N Engl J Med* 2005;352:1685-95.
4. Weber C, Zernecke A, Libby P. The multifaceted contributions of leukocyte subsets to atherosclerosis: lessons from mouse models. *Nat Rev Immunol* 2008;8:802-15.
5. Ait-Oufella H, Salomon BL, Potteaux S, Robertson AK, Gourdy P, Zoll J et al. Natural regulatory T cells control the development of atherosclerosis in mice. *Nat Med* 2006;12:178-80.
6. Pires NM, Schepers A, van der Hoeven BL, de Vries MR, Boesten LS, Jukema JW et al. Histopathologic alterations following local delivery of dexamethasone to inhibit restenosis in murine arteries. *Cardiovasc Res* 2005;68:415-24.
7. Lardenoye JH, Delsing DJ, de Vries MR, Deckers MM, Princen HM, Havekes LM et al. Accelerated atherosclerosis by placement of a perivascular cuff and a cholesterol-rich diet in ApoE*3Leiden transgenic mice. *Circ Res* 2000;87:248-53.
8. Gotsman I, Sharpe AH, Lichtman AH. T-cell costimulation and coinhibition in atherosclerosis. *Circ Res* 2008;103:1220-31.
9. Alegre ML, Frauwirth KA, Thompson CB. T-cell regulation by CD28 and CTLA-4. *Nat Rev Immunol* 2001;1:220-8.
10. Maszyra F, Hoff H, Kunkel D, Radbruch A, Brunner-Weinzierl MC. Diversity of clonal T cell proliferation is mediated by differential expression of CD152 (CTLA-4) on the cell surface of activated individual T lymphocytes. *J Immunol* 2003;171:3459-66.
11. Krummel MF, Allison JP. CD28 and CTLA-4 have opposing effects on the response of T cells to stimulation. *J Exp Med* 1995;182:459-65.
12. Chambers CA, Sullivan TJ, Allison JP. Lymphoproliferation in CTLA-4-deficient mice is mediated by costimulation-dependent activation of CD4+ T cells. *Immunity* 1997;7:885-95.
13. Chambers CA, Cado D, Truong T, Allison JP. Thymocyte development is normal in CTLA-4-deficient mice. *Proc Natl Acad Sci U S A* 1997;94:9296-301.
14. Platt AM, Gibson VB, Patakas A, Benson RA, Nadler SG, Brewer JM et al. Abatacept limits breach of self-tolerance in a murine model of arthritis via effects on the generation of T follicular helper cells. *J Immunol* 2010;185:1558-67.
15. Webb LM, Walmsley MJ, Feldmann M. Prevention and amelioration of collagen-induced arthritis by blockade of the CD28 co-stimulatory pathway: requirement for both B7-1 and B7-2. *Eur J Immunol* 1996;26:2320-8.
16. Fiocco U, Sfriso P, Oliviero F, Pagnin E, Scagliori E, Campana C et al. Co-stimulatory modulation in rheumatoid arthritis: the role of (CTLA4-Ig) abatacept. *Autoimmun Rev* 2008;8:76-82.
17. Ruderman EM, Pope RM. The evolving clinical profile of abatacept (CTLA4-Ig): a novel co-stimulatory modulator for the treatment of rheumatoid arthritis. *Arthritis Res Ther* 2005;7 Suppl 2:S21-S25.
18. Ruderman EM, Pope RM. Drug Insight: abatacept for the treatment of rheumatoid arthritis. *Nat Clin Pract Rheumatol* 2006;2:654-60.
19. Kremer JM, Westhovens R, Leon M, Di GE, Alten R, Steinfeld S et al. Treatment of rheumatoid arthritis by selective inhibition of T-cell activation with fusion protein CTLA4Ig. *N Engl J Med* 2003;349:1907-15.
20. Mallat Z, Taleb S, Ait-Oufella H, Tedgui A. The role of adaptive T cell immunity in atherosclerosis. *J Lipid Res* 2009;50 Suppl:S364-S369.
21. Zhou X, Robertson AK, Hjerpe C, Hansson GK. Adoptive transfer of CD4+ T cells reactive to modified low-density lipoprotein aggravates atherosclerosis. *Arterioscler Thromb Vasc Biol* 2006;26:864-70.
22. Buono C, Pang H, Uchida Y, Libby P, Sharpe AH, Lichtman AH. B7-1/B7-2 costimulation regulates plaque antigen-specific T-cell responses and atherogenesis in low-density lipoprotein receptor-deficient mice. *Circulation* 2004;109:2009-15.
23. Ewing MM, de Vries MR, Nordzell M, Pettersson K, de Boer HC, van Zonneveld AJ et al. Annexin A5 therapy attenuates vascular inflammation and remodeling and improves endothelial function in mice. *Arterioscler Thromb Vasc Biol* 2011;31:95-101.
24. Coats AJ, Shewan LG. Statement on authorship and publishing ethics in the International Jour-

- nal of Cardiology. *Int J Cardiol* 2011;153:239-40.
25. Arens R, Loewendorf A, Redeker A, Sierro S, Boon L, Klenerman P et al. Differential B7-CD28 costimulatory requirements for stable and inflationary mouse cytomegalovirus-specific memory CD8 T cell populations. *J Immunol* 2011;186:3874-81.
 26. Mallat Z, Ait-Oufella H, Tedgui A. Regulatory T cell responses: potential role in the control of atherosclerosis. *Curr Opin Lipidol* 2005;16:518-24.
 27. Zhou X, Robertson AK, Rudling M, Parini P, Hansson GK. Lesion development and response to immunization reveal a complex role for CD4 in atherosclerosis. *Circ Res* 2005;96:427-34.
 28. Robertson AK, Hansson GK. T cells in atherogenesis: for better or for worse? *Arterioscler Thromb Vasc Biol* 2006;26:2421-32.
 29. Vignali DA, Collison LW, Workman CJ. How regulatory T cells work. *Nat Rev Immunol* 2008;8:523-32.
 30. Sakaguchi S. Naturally arising Foxp3-expressing CD25+CD4+ regulatory T cells in immunological tolerance to self and non-self. *Nat Immunol* 2005;6:345-52.
 31. Salomon B, Lenschow DJ, Rhee L, Ashourian N, Singh B, Sharpe A et al. B7/CD28 costimulation is essential for the homeostasis of the CD4+CD25+ immunoregulatory T cells that control autoimmune diabetes. *Immunity* 2000;12:431-40.
 32. Hauer AD, Uyttenhove C, de VP, Stroobant V, Renauld JC, van Berkel TJ et al. Blockade of interleukin-12 function by protein vaccination attenuates atherosclerosis. *Circulation* 2005;112:1054-62.
 33. Dumitriu IE, Baruah P, Finlayson CJ, Loftus IM, Antunes RF, Lim P et al. High levels of costimulatory receptors OX40 and 4-1BB characterize CD4+CD28null T cells in patients with acute coronary syndrome. *Circ Res* 2012;110:857-69.
 34. Ammirati E, Cianflone D, Banfi M, Vecchio V, Palini A, De MM et al. Circulating CD4+CD25hiCD127lo regulatory T-Cell levels do not reflect the extent or severity of carotid and coronary atherosclerosis. *Arterioscler Thromb Vasc Biol* 2010;30:1832-41.
 35. Caligiuri G, Paulsson G, Nicoletti A, Maseri A, Hansson GK. Evidence for antigen-driven T-cell response in unstable angina. *Circulation* 2000;102:1114-9.
 36. Liuzzo G, Goronzy JJ, Yang H, Kopecky SL, Holmes DR, Frye RL et al. Monoclonal T-cell proliferation and plaque instability in acute coronary syndromes. *Circulation* 2000;101:2883-8.
 37. de Boer OJ, van der Meer JJ, Teeling P, van der Loos CM, van der Wal AC. Low numbers of FOXP3 positive regulatory T cells are present in all developmental stages of human atherosclerotic lesions. *PLoS One* 2007;2:e779.
 38. Ammirati E, Cianflone D, Vecchio V, et al. Effector memory T cells are associated with atherosclerosis in humans and animal models. *J Am Heart Assoc.* 2012;1:27- 41.
 39. Hoff H, Knieke K, Cabail Z, Hirsland H, Vratsanos G, Burmester GR et al. Surface CD152 (CTLA-4) expression and signaling dictates longevity of CD28null T cells. *J Immunol* 2009;182:5342-51.
 40. Yi-qun Z, Lorre K, de BM, Ceuppens JL. B7-blocking agents, alone or in combination with cyclosporin A, induce antigen-specific anergy of human memory T cells. *J Immunol* 1997;158:4734-40.
 41. Bluestone JA, Liu W, Yabu JM, Laszik ZG, Putnam A, Belingheri M et al. The effect of costimulatory and interleukin 2 receptor blockade on regulatory T cells in renal transplantation. *Am J Transplant* 2008;8:2086-96.
 42. Kormendy D, Hoff H, Hoff P, Broker BM, Burmester GR, Brunner-Weinzierl MC. The impact of the CTLA-4/CD28 axis on the processes of Joint Inflammation in Rheumatoid Arthritis. *Arthritis Rheum* 2012.

Online supplements

Materials and Methods

Mice

All experiments were approved by the Institutional Committee for Animal Welfare of the Leiden University Medical Center (LUMC). Male C57Bl/6J controls, CD4^{-/-} and CD80^{-/-}CD86^{-/-} mice on a C57Bl/6J background were purchased from the Jackson Laboratory (Bar Harbor) and transgenic male ApoE*3-Leiden mice, backcrossed for more than 20 generations on a C57Bl/6J background, were bred in our own laboratory. All animals used for this experiment were 10-12 weeks at the start of a dietary run-in period or surgery and were weighed before and at the end of the experimental period.

Diets

C57Bl/6J controls, CD4^{-/-} and CD80^{-/-}CD86^{-/-} mice received chow diet and transgenic male ApoE*3-Leiden mice were fed a Western-type diet containing 1% cholesterol and 0.05% cholate to induce hypercholesterolemia to desired levels in male ApoE3*Leiden mice (AB Diets). The Western-type diet was given three weeks prior to surgery and was continued throughout the experiment. All animals received food and water ad libitum during the entire experiment.

Treatment protocol

To investigate the role of CTLA-4 co-inhibition, C57Bl/6J control and ApoE3*Leiden animals were injected intraperitoneally (IP) with abatacept (Bristol-Myers Squibb B.V.) in a concentration of 10 mg/kg twice monthly (200 µl) or vehicle, starting at the time of surgery. CTLA-4 blockade in ApoE3*Leiden mice was induced by injecting animals IP with 200 µg of anti-mouse CTLA-4 IgG (clone 9H10¹) or control IgG diluted in 200 µl sterile phosphate-buffered saline (PBS) once every 2 days, starting at the time of surgery.

Blocking CTLA-4 IgG antibody generation

Anti-murine CTLA-4 IgG antibodies used in this study were isolated from supernatants from the 9H10 hybridoma line¹, first using Iscove's Modified Dulbecco's Medium (IMDM) (Invitrogen) with 8% FCS and 1% glutamine, followed by GIBCO™ protein-free hybridoma medium (PFHM)-II (Invitrogen) throughout T75, T175 and roller bottle culture systems (Sigma-Aldrich Chemie B.V), maintained at 37°C with 5% CO₂. Antibody concentration was performed using an artificial kidney (Fresenius Medical Care). The concentrated antibodies were protein G-purified (GE Healthcare Bio-Sciences AB) and antibody concentrations were determined using a Nanodrop spectrophotometer and stored at 2 mg/ml in sterile PBS at -20°C for further use.

Femoral artery cuff mouse model

To investigate the role of CD4 T lymphocytes, CD28-CD80/CD86 co-stimulation and CTLA-4 co-inhibition, mice were subjected to arterial femoral arterial cuff placement to induce intimal thickening and accelerated atherosclerosis development^{2,4}. In brief,

mice were anesthetized before surgery with a combination of IP injected Midazolam (5 mg/kg, Roche), Medetomidine (0.5 mg/kg, Orion) and Fentanyl (0.05 mg/kg, Janssen). The right femoral artery was isolated and sheathed with a rigid non-constrictive polyethylene cuff (Portex, 0.40mm inner diameter, 0.80mm outer diameter and an approximate length of 2.0mm). Using two ligatures, the polyethylene cuff was held in place, after which the wound was closed using continuous sutures.

Either 14 days (ApoE3*Leiden mice) or 21 days (normocholesterolemic mice) after cuff placement, mice were anesthetized as before and euthanized. At sacrifice, venous blood was drawn in EDTA collection tubes (Sarstedt B.V.) and subjected to centrifugation (6000 r.p.m. for 10 min at 4°C) to obtain plasma, which was stored at -20°C for further research. The spleen and draining inguinal lymph nodes were isolated and either snap frozen in liquid nitrogen for further analysis (stored at -80°C) or minced through a 70-mm cell strainer (BD Biosciences) to create single-cell suspensions and stored in 3% fetal calf serum-rich GIBCO™ RPMI 1640 medium (Invitrogen) on ice.

Next, the thorax was opened and mild pressure-perfusion (100mm Hg) with PBS for 4min by cardiac puncture in the left ventricle. After perfusion, the cuffed femoral artery was harvested, fixed overnight in 3.7% formaldehyde in water (w/v) and paraffin-embedded. Serial cross-sections (5 µm thick) were made from the entire length of the artery for analysis.

Biochemical analysis

Total plasma cholesterol (Roche Diagnostics, kit 1489437) concentration was measured enzymatically before randomization and at sacrifice. Plasma cholesterol concentrations (12.1±3.1 mmol/L) were similar in all groups throughout this study ($p>0.15$, table 2). To investigate effects of abatacept on systemic CD4 T-cell specific activation after surgery, interferon (IFN)- γ and interleukin-10 enzyme-linked immunosorbent assays (ELISAs) were performed (BD Biosciences) according to the manufacturer's instructions.

Quantification of cuffed femoral artery lesions

Immunohistochemical (IHC) staining was performed using positive and negative tissue-specific controls as indicated by the antibody manufacturer. Samples were stained with hematoxylin-phloxine-saffron (HPS) and specific vessel wall composition was visualized for elastin (Weigert's elastin staining), collagen (Sirius Red staining) and with antibodies against leukocytes (anti-CD45 antibodies 1:200, Pharmingen), macrophages (MAC3, 1:200, BD Biosciences), vascular SMCs (α -SMC actin 1:800, Dako), T-cells (anti-CD3, 1:100, AbD Serotec and anti-CD4, 1:250, Abcam), matrix metalloproteinase-9 (anti-MMP-9, 1:100, Santa Cruz), and CTLA-4 (anti-mouse CTLA-4, 1:200, Abbiotec), using hematoxylin for counterstaining to visualize all cells. The anti-CD4 antibody specificity for CD4 was confirmed on cuffed sections of CD4 knock-out mice (21d) (fig IIF).

Sections were deparaffinized by placement in xylene for 5 minutes, followed by ethanol 100% for 2 minutes, ethanol 70% for 2 minutes and ethanol 50% for 2 minutes and distilled water for 2 minutes. Sections underwent citrate buffer antigen retrieval (10mM sodium citrate, pH 6.0) for 10 minutes at 100°C, followed by 30 minutes cooling. PBS (1%) was used as a wash solution and for diluting antibodies. Novared

(Vector laboratories) was used as staining vector according to the manufacturer's instructions. Sections were dehydrated by placement in ethanol 50% for 2 minutes, ethanol 70% for 2 minutes and ethanol 100% for 2 minutes, followed by xylene for 5 minutes. The slides were mounted with xylene-based pertex and 24x60 mm coverslips.

The number of leukocytes, macrophages and cells expressing CTLA-4 attached to the endothelium, within the neointimal tissue or infiltrated in the medial layer of the femoral arteries was quantified and is displayed as a percentage of the total number of present cells. The area containing vascular SMCs, collagen or macrophages was quantified using computer-assisted morphometric analysis (Qwin, Leica) and is expressed as a percentage of the total cross-sectional arterial wall layer area. All quantification in this study was performed on six equally spaced (150 μ m distance) serial stained perpendicular cross-sections throughout the entire length of the vessel and was performed by blinded observers.

Flow cytometry

Spleens and draining inguinal lymph nodes were harvested and single-cell suspensions were prepared by mincing the tissue through a 70- μ m cell strainer (BD Biosciences). Erythrocytes were lysed using hypotonic (0.82%) ammonium chloride buffer. For cell surface staining, cells were resuspended in staining buffer (PBS + 3%P PFCS + 0.05% sodium azide) and incubated with fluorescent conjugated antibodies at 4C° for 30 minutes in 96-well plates. After washing and resuspension in staining buffer, cells were acquired using a BD LSRII flow cytometer and data was analyzed using FlowJo software (version 7.4.6., Tree Star).

Cells were stained with fluorochrome-conjugated monoclonal antibodies specific for CD3, CD4, CD44, CD25, CD62L CD69, CD127, CTLA-4, and KLRG1. All antibodies were purchased from eBioscience or BD Biosciences. Staining for intracellular FoxP3 was performed using the FoxP3 staining set from eBioscience (1:200, APC). 7-AAD was used to exclude dead cells.

Statistical analysis

All data are presented as mean \pm standard error of the mean (SEM). Groups were compared using a Mann-Whitney sum test for non-parametric data. All statistical analyses were performed with SPSS 17.0 software for Windows or using Prism software. P-values <0.05 were regarded as statistically significant and are indicated with an asterisk (*).

Reference List

1. Krummel MF, Allison JP. CD28 and CTLA-4 have opposing effects on the response of T cells to stimulation. *J Exp Med* 1995;182:459-465.
2. Lardenoye JH, Delsing DJ, de Vries MR, Deckers MM, Princen HM, Havekes LM et al. Accelerated atherosclerosis by placement of a perivascular cuff and a cholesterol-rich diet in ApoE*3Leiden transgenic mice. *Circ Res* 2000;87:248-253.
3. Pires NM, Schepers A, van der Hoeven BL, de Vries MR, Boesten LS, Jukema JW et al. Histopathologic alterations following local delivery of dexamethasone to inhibit restenosis in murine arteries. *Cardiovasc Res* 2005;68:415-424.
4. Ewing MM, de Vries MR, Nordzell M, Pettersson K, de Boer HC, van Zonneveld AJ et al. Annexin A5 therapy attenuates vascular inflammation and remodeling and improves endothelial function in mice. *Arterioscler Thromb Vasc Biol* 2011;31:95-101.

Supplemental figures

Group	Body weight (gram)	
	Surgery	Sacrifice
C57Bl/6J	22.6±0.4	24.8±0.4
CD4 ^{-/-}	26.7±0.4	29.0±0.4
CD80 ^{-/-} CD86 ^{-/-}	24.1±1.1	26.0±1.0
Abatacept	23.7±0.4	25.9±0.3

Table 1. Murine body weights at surgery and sacrifice. Body weight (gram) of control, CD4^{-/-}, CD80^{-/-}CD86^{-/-} and abatacept-treated (10 mg/kg/twice monthly) C57Bl/6J mice at surgery and sacrifice at day 21 (mean±SEM, n=10). No significant differences were observed.

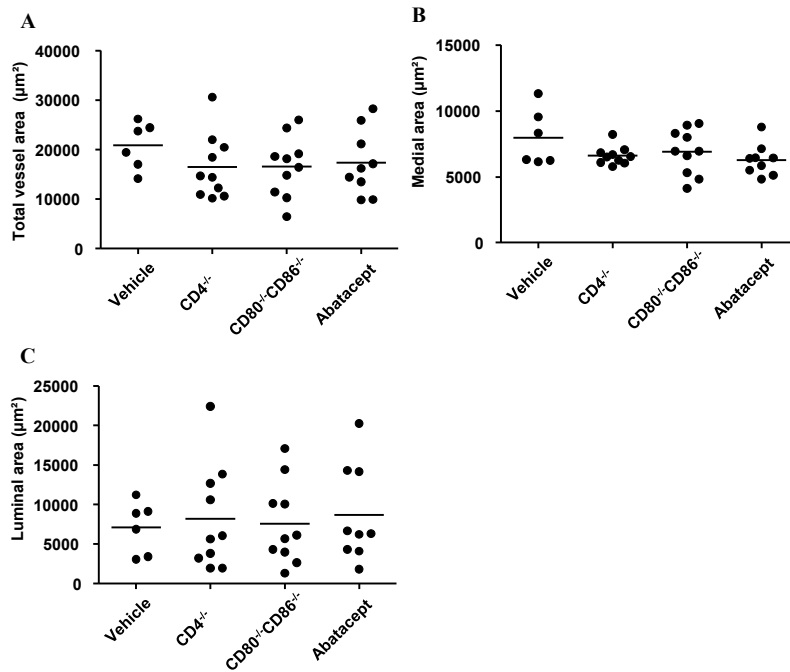
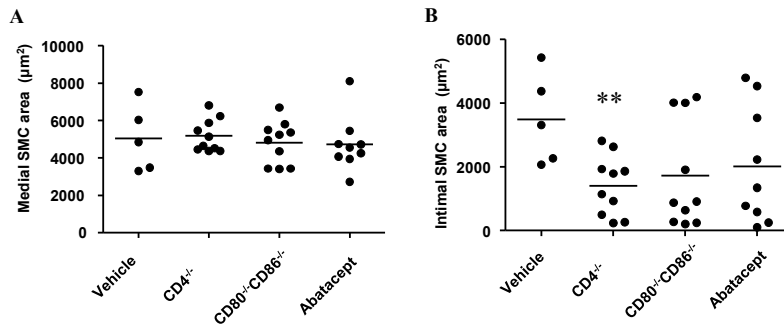


Figure I. Reduced vascular remodeling in CD4^{-/-} and CD80^{-/-}CD86^{-/-} and abatacept-treated mice. Quantification of total vessel area (μm²) (A), medial area (μm²) (B) and luminal area (μm²) (C) after 21 days. Horizontal bars indicate median values, n=10.



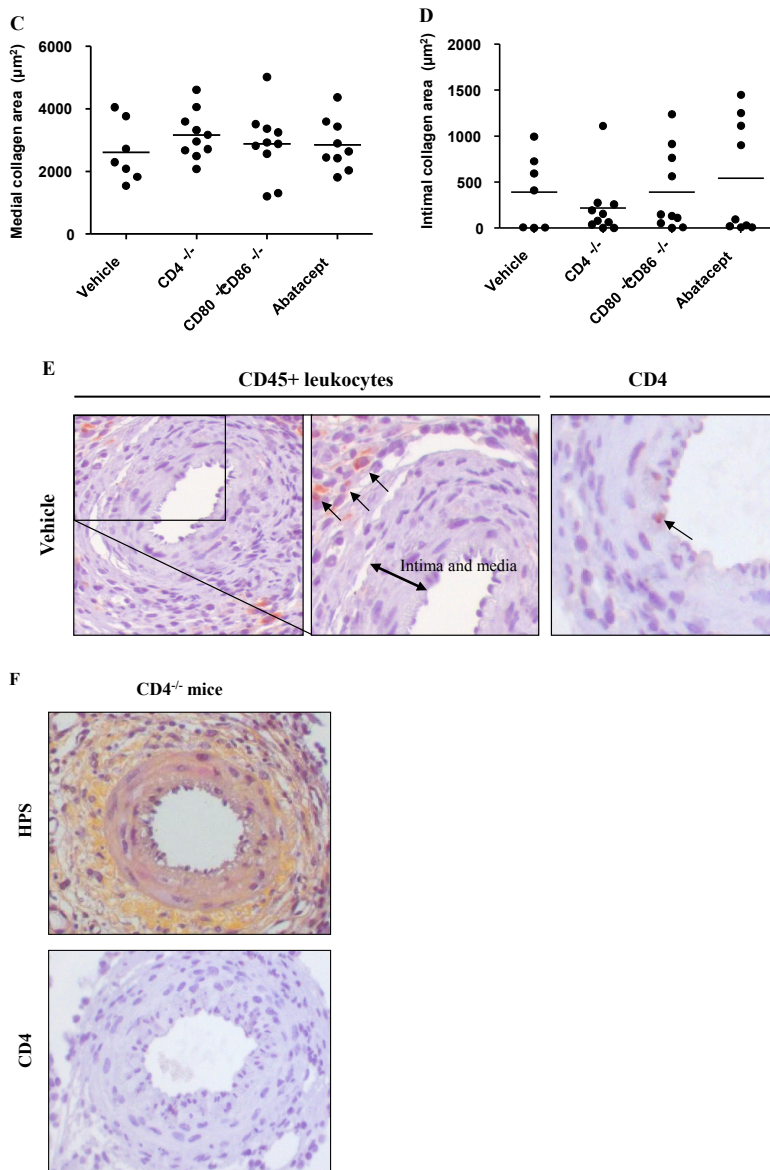


Figure II. CD4^{-/-}, CD80^{-/-}CD86^{-/-} and abatacept-treated mice display an altered lesion composition. Quantification of medial (A) and intimal (B) vascular α -SMC actin area (μm^2) and medial (C) and intimal (D) collagen area (μm^2) after 21 days. Horizontal bars indicate median values, $n=10$. ** $p<0.01$. Representative cross-sections of cuffed-femoral arteries of vehicle-treated C57Bl/6J mice (E) after 21d (CD45 leukocyte and CD4 T-cell staining, 80-160x). (F) Representative cross-sections of cuffed-femoral arteries of CD4 knock-out mice after 21d (HPS and CD4 staining, 80x).

Group	Body weight (gram)		Total cholesterol (mmol/L)	
	Surgery	Sacrifice	Surgery	Sacrifice
Vehicle	29.0±0.6	29.4±0.7	11.3±0.4	7.9±0.6
Abatacept	29.4±0.7	29.9±0.7	11.5±1.0	10.4±2.4
Anti-β gal IgG	28.8±0.6	29.0±0.6	13.4±1.4	8.9±0.9
Anti-CTLA-4 IgG	30.4±0.7	30.1±0.8	12.3±0.9	8.1±1.5

Table 2. Murine body weights and plasma total cholesterol at surgery and sacrifice. Body weight (gram) and plasma total cholesterol (mmol/L) of vehicle, abatacept (10 mg/kg/twice monthly), isotype control antibody (anti-β gal IgG 200 μg every 2 days) or anti-mouse CTLA-4 IgG (200 μg every 2 days)-treated ApoE3*Leiden mice measured at surgery and sacrifice (14 days) (mean±SEM, n=10). No significant differences were observed.

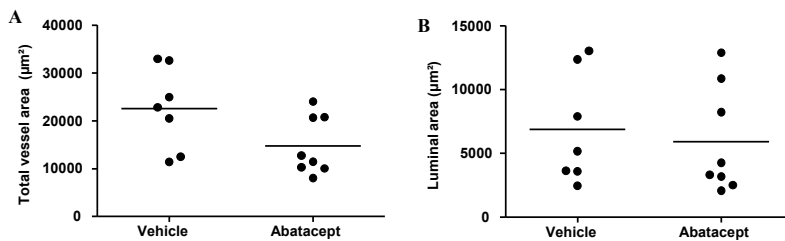


Figure III. Abatacept prevents accelerated atherosclerosis in hypercholesterolemic ApoE3*Leiden mice. Quantification of total vessel area (μm²) (A) and luminal area (μm²) (B) after day 14. Horizontal bars indicate median values, n=10.

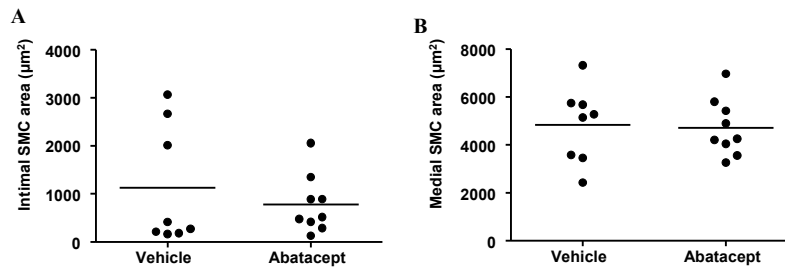


Figure IV. Abatacept positively affects accelerated atherosclerotic lesion composition. Quantification of total intimal (A) and medial (B) SMC areas (μm²) after day 14. Horizontal bars indicate median values, n=10.

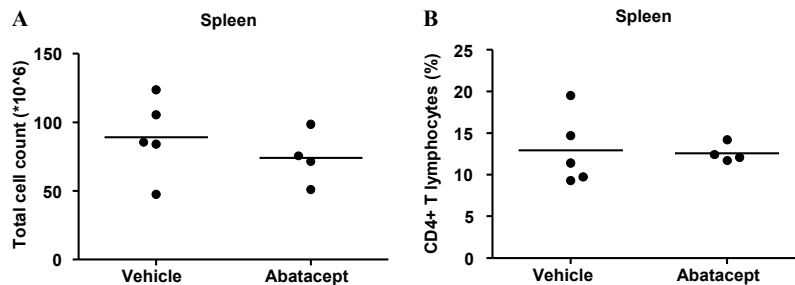


Figure V. Abatacept prevents systemic CD4 T-cell activation in ApoE3*Leiden mice. Quantification of splenic total cell count (*10⁶ cells) (A) and CD4 T-cell fractions (%) (B) 14 days after surgery. Horizontal bars indicate median values, n=5.

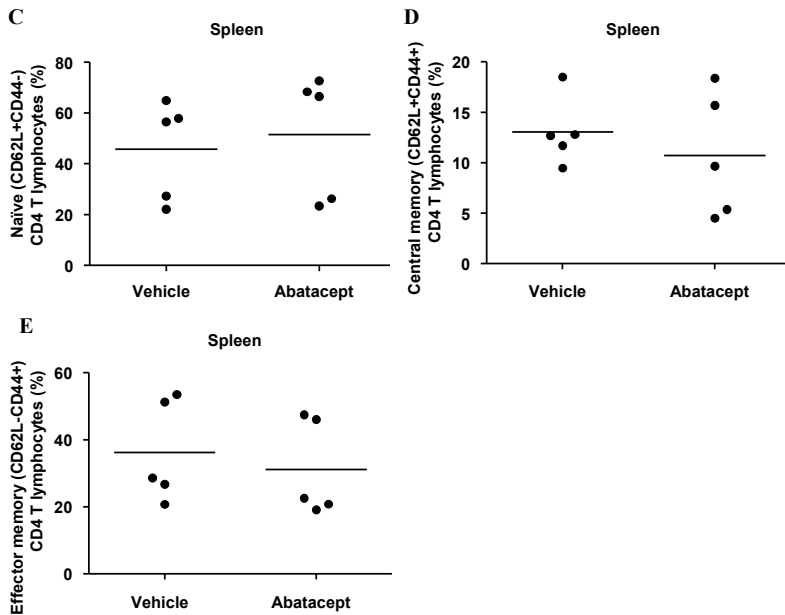


Figure V. Abatacept prevents systemic CD4 T-cell activation in ApoE3*Leiden mice. Quantification of splenic naïve (CD62L+CD44-) (C) and activated central-memory (CD62L+CD44+) (D) and effector-memory (CD62L-CD44+) (E) CD3+CD4+ T-cells (%) 14 days after surgery. Horizontal bars indicate median values, n=5.

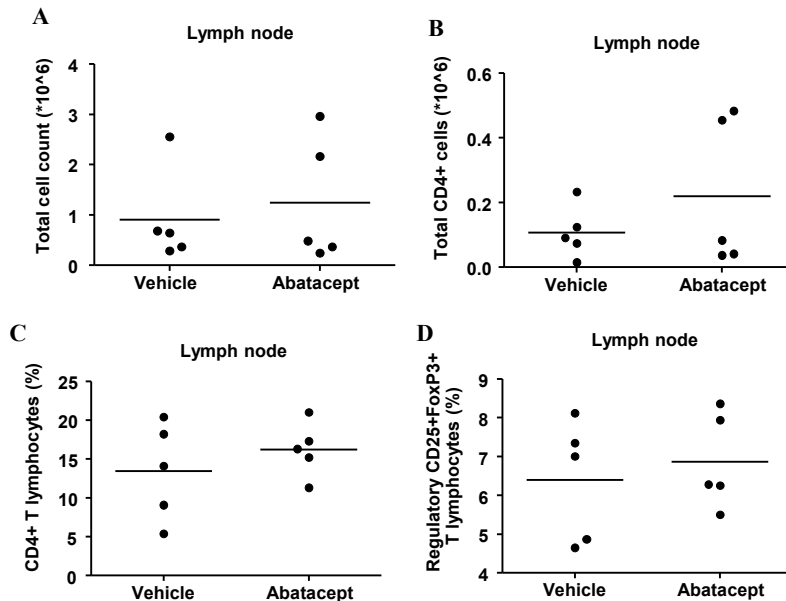


Figure VI. Abatacept does not affect draining inguinal lymph node T-cell activation status in hypercholesterolemic ApoE3*Leiden mice. Quantification of total cell count (*10⁶ cells) (A), total CD4 T-cells (*10⁶ cells) (B), CD4 T-cell fraction (%) (C) and regulatory CD4+CD25+FoxP3+ T-cells (%) (D) in draining inguinal lymph nodes, 14 days after surgery. Horizontal bars indicate median values, n=5.

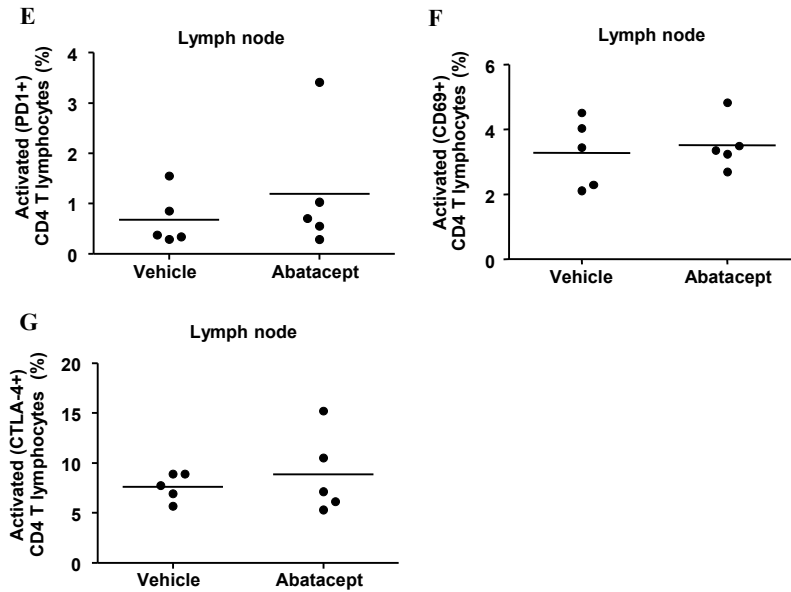


Figure VI. Abatacept does not affect draining inguinal lymph node T-cell activation status in hypercholesterolemic ApoE3*Leiden mice. Quantification of activated PD1+ (E), CD69+ (F) and CTLA-4+ (G) CD4 T-cells (%) in draining inguinal lymph nodes, 14 days after surgery. Horizontal bars indicate median values, n=5.

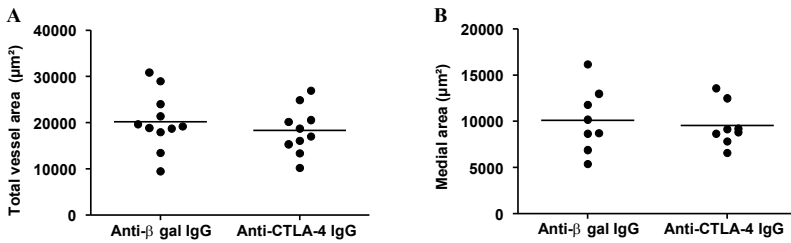


Figure VII. CTLA-4 blockade exacerbates accelerated atherosclerosis development in hypercholesterolemic ApoE3*Leiden mice. Quantification of total vessel area (μm^2) (A) and medial area (μm^2) (B), 14 days after surgery. Horizontal bars indicate median values, n=10.

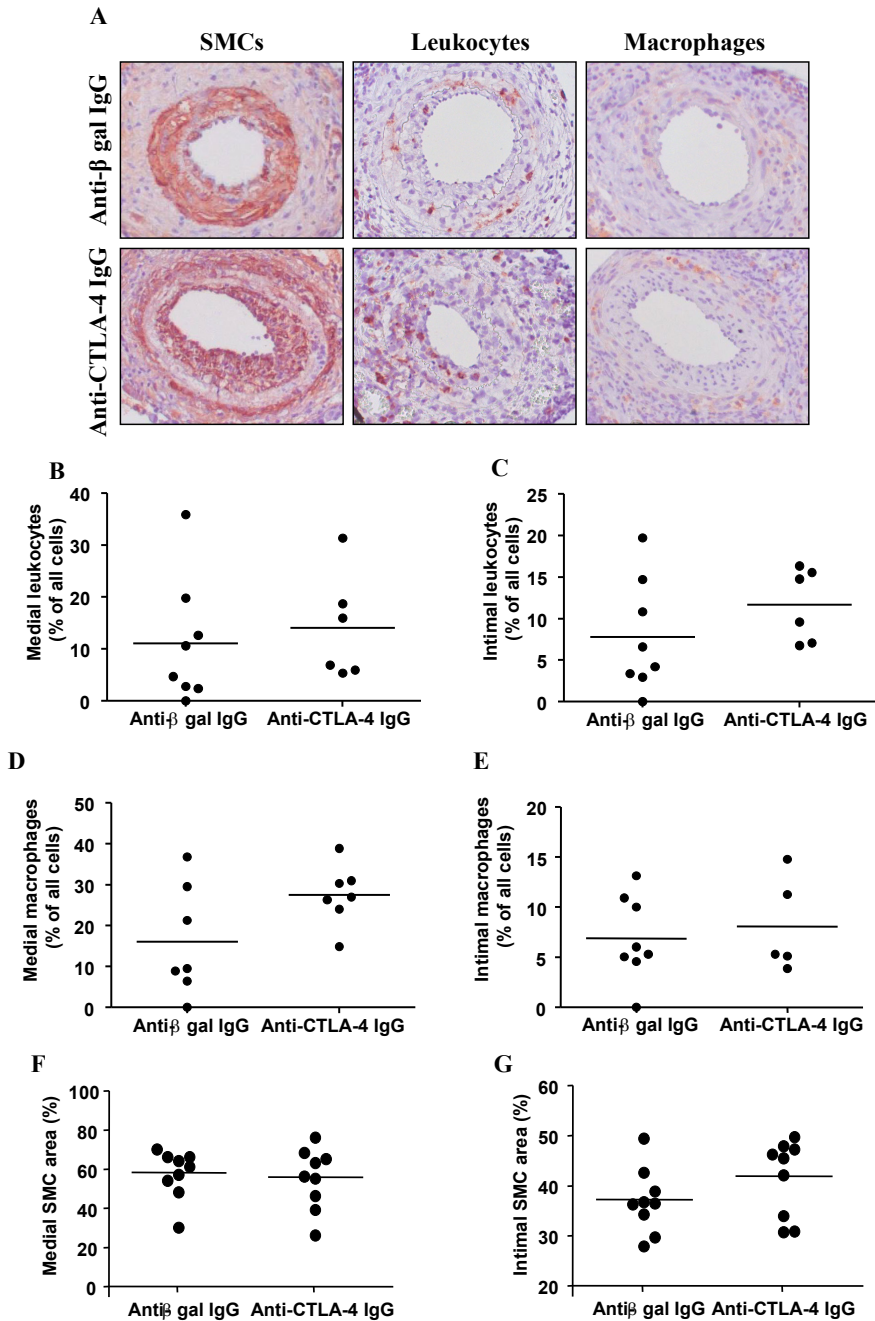


Figure VIII. Accelerated atherosclerotic lesion phenotype is preserved during CTLA-4 blockade. Representative cross-sections of cuffed-femoral arteries of ApoE3*Leiden mice following isotype antibody or anti-CTLA-4 IgG-treatment (A) after 14d (leukocyte, macrophage and α -SMC actin staining, 80x). Quantification of relative medial leukocyte (B), macrophage (D) and SMC (F) areas (%) and intimal leukocyte (C), macrophage (E) and SMC (G) areas (%) showed no significant differences. Horizontal bars indicate median values, n=10.

Chapter 9

Genetic variation in PCAF, a key mediator in epigenetics, is associated with reduced vascular morbidity and mortality

D. Pons^{1,2,3*}, S. Trompet^{1,4*}, A.J.M. de Craen⁴, P.E. Thijssen⁵, P.H.A. Quax^{3,5}, M.R. de Vries⁵, R.J. Wierda^{3,6}, P.J. van den Elsen^{3,6,7}, P.S. Monraats¹, M.M. Ewing^{1,3}, B.T. Heijmans⁸, P.E. Slagboom⁸, A.H. Zwinderman⁹, P.A.F.M. Doevendans^{2,10}, R.A. Tio^{2,11}, R.J. de Winter^{2,12}, M.P.M. de Maat¹³, O.A. Iakoubova¹⁴, N. Sattar¹⁵, J. Shepherd¹⁶, R.G.J. Westendorp⁴, J.W. Jukema^{1-3,17}

1 Dept. of Cardiology, Leiden University Medical Center (LUMC), Leiden, The Netherlands; 2 Interuniversity Cardiology Institute of the Netherlands, Utrecht, The Netherlands; 3 Eindhoven Laboratory for Experimental Vascular Medicine; 4 Dept. of Gerontology and Geriatrics; 5 Dept. of Vascular Surgery; 6 Dept. of Immunohematology and Blood Transfusion, LUMC, Leiden, The Netherlands; 7 Dept. of Pathology, VU University Medical Center, Amsterdam, The Netherlands; 8 Molecular Epidemiology Section, LUMC, Leiden, The Netherlands; 9 Dept. of Medical Statistics, Academic Medical Center (AMC), Amsterdam, The Netherlands; 10 Dept. of Cardiology, University Medical Center, Utrecht, The Netherlands; 11 Dept. of Cardiology, University Medical Center Groningen, Groningen, The Netherlands; 12 Dept. of Cardiology, AMC, Amsterdam, The Netherlands; 13 Dept. of Hematology, Erasmus University Medical Center, Rotterdam, The Netherlands; 14 Celera, Inc., Alameda, California; 15 BHF Glasgow Cardiovascular Research Centre, Faculty of Medicine, Glasgow, Scotland; 16 Dept. of Vascular Biochemistry, University of Glasgow, Scotland; 17 Durrer Center for Cardiogenetic Research, Amsterdam, The Netherlands. * These authors contributed equally to this work.

Abstract

Aims A major influence on gene expression is attributed to the counterbalancing action of lysine acetyltransferases (KATs) and lysine deacetylases (KDACs). This study was designed to investigate the influence of genetic variation in the promoter of the gene encoding P300/CBP associated factor (PCAF), a lysine acetyltransferase (KAT) on coronary heart disease (CHD) and mortality.

Methods and results We investigated the association of genetic variation in the promoter region of the PCAF-gene on CHD and mortality in two statin trials (PROSPER and WOSCOPS) and on restenosis risk in a third study of percutaneous coronary intervention (GENDER). We combined the results from these cohorts to examine 1) overall effects on CHD mortality and on 2) restenosis risk and determined the contribution of PCAF in an animal model of reactive stenosis. Compared with the homozygous -2481G allele in the PCAF promoter, we observed a significant reduction in CHD mortality risk with the homozygous -2481C PCAF promoter allele in PROSPER (risk reduction 22%; 2% to 37%), a non-significant trend towards reduction in WOSCOPS (risk reduction 17%; -14% to 39%), and a significant reduction of restenosis in GENDER (20%; 3% to 33%). A combined risk reduction for CHD death/ restenosis for the three studies was 21% (15%-26%; $p=8.1 \times 10^{-4}$). In elderly patients (>58 years) the effects were stronger and significant in all three studies. Furthermore, this PCAF allele was significantly associated with all cause mortality in PROSPER ($p=0.001$). Functional analysis showed that nuclear factors interact in vitro with the oligonucleotides encompassing this -2481 G/C polymorphism and that this interaction might be influenced in some cell types by this polymorphism in the PCAF promoter, and modulation of PCAF gene expression was detectable upon cuff-placement in an animal model of reactive stenosis.

Conclusion: We showed in three large prospective studies that the -2481C allele in the PCAF promoter is associated with a significant survival advantage in elderly patients while also protecting against clinical and angiographic restenosis after PCI. Our observations promote the concept that epigenetic processes are under genetic control and that, other than environment, genetic variation in genes encoding KATs may also determine susceptibility to CHD outcomes and mortality.

Introduction

Investigations into the pathogenetic mechanisms of human complex disease, such as cardiovascular disease and cancer, may lead to better risk prediction, treatment and new targets for future therapy. Cell proliferation regulatory pathways and pro-inflammatory transcription factors, such as NF κ B, have been associated with progression of these diseases¹. In the past decade, research into cardiovascular diseases such as atherosclerosis and restenosis, has been focused on the identification of genetic factors that determine disease risk. Several genes involved in inflammation and cell proliferation appeared to be common denominators of these diseases²⁻⁴. It has become clear, however, that part of the gene-environmental interactions relevant for complex diseases is regulated by epigenetic mechanisms such as histone acetylation and DNA methylation⁵. Epigenetic processes modulate gene expression patterns without modifying the actual DNA sequence and have profound effects on the cellular repertoire of expressed genes⁶. Evidence is growing that epigenetic mechanisms also regulate the expression of genes in the inflammatory and cell proliferation pathways^{7,8} and may therefore also play a role in cardiovascular disease⁹⁻¹¹.

A major influence on gene expression is attributed to the counterbalancing action of lysine acetyltransferases (KATs) and lysine deacetylases (KDACs)¹². KATs acetylate histones by transfer of an acetyl-group to the ϵ -portion of lysine residues, which results in an open modification of chromatin structure and in accessibility of DNA to transcription factors and recruitment of the basal transcription initiation machinery. Conversely, gene repression is mediated via KDACs, which remove acetyl groups and counteract the activity of KATs resulting in a closed chromatin structure. Thus far, the main focus has been to investigate the environmental influence on epigenetic processes. Research in this field has shown that epigenetic differences arise during the lifetime of monozygotic twins⁶. Furthermore, oxidative stress has been shown to influence the balance between KATs and KDACs in favour of KATs, leading to an increase in inflammation¹³. Notably, genetic variations in the genes encoding KATs and KDACs, which affect the activities of the enzymes they encode, have a bearing on the global and gene-specific levels of histone acetylation. As such, these genetic variations in the genes encoding KATs and KDACs could also be important determinants contributing to susceptibility to major human diseases.

P300/CBP associated factor (PCAF) is a transcriptional co-activator with intrinsic KAT-activity. Besides its role in lysine acetylation of histones at the site of NF κ B-regulated genes and the resultant inflammatory gene activation^{14,15}, PCAF is also found to act as a factor acetyltransferase (FAT) that acetylates non-histone proteins, including several tumor-suppressor proteins, such as p53^{16,17} and the phosphatase and tensin homolog (PTEN)¹⁸. Because PCAF is involved in proliferation and inflammation, common denominators of the major diseases determining human mortality, with clear evidence for inflammatory factors predicting incident CVD events^{19,20}, incident cancers²¹ and mortality, we hypothesized that the PCAF-gene could be of major importance in the development of cardiovascular disease and cancer, and death from such disease.

We investigated the impact of genetic variation in the promoter region of the PCAF-gene on all-cause mortality and mortality due to coronary heart disease and cancer in the PROSPER-study, a randomized controlled trial in which 5804 elderly patients

(age 70-82) at risk for vascular disease were randomized to pravastatin or placebo²². In order to validate the observed effects and to be able to extrapolate our findings to a younger population, we investigated the PCAF gene in the WOSCOPS study, a randomized controlled trial similar to the PROSPER-study, designed to determine the effect of pravastatin in middle-aged men with hypercholesterolemia without a history of cardiovascular disease. Finally, in order to further test the validity of results in the two statin trials, and to get insights in the mode of action, we investigated these variants in another large prospective study, the GENDER-study, a prospective follow-up study that included 3104 patients undergoing percutaneous coronary intervention (PCI)²³. The primary endpoint in this study was clinical restenosis, a process that is known to be mainly determined by inflammation and proliferation².

All participants in these three study groups were analyzed for 2 polymorphisms (SNPs) in the promoter region of the PCAF-gene. Of these polymorphisms, the -2481G/C SNP was found significantly associated with CHD mortality in elderly patients in PROSPER and WOSCOPS, and, in addition, with differential risk for restenosis in the GENDER study.

Methods

Study Design and Follow-up of the PROSPER Study

The protocol of PROSPER has been described elsewhere²⁴. PROSPER is a prospective multicenter randomized placebo-controlled trial to assess whether treatment with pravastatin diminishes the risk of major vascular events in elderly individuals. Between December 1997 and May 1999, we screened and enrolled subjects in Scotland (Glasgow), Ireland (Cork), and the Netherlands (Leiden). Men and women aged 70-82 years were recruited if they had pre-existing vascular disease or increased risk of such disease because of smoking, hypertension, or diabetes. A total number of 5804 subjects were randomly assigned to pravastatin or placebo. In this genetic sub-study, we evaluated the predefined endpoints all-cause mortality and mortality due to vascular events and cancer. Mean follow-up was 3.2 years (range 2.8-4.0) and 604 (10.4%) patients died during the study²². Of these patients, 292 (48%) died from vascular disease and 206 (31%) from cancer.

Study Design and Follow-up of the WOSCOPS Study

The WOSCOPS study (the West of Scotland Coronary Prevention Study), a primary prevention trial, included 6595 men, aged between 45 and 64 years old, who had LDL cholesterol levels between 174 and 232 mg/dL (4.5 and 6.0 mmol/L), who had no history of myocardial infarction, but were considered to be at enhanced risk for developing CHD²⁵. The first patient was enrolled on February 1, 1989, and the study ended on May 15, 1995. Mean follow up duration was 4.9 years. All participants were randomly assigned to receive 40 mg of pravastatin or placebo daily.

The present genetic study was performed in a previously described nested case-control cohort²⁶. In brief, the prospective nested case-control study included all of the 580 on-trial CHD events (death from CHD, nonfatal MI, or revascularization procedures) from the WOSCOPS cohort as case subjects and 1,160 control subjects matched to case subjects by age and smoking. In the present genetic study we used death from coronary heart disease as our primary endpoint.

Study Design and Follow-up of the GENDER Study

The present study sample has been described previously²³. In brief, the GENetic DEterminants of Restenosis project (GENDER) was a multicenter follow-up study designed to study the association between various gene polymorphisms and clinical restenosis. Patients eligible for inclusion in the GENDER-study were treated successfully for stable angina, non-ST-elevation acute coronary syndromes or silent ischemia by PCI in four out of 13-referral centers for interventional cardiology in the Netherlands. Patients treated for acute ST-elevation myocardial infarction were excluded. Experienced operators, using a radial or femoral approach, performed standard angioplasty and stent placement. During the study, no drug-eluting stents were used. Follow-up lasted for at least nine months, except when a coronary event occurred. Clinical restenosis, defined as TVR, either by PCI or coronary artery bypass grafting (CABG), was the primary endpoint. Median follow-up duration was 9.6 months (interquartile range 3.9) and 304 (9.8%) patients underwent TVR during follow-up. A prespecified subpopulation of 478 patients was scheduled for re-angiography at 6 months, according to standard procedures as described previously²⁷. Identical projections were used before, during and 6 months after the PCI for all assessed angiograms. Quantitative Computer Analyses (QCA) were independently performed by Heartcore (Leiden, the Netherlands).

For all three studies, all endpoints were adjudicated by independent clinical events committees. The protocols meet the criteria of the Declaration of Helsinki and were approved by the Medical Ethics Committees of each participating institution. Written informed consent was obtained from all participating patients.

Genotyping

Blood was collected in EDTA tubes at baseline and genomic DNA was extracted following standard procedures. As a first step to investigate this gene, we selected 2 validated polymorphisms in the PCAF-promoter. The -4556 C/T (rs2623074) and the -2481 G/C (rs2948080) polymorphisms were selected on the basis of their high minor allele frequency (>5%) and measured using the Sequenom Massarray genotyping platform. A multiplex assay was designed using Assay designer software (Sequenom). As quality controls, 5-10% of the samples were genotyped in duplo. No inconsistencies were observed. Cluster plots of the signals from the low and the high mass allele were drawn. Two independent researchers carried out scoring. Disagreements or vaguely positioned dots produced by Genotyper 4.0 (Sequenom Inc.) were left out of the results.

Cells and Cell Culture

The cell lines (HeLa, U251, Raji) used in this study were obtained through the ATCC (Rockville, MD, USA) and were cultured in Iscove's modified Dulbecco's medium (IMDM; BioWhittaker Europe, Verviers, Belgium) supplemented with 10% (v/v) heat-inactivated fetal calf serum (FCS; Greiner, Alphen a/d Rijn, The Netherlands), 100 IU/mL streptomycin and 100 IU/mL penicillin. For interferon- γ (IFN- γ) induction, cells were treated with 500U/mL of IFN- γ (Boehringer-Ingelheim, Alkmaar, The Netherlands) for 4 hours, hereafter nuclear extracts were prepared (see below). HUVECs were cultured in Medium 199 with Earl's salt and L-glutamine (Life Technologies,

Breda, The Netherlands), supplemented with 20% (v/v) FCS (PAA, Pasching, Austria), 100 IU/mL streptomycin and 100 IU/mL penicillin, 10 IU/mL heparine (Leo Pharma, Breda, The Netherlands) and 25 mg bovine pituitary extract (BPE; Life Technologies).

Transcription Factor Binding Site Search

Potential transcription factor binding sites were identified using the TFSEARCH program (<http://www.cbrc.jp/research/db/TFSEARCH.html>), which searches the TRANSFAC database²⁸. Cutoff was set at 75% of the consensus TF binding site.

Nuclear Extracts and Electrophoretic Mobility Shift Assay (EMSA)

Nuclear extracts and EMSAs were performed as described previously²⁹. In brief, 2 μ L of nuclear extracts (HeLa, HUVEC, U251, Raji) in binding buffer were incubated for 30 min on ice, with 2 ng of a [33P]-labeled dsDNA probe. The probe sequences were similar to either the C or G promoter variants of the PCAF-gene (PCAF-C: 5'-GCAAT-AAGCCTCCTCAATCCTTTGCCCTTG-3'; PCAF-G: 5'-GCAATAAGCCTCCTGAAT-CCTTTGCCCTTG-3'). Probe sequences for transcription factors MZF1 and GATA1-3 were similar to their previously described consensus sequence (MZF1 (zinc fingers 1-4): 5'- GATCTAAAAGTGGGGAGAAAA-3'; MZF1 (zinc fingers 5-13): 5'- GATC-CGGCTGGTGAGGGGGAATCG-3'; GATA: 5'- GGACCTTGATCTTATCTT-3')^{30,31}.

For competition assays, nuclear extracts from IFN- γ stimulated HeLa cells were incubated with unlabelled oligonucleotides in 100- and 200-fold excess for 30 min on ice, prior to incubation with the labeled probe. In case of IFN- γ treated samples, cells from five different cell types were stimulated with IFN γ (500U/mL; Boehringer-Ingelheim) for 4-hours prior to preparing nuclear extracts. Samples were run on a 6% polyacrylamide gel in 0.25x TBE-buffer. Gels were densitometrically analyzed using the ImageJ software³².

Mouse Model for Reactive Stenosis

The institutional committee on animal welfare approved all animal experiments. For all experiments hyperlipidemic male ApoE*3-Leiden mice³³ were fed a high-cholesterol diet (ArieBlok, Woerden, The Netherlands). Blood samples to determine plasma cholesterol were collected at time of surgery. After 3 weeks on diet, a non-constrictive polyethylene cuff was placed loosely around one femoral artery and mice were sacrificed at several time points after surgery. After sacrifice, at t=0 hours (control, no cuff placement), 6 hours, 24 hours, 2 days, 3 days, 7 days and 14 days, both femoral arteries were isolated and snap-frozen in liquid nitrogen (n=6 mice for each timepoint).

RNA Isolation and cDNA Synthesis from Femoral Artery Tissue

Per time point, cuffed segments of three femoral arteries were pooled to enable isolation of suitable amount of RNA, resulting in 4 pooled RNA samples obtained from n=6 mice, cuffed at two limbs. After RNA isolation, cDNA was synthesized and RT-PCR analysis was performed as previously described³⁴.

PCAF mRNA Quantification

Expression levels of PCAF were measured by virtue of quantitative RT-PCR using

TaqMan® gene expression assay (Mm00451387_m1). PCR runs were carried out in the ABI PRISM 7700 sequence detection system (Applied Biosystems, Foster City, CA, USA). HPRT was assayed as control gene and its cycle threshold (Ct) was subtracted from the Ct of the gene of interest, yielding Δ Ct. For each timepoint, $\Delta\Delta$ Ct was determined by subtracting the average Δ Ct at timepoint 0 hours from the Δ Ct at each other timepoint. This $\Delta\Delta$ Ct was used to calculate the displayed fold increase for each gene³⁵.

Statistical Analysis

Allele frequencies were determined by gene counting. The Chi-squared test was used to test the consistency of the genotype frequencies at the SNP locus with Hardy-Weinberg equilibrium. Hazard ratios (HR) with 95% confidence intervals (CI) were calculated using a Cox-proportional hazards model. All analyses with PROSPER and WOSCOPS data were adjusted for sex, age and pravastatin use. The analyses with PROSPER data were additionally adjusted for country. In the GENDER-study, polymorphisms were included in a multivariable model containing clinical and procedural risk factors for restenosis, such as diabetes, smoking, hypertension, stenting, total occlusion and residual stenosis >20%.

To reach statistical significance with an alpha of 0.05 and a beta of 0.8 in the association between the -2481 polymorphism and coronary heart disease death in this population, we need 168 cases of coronary heart disease death, for the -4556 we need 379 cases of coronary heart disease death. A combined-effect analysis was performed to pool the results of the effect of the -2481G/C polymorphism on study endpoints (all-cause mortality, CHD death and clinical restenosis) and coronary endpoints (CHD death in two studies and clinical restenosis in the third study) in the three separate studies at old age. The random-effects model was used to consider both the between-study and within-study variability. The pooled hazard ratio over the genotypes was assessed with ordinary logistic regression. The SPSS software (version 12.0.1, SPSS Inc, Chicago, IL) was used for all statistical analyses.

Results

PROSPER study

Participant characteristics are presented in table 1. Genotyping success rates were higher than 96% for all polymorphisms and there were no significant deviations from Hardy-Weinberg equilibrium.

Using a Cox proportional hazards model, which included several clinical variables such as sex, age, pravastatin use, and country, we found a significant association of the -2481 G/C promoter polymorphism with all-cause mortality in PROSPER. As presented in table 2 and figure 1, heterozygotes had a reduced mortality risk by 17% (2% to 30%, $p=0.03$), whereas individuals homozygous for the -2481C allele had a 39% lower mortality (16% to 56%, $p=0.003$). The effect of PCAF is more profound in the association with coronary heart disease (CHD) death (risk reduction 22% (2% to 37%), $p=0.03$) compared to the association with cancer mortality (risk reduction 13% (9% to 30%), $p=0.22$). Due to its proximity to the -2481 G/C polymorphism, we also present the data of the -4556 C/T polymorphism (table 2). It shows a small and non-significant trend towards a decrease in all-cause mortality. The linkage disequi-

librium (LD)-coefficient between these promoter polymorphisms was 0.79.

	PROSPER N=5595	WOSCOPS N=1092	GENDER N=2852
Continuous variates (mean, SD)			
Age (years)	75.3 (3.4)	56.8 (5.2)	62.1 (10.7)
Body mass index, (kg/m ²)	26.8 (4.2)	26.0 (3.2)	27.0 (3.9)
Categorical variates (%)			
Male sex	48	100	71
Current smoker	27	54	25
History of diabetes	11	2	15
History of hypertension	62	18	40
History of myocardial infarction	13	0	40
History of stable angina	27	8	67
Statins	50	48	55
Genotype, minor allele frequency (%)			
PCAF -4556 C/T	9	9	11
PCAF -2481 G/C	33	33	33

Table 1. Baseline characteristics of the PROSPER, the GENDER and the WOSCOPS study. All data are presented in % unless otherwise stated.

WOSCOPS study

To validate the association of the -2481 G/C polymorphism with CHD mortality, and to investigate whether its effect is also present in a population largely without established vascular disease, we aimed to replicate our findings in a previously described²⁶ nested case-control cohort of the WOSCOPS study. Baseline characteristics of the WOSCOPS study are presented in table 1.

	All cause mortality in PROSPER			CHD death in PROSPER			CHD death in WOSCOPS		
	N (%)*	HR (95%CI)	p-value	N (%)*	HR (95%CI)	p-value	N (%)*	HR (95%CI)	p-value
PCAF -4556 C/T									
C/C	491 (11)	1.0 (ref)		168 (4)	1.0 (ref)		83 (9)	1.0 (ref)	
C/T	81 (9)	0.81 (0.64-1.02)	0.09	32 (3)	0.94 (0.64-1.37)	0.75	11 (6)	0.65 (0.34-1.25)	0.20
T/T	4 (7)	0.63 (0.24-1.69)	0.38	3 (5)	1.31 (0.42-4.10)	0.65	2 (13)	1.4 (0.31-6.28)	0.66
Trend	576 (10)	0.80 (0.65-0.99)	0.04	203 (4)	0.99 (0.71-1.38)	0.95	96 (9)	0.80 (0.47-1.36)	0.41
PCAF -2481 G/C									
G/G	290 (12)	1.0 (ref)		103 (4)	1.0 (ref)		49 (10)	1.0 (ref)	
G/C	246 (10)	0.83 (0.70-0.98)	0.03	86 (3)	0.81 (0.61-1.08)	0.16	40 (9)	0.89 (0.58-1.39)	0.62
C/C	41 (7)	0.61 (0.44-0.84)	0.003	14 (3)	0.58 (0.33-1.00)	0.05	8 (6)	0.63 (0.29-1.36)	0.24
Trend	577 (10)	0.80 (0.70-0.91)	0.001	203 (4)	0.78 (0.63-0.98)	0.03	97 (9)	0.83 (0.61-1.14)	0.26

Table 2. Results of the association between two promoter polymorphisms in the PCAF gene and mortality endpoints within the PROSPER and WOSCOPS studies. HR=Hazard ratio. CI=Confidence interval. All hazard ratios and p-values were assessed with a Cox-proportional hazards model and adjusted for sex, age, country, and use of pravastatin. *Calculated for 5595 subjects in the PROSPER study and for 1092 in the WOSCOPS study.

In this case, the -2481 G/C polymorphism was associated with a non-significant trend towards protection against death from coronary heart disease (CHD) (risk reduction 17% (-14% to 39%), $p=0.26$) at all ages. Heterozygotes (risk reduction 11% (-39% to 42%), $p=0.62$) and homozygotes (risk reduction 37% (-36% to 71%), $p=0.24$) had a non-significantly lower mortality risk. Although these data did not reach statistical significance, the point estimate for CHD mortality in WOSCOPS was similar to that observed in the PROSPER study (figure 1). The -4556 C/T polymorphism was not significantly associated with the risk of CHD death (risk reduction 20% (-36% to 53%), $p=0.40$).

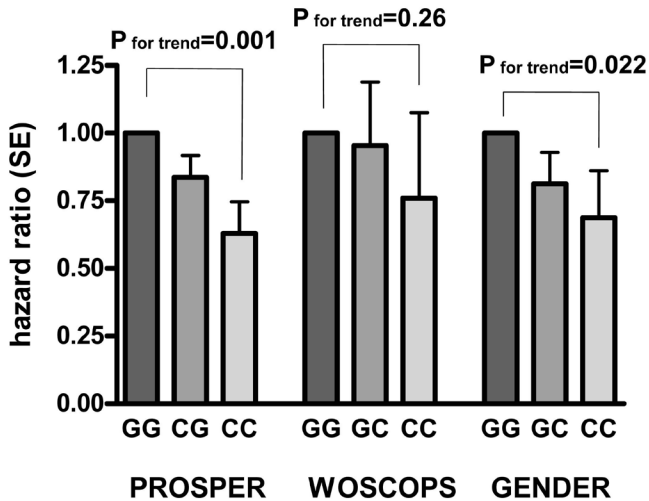


Figure 1. Hazard ratios for all-cause mortality in PROSPER, for coronary heart disease death in WOSCOPS, and for clinical restenosis in GENDER by PCAF -2481 G/C genotype at all ages. The PCAF -2481 G/C polymorphism is associated with mortality in the PROSPER study, with coronary heart disease death in the WOSCOPS study, and with clinical restenosis in the GENDER study in all age groups.

GENDER study

To extend the observed results in the PROSPER study, we tested the relevance of the gene to clinical conditions in which cell proliferation and inflammation play a role in a large patient population included in the GENDER-study. In this study patients were followed for at least 9 months after a PCI to determine absence or presence of clinical restenosis, as defined by the need for target vessel revascularization (TVR). We considered TVR a suitable intermediate endpoint as it is a direct consequence of mainly proliferative and inflammatory processes².

In agreement with the results from the PROSPER and WOSCOPS-study, the -4556 C/T polymorphism was not associated with the risk for TVR in the GENDER-study, whereas the -2481 G/C polymorphism showed a significant association with TVR (p -trend = 0.02) (table 3 and figure 1). Heterozygous patients were at lower risk for TVR (risk reduction 20% (-2% to 38%), $p=0.07$), and patients carrying two -2481C alleles had a greater protection against the development of restenosis (risk reduction 36% (0% to 59%), $p=0.05$).

In analogy of the clinical restenosis (TVR) results, carriers of the -2481C allele also

had less angiographic restenosis in a subpopulation of 478 patients undergoing angiography six months after the PCI (risk reduction 44% (4% to 67%), $p=0.03$) (table 3).

	Clinical restenosis			Angiographic restenosis ^a			Clinical restenosis in the stented subpopulation ^b		
	N (%)	HR (95%CI)	p-value	N (%)	HR (95%CI)	p-value	N (%)	HR (95%CI)	p-value
PCAF -4556 C/T									
C/C	218 (10)	1.0 (ref)		68 (21)	1.0 (ref)		148 (9)	1.0 (ref)	
C/T	54 (10)	0.98 (0.73-1.32)	0.90	16 (19)	0.80 (0.41-1.53)	0.50	31 (8)	0.86 (0.58-1.26)	0.43
T/T	2 (5)	0.46 (0.11-1.86)	0.28	0 (0)			1 (3)	0.34 (0.05-2.45)	0.34
Trend	274 (10)	0.92 (0.70-1.20)	0.54	84 (21)	0.77 (0.41-1.45)	0.42	180 (9)	0.80 (0.561.15)	0.23
PCAF -2481 G/C									
G/G	140 (11)	1.0 (ref)		47 (25)	1.0 (ref)		98 (10)	1.0 (ref)	
G/C	114 (9)	0.80 (0.62-1.02)	0.07	29 (16)	0.56 (0.33-0.96)	0.03	68 (7)	0.70 (0.51-0.95)	0.02
C/C	22 (7)	0.64 (0.41-1.00)	0.05	8 (18)	0.64 (0.27-1.52)	0.31	16 (7)	0.65 (0.38-1.10)	0.11
Trend	276 (10)	0.80 (0.67-0.97)	0.02	84 (21)	0.69 (0.47-1.02)	0.07	182 (9)	0.76 (0.60-0.95)	0.02

Table 3. Results of the association between two promoter polymorphisms in the PCAF gene and clinical and angiographic restenosis within the GENDER study. a measured in a subgroup of 478 subjects. b measured in a subgroup of 2309 subjects. HR=Hazard ratio. CI=Confidence interval. All hazard ratios and p-values were assessed with a Cox-proportional hazards model and adjusted for sex, age, and clinical and procedural risk factors for restenosis.

Combined Effect Analysis

Hazard ratios were almost remarkably equal in all three studies (figure 1). We formally test for homogeneity using a standard Olkin-type Q-test and found p-values of 0.91 and 0.77 for heterozygotic and homozygotic carriers of the minor allele of -2481G/C SNP between the three studies. Therefore and since all three studies have comparable endpoints, we conducted a combined effect analysis to show the effect of the -2481C on the study endpoints (CHD death in PROSPER and WOSCOPS, and clinical restenosis in GENDER) at all ages (figure 2, top panel). The pooled hazard ratio for the -2481C allele was 0.79 ((95%CI: 0.74-0.85), $p=8.1 \times 10^{-4}$). Heterozygotes had a reduced risk (HR: 0.82, 95%CI: 0.68-0.98, $p=0.03$), and this risk was lower in subjects homozygous for the -2481C allele (HR: 0.61 95%CI: 0.44-0.84, $p=0.002$).

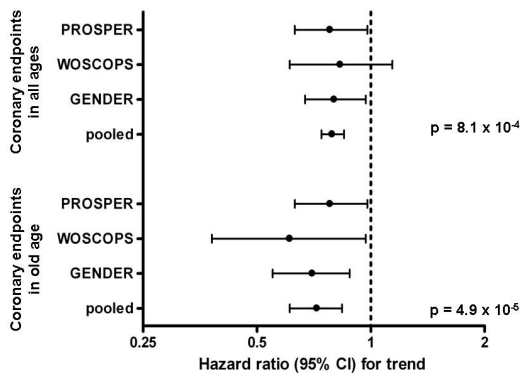


Figure 2. Combined effect estimate of the hazard ratios of the PROSPER, WOSCOPS, and GENDER studies for the PCAF -2481 G/C polymorphism. This figure represents the hazard ratios for the additive model of the PCAF -2481 G/C polymorphism. Coronary endpoints consist of CHD death for the PROSPER and WOSCOPS study, and clinical restenosis for the GENDER study. The top panel is the combined effect analysis for coronary endpoints at all ages, the bottom panel in subgroups with age > 58 years.

Examining for an Age Effect

We investigated an effect of the -2481C variant allele on vascular mortality in two age strata, older and younger than 58 years old. We could however not perform this analysis in the PROSPER cohort since all subjects were older than 70 years. In the WOSCOPS study, among participants ≥ 58 years old (median age), we found that the -2481C allele significantly reduced the risk of CHD death (risk reduction 39% (3% to 62%), $p = 0.035$), whereas there was no significant effect in the lower age group. We found similar results in the GENDER study. We again observed a strong protective effect of the C-allele in old patients (≥ 58 years, $n = 1800$) (risk reduction 30% (12% to 45%), $p = 0.003$) whereas there was no significant effect present in young patients (< 58 years, $n = 1052$).

We also conducted a combined effect analysis to show the effect of the -2481C allele at a high age only (median age > 58), shown in figure 2 bottom panel. The pooled hazard ratio for the -2481C allele on coronary events (CHD death or TVR) in this high age group was 0.72 (95%CI: 0.61-0.84), $p = 4.9 \times 10^{-5}$, which is somewhat stronger than the effect at all ages.

Functional Involvement: The -2481 Region Encompassing the C/G PCAF Variants

Using the EMSA technique we tested whether the observed polymorphism would lead to differential protein binding in vitro. Using nuclear extracts of different cell types, we studied complex formation at the -2481 region of PCAF. We could detect constitutive protein binding to both PCAF-C and G-variants (figure 3). In both human umbilical vein endothelial cells (HUVECs) and U251 cells nuclear factor binding is slightly enhanced by IFN- γ stimulation. Densitometric analysis revealed that the PCAF G-variant exhibits slightly stronger protein binding in some cell types than the C-variant, although these differences are not statistically significant. Competition assays also suggest a modest difference in binding affinity (figure 3B).

Using the TFSearch program, we identified possible binding sites for MZF1 and GATA1-3 in the PCAF C-variant promoter. However, ds-oligonucleotides representing binding sites for MZF1 and GATA1-3 did not compete with factor binding to the PCAF C-promoter variant (data not shown).

PCAF mRNA Expression in a Mouse Model of Reactive Stenosis

Placement of a small non-constrictive cuff around the femoral artery in hypercholesterolemic (13.9 ± 3.6 mmol/L) ApoE3Leiden mice results in induction of neointima formation. In the developing neointima a rapid upregulation of the PCAF expression was observed after cuff placement in a time dependent manner (figure 4). PCAF expression showed a peak two days after vascular injury (~ 1.5 fold increase) and reduces to baseline levels of expression after 7 days. PCAF expression at day 3, 7 and 14 differed significantly from the 24h measurement ($p < 0.05$).

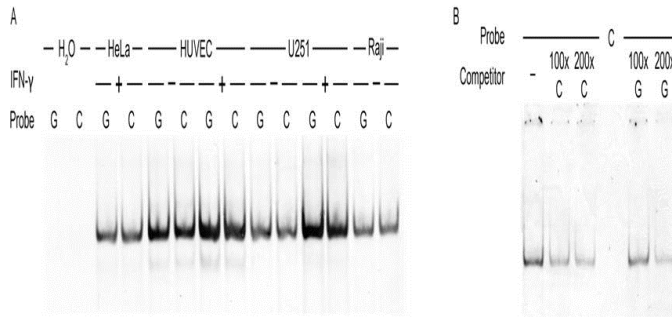


Figure 3. Protein binding to the C- and G-variant of the -2481 region. (A) EMSA showing binding of protein to the C- and G-variant of the -2481 region using nuclear extracts of various cell-lines. EMSA suggests slightly stronger binding of protein to the G-variant of the -2481 region, most pronounced in HUVECs and U251 cells. (B) Competition assay with nuclear extracts from HeLa cells stimulated with IFN- γ also suggests slightly increased binding affinity for the -2481 G-variant at high concentrations. The difference is best observed when unlabelled probe is added in 200-fold excess, indicating that the observed difference in affinity is weak. Shown are representatives of multiple independent experiments.

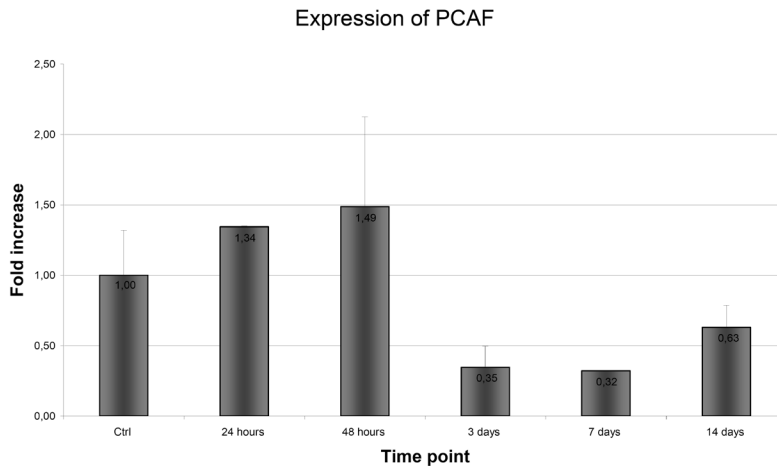


Figure 4. Expression of PCAF mRNA in a cuff-induced reactive stenosis mouse model. The figure shows PCAF differentially expressed upon activation of the vessel wall in a time dependent manner, with an expression peak 48 hours after vascular injury. The data is presented as fold increase compared to the control arteries, using HPRT as an internal control for cDNA input.

Discussion

Our data indicate that the -2481C allele in the gene encoding PCAF, a protein which has been shown to be a key mediator in epigenetics by acetylating histones and several non-histone proteins, such as the p53 tumor-suppressor proteins, is associated with a significant survival advantage in three independent studies. We found in the PROSPER-study an advantage in survival mainly due to a significant risk reduction in CHD death. In line with this observation we also observed that the -2481C allele was associated with a lower death by CHD in the WOSCOPS study in an age dependent manner. Furthermore, this allele also protects against clinical and

angiographic restenosis in the GENDER-study. The effects of the -2481C allele on mortality, CHD death and clinical restenosis were more profound at older age (>58 years). The -2481G/C polymorphism in the PCAF promoter affects transcription factor binding, as was demonstrated by an EMSA band shift analysis. A role for PCAF in vascular disease was further confirmed in a mouse model for reactive stenosis, in which modulation of PCAF expression was detected during vascular remodeling. Our observation in the PROSPER-study that this promoter variant associates to lower mortality from cardiovascular disease and cancer as well as clinical restenosis after PCI in GENDER, may indicate a role of PCAF in inhibiting cell proliferation also in more general terms. PCAF has been shown, for example, to activate p53-responsive enhancer elements within the p21waf1 promoter¹⁷ and activity of p21waf1 is known to induce cell-cycle arrest in vascular smooth muscle cells³⁶⁻³⁹. Furthermore, A20, a NF κ B-dependent gene that has been shown to inhibit proliferation of VSMCs via increased expression of p21waf1, was able to prevent neointima formation after balloon angioplasty in a rat model of carotid artery stenosis⁴⁰.

Apart from its well-described role in cell-cycle regulation, PCAF is also known to be required to co-activate p65-dependent transcription and has been shown to directly activate the transcription of several NF κ B-regulated genes known to be involved in cardiovascular disease⁴¹. Miao et al. has shown that PCAF could enhance the p65 mediated increase in TNF- α promoter activity and that high glucose increased the recruitment of PCAF to the TNF- α and COX-2 promoters¹⁴. Furthermore, they demonstrated concomitant acetylation of specific lysine residues of histone H3 and H4 at these promoters. Since TNF- α and COX-2 have been implicated in the development of atherosclerosis^{42,43}, and restenosis^{27,44}, and also cancer^{45,46}, our data suggest that PCAF may also play a role in the development of these diseases.

Our finding in the WOSCOPS and GENDER-study that the strong protective effect of the -2481C allele was more profound in patients older than 58 years old, whereas it seemed not present in young patients (<58 years old) is of particular interest⁴⁷. It could reveal the combined effect of a life-time dysregulation of expression of the lysine acetyltransferase -2481C PCAF variant, which affects global levels of histone acetylation, in addition to the accumulating effect of exposure to environmental factors which also affects histone acetylation profiles during life as observed by Fraga et al 6. In the PROSPER population such an age dependent effect was not observed as this trial included only patients >70 years old. As expected, here the effects on cardiovascular and cancer mortality associated with the PCAF -2481 G/C polymorphism were evident for the entire population. After observing an age-dependent effect in the WOSCOPS and GENDER study, we suggest that this polymorphism in PCAF is associated with an altered tendency to acetylate histones and non-histone proteins (such as the tumor-suppressor p53 whose function relies on acetylation, reviewed in Spange et al.³⁶) and may therefore become important especially in elderly patients, who may have been under the influence of altered PCAF activity for many years. This hypothesis needs however further investigation.

Although our findings in the GENDER-study do not directly replicate the effect of the -2481 G/C polymorphism on CHD mortality in the elderly, they are of much value as this study has a mechanistically linked and better defined concise endpoint. Thus in this way patho-physiologic insights would be obtained and not just replication only. Restenosis after a PCI is very well investigated and is now known to be mainly the

consequence of inflammatory and proliferative processes, which is underscored by the fact that stents eluting drugs that suppress these processes are highly efficacious in the prevention of restenosis. Therefore, we believe that our finding that the -2481C allele protects against restenosis in the GENDER-study could possibly confirm its functional significance, but could also provide mechanistic insights in its beneficial role in survival in the PROSPER and WOSCOPS studies. However this could only explain part of the causes by which CHD death risk is decreased in PROSPER and WOSCOPS studies, the exact mechanism is not known. We did not find any association between the strongly linked -4556C/T polymorphism and survival in any of the three studies. The estimated hazard ratio's were quite similar as expected, however, due to small numbers since the minor allele frequency of -4556C/T is three to four times smaller than of -2481G/C, no significant results were yielded. This could simply be due to lack of power.

Here we show a strong association between the PCAF locus involved in epigenetic control and clinical conditions in three large follow-up studies with a mechanistically linked endpoint, however our studies warrant further investigation into the influence of the -2481 G/C polymorphism on the activity of the PCAF promoter or expression levels of NF κ B-regulated genes. Here we hypothesize a new concept that differential transcription of the PCAF gene leads to differences in gene expression in various pathways mechanistically linked to CHD events, such as inflammatory regulatory pathways or pathways involved in proliferation. Hence, further research has to be performed to test this hypothesis.

In a first analysis we were able to demonstrate binding of nuclear factors to the specific region flanking the -2481 G/C polymorphism in the PCAF promoter. EMSA analysis showed that the G-variant possibly exhibits a slightly higher affinity for nuclear factor binding than the C-variant in some cell types tested (e.g. HUVECS and U251), albeit that this was not significant. It should also be noted that IFN- γ stimulation slightly increases nuclear factor binding in HUVECs and U251 cells, suggesting a role for IFN- γ induced nuclear factors. It remains to be established whether these interacting factors play a role in the transcriptional regulation of PCAF. However, provided that this SNP influences PCAF transcription and resulting protein levels, this could have a bearing on the cellular portrait of expressed genes and might lead to a dramatic different outcome if the effects accumulate over years. The fact that nuclear extracts do bind to the same region of the promoter in which the polymorphism is situated does strongly suggest that the SNP might affect the binding of transcription complexes and thus influences gene transcription, however this needs to be confirmed in future studies.

To further illustrate a possible role of PCAF in vascular disease, we quantified PCAF-transcripts in the stenotic vessel wall in a mouse model of cuff induced reactive stenosis in the femoral artery. During the stenotic process, the PCAF gene expression was rapidly upregulated, indicating that PCAF gene expression is activated upon vascular injury and suggesting that this transcriptional coactivator is involved in the development of reactive stenosis, at least in the early stages. Unfortunately it is not possible to measure the PCAF protein levels directly, however the rapid up and down regulation of the mRNA levels suggests that PCAF is not stable. The changes in mRNA levels are likely to reflect the changes in protein levels.

In conclusion, we showed in three large prospective studies that the -2481C allele

in the PCAF promoter is associated with a significant survival advantage in elderly patients while also protecting against clinical and angiographic restenosis after PCI. Although the exact mechanisms of these actions are thus far unknown, we suggest that the effect of this allele on these endpoints may be due to the well-known involvement of PCAF in inflammatory and proliferative processes. Our observations promote the concept that epigenetic processes are under genetic control and that, other than environment, genetic variation in genes encoding KATs may also determine susceptibility to CHD outcomes and mortality. Therefore epigenetic histone modification, when our results are confirmed in our studies, might become a target for future therapy.

Reference List

1. Ross JS, Stagliano NE, Donovan MJ, et al. Atherosclerosis and cancer: common molecular pathways of disease development and progression. *Ann N Y Acad Sci* 2001;947:271-292.
2. Agema WR, Jukema JW, Pimstone SN, et al. Genetic aspects of restenosis after percutaneous coronary interventions: towards more tailored therapy. *Eur Heart J* 2001;22:2058-2074.
3. Monraats PS, Pires NM, Agema WR, et al. Genetic inflammatory factors predict restenosis after percutaneous coronary interventions. *Circulation* 2005;112:2417-2425.
4. Nordlie MA, Wold LE, Kloner RA. Genetic contributors toward increased risk for ischemic heart disease. *J Mol Cell Cardiol* 2005;39:667-679.
5. Gosden RG, Feinberg AP. Genetics and epigenetics--nature's pen-and-pencil set. *N Engl J Med* 2007;356:731-733.
6. Fraga MF, Ballestar E, Paz MF, et al. Epigenetic differences arise during the lifetime of monozygotic twins. *Proc Natl Acad Sci U S A* 2005;102:10604-10609.
7. Ito K, Ito M, Elliott WM, et al. Decreased histone deacetylase activity in chronic obstructive pulmonary disease. *N Engl J Med* 2005;352:1967-1976.
8. Lill NL, Grossman SR, Ginsberg D, et al. Binding and modulation of p53 by p300/CBP coactivators. *Nature* 1997;387:823-827.
9. Pons D, de Vries FR, van den Elsen PJ, et al. Epigenetic histone acetylation modifiers in vascular remodelling: new targets for therapy in cardiovascular disease. *Eur Heart J* 2009;30:266-277.
10. Turunen MP, Aavik E, Yla-Herttuala S. Epigenetics and atherosclerosis. *Biochim Biophys Acta* 2009;1790:886-891.
11. Wei JQ, Shehadeh LA, Mitrani JM, et al. Quantitative control of adaptive cardiac hypertrophy by acetyltransferase p300. *Circulation* 2008;118:934-946.
12. Grunstein M. Histone acetylation in chromatin structure and transcription. *Nature* 1997;389:349-352.
13. Moodie FM, Marwick JA, Anderson CS, et al. Oxidative stress and cigarette smoke alter chromatin remodeling but differentially regulate NF-kappaB activation and proinflammatory cytokine release in alveolar epithelial cells. *FASEB J* 2004;18:1897-1899.
14. Miao F, Gonzalo IG, Lanting L, et al. In vivo chromatin remodeling events leading to inflammatory gene transcription under diabetic conditions. *J Biol Chem* 2004;279:18091-18097.
15. Vogel NL, Boeke M, Ashburner BP. Spermidine/Spermine N1-Acetyltransferase 2 (SSAT2) functions as a coactivator for NF-kappaB and cooperates with CBP and P/CAF to enhance NF-kappaB-dependent transcription. *Biochim Biophys Acta* 2006;1759:470-477.
16. Liu L, Scolnick DM, Trievel RC, et al. p53 sites acetylated in vitro by P/CAF and p300 are acetylated in vivo in response to DNA damage. *Mol Cell Biol* 1999;19:1202-1209.
17. Di S, V, Soddu S, Sacchi A, et al. HIPK2 contributes to P/CAF-mediated p53 acetylation and selective transactivation of p21Waf1 after nonapoptotic DNA damage. *Oncogene* 2005;24:5431-5442.
18. Okumura K, Mendoza M, Bachoo RM, et al. P/CAF modulates PTEN activity. *J Biol Chem* 2006;281:26562-26568.
19. Bucova M, Bernadic M, Buckingham T. C-reactive protein, cytokines and inflammation in cardiovascular diseases. *Bratisl Lek Listy* 2008; 109:333-340.
20. Lowe GD. Circulating inflammatory markers and risks of cardiovascular and non-cardiovascular disease. *J Thromb Haemost* 2005;3:1618-1627.
21. Allin KH, Bojesen SE, Nordestgaard BG. Baseline C-reactive protein is associated with incident cancer and survival in patients with cancer. *J Clin Oncol* 2009;27:2217-2224.
22. Shepherd J, Blauw GJ, Murphy MB, et al. Pravastatin in elderly individuals at risk of vascular disease (PROSPER): a randomised controlled trial. *Lancet* 2002; 360:1623-1630.
23. Agema WR, Monraats PS, Zwiderman AH, et al. Current PTCA practice and clinical outcomes in The Netherlands: the real world in the pre-drug-eluting stent era. *Eur Heart J* 2004;25:1163-1170.
24. Shepherd J, Blauw GJ, Murphy MB, et al. The design of a prospective study of Pravastatin in the Elderly at Risk (PROSPER). PROSPER Study Group. PROspective Study of Pravastatin in the Elderly at Risk. *Am J Cardiol* 1999;84:1192-1197.
25. Shepherd J, Cobbe SM, Ford I, et al. Prevention of coronary heart disease with pravastatin in men with hypercholesterolemia. West of Scotland Coronary Prevention Study Group. *N Engl J*

- Med 1995;333:1301-1307.
26. Packard CJ, O'Reilly DS, Caslake MJ, et al. Lipoprotein-associated phospholipase A2 as an independent predictor of coronary heart disease. West of Scotland Coronary Prevention Study Group. *N Engl J Med* 2000;343:1148-1155.
 27. Monraats PS, Pires NM, Schepers A, et al. Tumor necrosis factor-alpha plays an important role in restenosis development. *FASEB J* 2005;19:1998-2004.
 28. Heinemeyer T, Wingender E, Reuter I, et al. Databases on transcriptional regulation: TRANS-FAC, TRRD and COMPEL. *Nucleic Acids Res* 1998;26:362-367.
 29. Gobin SJ, Peijnenburg A, Keijsers V, et al. Site alpha is crucial for two routes of IFN gamma-induced MHC class I transactivation: the ISRE-mediated route and a novel pathway involving CIITA. *Immunity* 1997;6:601-611.
 30. Ko LJ, Engel JD. DNA-binding specificities of the GATA transcription factor family. *Mol Cell Biol* 1993;13:4011-4022.
 31. Morris JF, Hromas R, Rauscher FJ, III. Characterization of the DNA-binding properties of the myeloid zinc finger protein MZF1: two independent DNA-binding domains recognize two DNA consensus sequences with a common G-rich core. *Mol Cell Biol* 1994;14:1786-1795.
 32. Abramoff MD, Magelhaes PJ, Ram SJ. Image Processing with ImageJ. *Biophotonics International* 2004;11:36-42.
 33. van den Maagdenberg AM, Hofker MH, Krimpenfort PJ, et al. Transgenic mice carrying the apolipoprotein E3-Leiden gene exhibit hyperlipoproteinemia. *J Biol Chem* 1993;268:10540-10545.
 34. Pires NM, Eefting D, de Vries MR, et al. Sirolimus and paclitaxel provoke different vascular pathological responses after local delivery in a murine model for restenosis on underlying atherosclerotic arteries. *Heart* 2007;93:922-927.
 35. Pfaffl MW. A new mathematical model for relative quantification in real-time RT-PCR. *Nucleic Acids Res* 2001;29:e45.
 36. Mnjoyan ZH, Dutta R, Zhang D, et al. Paradoxical upregulation of tumor suppressor protein p53 in serum-stimulated vascular smooth muscle cells: a novel negative-feedback regulatory mechanism. *Circulation* 2003;108:464-471.
 37. Kusama H, Kikuchi S, Tazawa S, et al. Tranilast inhibits the proliferation of human coronary smooth muscle cell through the activation of p21waf1. *Atherosclerosis* 1999;143:307-313.
 38. Lee B, Kim CH, Moon SK. Honokiol causes the p21WAF1-mediated G(1)-phase arrest of the cell cycle through inducing p38 mitogen activated protein kinase in vascular smooth muscle cells. *FEBS Lett* 2006;580:5177-5184.
 39. Kato S, Ueda S, Yamaguchi M, et al. Overexpression of p21Waf1 induces apoptosis in immortalized human vascular smooth muscle cells. *J Atheroscler Thromb* 2003;10:239-245.
 40. Patel VI, Daniel S, Longo CR, et al. A20, a modulator of smooth muscle cell proliferation and apoptosis, prevents and induces regression of neointimal hyperplasia. *FASEB J* 2006;20:1418-1430.
 41. Kiernan R, Bres V, Ng RW, et al. Post-activation turn-off of NF-kappa B-dependent transcription is regulated by acetylation of p65. *J Biol Chem* 2003;278:2758-2766.
 42. Sarzi-Puttini P, Atzeni F, Doria A, et al. Tumor necrosis factor-alpha, biologic agents and cardiovascular risk. *Lupus* 2005;14:780-784.
 43. Cipollone F, Prontera C, Pini B, et al. Overexpression of functionally coupled cyclooxygenase-2 and prostaglandin E synthase in symptomatic atherosclerotic plaques as a basis of prostaglandin E(2)-dependent plaque instability. *Circulation* 2001;104:921-927.
 44. Wang K, Tarakji K, Zhou Z, et al. Celecoxib, a selective cyclooxygenase-2 inhibitor, decreases monocyte chemoattractant protein-1 expression and neointimal hyperplasia in the rabbit atherosclerotic balloon injury model. *J Cardiovasc Pharmacol* 2005;45:61-67.
 45. Mocellin S, Rossi CR, Pilati P, et al. Tumor necrosis factor, cancer and anticancer therapy. *Cytokine Growth Factor Rev* 2005;16:35-53.
 46. Williams CS, Mann M, DuBois RN. The role of cyclooxygenases in inflammation, cancer, and development. *Oncogene* 1999;18:7908-7916.
 47. Mayor S. Unravelling the secrets of ageing. *BMJ* 2009; 338:a3024.

Chapter 10

The epigenetic factor PCAF regulates vascular inflammation and is essential for accelerated atherosclerosis development

M.M. Ewing^{1,2,3}, J.C. Karper^{2,3}, A.J.N.M. Bastiaansen^{2,3}, H.A.B. Peters^{2,3}, M.R. de Vries^{2,3}, P.J. van den Elsen^{4,5}, K. Ozato⁶, T. Maurice^{7,8}, C. Gongora^{7,9}, J.W. Jukema^{1,3}, P.H.A. Quax^{2,3}

1 Dept. of Cardiology, Leiden University Medical Center (LUMC), Leiden, The Netherlands

2 Dept. of Surgery, LUMC, Leiden, The Netherlands

3 Einthoven Laboratory for Experimental Vascular Medicine, LUMC, Leiden, The Netherlands

4 Dept. of Immunohematology and Blood Transfusion, LUMC, Leiden, The Netherlands

5 Dept. of Pathology, VU University Medical Center, Amsterdam, the Netherlands

6 Laboratory of Molecular Growth Regulation, National Institute of Child Health and Human Development, National Institutes of Health, Bethesda, Maryland

7 Université de Montpellier 2, 34095 Montpellier, France

8 INSERM U 710, 34095, Montpellier, France

9 Institut de Recherche en Cancérologie de Montpellier INSERM U 896, 34298, Montpellier, France

Submitted for publication

Abstract

Objective Genetic P300/CBP-associated factor (PCAF) variation affects restenosis-risk in patients. PCAF has lysine acetylase activity and promotes inflammation, which drives post-interventional vascular remodeling and accelerated atherosclerosis development. We studied the contributing role of PCAF in post-interventional vascular remodeling.

Methods and Results PCAF contribution to inflammation and vascular remodeling was assessed in macrophages *in vitro* and in a mouse model for vascular remodeling and accelerated atherosclerosis. PCAF regulates MHC class-II, but not MHC class-I expression in macrophages through CIITA, inducing a pro-inflammatory reaction. PCAF^{-/-} mice are used to show that PCAF deficiency is associated with 73.2% ($p=0.001$) reduction of intimal hyperplasia, intima/media ratio and luminal stenosis by preventing smooth muscle cell (SMC) accumulation. This was confirmed using the potent natural PCAF inhibitor garcinol *in vivo* which reduced arterial leukocyte and macrophage adherence and infiltration following injury and accelerated atherosclerosis development by 71.9% ($p=0.004$) in operated hypercholesterolemic ApoE3*Leiden mice. This occurred due to downregulation of MCP-1 and TNF α expression by garcinol, similarly to PCAF siRNA, as demonstrated on cultured splenocytes, SMCs and macrophages and *in vivo*.

Conclusions These results identify a vital role for the epigenetic factor PCAF in the regulation of local inflammation after arterial injury, responsible for vascular remodeling and accelerated atherosclerosis development.

Introduction

Percutaneous coronary intervention (PCI) remains the main choice of revascularization therapy for coronary artery disease. However, restenosis is a common complication and inflammation plays a pivotal role in its development¹⁻³. Endothelial injury and underlying plaque exposure during PCI, together with sub-endothelial LDL cholesterol retention evoke thrombocyte adhesion and activation, promoting leukocyte attachment and extravasation^{2,4}. Macrophages and T-cells play a central role and their pro-atherogenic cytokine expression is responsible for further chemotaxis. T-cells secrete interferon (IFN) γ , which enhances class II transactivator (CIITA) and MHC class II-molecule expression in macrophages. Although it can both stimulate SMC proliferation and lead to SMC apoptosis *in vitro*⁵, it has been shown to function as an important pro-atherogenic cytokine in (accelerated) atherosclerosis development⁶. Gene-environmental interactions that stimulate nuclear factor kappa-beta (NF κ B) expression are regulated by epigenetic factors that strongly modulate gene expression patterns without DNA sequence modification, mainly by regulating histone acetylation and de-acetylation⁷. Inflammatory gene expression is the result of the counterbalancing and reversible actions of lysine acetyltransferases (KATs) and lysine deacetylases (KDACs), which together determine chromatin structure modification and accessibility to transcription factors^{8,9}. P300/CBP associated factor (PCAF/KAT2B) is a transcriptional co-activator with intrinsic KAT-activity and is involved in lysine acetylation of histones at the site of NF κ B-regulated genes^{9,10}. PCAF binds the cyclooxygenase (COX)-2 promoter region following cellular exposure to inflammatory mediators and thereby regulates the general inflammatory response through prostaglandin H₂ formation¹¹. PCAF also enhances the p65-mediated increase in tumor necrosis factor (TNF) α promoter activity and both TNF α and COX-2 regulate the inflammatory response that lead to atherosclerosis^{12,13}.

Few natural inhibitors of PCAF have been described, of which only the natural inhibitor garcinol, derived from the *Garcinia Indica* fruit rind, has been shown to be extremely potent¹⁴. It inactivates PCAF activity within 3min¹⁵ and has strong apoptosis-inducing effect on leukemia cell lines¹⁶ and prostate and pancreatic cancer cells¹⁷ through NF κ B downregulation. These properties make garcinol an extremely potent inhibitor of PCAF-regulated inflammation in vascular remodeling and accelerated atherosclerosis development.

Previously, association between the -2481C variant allele of the PCAF gene and reduced vascular mortality was shown in three independent large prospective studies¹⁸⁻²⁰, identifying PCAF as possible diagnostic marker for CHD mortality and restenosis²¹. Increased intravascular PCAF mRNA levels after injury suggested PCAF involvement in inflammatory-mediated remodeling, although the nature of this elevation remained unexplored²¹.

In the present study, PCAF knock-out mice^{22,23} were used to investigate the PCAF contribution to the inflammatory response following vascular injury in a reactive stenosis mouse model^{24,25}. Mice lacking PCAF are developmentally normal without a distinct phenotype, although they have been shown to be resistant to amyloid toxicity²² and display an altered memory capacity in response to stress²². Furthermore, PCAF inhibition with siRNA and garcinol is shown to functionally affect the cellular inflammation reaction after stimulation, resulting in reduced inflammatory cell re-

cruitment to the site of vascular injury and eventually attenuated accelerated atherosclerosis development in vivo. This highlights inflammation-regulation by PCAF as a contributing factor in post-interventional vascular remodeling.

Materials and methods

PCAF^{-/-} and control macrophages were used to study expression of MHC-I, II and CIITA, the master regulator of class II MHC transcription, at RNA and protein level using quantitative real-time PCR and flow cytometry in resting conditions and following IFN γ stimulation. We performed multiple in vivo studies in which control, PCAF^{-/-} and garcinol-treated hypercholesterolemic ApoE3*Leiden mice were subjected to femoral artery cuff placement to induce vascular remodeling. This evokes rapid leukocyte recruitment and infiltration (3d) and inflammation-dependent concentric intimal lesions (21d) that consists predominately of SMCs and connective tissue. In these vascular segments, inflammatory cell adhesion, infiltration, intimal thickening and lesion composition were assessed using histology, morphometry and immunohistochemistry (IHC). Cultured splenocytes, SMCs and macrophages were used to study the effects of PCAF inhibition by siRNA and garcinol on the expression of MCP-1 and TNF α by ELISA. A detailed description of materials and methods can be found in the supplemental material section.

Results

PCAF is essential for CTIIA and MHCII, but not MHCI, expression in macrophages

We analyzed the expression of MHC-I and II at the RNA and protein levels and the expression of the master regulator of class II MHC transcription, CIITA, at the RNA level. First we confirmed by quantitative real-time PCR (QPCR) analysis that PCAF is not expressed in PCAF^{-/-} mice (fig 1A) and we observed that PCAF expression is not induced by IFN γ .

We compared IFN γ -induced MHC-II expression in WT and PCAF^{-/-} macrophages. Constitutive MHC-II and IFN γ expression was inhibited in PCAF^{-/-} macrophages, compared to the WT macrophages at the mRNA level measured by QPCR (fig 1B) and at the protein level at the cell surface, both constitutively and following IFN γ induction, measured by flow cytometry (fig 1C). The mRNA level of CIITA was assessed by QPCR and we observed that WT and PCAF^{-/-} macrophages displayed the same level (fig 1D), indicating that the levels of IFN γ -induced CIITA transcription are not modulated in these macrophages, but its activity is impaired due to the lack of PCAF. As CIITA also contributes to MHC-I gene transcription, the cell surface expression of MHC-I in macrophages incubated or untreated with IFN γ was measured in WT and PCAF^{-/-} cells (fig 1E). We observed that the MHC-I expression was not altered in PCAF^{-/-} macrophages.

Intimal thickening is significantly reduced in PCAF^{-/-} mice

Quantitative analysis of cuffed femoral artery segments of C57Bl/6 control and PCAF^{-/-} mice stained with Weigert's elastin revealed, despite similar plasma total choleste

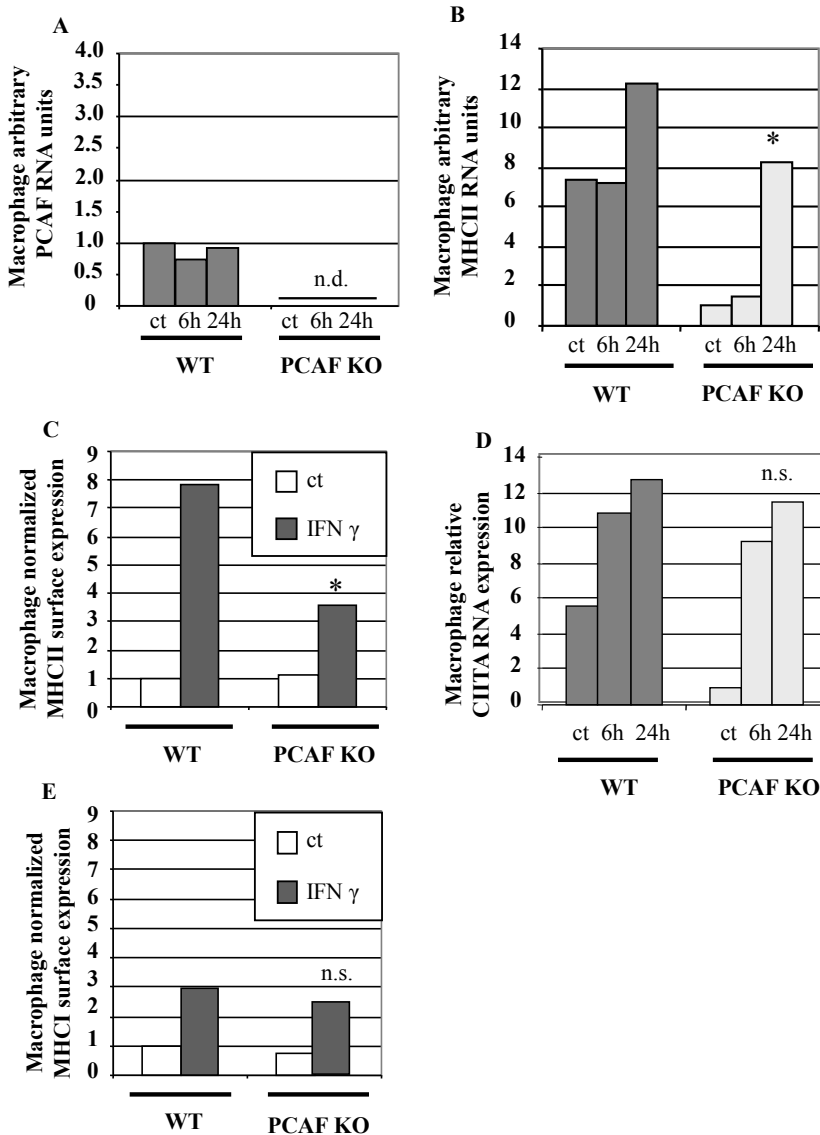


Figure 1. PCAF is necessary for MHC-II expression in macrophages. The loss of PCAF inhibits IFN γ -induced MHC-II expression in peritoneal macrophages at RNA and protein level. A, B and D: Analysis of mRNA levels by semi-quantitative Q-PCR of PCAF, MHCII and CIITA respectively. Constitutive and IFN γ -induced levels of transcripts were analyzed at times 0, 6 and 24h following IFN γ exposure respectively. C and E: Analysis of protein expression at the cell surface by flow cytometry of MHCII and MHCII respectively. Endogenous and IFN γ -treated cells during 24h were analyzed and displayed against untreated cells (ct: consecutively, n.d.: non-detectable, n.s.: not-significant). Results are representative of three separate experiments (mean \pm SEM, n=3, * p<0.05).

rol concentrations (supplemental table I), 73.2% reduced intimal thickening in PCAF^{-/-} mice when compared to controls (WT: 9777 \pm 1608 μ m², PCAF^{-/-}: 2623 \pm 368 μ m², n=10, p=0.001, fig 2A). Since the media area was similar, this was accompanied by a reduced intima/media ratio by 73.7% (WT: 0.94 \pm 0.18, PCAF^{-/-}: 0.25 \pm 0.03, n=10, p=0.001, fig 2B) and reduced luminal stenosis by 60.1% after 21d (WT: 51.5 \pm 4.6%,

PCAF^{-/-}: 20.5±2.5%, n=10, p=0.001, fig 2C). IHC was performed to assess lesion composition (fig 2D) and it was observed that PCAF^{-/-} mice displayed a significantly smaller area of α -SMC actin expressing cells (positively-stained area per cross section in μm^2) by 61.8% (p=0.028) within the intimal layer (fig 2E).

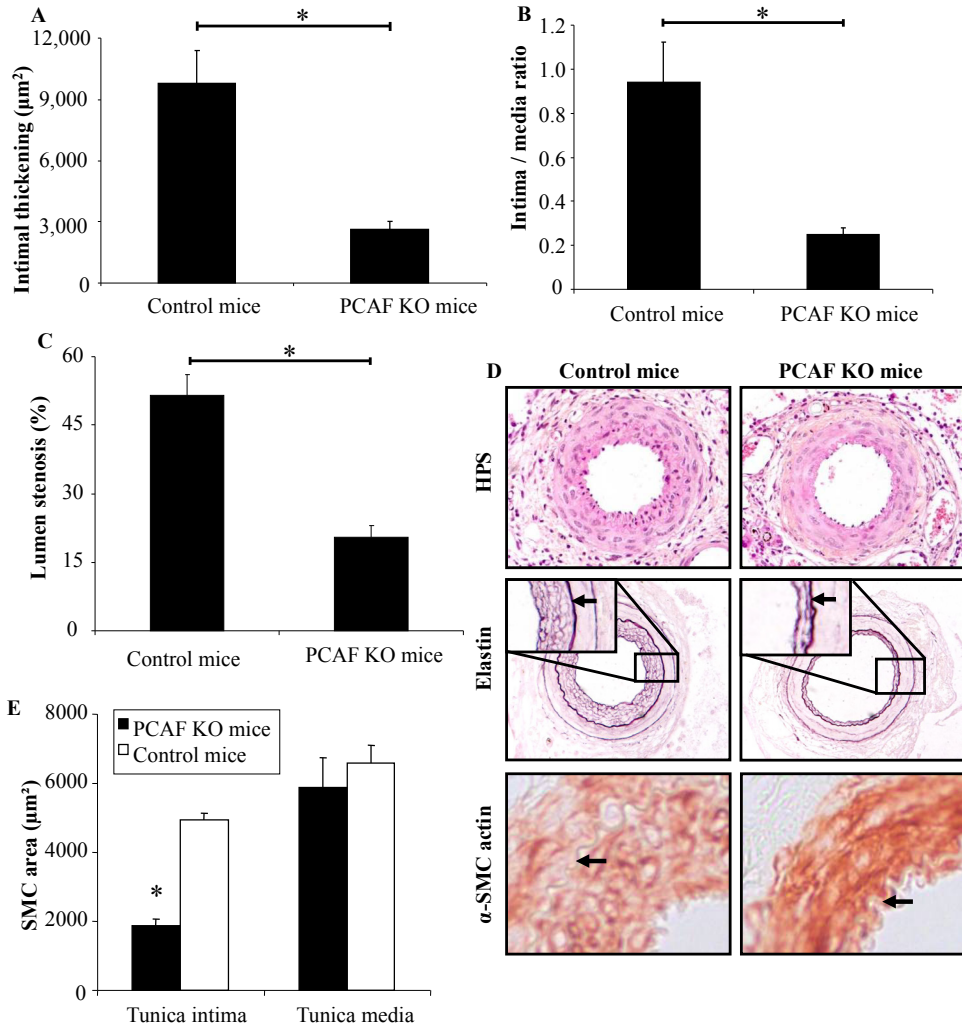


Figure 2. Reduced vascular remodeling in PCAF^{-/-} mice. A: intimal thickening (μm^2), (B) intima / media ratio and (C) luminal stenosis (%) in wildtype and PCAF^{-/-} mice, 21d after femoral arterial cuff placement (mean±SEM, n=10, * p<0.05). D: representative cross-sections of cuffed arterial segments, stained with HPS (200x), Weigert's elastin 200x (arrows in inserts (400x) indicate internal elastic lamina) and for SMC α -actin (200x). E: quantification of SMC area (μm^2) in the intimal and medial layers of wildtype and PCAF^{-/-} mice (mean±SEM, n=10, * p<0.05).

PCAF regulates the functional leukocyte and SMC inflammatory response

Vascular injury leads to inflammatory cytokine expression by recruited leukocytes and resident VSMCs which drives subsequent vascular remodeling. The anti-inflammatory potential of pharmacological PCAF inhibition through garcinol, the most po-

tent natural PCAF inhibitor described, was first tested *in vitro*. Analysis of garcinol-treated wildtype and PCAF^{-/-} cultured splenocytes showed reduced expression of TNF α by 25.7% ($p=0.037$) and 42.3% ($p=0.030$) respectively (fig 3A) and of MCP-1 by 41.3% ($p=0.057$) and 71.4% ($p=0.029$) respectively (fig 3B) after overnight lipopolysaccharide (LPS) stimulation. Next, splenocytes were subjected to siRNA-mediated knock-down of PCAF, incorporation assessed with siRNA luciferase (fig 3C) and control siRNA as controls and were again exposed to LPS. When compared to vehicle-treated splenocytes (which responded similarly to control siRNA-exposed cells, $p=0.240$), knockdown of PCAF led to reduced TNF α expression by 41.2% ($p=0.029$) as did PCAF^{-/-} splenocytes by 55.5% ($p=0.004$). No differences in TNF α expression were measured between PCAF deficient splenocytes and wildtype splenocytes following PCAF knockdown (fig 3D).

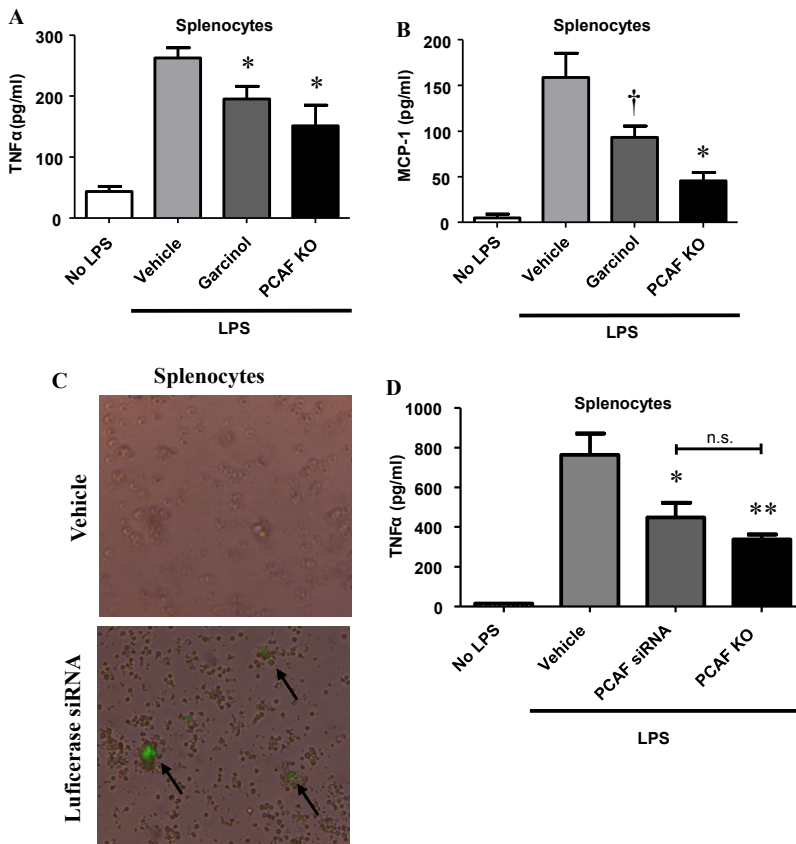


Figure 3. PCAF inhibition prevents inflammatory cytokine expression *in vitro*. Compared to overnight LPS-stimulated (100 ng/ml) wildtype splenocytes, garcinol-incubated (15 μ M) and PCAF^{-/-} splenocytes display a reduced expression of TNF α (pg/ml) (A) and MCP-1 (pg/ml) (B). Luciferase siRNA controls display effective splenocyte transfection after 24h (C). TNF α expression (pg/ml) is also reduced after siRNA-mediated PCAF knockdown in wildtype splenocytes following overnight LPS-stimulation (300 ng/ml) as effectively as in PCAF^{-/-} splenocytes (D). Results are representative of three separate experiments (mean \pm SEM, $n=3$, * $p<0.05$, † $0.05<p<0.10$, n.s. not significant, n.d. not detectable).

PCAF was shown to regulate macrophage MHCII expression through CTIIA. Functional macrophage dampening was investigated and it was found that TNF α expression after overnight LPS stimulation was profoundly reduced by simultaneous garcinol incubation (fig 3E) ($p=0.0*10^{-6}$) in vitro. Finally, MCP-1 expression by LPS-stimulated SMCs was reduced by 24.5% ($p=0.043$, fig 3F) in the presence of garcinol (15 μ M), although this could not be demonstrated at the lowest garcinol concentration (5.0 μ M). Next, analysis to which extent PCAF contributes to MCP-1 expression by VSMCs was performed in a dose-response experiment using (0.1-10.0 ng/ml) LPS. It is shown that VSMC-secreted level of MCP-1 (pg/ml) is reduced by garcinol by 19.2-26.0% at LPS concentrations of 0.1, 1.0 and 10 ng/ml respectively (fig 3G, $p=0.049$, $p=0.021$ and $p=0.043$ respectively), measured by ELISA.

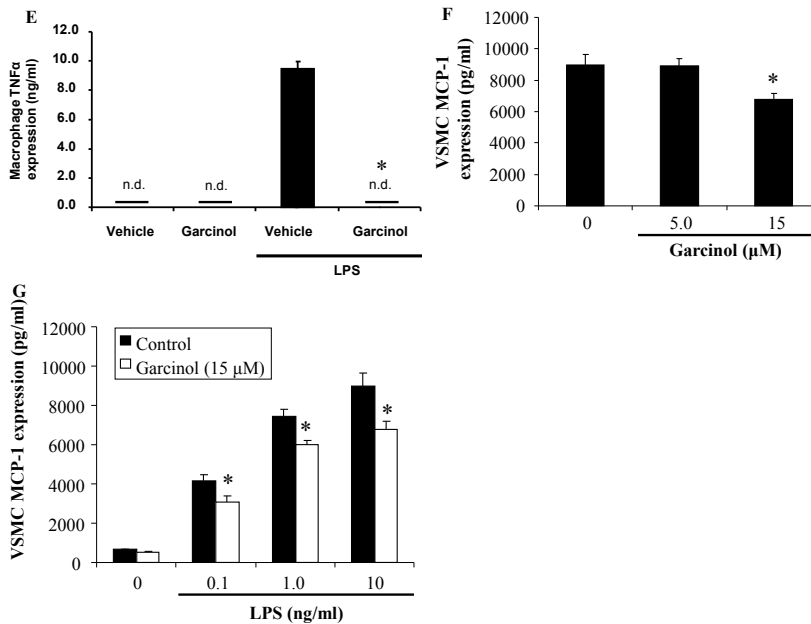


Figure 3. PCAF inhibition prevents inflammatory cytokine expression in vitro. Macrophage TNF α (ng/ml) expression following overnight inflammatory mediator (LPS) stimulation is significantly reduced by garcinol (15 μ M) to non-detectable levels (E). Garcinol (15 μ M) downregulates MCP-1 (pg/ml) expression by cultured vascular SMCs (F) and reduces vascular SMC MCP-1 (pg/ml) expression following a dose-dependent increase of LPS (0.1-10 ng/ml) (G). Results are representative of three separate experiments (mean \pm SEM, n=3, * $p<0.05$, † $0.05<p<0.10$, n.s. not significant, n.d. not detectable).

PCAF inhibition prevents injury-induced leukocyte recruitment in vivo

PCAF inhibition to prevent post-interventional remodeling and accelerated atherosclerosis development was investigated by garcinol in the femoral artery cuff model in hypercholesterolemic ApoE3*Leiden mice. Viability of circulating leukocytes in the presence of garcinol (0-250 μ M) was investigated using the redox indicator Alamar blue. Fluorescence intensity (FI) remained constant at ~5700 AU (615 nm) at garcinol concentrations 0-20 μ M, indicating complete cellular viability compared to positive controls (100%) ($p=0.448$, fig 4A), with cytotoxicity at concentrations ≥ 30 μ M (FI: ~900 AU).

Independently of elevated total plasma cholesterol concentrations (supplementary

table I), garcinol in pluronic gel (10 μ l of 41.5 mmol/L lubricated around operated arterial segment) reduced the percentage of endothelial leukocyte adhesion out of all cells within the internal elastic lamina by 62.1% ($p=0.028$) and of macrophages by 54.6% ($p=0.010$) after 3d compared to vehicle only. Medial leukocyte infiltration was reduced by garcinol by 61.7% ($p=0.005$) and macrophages by 84.5% ($p=0.004$) (fig 4C, D). Garcinol reduced the percentage of cells in the tunica intima (predominately endothelial cells) that expressed MCP-1 by 65.0% ($p=0.003$) and of cells in the tunica media by 57.1% ($p=0.010$) (fig 4E), suggesting that garcinol reduced leukocyte adherence and infiltration by affecting chemo-attracting factors.

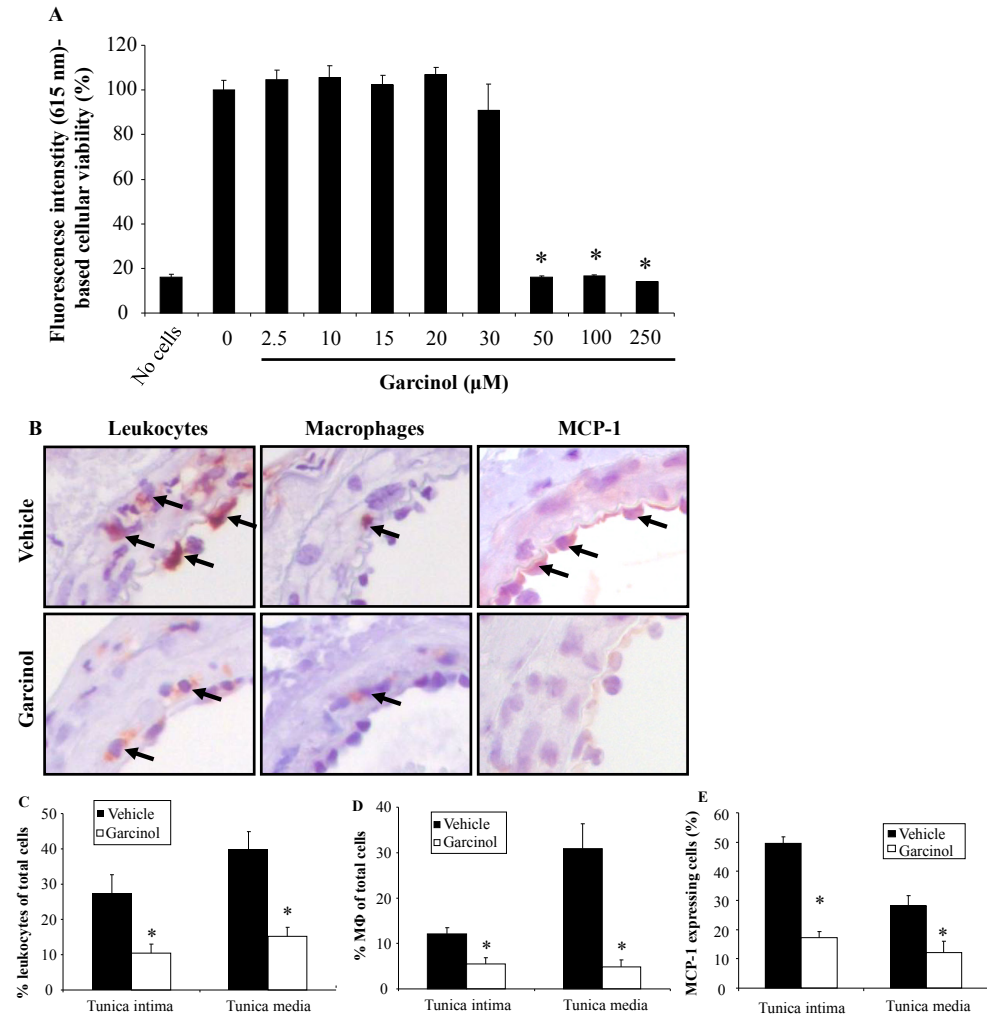


Figure 4. Garcinol-mediated PCAF inhibition reduces the leukocyte inflammatory response. A: ApoE3*Leiden-derived whole blood viability assay after overnight 0-250 μ M garcinol incubation using Alamar blue conversion (emission 615 nm), expressed as percentage fluorescence intensity (of positive controls) (mean \pm SEM, $n=10$, * $p<0.05$). B: representative cross-sections of cuffed arterial segments of ApoE3*Leiden mice, 3d after surgery (CD45+ leukocytes, macrophages and MCP-1 expressing cells, 400x, arrows indicate positive staining). Quantification of (endothelial)-adhered or medial infiltrated leukocytes (C), macrophages (D) and MCP-1 expressing cells (E), expressed as the percentage of all cells

adhering to the endothelium or in the media. The entire length of the cuffed femoral artery segment was used for analysis (mean±SEM, n=10, * p<0.05).

PCAF inhibition prevents accelerated atherosclerosis development

IHC showed that PCAF expression is absent in non-injured hypercholesterolemic arteries (fig 5A). Negative staining was confirmed in PCAF^{-/-} arteries (fig 5B). PCAF presence was increased 3d after surgery in ApoE3*Leiden mice (fig 5C). Staining was observed in both endothelial-adhering leukocytes and in the SMC-rich tunica media. Garcinol reduced PCAF staining (fig 5C) after 3d.

Early anti-inflammatory effects of PCAF-inhibition were substantiated by garcinol application during femoral artery cuff placement. Despite similarly elevated total plasma cholesterol concentrations (supplementary table I), garcinol (10 µl of 41.5 mmol/L concentration lubricated around operated arterial segment) significantly reduced intimal thickening by 71.9% (p=0.004) in ApoE3*Leiden mice when compared to vehicle only (fig 5D, G). Since medial surface was similar, this was accompanied by a reduced intima / media ratio by 72.5% (p=0.002) (fig 5E) and reduced luminal stenosis by 63.3% (p=0.001) after 14d (fig 5F).

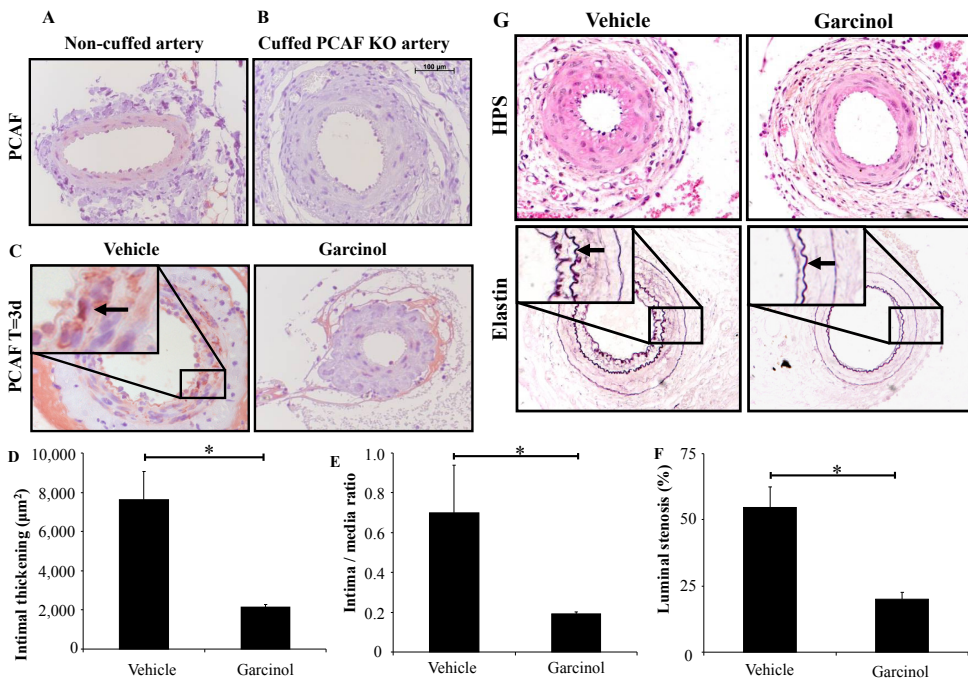


Figure 5. PCAF inhibition prevents vascular remodeling. Representative cross-sections of (un)cuffed-femoral arterial segments, stained for the presence of PCAF (200x). A: non-cuffed artery from ApoE3*Leiden mouse. B: cuffed femoral artery of PCAF^{-/-} mouse (negative control). C: PCAF expression in cuffed femoral arteries of ApoE3*Leiden mice ± garcinol treatment, 3d and 14d after surgery. Arrow in insert indicates positive medial staining. Garcinol-treatment in ApoE3*Leiden mice reduced intimal thickening (µm²) (D), intima / media ratio (E) and luminal stenosis (%) (F), 14d after femoral arterial cuff placement (mean±SEM, n=10, * p<0.05). G: representative cross-sections of cuffed femoral arteries (HPS and Weigert's elastin staining, 200x, arrow in inserts (400x) indicate internal elastic lamina).

PCAF inhibition affects vessel wall composition

IHC was performed to assess lesion composition in vehicle and garcinol-treated animals (fig 6A), revealing a reduced inflammatory phenotype following garcinol treatment. This led to reduced relative macrophage presence (in %) by 75.7% in the intimal layer ($p=0.023$) and by 74.7% in the medial layer ($p=0.004$) (fig 6B). In garcinol-treated arteries, the relative α SMC actin+ area (%) was 14.6% ($p=0.042$) higher in the tunica media, although there were no relative differences measured in the tunica intima (fig 6C). However, absolute α SMC actin intimal thickening was prevented by garcinol, indicated by 40.0% ($p=0.042$) reduced SMC surface area (μm^2) (fig 6D). Cellular proliferation in the arterial wall was assessed using BrdU staining, injected once daily for 3d after surgery. Control arteries displayed more elaborate BrdU staining, suggesting PCAF inhibition could affect injury-induced cellular proliferation in vivo (fig 6A). Together, these data identify clear effects of PCAF inhibition on vascular inflammatory phenotype.

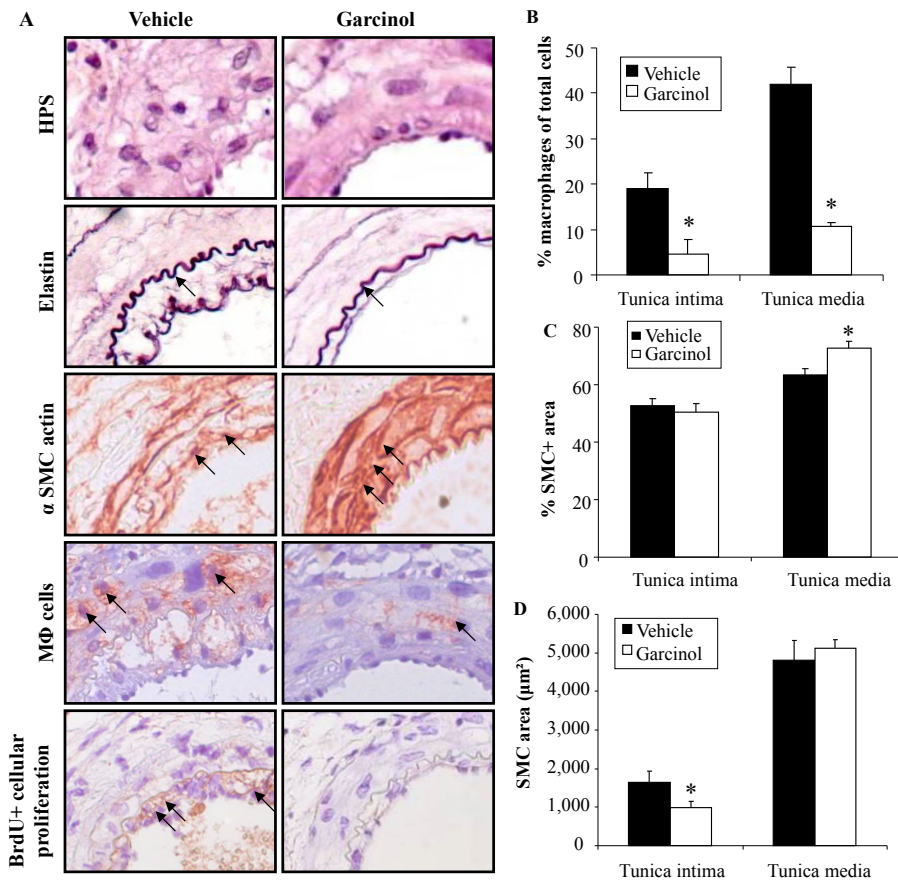


Figure 6. PCAF inhibition affects accelerated atherosclerotic lesion morphology. A: cross-sections of cuffed arterial segments of ApoE3*Leiden mice, 14d after surgery, treated with vehicle only or garcinol-containing pluronic gel, 200x. Arteries are stained with HPS, Weigert’s elastin (arrows indicate internal elastic lamina) and for SMC α -actin, macrophages and BrdU-incorporation (arrows indicate positive staining). Quantification of macrophages (B) and relative SMC α -actin+ surface area (C) in the intimal and medial layers, expressed as the positively-stained area as percentage of the total area. D: quantification of α -actin SMC area (μm^2) in the tunica intima and media (mean \pm SEM, n=10, * $p<0.05$).

Discussion

Here we demonstrate that compared to controls, post-interventional vascular remodeling is reduced in PCAF^{-/-} mice, as is post-interventional accelerated atherosclerosis development in hypercholesterolemic mice treated with a PCAF inhibitor. Furthermore, we demonstrate that this reduced remodeling is due to an attenuated inflammatory response, shown by reduced MCP-1 and TNF α -expression *in vivo* and in cultured cells. It was shown that PCAF regulates MHC class II, but not I, expression in macrophages through CIITA and becomes upregulated in the early period following vascular injury. To our knowledge, this is the first paper to show that PCAF has a contributing role in vascular remodeling by regulating the inflammatory response. PCAF^{-/-} mice were used to demonstrate clear effects of PCAF deficiency on inflammatory-regulated vascular remodeling. Animals developed significantly smaller SMC-rich neointimal lesions with reduced luminal stenosis. The only described natural potent PCAF inhibitor garcinol, was used next to siRNA-mediated PCAF knock-down and PCAF^{-/-} cells to demonstrate its essential contribution in the production of pro-inflammatory cytokines (MCP-1 and TNF α) by various cell types including splenocytes, macrophages and vascular SMCs. This contribution was confirmed *in vivo* where garcinol prevented post-interventional leukocyte recruitment to the site of arterial injury and accelerated atherosclerosis development in operated hypercholesterolemic mice. These results demonstrate an important role for the epigenetic factor PCAF in the post-interventional arterial inflammatory response²⁶.

The role of PCAF was further investigated in macrophages, which play a vital role in the progression of accelerated atherosclerotic lesions. MHC class II, but not class I, expression was found to be inhibited in PCAF^{-/-} macrophages at both mRNA and protein level, whilst CIITA mRNA was normalized. This indicates that IFN γ -induced CIITA transcription is not affected by PCAF deficiency, but its activity is impaired due to the lack of PCAF^{27, 28}, suggesting PCAF-requirement for adequate adaptive immune responses in this leukocyte subset. Although PCAF is important for MHC class II expression, it cannot be fully excluded that other inflammatory genes are also affected by PCAF inhibition (e.g. COX-2), albeit not MHC class I.

Previously, mouse PCAF mRNA levels were demonstrated to be reactively increased within 48h after vascular injury, after which levels were reduced below resting values²¹. Using IHC, we show abundant PCAF protein expression 72h after surgery in endothelial-adhering cells (e.g. macrophages) and in the SMC-rich tunica media. Since vascular injury is known to elicit inflammation and provoke SMC proliferation, regulation of inflammation by PCAF could strongly contribute to vascular remodeling. Indeed, short-term PCAF inhibition early after surgery led to reduced PCAF expression after 14 days, indicative of a reduced inflammatory phenotype of arterial wall. Consistent with PCAF expression by SMC, SMC-rich intimal lesions which occurred in wildtype mice were significantly less present in PCAF^{-/-} mice (fig 2E), indicating that PCAF-regulated inflammation contributes strongly to lesion formation in these animals.

An *ex vivo* LPS stimulation experiment in splenocytes, macrophages and vascular SMCs from either wildtype or PCAF^{-/-} mice was performed to test if PCAF was involved in inflammatory cytokine expression by these various cell types. Indeed, TNF α expression by splenocytes and macrophages was severely compromised in

PCAF deficient animals and similarly in wildtype cells subjected to siRNA-mediated PCAF knockdown or garcinol-treatment, indicating a vital role for PCAF in inflammatory gene transcription. Since cytokine levels were differently affected in different cell types such as VSMCs and macrophages, this might differences in PCAF expression concentrations in different cell types or altered histone acetylation status between cells.

Garcinol was used successfully in preclinical cancer studies in rats, where oral garcinol application reduced the severity of tongue carcinoma by inhibiting tumor cell proliferation^{29, 30}. Anti-proliferative drugs, originally applied as cytostatic anti-cancer agents such as sirolimus and paclitaxel, have been extensively used against restenosis in drug-eluting stents^{31, 32}. However, they affect cellular proliferation non-specifically, whereas PCAF inhibition could be a potent promising anti-restenotic therapy. It is speculated that the protective function of garcinol is primarily through PCAF inactivation in macrophages, affecting their MHCII expression. However, garcinol also downregulates KDAC-induced tissue-type plasminogen activator in endothelial cells³³. Unlike the quiescent state in an uninjured artery, the fibrinolytic system becomes activated after vascular trauma with strong t-PA expression in SMC, endothelial cells and platelets³⁴ and can increase SMC migration. Inhibition of plasmin activity at the cell surface inhibits intimal thickening in our mouse model for reactive stenosis³⁵ and it can therefore not be ruled out that garcinol affects intimal thickening by influencing plasmin activity, provided this is KDAC-induced.

It is also conceivable that PCAF itself influences post-interventional vascular remodeling through indirect effects on macrophages. High mobility group 1 protein (HMGB1) is a chromatin component that can be secreted by activated monocytes and macrophages and functions as a late mediator of inflammation. These cells can tilt the acetylation / deacetylation balance in favor of acetylation upon activation and PCAF is known to acetylate HMGB1⁸, which occurs extensively upon activation with LPS³⁶. LPS also provokes significant intimal thickening, which could indicate that PCAF may not directly affect inflammatory gene transcription, but indirectly through LPS-induced HMGB1 acetylation in stimulated monocytes and macrophages. Moreover, HMGB1 may act as an endogenous ligand for TLR4 and TLR4 signaling is also a key regulatory process in vascular remodeling³⁷. A significantly impaired inflammatory response by LPS-stimulated PCAF^{-/-} whole blood ex vivo is supportive of this possibility.

In conclusion, using PCAF^{-/-} mice, evidence is provided that PCAF contributes to post-interventional vascular remodeling. Further, local delivery of the PCAF-inhibitor garcinol inhibited reactive stenosis and accelerated atherosclerosis development in hypercholesterolemic ApoE*3-Leiden transgenic mice. This could be explained by an as yet unrecognized direct or indirect effect of PCAF on inflammation and SMC proliferation, leading to reduced post-interventional remodeling. These results might therefore shed light on the possible contribution of PCAF as an important epigenetic factor in vascular remodeling and accelerated atherosclerosis development in stenosed human coronary lesions and identify it as a possible new clinical target against vascular remodeling after PCI.

Reference List

1. Lee MS, David EM, Makkar RR, Wilentz JR. Molecular and cellular basis of restenosis after percutaneous coronary intervention: the intertwining roles of platelets, leukocytes, and the coagulation-fibrinolysis system. *J Pathol* 2004;203:861-870.
2. Pires NM, Jukema JW, Daemen MJ, Quax PH. Drug-eluting stents studies in mice: do we need atherosclerosis to study restenosis? *Vascul Pharmacol* 2006;44:257-264.
3. Pons D, Monraats PS, de Maat MP, Pires NM, Quax PH, van Vlijmen BJ, Rosendaal FR, Zwinderman AH, Doevendans PA, Waltenberger J, de Winter RJ, Tio RA, Frants RR, van der LA, van der Wall EE, Jukema JW. The influence of established genetic variation in the haemostatic system on clinical restenosis after percutaneous coronary interventions. *Thromb Haemost* 2007;98:1323-1328.
4. Hansson GK. Inflammation, atherosclerosis, and coronary artery disease. *N Engl J Med* 2005;352:1685-1695.
5. Geng YJ, Wu Q, Muszynski M, Hansson GK, Libby P. Apoptosis of vascular smooth muscle cells induced by in vitro stimulation with interferon-gamma, tumor necrosis factor-alpha, and interleukin-1 beta. *Arterioscler Thromb Vasc Biol* 1996;16:19-27.
6. Weber C, Zernecke A, Libby P. The multifaceted contributions of leukocyte subsets to atherosclerosis: lessons from mouse models. *Nat Rev Immunol* 2008;8:802-815.
7. Barnes PJ, Karin M. Nuclear factor-kappaB: a pivotal transcription factor in chronic inflammatory diseases. *N Engl J Med* 1997;336:1066-1071.
8. Pasheva E, Sarov M, Bidjekov K, Ugrinova I, Sarg B, Lindner H, Pashev IG. In vitro acetylation of HMGB-1 and -2 proteins by CBP: the role of the acidic tail. *Biochemistry* 2004;43:2935-2940.
9. Pons D, de Vries FR, van den Elsen PJ, Heijmans BT, Quax PH, Jukema JW. Epigenetic histone acetylation modifiers in vascular remodelling: new targets for therapy in cardiovascular disease. *Eur Heart J* 2009;30:266-277.
10. Maurice T, Duclot F, Meunier J, Naert G, Givalois L, Meffre J, Celerier A, Jacquet C, Copois V, Mechti N, Ozato K, Gongora C. Altered memory capacities and response to stress in p300/CBP-associated factor (PCAF) histone acetylase knockout mice. *Neuropsychopharmacology* 2008;33:1584-1602.
11. Deng WG, Zhu Y, Wu KK. Role of p300 and PCAF in regulating cyclooxygenase-2 promoter activation by inflammatory mediators. *Blood* 2004;103:2135-2142.
12. Monraats PS, Pires NM, Schepers A, Agema WR, Boesten LS, de Vries MR, Zwinderman AH, de Maat MP, Doevendans PA, de Winter RJ, Tio RA, Waltenberger J, 't Hart LM, Frants RR, Quax PH, van Vlijmen BJ, Havekes LM, van der Laarse A, van der Wall EE, Jukema JW. Tumor necrosis factor-alpha plays an important role in restenosis development. *FASEB J* 2005;19:1998-2004.
13. Narasimha AJ, Watanabe J, Ishikawa TO, Priceman SJ, Wu L, Herschman HR, Reddy ST. Absence of myeloid COX-2 attenuates acute inflammation but does not influence development of atherosclerosis in apolipoprotein E null mice. *Arterioscler Thromb Vasc Biol* 2010;30:260-268.
14. Balasubramanyam K, Altaf M, Varier RA, Swaminathan V, Ravindran A, Sadhale PP, Kundu TK. Polyisoprenylated benzophenone, garcinol, a natural histone acetyltransferase inhibitor, represses chromatin transcription and alters global gene expression. *J Biol Chem* 2004;279:33716-33726.
15. Arif M, Pradhan SK, Thanuja GR, Vedamurthy BM, Agrawal S, Dasgupta D, Kundu TK. Mechanism of p300 specific histone acetyltransferase inhibition by small molecules. *J Med Chem* 2009;52:267-277.
16. Matsumoto K, Akao Y, Kobayashi E, Ito T, Ohguchi K, Tanaka T, Iinuma M, Nozawa Y. Cytotoxic benzophenone derivatives from *Garcinia* species display a strong apoptosis-inducing effect against human leukemia cell lines. *Biol Pharm Bull* 2003;26:569-571.
17. Ahmad A, Wang Z, Wojewoda C, Ali R, Kong D, Maitah MY, Banerjee S, Bao B, Padhye S, Sarkar FH. Garcinol-induced apoptosis in prostate and pancreatic cancer cells is mediated by NF- KappaB signaling. *Front Biosci (Elite Ed)* 2011;3:1483-1492.
18. Monraats PS, Pires NM, Agema WR, Zwinderman AH, Schepers A, de Maat MP, Doevendans PA, de Winter RJ, Tio RA, Waltenberger J, Frants RR, Quax PH, van Vlijmen BJ, Atsma DE, van der Laarse A, van der Wall EE, Jukema JW. Genetic inflammatory factors predict restenosis after percutaneous coronary interventions. *Circulation* 2005;112:2417-2425.
19. Shepherd J, Blauw GJ, Murphy MB, Bollen EL, Buckley BM, Cobbe SM, Ford I, Gaw A, Hyland

- M, Jukema JW, Kamper AM, Macfarlane PW, Meinders AE, Norrie J, Packard CJ, Perry IJ, Stott DJ, Sweeney BJ, Twomey C, Westendorp RG. Pravastatin in elderly individuals at risk of vascular disease (PROSPER): a randomised controlled trial. *Lancet* 2002;360:1623-1630.
20. Shepherd J, Cobbe SM, Ford I, Isles CG, Lorimer AR, Macfarlane PW, McKillop JH, Packard CJ. Prevention of coronary heart disease with pravastatin in men with hypercholesterolemia. West of Scotland Coronary Prevention Study Group. *N Engl J Med* 1995;333:1301-1307.
 21. Pons D, Trompet S, de Craen AJ, Thijssen PE, Quax PH, de Vries MR, Wierda RJ, van den Elsen PJ, Monraats PS, Ewing MM, Heijmans BT, Slagboom PE, Zwinderman AH, Doevendans PA, Tio RA, de Winter RJ, de Maat MP, Iakoubova OA, Sattar N, Shepherd J, Westendorp RG, Jukema JW. Genetic variation in PCAF, a key mediator in epigenetics, is associated with reduced vascular morbidity and mortality: evidence for a new concept from three independent prospective studies. *Heart* 2011;97:143-150.
 22. Duclot F, Meffre J, Jacquet C, Gongora C, Maurice T. Mice knock out for the histone acetyltransferase p300/CREB binding protein-associated factor develop a resistance to amyloid toxicity. *Neuroscience* 2010;167:850-863.
 23. Duclot F, Jacquet C, Gongora C, Maurice T. Alteration of working memory but not in anxiety or stress response in p300/CBP associated factor (PCAF) histone acetylase knockout mice bred on a C57BL/6 background. *Neurosci Lett* 2010;475:179-183.
 24. Ewing MM, de Vries MR, Nordzell M, Pettersson K, de Boer HC, van Zonneveld AJ, Frostegard J, Jukema JW, Quax PH. Annexin A5 treatment attenuates vascular inflammation and remodeling and improves endothelial function in mice. *Arterioscler Thromb Vasc Biol* 2011;31:95-101.
 25. Lardenoye JH, Delsing DJ, de Vries MR, Deckers MM, Princen HM, Havekes LM, van Hinsbergh VW, van Bockel JH, Quax PH. Accelerated atherosclerosis by placement of a perivascular cuff and a cholesterol-rich diet in ApoE*3Leiden transgenic mice. *Circ Res* 2000;87:248-253.
 26. Wierda RJ, Geutskens SB, Jukema JW, Quax PH, van den Elsen PJ. Epigenetics in atherosclerosis and inflammation. *J Cell Mol Med* 2010;14:1225-1240.
 27. Harton JA, Zika E, Ting JP. The histone acetyltransferase domains of CREB-binding protein (CBP) and p300/CBP-associated factor are not necessary for cooperativity with the class II transactivator. *J Biol Chem* 2001;276:38715-38720.
 28. Spilianakis C, Papamatheakis J, Kretsovali A. Acetylation by PCAF enhances CIITA nuclear accumulation and transactivation of major histocompatibility complex class II genes. *Mol Cell Biol* 2000;20:8489-8498.
 29. Tanaka T, Kohno H, Shimada R, Kagami S, Yamaguchi F, Kataoka S, Ariga T, Murakami A, Koshimizu K, Ohgishi H. Prevention of colonic aberrant crypt foci by dietary feeding of garcinol in male F344 rats. *Carcinogenesis* 2000;21:1183-1189.
 30. Yoshida K, Tanaka T, Hirose Y, Yamaguchi F, Kohno H, Toida M, Hara A, Sugie S, Shibata T, Mori H. Dietary garcinol inhibits 4-nitroquinoline 1-oxide-induced tongue carcinogenesis in rats. *Cancer Lett* 2005;221:29-39.
 31. Moses JW, Leon MB, Popma JJ, Fitzgerald PJ, Holmes DR, O'Shaughnessy C, Caputo RP, Kereiakes DJ, Williams DO, Teirstein PS, Jaeger JL, Kuntz RE. Sirolimus-eluting stents versus standard stents in patients with stenosis in a native coronary artery. *N Engl J Med* 2003;349:1315-1323.
 32. Stone GW, Ellis SG, Cox DA, Hermiller J, O'Shaughnessy C, Mann JT, Turco M, Caputo R, Bergin P, Greenberg J, Popma JJ, Russell ME. A polymer-based, paclitaxel-eluting stent in patients with coronary artery disease. *N Engl J Med* 2004;350:221-231.
 33. Dunoyer-Geindre S, Kruihof EK. Epigenetic control of tissue-type plasminogen activator synthesis in human endothelial cells. *Cardiovasc Res* 2011;90:457-463.
 34. Clowes AW, Clowes MM, Au YP, Reidy MA, Belin D. Smooth muscle cells express urokinase during mitogenesis and tissue-type plasminogen activator during migration in injured rat carotid artery. *Circ Res* 1990;67:61-67.
 35. Quax PH, Lamfers ML, Lardenoye JH, Grimbergen JM, de Vries MR, Slomp J, de Ruyter MC, Kockx MM, Verheijen JH, van Hinsbergh VW. Adenoviral expression of a urokinase receptor-targeted protease inhibitor inhibits neointima formation in murine and human blood vessels. *Circulation* 2001;103:562-529.
 36. Aneja RK, Tsung A, Sjodin H, Geffer JV, Delude RL, Billiar TR, Fink MP. Preconditioning with high mobility group box 1 (HMGB1) induces lipopolysaccharide (LPS) tolerance. *J Leukoc Biol* 2008;84:1326-1334.
 37. Karper JC, de Vries MR, van den Brand BT, Hofer IE, Fischer JW, Jukema JW, Niessen HW, Quax PH. Toll-Like Receptor 4 Is Involved in Human and Mouse Vein Graft Remodeling, and

Local Gene Silencing Reduces Vein Graft Disease in Hypercholesterolemic APOE*3Leiden Mice. *Arterioscler Thromb Vasc Biol* 2011;31:1033-1040.

Supplemental material

Materials and Methods

Mice

All experiments were approved by the Institutional Committee for Animal Welfare at the LUMC. The generation of PCAF knockout (KO) mice has been described previously¹. Male C57Bl/6 PCAF KO mice² and wildtype (WT) C57Bl/6 controls were used, as were transgenic male ApoE*3-Leiden mice (both bred in our own laboratory), backcrossed for more than 20 generations on a C57BL/6 background. ApoE*3-Leiden (at the start of a dietary run-in period) and WT and PCAF KO mice aged 10-12 weeks, were used for femoral artery cuff experiments.

Peritoneal macrophage culture

Peritoneal macrophages (PM) were elicited by intraperitoneal (IP) injection with thioglycollate broth. 2 ml of thioglycollate was administered IP to 4-6 week old control or PCAF KO mice and PM were harvested 3d later under anesthesia, as described in the section below. Thioglycollate elicited PM were plated at 5×10^6 cells/dish in 100 mm tissue culture dish in RPMI 5% fetal calf serum (FCS) overnight. The PM were then washed with RPMI 5% FCS and were either treated or untreated with IFN γ (100 U/ml) for 24 or 48 hours.

Peritoneal macrophage RNA isolation and real time (RT) PCR

Real time PCR analysis was done with an ABI PRISM 7700 sequence detection system (Applied Biosystems). Real-time PCR was used in analysis of RNA samples from macrophages-like cells isolated from PCAF WT and KO mice. RT-PCR reactions were done with a kit from Perkin Elmer (SYBR Green PCR master kit). Primer sets for CIITA, MHC-II and HPRT cDNAs were (forward and reverse) 5'-TGCAGG-CGACCAGGAGAGACA-3' and 5'-GAAGCTGGGCACCTCAAAGAT-3'; 5'-TATG-TGGACTTGGATAAGAAG-3' and 5'-ACAAAGCAGATAAGGGTGTGG-3'; 5'-GGGAGGCCATCACATTGTG -3' and 5'-TCCAGCAGGTCAGCAAAGAAC-3', respectively. Real time PCR values were determined by reference to a standard curve generated by real time PCR amplification of serial dilution of cDNA using CIITA, MHC-II and HPRT primers. Values obtained for levels of CIITA and MHC-II mRNAs were normalized to the levels of HPRT mRNA expression as determined by real time PCR. Data are representative of at least three separate experiments on different RNA.

Flow cytometry analysis

Macrophages-like cells were plated at a concentration of $0.5-1 \times 10^6$ /ml and were either treated or untreated by IFN γ for 48h. Cells were removed from the plates, washed in PBS and resuspended in medium. For surface marker analysis, cells were first blocked with anti-mouse Fc γ R antibody (CD16/CD32 2.4G2, BD Pharmingen) followed by incubation with specific antibodies or isotype control for 30 min at 4°C. FITC-conjugated antibodies against H-2Kb (AF6-88.5), PE-conjugated anti-mouse I-A/I-E (M5/114.15.21), were purchased from BD Pharmingen. PE-conjugated anti-

F4/80 (Ly-71) antibody was obtained from Caltag. Cells were collected on FACS Caliber and analyzed using Cell Quest software (Becton Dickinson).

Diet

PCAF KO and WT mice received chow diet. Transgenic male ApoE*3-Leiden mice were fed a Western-type diet containing 1% cholesterol and 0.05% cholate to induce hypercholesterolemia (AB Diets). The diet was given three weeks prior to surgery and was continued throughout the experiment. All animals received food and water ad libitum during the entire experiment.

Femoral artery cuff mouse model

To investigate the role of PCAF in restenosis development, mice underwent a non-constrictive cuff placement around the femoral artery after three weeks of diet to induce vascular inflammation and remodeling. Mice were anesthetized before surgery with a combination of intraperitoneally (IP) injected Midazolam (5mg/kg, Roche), Medetomidine (0.5mg/kg, Orion) and Fentanyl (0.05mg/kg, Janssen). The right femoral artery was isolated and sheathed with a rigid non-constrictive polyethylene cuff (Portex, 0.40mm inner diameter, 0.80mm outer diameter and an approximate length of 2.0mm). 3d, 14d or 21d after cuff placement, mice were anesthetized as before and euthanized.

The thorax was opened and pressure-perfusion (100mm Hg) with 3.7% formaldehyde in water (w/v) was performed for 5 minutes by cardiac puncture in the left ventricle. After perfusion, the cuffed femoral artery was harvested, fixed overnight in 3.7% formaldehyde in water (w/v) and paraffin-embedded. Serial perpendicular cross-sections (5µm thick) were taken from the entire length of the artery for analysis.

In vivo garcinol treatment

During non-constrictive cuff placement, ApoE*3Leiden mice were treated with 10 µl pluronic gel (40%, maintained at 0°C, Sigma Aldrich) ± 25 mg/ml garcinol (Enzo Life Sciences), which was lubricated around the isolated femoral artery and was allowed to harden out and settle around the artery, which occurred within 20 seconds after application.

Biochemical analysis

Total plasma cholesterol concentration (Roche Diagnostics, kit 1489437) was measured enzymatically. Inflammatory cytokine concentration of monocyte chemoattractant protein (MCP)-1 and TNFα were determined using ELISA kits (2665KI and 558534, both Becton Dickinson), according to the manufacturer's instructions.

Immunohistochemistry (IHC)

To detect the presence of PCAF, inflammatory cells, vessel wall characteristics and effects of garcinol therapy, IHC was performed on paraffin-embedded sections of cuffs harvested after 3 and 14 days (ApoE3*Leiden) or 21 days respectively (PCAF KO and WT mice). All samples were stained with hematoxylin-phloxine-saffron (HPS) and Weigert's elastin staining was used to visualize elastic laminae. Presence of PCAF was assessed using an anti-PCAF antibody (1:500, Abcam). Inflammatory

cell presence in the vascular wall was visualized using antibodies against leukocytes (anti-CD45 antibodies 1:200, Pharmingen) and macrophages (MAC3, 1:200, Pharmingen). To assess vessel wall morphology, smooth muscle cells (SMC) were stained using anti-smooth muscle α -actin (1:800, Dako). Since garcinol can alter global gene expression and can inhibit proliferation, incorporation of 5-bromo-2'-deoxyuridine (BrdU) into DNA as a marker of DNA synthesis was used to determine the rate of cell proliferation in cuffed vessel segments. Mice (n=5 per group) were injected IP with 25 mg/kg (in 100 μ l) BrdU (Sigma Aldrich) three times, once daily starting at time of surgery or 72, 48 and 24h prior to sacrifice. Sections were incubated with a rat anti-BrdU antibody (1:200, Abcam).

Immunohistochemical analysis

All quantification in this study was performed on six equally spaced (150 μ m distance) serial stained perpendicular cross-sections throughout the entire length of the vessel and was performed by (at least) two blinded observers. The number of leukocytes, macrophages and proliferating cells were counted and expressed as a percentage of the total number of cells (stained with hematoxylin). Vessel wall morphology after 14d is expressed as the percentage of total medial and intimal area stained positive for SMC α -actin or MAC3. Using image analysis software, (Qwin, Leica), total cross-sectional medial area (between both elastic laminae), neointimal area (between internal elastic lamina and lumen) and luminal area was measured. These values were used to calculate the intima / media ratio and percentage luminal stenosis.

Cell-cultures

Murine aortas were harvested from C57Bl/6 PCAF KO mice and WT controls. The aortas were cut longitudinally to expose the luminal side. The endothelial cells were removed by gently scraping. The aortas were cut in small pieces and placed on gelatin-coated culture dishes. The explants were cultured in DMEM (PAA laboratories) containing 20% FCS heat-inactivated (Lonza), 1% penicillin/streptomycin (Invitrogen) and 1% NEAA (PAA laboratories). Cells were cultured and used for experiments at passages 2 to 4.

Splenocytes were isolated from PCAF^{-/-} and control WT mice and were transfected during 24 hours with 100 nmol/L control short-interfering (si) RNA or directed towards murine KAT2B (PCAF) 1, KAT2B 5, KAT2B 6 and KAT2B 7 (all from Qiagen) using Lipofectamine 2000 (Invitrogen).

Bone-marrow derived cells were isolated from PCAF^{-/-} and control mice and subjected to murine macrophage colony-stimulating factor (M-CSF) (20 ng/ μ l; Miltenyi Biotec) to stimulate differentiation into macrophages. To evaluate the effects of inflammation on inflammatory cytokine expression, confluent layers of human SMC were trypsinized and seeded out in DMEM supplemented with 8% FCS and 1% penicillin/streptomycin and cultured for 24h. SMCs, splenocytes and macrophages were stimulated by exposure to 8% FCS in the presence and absence of 10-100 ng/ml lipopolysaccharide (LPS) from *Escherichia coli* K-235 L2018 (Sigma Aldrich) alone or together with a serial dilution of garcinol (0, 5 or 15 μ M). The cells were incubated overnight at 37°C in 5% CO₂ atmosphere. After 24 hr incubation the supernatants were collected and analyzed by ELISA. Data are one representative of three independent experiments.

Cell viability assay

Since garcinol can affect cellular viability in high concentrations, garcinol-induced apoptosis in ex vivo whole blood was assessed in heparinized venous whole blood drawn from WT mice. Blood was diluted 1:25 in RPMI together with (0, 2.5, 10, 15, 20, 30, 50, 100 or 250 μ M) garcinol for 24h at 37°C in 5% CO₂ atmosphere. After 24h incubation, the medium of all cells including garcinol treated cells was refreshed with RPMI supplemented with 8% FCS and 10% (vol/vol) Alamar blue (Invitrogen). The optical density of each well was measured in a Millipore CytoFluor 2300 plate-reading Fluor meter with excitation at 560 nm and emission at 615 nm when medium in untreated samples turned pink (\pm 4h). Cell viability (%) was calculated compared with positive (untreated) control cells.

Statistical analysis

All data are presented as mean \pm standard error of the mean (SEM), unless otherwise indicated. Overall comparisons between data from groups were performed using the Kruskal-Wallis test. If a significant difference was found, groups were compared using a Mann-Whitney sum test. All statistical analyses were performed with SPSS 14.0 software for Windows. P-values less than 0.05 were regarded as statistically significant and are indicated with an asterisk (*).

Supplemental figures

	Body Weight (g)	Total plasma cholesterol (mmol/L)
Control mice	24.9 \pm 0.3	2.5 \pm 0.2
PCAF ^{-/-} mice	27.0 \pm 1.3	2.4 \pm 0.2
Leukocyte adhesion (3d)		
ApoE3*Leiden + vehicle	27.0 \pm 0.7	10.9 \pm 0.9
ApoE3*Leiden + garcinol	26.9 \pm 0.9	11.4 \pm 1.2
Vascular remodeling (14d)		
ApoE3*Leiden + vehicle	30.5 \pm 0.5	13.3 \pm 0.9
ApoE3*Leiden + garcinol	30.8 \pm 1.0	12.4 \pm 1.1

Table I. Mean body weights (gram) and total plasma cholesterol (mmol/L) at surgery. Values are shown as mean \pm SEM (n=10/group). No significant differences were observed between groups.

Reference List

1. Yamauchi T, Yamauchi J, Kuwata T, Tamura T, Yamashita T, Bae N, Westphal H, Ozato K, Nakatani Y. Distinct but overlapping roles of histone acetylase PCAF and of the closely related PCAF-B/GCN5 in mouse embryogenesis. *Proc Natl Acad Sci U S A* 2000;97:11303-11306.
2. Duclot F, Jacquet C, Gongora C, Maurice T. Alteration of working memory but not in anxiety or stress response in p300/CBP associated factor (PCAF) histone acetylase knockout mice bred on a C57BL/6 background. *Neurosci Lett* 2010;475:179-183.

Chapter 11

The lysine acetyltransferase PCAF is a key regulator of arteriogenesis

A.J. Bastiaansen^{1,2}, M.M. Ewing^{1,2,3}, H.C. de Boer^{2,4}, T.C. van der Pouw Kraan⁵, M.R. de Vries^{1,2}, E.A. Peters^{1,2}, R. Arens⁶, S.M. Moore⁷, J.E. Faber⁷, J.W. Jukema^{2,3,8}, J.F. Hamming¹, A.Y. Nossent^{1,2}, P.H. Quax^{1,2}

1 Dept. of Surgery, Leiden University Medical Center (LUMC), Leiden, the Netherlands

2 Einthoven Laboratory for Experimental Vascular Medicine, LUMC, Leiden, the Netherlands

3 Dept. of Cardiology, LUMC, Leiden, the Netherlands

4 Dept. of Nephrology, LUMC, Leiden, the Netherlands

5 Dept. of Molecular Cell Biology and Immunology, VU University Medical Center, Amsterdam, the Netherlands

6 Dept. of Immunohematology and Blood Transfusion, LUMC, Leiden, the Netherlands

7 Dept. of Cell and Molecular Physiology, University of North Carolina, Chapel Hill, USA

8 Durrer Institute for Cardiogenetic Research/Interuniversity Cardiology Institute of the Netherlands, the Netherlands.

Submitted for publication

Abstract

Therapeutic arteriogenesis, i.e., expansive remodeling of pre-existing collaterals, using single-action factor therapies has not been as successful as anticipated. Transcriptional co-activator P300/CBP-associated factor (PCAF) has histone acetylating activity and promotes transcription of multiple inflammatory genes. Because arteriogenesis is an inflammation-driven process, we hypothesized that PCAF acts as multifactorial regulator of arteriogenesis.

After induction of hind limb ischemia (HLI), blood flow recovery was impaired in both PCAF^{-/-} mice and healthy wild type (WT) mice treated with the pharmacological PCAF inhibitor Garcinol, demonstrating an important role for PCAF in arteriogenesis. PCAF deficiency reduced the *in vitro* inflammatory response in leukocytes and vascular cells involved in arteriogenesis. *In vivo* gene expression profiling revealed that PCAF deficiency results in differential expression of 3505 genes during arteriogenesis and, more specifically, in impaired induction of multiple pro-inflammatory genes. Additionally, recruitment from the bone marrow of inflammatory cells, in particular “pro-inflammatory” Ly6Chi monocytes, was severely impaired in PCAF^{-/-} mice. These findings indicate that PCAF acts as master switch in the inflammatory processes required for effective arteriogenesis.

Introduction

Peripheral arterial occlusive disease is a leading cause of morbidity and mortality. Blood flow to ischemic tissues in the affected limb can be restored by distinct processes (van Oostrom et al, 2008), namely vasculogenesis, angiogenesis and arteriogenesis, of which arteriogenesis, the remodeling of pre-existing collateral arterioles into larger arteries, has the greatest impact (Heil & Schaper, 2004).

Effective arteriogenesis requires coordination of multiple events. Arteriogenesis is triggered by an increase in fluid shear stress across pre-existing collaterals cross-connecting adjacent arterial trees, which is caused by a pressure gradient created by occlusion or atherosclerotic stenosis of one of the trees. This leads to activation of the endothelial cells and adjacent vascular smooth muscle cells (VSMCs) of the collateral wall. Induction of adhesion molecules, cytokines and chemokines then follows as the first step of an inflammatory cascade essential for arteriogenesis. Recruitment of leukocytes from blood and bone marrow follows, in particular monocytes (Bergmann et al, 2006; Heil et al, 2002; Schaper et al, 1976; Voskuil et al, 2004) but also CD4⁺, CD8⁺ and regulatory T cells and natural killer cells (Hellingman et al, 2012; Stabile et al, 2003; Stabile et al, 2006; van Weel et al, 2007; Zougari et al, 2009). These cells infiltrate into the perivascular space around collaterals and release additional paracrine signaling molecules and growth factors. Subsequent degradation and reorganization of the extracellular matrix by released matrix metalloproteases (MMPs), including MMP2 and MMP9, creates space required for expansive remodeling of the pre-existing collaterals. Proliferation of collateral endothelial cells, VSMCs and fibroblasts is stimulated, resulting in an increased anatomic lumen diameter. All of the steps described above underline the crucial role of inflammation in effective arteriogenesis.

Although stimulation of collateral remodeling is regarded as a promising therapeutic alternative to surgical interventions, clinical trials aimed at modulating individual growth factors or cytokines have thus far not been as successful as anticipated (Schirmer et al, 2009). We now know that the coordinated inflammatory and immune modulatory processes driving collateral growth are multifactorial and too complex to be modulated by therapeutics that target a single gene or pathway. In contrast, modulation of a factor that acts as a master switch for multiple relevant gene programs may be a more effective strategy to augment arteriogenesis.

A recently described protein with such master switch potential is P300/CBP-Associated Factor (PCAF), a transcriptional co-activator with intrinsic histone acetyltransferase activity. PCAF acetylates histones H3 and H4, but there is also increasing evidence that PCAF modulates non-histone proteins (Imhof et al, 1997; Itoh et al, 2000; Liu et al, 1999; Sartorelli et al, 1999), including hypoxia-inducible factor 1 α (Hif-1 α) (Lim et al, 2010) and Notch (Guarani et al, 2011). Furthermore, the histone acetylating activity of PCAF is essential for NF- κ B-mediated gene transcription (Sheppard et al, 1999) and facilitates inflammatory gene regulation (Miao et al, 2004). Since arteriogenesis is an inflammatory-like process, we hypothesized that PCAF acts as master switch that stimulates multiple inflammatory processes important for collateral remodeling.

Recently, it was shown in a large patient population study (>3000 individuals) (Monraats et al, 2005) that a variation in the promoter region of PCAF is associated with

coronary heart disease-related mortality (Pons et al, 2011). In support of this observation, we recently demonstrated a role for PCAF in vascular remodeling in a mouse model for reactive stenosis. However, whether PCAF participates in arteriogenesis has not yet been investigated.

In the present study, we investigated the contribution of PCAF to post-ischemic neovascularization in a hind limb ischemia (HLI) model, using PCAF deficient (PCAF^{-/-}) mice. When studying arteriogenesis in a knockout model, it is possible that the gene deletion may affect vascular development in the embryo, including collateralogenesis, thus affecting the number of collaterals available for remodeling after an occlusive event in the adult. To investigate whether observed effects were caused by differences in arteriogenesis, in the native collateral circulation or a combination of both, we examined the pre-existing collateral density as well as the effect of administration of the PCAF inhibitor Garcinol to wild type (WT) mice after induction of HLI. We also studied gene expression and leukocyte recruitment in PCAF^{-/-} and WT mice after induction of HLI to examine potential mechanisms by which PCAF regulates arteriogenesis.

Materials and Methods

Animals

Experiments were approved by the committee on animal welfare of the Leiden University Medical Center (Leiden, The Netherlands). Male C57BL/6 mice were purchased from Charles River (France). The generation of PCAF^{-/-} mice (C57BL/6 background) has previously been described (Duclot et al, 2010; Yamauchi et al, 2000) and the animals were kindly provided by Dr. C. Gongora (Montpellier, France). All animals received regular chow diet and water ad libitum.

Induction of hind limb ischemia

Mice were anesthetized by intraperitoneal (i.p.) injection of midazolam (8 mg/kg, Roche Diagnostics), medetomidine (0.4 mg/kg, Orion) and fentanyl (0.08 mg/kg, Janssen Pharmaceutica). Unilateral HLI was induced by electrocoagulation of the left femoral artery proximal to the superficial epigastric arteries alone, or combined with electrocoagulation of the distal femoral artery proximal to the bifurcation of the popliteal and saphenous artery (Hellingman et al, 2010). After surgery, anesthesia was antagonized with flumazenil (0.7 mg/kg, Fresenius Kabi), atipamezole (3.3 mg/kg, Orion) and buprenorphine (0.2 mg/kg, MSD Animal Health). For pharmacological PCAF inhibition in WT mice, 20 μ l 40% pluronic gel (Sigma-Aldrich) with or without 25 mg/ml Garcinol (Santa Cruz Biotechnology) was applied topically to the adductor muscle before skin closure.

Laser Doppler perfusion imaging

Hind limb perfusion was measured with laser Doppler perfusion imaging (LDPI) (Moor Instruments) after intraperitoneal injection of midazolam (8 mg/kg) and medetomidine (0.4 mg/kg). The regions of interest analyzed consisted of the foot distal to the base of the first digit. Perfusion was expressed as the ratio of ligated to non-ligated foot. After measurement, anesthesia was antagonized with flumazenil (0.7 mg/kg) and atipamezole (3.3 mg/kg).

Pre-existing collateral density

Pre-existing collateral density in the pial circulation of the dorsal cerebral cortex predicts collateral density in skeletal muscle and other vascular beds (Chalothorn et al, 2010; Wang et al, 2010; Zhang et al, 2010). However, unlike in other tissues where arterial trees are arranged three-dimensionally and difficult to image with fidelity, all cerebral collaterals are contained within the pia and can thus be directly identified and counted. Methods for measurement of collateral density between the anterior cerebral artery (ACA), middle cerebral artery (MCA), and posterior cerebral artery (PCA) were described elsewhere (Chalothorn et al, 2010; Wang et al, 2010; Zhang et al, 2010). Briefly, animals were heparinized systemically and anesthetized with ketamine (100 mg/kg) and xylazine (10 mg/kg) prior to vascular casting. Maximal dilation was accomplished by cannulation of the thoracic aorta and infusion of sodium-nitroprusside (30 $\mu\text{g/ml}$) and papaverine (40 $\mu\text{g/ml}$) in PBS at 100 mmHg for 3 minutes. Yellow Microfil™ (Flow Tech Inc.) with viscosity adjusted to prevent capillary and venous filling was infused under a stereomicroscope after craniotomy. The dorsal cerebral circulation was fixed with topical application of 4% paraformaldehyde to prevent any reduction in vessel dimensions after Microfil injection. Brains were incubated in Evans Blue (2 $\mu\text{g/ml}$) for several days to improve contrast for visualization of the vasculature. Digital images were obtained at 13X (Leica) of the dorsal brain surface and processed with ImageJ software (NIH). Collateral density was calculated by determining the total number of pial collaterals between the ACA-MCA, ACA-PCA and MCA-PCA and dividing by the dorsal surface area of the cerebral hemispheres. Areas that sustained damage, were incompletely filled, or were otherwise uncountable were excluded from analysis.

Immunostaining and analysis

Mice were sacrificed and the adductor muscle group medial to the femur was excised en bloc. Tissues were snap frozen in liquid nitrogen or fixed in 3.7% formaldehyde. Serial 5- μm -thick paraffin-embedded sections were used for histological analysis of collateral artery number and size. Vessels at the midpoint of the adductor muscle group, stained using anti-smooth muscle α -actin (αSMA) (DAKO), are likely composed of collaterals but may also include arterioles of the opposing tree. Randomly photographed images through the central part of the adductor muscle group were used to quantify the number and lumen diameter of αSMA^+ vessels using ImageJ software (total of 9 images of 3 sections per mouse). To correct for non-perpendicularly cut sections, the circular lumen area of αSMA^+ vessels was calculated from the lumen diameter measured at the narrowest point.

Frozen 5- μm -thick sections were fixed in ice-cold acetone and stained with anti-PCAF (Abcam) and Cy3 conjugated anti- αSMA (Sigma-Aldrich). PCAF was visualized using Alexa 488 conjugated secondary antibody (Invitrogen). Nuclei were stained using Vectashield with DAPI (Vector Laboratories). Fluorescent images were taken on a LSM700 microscope (Carl Zeiss) and contrast-stretched using Zen 2009 software (Carl Zeiss). Collaterals were detected with Cy3 conjugated anti- αSMA , and perivascular monocytes with anti-MOMA-2 (Millipore), visualized using Alexa 488 conjugated secondary antibody (Invitrogen). Monocytes were quantified from at least six consecutive sections per mouse and expressed as the number of MOMA-2

positive cells in the perivascular space of α SMA+ vessels.

In vitro immune response

Whole blood

Blood was collected from the tail vein of PCAF^{-/-} and WT mice and diluted 1:25 with RPMI 1640 (Invitrogen) supplemented with non-essential amino acids (PAA Laboratories) and glutamax (Invitrogen). Blood was incubated overnight at 37°C, 5% CO₂, in the presence of lipopolysaccharide (LPS) (0-500 ng/ml) from *Escherichia coli* K-235 (Sigma-Aldrich). Cell-free supernatant was collected and TNF α level was measured by ELISA (BD Biosciences).

Splenocytes

Spleens were isolated from PCAF^{-/-} and WT mice, minced through a 40 μ m-cell strainer (Biosciences) and, after erythrolysis with ammonium chloride solution, single cell suspensions were resuspended in DMEM (PAA Laboratories) supplemented with 10% heat-inactivated FCS (Lonza). Splenocytes (1x10⁶) from PCAF^{-/-} and WT mice were plated and incubated for 24 hours with LPS (300 ng/ml) or control. Splenocytes of WT mice were also incubated with Garcinol (20 μ M) in combination with LPS (300 ng/ml) or control. MCP-1 level in the cell-free supernatant was measured by ELISA (BD Biosciences).

Vascular smooth muscle cells

VSMCs were isolated from abdominal aortas from PCAF^{-/-} and WT mice. For stimulation assays, cells (passage 2-4) were plated (5x10³) and incubated for 24 hours with LPS (0.1 and 1 ng/ml) or control. VSMCs of WT mice were also incubated with Garcinol (15 μ M) in combination with LPS (0.1 and 1 ng/ml) or control. MCP-1 level in the cell-free supernatant was measured by ELISA (BD Biosciences). RNA was isolated from LPS stimulated (1 ng/ml) WT and PCAF^{-/-} VSMCs (1x10⁵) using RNeasy minikits (Qiagen).

Whole-genome expression

The adductor muscle group of PCAF^{-/-} and WT mice was harvested before (t0) and 1 day after (t1) induction of HLI, and total RNA was extracted using RNeasy fibrous tissue minikit (Qiagen). RNA integrity was checked by NanoDrop 1000 Spectrophotometer (NanoDrop Technologies) and 2100 Bioanalyzer (Agilent Technologies). For whole-genome expression profiling, amplified biotinylated RNA was generated using the Illumina TotalPrep RNA Amplification Kit. For array analysis, MouseWG-6 v2.0 Expression Beadchips (Illumina), which contain more than 45,200 transcripts, were used. Expression levels were Log₂-transformed and after quantile normalization, transcripts showing background intensity, both at baseline and after induction of HLI, were removed from the analysis. Gene expression levels at t1 were expressed relative to average baseline levels generating t1/t0avg ratios for all 15,555 regulated genes, and compared between both mouse strains. To define the effect of PCAF on inflammatory gene transcription, gene descriptions, as provided by Illumina, containing any of these criteria (interleukin, chemokine, interferon, TGF, TNF, NF- κ B) were selected and ratios were tested for significance.

Real-time quantitative PCR

RNA was reverse transcribed using High Capacity RNA-to-cDNA kit (Applied Bio-

systems). Quantitative PCR was performed on the ABI 7500 Fast system, using commercially available TaqMan gene expression assays for HPRT1, MCP-1, MMP9, TNF α , CCL9, CXCL12 and IRF7 (Applied Biosystems).

Flow cytometry

Blood, spleen, bone marrow and non-draining lymph nodes were harvested before (t0) and 1 day after (t1) induction of HLI. Draining lymph nodes were dissected from the inguinal region. Total circulating leukocytes were measured using the KX-21N Hematology Analyzer (Sysmex). Tissues were minced through a 40 μ m-cell strainer (BD Biosciences) to obtain single cell suspensions which were resuspended in IMDM (Lonza) with 2% FCS. For dendritic cell-specific cell surface staining, the spleen and lymph nodes were first perfused with collagenase (1mg/ml) and DNase (0.02mg/ml) for 10 minutes and minced. Erythrocytes were lysed and samples for intracellular staining were permeabilized. Fluorochrome-conjugated monoclonal antibodies specific for CD3, CD4, CD8, CD11c, CD11b, CD19, CD25, CD86, CD115, FoxP3, Ly6C, Ly6G, B220, DX5 were used. Cells were measured on a LSRII flow cytometer (BD Biosciences) and data was analyzed using FlowJo software (Tree Star, Inc.).

Statistical analysis

All results are presented as mean \pm standard error of the mean (SEM) or as scatter plot. Comparisons between groups were performed using Student's T-test. All statistical analyses were performed using SPSS 17.0 software. P-values < 0.05 were considered statistically significant and are indicated with *; p-values < 0.01 and < 0.001 are indicated by ** and ***, respectively. Statistical Analysis of Microarray data (SAM) (Tusher et al, 2001) was used for the analysis on t1/t0avg ratios in the whole-genome expression array. A false discovery rate (expressed as q-values) of less than 5% was considered significant.

Results

PCAF contributes to collateral remodeling

PCAF^{-/-} mice showed impaired blood flow recovery after HLI (Fig 1A-B). Postoperative blood flow was decreased to approximately 6% of blood flow in the contralateral limb in both groups, with a trend towards reduced blood flow in PCAF^{-/-} mice compared to WT mice (Fig 1C, p=0.07). Thereafter, blood flow recovery in PCAF^{-/-} mice was reduced and did not recover completely before termination at 28 days. Moreover, PCAF^{-/-} mice showed significantly more necrotic toe nails than WT mice (PCAF^{-/-} 2.9 \pm 0.6 vs WT 0.45 \pm 0.2, p<0.001) (Fig 1D). No auto-amputation of hind limb digits was observed in either group. The reduced blood flow recovery in PCAF^{-/-} mice was confirmed by quantification of α SMA⁺ vessels in the adductor muscle group, 28 days after HLI (Fig 1E). Although the number of α SMA⁺ vessels was nearly similar (Fig 1F), the size of α SMA⁺ vessels in PCAF^{-/-} mice was significantly reduced, resulting in a reduced blood flow. The mean lumen area per α SMA⁺ vessel (PCAF^{-/-} 139 \pm 15 μ m² vs WT 297 \pm 26 μ m², p<0.001) and total lumen area per section (PCAF^{-/-} 447 \pm 46 μ m² vs WT 1253 \pm 117 μ m², p<0.001) were severely reduced in PCAF^{-/-} mice (Fig 1G-H). Thus, PCAF deficiency leads to reduced arteriogenesis after induction of HLI.

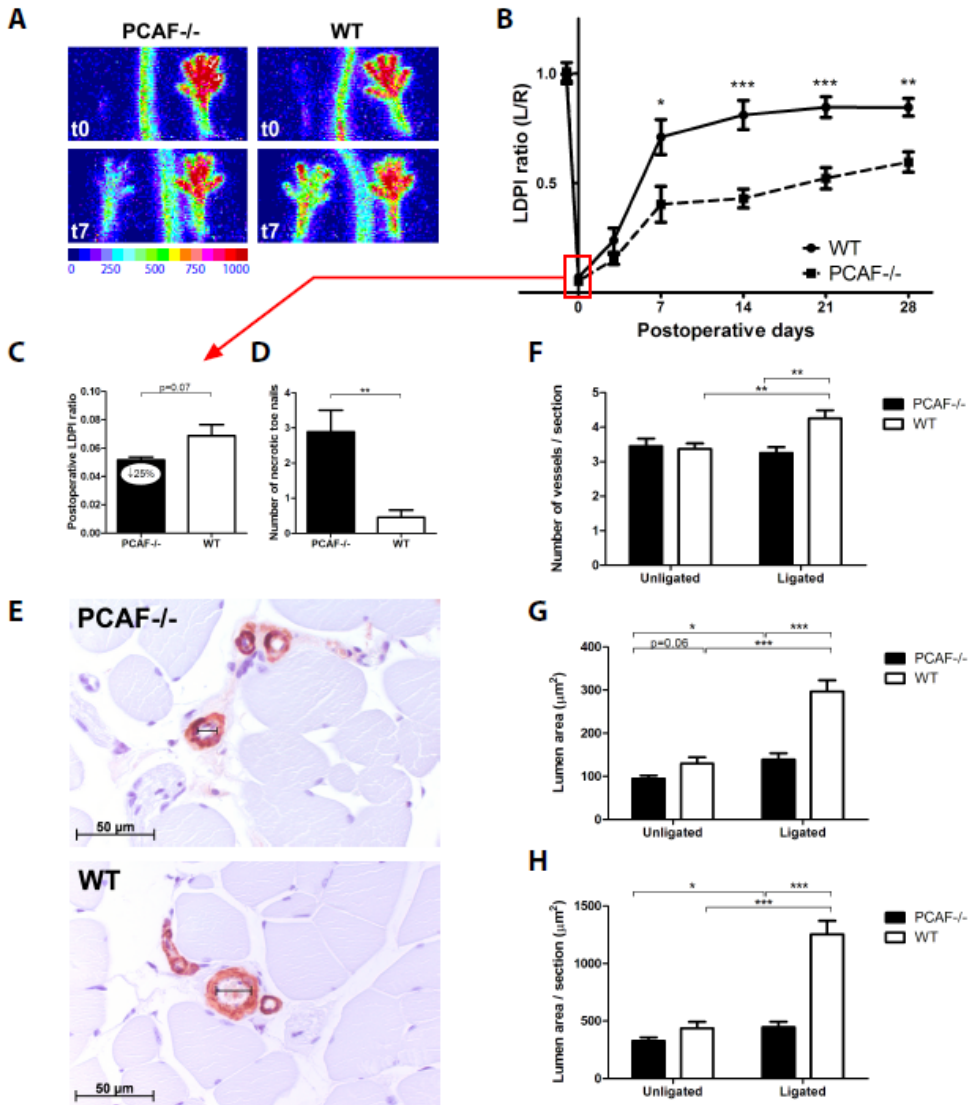


Figure 1. Arteriogenesis in PCAF^{-/-} mice. **A.** Representative LDPI images of paws from PCAF^{-/-} and WT mice directly and 7 days after induction of HLI in the left limb. High blood flow is displayed in red. **B.** Quantification of LDPI measurements of PCAF^{-/-} and WT mice over time. Data are calculated as the ratio of ligated over non-ligated paw. **C.** Quantification of LDPI measurements of PCAF^{-/-} and WT mice directly after induction of HLI. Data are calculated as the ratio of ligated over non-ligated paw. **D.** Quantification of necrotic toe nails of the ligated limb in PCAF^{-/-} and WT mice counted 28 days after HLI. **E.** Immunohistochemical staining of paraffin-embedded adductor muscle group of PCAF^{-/-} and WT mice 28 days after HLI using anti- α SMA (red) antibodies. Lumen diameter of α SMA⁺ vessels is indicated by black bars. Scale bars = 50 μ m. **F-H.** Number, mean lumen area (μ m²) and total lumen area per section (μ m² / section) of α SMA⁺ vessels, measured at the center of the adductor muscle group in ligated and non-ligated limbs of PCAF^{-/-} and WT mice. All values are presented as the mean \pm SEM. * $P < 0.05$, ** $P < 0.01$, *** $P < 0.001$.

To assess whether the reduction in blood flow recovery in PCAF^{-/-} mice was caused by reduced collateral remodeling or by fewer pre-existing collaterals, we performed

two additional experiments. First, we inhibited PCAF by pharmacological intervention with Garcinol to rule out any effects on number of pre-existing collaterals in the PCAF^{-/-} mice. In WT mice, local PCAF inhibition by Garcinol resulted in reduced blood flow restoration compared to the empty pluronic gel control group (Fig 2A-B).

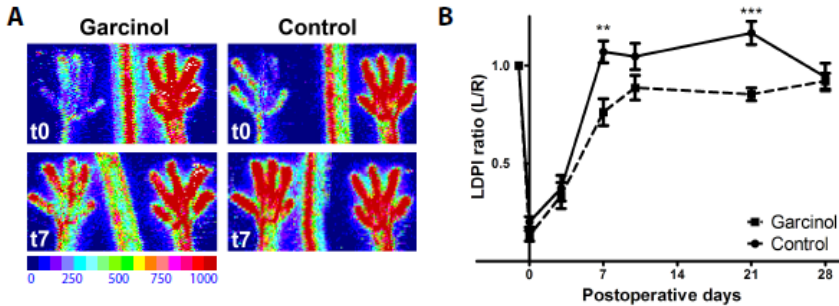


Figure 2. Arteriogenesis after pharmacological inhibition of PCAF. A. Representative LDPI images of paws directly and 7 days after induction of HLI in the left limb. In WT mice, pluronic gel with or without 25 mg/ml Garcinol was applied topically to the adductor muscle before skin closure. High blood flow is displayed in red. B. Quantification of LDPI measurements of WT mice treated with Garcinol or control over time. Data are calculated as the ratio of ligated over non-ligated paw. All values are presented as the mean ± SEM. **P < 0.01, ***P < 0.001, Garcinol versus control.

Secondly, the pre-existing vascular bed of PCAF^{-/-} and WT mice was assessed in the pial circulation using an arterial vascular casting (Fig 3A). Pial collateral density in PCAF^{-/-} mice was reduced by 11% compared to WT mice, reflecting a moderate but significant contribution of PCAF in determining the abundance of the native collateral circulation (Fig 3B-C, p=0.02). This was in agreement with the trend towards decreased blood flow perfusion in PCAF^{-/-} mice directly after HLI.

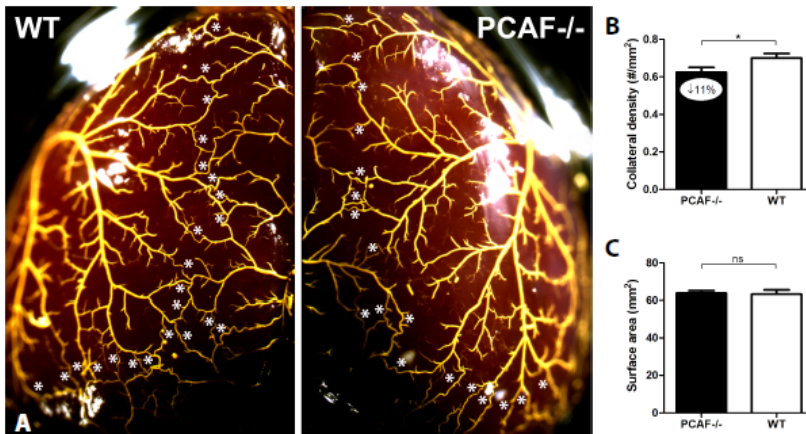


Figure 3. Pre-existing collateral bed in PCAF^{-/-} mice. A. Representative images of the pial circulation in PCAF^{-/-} and WT mice. White asterisks indicate collateral arteries between anterior, middle and posterior cerebral arteries (ACA, MCA and PCA, respectively). Following exsanguination and maximal dilation of the dorsal cerebral circulation, Microfil™ was used as a casting agent, after which the whole brain was fixed in 4% PFA. B. Pial collateral density was calculated in PCAF^{-/-} and WT mice by dividing the sum of ACA to MCA, ACA to PCA and MCA to PCA by the surface area of the cerebral hemispheres. C. Region of the brain utilized for calculation of pial density. Areas were excluded when they were damaged, had poor filling with Microfil™, or were otherwise uncountable. NS = non-significant. All values are presented as the mean ± SEM. *P < 0.05, PCAF^{-/-} versus WT.

PCAF is required for in vitro inflammatory response

We investigated the role of PCAF in the inflammatory response of multiple cell types, given the above evidence for decreased collateral remodeling and the known involvement of these cells in arteriogenesis. Analysis of circulating cells in a whole blood LPS stimulation assay showed dose-dependent increase of TNF α in blood from WT mice, which was significantly reduced in blood from PCAF $^{-/-}$ mice (Fig 4A). Next, the splenic cell reservoir was subjected to LPS stimulation and pharmacological PCAF inhibition with Garcinol. LPS (300 ng/ml)-stimulated MCP-1 levels of splenocytes from both PCAF $^{-/-}$ mice (63 \pm 32pg/ml) and WT splenocytes treated with 20 μ M Garcinol (195 \pm 35 pg/ml) were both significantly reduced in comparison to WT splenocytes (372 \pm 13 pg/ml, $p=0.005$ and $p=0.04$ respectively) (Fig 4B). Also the inflammatory phenotype of PCAF $^{-/-}$ VSMCs was assessed. Similar to the splenocyte stimulation, MCP-1 levels were markedly reduced after LPS (0.1 ng/ml) stimulation of PCAF $^{-/-}$ VSMCs (689 \pm 49 pg/ml) and WT VSMCs when exposed to 15 μ M Garcinol (3087 \pm 284 pg/ml) compared with untreated WT VSMCs (4175 \pm 264 pg/ml, $p<0.001$ and $p=0.049$ respectively) (Fig 4C). In addition, upregulation of MCP-1 mRNA was significantly reduced by 53% in PCAF $^{-/-}$ VSMCs (Fig 4D, $p=0.01$). To exclude non-specific effects of Garcinol, these experiments were repeated in WT VSMCs treated with siRNAs against PCAF mRNA instead of Garcinol. Transfection with siRNAs targeting PCAF mRNA efficiently decreased PCAF mRNA expression by 61% and, like Garcinol, inhibited MCP-1 production (Supporting Information Fig 1A-C).

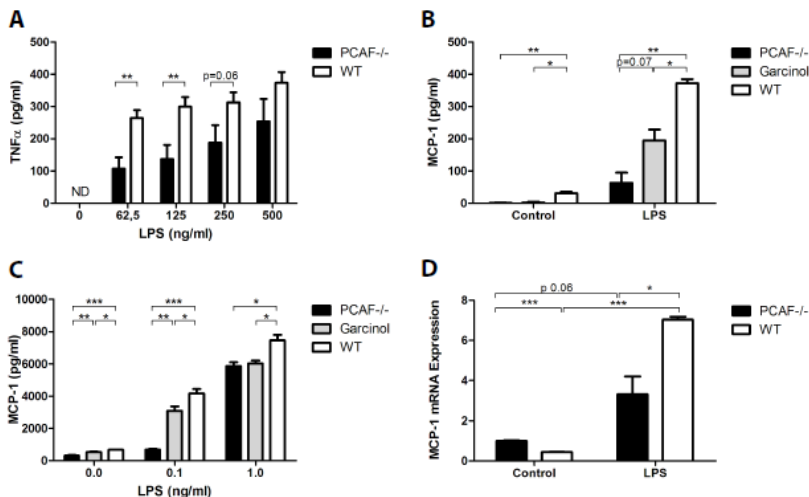


Figure 4. The role of PCAF in in vitro inflammatory response. A. Inflammatory response of whole blood from PCAF $^{-/-}$ and WT mice was evaluated. Blood from tail vein was collected, diluted (1:25) and incubated 24 h with LPS (0-500 ng/ml). TNF α (pg/ml) level in cell-free supernatant was measured by ELISA. ND = non-detectable. B. Splenocytes of PCAF $^{-/-}$ and WT mice were cultured and incubated for 24 h with LPS (300 ng/ml) or control. Splenocytes of WT mice were also incubated with Garcinol (20 μ M) in combination with LPS (300 ng/ml) or control. Cell-free supernatant MCP-1 (pg/ml) level was measured by ELISA. C. VSMCs of PCAF $^{-/-}$ and WT mice were cultured and incubated for 24 h with LPS (0.1 and 1 ng/ml) or control. VSMCs of WT mice were also incubated with Garcinol (15 μ M) in combination with LPS (0.1 and 1 ng/ml) or control. Cell-free supernatant MCP-1 (pg/ml) level was measured by ELISA. D. Vascular smooth muscle cells (VSMCs) of PCAF $^{-/-}$ and WT mice were cultured and incubated for 24 h with LPS (1 ng/ml) or control. MCP-1 mRNA expression was measured by real-time quantitative PCR. Cts were normalized against Cts of HPRT1. All values are presented as the mean \pm SEM of triplicates. * $P < 0.05$, ** $P < 0.01$, *** $P < 0.001$.

PCAF modulates post-ischemic gene regulation

PCAF staining showed enhanced expression in cells of large developing collaterals in the adductor muscle group compared to surrounding skeletal muscle (Fig 5A). To study differential gene expression after HLI between PCAF^{-/-} and WT mice, total RNA isolated from the adductor muscle group was used in a whole-genome expression analysis using Illumina Beadchips. Statistical analysis by SAM on t1/t0avg ratios identified 1963 genes with a significant lower ratio and 1542 genes with a higher ratio in PCAF^{-/-} relative to WT mice ($q < 5\%$), indicating that PCAF exhibits a large effect on gene transcription after HLI (Fig 5B).

Supporting Information Table 1 shows the top 50 genes with impaired upregulation in PCAF^{-/-} mice compared to WT mice, including MMP9, critical in matrix degradation required for collateral artery expansion. Since PCAF has been shown to regulate inflammatory gene transcription, we selected inflammatory genes that were significantly regulated (Supporting Information Table 2 and Supporting Information Fig 2). Among the inflammatory genes showing a more pronounced induction in WT mice compared to PCAF^{-/-} mice were genes encoding cytokines CXCL12, CCL9 and TNF α , chemokine receptor CXCR1, transcription factor IRF7, TNF receptor associated factors TRAF2 and TRAF3, TNF receptor associated protein TRAP1 and members of the TNF receptor superfamily TNFRSF19 and TNFRSF11a (also known as RANK). The total of inflammatory genes with greater induction in PCAF^{-/-} mice was much smaller than the number of genes more strongly induced in WT, and included inhibitors of the NF- κ B pathway like NFKBIA and NKIRAS1. Aberrant regulation of several relevant regulated factors (MMP9, TNF α , CCL9, CXCL12, IRF7) were confirmed using real-time quantitative PCR (Fig 5C-G).

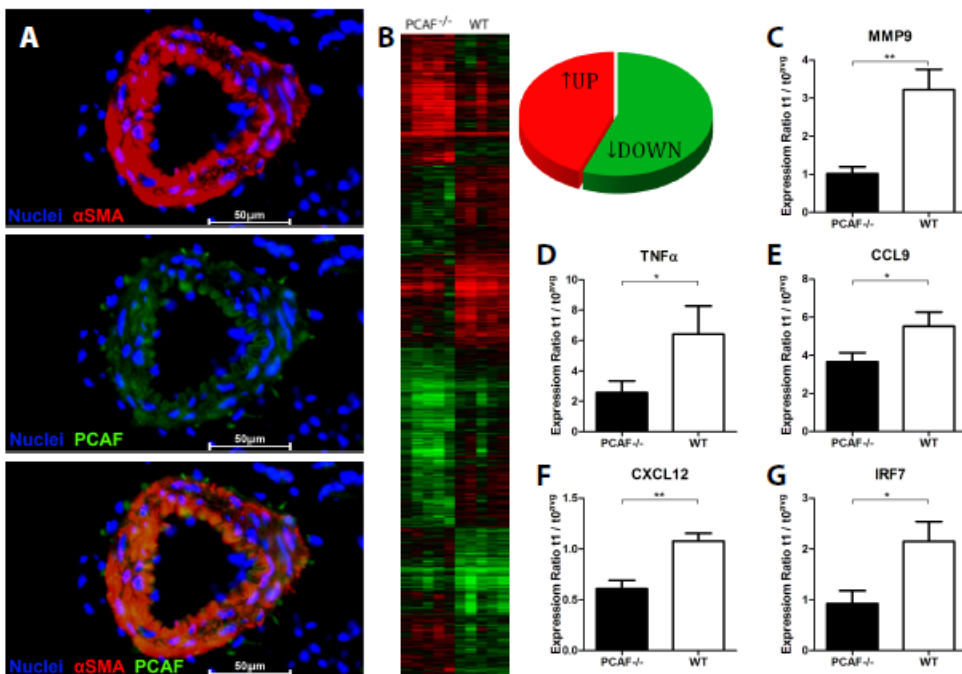


Figure 5. Gene regulation in PCAF^{-/-} mice after HLI. A. Immunohistochemical staining on fresh frozen sections of WT adductor muscle 1 day after HLI, using anti- α SMA (red) and anti-PCAF (green) antibodies. Cell nuclei were stained with DAPI (blue). Scale bars = 50 μ m. B. Heatmap of differentially regulated genes in whole-genome expression analysis, comparing PCAF^{-/-} and WT mice. Included are genes that were significantly different between PCAF^{-/-} and WT mice (q-value < 5). Data are presented as the fold change in expression between day 1 (t1) and average preoperative baseline levels (t0), generating t1/t0avg ratios. Red indicates increased and green indicates reduced expression relative to average baseline levels. The pie graph illustrates a significant decrease of 1963 genes (green) and increase of 1542 (red) genes in PCAF^{-/-} relative to WT mice. C-G. Microarray validation by real-time quantitative PCR of a selection of relevant regulated inflammatory factors MMP9, TNF α , CCL9, CXCL12 and IRF7. Cts were normalized against Cts of HPRT1. All values are presented as the mean \pm SEM. *P < 0.05, **P < 0.01, PCAF^{-/-} versus WT.

PCAF deficiency alters leukocyte recruitment

We quantified leukocyte subtypes that are involved in arteriogenesis, including T cells (helper CD4⁺, cytotoxic CD8⁺ and regulatory T cells) and natural killer cells, and subtypes which have not been previously implicated in arteriogenesis, including B cells and dendritic cells. Blood samples from before (t0) and 1 day after (t1) HLI, were analyzed by FACS. PCAF deficiency had effects on most of the leukocyte subtypes examined. Following HLI, circulatory T cells were significantly decreased in PCAF^{-/-} mice compared to WT mice. This difference was caused mainly by a reduction in CD4⁺ T cells, especially by the fraction of activated CD4⁺ T cells, defined by the loss of CD62L (L-selectin), and regulatory T cells (CD4⁺CD25⁺FoxP3⁺ T cells). The number of circulatory CD8⁺ T cells did not differ between WT and PCAF^{-/-} mice. Also counts of other leukocyte subtypes, including B cells and natural killer cells were decreased by PCAF deficiency.

To investigate the migratory behavior of the leukocyte subtypes, the spleen, bone marrow and lymph nodes were harvested from both mouse strains before (t0) and 1 day after (t1) HLI. Compared to WT mice, we observed reduced numbers of dendritic cells in the draining inguinal lymph nodes of PCAF^{-/-} mice after HLI. Accordingly, the fraction of dendritic cells expressing the co-stimulatory molecule CD86⁺ was smaller in the draining lymph nodes of PCAF^{-/-} mice. Furthermore, nearly all tested leukocyte subtypes were increased in the bone marrow of PCAF^{-/-} mice compared to WT mice, including CD4⁺ and CD8⁺ T cells, natural killer cells and dendritic cells, suggesting that these subpopulations are retained in the bone marrow of PCAF^{-/-} mice during recovery after HLI (Supporting Information Fig 3A-I).

Because monocytes play a key role in arteriogenesis and are among the first leukocytes recruited to remodeling collaterals, we evaluated different monocyte populations in blood, spleen and bone marrow. After HLI, the absolute number of circulating monocytes in WT mice was equal to baseline numbers, but monocytes in PCAF^{-/-} mice significantly decreased compared to baseline (PCAF^{-/-} $0.13 \pm 0.05 \times 10^6$ /mL vs WT $0.37 \pm 0.02 \times 10^6$ /mL, $p = 0.002$) (Fig 6A). In WT mice, the monocyte population increased in the spleen and decreased in the bone marrow after HLI. In contrast, bone marrow monocytes in PCAF^{-/-} mice increased compared to baseline and were significantly higher after HLI compared to WT mice (Fig 6B-C). The differences in monocyte numbers were caused mainly by the specific subtype of “pro-inflammatory” Ly6Chi monocytes (Fig 6D-F). The activation state of total and Ly6Chi monocytes did not differ between the two strains, measured by mean fluorescent intensity of the adhesion molecule CD11b (Fig 6G-H).

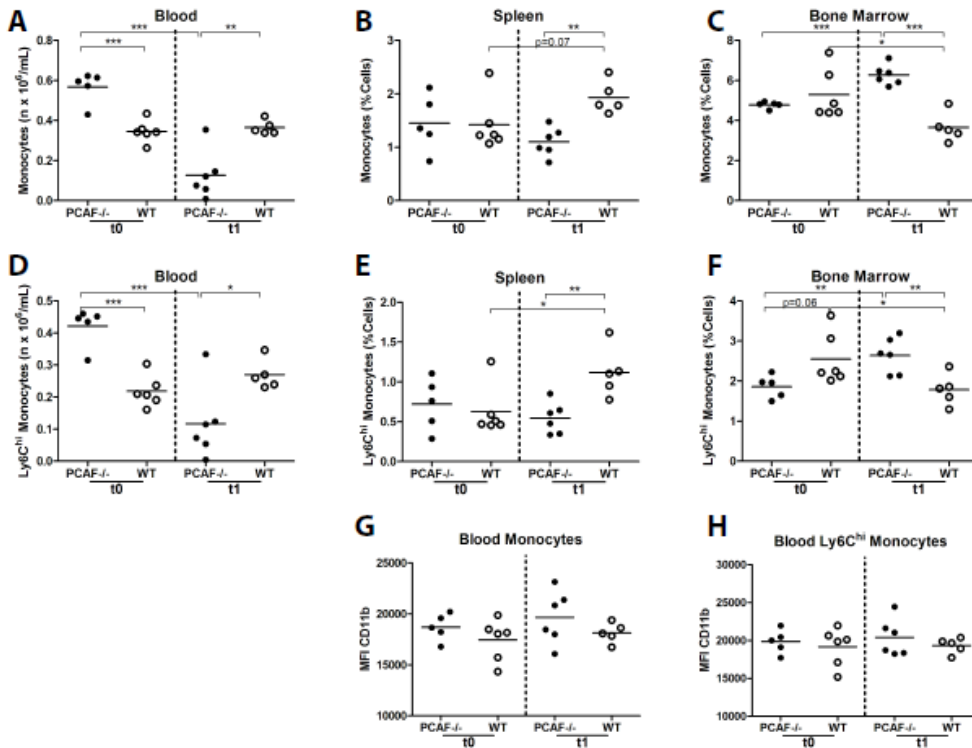


Figure 6. Monocyte recruitment in PCAF^{-/-} mice after HLI. A-C. Flow cytometry analysis of monocytes before (t0) and one day after (t1) HLI in PCAF^{-/-} and WT mice. Values are presented as total monocyte counts in blood (nx10⁶/mL), spleen (% of total cells) and bone marrow (% of total cells). D-F. Flow cytometry analysis of “pro-inflammatory” Ly6Chi monocytes after HLI in PCAF^{-/-} and WT mice. Values are presented as total Ly6Chi monocyte counts in blood (nx10⁶/mL), spleen (% of total cells) and bone marrow (% of total cells). G-H. Activation state of monocytes and Ly6Chi monocytes measured by mean fluorescence intensity (MFI) of CD11b. *P < 0.05, **P < 0.01, ***P < 0.001.

Finally, we assessed the number of monocytes/macrophages in the adductor muscle group by fluorescent staining with antibodies against MOMA-2 and smooth muscle α -actin (Fig 7A). Although PCAF^{-/-} mice showed a significant increase in MOMA-2-positive cells 24 hours after HLI, the increase in WT mice was significantly higher (PCAF^{-/-} 3.2 \pm 0.35/section vs WT 6.0 \pm 0.43/section, p=0.001) (Fig 7B). Differences were most evident in the perivascular space of remodeling collaterals (PCAF^{-/-} 1.4 \pm 0.16/section vs WT 3.5 \pm 0.76/section, p=0.01) (Fig 7C).

Discussion

We demonstrate that blood flow recovery after induction of HLI is strongly impaired in PCAF^{-/-} mice, in association with reduced expansive remodeling of collaterals. Furthermore, local PCAF inhibition by Garcinol in WT mice also reduces recovery, indicating that PCAF is directly required for normal arteriogenesis. PCAF gene deficiency results in a repressed *in vitro* inflammatory response in many cell types known to be involved in arteriogenesis. One day after induction of HLI, 3505 genes are differentially regulated in the adductor muscle group of PCAF^{-/-} mice compared to

WT mice. Additionally, recruitment of different pro-arteriogenic leukocyte subtypes in PCAF^{-/-} mice, in particular “inflammatory” monocytes, is significantly impaired at this time. Our data therefore demonstrate that PCAF plays a key role in post-ischemic arteriogenesis.

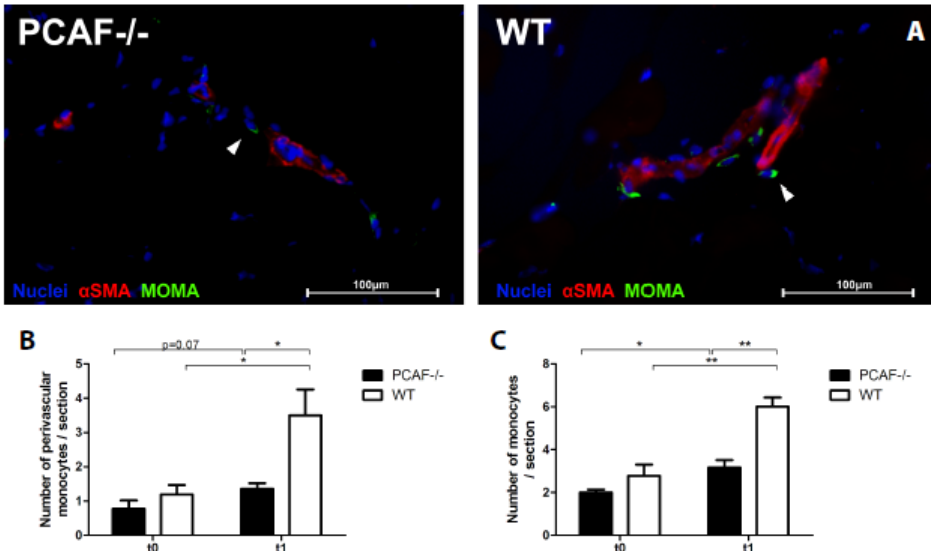


Figure 7. Monocyte recruitment to collateral arteries in PCAF^{-/-} mice after HLI. A. Immunohistochemical staining on fresh frozen sections of the adductor muscle group from PCAF^{-/-} and WT mice 1 day after HLI, using anti-αSMA (red) and anti-MOMA-2 (green) antibodies. Cell nuclei were labeled with DAPI (blue). Scale bars = 100 μm. B-C. Quantification of MOMA-2 positive cells in the adductor muscle group of PCAF^{-/-} and WT before (t0) and 1 day after (t1) HLI. Monocytes were quantified from at least six consecutive sections per mouse and expressed as the number of MOMA-2 positive cells per section and as the number of MOMA-2 positive cells in the perivascular space of αSMA⁺ vessels per section. *P < 0.05, **P < 0.01.

Compared to WT mice, PCAF^{-/-} mice showed an impaired blood flow recovery after HLI. Our findings suggest that two deficiencies caused by a lack of PCAF are involved. First, the expansive remodeling of αSMA⁺ arterioles at the center of the adductor muscle group, of which most are collaterals, was reduced by 53% in PCAF^{-/-} mice compared to WT mice. Correspondingly, local application of PCAF inhibitor Garcinol in healthy WT mice also resulted in impaired blood flow recovery compared to control animals. Hence, PCAF has a major impact on arteriogenesis. Secondly, we observed that the density of native pre-existing collaterals in the pial circulation of PCAF^{-/-} mice was reduced by 11%. Even changes of this magnitude have significant effects on collateral-dependent perfusion of tissue downstream from an arterial obstruction (Chalothorn & Faber, 2010; Wang et al, 2010; Zhang et al, 2010). Previous studies have shown that genetic-dependent variation in collateral number in the cerebral pial circulation is shared, at least qualitatively, by similar differences in collateral density in other tissues (Chalothorn et al, 2010; Wang et al, 2010; Zhang et al, 2010). Accordingly, we also observed a trend towards a decrease in blood flow directly after induction of HLI in PCAF^{-/-} mice. In mice, the density of the native collaterals in tissues varies widely among strains from differences in genetic background (Chalothorn et al, 2010; Wang et al, 2010; Zhang et al, 2010). Hence, besides collateral remodeling, genetic PCAF deficiency also contributes to reduced formation of

the collateral circulation which occurs during embryonic development.

In a clinical setting, the outcome after an ischemic event varies among individuals, and differences in abundance of the native collateral circulation have also been reported in patients (Meier et al, 2007; Menon et al, 2012). Moreover, a previous study found that the -2481G allele in the promoter region of the PCAF gene associates with an increased risk of mortality in patients with coronary heart disease (Pons et al, 2011), which further supports our findings that PCAF deficiency impairs collateral function.

In order for PCAF to serve as a master switch in collateral remodeling, it needs to impact multiple critical phases in the process, namely activation of the endothelium and vessel wall, leukocyte recruitment, matrix degradation and arteriolar expansion. We examined gene expression in the adductor muscle group containing remodeling collaterals in the initial phase after HLI. Over 3500 genes were differentially regulated between PCAF^{-/-} and WT mice. This suggests that PCAF impacts expression of a large number of genes activated in this setting. More specifically, PCAF^{-/-} mice showed impaired induction of multiple pro-arteriogenic and pro-inflammatory genes, including matrix metalloproteinase (MMP) 9 and chemokines CXCL12 (SDF1) and CCL9.

MMP9 is critical in degradation and remodeling of the extracellular matrix allowing cell migration and outward expansion of the collaterals and thus effective arteriogenesis (Huang et al, 2009). CXCL12 is elevated in ischemic skeletal muscle of patients with critical limb ischemia (Ho et al, 2010) and acts as chemoattractant for CXCR4⁺ cells, including leukocytes and progenitor cells. CXCL12-mediated recruitment of bone marrow-derived cells to ischemic tissues results in enhanced neovascularization (Hiasa et al, 2004; Shao et al, 2008). Also CCL9, which is a strong chemoattractant for bone marrow derived cells (Yang & Odgren, 2005), is upregulated after muscle injury (Shireman, 2007).

In addition, PCAF^{-/-} mice showed impaired induction of multiple factors related to the pro-inflammatory TNF α pathway (Silke & Brink, 2010). TNF α ^{-/-} mice have reduced collateral artery perfusion (Hofer et al, 2002) and anti-TNF α therapy attenuates arteriogenesis (Grundmann et al, 2005). Thus, reduced TNF α expression in PCAF^{-/-} mice likely contributes to the impaired arteriogenesis in these mice. Our data suggest that PCAF regulates many factors that have previously been described to play an important role in both inflammation and arteriogenesis (Lee et al, 2004).

It should be noted that RNA was isolated from the adductor muscle group as a whole (Lee et al, 2004) and not from the embedded collateral arteries alone, as was described previously (Dai & Faber, 2010). In that report, a whole-genome microarray analysis was performed on collaterals microdissected from the gracilis muscle 24 hours after HLI. Here we found exceedingly more differentially expressed genes, then the 404 genes that were found upregulated in gracilis collaterals of WT mice (Dai et al, 2010). Using the entire adductor muscle group for microarray analysis, not only the collaterals but also infiltrating leukocytes and surrounding non-vascular tissues were included in these analyses.

As discussed in the introduction, an inflammatory-like process plays a role in all stages of arteriogenesis. To investigate the impact of PCAF on the inflammatory response of the different cell types involved in arteriogenesis, we studied circulating cells in whole blood, splenic leukocytes and VSMCs in vitro. PCAF is critical for

the regulation of transcription factor NF- κ B, that consists of a p65 and p50 subunit bound to inhibitory proteins in the cytoplasm. Upon stimulation NF- κ B is translocated to the nucleus and regulates the expression of multiple genes, including TNF α and MCP-1 (Lenardo & Baltimore, 1989; Miao et al, 2004). PCAF binds to the NF- κ B p65 subunit and activates NF- κ B-related inflammatory gene expression (Miao et al, 2004; Sheppard et al, 1999). We clearly demonstrate that PCAF deficiency results in decreased production of pro-inflammatory cytokines by multiple cell types after stimulation with LPS. LPS stimulated whole blood from PCAF^{-/-} mice produced less TNF α than blood from WT mice, indicating a reduced inflammatory phenotype of circulating cells. Also PCAF^{-/-} cells isolated from the spleen, one of the major leukocyte reservoirs, showed a reduced inflammatory response compared to splenocytes from WT mice. PCAF^{-/-} VSMCs produced less MCP-1 than WT VSMCs in response to LPS, which would favor reduced monocyte recruitment and therefore reduced VSMC proliferation, which is essential for collateral remodeling. We obtained similar results using either Garcinol or PCAF-specific siRNA knockdown in WT VSMCs, thus excluding effects of any pre-existing differences in PCAF deficient cells. Our data correspond with a report that TNF α -induced NF- κ B activity increases in human airway smooth muscle cells overexpressing PCAF (Clarke et al, 2008) and provide strong evidence for a wide effect of PCAF on inflammatory gene transcription.

The p65 subunit of NF- κ B recruits co-activator PCAF and activates NF- κ B-mediated gene transcription. In contrast, the NF- κ B p50 subunit lacks the transcriptional activation domain and inhibits gene transcription (Driessler et al, 2004). Mice deficient of the NF- κ B p50 subunit showed enhanced blood flow recovery after HLI as the result of increased monocyte recruitment to the perivascular space of collaterals (de Groot D. et al, 2010). Whereas arteriogenesis and monocyte recruitment is enhanced by NF- κ B activation in NF- κ B p50^{-/-} mice, reduced regulation of the NF- κ B p65 subunit in PCAF^{-/-} mice could likely explain the impaired arteriogenesis by inhibition of monocyte recruitment. In WT mice, the monocyte population increased in the spleen and decreased in the bone marrow after HLI. This is in line with earlier reports that monocytes are mobilized from the bone marrow after HLI (Cochain et al, 2010). In that report, the pro-arteriogenic potential of monocytes was described to originate from a specific “pro-inflammatory” subtype, which is characterized by high expression of Ly6C. These Ly6Chi monocytes are recruited in the early stage of collateral remodeling (Capoccia et al, 2008; Cochain et al, 2010) and our data confirm that they are mobilized from the bone marrow in WT mice. In contrast, recruitment of monocytes proved to be severely impaired in PCAF^{-/-} mice. PCAF^{-/-} mice showed reduced numbers of circulating monocytes following HLI, particularly reduced numbers of Ly6Chi monocytes. Whereas monocytes migrated away from the bone marrow in WT mice, PCAF^{-/-} mice showed an increase in bone marrow monocytes, suggesting a defect in monocyte mobilization. Concomitantly, 24 hours after HLI fewer monocytes were recruited to the collaterals in PCAF^{-/-} mice. Monocytes stimulate arteriogenesis by secretion of growth factors and degradation of extracellular matrix at the site of collateral remodeling. Therefore, the lack of monocyte accumulation along collaterals likely contributes to the impaired arteriogenesis in PCAF^{-/-} mice.

Besides monocytes, PCAF also affected numerous other leukocyte subtypes. In PCAF^{-/-} mice, we demonstrated decreased numbers of circulating leukocytes involved in arteriogenesis, like T cells (Couffinhal et al, 1999) (predominantly activated

CD4⁺ T cells (Stabile et al, 2003; van Weel et al, 2007)), natural killer cells (van Weel et al, 2007) and regulatory T cells (Hellingman et al, 2012; Zougari et al, 2009), and also in those cells that have not previously been implicated in arteriogenesis, including B cells. Furthermore, fewer dendritic cells were found in draining inguinal lymph nodes compared to WT mice, where the interaction between antigen-presenting dendritic cells and T cells takes place. Interestingly, nearly all subtypes were increased in the bone marrow of PCAF^{-/-} mice, after HLI. This indicates that PCAF deficiency interferes with recruitment of pro-arteriogenic leukocytes from the bone marrow reservoir (Meisner & Price, 2010).

In conclusion, PCAF^{-/-} mice demonstrated impaired collateral remodeling after HLI, together with a reduction in the number of native pre-existing collaterals present before arterial obstruction. PCAF deficiency resulted in altered expression of a large number of genes, including those in immune and inflammatory pathways, and an attenuated inflammatory response in multiple cell types involved in arteriogenesis. These findings indicate that PCAF is a key regulator in post-ischemic blood flow recovery by impacting the inflammatory processes required for robust arteriogenesis.

References

1. Bergmann CE, Hoefler IE, Meder B, Roth H, van Royen N., Breit SM, Jost MM, Aharinejad S, Hartmann S, and Buschmann IR (2006) Arteriogenesis depends on circulating monocytes and macrophage accumulation and is severely depressed in op/op mice. *J Leukoc Biol* 80: 59-65
2. Capoccia BJ, Gregory AD, and Link DC (2008) Recruitment of the inflammatory subset of monocytes to sites of ischemia induces angiogenesis in a monocyte chemoattractant protein-1-dependent fashion. *J Leukoc Biol* 84: 760-768
3. Chalothorn D and Faber JE (2010) Strain-dependent variation in collateral circulatory function in mouse hindlimb. *Physiol Genomics* 42: 469-479
4. Clarke DL, Sutcliffe A, Deacon K, Bradbury D, Corbett L, and Knox AJ (2008) PKC β 1 augments NF- κ B-dependent transcription at the CCL11 promoter via p300/CBP-associated factor recruitment and histone H4 acetylation. *J Immunol* 181: 3503-3514
5. Cochain C, Rodero MP, Vilar J, Recalde A, Richart AL, Loinard C, Zouggar Y, Guerin C, Duriez M, Combadiere B, Poupel L, Levy BI, Mallat Z, Combadiere C, and Silvestre JS (2010) Regulation of monocyte subset systemic levels by distinct chemokine receptors controls post-ischaemic neovascularization. *Cardiovasc Res* 88: 186-195
6. Couffinhal T, Silver M, Kearney M, Sullivan A, Witzenbichler B, Magner M, Annex B, Peters K, and Isner JM (1999) Impaired collateral vessel development associated with reduced expression of vascular endothelial growth factor in ApoE $^{-/-}$ mice. *Circulation* 99: 3188-3198
7. Dai X and Faber JE (2010) Endothelial nitric oxide synthase deficiency causes collateral vessel rarefaction and impairs activation of a cell cycle gene network during arteriogenesis. *Circ Res* 106: 1870-1881
8. de Groot D., Haverslag RT, Pasterkamp G, de Kleijn DP, and Hoefler IE (2010) Targeted deletion of the inhibitory NF- κ B p50 subunit in bone marrow-derived cells improves collateral growth after arterial occlusion. *Cardiovasc Res* 88: 179-185
9. Driessler F, Venstrom K, Sabat R, Asadullah K, and Schottelius AJ (2004) Molecular mechanisms of interleukin-10-mediated inhibition of NF- κ B activity: a role for p50. *Clin Exp Immunol* 135: 64-73
10. Duclot F, Jacquet C, Gongora C, and Maurice T (2010) Alteration of working memory but not in anxiety or stress response in p300/CBP associated factor (PCAF) histone acetylase knockout mice bred on a C57BL/6 background. *Neurosci Lett* 475: 179-183
11. Grundmann S, Hoefler I, Ulusans S, van RN, Schirmer SH, Ozaki CK, Bode C, Piek JJ, and Buschmann I (2005) Anti-tumor necrosis factor- α therapies attenuate adaptive arteriogenesis in the rabbit. *Am J Physiol Heart Circ Physiol* 289: H1497-H1505
12. Guarani V, Deflorian G, Franco CA, Kruger M, Phng LK, Bentley K, Toussaint L, Dequiedt F, Mostoslavsky R, Schmidt MH, Zimmermann B, Brandes RP, Mione M, Westphal CH, Braun T, Zeiher AM, Gerhardt H, Dimmeler S, and Potente M (2011) Acetylation-dependent regulation of endothelial Notch signalling by the SIRT1 deacetylase. *Nature* 473: 234-238
13. Heil M and Schaper W (2004) Influence of mechanical, cellular, and molecular factors on collateral artery growth (arteriogenesis). *Circ Res* 95: 449-458
14. Heil M, Ziegelhoeffer T, Pipp F, Kostin S, Martin S, Clauss M, and Schaper W (2002) Blood monocyte concentration is critical for enhancement of collateral artery growth. *Am J Physiol Heart Circ Physiol* 283: H2411-H2419
15. Hellingman AA, Bastiaansen AJ, de Vries MR, Seghers L, Lijkwan MA, Lowik CW, Hamming JF, and Quax PH (2010) Variations in surgical procedures for hind limb ischaemia mouse models result in differences in collateral formation. *Eur J Vasc Endovasc Surg* 40: 796-803
16. Hellingman AA, van der Vlugt LE, Lijkwan MA, Bastiaansen AJ, Sparwasser T, Smits HH, Hamming JF, and Quax PH (2012) A limited role for regulatory T cells in post-ischemic neovascularization. *J Cell Mol Med* 16: 328-336
17. Hiasa K, Ishibashi M, Ohtani K, Inoue S, Zhao Q, Kitamoto S, Sata M, Ichiki T, Takeshita A, and Egashira K (2004) Gene transfer of stromal cell-derived factor-1 α enhances ischemic vasculogenesis and angiogenesis via vascular endothelial growth factor/endothelial nitric oxide synthase-related pathway: next-generation chemokine therapy for therapeutic neovascularization. *Circulation* 109: 2454-2461
18. Ho TK, Tsui J, Xu S, Leoni P, Abraham DJ, and Baker DM (2010) Angiogenic effects of stromal cell-derived factor-1 (SDF-1/CXCL12) variants in vitro and the in vivo expressions of CXCL12 variants and CXCR4 in human critical leg ischemia. *J Vasc Surg* 51: 689-699

19. Hoefler IE, van Royen N, Rectenwald JE, Bray EJ, Abouhamze Z, Moldawer LL, Voskuil M, Piek JJ, Buschmann IR, and Ozaki CK (2002) Direct evidence for tumor necrosis factor-alpha signaling in arteriogenesis. *Circulation* 105: 1639-1641
20. Huang PH, Chen YH, Wang CH, Chen JS, Tsai HY, Lin FY, Lo WY, Wu TC, Sata M, Chen JW, and Lin SJ (2009) Matrix metalloproteinase-9 is essential for ischemia-induced neovascularization by modulating bone marrow-derived endothelial progenitor cells. *Arterioscler Thromb Vasc Biol* 29: 1179-1184
21. Imhof A, Yang XJ, Ogryzko VV, Nakatani Y, Wolffe AP, and Ge H (1997) Acetylation of general transcription factors by histone acetyltransferases. *Curr Biol* 7: 689-692
22. Itoh S, Ericsson J, Nishikawa J, Heldin CH, and ten Dijke P (2000) The transcriptional coactivator P/CAF potentiates TGF-beta/Smad signaling. *Nucleic Acids Res* 28: 4291-4298
23. Lee CW, Stabile E, Kinnaird T, Shou M, Devaney JM, Epstein SE, and Burnett MS (2004) Temporal patterns of gene expression after acute hindlimb ischemia in mice: insights into the genomic program for collateral vessel development. *J Am Coll Cardiol* 43: 474-482
24. Lenardo MJ and Baltimore D (1989) NF-kappa B: a pleiotropic mediator of inducible and tissue-specific gene control. *Cell* 58: 227-229
25. Lim JH, Lee YM, Chun YS, Chen J, Kim JE, and Park JW (2010) Sirtuin 1 modulates cellular responses to hypoxia by deacetylating hypoxia-inducible factor 1alpha. *Mol Cell* 38: 864-878
26. Liu L, Scolnick DM, Trievel RC, Zhang HB, Marmorstein R, Halazonetis TD, and Berger SL (1999) p53 sites acetylated in vitro by PCAF and p300 are acetylated in vivo in response to DNA damage. *Mol Cell Biol* 19: 1202-1209
27. Meier P, Gloekler S, Zbinden R, Beckh S, de Marchi SF, Zbinden S, Wustmann K, Billinger M, Vogel R, Cook S, Wenaweser P, Togni M, Windecker S, Meier B, and Seiler C (2007) Beneficial effect of recruitable collaterals: a 10-year follow-up study in patients with stable coronary artery disease undergoing quantitative collateral measurements. *Circulation* 116: 975-983
28. Meisner JK and Price RJ (2010) Spatial and temporal coordination of bone marrow-derived cell activity during arteriogenesis: regulation of the endogenous response and therapeutic implications. *Microcirculation* 17: 583-599
29. Menon BK, Bal S, Modi J, Sohn SI, Watson TW, Hill MD, Demchuk AM, and Goyal M (2012) Anterior temporal artery sign in CT angiography predicts reduced fatal brain edema and mortality in acute M1 middle cerebral artery occlusions. *J Neuroimaging* 22: 145-148
30. Miao F, Gonzalo IG, Lanting L, and Natarajan R (2004) In vivo chromatin remodeling events leading to inflammatory gene transcription under diabetic conditions. *J Biol Chem* 279: 18091-18097
31. Monraats PS, Rana JS, Zwinderman AH, de Maat MP, Kastelein JP, Agema WR, Doevendans PA, de Winter RJ, Tio RA, Waltenberger J, Frants RR, van der Laarse A, van der Wall EE, and Jukema JW (2005) -455G/A polymorphism and preprocedural plasma levels of fibrinogen show no association with the risk of clinical restenosis in patients with coronary stent placement. *Thromb Haemost* 93: 564-569
32. Pons D, Trompet S, de Craen AJ, Thijssen PE, Quax PH, de Vries MR, Wierda RJ, van den Elsen PJ, Monraats PS, Ewing MM, Heijmans BT, Slagboom PE, Zwinderman AH, Doevendans PA, Tio RA, de Winter RJ, de Maat MP, Iakoubova OA, Sattar N, Shepherd J, Westendorp RG, and Jukema JW (2011) Genetic variation in PCAF, a key mediator in epigenetics, is associated with reduced vascular morbidity and mortality: evidence for a new concept from three independent prospective studies. *Heart* 97: 143-150
33. Sartorelli V, Puri PL, Hamamori Y, Ogryzko V, Chung G, Nakatani Y, Wang JY, and Kedes L (1999) Acetylation of MyoD directed by PCAF is necessary for the execution of the muscle program. *Mol Cell* 4: 725-734
34. Schaper J, Konig R, Franz D, and Schaper W (1976) The endothelial surface of growing coronary collateral arteries. Intimal margination and diapedesis of monocytes. A combined SEM and TEM study. *Virchows Arch A Pathol Anat Histol* 370: 193-205
35. Schirmer SH, van Nooijen FC, Piek JJ, and van Royen N. (2009) Stimulation of collateral artery growth: travelling further down the road to clinical application. *Heart* 95: 191-197
36. Shao H, Tan Y, Eton D, Yang Z, Uberty MG, Li S, Schulick A, and Yu H (2008) Statin and stromal cell-derived factor-1 additively promote angiogenesis by enhancement of progenitor cells incorporation into new vessels. *Stem Cells* 26: 1376-1384
37. Sheppard KA, Rose DW, Haque ZK, Kurokawa R, McInerney E, Westin S, Thanos D, Rosenfeld MG, Glass CK, and Collins T (1999) Transcriptional activation by NF-kappaB requires multiple coactivators. *Mol Cell Biol* 19: 6367-6378

38. Shireman PK (2007) The chemokine system in arteriogenesis and hind limb ischemia. *J Vasc Surg* 45 Suppl A: A48-A56
39. Silke J and Brink R (2010) Regulation of TNFRSF and innate immune signalling complexes by TRAFs and cIAPs. *Cell Death Differ* 17: 35-45
40. Stabile E, Burnett MS, Watkins C, Kinnaird T, Bachis A, la Sala A, Miller JM, Shou M, Epstein SE, and Fuchs S (2003) Impaired arteriogenic response to acute hindlimb ischemia in CD4-knockout mice. *Circulation* 108: 205-210
41. Stabile E, Kinnaird T, la Sala A, Hanson SK, Watkins C, Campia U, Shou M, Zbinden S, Fuchs S, Kornfeld H, Epstein SE, and Burnett MS (2006) CD8+ T lymphocytes regulate the arteriogenic response to ischemia by infiltrating the site of collateral vessel development and recruiting CD4+ mononuclear cells through the expression of interleukin-16. *Circulation* 113: 118-124
42. Tusher VG, Tibshirani R, and Chu G (2001) Significance analysis of microarrays applied to the ionizing radiation response. *Proc Natl Acad Sci U S A* 98: 5116-5121
43. van Oostrom MC, van Oostrom O, Quax PH, Verhaar MC, and Hoefer IE (2008) Insights into mechanisms behind arteriogenesis: what does the future hold? *J Leukoc Biol* 84: 1379-1391
44. van Weel V, Toes RE, Seghers L, Deckers MM, de Vries MR, Eilers PH, Sipkens J, Schepers A, Eefting D, van H, V, van Bockel JH, and Quax PH (2007) Natural killer cells and CD4+ T-cells modulate collateral artery development. *Arterioscler Thromb Vasc Biol* 27: 2310-2318
45. Voskuil M, Hoefer IE, van Royen N, Hua J, de GS, Bode C, Buschmann IR, and Piek JJ (2004) Abnormal monocyte recruitment and collateral artery formation in monocyte chemoattractant protein-1 deficient mice. *Vasc Med* 9: 287-292
46. Wang S, Zhang H, Dai X, Sealock R, and Faber JE (2010) Genetic architecture underlying variation in extent and remodeling of the collateral circulation. *Circ Res* 107: 558-568
47. Yamauchi T, Yamauchi J, Kuwata T, Tamura T, Yamashita T, Bae N, Westphal H, Ozato K, and Nakatani Y (2000) Distinct but overlapping roles of histone acetylase PCAF and of the closely related PCAF-B/GCN5 in mouse embryogenesis. *Proc Natl Acad Sci U S A* 97: 11303-11306
48. Yang M and Odgren PR (2005) Molecular cloning and characterization of rat CCL9 (MIP-1gamma), the ortholog of mouse CCL9. *Cytokine* 31: 94-102
49. Zhang H, Prabhakar P, Sealock R, and Faber JE (2010) Wide genetic variation in the native pial collateral circulation is a major determinant of variation in severity of stroke. *J Cereb Blood Flow Metab* 30: 923-934
50. Zouggari Y, Ait-Oufella H, Waeckel L, Vilar J, Loinard C, Cochain C, Recalde A, Duriez M, Levy BI, Lutgens E, Mallat Z, and Silvestre JS (2009) Regulatory T cells modulate postischemic neovascularization. *Circulation* 120: 1415-1425

Supplementary figures

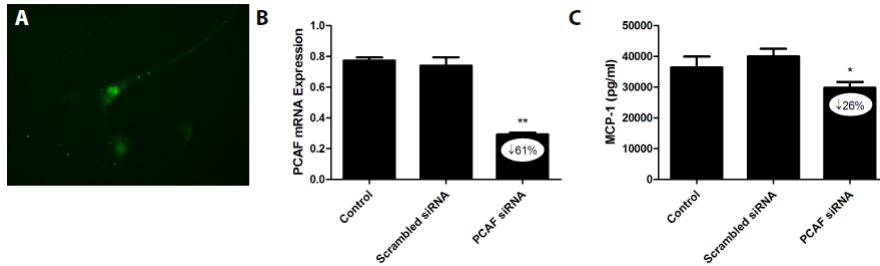


Figure 1. PCAF knockdown by siRNA in vascular smooth muscle cells. A. Vascular smooth muscle cells (VSMCs) were transfected with nontarget fluorescent siGlow (Dharmacon) to test transfection efficiency, using Lipofectamine 2000 according to the manufacturer's instructions. VSMCs were visualized on a Leica fluorescence microscope. B. VSMCs were plated and transfected with control short-interfering RNA (siRNA) or a combination of 4 siRNAs directed towards PCAF for 4 hours. Untransfected VSMCs were used as control.

VSMCs were incubated with LPS (1 ng/ml) for 24 hours. To confirm PCAF knockdown, PCAF mRNA was measured by real-time quantitative PCR. Levels were normalized against the expression of HPRT1. PCAF specific siRNA reduced PCAF expression with 61% in comparison to scrambled siRNA. C. Cell-free supernatant of LPS stimulated VSMCs was collected for MCP-1 quantification, measured by ELISA. Transfection with PCAF specific siRNA inhibited MCP-1 production of VSMCs in comparison to scrambled siRNA. All samples were performed in triplicates. *P < .05, **P < .01, scrambled siRNA versus PCAF siRNA.

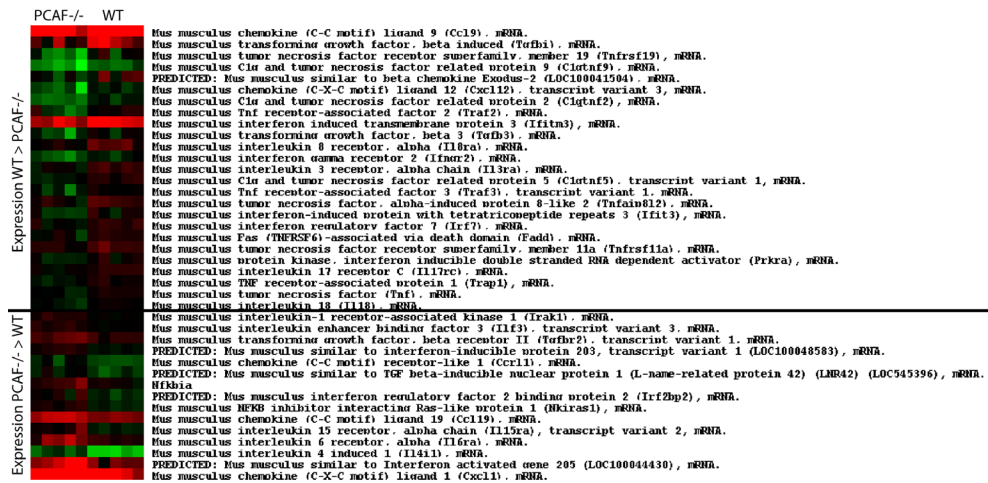
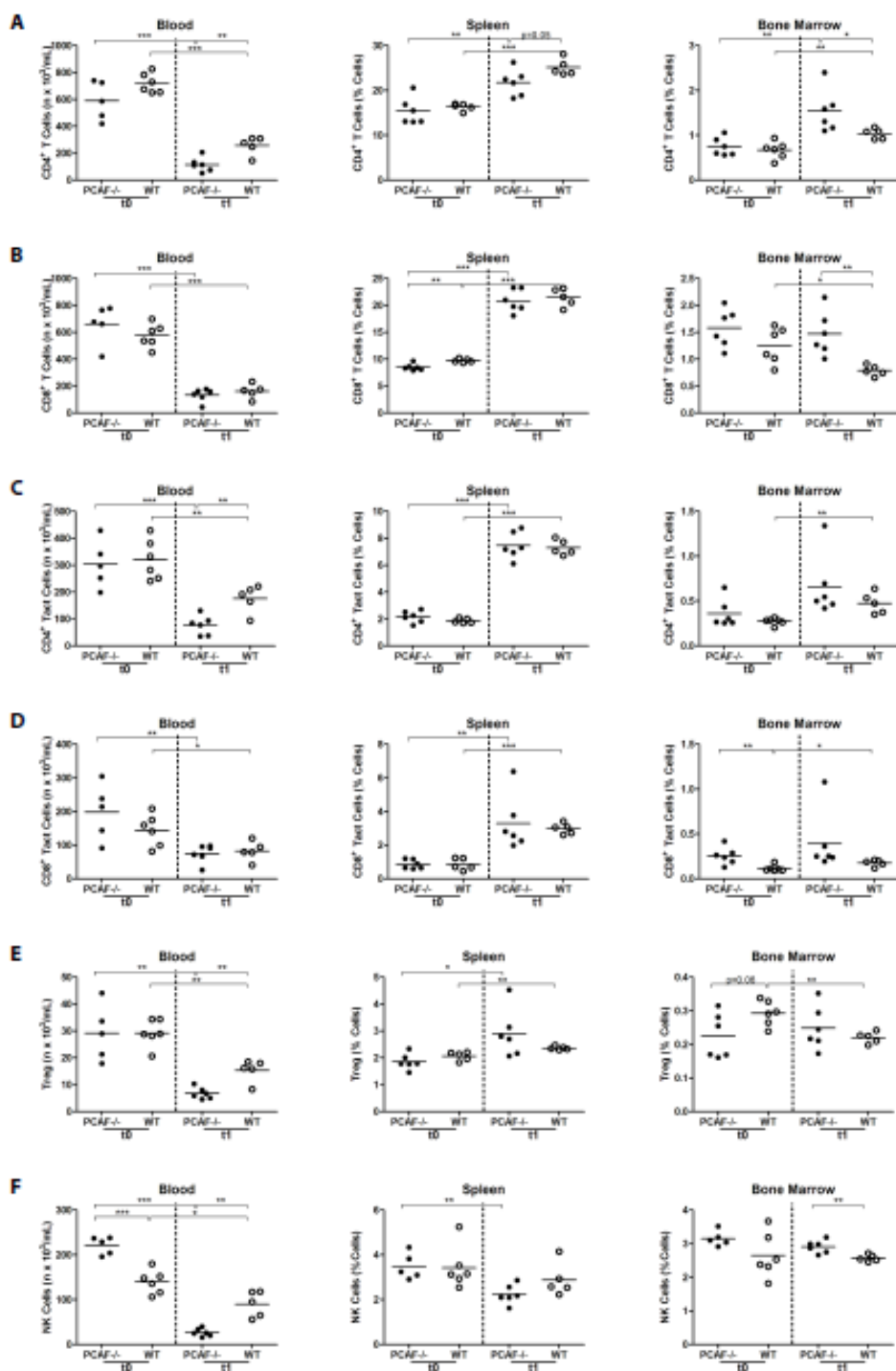


Figure 2. Differential inflammatory gene expression in PCAF^{-/-} and WT mice. Heatmap of differentially expressed inflammatory genes in adductor muscle group of PCAF^{-/-} and WT mice, 1 day after HLI. Gene definitions containing any of these criteria (interleukin, chemokine, interferon, TGF, TNF, NFKB) were selected. Included are genes that were significantly different between PCAF^{-/-} and WT mice (q-value < 5). Data are presented as the fold change in expression between day 1 and average preoperative baseline levels, generating t1/t0avg ratios. Red indicates increased and green indicates reduced expression relative to average baseline levels.



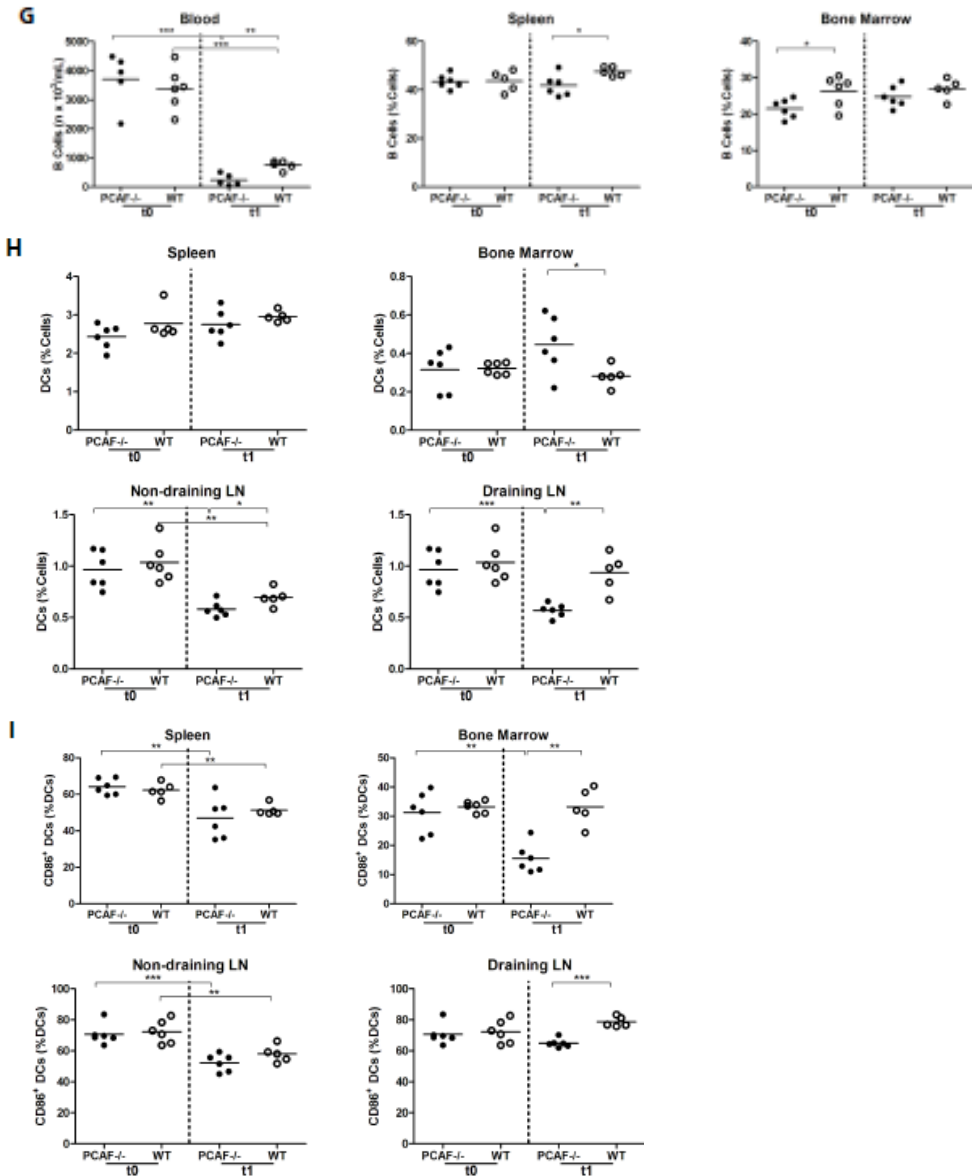


Figure 3. Leukocyte subtypes in PCAF^{-/-} and WT mice after HLI. Flow cytometry analysis of lymphocytes in blood ($n \times 10^3/\text{mL}$), spleen and bone marrow (% of total cells). In succession, values are presented for (A) CD4⁺ T helper cells, (B) CD8⁺ cytotoxic T cells, (C) activated CD4⁺ T helper cells, (D) activated CD8⁺ cytotoxic T cells, (E) regulatory T cells (Treg), (F) Natural Killer (NK) cells and (G) B lymphocytes. (H) Dendritic cells (DCs) in spleen, bone marrow, nondraining and draining (inguinal) lymph nodes (LN). (I) Activated DCs in spleen, bone marrow, non-draining and draining (inguinal) lymph nodes.

Symbol	Gene Name	PCAF ^{-/-} WT			Ratio
		logFC	logFC	q-value	PCAF ^{+/+} vs WT FC
Arg1	arginase 1, liver	1,55	3,11	4,39	0,34
Pdk4	pyruvate dehydrogenase kinase, isoenzyme 4	0,17	1,29	3,00	0,46
Ptpn6	protein tyrosine phosphatase, non-receptor type 6, transcript variant 2	0,55	1,54	0,86	0,50
Lst1		0,37	1,36	0,86	0,50
Anxa2	annexin A2 (Anxa2), mRNA.	0,39	1,37	0,69	0,51
Serpinb1a	serine (or cysteine) peptidase inhibitor, clade B, member 1a	0,31	1,28	1,23	0,51
Slnf1	schlafen 1	0,79	1,74	1,66	0,52
Mmp9	matrix metalloproteinase 9	0,07	1,01	0,69	0,52
Cott1	coactosin-like 1	0,66	1,60	1,23	0,52
Cd52	CD52 antigen	1,41	2,33	4,39	0,53
Tagln2	transgelin 2	0,23	1,15	0,86	0,53
Ccl9	chemokine (C-C motif) ligand 9	1,91	2,81	3,60	0,54
LOC100046120	PREDICTED: similar to clusterin	1,06	1,94	1,23	0,54
Angptl4	angiopoietin-like 4	0,43	1,31	3,60	0,54
Cfp	complement factor properdin	0,37	1,23	0,40	0,55
Cott1	coactosin-like 1	0,42	1,25	0,59	0,56
Kcnab2	potassium voltage-gated channel, shaker-related subfamily, beta member 2	0,37	1,16	0,59	0,58
LOC100044439	PREDICTED: similar to cytochrome P450 CYP4F18	0,40	1,19	1,66	0,58
Sirpa	signal-regulatory protein alpha	0,55	1,33	1,94	0,58
Fbxo32	F-box protein 32	0,86	1,63	4,39	0,59
Alox5ap	arachidonate 5-lipoxygenase activating protein	1,13	1,87	1,94	0,60
Arhgdib	Rho, GDP dissociation inhibitor (GDI) beta	0,32	1,04	1,23	0,61
Emilin2	elastin microfibril interfacer 2	0,10	0,82	0,86	0,61
Lrrc33	leucine rich repeat containing 33	0,42	1,12	0,86	0,62
Fbxl22	F-box and leucine-rich repeat protein 22	0,26	0,96	2,42	0,62
Emilin2	elastin microfibril interfacer 2	0,12	0,80	1,94	0,62
Cyth4	cytohesin 4	0,74	1,41	4,39	0,63
Laptm5	lysosomal-associated protein transmembrane 5	0,92	1,59	0,98	0,63
Sdc3	syndecan 3	0,07	0,73	0,86	0,64
Ly6e	lymphocyte antigen 6 complex, locus E	0,01	0,66	0,33	0,64
Hdac4	histone deacetylase 4	0,02	0,66	0,00	0,64
Dok2	docking protein 2	0,50	1,14	1,94	0,64
Fcgr4	Fc receptor, IgG, low affinity IV	1,63	2,26	3,60	0,64
Alox5ap	arachidonate 5-lipoxygenase activating protein	0,85	1,48	2,42	0,65
Cap1	CAP, adenylate cyclase-associated protein 1	0,26	0,89	0,98	0,65
Tgfb1	transforming growth factor, beta induced	0,36	0,99	3,00	0,65
Aif1	allograft inflammatory factor 1	0,23	0,84	1,23	0,65
Mcm5	minichromosome maintenance deficient 5, cell division cycle 46	0,07	0,68	0,00	0,65
Fes	feline sarcoma oncogene	0,33	0,95	0,45	0,65
Gnb2	guanine nucleotide binding protein (G protein), beta 2	0,07	0,68	0,00	0,66
Cyba	cytochrome b-245, alpha polypeptide	0,56	1,17	1,23	0,66
Gm	granulin	0,21	0,81	0,00	0,66
Fxyd5	FXYD domain-containing ion transport regulator 5	0,78	1,38	3,60	0,66
Cdh15	cadherin 15	0,09	0,69	0,33	0,66
Rabgef1	RAB guanine nucleotide exchange factor	0,24	0,82	0,45	0,67
Oas1g	2'-5' oligoadenylate synthetase 1G	0,04	0,62	0,98	0,67
Arrib2	arrestin, beta 2	0,04	0,62	0,40	0,67
Emp3	epithelial membrane protein 3	0,33	0,90	3,60	0,67
Sh3bgrt3	SH3 domain binding glutamic acid-rich protein-like 3	0,60	1,16	1,23	0,68
S100a11	S100 calcium binding protein A11	0,54	1,11	4,39	0,68

Table 1. List of differentially expressed genes in the adductor muscle group of PCAF^{-/-} and WT mice. Data are presented as the log fold change in expression between day 1 after HLI and average preoperative baseline levels, generating t1/t0avg ratios. Listed are the top 50 genes which showed an impaired up-regulation in PCAF^{-/-} mice compared to WT mice. Q-values less than 5% were considered significant. FC = fold change.

Symbol	Gene Name	PCAF ^{-/-}	WT	q-value
		logFC	logFC	
Ccl9	chemokine (C-C motif) ligand 9	1,91	2,81	3,60
Tgfb1	transforming growth factor, beta induced	0,36	0,99	3,00
Tnfrsf19	tumor necrosis factor receptor superfamily, member 19	-0,64	-0,04	1,66
C1qtnf9	C1q and tumor necrosis factor related protein 9	-0,95	-0,50	3,00
LOC100041504	PREDICTED: similar to beta chemokine Exodus-2	-0,16	0,27	3,60
Cxcl12	chemokine (C-X-C motif) ligand 12, transcript variant 3	-0,58	-0,16	3,60
C1qtnf2	C1q and tumor necrosis factor related protein 2	-0,57	-0,16	0,00
Traf2	Tnf receptor-associated factor 2	-0,28	0,12	3,60
Ifitm3	interferon induced transmembrane protein 3	1,00	1,39	2,42
Tgfb3	transforming growth factor, beta 3	-0,40	-0,02	4,39
Il8ra	interleukin 8 receptor, alpha	0,07	0,43	0,98
Ifngr2	interferon gamma receptor 2	-0,48	-0,15	1,94
Il3ra	interleukin 3 receptor, alpha chain	-0,02	0,30	0,69
C1qtnf5	C1q and tumor necrosis factor related protein 5, transcript variant 1	-0,11	0,19	0,33
Traf3	Tnf receptor-associated factor 3, transcript variant 1	-0,26	0,04	4,39
Tnfaip8l2	tumor necrosis factor, alpha-induced protein 8-like 2	0,07	0,36	1,94
Ifit3	interferon-induced protein with tetratricopeptide repeats 3	-0,23	0,06	4,39
Irf7	interferon regulatory factor 7	0,00	0,24	1,94
Fadd	Fas (TNFRSF6)-associated via death domain	-0,04	0,19	4,39
Tnfrsf11a	tumor necrosis factor receptor superfamily, member 11a	0,14	0,37	2,42
Prkra	protein kinase, interferon inducible double stranded RNA dependent activator	-0,14	0,08	4,39
Il17rc	interleukin 17 receptor C	0,01	0,23	0,98
Trap1	TNF receptor-associated protein 1	-0,10	0,11	1,66
Tnf	tumor necrosis factor	-0,08	0,11	1,94
Il18	interleukin 18	-0,12	0,04	4,39

Symbol	Gene Name	PCAF ^{-/-}	WT	q-value
		logFC	logFC	
Irak1	interleukin-1 receptor-associated kinase 1	0,18	0,00	1,66
Ilf3	interleukin enhancer binding factor 3, transcript variant 3	0,19	0,00	0,98
Tgfb2	transforming growth factor, beta receptor II, transcript variant 1	0,47	0,24	3,60
LOC100048583	PREDICTED: similar to interferon-inducible protein 203, transcript variant 1	0,16	-0,08	0,33
Ccr1	chemokine (C-C motif) receptor-like 1	-0,15	-0,42	3,00
LOC545396	PREDICTED: similar to TGF beta-inducible nuclear protein 1	-0,06	-0,33	3,00
Nfkbia	nuclear factor of kappa light polypeptide gene enhancer in B-cells inhibitor, alpha	0,36	0,06	3,60
Irf2bp2	PREDICTED: interferon regulatory factor 2 binding protein 2	0,09	-0,22	3,00
Nkiras1	NFKB inhibitor interacting Ras-like protein 1	0,15	-0,17	0,00
Ccl19	chemokine (C-C motif) ligand 19	1,02	0,68	0,40
Il15ra	interleukin 15 receptor, alpha chain, transcript variant 2	0,20	-0,15	2,42
Il6ra	interleukin 6 receptor, alpha	0,69	0,21	1,66
Il4i1	interleukin 4 induced 1	-0,39	-1,10	0,00
LOC100044430	PREDICTED: similar to Interferon activated gene 205	1,27	0,50	1,23
Cxcl1	chemokine (C-X-C motif) ligand 1	2,93	1,45	1,66

Table 2. List of significantly differentially expressed inflammatory genes in the adductor muscle group of PCAF^{-/-} and WT mice. Data are presented as the log fold change in expression between day 1 after HLI and average preoperative baseline levels, generating t1/t0avg ratios. Gene definitions containing any of these criteria (interleukin, chemokine, interferon, TGF, TNF, NFKB) were selected. Q-values less than 5% were considered significant. FC = fold change.

Chapter 12

Summary and general discussion

Summary and general discussion

Cardiovascular diseases remain the major cause of death throughout the world and can be primarily attributed to atherosclerotic vascular disease leading to stroke and coronary heart disease (CHD). Improved primary prevention and the introduction and subsequent optimization of percutaneous coronary interventions (PCI) for myocardial ischemia due to obstructive CHD have significantly improved patient outcome and reduced morbidity and mortality. The insight into disease pathology has however expanded tremendously over the past decade and continuing research has shifted the focus of interest towards post-interventional accelerated atherosclerosis development due to a dysfunctional (auto) immune inflammatory response, responsible for vascular remodeling, re-occlusion and recurrence of symptoms.

The aim of this thesis therefore was to investigate the role of the immune system in this pathophysiological process that ultimately results in post-interventional atherosclerotic vascular remodeling and apply this insight for the development of new immune-modulatory therapies in a preclinical setting. The important contribution of the various parts of the immune system involved in both clinical and preclinical vascular remodeling are described in **chapter 1**. Preclinical screening and testing of immune-modulatory therapy effectiveness is a vital step towards clinical application of such interventions at the time of PCI or CABG-surgical procedures to prevent vascular re-occlusion and the necessity for re-interventions. Insight into the evoked immune responses, both in mouse and man, during these procedures lies at the basis for the discovery and application of new therapies with ultimate clinical potential.

Chapter 2 provides an overview of the immune reactions of the innate and adaptive immune systems that develop during native atherogenesis, as well as those which are evoked by vascular injury during revascularization strategies. Specific leukocyte receptors, ligands, co-stimulatory molecules and inflammatory cytokines are highlighted and are shown to be involved in disease initiation and lesion progression during inflammation. In addition, their association with disease severity is independent of traditional risk factors such as smoking and hypertension and they could serve as helpful tools for biomarker-based risk stratification or and diagnosis. This includes diagnostic assessment of patients eligible for intensified treatment evaluated clinicians performing target lesion revascularization interventions. Moreover, future biomarkers could be helpful in assessing treatment effectiveness in a way that traditional makers such as plasma lipoprotein levels or electrocardiographic do not provide adequate insight. Plasma measurements are above all strongly preferred over diagnostic angioplasty procedures and local biomarkers in the arterial segments of interest could improve optimal disease severity assessment. The search for new biomarkers is therefore essential and markers of inflammation that are causally linked to post-interventional vascular remodeling could prove to be the most valuable makers available to clinicians.

Chapter 3 illustrates that investigational screening of the therapeutic effects of drug therapy on vascular remodeling and accelerated atherosclerosis development requires preclinical models that optimally mimic the clinical situation of the vessel after intervention, not only in vascular anatomical aspects such as size, diameter and wall thickness, but also in features of disease stage aspects such as hypercholesterole-

mia and other conventional risk factors for atherosclerosis. To this end, humanized animal models are discussed that have the best predictive value for the pathophysiological process in the development of restenosis, intimal hyperplasia and accelerated atherosclerotic lesions. Various vascular interventions in transgenic mouse models are mentioned, with a strong focus on the mouse femoral artery cuff model. To study effects of (local) drug therapy, animals should be susceptible to the treatment of interest, have similar metabolic levels, coagulatory phenotype and react in a human-like fashion. The use of humanized (transgenic) animal models has extensively increased the similarity between human and animal lesions and the translation of new therapies into the clinical setting. Furthermore, mechanistic and pathophysiological studies have shown that local vessel wall inflammation, proliferation and proteolysis are central in post-interventional vascular remodeling. It was therefore concluded that highly-reproducible animal models for post-interventional vascular remodeling are essential for studying the process of restenosis and the development of future anti-restenotic therapies.

Specific stages of the immune response and their usefulness as target of immune-directed interventions are discussed below. Vascular remodeling is originally initiated by endothelial damage and injury to the underlying plaque by balloon inflation, stent deployment or surgical harvesting and engraftment procedures during revascularization interventions. Exposure of thrombogenic tissue will evoke platelet adherence, activation and thrombosis formation and support the recruitment of leukocytes to the site of vascular injury. Platelet activation and binding is supported by the presence of phosphatidylserine (PS) on activated and apoptotic cells. **Chapter 4** shows a therapeutic role for the PS-binding annexin A5 protein against vascular inflammation, remodeling and dysfunction in mouse models for accelerated atherosclerosis development. It was demonstrated that annexin A5 injection resulted in a marked reduction in circulating plasma cytokine concentrations and early inflammatory cell recruitment to the vessel wall after injury, eventually leading to decreased intimal hyperplasia with less plaque instability features. Although the exact role through which annexin A5 led to these effects was not completely clarified, annexin A5 was shown to act through local platelet-supported leukocyte binding and prevention of the subsequent immune response, thus extending the role of annexin A5 as a regulator of inflammatory processes and demonstrated its potential therapeutic use in inflammation-associated vascular disease.

In **chapter 5** it is demonstrated that a strong association exists between genetic polymorphisms in the human annexin A5 gene and increased restenosis-risk in patients undergoing PCI enrolled in the GENDER study, composed of 866 patients of which 295 cases developed restenosis within 1 year following PCI and 571 controls were free of restenosis. Although association exists, this does not implicate a direct causal link between this polymorphism and clinical outcome. To this end, measurement of patient plasma annexin A5 concentration could provide insight, since reduced annexin A5 concentrations are linked to increased coronary stenosis severity, whilst increased concentrations occurs following myocardial infarction. Nevertheless, these results do suggest that annexin A5 genotype could function as a risk marker for restenosis. Together, these data indicate high diagnostic and therapeutic clinical potential for annexin A5 against post-PCI vascular remodeling.

Chapter 6 describes the process of optimization of a natural occurring protective

anti-phosphorylcholine (PC) T15/E06 IgM antibody into a recombinant chimeric IgG which was first evaluated for *in vitro* anti-inflammatory effectiveness. Remarkably, the inhibitory effects on oxidized low density lipoprotein (oxLDL) uptake by scavenger receptor-bearing macrophages was lost after transition of the constant antibody region from an IgM to an IgG chain. Despite this loss, the recombinant anti-PC T15 IgG was nevertheless effective in preventing monocyte chemotactic protein (MCP)-1 expression by macrophages and passive immunization of cuffed hypercholesterolemic mice with this antibody prevented accelerated atherosclerosis development. These results suggest that although the chimeric antibody did not prevent oxLDL uptake, it did inhibit inflammatory responses towards oxLDL, possibly by masking the immunogenic epitope or by supporting its degradation and clearance from the circulation.

Using the Dyax library, phage display selection allowed identification of phosphorylcholine-specific phages that were converted to full IgGs and could still block oxLDL-uptake by macrophages and subsequent MCP-1 expression. A selection of antibodies was then tested *in vivo* and yielded potent fully human monoclonal anti-PC T15 IgG (M99-B05) antibodies that were effective in preventing intimal thickening in cuffed hypercholesterolemic animals. Codon optimization of M99-B05 produced the X19-A05 antibody with high specificity for PC and strong anti-inflammatory effects that could inhibit oxLDL uptake *in vitro* and vascular remodeling *in vivo*, even in low concentrations. This study, like those performed previously, showed that PC is a promising therapeutic target in the prevention and treatment of accelerated atherosclerosis development in mice and anti-PC IgG antibodies can prevent vascular remodeling. However, the vital new aspect of this study is that it is the first to develop new fully human anti-PC IgG antibodies that are atheroprotective. Others used IgM antibodies passively in mice or induced anti-PC IgM and IgG through active immunization. These techniques are promising, but not applicable in the clinical setting, since active immunization with a pneumococcal polysaccharide vaccine previously did not lead to adequate titers of oxLDL-recognizing anti-PC antibodies. We developed, screened and tested recombinant monoclonal anti-PC IgG antibodies that are suitable for passive therapeutic immunization in humans. By providing immediate and direct control of the patient's immune response with restriction to a single immunogenic epitope, this immunization approach could prove to be an effective treatment modality against post-interventional atherosclerotic vascular remodeling in patients undergoing PCI or CABG-surgery.

The important role of the innate immune system was confirmed in **chapter 7**, where a novel TLR7/9 dual antagonist was tested in a mouse restenosis model. Toll-like receptors are a vital part of the innate immune system and serve as pattern recognition receptors (PRR) that recognize extracellular ligands that originate from bacteria or viruses (TLR2, 4 and 5), as well as intracellular ligand such as damaged or viral (double stranded) RNA (TLR3, 7 and 9). These endogenous ligands may be released after tissue damage or cell stress, processes that may be initiated by PCI. TLR7 or TLR9 presence occurred in vascular lesions at the location of macrophage accumulation. *In vitro*, these cells responded to TLR7 or TLR9 activation by increased oxLDL uptake and TNF α production, which could be inhibited by the novel TLR7/9 dual antagonist. These effects led to reduced intimal thickening when applied *in vivo*. The magnitude of individual TLR signaling remains unknown, but

the therapeutic potential of targeting TLR7 and TLR9 to prevent restenosis and accelerated atherosclerosis has been made clear. Since TLRs are easily accessible for circulating drugs (directly or after cellular infiltration) and form the first line of defense of the innate immune system, they are favorable as therapeutic targets in the acute phase of vascular injury and can be readily silenced or stimulated. Novel inhibitors can be designed to bear desired drug properties, whilst effectively targeting a TLR of great interest. Dual targeting of multiple receptors greatly increases drug effectiveness, clearly demonstrated in this study.

In **chapter 8**, the contribution of the adaptive immune system to post-interventional atherosclerotic vascular remodeling was elucidated by investigating the role of CD4⁺ T-cells and CD28-CD80/86 co-stimulatory pathways. Post-interventional vascular remodeling was significantly attenuated in CD4^{-/-} and CD80^{-/-}CD86^{-/-} mice compared to controls. To show that CTLA-4 is a key and vital regulator in this process, abatacept was injected in control mice that then failed to develop significant intimal thickening. Next, this was repeated in hypercholesterolemic ApoE3*Leiden mice, producing similar striking results. Flow cytometry analysis of activated lymphocytes in spleen and draining lymph nodes revealed that abatacept prevented effector CD4⁺ T-cell activation and led to a reduced number of regulatory T-cells in the spleen, although without affecting Teff : Treg ratio. However, abatacept did not affect cellular activation status in draining lymph nodes. These findings were later linked to reduced plasma levels of interferon γ in abatacept-treated animals. The role of CTLA-4 co-inhibition in this process was finally confirmed by treating ApoE3*Leiden mice with hybridoma-derived blocking anti-CTLA-4 IgG antibodies, which developed significantly larger lesions.

Immune-mediated interventions directed towards therapeutically controlling the inflammatory T-cell response such as abatacept are widely applied in other immune (e.g. rheumatoid) disorders and could now be used in an early phase following vascular interventions to prevent subsequent vascular remodeling. Abatacept is a registered drug with an established efficacy and safety profile in patients, which can dramatically shorten the time necessary for bench-to-bedside translation for this specific drug. Although initial beneficial effects of abatacept were observed, these need to be reproduced in the prolonged treatment setting before they can be applied in the clinic. In addition, effects of abatacept treatment on other CD28-expressing cell types such as B-cells should be fully clear before application during vascular revascularization interventions. Nevertheless, this study clearly demonstrates the important role of CD4 T-cells and the CD28/CTLA-4-CD80/CD86 co-stimulatory pathway in the inflammatory reaction as part of the adaptive immune system that occurs after vascular intervention in vivo.

In **chapter 9** it is shown in three large prospective studies that the -2481C allele in the PCAF promoter is associated with a significant survival advantage in elderly patients while also protecting against clinical and angiographic restenosis after PCI. It is suggested that the effect of this allele on these endpoints may be due to the well-known involvement of PCAF in inflammatory and proliferative processes. These results not shed light on a causal role of this polymorphism in the development of restenosis, but do promote the concept that epigenetic processes are under genetic control and that, other than environment, genetic variation in genes encoding KATs may also determine susceptibility to CHD outcomes and mortality. Until this point,

it remains to be established whether this SNP functionally affects transcriptional regulation of P300/CBP-associated factor (PCAF). Provided that this SNP influences PCAF transcription and resulting protein levels, this could have a bearing on the cellular portrait of expressed genes and might lead to a dramatic different outcome if the effects accumulate over years. Until this can be established, this SNP could serve as risk marker for both mortality and restenosis risk in patients undergoing PCI. Furthermore, it has provided insight into the association between PCAF and vascular remodeling, the exact role of which was further investigated in the next chapters. **Chapter 10** describes the investigations performed into the causal role of PCAF in controlling the inflammatory response responsible for post-interventional atherosclerotic vascular remodeling. It was found that PCAF regulates MHC class II, but not I, expression in macrophages through CIITA and is upregulated in the arterial wall in the early period following vascular injury at both mRNA and at protein level. It is demonstrated that post-interventional vascular remodeling is reduced in PCAF^{-/-} mice and accelerated atherosclerosis development in hypercholesterolemic mice treated with the natural potent PCAF inhibitor garcinol. Furthermore, it was shown that this reduced remodeling was due to an attenuated inflammatory response, identified by reduced MCP-1 and TNF α -expression in vivo and in cultured SMCs and macrophages in vitro.

Although the role of PCAF in the regulation of inflammation is clear and was shown to affect macrophage recruitment, activation and cytokine expression, the specificity of garcinol for PCAF in this process needs to be further elucidated. Garcinol was shown to be extremely potent and can inactivate PCAF activity within 3 minutes in vitro, but also affects the expression of many other genes and is known to induce apoptosis in high concentrations. Indeed, the anti-inflammatory effects of short-term applied garcinol to inhibit PCAF expression at the time of vascular interventions was lost with prolonged garcinol application in high concentrations in the femoral drug-eluting cuff model (unpublished data). This highlights the necessity of the search towards new and potent PCAF inhibitors that do not display as many or severe side-effects as garcinol does, before effective PCAF inhibition can be applied in the clinical setting. Nevertheless, the results highlight inflammation-regulation by the epigenetic factor in the acute setting as a causal factor in post-interventional vascular remodeling.

The role of PCAF in inflammation and vascular remodeling was further investigated in **chapter 11**, where PCAF^{-/-} mice were shown to display impaired arteriogenesis capability following acute arterial occlusion. This process, a form of collateral artery growth from pre-existing arterioles to arterial occlusion, is initiated by flow and shear-stress-increase and is highly dependent of the activation of circulating inflammatory cells. Using a hind-limb ischemia mouse model based upon surgically-induced acute femoral artery occlusion, PCAF was identified to be vital in this inflammatory process. PCAF^{-/-} animals were shown to display an impaired inflammatory response with functionally less activated dendritic cells, T-cells and reduced inflammatory cytokine expression in vivo and following a LPS-challenge ex vivo. Although exactly which inflammatory genes and to what extent these are regulated by PCAF remains to be further investigated, it has been made clear that PCAF is causally involved in post-interventional vascular remodeling.

PCAF regulation of inflammatory gene transcription was shown to occur in multiple

cell types involved in the innate and adaptive immune responses, including antigen-presenting cells, lymphocytes and smooth muscle cells. By exerting a regulatory function in controlling acute inflammation, PCAF was shown to dominantly affect pro-inflammatory genes and by serving as central-regulating factor with intrinsic histone acetyltransferase activity, it might provide clinicians with an interesting and controllable epigenetic target for anti-inflammatory preventive therapy.

Therapy directed towards expression of such an epigenetic factor as PCAF might be more effective in preventing vascular remodeling than a single gene or single protein treatment approach, since a factor like PCAF can affect chromatin structure throughout the nucleus.

How do we proceed beyond our promising newly discovered therapies?

The aim of this thesis was to investigate the role of the immune system in the pathophysiological process leading to the development of post-interventional atherosclerotic vascular remodeling. This research has yielded multiple new therapeutic applications that could be translated into the clinic within a varying range of time. Although statements naming time units are mere predictions, it is wrong not to pursue such goals and leave promising drugs for what they are simply because investigations into their application might take a long time. Abatacept is already a registered drug treatment drug for rheumatoid arthritis and could be relatively quickly (<1 year) tested in a revascularization setting, once therapeutic effectiveness is confirmed in long-term animal studies. Annexin A5, recombinant monoclonal X19-A05 anti-PC IgG antibodies and our novel TLR7/9 antagonist have been tested and found effective in our animal models, but still require additional investigations into their efficacy and safety profiles, before clinical application could be initiated. This should be able to be performed within the foreseeable future (<2 years). Our PCAF results have identified a new factor involved in post-interventional vascular remodeling and still require more work before patients can receive their 'anti-PCAF pill' when undergoing PCI or CABG surgery. Specifically, the target genes other than CIITA and NF κ B affected by PCAF modulation need to be fully investigated, in order to provide insight into possible adverse effects. Once this is achieved, new PCAF modulators could be developed (e.g. using phage display selection) with the optimal drug characteristics of our desire (<3-4 years).

Nonetheless, this research was able for a large extent to fulfill the aim of this thesis stated in chapter 1. This has been clearly the result of fruitful collaboration between many departments within the LUMC and pharmaceutical partners and such joint efforts should to be pursued continuously and vigorously to improve patient outcome and reduce morbidity and mortality in clinics worldwide.

Nederlandse samenvatting

Cardiovasculaire ziekten zijn verantwoordelijk voor het grootste aantal sterfgevallen wereldwijd en dit kan in het bijzonder worden toegeschreven aan atherosclerotische vaatziekten, die aanleiding geven tot beroertes of coronaire hartziekten. Verbeterde primaire preventie en de introductie en optimalisatie van percutane coronaire interventies (PCI), dotteren, heeft sterk bijgedragen aan de verbeteringen van mortaliteit en morbiditeit ten gevolge van deze aandoeningen. Het inzicht in de ziektepathofysiologie is in het afgelopen decennium enorm toegenomen. Nieuw onderzoek naar het ontstaan van post-interventionele atherosclerotische vasculaire veranderingen heeft de focus gelegd op een disfunctionele (auto)immuun respons en ontstekingsreactie. Ten gevolge hiervan ontstaan vaatwand verdikking, re-occlusie en de daaraan gerelateerde symptomen.

Het doel van dit promotieonderzoek was daarom gericht op het onderzoeken van de rol van het immuunsysteem in dit pathofysiologische proces, verantwoordelijk voor het optreden van vaatwandveranderingen. Deze nieuw verkregen inzichten werden toegepast bij de ontwikkeling van immuun modulerende therapieën in preklinische modellen. De belangrijke bijdragen van de verschillende delen van het immuunsysteem aan het ontstaan van vaatwandveranderingen in de klinische en preklinische situaties worden besproken in **hoofdstuk 1**. Het preklinisch screenen en testen van immuun modulerende therapie-effectiviteit is een belangrijke stap naar de klinische toepassing van dergelijke interventies ten tijde van PCI of coronaire arteriële bypass graft (CABG) operaties, om het ontstaan van vaatwand veranderingen en daarmee de noodzaak van re-interventies te voorkomen. Inzicht in de uitgelokte immuunreactie tijdens vasculaire ingrepen, zowel in de muis als in de mens, ligt aan de basis van de ontdekking en toepassing van nieuwe therapieën met de maximale klinische potentie.

Hoofdstuk 2 biedt een overzicht van de immuunreacties van het aangeboren en verworven immuunsysteem die plaatsvinden tijdens het ontstaan van atherosclerose en uitgelokt worden door revascularisatie procedures. Specifieke leukocyten receptoren, liganden, co-stimulatoire moleculen en ontstekingsmediatoren zoals cytokines, worden belicht. De nadruk ligt op hun rol bij het ontstaan en de progressie van de ontstekingsreactie in de vaatwand. Bovendien wordt hun associatie met de ernst van het ziekteproces beschreven, onafhankelijk van de traditionele risicofactoren zoals roken en hypertensie. Op basis hiervan zouden zij geschikt kunnen zijn om te dienen als biomarkers voor ziektestratificatie en diagnose. Hieronder valt hun geschiktheid om te dienen als markers voor patiënten die geïntensifieerde zorg behoeven, gericht op clinici die in deze patiëntengroep revascularisatie procedures uitoefenen. Daarnaast zouden dergelijke toekomstige biomarkers nuttig kunnen zijn voor het beoordelen van therapie-effectiviteit, hetgeen met de huidige meetbare risicofactoren, zoals plasma lipoproteïnen, niet mogelijk is. Plasmametingen verdienen de voorkeur boven metingen uitgevoerd ter plaatse van en tijdens angioplastiek. Desondanks kunnen lokale markers in de vaatwand op dit punt ook additionele informatie opleveren om de ernst van de laesies optimaal in te kunnen schatten. De

continue zoektocht naar nieuwe biomarkers is daarom essentieel. Met name markers van ontsteking, die causaal gerelateerd zijn met post-interventionele vasculaire veranderingen, bieden de meeste potentie en zijn van grote waarde voor klinici.

Hoofdstuk 3 illustreert dat het onderzoeksmatig screenen van therapeutische effectiviteit van medicamenteuze therapieën tegen vasculaire veranderingen en het optreden van versnelde atherosclerose niet mogelijk zou zijn zonder preklinische modellen. Zij bootsen de klinische situatie na vasculaire interventies optimaal na. Dit is niet slechts het geval op het gebied van anatomische aspecten van het vat zoals grootte, diameter en vaatwanddikte, maar ook in kenmerken van ziektestadia, conventionele risicofactoren en andere factoren voor atherosclerose. Voorts worden de gehumaniseerde muismodellen besproken die de pathofysiologische reactie, zoals deze optreedt ten tijde van restenose, alsmede de vasculaire veranderingen en versnelde atherosclerose het dichtst benaderen. Verscheidene vasculaire interventies in transgene muismodellen worden belicht met de sterkste focus op het arteria femoralis cuff model. Om effecten van lokale medicamenteuze therapie te kunnen bestuderen dienen de dieren ontvankelijk te zijn voor de specifieke therapie, maar behoren zij daarnaast ook een vergelijkbare metabole status, coaguloir fenotype en reactievermogen te hebben gelijk aan de mens. De toepassing van transgene muismodellen heeft de vergelijkbaarheid van humane en muislaesies sterk vergroot en daarmee de translatie van nieuwe therapieën richting de kliniek. Daarnaast hebben mechanistische en pathofysiologische studies aangetoond dat lokale vaatwand ontsteking, proliferatie en proteolyse centraal staan in het optreden van post-interventionele vaatwand veranderingen. Om deze redenen werd geconcludeerd dat sterk reproduceerbare diermodellen voor post-interventionele vaatwand veranderingen essentieel zijn voor het bestuderen van het ontstaan van restenose en het vinden van nieuwe medicamenteuze therapieën. Specifieke onderdelen van het immuunsysteem en hun geschiktheid om te dienen als doel van immuunmodulerende therapie worden tevens besproken. Vasculaire veranderingen worden geïnitieerd door schade aan het endotheel en aan de onderliggende atherosclerotische plaque tijdens ballon inflatie, stent positioneringen of de chirurgische procedure tijdens het prepareren van het bypass vaatsegment. Blootstelling van onderliggend trombose materiaal aan circulerend bloed geeft plaatjesadhesie, activering en trombusvorming, wat voor aantrekking van leukocyten naar het beschadigde vaatsegment zorgt. Plaatjesactivering en binding wordt ondersteund door de aanwezigheid van fosfatidylserine (PS) op geactiveerde en apoptotische cellen.

Hoofdstuk 4 toont een therapeutische rol aan voor het PS-bindende annexine A5 eiwit tegen vasculaire inflammatie, verdikkingen en disfunctie in verschillende muismodellen voor versnelde atherosclerose. Aangetoond werd dat annexine A5 injecties resulteren in een significante reductie van inflammatoire cytokine concentraties in plasma en daarmee de aantrekking van inflammatoire cellen naar de vaatwand na chirurgische interventie. Dit gaf uiteindelijk een verminderde intimale hyperplasie en ging gepaard met minder tekenen van plaque instabiliteit. Ondanks dat het niet volledig duidelijk werd waarom annexine A5 aanleiding gaf tot deze effecten, kon wel worden aangetoond dat annexine A5 functioneert via de aanhechting van leukocyten aan gebonden trombocyten en dat het de hierop volgende inflammatoire respons kan voorkomen. Deze bevindingen breiden de rol van annexine A5 uit als regulator eiwit van inflammatoire processen met een therapeutische toepassing in

inflammatoir-gedreven vaatziekten.

In **hoofdstuk 5** werd aangetoond dat er een sterke associatie bestaat tussen genetische polymorfismen in het humane annexine A5 gen en een toegenomen risico op het ontwikkelen van restenose bij patiënten die PCI ondergaan. Deze associatie werd gevonden bij 866 patiënten uit de GENDER studie. Binnen één jaar na PCI ontwikkelde 295 patiënten hiervan restenose, terwijl 571 patiënten vrij bleven van herhaalde klachten. Ondanks dat een sterke associatie bestaat, is hiermee nog niet bewezen dat er een direct causaal verband bestaat tussen deze polymorfismen en klinische uitkomsten. Om het inzicht hierin te vergroten zouden plasmametingen uitgevoerd kunnen worden naar de concentratie van circulerend annexine A5 bij deze patiënten. Verlaagde annexine A5 concentraties zijn immers al eerder gerelateerd aan een toegenomen ernst van coronairsclerose, terwijl verhoogde plasma niveaus meetbaar zijn na een myocard infarct. Desalniettemin tonen deze resultaten wel aan dat het annexine A5 genotype zou kunnen dienen als risicomarker voor het ontstaan van restenose na PCI. Deze resultaten tonen een hoge diagnostische en therapeutische potentiële waarde aan voor annexine A5 tegen PCI-geïnduceerde vaatwand veranderingen.

Hoofdstuk 6 beschrijft het proces van optimalisatie van het natuurlijk voorkomende en beschermende anti-phosphorylcholine (PC) T15/E06 IgM antilichaam naar een recombinant chimeer IgG antilichaam. Opmerkelijk genoeg gingen de beschermende effecten van het voorkomen van geoxideerd LDL (oxLDL) cholesterol opname door macrofagen met scavenger receptoren verloren na de transitie van een IgM naar een IgG antilichaam. Ondanks dit verlies was het recombinante anti-PC T15 IgG antilichaam effectief in het remmen van de monocyt-chemotactische eiwit (MCP)-1 expressie door macrofagen. Ook kon met passieve immunisatie van dit antilichaam versnelde atherosclerose vorming in gecuffde hypercholesterolemische muizen sterk geremd worden. Deze resultaten suggereren dat de inflammatoire reactie op oxLDL voorkomen wordt zonder dat het chimeer antilichaam een remming geeft van oxLDL opname. Wellicht komt dit door het maskeren van dit immunogene epitoom of door het stimuleren van de degradatie ervan en hiermee de verwijdering uit de circulatie. Volledig humane IgGs werden verkregen met behulp van phage display selectie van PC-specifieke fagen. Deze waren wel in staat om oxLDL opname door macrofagen te blokkeren en de MCP-1 expressie te remmen. Een selecte groep antilichamen werd in vivo getest en dit leverde het potente volledige humane monoclonale anti-PC T15 IgG (M99-B05) antilichaam op, dat zeer effectief was in het voorkomen van intimale verdikking in gecuffde hypercholesterolemische muizen. Deze studie bevestigt de bevindingen uit eerdere studies dat PC als een veelbelovende therapeutisch doel kan functioneren om versnelde atherosclerosevorming te voorkomen en te behandelen. Het unieke aan deze studie is echter dat er voor het eerst volledig humane anti-PC IgG antilichamen geproduceerd zijn die een atheroprotectieve functie hebben. Eerdere onderzoekers hebben anti-PC IgM antilichamen passief toegediend of muizen anti-PC IgM opgewekt via actieve immunisatie. Dit zijn veelbelovende technieken, maar zijn niet klinisch toepasbaar en eerdere actieve immunisatie met een pneumococcon-polysacharride vaccin gaf onvoldoende plasma titers van oxLDL-specifieke anti-PC antilichamen. In onze studie werden echter recombinante monoclonale anti-PC IgG antilichamen ontwikkeld, gescreend en getest welke geschikt zijn voor passieve therapeutische immunisatie in patiënten. Door

het verzorgen van directe en acute controle over de immunoreactie van de patiënt, specifiek voor één enkel immunogeen epitoom, kan deze immunisatie aanpak als een effectieve therapie dienen tegen post-PCI atherosclerotische vasculaire veranderingen.

De belangrijke rol van het aangeboren immuunsysteem werd bevestigd in **hoofdstuk 7**. In dit hoofdstuk werd in het arteria femoralis cuff model een nieuw ontwikkelde duale toll-like receptor (TLR) 7 en 9 antagonist getest. TLRs vormen een zeer belangrijk onderdeel van het aangeboren immuunsysteem en functioneren als pathogene herkenningsreceptoren (PRRs). Zij herkennen in deze functie zowel extracellulaire liganden die voorkomen op bacteriën en virussen (TLR2, 4 en 5), alsmede intracellulaire (endogene) liganden zoals beschadigd of viraal (dubbelstrengs) RNA (TLR3, 7 en 9). Deze endogene liganden kunnen vrijkomen na weefselschade of stress, zoals optreedt tijdens PCI procedures. Aanwezigheid van TLR7 en TLR9 werd aangetoond in de gebieden met uitgesproken macrofagen accumulatie in vasculaire laesies. In vitro reageerden deze cellen op TLR7 of TLR9 stimulatie met een toegenomen opname van oxLDL en secretie van tumor necrosis factor (TNF) α , wat voorkomen werd door simultane incubatie met de nieuwe inhibitor. Na cuff plaatsing in vivo leidden deze effecten tot een afname van de intimale verdikking. De bijdrage van individuele TLR signalering is nog onduidelijk, maar de therapeutische potentie van het remmen van TLR7 en TLR9 om het ontstaan van restenose en versnelde atherosclerose te voorkomen is duidelijk aangetoond. Aangezien TLRs gemakkelijk benaderbaar zijn voor circulerende medicijnen (direct of na cellulaire opname) en de eerste verdedigingslinie vormen van het aangeboren immuunsysteem, zijn zij geschikte therapeutische doelen voor medicamenteuze inhibitie of stimulatie tijdens de acute fase van vaatwand beschadiging. Nieuwe inhibitoren kunnen zo ontwikkeld worden dat zij de gewenste eigenschappen bezitten, terwijl ze specifiek gericht zijn tegen de gewenste TLRs. Tevens kunnen zij ontwikkeld worden met specificiteit voor meerdere receptoren, waardoor hun effectiviteit sterk kan toenemen, zoals werd aangetoond in deze studie.

In **hoofdstuk 8** werd de bijdrage van het verworven immuunsysteem onderzocht bij het optreden van post-interventionele atherosclerotische vaatwand veranderingen, door de rol van CD4⁺ T lymfocyten en CD28-CD80/86 co-stimulatoire moleculen te onderzoeken. Post-interventionele vasculaire veranderingen waren significant geremd in CD4^{-/-} en CD80^{-/-}CD86^{-/-} muizen. Om aan te tonen dat cytotoxic T-lymfocyt-antigen (CTLA)-4 een vitale factor is in de fysiologische co-stimulatie en betrokken is bij de T cel reacties tijdens vaatwand veranderingen, ontvingen controledieren injecties met abatacept. Dit gaf aanleiding tot een verminderde intimale verdikking. Deze methode werd herhaald in hypercholesterolemische ApoE3*Leiden muizen en gaf vergelijkbare opmerkelijke resultaten. Flow cytometrie analyse van geactiveerde lymfocyten in de milt en drainerende lymfeknopen toonde aan dat door abatacept de activering van CD4⁺ T cellen voorkomen werd en dit leidde tot een afname van de hoeveelheid regulatoire T cellen in de milt. De ratio tussen effector en regulatoire T cellen werd echter niet veranderd ten opzichte van de controledieren. Abatacept gaf geen aanleiding tot verschillen in cellulaire activeringsstatus in de drainerende lymfeknopen, hetgeen voor een systemische werkzaamheid pleit. Deze bevindingen werden later gecorreleerd met afgenomen plasma concentraties van interferon γ in dieren die met abatacept waren behandeld. De rol van CTLA-4 co-inhibitie in dit

proces werd uiteindelijk bevestigd door de behandeling van ApoE3*Leiden muizen met blokkerende anti-CLTA-4 antilichamen, afkomstig uit hybridoma's, die daardoor significant grotere laesies ontwikkelden. Immuun-gemedieerde interventies gericht op het therapeutisch controleren van de inflammatoire T cel reactie, zoals met abatacept, worden in een breed scala toegepast in andere immuunafwijkingen, waaronder reumatische ziekten. Deze interventies kunnen nu ook toegepast worden in de acute fase na vasculaire interventies om hierop volgende vaatwandveranderingen te voorkomen. Abatacept is een geregistreerd medicijn met een bewezen effectiviteit en veiligheid in patiënten. Toepassing hiervan kan de benodigde tijd voor de translatie van bench-to bedside sterk reduceren. Ondanks dat initiële positieve effecten geobserveerd zijn, moeten deze gereproduceerd worden op lange termijn na langdurige toepassing voordat abatacept klinisch toegepast zou kunnen worden. Daarnaast dienen de effecten op andere celtypen die CD28 tot expressie brengen, zoals B lymfocyten. Ondanks deze eisen heeft de huidige studie laten zien dat CD4 T cellen en de CD28-CD80/86 co-stimulatie een belangrijke rol spelen bij de inflammatoire reactie die optreedt als onderdeel van het verworven immuunsysteem na vasculaire interventies in vivo.

In **hoofdstuk 9** laten drie grote individuele prospectieve studies zien dat een significante associatie bestaat tussen het -2481C allel in de promotor regio van het P300/CBP-geassocieerde factor (PCAF) gen en een toegenomen overleving na PCI vanwege minder restenose. Dit suggereert dat de effecten van dit allel op deze klinisch eindpunten het resultaat kunnen zijn van de betrokkenheid van PCAF bij het optreden van inflammatoire en proliferatieve processen. De resultaten bieden geen inzicht in de mogelijke causale rol van dit polymorfisme bij de ontwikkeling van restenose, maar ondersteunen wel het concept dat epigenetische processen onder genetische controle staan. Tevens suggereren deze studies dat, anders dan de effecten van het milieu, genetische variatie in genen (die coderen voor K lysine acetyltransferasen (KATs)) mede het risico bepalen op het optreden van cardiovasculaire ziekten en sterfte. Het blijft tot op dit moment onduidelijk of de gevonden SNP functionele invloed heeft op de transcriptie en regulatie van PCAF. Op voorwaarde dat deze SNP een effect heeft op PCAF transcriptie of resulterende eiwit niveau, zou dit een sterk effect kunnen betekenen op de cellulaire expressie van genen, welke geaccumuleerd over vele jaren een verschil kan opleveren in uitkomst op cardiovasculair gebied. Tot het moment waarop dit bevestigd kan worden, kan deze SNP dienen als risicomarker voor mortaliteit en restenoserisico in patiënten die PCI ondergaan. Daarnaast biedt de SNP inzicht in de betrokkenheid tussen PCAF en vasculaire veranderingen, waarvan de exacte rol verder onderzocht werd in de volgende hoofdstukken.

Hoofdstuk 10 beschrijft het onderzoek dat uitgevoerd is naar de causale rol van PCAF bij de regulatie van de inflammatoire reactie, die leidt tot post-interventionele atherosclerotische vasculaire veranderingen. In het onderzoek komt naar voren dat PCAF de expressie van MHC klasse II, maar niet I, door macrofagen reguleert via klasse II-transactivator (CIITA) en in toegenomen mate tot expressie komt in de vaatwand in de vroege periode na vasculaire beschadigingen op zowel mRNA als eiwit niveau. Voorts werd aangetoond dat post-interventionele vasculaire veranderingen sterk verminderd waren in PCAF^{-/-} muizen, evenals de vorming van versnelde atherosclerose in hypercholesterolemische muizen die behandeld werden met de na-

tuurlijke PCAF-remmer garcinol. Daarnaast kwam naar voren dat een verminderde inflammatoire reactie, ten gevolge van kortdurende garcinol therapie, ten grondslag lag aan deze afgenomen intimale verdikking. Dit kwam mogelijk doordat garcinol de expressie van MCP-1 en TNF α , geproduceerd door inflammatoir gestimuleerde SMCs en macrofagen, sterk deed verminderen. Ondanks dat de rol van PCAF in de regulatie van inflammatie duidelijk is en dat PCAF betrokken is bij macrofagen aantrekking, activering en cytokine expressie, dient de specificiteit van garcinol voor PCAF in dit proces verder verduidelijkt te worden. Garcinol is uiterst potent en kan de activiteit van PCAF binnen 3 minuten inactiveren *in vitro*, maar beïnvloedt ook de expressie van andere genen en kan in hoge concentraties apoptose veroorzaken. Dit volgde ook uit andere (ongepubliceerde) experimenten in het arteria femoralis drug-eluting cuff model, waarbij de anti-inflammatoire effecten van kortdurige garcinol toepassing om PCAF te remmen verloren ging bij langdurige blootstelling van de vaatwand aan garcinol. Dit benadrukt de noodzaak van verder onderzoek naar nieuwe en potente PCAF remmers die niet zoveel, of niet in een dergelijke ernstige mate, bijwerkingen geven als garcinol. Pas dan kan PCAF inhibitie effectief worden toegepast in de kliniek. Desalniettemin tonen deze resultaten een regulatie aan van de inflammatoire reactie door een epigenetische factor in de acute fase volgend na interventie en belichten PCAF als een causale factor in dit proces.

De rol van PCAF in inflammatie en vasculaire verandering is verder onderzocht in **hoofdstuk 11**, waar PCAF^{-/-} muizen een verminderde mate van arteriogenese lieten zien na acute arteriële occlusie. Dit proces, een vorm van collaterale arteriegroei uit pre-existente arteriolen van een geoccludeerde arterie, wordt geïnduceerd door een toename in flow en shear-stress en is erg afhankelijk van de activering van circulerende inflammatoire cellen. Met behulp van een achterpoot ischemie muismodel, gebaseerd op een chirurgisch geïnduceerde acute arteria femoralis occlusie, werd de vitale betrokkenheid van PCAF in dit proces aangetoond. PCAF^{-/-} muizen lieten een verminderde inflammatoire reactie zien met afname van geactiveerde dendritische cellen, T cellen en cytokine expressie *in vivo*. Dit was ook het geval na een gift lipopolysaccharide *ex vivo*. Ondanks dat verder onderzocht dient te worden welke inflammatoire genen en in welke mate deze door PCAF gereguleerd worden, is aangetoond dat PCAF causaal betrokken is bij post-interventionele vaatwand veranderingen. PCAF regulatie van inflammatoire gen transcriptie vindt plaats in meerdere cel types van zowel het aangeboren als verworven immuunsysteem, inclusief antigeen presenterende cellen, lymfocyten en gladde spiercellen. Door een regulerende functie uit te oefenen in de acute inflammatoire reactie beïnvloedt PCAF met name pro-inflammatoire genen. PCAF functioneert hierbij als centrale factor met intrinsieke histon acetyltransferase activiteit. Dit kan klinici een interessante controleerbare epigenetische factor bieden als doel voor anti-inflammatoire preventieve therapie. Behandeling gericht op expressie van een dergelijke epigenetische factor zoals PCAF zou daarom wellicht effectiever zijn in het voorkomen van vasculaire veranderingen dan therapie gericht op een enkel gen of eiwit.

Hoe gaan we verder met deze nieuwe veelbelovende therapieën?

Het doel van dit promotieonderzoek was om de rol van het immuunsysteem in het pathofysiologische proces, wat leidt tot de ontwikkeling van post-interventionele atherosclerotische vaatwand veranderingen, te onderzoeken. Dit onderzoek heeft

meerdere nieuwe therapeutische toepassingen opgeleverd die vertaald kunnen worden naar de kliniek binnen niet afzienbare tijd. Ondanks dat dergelijke tijdsindicaties per definitie speculatief zijn, is het onjuist om zich niet aan dergelijke voorspellingen te wagen. Daarnaast is het contraproductief om veelbelovende vindingen niet verder uit te zoeken, enkel omdat de translatie naar de kliniek mogelijk erg lang kan duren. Abatacept is een reeds geregistreerde medicamenteuze therapie voor de behandeling van rheumatoïde artritis en kan in een relatieve korte tijd (<1 jaar) getest worden tijdens revascularisatie technieken, op voorwaarde dat de therapeutische effectiviteit bevestigd wordt in langdurige dierstudies. Annexine A5, recombinante monoclonale X19-A05 anti-PC IgG antilichamen en onze nieuwe TLR7/9 antagonist zijn getest en effectief bevonden in onze diermodellen, maar voordat gestart kan worden met klinische toepassing behoeven zij extra onderzoek naar de effectiviteit en veiligheidsprofielen. Dit zou voltooid kunnen worden binnen de nabije toekomst (<2 jaar). De PCAF resultaten hebben een nieuwe factor geïdentificeerd die betrokken is bij post-interventionele vasculaire veranderingen en heeft nog extra onderzoek voordat patiënten die PCI of CABG-chirurgie ondergaan een 'anti-PCAF pil' kunnen ontvangen. Om inzicht te geven in mogelijke bijwerkingen dienen in het bijzonder de genen onderzocht te worden die naast CIITA en NFκB door PCAF modulering beïnvloed worden. Wanneer dit voltooid is kunnen nieuwe PCAF modulatoren worden ontwikkeld (bijvoorbeeld via phage display selectie) met de optimale en gewenste medicamenteuze eigenschappen (<3-4 jaar). Het promotieonderzoek heeft in grote mate voldaan aan de doelstellingen die gesteld werden in hoofdstuk 1. Dit is te danken aan een goede samenwerking tussen vele afdelingen binnen het LUMC en farmaceutische partners. Dergelijke samenwerkingsprojecten dienen dan ook optimaal en continu nagestreefd te worden om patiëntresultaten te verbeteren en de morbiditeit en mortaliteit in klinieken wereldwijd te reduceren.

List of publications

Book chapters

1. Ewing MM, Karper JC, de Vries MR, Jukema JW, Quax PHA. Small Animal Models to Study Restenosis and Effects of (Local) Drug Therapy. *Coronary stent restenosis*. Editor: IC Tintoiu. Bucharest: The Publishing House of the Romanian Academy, 2011.

Full papers

2. Ewing MM, Karper JC, Abdul S, de Jong RCM, Peters HAB, de Vries MR, Redeker A, Kuiper J, Toes RE, Arens R, Jukema JW, Quax PHA. T-cell co-stimulation by CD28-CD80/86 and its negative regulator CTLA-4 strongly influence accelerated atherosclerosis development. *Int J Cardiol*. 2013; in press.
3. Karper JC, Ewing MM, Habets KLL, de Vries MR, Peters HAB, van Oeveren-Rietdijk AM, de Boer HC, Hamming JF, Kuiper J, Kandimalla ER, La Monica N, Jukema JW, Quax PHA. Blocking toll-like receptors 7 and 9 reduces postinterventional remodeling via reduced macrophage activation, foam cell formation, and migration. *Arterioscler Thromb Vasc Biol*. 2012;32:e72-80.
4. Ewing MM, Karper JC, Sampietro ML, de Vries MR, Pettersson K, Jukema JW, Quax PHA. Annexin A5 prevents post-interventional accelerated atherosclerosis development in a dose-dependent fashion. *Atherosclerosis* 2012;221:333-340.
5. Ewing MM, Karper JC, Jukema JW, Quax PH. Future potential biomarkers for postinterventional restenosis and accelerated atherosclerosis. *Biomark Med*. 2012;6:53-66.
6. Verschuren JJ, Sampietro ML, Pons D, Trompet S, Ewing MM, Quax PH, de Knijff P, Zwinderman AH, de Winter RJ, Tio RA, de Maat MP, Doevendans PA, Jukema JW. Matrix metalloproteinases 2 and 3 gene polymorphisms and the risk of target vessel revascularization after percutaneous coronary intervention: Is there still room for determining genetic variation of MMPs for assessment of an increased risk of restenosis? *Dis Markers*. 2010;29:265-73.
7. Pons D, Trompet S, de Craen AJ, Thijssen PE, Quax PH, de Vries MR, Wierda RJ, van den Elsen PJ, Monraats PS, Ewing MM, Heijmans BT, Slagboom PE, Zwinderman AH, Doevendans PA, Tio RA, de Winter RJ, de Maat MP, Iakoubova OA, Sattar N, Shepherd J, Westendorp RG, Jukema JW. Genetic variation in PCAF, a key mediator in epigenetics, is associated with reduced vascular morbidity and mortality: evidence for a new concept from three independent prospective studies. *Heart*. 2011;97:143-50.

8. Ewing MM, de Vries MR, Nordzell M, Pettersson K, de Boer HC, van Zonneveld AJ, Frostegård J, Jukema JW, Quax PH. Annexin A5 therapy attenuates vascular inflammation and remodeling and improves endothelial function in mice. *Arterioscler Thromb Vasc Biol.* 2011;31:95-101.
9. Bergheanu SC, Pons D, Karalis I, Ozsoy O, Verschuren JJW, Ewing MM, Quax PHA, Jukema JW. Genetic determinants of adverse outcome (restenosis, malapposition and thrombosis) after stent implantation. *Interventional Cardiology.* 2010;2:147-157.
10. Ewing MM, Karabina SAP, Nordzell M, Atout R, Sexton D, Lettesjö H, Karper JC, de Vries MR, Dahlbom I, Camber O, Frostegård J, Ninio E, Jukema JW, Pettersson K, Quax PHA. Optimizing Natural Occurring IgM Antibodies for Therapeutic Use: Inflammatory Vascular Disease Treatment with Anti-Phosphorylcholine IgG. *Submitted for publication.*
11. Ewing MM, Karper JC, Peters HAB, Bastiaansen AJNM, de Vries MR, van den Elsen PJ, Gongora C, Maurice T, Jukema JW, Quax PHA. The epigenetic factor PCAF regulates vascular inflammation and is essential for accelerated atherosclerosis development. *Submitted for publication.*
12. Bastiaansen AJ, Ewing MM, de Boer HC, van der Pouw Kraan TC, de Vries MR, Peters HAB, Arens R, Moore SM, Faber JE, Jukema JW, Hamming JF, Nossent AY, Quax PHA. The lysine acetyltransferase PCAF is a key regulator of arteriogenesis. *Submitted for publication.*
13. Karper JC, de Jager SCA, Ewing MM, de Vries MR, Bot I, van Santbrink PJ, Redeker A, Mallat Z, Binder CJ, Arens R, Jukema JW, Kuiper J, Quax PHA. The extracellular Toll Like Receptor 4 regulator RP105 (CD180) ameliorates atherosclerosis via its role on B-cells. *Submitted for publication.*
14. Karper JC, Ewing MM, de Vries MR, de Jager SCA, el Otmani H, Peters HAB, Sampietro ML, de Boer HC, van Zonneveld AJ, Kuiper J, Huizinga EG, Brondijk THC, Jukema JW, Quax PHA. TLR accessory molecule RP105 (CD180) is involved in post-interventional vascular remodeling and soluble RP105 modulates neointima formation. *Submitted for publication.*

Abstracts

15. Ewing MM, Verschuren JJW, Sampietro ML, de Vries MR, De Knijff P, Quax PHA, Jukema JW. Annexin A5: Genotypic risk marker for clinical restenosis after percutaneous coronary intervention. *Eur Heart J.* 2010;31:803.
16. Karper JC, Ewing MM, de Vries MR, Sampietro ML, Jukema JW, Quax PHA. RP105, a Toll Like Receptor 4 (TLR4) homolog, moderates restenosis and outward remodeling. *Circulation.* 2010;122: A14280.

17. Ewing MM, Karabina SAP, Pettersson K, Atout R, de Vries Mr, Sexton D, Lettesjö H, Frostegård J, Jukema JW, Ninio E, Quax PHA. Anti-Phosphorylcholine IgG Antibodies Reduce Restenosis and Vascular Inflammation by Inhibition of the Unfolded Protein Response in a Mouse Model of Accelerated Atherosclerosis. *Circulation*. 2010;122: A14320.
18. Ewing MM, de Vries MR, Nordzell M, Jukema JW, Frostegård J, Pettersson K, Quax PHA. Annexin A5 Reduces Inflammation Mediated Vascular Remodelling and Post-interventional Atherosclerosis and Improves Vascular Function in Hypercholesterolemic Mice. *Circulation*. 2009;120:S1113.

Curriculum vitae

Mark M. Ewing was born on June 29th 1986 in Alkmaar. He attended the *atheneum* at the Openbare Scholengemeenschap Willem Blaeu in Alkmaar, where he graduated *cum laude* in 2004. During the same year, he started his medical study at the Leiden University Medical Center (LUMC) in Leiden, The Netherlands.

During his study, he took up a position of student-assistant in teaching anatomy lessons for medical students and was involved in research into preclinical models for screening of immune system-based modulatory therapy for post-interventional vascular remodeling under the supervision of prof. dr. J.W. Jukema at the department of Cardiology at the LUMC and prof. dr. P.H.A. Quax at the Gaubius Laboratorium at TNO, Quality for Life, both in Leiden. He obtained his medical doctoral exam *cum laude* in 2008.

Thereafter, he continued his research which formed the basis of his PhD program conducted in the LUMC under prof. Jukema and prof. Quax at both the department of Cardiology and Surgery. This was funded by the European Sixth Framework program for research and technological development and the Circulating Cells project under auspices of the Center for Translation Molecular Medicine and is described in this thesis. In 2010, he won the prize for best oral presentation at the Vascular Medicine Symposium of the Rembrandt Institute for Cardiovascular Science hosted by the LUMC and Amsterdam Medical Center.

Starting October 2011, he is performing his medical rotations at the LUMC and the University of Leiden. From November 2013 onwards, he will continue his training as *Arts in Opleiding tot Specialist (AIOS)* Cardiology at the Onze Lieve Vrouwe Gasthuis (OLVG) in Amsterdam under supervision of dr. G.A. Somsen (department of Cardiology) and dr. Y.F.C. Smets (department of Internal Medicine). He lives in Amsterdam together with his partner Hinka.

